

The Science of Nutrition

Josie Frazier

An abstract graphic on the left side of the cover, composed of several overlapping, curved shapes in various shades of teal and blue. The shapes flow from the top left towards the bottom right, creating a sense of movement and depth. The colors range from a light, airy teal to a deep, dark blue.

The Science of Nutrition

The Science of Nutrition

Edited by Josie Frazier

Published by White Word Publications,
5 Penn Plaza,
19th Floor,
New York, NY 10001, USA

The Science of Nutrition

Edited by Josie Frazier

© 2021 White Word Publications

International Standard Book Number: 978-1-9789-7366-4

This book contains information obtained from authentic and highly regarded sources. Copyright for all individual chapters remain with the respective authors as indicated. All chapters are published with permission under the Creative Commons Attribution License or equivalent. A wide variety of references are listed. Permission and sources are indicated; for detailed attributions, please refer to the permissions page and list of contributors. Reasonable efforts have been made to publish reliable data and information, but the authors, editors and publisher cannot assume any responsibility for the validity of all materials or the consequences of their use.

Copyright of this ebook is with White Word Publications, rights acquired from the original print publisher, Syrawood Publishing House.

The publisher's policy is to use permanent paper from mills that operate a sustainable forestry policy. Furthermore, the publisher ensures that the text paper and cover boards used have met acceptable environmental accreditation standards.

Trademark Notice: Registered trademark of products or corporate names are used only for explanation and identification without intent to infringe.

Cataloging-in-Publication Data

The science of nutrition / edited by Josie Frazier.

p. cm.

Includes bibliographical references and index.

ISBN 978-1-9789-7366-4

1. Nutrition. 2. Diet. 3. Dietetics. 4. Food. 5. Physiology. 6. Health. I. Frazier, Josie.

QP141 .S35 2021

613.2--dc23

TABLE OF CONTENTS

Preface.....	VII
Chapter 1 Short-term cactus pear [<i>Opuntia ficus-indica</i> (L.) Mill] fruit supplementation ameliorates the inflammatory profile and is associated with improved antioxidant status among healthy humans	1
Alessandro Attanzio, Luisa Tesoriere, Sonya Vasto, Anna Maria Pintaudi, Maria A. Livrea and Mario Allegra	
Chapter 2 Nutritional quality of heat-sensitive food materials in intermittent microwave convective drying	10
Nghia Duc Pham, W. Martens, M. A. Karim and M. U. H. Joardder	
Chapter 3 Bitter melon extract ameliorates palmitate-induced apoptosis via inhibition of endoplasmic reticulum stress in HepG2 cells and high-fat/high-fructose-diet-induced fatty liver	21
Hwa Joung Lee, Rihua Cui, Sung-E Choi, Ja Young Jeon, Hae Jin Kim, Tae Ho Kim, Yup Kang and Kwan-Woo Lee	
Chapter 4 Assessment of nutritional status in the elderly: a proposed function-driven model	31
Stina Engelheart and Robert Brummer	
Chapter 5 Antioxidant effects of compound walnut oil capsule in mice aging model induced by D-galactose	37
Huandong Zhao, Jian Li, Juan Zhao, Yang Chen, Caiping Ren and Yuxiang Chen	
Chapter 6 Efficacy and safety of <i>Eurycoma longifolia</i> (Physta®) water extract plus multivitamins on quality of life, mood and stress.....	47
Annie George, Jay Udani, Nurhayati Zainal Abidin and Ashril Yusof	
Chapter 7 Rice bran triterpenoids improve postprandial hyperglycemia in healthy male adults	63
Koichi Misawa, Hiroko Jokura and Akira Shimotoyodome	
Chapter 8 Grape seed proanthocyanidin extract supplementation affects exhaustive exercise-induced fatigue in mice	70
Liu Xianchu, Liu Ming, Liu Xiangbin and Zheng Lan	
Chapter 9 Sufficient iodine status among Norwegian toddlers 18 months of age.....	77
Inger Aakre, Maria Wik Markhus, Marian Kjellefold, Vibeke Moe, Lars Smith and Lisbeth Dahl	
Chapter 10 Cholesterol-lowering effects and potential mechanisms of chitoooligosaccharide capsules in hyperlipidemic rats.....	86
Yao Jiang, Chuhan Fu, Guihua Liu, Jiao Guo and Zhengquan Su	

Chapter 11	Mulberry leaf extract displays antidiabetic activity in <i>db/db</i> mice via Akt and AMP-activated protein kinase phosphorylation	101
	Ui-Jin Bae, Eun-Soo Jung, Su-Jin Jung, Soo-Wan Chae and Byung-Hyun Park	
Chapter 12	Green tea (<i>Camellia sinensis</i>) aqueous extract alleviates postmenopausal osteoporosis in ovariectomized rats and prevents RANKL-induced osteoclastogenesis <i>in vitro</i>	110
	Xin Wu, Chuan-qi Xie, Qiang-qiang Zhu, Ming-yue Wang, Bin Sun, Yan-ping Huang, Chang Shen, Meng-fei An, Yun-li Zhao, Xuan-jun Wang and Jun Sheng	
Chapter 13	TLR2/4-mediated NF-κB pathway combined with the histone modification regulates β-defensins and interleukins expression by sodium phenyl butyrate in porcine intestinal epithelial cells	121
	Xiujing Dou, Junlan Han, Qiuyuan Ma, Baojing Cheng, Anshan Shan, Nan Gao and Yu Yang	
Chapter 14	Phoenix Dan Cong Tea: An Oolong Tea variety with promising antioxidant and <i>in vitro</i> anticancer activity	134
	Xiaobin Zhang, Zhenhuan Song, Yuanyuan You, Xiaoling Li and Tianfeng Chen	
Chapter 15	Nutritional, biochemical and sensory properties of instant beverage powder made from two different varieties of pearl millet	145
	Anthony O. Obilana, Barthi Odhav and Victoria A. Jideani	
Chapter 16	Oolong tea polysaccharide and polyphenols prevent obesity development in Sprague-Dawley rats	156
	Tao Wu, Jinling Xu, Yijun Chen, Rui Liu and Min Zhang	
Chapter 17	Sodium and potassium urinary excretion and their ratio in the elderly: results from the Nutrition UP 65 study	164
	Pedro Moreira, Ana S. Sousa, Rita S. Guerra, Alejandro Santos, Nuno Borges, Cláudia Afonso, Teresa F. Amaral and Patrícia Padrão	
Chapter 18	Mung bean proteins and peptides: nutritional, functional and bioactive properties	174
	Zhu Yi-Shen, Sun Shuai and Richard FitzGerald	
Chapter 19	Iodine content of six fish species, Norwegian dairy products and hen's egg	185
	Ive Nerhus, Maria Wik Markhus, Bente M. Nilsen, Jannike Øyen, Amund Maage, Elisabeth Rasmussen Ødegård, Lisa Kolden Midtbø, Sylvia Frantzen, Tanja Kögel, Ingvild Eide Graff, Øyvind Lie, Lisbeth Dahl and Marian Kjelleevold	
Chapter 20	A novel polysaccharide from the <i>Sarcodon aspratus</i> triggers apoptosis in Hela cells via induction of mitochondrial dysfunction	198
	Dan-Dan Wang, Qing-Xi Wu, Wen-Juan Pan, Sajid Hussain, Shomaila Mehmood and Yan Chen	

Permissions

List of Contributors

Index

PREFACE

Over the recent decade, advancements and applications have progressed exponentially. This has led to the increased interest in this field and projects are being conducted to enhance knowledge. The main objective of this book is to present some of the critical challenges and provide insights into possible solutions. This book will answer the varied questions that arise in the field and also provide an increased scope for furthering studies.

The science which interprets the interaction of different substances in food along with nutrients with respect to an organism is known nutrition. It takes into consideration the maintenance, growth, reproduction, disease and health of the organism. When the nutrient intake is not enough or if the intake is too much, it can cause a condition known as malnutrition. Deficiency of nutrients, also known as undernutrition, can cause various diseases such as scurvy, anemia and blindness. The excess of nutrients, also called overnutrition, can also cause several diseases like obesity and metabolic syndrome. Nutrients are primarily divided into two categories, macronutrients and micronutrients. Carbohydrates, fats, fiber and protein are some of the macronutrients. Minerals and vitamins are some examples of micronutrients. The topics included in this book on nutrition are of utmost significance and bound to provide incredible insights to readers. It includes contributions of experts and scientists which will provide innovative insights into this field. This book will serve as a valuable source of reference for graduate and post graduate students.

I hope that this book, with its visionary approach, will be a valuable addition and will promote interest among readers. Each of the authors has provided their extraordinary competence in their specific fields by providing different perspectives as they come from diverse nations and regions. I thank them for their contributions.

Editor

WWT

Short-term cactus pear [*Opuntia ficus-indica* (L.) Mill] fruit supplementation ameliorates the inflammatory profile and is associated with improved antioxidant status among healthy humans

Alessandro Attanzio, Luisa Tesoriere, Sonya Vasto, Anna Maria Pintaudi, Maria A. Livrea and Mario Allegra*

Dipartimento di Scienze e Tecnologie Biologiche, Chimiche e Farmaceutiche, Università degli Studi di Palermo, Palermo, Italy.

Abstract

Background: Dietary ingredients and food components are major modifiable factors protecting immune system and preventing the progression of a low-grade chronic inflammation responsible for age-related diseases.

Objective: Our study explored whether cactus pear (*Opuntia ficus-indica*, *Surfarina* cultivar) fruit supplementation modulates plasma inflammatory biomarkers in healthy adults. Correlations between inflammatory parameters and antioxidant status were also assessed in parallel.

Design: In a randomised, 2-period (2 weeks/period), crossover, controlled-feeding study, conducted in 28 healthy volunteers [mean age 39.96 (\pm 9.15) years, BMI 23.1 (\pm 1.5) kg/m²], the effects of a diet supplemented with cactus pear fruit pulp (200 g, twice a day) were compared with those of an equivalent diet with isocaloric fresh fruit substitution.

Results: With respect to control, cactus pear diet decreased ($p < 0.05$) the pro-inflammatory markers such as tumour necrosis factor- α (TNF- α), interleukin (IL)-1 β , interferon- γ (INF)- γ , IL-8, C-reactive protein (CRP) and erythrocyte sedimentation rate (ESR), whereas it increased ($p < 0.05$) the anti-inflammatory marker IL-10. Moreover, the diet decreased ratios between pro-inflammatory biomarkers (CRP, IL-6, IL-8, TNF- α) and anti-inflammatory biomarker (IL-10) ($p < 0.05$). Cactus pear supplementation caused an increase ($p < 0.05$) in dermal carotenoids (skin carotenoid score, SCS), a biomarker of the body antioxidant status, with correlations between SCS and CRP ($r = -0.905, p < 0.0001$), IL-8 ($r = -0.835, p < 0.0001$) and IL-10 ($r = 0.889, p < 0.0001$).

Conclusions: The presently observed modulation of both inflammatory markers and antioxidant balance suggests cactus pear fruit as a novel and beneficial component to be incorporated into current healthy dietary habits.

Keywords: *cactus pear fruit; healthy subjects; inflammatory biomarkers; antioxidant network; skin carotenoids*

Dietary patterns based on plant-derived food have consistently been associated with reduced risk of age-related pathologies, such as cardiovascular diseases, cancer, metabolic syndrome, inflammatory conditions and neurodegenerative disorders (1). A slowly increasing systemic inflammation is related to the onset and the evolution of virtually all the above-mentioned pathologies. Indeed, serum concentrations of inflammatory mediators typically increase with age even in the absence of acute infection or other pathological stress. In this context in order to examine the 'diet-health' relationship, dietary

interventions targeting disease prevention are critically dependent on the evaluation of inflammatory biomarkers, even within the reference range, to monitor underlying inflammatory state and progression. Notwithstanding the complexity and the discordance of the available literature in this regard, a suite of biomarkers reliable even in low-grade inflammation has emerged in the recent years (2).

Inflammation-induced tissue damage occurs in an organ-specific manner in different diseases or conditions; nonetheless, responses and markers in different organs and molecules involved in the inflammatory reaction are

remarkably similar. Along with an increased number of peripheral leukocytes, an overproduction of inflammatory cytokines and chemokines, including tumour necrosis factor- α (TNF- α), interleukin (IL)-1 β , IL-6, IL-8 and interferon- γ (INF- γ), is observed (3, 4). These mediators act to amplify the inflammatory process and elicit systemic effects, such as generation of high amounts of hepatic acute-phase reactant C-reactive protein (CRP), eventually leading to tissue injury. All these parameters have then been identified as a set of 'general' biomarkers that can provide quantitative assessments of the inflammatory condition [2]. On the contrary, the concentration of anti-inflammatory cytokine IL-10 (5, 6) and its relationship and balance with the pro-inflammatory ones has to be taken into consideration when evaluating ongoing inflammatory processes and specifically age-related low-grade inflammation (7).

Within the abundance of fruits and vegetables, the *Opuntia ficus-indica* fruit has received a reasonable amount of attention over the last decade for its health-promoting properties mainly related to its betalain content (8–17). In particular, human studies showed that consumption of cactus pear at dietary-achievable amounts was associated with a remarkable reduction of oxidative stress in healthy subjects (18). Moreover, nutritionally relevant supplementation of either whole fruit extracts or its characteristic betalain and indicaxanthin has been reported to exert strong anti-inflammatory effects in several experimental models both *in vitro* and *in vivo* (11–15, 17).

Inflammatory biomarkers undergo an age-related increase, though remaining within a normal range, in healthy subjects (7). In this context, the primary objective of this short-term dietary intervention study was to investigate whether dietary amounts of cactus pear fruit, daily supplemented for 2 weeks, could affect inflammatory status and plasma concentration of inflammatory biomarkers of healthy men and women. Currently, no single marker can predict the effect of a dietary intervention, and very few studies have considered multiple markers simultaneously, most focusing on non-specific biochemical markers such as CRP and/or IL-6 (19–23). Conversely, in our study both clinical biomarkers, such as CRP and erythrocyte sedimentation rate (ESR), and a large panel of pro- and anti-inflammatory cytokines have been considered. Moreover, owing to the interconnections between inflammation and oxidative stress (24), we concurrently assessed the effects from cactus pear supplementation on the global body antioxidant balance and sought to correlate them with the anti-inflammatory ones.

Subjects and methods

Fruit

Cactus pear fruits from the yellow Sicilian *Surfarina* cultivar, from the same area (San Cono, Catania, Italy), at

comparable ripening stages and 1-week old, were obtained from the producer from October to December 2016, and the study was carried out within the same time interval. The necessary amounts were delivered to our laboratory twice a week. Fruits were peeled and pulp consumed according to the design below. The phytochemical content of the fruit was randomly checked at the beginning of the study and once a week during the time of supplementation according to methods reported elsewhere (8, 25).

Participants, study design and compliance

The study population consisted of 28 volunteers aged 30–69 years (14 women, 14 men; age 31–40 years, $n = 15$; 40–50 years, $n = 10$; 50–60 years, $n = 2$; >60 years, $n = 1$; $x \pm SD = 39.96 \pm 9.15$); body mass index (kg/m^2): 23.1 ± 1.5 . All participants were highly educated, working at our university ($n = 12$), professionals ($n = 6$) or postdoc students ($n = 10$). Among them, some worked in the field of health science ($n = 13$). Some participants performed habitual physical activity ($n = 4$), and some were smokers ($n = 6$). They provided written informed consent to participate and none of them withdrew from the study. All participants were in good general health as determined by a medical history questionnaire, physical examination and clinical laboratory tests. Subjects fulfilled the following eligibility criteria: (1) no history of cardiovascular, hepatic, gastrointestinal or renal disease, hypertension, diabetes mellitus and dyslipidaemia; (2) no antibiotic, vitamin or mineral use for > 6 weeks before the beginning of the study. The women were not using exogenous hormones. The study protocol was in accordance with the Helsinki Declaration of 1964 and its later amendments.

The study was a randomised, crossover, 2-period (2 weeks/period), controlled-feeding study designed to evaluate the effects of cactus pear fruit pulp consumption (200 g, twice a day) in the context of a planned dietary regimen, on both a number of inflammatory parameters and the whole body antioxidative status. Blood samples, collected in EDTA-coated tubes (1 mg/mL) after an overnight fasting, were obtained from the subjects at the beginning (baseline, B) and at the end of each diet period, that is, control diet (CD) and cactus pear diet (CPD). Diet periods were separated by a 3-week compliance break after which blood was drawn. Plasma was separated from blood cells by centrifugation at 4°C and $2,000 \times g$ for 10 min. Suitable aliquots of plasma were portioned, stored at -80°C and analysed within 2 weeks. The trial design is depicted in Fig. 1. With the exception of the substitution of seasonal fruit with cactus pear fruits, participants consumed individual but comparable meals. Energy, macronutrient, total lipids, cholesterol, saturated fatty acids and vitamins were calculated by WinFood Software based on the Italian Food Composition Table from the National Institute of Nutrition

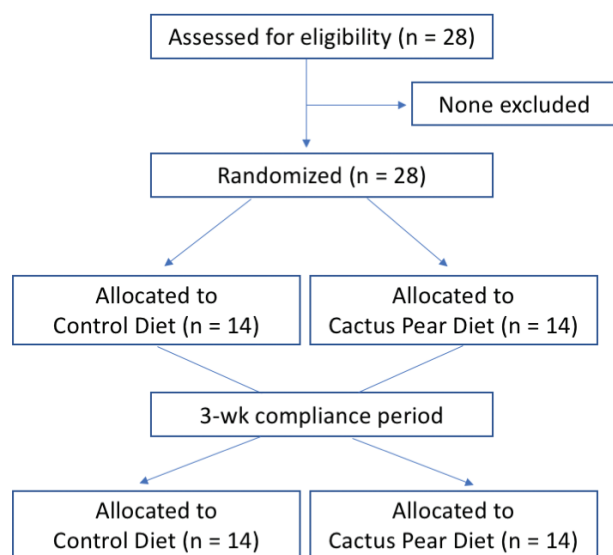


Fig. 1. Scheme of participant flow through the study.

(INRAN). The individual dietary plans were composed using information from each subject with the objective of respecting the personal food tastes and according to the total energy expenditure for each participant. Macronutrient distribution was adjusted in accordance with the Acceptable Macronutrient Distribution Range (26). Participants committed themselves to substitute equivalent foods using a food replacement list based on MyPlate's food groups, as vegetables, grains, protein, dairy and others (oil, sugar and salt) (27). Food portion size was based on Italian standard kitchen utensils, and all participants were recommended by the dietician to use them to measure their own consumption. Dietary composition reported in Table 1 was based on the planned dietary protocols and consisted of five meals daily, that is, *breakfast*: milk or yogurt, coffee, whole-grain bread with jam; *snack 1*: 200 g of seasonal fresh fruit (CD, Table 2) or 200 g of cactus pear fruit pulp (CPD); *lunch*: pasta or bread or rice, grilled fish, salad or cooked vegetables; *snack 2*: 200 g of seasonal fresh fruits (CD, Table 2) or 200 g cactus pear fruit pulp (CPD); *dinner*: bread, legumes or grilled fish, cooked vegetables or salad. Food intake was assessed using 3-day food records, applied four times for each patient (1 week, 3 weeks, 5 weeks and 7 weeks). All raw dietary components were provided to participants twice a week, and the subjects were instructed for the meal preparation by written recipes. Record methodology, portion size estimate and validation were conducted in agreement with published protocols (27). Participants were recommended to maintain their lifestyle habits.

Assessment of hematologic indexes and inflammatory markers

Glucose was measured using the hexokinase method; total cholesterol, high-density lipoprotein (HDL) cholesterol

Table 1. Macro- and micro-nutrient composition of cactus pear diet (CPD) and control diet (CD), on the basis of 2100 kcal/day and averaged across a 5-day menu cycle.

	CPD	CD
Protein, % of kcal (g)	13.5 (71)	14.3 (75)
Carbohydrate, % of kcal (g)	59.8 (314)	58.7 (308)
Fat, % of kcal (g)	26.6 (62)	27.0 (63)
SFA, % of kcal (g)	7.4 (18)	7.6 (18)
MUFA, % of kcal (g)	10.1 (24)	10.3 (24)
PUFA, % of kcal (g)	6.1 (15)	6.3 (15)
Cholesterol, mg	125	120
Fiber, g	24.1	25.1
Sodium, mg	3012	3018
Potassium, mg	2860	2855
Calcium, mg	1329	1331
Iron, mg	14	16
Ascorbic acid, mg	130	120

Note: All values were determined using The Food Processor SQL (version 10.8.0; ESHA Research, Salem, OR). MUFA indicates monounsaturated fatty acids; PUFA, polyunsaturated fatty acids; SFA, saturated fatty acids.

Table 2. Types of fruit consumed in the CD.

Snack 1	Strawberry
	Pineapple
	Apple
	Tangerine
Snack 2	Orange
	Melon
	Pear
	Grapefruit

and triglycerides were measured using enzymatic colorimetric methods (Abbott ARCHITECT System; Abbott Diagnostics, Abbott Park, Ill). Low-density lipoprotein (LDL) cholesterol was calculated using the Friedewald formula.

Serum concentrations of all plasma cytokines were measured by high-sensitivity magnetic luminex performance assay (R&D Systems, Minneapolis, MN) in triplicate. Serum high-sensitivity CRP was measured by latex-enhanced immuno-nephelometry (Quest Diagnostics, Madison, NJ). ESR was determined as reported by Strojnik et al. (28).

Measurement of skin carotenoids as index of body antioxidant status

A portable Raman spectroscope, Pharmanex® Bio-Photonic Scanner S2 (NuSkin, Provo, Utah, USA), designed to monitor carotenoids in the 0.1 mm stratum corneum of the skin of the hand, has been used for the measurement of the global antioxidant status (29). A

low-intensity 471.3–473 nm radiation from light emitting diodes interacts with the skin carotenoids. The scattered light is detected at 507.8–509.8 nm by the scanner that converts the Raman intensity in counts (skin carotenoid score, SCS). A computer then transforms the scanner signals in a coloured scale going from red (poor SCS, <19,000) to dark blue (high SCS, >50,000). SCS can be converted to laboratory measurements using the equation [$Y = 12703X + 5891.7$], where 'Y' is the SCS value and 'X' is the carotenoid concentration expressed as micrograms (μg)/mL of serum.

Statistical analysis

Data are expressed as means \pm SD. Comparisons were made using one-way ANOVA followed by Sidak's multiple comparison test. In all cases, significance was accepted when the null hypothesis was rejected at $p < 0.05$ level. Pearson's correlational analysis was run on comparisons of IL-10, IL-8 and CRP versus SCS.

Results

Compliance of subjects to the study

The compliance of each patient to his/her dietary schedule was assessed by nutritionists every week during the intervention and was very good as no one dropped out of the study or reported problems in the self-management of meals; no adverse events were identified in both CD and CPD over the study period, and all 28 subjects (14 in the CD group and 14 in the CPD group) completed the study and were included in the analyses (Fig. 1).

Phytochemical profile of cactus pear fruits

The fruit content was checked for antioxidant vitamins, betalain pigments and polyphenols and results are shown in Table 3. Significant amounts of ascorbic acid and indicaxanthin and minor amounts of β -carotene were measured,

Table 3. Phytochemicals, vitamins, antioxidants and total reducing power (TEAC) of the cactus pear pulp employed in the study.

	Content/100 g edible pulp
Indicaxanthin (mg)	8.51 \pm 0.33
Betanin (mg)	1.05 \pm 0.19
Ascorbic acid (mg)	29 \pm 2
α -Tocopherol (μg)	75 \pm 6
β -Carotene (μg)	1.3 \pm 0.5
Glutathione (mg)	7.8 \pm 0.5
Cysteine (mg)	0.67 \pm 0.04
Kaempferol (μg)	2.1 \pm 0.3

Note: All values are the mean \pm SD of five determinations performed in triplicate on four lots of fruits.

whereas polyphenols were almost absent, with the exception of minor amounts of kaempferol.

Effect of cactus pear supplementation on CRP and ESR

Characteristics of the participants to the study are summarised in Table 4. All parameters measured were within the reference range at the beginning of the study (baseline), and their level did not vary significantly at the end of neither the control diet nor the cactus pear diet.

Levels of CRP and ESR were measured as non-specific markers of the global inflammatory status. CRP and ESR should not exceed 10 mg/L and 15 mm/h, respectively, in healthy subjects (30). In our study, both values were in the reference range at the baseline (CRP = 0.47 ± 0.12 ; ESR = 5.5 ± 2.38) and were not significantly modified by CD; however, they showed a significant ($p < 0.02$ for CRP and $p < 0.0001$ for ESR) decrease after the cactus pear supplementation (Fig. 2).

Level of CRP and ESR evaluated at the end of the 3-week compliance period was not significantly different from baseline values (not reported).

Effect of cactus pear supplementation on inflammatory markers

Taking into account the strong relationship between CRP and cytokine production (31, 32), we next evaluated the effect of cactus pear fruit supplementation on several plasma cytokines. With respect to CD, almost all cytokines tested varied significantly after CPD ($p < 0.05$) (Fig.3). Noteworthy, while remaining within a physiological range, levels of pro-inflammatory cytokines (i.e. TNF- α , IL-1 β , INF- γ and IL-8) decreased, whereas that of IL-10, a potent anti-inflammatory cytokine, increased. IL-6 did not show any significant variation (Fig. 3).

The level of cytokines at the end of the 3-week compliance period was not significantly different from the baseline level (not reported).

Ratios between pro- and anti-inflammatory markers can help to define asymptomatic low-grade inflammation (33). Table 5 reports the calculated ratios between

Table 4. Lipid haematological parameters of the subjects enrolled at baseline, after CPD and after CD.

	Baseline	CPD	CD
Glucose (mmol/L)	4.60 \pm 0.41	4.38 \pm 0.39	4.94 \pm 0.42
Cholesterol (mmol/L)	4.84 \pm 0.42	4.69 \pm 0.44	4.94 \pm 0.39
HDL-cholesterol (mmol/L)	2.56 \pm 0.2	2.46 \pm 0.1	2.61 \pm 0.2
LDL-cholesterol (mmol/L)	2.28 \pm 0.2	2.23 \pm 0.2	2.33 \pm 0.2
Triglycerides (mmol/L)	1.12 \pm 0.09	1.07 \pm 0.09	1.14 \pm 0.1

Note: All values are the mean \pm SD of separate determinations performed in triplicate on blood samples from different subjects, $n=28$. With respect to baseline, no value was significantly different. One-way ANOVA with Sidak's multiple comparison test.

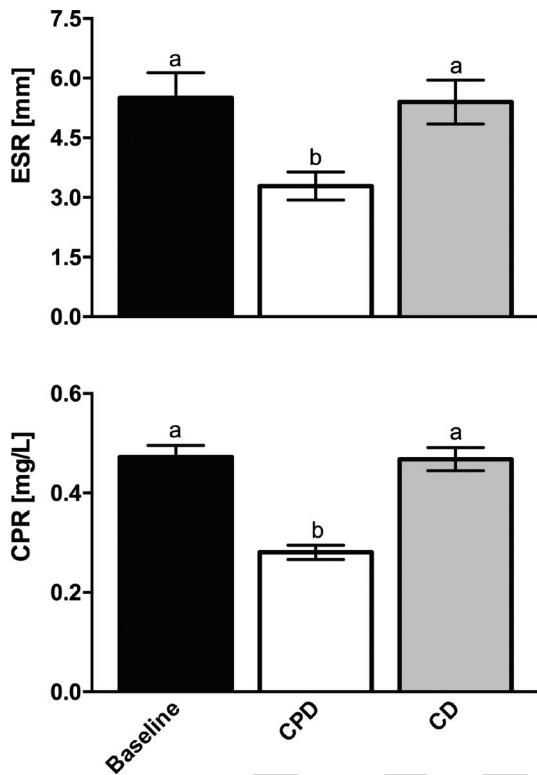


Fig. 2. Plasma ESR and CRP values of the subjects enrolled at baseline, after CPD and after CD. All values are the mean \pm SD of separate determinations performed in triplicate on samples from different subjects, $n = 28$. Labelled means without a common letter differ with a $p < 0.05$. One-way ANOVA with Sidak's multiple comparison test.

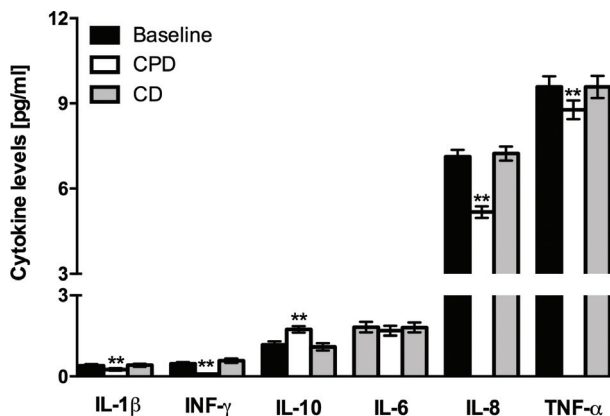


Fig. 3. Plasma cytokine levels of the subjects enrolled at baseline, after CPD and after CD. All values are the mean \pm SD of separate determinations performed in triplicate on samples from different subjects, $n = 28$. Within each set, asterisks indicate that means differ with a $p < 0.05$. One-way ANOVA with Sidak's multiple comparison test.

CRP, IL-6, IL-8, TNF- α and IL-10 at baseline and at the end of CPD and CD. Although serum concentration of IL-6 did not vary at any dietary condition, a significant

Table 5 Ratio between selected inflammatory parameter (IL-6, IL-8, TNF- α , CRP) and IL-10 at baseline, after CPD and after CD.

	Baseline	CPD	CD
IL-6/IL-10	1.84 \pm 0.98	1.02 \pm 0.52*	2.05 \pm 1.18
IL-8/IL-10	7.36 \pm 3.03	3.26 \pm 1.26**	8.35 \pm 3.95
TNF- α /IL-10	10.30 \pm 5.10	5.55 \pm 2.14**	11.60 \pm 6.80
CRP/IL-10	0.46 \pm 0.27	0.17 \pm 0.10**	0.49 \pm 0.31

Note: All values are the mean \pm SD of separate determinations performed in triplicate on blood samples from different subjects, $n = 28$. With respect to baseline, values significantly differ (*) with $p = 0.0002$, (**) with $p < 0.0001$. One-way ANOVA with Sidak's multiple comparison test.

decrease ($p < 0.0002$) in IL-6/IL-10 ratios was observed after CPD as compared with CD. Likewise, there was a decrease of all other pro-inflammatory mediators/IL-10 ratios ($p < 0.0001$).

Effect of cactus pear supplementation on antioxidant state

The antioxidant status of the subjects was assessed through Raman spectroscopy-based measurements of skin carotenoids. At the baseline, SCS was 30×10^3 to 40×10^3 (Fig. 4). In comparison with CD, CPD significantly ($p < 0.05$) improved the SCS (40×10^3 to 50×10^3). Remarkably, a negative correlation existed at the end of CPD between the change of the skin carotenoid levels and either CRP or IL-8, whereas a positive correlation was observed with the anti-inflammatory IL-10 (Fig. 5). On the contrary, no significant correlation was found between the change of the SCS and the change of ESR, TNF- α , IL-1 β and TNF- γ .

Discussion

Monitoring the inflammatory status of healthy subjects following specific dietary approaches may help to reveal food components that may protect the immune system and counteract its progressive dysfunction. By comparing the effects of a cactus pear fruit including diet with those of a comparable diet with a seasonal fresh fruit substitution, this study showed that a 2-week supplementation with dietary amounts of cactus pear fruit significantly modulated a large panel of critical inflammatory biomarkers, this being correlated with concurrent amelioration of the body antioxidant status, in healthy adults.

Serum CRP and ESR are general but definite inflammatory biomarkers; in line with current literature data showing that consumption of healthy dietary patterns rich in vegetables, fruits and legumes is associated with a significant reduction of both CRP and ESR (1, 34), we here observed a remarkable decrease of both these parameters after cactus pear supplementation. In addition, beside its significance in the inflammatory reaction, CRP is considered among risk factors for CVD and independent

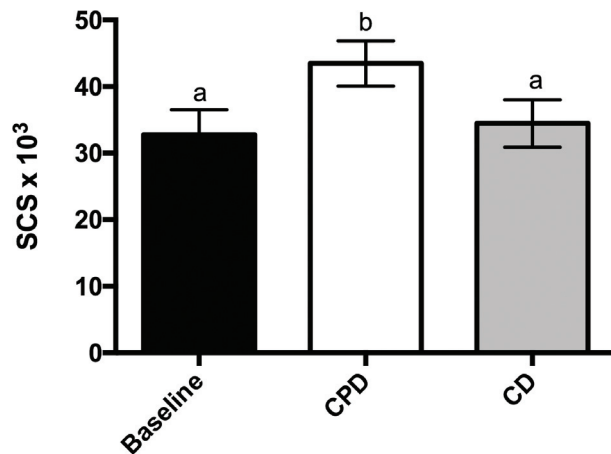


Fig. 4. SCS values of the subjects enrolled at baseline, after CPD and after CD. All values are the mean \pm SD of separate determinations performed in triplicate on samples from different subjects, $n = 28$. Labelled means without a common letter differ with a $p < 0.05$. One-way ANOVA with Sidak's multiple comparison test.

predictor of cardiovascular events (35). The reported significant reduction of plasma CRP by cactus pear fruit supplementation may suggest further benefits from diets enriched with these fruits.

The effects from cactus pear supplementation on CRP levels were paralleled by those on several plasma cytokines, with the exception of IL-6. The latter plays an important role in the inflammatory response and is a key stimulus for the acute-phase response that drives downstream events, including the hepatic synthesis of CRP (36). For this reason, a positive correlation between levels of IL-6 and CRP usually exists under inflammatory conditions. As stated by our measurements, despite the remarkable decrease in CRP, IL-6 was not affected by the supplementation. Dietary components may possibly affect the levels of CRP in different ways in healthy subjects. Liver pathways regulating CRP production are indeed controlled by a number of pro- and anti-inflammatory factors, including IL-10 (33, 37, 38). The increase in this anti-inflammatory cytokine, caused by cactus pear supplementation, may have altered the cytokine balance eventually preventing the activation of the CRP synthesis.

Besides the serum levels of inflammatory mediators, ratios between pro- and anti-inflammatory markers can help to define asymptomatic low-grade inflammation (33) and should therefore be considered in healthy subjects. We observed a significant decrease in the ratio between CRP, IL-6, IL-8, TNF- α , all factors that may undergo a life-long variation within their normal range in healthy population (7), and IL-10. Although serum concentration of IL-6 did not vary, the decrease in IL-6/IL-10 ratio further indicates the positive effect of cactus pear on the inflammatory

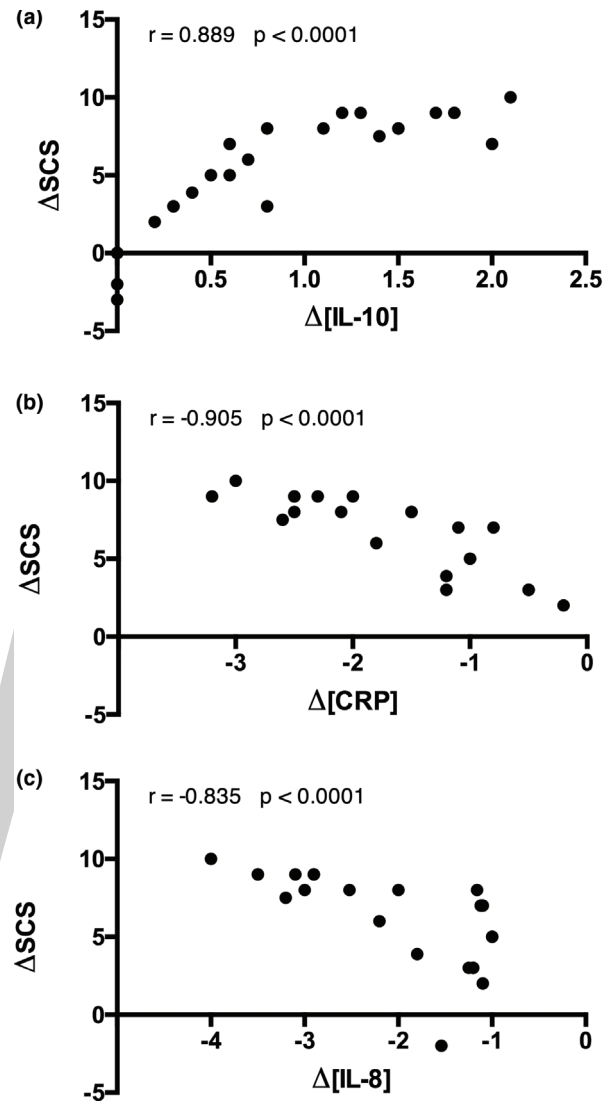


Fig. 5. Correlation between changes of SCS and IL-10 (a), CRP (b) and IL-8 (c) values of the subjects enrolled at baseline and after CPD. All values are the mean \pm SD of separate determinations performed in triplicate on samples from different subjects, $n = 28$. The Pearson's correlation coefficients and p -values are stated in the corresponding plots.

status of the subjects and confirms a prevalence of activation of anti-inflammatory pathways. Then, cactus pear fruit supplementation might have, by some means, affected physiological mechanisms of control, in turn causing a decrease in pro-inflammatory factors and an increase in anti-inflammatory factor.

Anti-inflammatory effects arising from dietary fruits and vegetables have possibly been related to the flavonoid content (34). Interestingly, only minor amounts of kaempferol occurred in our cactus pear fruits. A modulation of redox-dependent inflammatory pathways by indicaxanthin (13), the main and highly bioavailable (39) phytochemical of this yellow cultivar of cactus pear

fruit that was used, may be implicated. In addition, although we demonstrated that vitamin C was not involved in the beneficial effects by cactus pear supplementation on the oxidative stress (18), present findings cannot rule out a positive role for ascorbate or for a combination of betalain pigments with ascorbate on the inflammatory status.

The global body's antioxidant status is a result of a balance between the level of antioxidants in cells and body fluids, including blood, and pro-oxidant species endogenously produced or coming from external sources. Body's molecular antioxidants work in concert and preserve each other, so the level of each one in the pool reflects the level of the whole antioxidant pool. On this basis, dermal carotenoids are a feasible marker of the body antioxidative network and may provide a useful, though indirect, indication of a moderate to severe individual oxidative stress (40). By a non-invasive laser spectroscopy-based measurement of skin carotenoids, we showed that cactus pear consumption caused an increase of skin carotenoids by around 30%, showing that the antioxidant balance of the subjects varied positively. Data from the present approach are substantially in accordance with those from blood measurements previously reported by our research group, showing reduction of oxidative stress arising in healthy subjects from cactus pear fruit consumption (18). It is not realistic to suppose that the very minute amounts of β -carotene in the fruits might vary the blood amounts of β -carotene (of the order of 10^{-6} M in healthy people), and then the skin content, to the observed extent. Rather, we suggest that the ingestion of the whole fruit and its phytochemical components, including betalains, can favourably affect cell pathways concurring to the maintenance of a proper antioxidant status (41). Moreover, in accordance with the interconnections between inflammation and oxidative stress (24), we observed that the antioxidative effects from cactus pear ingestion had a meaningful correlation with the anti-inflammatory factor. Specifically, the increase in the changes of SCS negatively correlated with the changes of CRP and IL-8 and positively with those of the anti-inflammatory IL-10.

A limitation of the study is the rather small sample size including young- to middle-aged healthy subjects from the same area. A second limitation is the short duration of the intervention. Nonetheless, the experimental design is quite coherent with previous nutritional investigations from this group (18), showing reduction of oxidative stress in healthy volunteers by regular consumption of cactus pear fruits. Exploring the effect of cactus pear fruit supplementation on the immune system in different age groups, as well as subjects at risk or affected by inflammatory diseases, should deserve further studies.

Conclusive remarks and perspectives

Dietary ingredients and food components are major modifiable factors affecting immune function and may lifelong counteract ongoing alterations of the inflammatory state associated with ageing and age-related disorders (33, 42). In this context, our randomised, crossover, controlled-feeding study in healthy men and women provides a good indication of the potential of this fruit to positively affect mechanisms regulating the immune system. Moreover, by providing evidence that relationships between the circulating levels of inflammatory biomarkers and the individual oxidative status may be revealed in healthy humans, our findings may suggest an interesting issue for nutritional investigations. Since inflammation and oxidative stress contribute to the pathogenesis of many of chronic pathologies, assessment of their relationships in healthy populations may help to predict risk of age-related chronic conditions and eventually validate the effects of dietary interventions.

Present findings may suggest cactus pear fruit as a novel habit to be incorporated into the dietary portion of beneficial lifestyle changes.

Conflict of interest and funding

On behalf of all authors, the corresponding author states that there is no conflict of interest.

References

1. Neale EP, Batterham MJ, Tapsell LC. Consumption of a healthy dietary pattern results in significant reductions in C-reactive protein levels in adults: a meta-analysis. *Nutr Res* 2016; 36(5): 391–401.
2. Calder PC, Ahluwalia N, Albers R, Bosco N, Bourdet-Sicard R, Haller D, et al. A consideration of biomarkers to be used for evaluation of inflammation in human nutritional studies. *Br J Nutr* 2013; 109(Suppl 1): S1–34.
3. Danesh J, Kaptoge S, Mann AG, Sarwar N, Wood A, Angleman SB, et al. Long-term interleukin-6 levels and subsequent risk of coronary heart disease: two new prospective studies and a systematic review. *PLoS Med* 2008; 5(4): e78.
4. Clearfield MB. C-reactive protein: a new risk assessment tool for cardiovascular disease. *J Am Osteopath Assoc* 2005; 105(9): 409–16.
5. Sabat R, Grutz G, Warszawska K, Kirsch S, Witte E, Wolk K, et al. Biology of interleukin-10. *Cytokine Growth Factor Rev* 2010; 21(5): 331–44.
6. Filippi CM, von Herrath MG. IL-10 and the resolution of infections. *J Pathol* 2008; 214(2): 224–30.
7. Wyczalkowska-Tomasik A, Czarkowska-Paczek B, Zielenkiewicz M, Paczek L. Inflammatory markers change with age, but do not fall beyond reported normal ranges. *Arch Immunol Ther Exp (Warsz)*. 2016; 64(3): 249–54.
8. Butera D, Tesoriere L, Di Gaudio F, Bongiorno A, Allegra M, Pintaudi AM, et al. Antioxidant activities of Sicilian prickly pear (*Opuntia ficus indica*) fruit extracts and reducing properties of its betalains: betanin and indicaxanthin. *J Agr Food Chem* 2002; 50(23): 6895–901.

9. Tesoriere L, Allegra M, Butera D, Gentile C, Livrea MA. Cytoprotective effects of the antioxidant phytochemical indicaxanthin in beta-thalassemia red blood cells. *Free Radic Res* 2006; 40(7): 753–61.
10. Tesoriere L, Allegra M, Butera D, Gentile C, Livrea MA. Kinetics of the lipoperoxyl radical-scavenging activity of indicaxanthin in solution and unilamellar liposomes. *Free Radic Res* 2007; 41(2): 226–33.
11. Tesoriere L, Attanzio A, Allegra M, Gentile C, Livrea MA. Phytochemical indicaxanthin suppresses 7-ketocholesterol-induced THP-1 cell apoptosis by preventing cytosolic Ca(2+) increase and oxidative stress. *Br J Nutr* 2013; 110(2): 230–40.
12. Tesoriere L, Gentile C, Angileri F, Attanzio A, Tutone M, Allegra M, et al. Trans-epithelial transport of the betalain pigments indicaxanthin and betanin across Caco-2 cell monolayers and influence of food matrix. *Eur J Nutr* 2013; 52(3): 1077–87.
13. Allegra M, D'Acquisto F, Tesoriere L, Attanzio A, Livrea MA. Pro-oxidant activity of indicaxanthin from *Opuntia ficus indica* modulates arachidonate metabolism and prostaglandin synthesis through lipid peroxide production in LPS-stimulated RAW 264.7 macrophages. *Redox Biol* 2014; 2: 892–900.
14. Allegra M, Ianaro A, Tersigni M, Panza E, Tesoriere L, Livrea MA. Indicaxanthin from cactus pear fruit exerts anti-inflammatory effects in carrageenin-induced rat pleurisy. *J Nutr* 2014; 144(2): 185–92.
15. Tesoriere L, Attanzio A, Allegra M, Gentile C, Livrea MA. Indicaxanthin inhibits NADPH oxidase (NOX)-1 activation and NF-kappaB-dependent release of inflammatory mediators and prevents the increase of epithelial permeability in IL-1beta-exposed Caco-2 cells. *Br J Nutr* 2014; 111(3): 415–23.
16. Allegra M, Carletti F, Gambino G, Tutone M, Attanzio A, Tesoriere L, et al. Indicaxanthin from *Opuntia ficus-indica* crosses the blood-brain barrier and modulates neuronal bioelectric activity in rat hippocampus at dietary-consistent amounts. *J Agr Food Chem*. 2015; 63(33): 7353–60.
17. Tesoriere L, Attanzio A, Allegra M, Livrea MA. Dietary indicaxanthin from cactus pear (*Opuntia ficus-indica*, L. Mill) fruit prevents eryptosis induced by oxysterols in a hypercholesterolaemia-relevant proportion and adhesion of human erythrocytes to endothelial cell layers. *Br J Nutr* 2015; 114(3): 368–75.
18. Tesoriere L, Butera D, Pintaudi AM, Allegra M, Livrea MA. Supplementation with cactus pear (*Opuntia ficus-indica*) fruit decreases oxidative stress in healthy humans: a comparative study with vitamin C. *Am J Clin Nutr* 2004; 80(2): 391–5.
19. Bonaccio M, Cerletti C, Iacoviello L, de Gaetano G. Mediterranean diet and low-grade subclinical inflammation: the Moli-sani study. *Endocr Metab Immune Disord Drug Targets* 2015; 15(1): 18–24.
20. Rocha VZ, Ras RT, Gagliardi AC, Mangili LC, Trautwein EA, Santos RD. Effects of phytosterols on markers of inflammation: a systematic review and meta-analysis. *Atherosclerosis* 2016; 248: 76–83.
21. Devaraj S, Autret BC, Jialal I. Reduced-calorie orange juice beverage with plant sterols lowers C-reactive protein concentrations and improves the lipid profile in human volunteers. *Am J Clin Nutr* 2006; 84(4): 756–61.
22. Labonte ME, Cyr A, Abdullah MM, Lepine MC, Vohl MC, Jones P, et al. Dairy product consumption has no impact on biomarkers of inflammation among men and women with low-grade systemic inflammation. *J Nutr* 2014; 144(11): 1760–7.
23. Yu Z, Malik VS, Keum N, Hu FB, Giovannucci EL, Stampfer MJ, et al. Associations between nut consumption and inflammatory biomarkers. *Am J Clin Nutr* 2016; 104(3): 722–8.
24. Reuter S, Gupta SC, Chaturvedi MM, Aggarwal BB. Oxidative stress, inflammation, and cancer: how are they linked? *Free Radic Biol Med* 2010; 49(11): 1603–16.
25. Tesoriere L, Fazzari M, Allegra M, Livrea MA. Biothiols, taurine, and lipid-soluble antioxidants in the edible pulp of Sicilian cactus pear (*Opuntia ficus-indica*) fruits and changes of bioactive juice components upon industrial processing. *J Agric Food Chem* 2005; 53(20): 7851–5.
26. Zello GA. Dietary Reference Intakes for the macronutrients and energy: considerations for physical activity. *Appl Physiol Nutr Metab* 2006; 31(1): 74–9.
27. Chang S, Koegel K. Back to basics: all about myPlate food groups. *J Acad Nutr Diet*. 2017; 117(9): 1351–3.
28. Strojnik T, Smigoc T, Lah TT. Prognostic value of erythrocyte sedimentation rate and C-reactive protein in the blood of patients with glioma. *Anticancer Res* 2014; 34(1): 339–47.
29. Perrone A, Pintaudi AM, Traina A, Carruba G, Attanzio A, Gentile C, et al. Raman spectroscopic measurements of dermal carotenoids in breast cancer operated patients provide evidence for the positive impact of a dietary regimen rich in fruit and vegetables on body oxidative stress and BC prognostic anthropometric parameters: a five-year study. *Oxid Med Cell Longev* 2016; 2016: 2727403.
30. Devaraj S, O'Keefe G, Jialal I. Defining the proinflammatory phenotype using high sensitive C-reactive protein levels as the biomarker. *J Clin Endocrinol Metab* 2005; 90(8): 4549–54.
31. Wang XH, Liu SQ, Wang YL, Jin Y. Correlation of serum high-sensitivity C-reactive protein and interleukin-6 in patients with acute coronary syndrome. *Genet Mol Res* 2014; 13(2): 4260–6.
32. Ridker PM. From C-reactive protein to interleukin-6 to interleukin-1: moving upstream to identify novel targets for atheroprotection. *Circ Res* 2016; 118(1): 145–56.
33. Albers R, Bourdet-Sicard R, Braun D, Calder PC, Herz U, Lambert C, et al. Monitoring immune modulation by nutrition in the general population: identifying and substantiating effects on human health. *Br J Nutr* 2013; 110(Suppl 2): S1–30.
34. Gonzalez-Gallego J, Garcia-Mediavilla MV, Sanchez-Campos S, Tunon MJ. Fruit polyphenols, immunity and inflammation. *Br J Nutr* 2010; 104(Suppl 3): S15–27.
35. Koenig W. Predicting risk and treatment benefit in atherosclerosis: the role of C-reactive protein. *Int J Cardiol* 2005; 98(2): 199–206.
36. Il'yasova D, Ivanova A, Morrow JD, Cesari M, Pahor M. Correlation between two markers of inflammation, serum C-reactive protein and interleukin 6, and indices of oxidative stress in patients with high risk of cardiovascular disease. *Biomarkers* 2008; 13(1): 41–51.
37. Ivashchenko Y, Kramer F, Schafer S, Bucher A, Veit K, Hombach V, et al. Protein kinase C pathway is involved in transcriptional regulation of C-reactive protein synthesis in human hepatocytes. *Arterioscler Thromb Vasc Biol* 2005; 25(1): 186–92.
38. Kluff C, de Maat MP. Genetics of C-reactive protein: new possibilities and complications. *Arterioscler Thromb Vasc Biol* 2003; 23(11): 1956–9.
39. Tesoriere L, Allegra M, Butera D, Livrea MA. Absorption, excretion, and distribution of dietary antioxidant betalains in LDLs: potential health effects of betalains in humans. *Am J Clin Nutr* 2004; 80(4): 941–5.
40. Mayne ST, Cartmel B, Scarmo S, Jahns L, Ermakov IV, Gellermann W. Resonance Raman spectroscopic evaluation of skin carotenoids as a biomarker of carotenoid status for human studies. *Arch Biochem Biophys* 2013; 539(2): 163–70.

41. Forman HJ, Davies KJ, Ursini F. How do nutritional antioxidants really work: nucleophilic tone and para-hormesis versus free radical scavenging in vivo. *Free Radic Biol Med* 2014; 66: 24–35.
42. Panickar KS, Jewell DE. The beneficial role of anti-inflammatory dietary ingredients in attenuating markers of chronic low-grade inflammation in aging. *Horm Mol Biol Clin Investig* 2015; 23(2): 59–70.

***Mario Allegra**

Dipartimento di Scienze e Tecnologie Biologiche,
Chimiche e Farmaceutiche,
Università degli Studi di Palermo,
Via Archirafi 28, 90123 – Palermo, Italy
Email: mario.allegra@unipa.it

WWT

Nutritional quality of heat-sensitive food materials in intermittent microwave convective drying

Nghia Duc Pham^{1,2}, W. Martens¹, M.A. Karim^{1*} and M.U.H. Joardder¹

¹Science and Engineering Faculty, Queensland University of Technology 2 George street, Brisbane, QLD 4001, Australia

²Engineering Faculty, Vietnam National University of Agriculture, Vietnam

Abstract

Background: The retention of health promoting components in nutrient-rich dried food is significantly affected by the dehydration method. Theoretical and experimental investigations reported in the literature have demonstrated that intermittent microwave convective drying (IMCD) can effectively improve the drying performance. However, the impact of this advanced drying method on the quality food has not been adequately investigated.

Design: A programmable NN-SD691S Panasonic inverter microwave oven (1100 W, 2450 MHz) was employed for the experiments. The microwave power level was set at 100 W and ran for 20 seconds at different power ratios and the constant hot air conditions was set to a temperature of 60°C and 0.86 m/s air velocity.

Objective: In this study, natural bioactive compounds (ascorbic acid and total polyphenol), water activity, colour and microstructure modifications which can occur in IMCD were investigated, taking kiwifruit as a sample.

Results and Discussion: The microwave (MW) power ratio (PR) had significant impact on different quality attributes of dried samples. The results demonstrate that applying optimum level MW power and intermittency could be an appropriate strategy to significantly improve the preservation of nutrient contents, microstructure and colour of the dried sample. The IMCD at PR 1:4 was found to be the ideal drying condition with the highest ascorbic acid retention (3.944 mg/g DM), lowest colour change ($\Delta_{\text{ERGB}} = 43.86$) and a porous microstructure. However, the total polyphenol content was better maintained (3.701 mg GAE/g DM) at higher microwave density (PR 1:3). All samples attained a desirable level of water activity which is unsusceptible for microorganism growth and reproduction.

Conclusion: Overall, IMCD significantly improved the drying performance and product quality compared to traditional convective drying.

Keywords: *intermittent microwave convective drying; Kiwifruit; microstructure; ascorbic acid; Polyphenol; colour analysis; nutritional quality; drying characteristics*

Nomenclature

IMCD	Intermittent microwave convective drying	PR	Power ratio
h	Hue angle	Rpm	Round per minute
M	Moisture content of the material (g/g DM)	a_w	Water activity
M_e	Equilibrium moisture content (g/g DM)	DM	Dry mass (g)
M_o	Initial moisture content (g/g DM)	t_{on}	Microwave on time
ΔE_{RGB}	Total colour difference	t_{off}	Microwave off time
AAC	Ascorbic acid content (mg/ g DM)	RGB	Red – green – blue
GAE	Gallic acid equivalents (mg/ g DM)	TPC	Total polyphenol content

One of the major processes in food industries is drying. Drying adds value to a product, reduces transportation and storage costs, increases a product shelf life and has the ability to improve the bio-accessibility and bio-availability of health-promoting compounds in food (1). However, the quality of heat-sensitive plant-based food rapidly deteriorates during conventional drying, which results in considerable destruction of bioactive components and development of undesirable colour, flavour, texture and microbiological spoilage (2). In order to shorten the lengthy processing time in traditional convective drying, high-temperature drying medium can be used. However, these types of drying methods generally result in quality deterioration, in particular, a high reduction in their nutritional value (3, 4). To overcome this issue, an integrated convective and microwave (MW) drying method has been proposed. This hybrid drying method has a potential to improve energy efficiency while maintaining desirable product quality by utilising the advantages of each drying method (2, 5). This hybrid drying method can significantly reduce the processing time due to rapid volumetric heating caused by MW radiation. However, continuously applying the MW and convective heating can result in higher and localised temperatures. These elevated temperatures can cause significant quality deterioration in thermo-labile foods like fruits and vegetables (6). Due to the continuous supply of heat, the atoms and molecules of bioactive components' movement are accelerated, which increases the frequency of collisions until the products reach the sufficient energy to start the chemical reaction. The rate of biological reaction approximately doubles for every 10°C increase in temperature (7–9). Prolonged exposure of samples to a drying environment can facilitate the degradative reactions (i.e. vitamin C, polyphenol oxidation, protein hydrolysis and beta-carotene isomerisation), which eventually reduces the health-promoting benefits and antioxidant activity of bioactive ingredients in plant-based food materials. One such drying method which has received attention recently is intermittent microwave convective drying (IMCD). Applying MW radiation intermittently during convective food drying has shown huge potential to reduce browning effects, reduce mitigation of hydro-thermo-mechanical stresses generated inside the sample, and minimise the chemical reactions that lead to health-beneficial component losses and adverse physical quality modifications (10–13). The results show that this style of drying is a promising alternative for drying of thermo-labile plant-based food materials. This advanced hybrid drying method has two sections within the drying cycle, the active drying period and the tempering period (2, 14). During the active drying period (when MW is on), moisture from the food surface is evaporated and carried away, while in the tempering period (when MW is off) the temperature and moisture are redistributed from the

high- to low-concentration regions. Due to the moisture gradient, moisture still migrates from the interior region to the surface in the tempering period of the drying cycle. This allows the high drying rate to be maintained for the next active cycle. This cycle of cooling and rewetting the sample during the tempering period prevents samples from overheating and quality deterioration. Overheating can also be avoided by controlling the MW supply to the sample allowing the energy to be wisely utilised, and therefore, the sample is heated within the safe region ensuring the food quality. Hence, IMCD has the potential to provide an optimal drying process by overcoming the issues associated with continuous hot air and/or continuous MW drying (15–17).

Currently, despite the considerable potential of IMCD, the impact of IMCD on food quality has not been extensively examined (2, 18, 19), particularly no study has investigated the effect of IMCD on the nutritional quality attributes of kiwifruit. Kiwifruit (*Actinidia chinensis Planch*) is an attractive, valuable and nutrient-dense fruit with inviting green/yellow flesh colour, distinctive flavour, taste and many health beneficial ingredients. It is an abundant source of chlorophyll, actinidin, total polyphenol, vitamin E and vitamin C with a high level of antioxidant capacity while containing no fat or cholesterol (20). Because of its abundant health benefits, a growing interest is being observed in the impact of thermal dehydration on the properties of these compounds and their relation to other quality characteristics. Kiwifruit is one of the highly perishable foods with seasonal availability; many preservation methods have been attempted to prolong their storage life and make this healthy product commercially available to consumers (21–25). IMCD drying could be one potential dehydration method able to extend kiwifruits shelf life and add value by efficiently reducing moisture content, hence inhibiting microbial growth and deteriorative chemical and enzymatic reactions (26).

Kiwifruit has been investigated for convective drying by several researchers (21, 27–30). Similarly, changes in colour (25, 31, 32) and physical properties (33, 34) of hot air convective dried kiwifruit have been published. The influence of conventional drying conditions on bioactive compounds in fresh and dried kiwifruit has also been examined by Tian et al. (22), Orikasa et al. (23) and Kaya et al. (24). However, no study exists of the impact of IMCD conditions on the drying characteristics and quality attributes of kiwifruit. It is especially challenging to produce high-quality dried kiwifruit as the fresh kiwi contains high amount of thermal-sensitive elements while intensive heating treatments generally have detrimental effects on the bioactive compounds, colour, water activity and microstructure of the product. Therefore, a comprehensive research is required to obtain an appropriate drying method to ensure the quality of nutrition-rich fruits like kiwifruit.

In this context, the primary aim of this study is to investigate the quality characteristic change of kiwifruits under different IMCD conditions. The retention of AAC and total polyphenol content, water activity, colour degradation and microstructure modification were investigated under different IMCD PRs, taking convective air-dried sample as a reference.

Materials and methods

Sample preparation for drying

Fresh green Nutri kiwifruits were used for the IMCD experiments. They were carefully chosen to be identical in shape, size, firmness and ripeness. The fresh samples were stored at $4 \pm 1^\circ\text{C}$ before experiments. The kiwifruits taken from the laboratory fridge were washed with distilled water to remove residue and dirt and then allowed to reach room temperature before conducting each drying experiment. The initial moisture content of the fresh kiwi slices was estimated to be approximately 83.4 ± 0.03 (% w.b.). The kiwifruit skin was peeled, and then slices of 50 mm diameter and 7mm thickness were made by cutting perpendicularly to the main core fruit axis using a food slicer. One slice of kiwifruit was dried in each IMCD condition and three replicates were carried out.

Drying equipment and experimental procedure

For IMCD experiment, a programmable NN-SD691S Panasonic inverter MW oven with a maximum energy output of 1,100 W (2,450 MHz) was employed for the experiments. The inverter MW oven provides constantly true power transmission at the setting values. The MW power level was set at 100 W and was turned on for 20 sec at different PRs, and the hot air drying time was in accordant with PR during the MW time off. The hot air condition was set to a temperature of 60°C and 0.86 m/s air velocity. The kiwifruit slice was placed in the centre of the MW cavity, for an even absorption of MW energy. The moisture loss was recorded at regular intervals at the end of power-off times by placing the sample slice on the digital balance. Once the kiwifruit had reached a moisture content of approximately 19.5 ± 0.4 (% w.b.), the drying process was stopped. Sample temperature was regularly checked during the drying process by aFlir E5 thermal imaging camera to record the maximum sample temperature.

The PR ($\text{PR} = t_{\text{on}} : t_{\text{off}}$) was set at four different modes: 1:1, 1:2, 1:3 and 1:4. Here t_{on} was the MW on time in seconds and t_{off} was the MW off time in seconds.

An independent hot air convective drying experiment was also conducted to compare with the results from IMCD, which had the same experimental conditions as in IMCD method.

The decrease in the moisture ratio (MR) with the drying time was used to examine the experimental data. The MR denotes the remaining moisture in the kiwifruit samples in relation to the initial moisture content, which can be calculated by Equation (1).

$$MR = \frac{M - M_e}{M_o - M_e} \quad (1)$$

Where M is the moisture content of the material on a dry basis, M_e is the equilibrium moisture content, and M_o is the initial moisture content. For an extended period, the M_e becomes very insignificant and considerably small as compared to M and M_o , and therefore, Equation (1) can also be written as $MR = M/M_o$ (35, 36).

Water activity measurement

The water activity (a_w) was measured using an Aqualab water activity meter (Decagon Devices, Pawkit, USA) in stable laboratory condition at $24 \pm 0.3^\circ\text{C}$. The dried samples of different drying conditions were kept in a desiccant chamber until the sample temperature reach the room temperature before placing in the sample cup of the water activity meter. The water activity measurements of dried product were performed in triplicate.

HPLC analysis of AAC content

About 4 g of the fresh sample or 1 g of dried sample was homogenised for 1 min at maximum speed in a UltraTurrax T25 homogeniser in 25 ml of metaphosphoric acid buffer (3% metaphosphoric acid, 1 mM Na_2EDTA) under low light condition, purging with nitrogen to prevent the oxidation process. The homogenised samples were vortexed, then filtered through a Whatman no. 3 filter paper and diluted again to 25 mL of the extractant solution and centrifuged at 10,000 g for 15 min at ambient temperature.

AAC contents were determined based on the HPLC method proposed by Asami et al. (37) with some modifications. The analysis was carried out using an Agilent HPLC 1100, G1311A dual pump, G4225A 1260 HiP Degasser, equipped with a G1315B DAD absorbance detector. The reverse-phase separation was obtained using a Waters Symmetry C18 column (4.6×250 mm, $5 \mu\text{m}$). The isocratic mobile phase was HPLC graded water brought to pH 3.0 by metaphosphoric acid. The flow rate was 0.5 mL/min; injection volume was 20 μL , and the applied wavelength was 254 nm. Supernatants of the extracted samples were filtered through a 0.22 μm Acrodisc syringe Nylon membrane filter before injection. The retention time of AAC peak was archived at 2.6 min. A 5-point standard curve was established to calculate the ascorbic content of samples. All samples were tested in triplicate.

Total polyphenol extraction and measurement

The amount of total polyphenols in the samples was determined by Folin–Ciocalteu method (38) with some modification. About 4 g of the fresh sample or about 1 g of dried sample was homogenised in 25 mL of a mixture of acetone and distilled water (70:30 v/v) for 1 min at maximum speed (25,000 rpm) in a UltraTurrax T25 homogeniser. The homogenised samples were shaken and then allowed to settle for 1 h at ambient temperature. Extracts were centrifuged at 10,000 g for 15 min at 20°C. The supernatant added with 5 mL extractant was filtered through a Whatman no. 3 filter paper. Extraction processes were repeated three times to get reliable data, and the extracts were diluted 10 times with distilled water. Then, 1 ml of the diluted extract solution was mixed with 5 ml of Folin–Ciocalteu reagent (10%) and 4 ml of 7.5% Na₂CO₃ solution. After 30 min of incubation in a water bath at 37°C, the absorbance was measured against water at the highest absorption wavelength with kiwifruit extraction solution, 760 nm (Cary50 UV Spectrophotometer). A standard curve with gallic acid standard solutions was established. The amount of total phenolic content (TPC) was in milligrams of gallic acid equivalents/gram (GAE) on the dry mass basis.

Microstructure

A scanning electron microscope (Model Mira 3 Tescan, Kohoutovice, Česká Republika) was used to examine the microstructure of the dried kiwifruit slices. The scanning electron microscopy (SEM) analysis was used in order to determine the degree of change/damage of the kiwi cells caused by the drying process. The fresh/dried kiwifruit samples were cut into cubes of 5–8 mm³ by shaft razor blade, placed on a SEM stub by carbon strip, then sputter coated with 10 nm gold before observation (Leica EM SCD005 sputter coater). Fresh samples were scanned under low vacuum conditions (40 Pa), LVSTD detector, at an accelerating voltage of 10 kV; while dried samples were scanned under high vacuum mode, 10kV voltage, SE detector.

Image acquisition and colour analysis

Digital images were obtained using 8.0 megapixels Samsung camera. These images were stored in the bitmap graphic format. ImageJ software was employed to analyse digital images in the RGB (Red–green–blue) colour. RGB-triplets for every pixel in the image represent the intensities of RGB colours in the range 0–255. Before processing of the sample images, the preprocessing was carried out based on a method proposed by Sharifian et al. (39) to avoid the non-uniform light distribution in the background and to remove surrounding noises. Colour measurement was performed in triplicate in each drying

condition to determine hue angle and colour change (6). The hue angle h° is defined as:

$$h^\circ = \tan^{-1} \left(\frac{\sqrt{3}(G-B)}{2R-G-B} \right) \quad (2)$$

Therefore,

$$\tan h^\circ = \left(\frac{\sqrt{3}(G-B)}{2R-G-B} \right) \quad (3)$$

Colour changes were defined as in Equation (4):

$$\Delta E_{RGB} = \sqrt{(\Delta R)^2 + (\Delta G)^2 + (\Delta B)^2} \quad (4)$$

Where ΔE_{RGB} represents the total colour changes of IMCD dried kiwifruit slices compared to the fresh sample.

Statistical analysis

The investigated characteristics were independently performed in triplicate. The mean data were analysed by analysis of variance (ANOVA) using SAS (version 9.1; SAS Institute Inc., Cary, NC, USA). Least significance difference (LSD) tests were employed to determine the difference of means, and statistical significance with a confidence interval of 95% ($p \leq 0.05$).

Results and discussion

Drying process

Experimental drying curves for different PRs of IMCD and the reference convective drying curve are presented in Fig. 1. It can be seen that the processing times required to attain the same final moisture content were different at different drying conditions (PRs). The drying time required to reach the moisture content of 19.5 ± 0.4 (% w.b.) from the fresh condition of 83.4 ± 0.03 (% w.b.) at PR 1:1, 1:2, 1:3 and 1:4 were 88 min, 93 min, 108 min and 151 min, respectively, whereas convective drying took 528 min to bring the sample to the same moisture content. While in all IMCD settings, the moisture content reached <20% within 150 min, the convective sample still remained at a high moisture content, approximately 75 (% w.b.) or 3.04 (g water/g dry mass). The results demonstrate that IMCD can significantly reduce the drying time compared to convective drying.

The drying rate was significantly high at the beginning of the IMCD process as the initial available moisture content in the samples was high. The drying rate was then gradually reduced towards the end of the drying process. It can be concluded that in the early drying stage, the MW energy was mainly absorbed by water near the sample

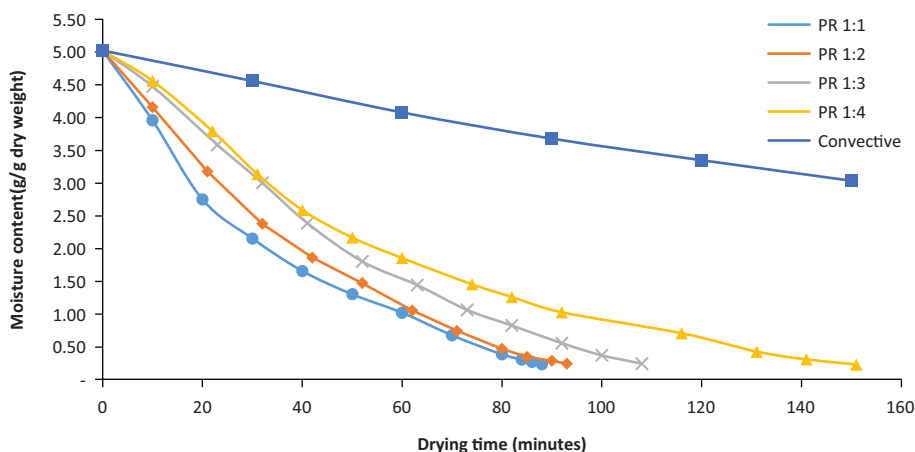


Fig. 1. Drying curves at different drying conditions.

surface, the free and loosely bound water of the sample, which was easily removed (40).

It is clear from Fig. 1 that a higher PR led to higher drying rate during the drying process, resulting in a shorter drying time. Because of the volumetric heating characteristics of MW, the MW energy directly penetrated inside the sample and excited water inside the sample. At the same time, the sample was gradually heated from the outer surface of the sample by the hot air (Kumar et al. 2016). The moisture outward flux was eventually increased, and drying rate increased considerably. However, there was an insignificant difference in the drying times between drying PR 1:1 and 1:2, especially in the final drying period (when the moisture content was <1 g/g dry basis), indicating that determining right PR in IMCD is critical to increase the drying rate and achieve shorter drying times.

Water activity

Another essential quality indicator measured in this study was water activity, which allowed determining the product stability and safety (41). Water activity characteristics determine many chemical or enzyme reaction and biochemical processes, which are important for the control of food product safety and quality. The results of water activity measurement in fresh and dried kiwi-fruit are presented in Table 1. The fresh material was characterised by the average water activity of 0.97 ± 0.012 . According to Sablani et al. (42), the growth of microorganisms, the microbiological stability of food materials, depends on the value of water activity. Moreover, a change in water activity affects the relative speed of chemical, enzymatic and biological reaction (42, 43). This can be seen in Table 1; the water activity of all dried samples was less than 0.6, which means that the growth of bacteria, yeasts and moulds will be inhibited

Table 1. Water activity of samples under different drying conditions

Samples	Water activity
Fresh sample	0.97 ± 0.012
Convective drying sample	$0.57^a \pm 0.011$
IMCD PR 1:1 sample	$0.34^d \pm 0.004$
IMCD PR 1:2 sample	$0.41^c \pm 0.005$
IMCD PR 1:3 sample	$0.43^c \pm 0.011$
IMCD PR 1:4 sample	$0.52^b \pm 0.005$

Different superscript letters (a, b, c, d) indicate significant differences ($p \leq 0.05$) among the samples under different drying conditions. Identical superscript letters indicate no significant difference.

and the degradation of chemical reactions will be minimised in all the drying conditions considered. However, the highest a_w value was obtained in convective drying (0.57 ± 0.011) and the lowest a_w value was observed in IMCD at PR 1:1 (0.34 ± 0.004), which was about 40% lower compared to convective drying. In drying pumpkin slices, Junqueira et al. (44) found similar results that MW drying provided lower water activity in the samples than other methods. Water activity describes the bound of moisture to a food's structure and it is related to the energy required to remove moisture from the sample. It also takes part in chemical/biochemical reactions and growth of microorganisms. Therefore, the results demonstrated that the intensity of MW heating takes a significant part in the rate of bound water removal from the sample, which is considered as the most time-consuming process and ineffective energy use in conventional hot air drying. The result suggests that MW effectively reduced the sample water activity to the optimum stability level. Attaining low water activity at desired moisture level helped to extend product shelf life while maintaining its expected quality characteristics.

Ascorbic acid

AAC is one of the most thermo-labile bioactive compounds in plant-based foods. Therefore, the thermal drying processes should be carried out in a way that ensures the highest preservation of AAC in the dried food products. The effects of IMCD at different PRs and convective drying on the retention of AAC in dehydrated kiwifruit are shown in Fig. 2. It can be seen that drying conditions greatly affected the retention of AAC and its content decreased in all drying conditions in comparison with the fresh samples. This phenomenon could be due to the thermal destruction during drying and the exposure of the samples to the drying medium. The degradative chemical reactions of natural bioactive compounds are catalysed by heat and ascorbate oxidase enzyme released from disrupted cell membranes during the drying process. The average total AAC found in fresh kiwifruit was 91.64 mg/100 g fresh sample (5.520 mg/g DM), which is consistent with those reported in several varieties and genotypes of fresh green kiwi: 59.65 mg/100 g (45), 65–120 mg/100 g (46), and 117.65 mg/100 g (24). Because AAC is a heat-sensitive nutrient, higher degradation of AAC was observed in convective drying and IMCD at higher PR (e.g. 1:1 and 1:2) and the retention of AAC was approximately 52%. The temperatures of samples were found fluctuated during each IMCD cycle, which was at peak point at the end of the MV heating period and lowest point at the end of the tempering period. The maximum temperatures recorded were 70°C, 76°C, 81°C and 85°C at PR 1:4, PR 1:3, PR 1:2 and PR 1:1, respectively. The higher frequency of MV radiation (PR) increased the sample temperature during IMCD, which generally degrades the heat-sensitive bioactive compounds within the sample. This result affirms the thermal sensitivity of AAC at intensive heating conditions and lengthy drying process of the samples. The results of this study show that the highest retention of AAC ($p \leq 0.05$) can be obtained at

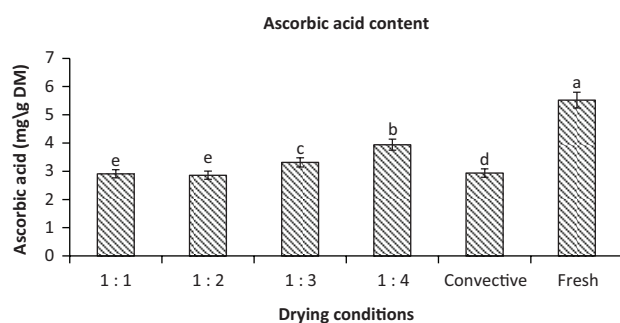


Fig. 2. Ascorbic acid content of fresh and dried sample slices under different PRs 1:1, 1:2, 1:3, 1:4 and convective drying. Different letters (a, b, c, d) indicate significant differences ($p \leq 0.05$) among the samples under different drying conditions. Identical letters indicate no significant difference.

drying conditions of PR 1:4 (3.994 mg/g DM) which is a pretty mild condition and relatively short total drying time, retaining approximately 71.5% of AAC from the fresh sample, whereas samples dried with hot air drying at 60°C retained only 53.2% of AAC (2.938 mg/g DM), which was slightly higher than the retention of AAC at PR 1:1 and PR 1:2. It is also noted that the total drying time is significantly longer in convective drying.

Total polyphenols content

The retention of total polyphenol content of the fresh and dried kiwi slices is shown in Fig. 3. The average concentration of the total polyphenol in fresh kiwifruits was 4.523 mg GAE/g DM. At the end of the drying process, the highest loss of 30.4% of the TPC had occurred at PR 1:1 (3.150 mg GAE/g DM), followed by 22.7 and 23.5% loss in PR 1:2 and PR 1:4 samples, respectively, while the loss of TPC was lowest (14%) at PR 1:3. A significant difference ($p \leq 0.05$) in the TPC between PR 1:4 and PR 1:3 was observed. In spite of the fact that the drying condition in PR 1:3 was more heat-intensive than PR 1:4, it is interesting to observe the highest polyphenol retention at PR 1:3 (3.701 mg GAE/g DM). The above-mentioned results also demonstrated that the level of TPC retention in IMCD is higher than that of AAC. It can be concluded that TPC is less heat sensitive than AAC. Also, the MW radiation at PR 1:3 might be sufficient to release the bound polyphenols by breaking the cellular food matrix for better extraction in chemical analysis. The discharge of the oxidative and hydrolytic enzymes from the collapsed food cells can decompose long-chain polyphenols into simple phenolic compounds. Also, newly formed phenolic compounds were the result of the complex heat catalysed chemical reaction of the released enzymes and bioactive compounds. In addition, more phenolic products can be

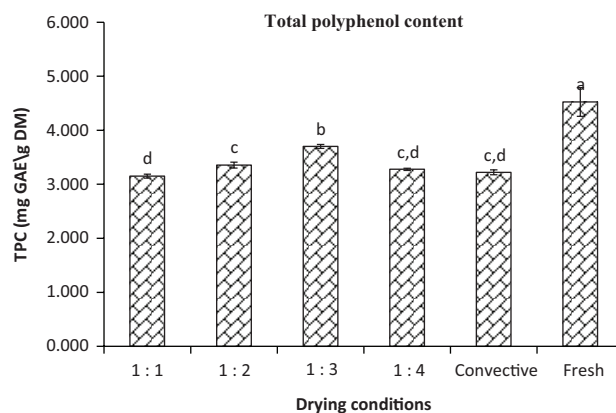


Fig. 3. Total polyphenol content of fresh and dried sample slices under different PRs 1:1, 1:2, 1:3, 1:4, and convective drying. Different letters (a, b, c, d) indicate significant differences ($p \leq 0.05$) among the samples under different drying conditions. Identical letters indicate no significant difference.

produced as the result of Maillard reaction under PR 1:3. In contrast, thermal destruction by intensive MW heating in PR 1:2 diminished polyphenols and longer drying time in PR 1:4 and convective drying gained sufficient time to facilitate oxidative deterioration of polyphenols (47–49). The obtained results also highlighted the advantages of combining hot air and intermittent MV to enhance extraction efficiency of the bioactive compounds due to its combined effect on the cell membrane. Moreover, the elevated temperature induced by MW radiation at suitable PR can reduce the degradation of polyphenols by inactivating the polyphenol oxidase, lipoxygenase and peroxidase enzymes released from the collapsed tissue (50). Many published articles (51–53) reported that MW drying retains high total polyphenol. On the contrary, an insignificant difference ($p > 0.05$) in the TPC was observed between drying mode PR 1:4 and convective drying, with the retention of approximately 75% (3.277 mg GAE/g DM). Overall, compared to fresh samples, all the dried samples retained high level of phenolic contents. The lowest phenolic retention was approximately a third from fresh sample observed in IMCD at PR 1:1 as well as in the case of convective drying.

Microstructure

As MW penetrating deep into the samples causes volumetric heating and rapid moisture evaporation, it is

suspected that significant microstructural changes may take place during IMCD. However, no investigation on microstructural changes in IMCD can be found in the literature. Illustration of the microstructure of fresh and dried samples derived from different drying conditions has been presented in Fig. 4. Prolonged external heating in convective drying (60°C) causes case hardening and collapses as shown in Fig. 4d. A limited number of pores and cell opening can be observed. The hot air drying induced slow water migration with high turgor reduction, structural shrinkage and collapse, whereas hot air drying coupled with periodic MW heating provided a more porous structure compared to the purely convective drying method as depicted in Fig. 4.

The MW reduces the drying time due to rapid moisture evaporation from inside the material. However, cell collapse can also be observed due to overheated regions resulted from uneven heating during MW heating at higher PR. This incident is observed from Fig. 4b and c that represents the cracked and collapsed microstructure of sample dried at PR 1:1 and PR 1:2.

It is also noted that there is swelling, loss of stability and disappearance of many cell walls of kiwifruit structure in the convective dried sample as well as IMCD samples at high PRs. It can be explained that the kiwifruit cells are composed of a small amount of cellulose, and a high amount of pectic polysaccharides (54), which were

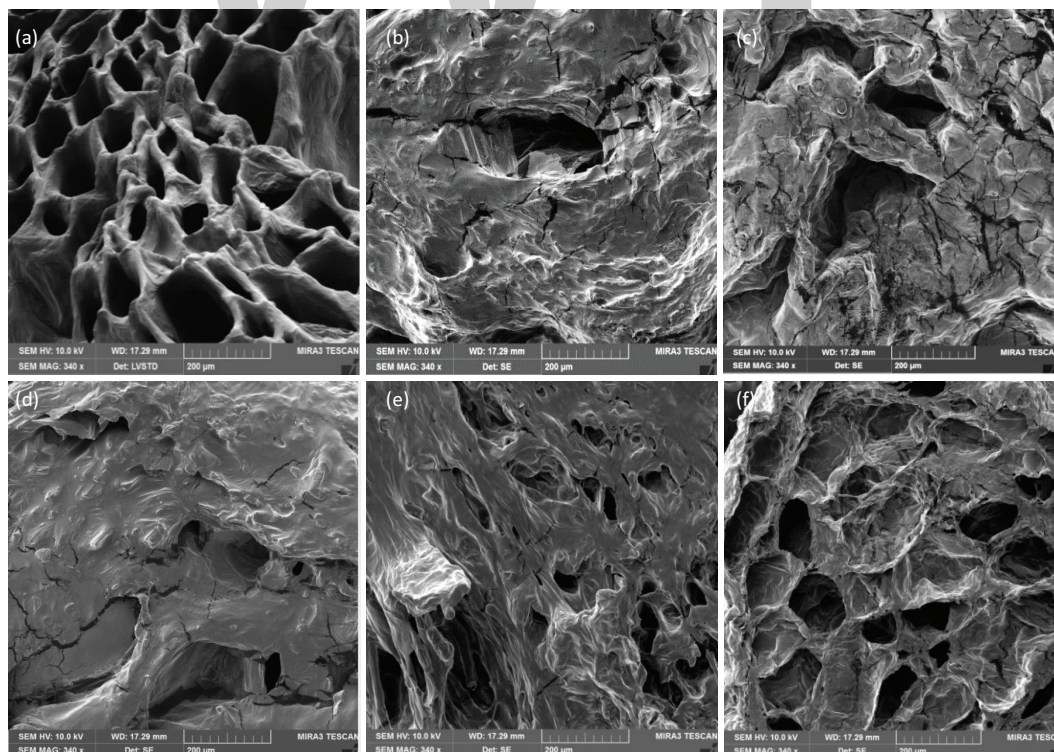








Fig. 4. Microstructure of sample slice in fresh condition and dried state under different drying conditions. (a) Fresh samples, (b) PR 1:1 sample, (c) PR 1:2 sample, (d) convective sample, (e) PR 1:3 sample, and (f) PR 1:4 sample.

Table 2. RGB values and total colour changes of samples under different drying conditions.

Factor	Sample PR 1:1	Sample PR 1:2	Sample PR 1:3	Sample PR 1:4	Sample convective	Fresh sample
						
Red	119.97 ± 21.88	127.42 ± 20.28	119.25 ± 24.51	146.67 ± 20.29	166.45 ± 32.35	105.45 ± 16.00
Green	103.22 ± 21.62	109.77 ± 21.53	102.26 ± 25.39	159.17 ± 22.79	123.25 ± 30.87	144.61 ± 17.73
Blue	41.03 ± 16.02	51.66 ± 16.79	49.51 ± 18.32	71.76 ± 25.17	42.52 ± 23.56	68.22 ± 15.72
ΔE_{RGB}	51.60 ± 2.58 ^b	44.40 ± 2.04 ^c	48.31 ± 2.32 ^{b,c}	43.86 ± 2.06 ^c	69.55 ± 3.37 ^a	-

Different superscript letters (a, b, c, d) indicate significant differences ($p \leq 0.05$) among the samples under different drying conditions. Identical superscript letters indicate no significant difference.

degraded significantly during severe thermal stresses in hot air convective and higher PRs in IMCD. Therefore, the prolonged heating time in continuous hot air drying and/or intensive MW heating (PR 1:1 and PR 1:2) resulted in the adverse microstructural changes in kiwifruit. The IMCD drying condition PR 1:3 and PR 1:4 maintained better kiwifruit microstructure. IMCD at PR 1:4 obtained a porous structure resembling the structure of the fresh sample, less shrinkage and collapses (Fig. 4f) compared to the other drying modes. Tian et al. (22) reported similar results for MW-assisted vacuum drying which indicated that convective sample had a less porous structure with severe cell disruption, while MW vacuum drying maintained open pore structure with good appearance. The modification of sample microstructure might also affect the other sensor properties, for example, hardness and crispiness. Highly porous structure obtained at PR 1:3 and PR 1:4 tends to produce crunchy and crispy products, while dense and collapsed structure in dried products at PR 1:1 and PR 1:2 usually results in chewy and hard products.

Colour degradation

During drying, sample colour can be considerably affected by pigment degradation (55, 56), enzymatic activity (57), and Maillard nonenzymatic browning reaction (58). The changes in porosity and surface texture also vary the reflectance of light on food surface, which ultimately affects viewers' colour perception (5, 59–61).

The visual appearance, average RGB values along with total colour changes altered by different drying conditions are presented in Table 1. It is clearly seen that higher PR caused more colour degradation in the sample.

Similar to the change of nutrient content, sample colour was also negatively influenced by higher PR because of the accelerated colour degradation reaction occurred within the sample due to higher MW irradiation. The application of MW heating brought about the rapid colour change of the samples, caused by intense thermal effect and browning reaction during drying. It is also noted that extended drying time in convective drying significantly

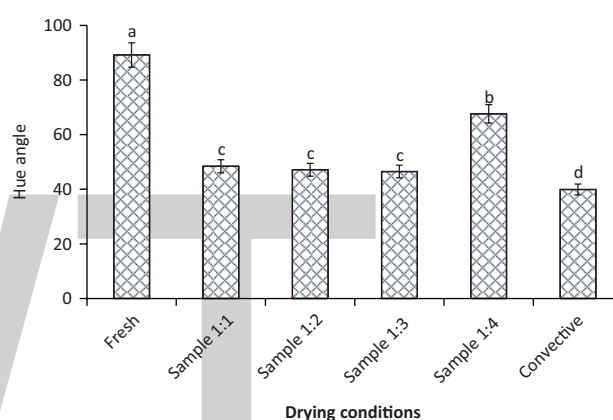


Fig. 5. Average hue angle of the dried sample under different PRs 1:1, 1:2, 1:3, 1:4, and convective drying. Different letters (a, b, c, d) indicate significant differences ($p \leq 0.05$) among the samples under different drying conditions. Identical superscript letters above the bars indicate no significant difference.

degraded the colour of the dried product. From Table 2, it can be stated that a higher PR led to higher colour changes in the sample. However, the maximum colour change ($\Delta E_{RGB} = 69.56$) ($p \leq 0.05$) was found in the case of hot air drying, while minimum colour changes ($p \leq 0.05$) took place in PR 1:2, 1:3 and 1:4 IMCD mode.

In addition to colour changes, the hue angle of the dried samples in convective drying, as well as IMCD, was considerably different from the fresh sample as shown in Fig. 5. In light of this finding, it is clear that the hue angle (values from 40 to 68) implies high colour changes at IMCD PR 1:1, 1:2 and 1:3, but there was an insignificant difference among these IMCD conditions ($p > 0.05$). However, the colour of the product under these conditions was still better than in the case of convective drying ($p \leq 0.05$). Hue angle of the sample dried in IMCD with the lowest PR (PR 1:4) resulted in the closest hue angle to the fresh sample ($p \leq 0.05$). Reducing the PR further may result in less degradation of colour (closer to the hue angle of the fresh sample). However, it will increase the total drying time, which might also negatively affect

colour as extended time exposure to drying environment facilitated browning reaction as in the case of convective drying. Therefore, PR 1:4 can be considered the best operating condition for the best colour, AAC retention and achievement of shorter drying time.

The product qualities, as described in the above sections, decrease with the increase of PR due to higher temperature induced by intensive MW heating. Although some reports in the literature claimed that decreasing PR might provide better food quality, it would prolong the drying time and increase the overall energy consumption (3, 62, 63). Moreover, as demonstrated above, prolonged drying time can cause undesirable effects on the quality of the samples. Therefore, an appropriate/optimum PR should be determined for the optimisation of drying time and food quality. In the experiments of IMCD, the tempering period supported the redistribution of the temperature and moisture, especially at lower PR as it allowed sufficient time to even out the temperature and moisture difference in the sample (64). Therefore, the product quality was better maintained in IMCD at lower PRs.

Considering the above discussion, it can be concluded that better appearance and quality of dried food can be achieved by appropriately setting the MW power-on/off time in IMCD drying.

Conclusion

Effect of the operating variable (e.g. PR) of IMCD on the drying process and product quality were investigated in this study. In the IMCD experiments, the drying time was significantly reduced in comparison with conventional hot air drying process. The water activity of all dried samples was attained at a safe level for extended storage. Thus, the microbial growth has been inhibited, and degradation of chemical reactions has been retarded. In addition, water activity decreased with the increase in PR of IMCD resulting in safer products with a longer shelf life. Higher PR and/or extended exposure time to the drying environment resulted in a greater degradation of the total polyphenol and AAC values. It was observed that the PR was a profound factor in the IMCD on the health-promoting compounds (AAC and total polyphenols) and colour as well as the microstructure. The best drying conditions in this study were identified at PR 1:4 (MW 20 sec on/80 sec off at 60°C hot air) in terms of colour and AAC retention. However, it should be noted that IMCD at PR 1:3 retained the best total polyphenol. It was found that the IMCD method was substantially more efficient than convective drying as it significantly decreased the drying time and enhanced the product nutrient and colour quality with a porous microstructure. In addition, the highly porous microstructure of IMCD samples suggests better texture compared to hot air dried product.

However, further lowering PR might not guarantee better quality product (e.g. PR 1:4 attain lower total polyphenol content than at PR 1:3) and efficient drying performance due to prolonged exposure of the products to the drying environment. Therefore, the PR should be carefully chosen based on product quality, MW power and drying performance to achieve optimal drying conditions.

Acknowledgement

Authors acknowledge the financial support of Advance Queensland Fellowship (AQF), the facilities, and the scientific and technical assistance of the Australian Microscopy & Microanalysis Research Facility at the Central Analytical Research Facility (CARF), Queensland University of Technology. Authors also acknowledge the contribution of Zachary Welsh and Dr. Chandan Kumar for their assistance with the manuscript proofreading.

Conflict of interest and funding

The authors have not received any funding or benefits from industry or elsewhere to conduct this study

Author contributions

Nghia Duc Pham and Wayde Martens conceived and designed the experiments; Nghia Duc Pham performed the experiments; Nghia Duc Pham and M U H Joardder analysed the data. M.A. Karim is the leader of the project, developed main research plan and contributed to drafting the paper.

References

1. Mujumdar AS. Handbook of industrial drying, Boca Raton, FL: CRC/Taylor & Francis; 2007.
2. Kumar C, Karim MA, Joardder MUH. Intermittent drying of food products: A critical review. *J Food Enging* 2014; 121: 48–57. doi: <https://doi.org/10.1016/j.jfoodeng.2013.08.014>.
3. Botha GE, Oliveira JC, Ahrné L. Microwave assisted air drying of osmotically treated pineapple with variable power programmes. *J Food Eng* 2012; 108(2): 304–11. doi: <https://doi.org/10.1016/j.jfoodeng.2011.08.009>.
4. Kumar C, Kumar C, Karim A, Saha S, Joardder UH, J Brown R, Biswas D. Multiphysics modelling of convective drying of food materials. Proceedings of the Global Engineering, Science and Technology Conference, Dhaka, Bangladesh, 2012; 28–29.
5. Joardder MUH, Kumar C, Karim MA. Food structure: its formation and relationships with other properties. *Crit Rev Food Sci Nutr* 2017; 57(6): 1190–205. doi: 10.1080/10408398.2014.971354.
6. Joardder MUH, Kumar C, Karim AA. Effect of temperature distribution on predicting quality of microwave dehydrated food. *J Mech Eng Sci* 2013; 5: 562–8. doi: <http://dx.doi.org/10.15282/jmes.5.2013.2.0053>.
7. Sablani SS. Drying of fruits and vegetables: retention of nutritional/functional quality. *Drying Technol* 2006; 24(2): 123–35. doi: 10.1080/07373930600558904.

8. Barsa CS, Normand MD, Peleg M. On models of the temperature effect on the rate of chemical reactions and biological processes in foods. *Food Eng Rev* 2012; 4(4): 191–202. doi: 10.1007/s12393-012-9056-x.
9. Defraeye T, Nicolaï B, Mannes D, Aregawi W, Verboven P, Derome D. Probing inside fruit slices during convective drying by quantitative neutron imaging. *J Food Eng* 2016; 178: 198–202. doi: <https://doi.org/10.1016/j.jfoodeng.2016.01.023>.
10. Chou SK, Chua KJ, Mujumdar AS, Hawlader MNA, Ho JC. On the intermittent drying of an agricultural product. *Food Bioprocess Process* 2000; 78(4): 193–203. doi: 10.1205/09603080051065296.
11. Chua KJ, Mujumdar AS, Chou SK, Hawlader MNA, Ho JC. Convective drying of banana, guava and potato pieces: effect of cyclical variations of air temperature on drying kinetics and color change. *Drying Technol* 2000; 18(4): 907–36. doi: 10.1080/07373930008917744.
12. Jumah R, Al-Kteimat E, Al-Hamad A, Telfah E. Constant and intermittent drying characteristics of olive cake. *Drying Technol* 2007; 25(9): 1421–6. doi: 10.1080/07373930701536668.
13. Thomkapanich O, Suvarnakuta P, Devahastin S. Study of intermittent low-pressure superheated steam and vacuum drying of a heat-sensitive material. *Drying Technol* 2007; 25(1): 205–23. doi: 10.1080/07373930601161146.
14. Chua KJ, Mujumdar AS, Chou SK. Intermittent drying of bioproducts – An overview. *Bioresour Technol* 2003; 90(3): 285–95. doi: 10.1016/S0960-8524(03)00133-0.
15. Joardder MUH, Kumar C, Karim MA. Multiphase transfer model for intermittent microwave-convective drying of food: Considering shrinkage and pore evolution. *International Journal of Multiphase Flow*. 2017; 95: 101–19. doi: <https://doi.org/10.1016/j.ijmultiphaseflow.2017.03.018>.
16. Kumar C, Joardder MUH, Farrell TW, Millar GJ, Karim MA. Mathematical model for intermittent microwave convective drying of food materials. *Drying Technol* 2016; 34(8): 962–73. doi: 10.1080/07373937.2015.1087408.
17. Kumar C, Joardder MUH, Farrell TW, Karim MA. Multiphase porous media model for intermittent microwave convective drying (IMCD) of food. *Int J Therm Sci* 2016; 104: 304–14. doi: <http://dx.doi.org/10.1016/j.ijthermalsci.2016.01.018>.
18. Barbosa de Lima AG, Delgado JMPQ, Neto SRF, Franco CMR. Intermittent drying: fundamentals, modeling and applications. In J. M. P. Q. Delgado & A. G. Barbosa de Lima (Eds.), *Drying and Energy Technologies* 2016; 19–41. Cham: Springer International Publishing.
19. Allaf K, Mounir S, Negm M, Allaf T, Ferrasse H, Mujumdar A. Intermittent Drying. In Arun S. Mujumdar, eds. *Handbook of Industrial Drying*, 4th ed, Boca Raton, Florida: CRC Press; 2015; 491–501.
20. Ferguson AR, Seal AG, Kiwifruit. In J. Hancock (Ed.), *Temperate Fruit Crop Breeding* 2014; 235–64. Springer Netherlands.
21. Darıcı S, Şen S. Experimental investigation of convective drying kinetics of kiwi under different conditions. *Heat Mass Trans* 2015; 51(8): 1167–76. doi: 10.1007/s00231-014-1487-x.
22. Tian Y, Wu S, Zhao Y, Zhang Q, Huang J, Zheng B. Drying characteristics and processing parameters for microwave-vacuum drying of Kiwifruit (*Actinidia deliciosa*) slices. *J Food Process Preserv* 2015; 39(6): 2620–9. doi: 10.1111/jfpp.12512.
23. Orikasa T, Koide S, Okamoto S, Imaizumi T, Muramatsu Y, Takeda J-i, Tagawa A. Impacts of hot air and vacuum drying on the quality attributes of kiwifruit slices. *J Food Eng* 2014; 125(0): 51–8. doi: <http://dx.doi.org/10.1016/j.jfoodeng.2013.10.027>.
24. Kaya A, Aydın O, Kolaylı S. Effect of different drying conditions on the vitamin C (ascorbic acid) content of Hayward kiwifruits (*Actinidia deliciosa* Planch). *Food Bioprocess Process* 2010; 88(2–3): 165–73. <http://dx.doi.org/10.1016/j.fbp.2008.12.001>.
25. Maskan M. Kinetics of colour change of kiwifruits during hot air and microwave drying. *J Food Eng* 2001; 48(2): 169–75. doi: [http://dx.doi.org/10.1016/S0260-8774\(00\)00154-0](http://dx.doi.org/10.1016/S0260-8774(00)00154-0).
26. Joardder MUH, Brown RJ, Kumar C, Karim MA. Effect of cell wall properties on porosity and shrinkage of Dried Apple. *Int J Food Properties* 2015; 18(10): 2327–37. doi: 10.1080/10942912.2014.980945.
27. Darvishi H, Zarein M, Farhudi Z. Energetic and exergetic performance analysis and modeling of drying kinetics of kiwi slices. *J Food Sci Technol* 2016; 53(5): 2317–33. doi: 10.1007/s13197-016-2199-7.
28. Kaya A, Aydın O, Dincer I. Experimental and numerical investigation of heat and mass transfer during drying of Hayward kiwi fruits (*Actinidia Deliciosa* Planch). *J Food Eng* 2008; 88(3): 323–30. doi: 10.1016/j.jfoodeng.2008.02.017.
29. Simal S, Femenia A, Garau MC, Rosselló C. Use of exponential, Page's and diffusional models to simulate the drying kinetics of kiwi fruit. *J Food Eng* 2005; 66(3): 323–8. doi: <https://doi.org/10.1016/j.jfoodeng.2004.03.025>.
30. Orikasa T, Wu L, Shiina T, Tagawa A. Drying characteristics of kiwifruit during hot air drying. *J Food Eng* 2008; 85(2): 303–8. <http://dx.doi.org/10.1016/j.jfoodeng.2007.07.005>.
31. Benlloch-Tinoco M, Kaulmann A, Corte-Real J, Rodrigo D, Martínez-Navarrete N, Bohn T. Chlorophylls and carotenoids of kiwifruit puree are affected similarly or less by microwave than by conventional heat processing and storage. *Food Chem* 2015; 187: 254–62. doi: 10.1016/j.foodchem.2015.04.052.
32. Fathi M, Mohebbi M, Razavi S. Application of image analysis and artificial neural network to predict mass transfer kinetics and color changes of osmotically dehydrated Kiwifruit. *Food Bioprocess Technol* 2011; 4(8): 1357–66. doi: 10.1007/s11947-009-0222-y.
33. An K, Li H, Zhao D, Ding S, Tao H, Wang Z. Effect of osmotic dehydration with pulsed vacuum on hot-air drying kinetics and quality attributes of Cherry Tomatoes. *Drying Technol* 2013; 31(6): 698–706. doi: 10.1080/07373937.2012.755192.
34. Huang D, Li W, Shao H, Gao A, Yang X. Colour, texture, microstructure and nutrient retention of Kiwifruit slices subjected to combined air-impingement jet drying and freeze drying. *Int J Food Eng* 2017; 13(7), doi: 10.1515/ijfe-2016-0344.
35. Bhattacharya M, Srivastav PP, Mishra HN. Thin-layer modeling of convective and microwave-convective drying of oyster mushroom (*Pleurotus ostreatus*). *J Food Sci Technol* 2015; 52(4): 2013–22. doi: 10.1007/s13197-013-1209-2.
36. Schossler K, Jager H, Knorr D. Effect of continuous and intermittent ultrasound on drying time and effective diffusivity during convective drying of apple and red bell pepper. *J Food Eng* 2012; 108(1): 103. doi: 10.1016/j.jfoodeng.2011.07.018.
37. Asami DK, Hong Y-J, Barrett DM, Mitchell AE. Comparison of the total phenolic and ascorbic acid content of freeze-dried and air-dried marionberry, strawberry, and corn grown using conventional, organic, and sustainable agricultural practices. *J Agric Food Chem* 2003; 51(5): 1237–41. doi: 10.1021/jf020635c.
38. Socha R, Juszczak L, Pietrzyk S, Fortuna T. Antioxidant activity and phenolic composition of herbhoneys. *Food Chem* 2009; 113(2): 568–74. doi: 10.1016/j.foodchem.2008.08.029.
39. Sharifian F, Modarres-Motlagh A, Komarizade MH, Nikbakht AM. Colour change analysis of fig fruit during microwave drying. *Int J Food Eng* 2013; 9(1): 107–14. doi: 10.1515/ijfe-2012-0211.

40. Khan MIH, Wellard RM, Pham ND, Karim A. Investigation of cellular level of water in plant-based food material. *International Drying Symposium*, 2016; 7–10. Gifu, Japan.
41. Moreno JJ. *Innovative processing technologies for foods with bioactive compounds*. Milton: CRC Press; 2016.
42. Sablani SS, Kasapis S, Rahman MS. Evaluating water activity and glass transition concepts for food stability. *J Food Eng* 2007; 78(1): 266–71. doi: 10.1016/j.jfoodeng.2005.09.025.
43. Pittia P, Antonello P. Chapter 2 – safety by control of water activity: drying, smoking, and salt or sugar addition A2 – Prakash, Vishweshwaraiah. In: Martín-Belloso O, Keener L, Astley S, Braun S, McMahon H, Lelieveld H. (Eds.), *Regulating safety of traditional and ethnic foods*. San Diego: Academic Press; 2016; 7–28.
44. Junqueira JRDJ, Corrêa JLG, Ernesto DB. Microwave, convective, and intermittent microwave-convective drying of pulsed vacuum osmotic-hydrated pumpkin slices. *J Food Process Preserv* 2017; 41(6): e13250. doi: 10.1111/jfpp.13250.
45. Guldás M. Peeling and the physical and chemical properties of kiwi fruit. *J Food Process Preserv* 2003; 27(4): 271–84. doi: 10.1111/j.1745-4549.2003.tb00517.x.
46. Vissers MCM, Carr AC, Pullar JM, Bozonet SM. Chapter seven – the bioavailability of vitamin C from Kiwifruit. In: Mike B, Paul JM, editors, *Advances in food and nutrition research*. San Diego: Academic Press; 2013; 68: 125–47.
47. Joardder MUH, Brown RJ, Kumar C, Karim MA. Effect of cell wall properties on porosity and shrinkage of dried apple. *Int J Food Properties* 2015; 18(10): 2327–37. doi: 10.1080/10942912.2014.980945
48. Aguilera JM. Why food microstructure? *J Food Eng* 2005; 67(1): 3–11. doi: 10.1016/j.jfoodeng.2004.05.050.
49. De Roos KB. Effect of texture and microstructure on flavour retention and release. *Int Dairy J* 2003; 13(8): 593–605. doi: http://dx.doi.org/10.1016/S0958-6946(03)00108-0.
50. McSweeney M, Seetharaman K. State of polyphenols in the drying process of fruits and vegetables. *Crit Rev Food Sci Nutr* 2015; 55(5): 660–9. doi: 10.1080/10408398.2012.670673.
51. Degirmencioglu N, Gürbüz O, Herken EN, Yıldız AY. The impact of drying techniques on phenolic compound, total phenolic content and antioxidant capacity of oat flour tarhana. *Food Chem* 2016; 194: 587–94. doi: http://dx.doi.org/10.1016/j.foodchem.2015.08.065.
52. Horuz E, Bozkurt H, Karataş H, Maskan M. Effects of hybrid (microwave-convective) and convective drying on drying kinetics, total phenolics, antioxidant capacity, vitamin C, color and rehydration capacity of sour cherries. *Food Chem* 2017; 230: 295–305. doi: http://dx.doi.org/10.1016/j.foodchem.2017.03.046.
53. Wang R, Ding S, Zhao D, Wang Z, Wu J, Hu X. Effect of dehydration methods on antioxidant activities, phenolic contents, cyclic nucleotides, and volatiles of jujube fruits. *Food Sci Biotechnol* 2016; 25(1): 137–43. doi: 10.1007/s10068-016-0021-y.
54. Cangi R, Altuntas E, Kaya C, Saracoglu O. Some chemical and physical properties at physiological maturity and ripening period of kiwifruit ('Hayward'). *Afr J Biotechnol* 2011; 10(27): 5304–10. doi: 10.5897/AJB11.192.
55. Grabowski S, Marcotte M, Poirier M, Kudra T. Drying characteristics of osmotically pre-treated cranberries-energy and quality aspects*. *Drying Technol* 2007; 20(10): 1989–2004. doi: 10.1081/DRT-120015580.
56. Reyes A, Alvarez PI, Marquardt FH. Drying of carrots in fluidized bed. I. Effect of drying conditions and modelling. *Drying Technol* 2002; 20(7): 1463–83. doi: 10.1081/DRT-120005862.
57. Hansmann CF, Joubert E, Britz TJ. Dehydration of peaches without sulphur dioxide. *Drying Technol* 1998; 16(1–2): 101–21. doi: 10.1080/07373939808917394.
58. Ho JC, Chou SK, Chua KJ, Mujumdar AS, Hawlader MNA. Analytical study of cyclic temperature drying: effect on drying kinetics and product quality. *J Food Eng* 2002; 51(1): 65–75. doi: 10.1016/S0260-8774(01)00038-3.
59. Lewicki PP, Pawlak G. Effect of drying on microstructure of plant tissue. *Drying Technol* 2003; 21(4): 657–83. doi: 10.1081/DRT-120019057.
60. Lewicki PP, Duszczak E. Color change of selected vegetables during convective air drying. *Int J Food Properties* 1998; 1(3): 263–73. doi: 10.1080/10942919809524582.
61. Fornal J. The changes of plant materials microstructure during processing. *Polish J Food Nutr Sci* 1998; 7(3): 9–23.
62. Kowalski SJ, Pawłowski A. Energy consumption and quality aspect by intermittent drying. *Chem Eng Process Process Intensif* 2011; 50(4): 384–90. doi: 10.1016/j.cep.2011.02.012.
63. Chaikham P, Kreungngern D, Apichartsrangkoon A. Combined microwave and hot air convective dehydration on physical and biochemical qualities of dried longan flesh. *Int Food Res J* 2013; 20(5): 2145–51.
64. Kumar C, Joardder MUH, Karim A, Millar GJ, Amin Z. Temperature redistribution modelling during intermittent microwave convective heating. *Procedia Engineering* 2014; 90: 544–549. doi: https://doi.org/10.1016/j.proeng.2014.11.770.

***Azharul Karim**

Mechanical Engineering
Drying Technology
Queensland University of Technology
2 George Street, QLD 4001 Australia
Email: azharul.karim@qut.edu.au

Bitter melon extract ameliorates palmitate-induced apoptosis via inhibition of endoplasmic reticulum stress in HepG2 cells and high-fat/high-fructose-diet-induced fatty liver

Hwa Joung Lee^{1†}, Rihua Cui^{1†}, Sung-E Choi^{2†}, Ja Young Jeon¹, Hae Jin Kim¹, Tae Ho Kim³, Yup Kang² and Kwan-Woo Lee^{1*}

¹Department of Endocrinology and Metabolism, Ajou University School of Medicine, Suwon, Republic of Korea;

²Department of Physiology, Ajou University School of Medicine, Suwon, Republic of Korea; ³Division of Endocrine and Metabolism, Department of Internal Medicine, Seoul Medical Center, Seoul, Republic of Korea

Abstract

Background: Bitter melon (BM) improves glucose level, lipid homeostasis, and insulin resistance *in vivo*. However, the preventive mechanism of BM in nonalcoholic fatty liver disease (NAFLD) has not been elucidated yet.

Aim & Design: To determine the protective mechanism of bitter melon extract (BME), we performed experiments *in vitro* and *in vivo*. BME were treated palmitate (PA)-administrated HepG2 cells. C57BL/6J mice were divided into two groups: high-fat/high-fructose (HF/HFr) without or with BME supplementation (100 mg/kg body weight). Endoplasmic reticulum (ER) stress, apoptosis, and biochemical markers were then examined by western blot and real-time PCR analyses.

Results: BME significantly decreased expression levels of ER-stress markers (including phospho-eIF2 α , CHOP, and phospho-JNK [Jun N-terminal kinases]) in PA-treated HepG2 cells. BME also significantly decreased the activity of cleaved caspase-3 (a well known apoptotic-induced molecule) and DNA fragmentation. The effect of BME on ER stress-mediated apoptosis *in vitro* was similarly observed in HF/HFr-fed mice *in vivo*. BME significantly reduced HF/HFr-induced hepatic triglyceride (TG) and serum alanine aminotransferase (ALT) as markers of hepatic damage in mice. In addition, BME ameliorated HF/HFr-induced serum TG and serum-free fatty acids.

Conclusion: These data indicate that BME has protective effects against ER stress mediated apoptosis in HepG2 cells as well as in HF/HFr-induced fatty liver of mouse. Therefore, BME might be useful for preventing and treating NAFLD.

Keywords: bitter melon extract; palmitate; high-fat/high-fructose diet; nonalcoholic fatty liver disease; endoplasmic reticulum stress; apoptosis

In recent years, nonalcoholic fatty liver disease (NAFLD) is commonly found in many people worldwide (1). NAFLD ranges from steatosis to nonalcoholic steatohepatitis (NASH) that can lead to hepatocellular carcinoma and liver failure (2). Obesity-related mortality, type 2 diabetes, and cardiovascular risk are particularly high in patients with NAFLD (3). Liver steatosis, a typical feature of NAFLD, appears when the sum of *de novo* fatty acid synthesis and free fatty acids (FFA) imported into liver is greater than the sum of FFA oxidation and FFA exported from the liver. Therefore, an increment in FFA level in the liver may play a key role in the development of

NAFLD. Excess FFA evokes endoplasmic reticulum (ER) stress and leads to ER dysfunction (4).

Sustained exposure to FFA induces excessive protein synthesis that exceeds ER capacity, resulting in the accumulation of unfolded or misfolded proteins in the ER lumen. To solve this problem, unfolded protein response (UPR) is induced to maintain ER homeostasis. Binding immunoglobulin protein (BiP) is a member of the heat-shock protein-70 (HSP70) family protein chaperone. It is associated with ER-stress sensors such as inositol requiring enzyme-1 (IRE1), Protein kinase ribonucleic acid-like endoplasmic reticulum kinase (PERK), and activating transcription factor 6 (ATF6) in

[†]Hwa Joung Lee, Rihua Cui, and Sung-E Choi contributed equally to this study.

the ER membrane to detect unfolded or misfolded proteins and move them from membrane to ER lumen for repairing (5). When ER-stress sensors are dissociated from BiP, they are activated to participate in three signaling pathways of ER stress. The activation degree of IRE1, PERK, and ATF6 under UPR determines cell fate such as cell survival and cell death (6). Persistent and intense ER stress will cause ER dysfunction, eventually leading to apoptosis. Expression of C/EBP homologous protein (CHOP), a typical ER-stress marker regulated by UPR, plays a key role in inducing the apoptotic process. Expression of CHOP is known to be regulated by IRE1, PERK, and ATF6 pathways. The PERK-eIF2 α -ATF4 pathway has been reported to be the most important for the expression of CHOP (7). DeZwaan et al. have reported that expression of CHOP can accelerate cell death in a variety of chronic liver diseases (8). In addition, caspase-12, an apoptotic regulator, is activated by the IRE-TRAF2-JNK pathway. It then induces apoptosis by sequentially activating caspase-9 and effector caspase-3 (9). Strong ER stress induces nuclear condensation, DNA fragmentation, and formation of apoptotic bodies containing cleaved DNA and proteolytic fragments. Since apoptosis is associated with ER-stress seen in the progression of NAFLD and is positively correlated with disease severity, and it can be used as a disease progression marker (7).

Bitter melon (BM) belongs to the family of Cucurbitaceae. It is cultivated in tropical regions of Asia, Africa, and South America. BM has long been used as traditional medicines in Asia. It is widely known to have antidiabetic, antioxidant, antiviral, and anticancer effects. The efficacy of BM for several diseases has been proven. It has been reported that bitter melon extract (BME) can reduce the expression of ER-stress proteins such as ATF6, XBP1, PERK, and CHOP in colonic epithelial cells. BME is also known for improving high fat diet (HFD)-induced obesity and hyperlipidemia in animal models (10, 11). Beneficial effects of BME on obesity and hyperlipidemia in liver and skeletal muscle are regulated by fat metabolizing kinases and nuclear factors (12). The liver protective effect of BME is mainly due to its antioxidant effects by scavenging free radicals and reducing inflammation caused by harmful stimuli (13).

Although several possible mechanisms have been proposed for the hepatoprotective effect of BME, few studies have examined the effect of BME on ER stress-mediated apoptosis in NAFLD. Therefore, the objective of the present study was to determine the effect of BME on palmitate (PA)-treated HepG2 cells (*in vitro*) and a mouse model of NAFLD (*in vivo*).

Materials and methods

Materials

PA and 4,6-diamidino-2-phenylindole diHCl (DAPI) were purchased from Sigma-Aldrich (St. Louis, MO,

USA). Anti-phospho-Akt (#9271), Anti-Akt (#9272), Anti-caspase-3 (#9962), anti-cleaved caspase-3 (#9961), anti-calnexin (#2679), anti-CHOP (#2895), anti-phospho-c-Jun (#9164), anti-phospho-eIF2 α (#9721), anti-eIF2 α (#9722), anti-I κ B α (#9242), anti-phospho-JNK (#9251), anti-JNK (#9252), anti-phospho-NF κ B (#3031), anti-NF κ B (#4764), and anti-PARP (#9542) antibodies were obtained from Cell Signaling Technology (Danvers, MA, USA). Anti-actin (sc1616) and anti-c-Jun (sc1694) antibodies were purchased from Santa Cruz Biotechnology (Santa Cruz, CA, USA).

Cells and culture

Commercially available HepG2 human hepatoma cell line was purchased from the American Type Culture Collection (ATCC, Manassas, VA). HepG2 cells were seeded into 12-well plates, at a density of 1×10^5 cells per well, and then maintained in Dulbecco's modified Eagle's medium (DMEM) supplemented with 10% fetal bovine serum (FBS; Gibco, Grand Island, NY, USA), 100 U/mL penicillin, and 100 g/mL streptomycin at 37°C, in a humidified atmosphere containing 95% air and 5% CO₂. After 24 h of incubation, HepG2 cells were treated with different concentrations of BME and 300 μ M PA. Cells were treated with Dimethyl sulfoxide (DMSO) which was used as a vehicle control. PA and BME were treated for 12 h and subsequently, the cells were harvested using trypsin and washed with phosphate-buffered saline (PBS). The harvested HepG2 cells were suspended in Radioimmunoprecipitation assay (RIPA) buffer for western blotting or homogenized in RNAiso Plus reagent for real-time polymerase chain reaction (PCR).

Preparation of PA

PA/bovine serum albumin (BSA) conjugate was prepared by saponifying PA with sodium hydroxide followed by mixing with BSA. PA (20 mM in 0.01 M NaOH) was incubated at 70°C for 30 min (14). Fatty acid soaps were then complexed with 5% fatty acid-free BSA in PBS at a 1:3 volume ratio. Complexed fatty acids consisted of 5 mM PA and 3.75% BSA. PA/BSA conjugate was then diluted in DMEM containing 10% FBS and administered to cell cultures.

Preparation of BME

BM (*Momordica charantia*) was purchased at the BM farm located in Cheorwon-gun, South Korea. After washing it thoroughly, the fruit of BM was cut and dried naturally at room temperature; it was powdered using an electric grinder and stored at 4°C. BME was prepared from 10 g of dried BM powder using 100% ethanol. Extract was filtered and dried at 37°C for 24 h. Dried BME was dissolved in dimethyl sulfoxide (Supplementary Fig. 1). BME was stored in airtight containers at -20°C until use.

Animal experiments

C57BL/6J male mice were purchased from Japan SLC, Inc. (Hamamatsu, Japan). All animal experiments were approved by the Animal Ethics Committee of the Laboratory Animal Research Center, Ajou University Medical Center, Suwon, South Korea. These mice were housed in a temperature controlled room ($22 \pm 2^\circ\text{C}$) with a 12/12 h light/dark cycle and fed *ad libitum*. To prepare the dietary NAFLD mouse model, 8-week-old male C57BL/6J mice were fed HFD (pellet containing 60% kcal fat; Research Diets, New Brunswick, USA, Cat#12492) and drinking water containing 30% high fructose (HFr) for 7 weeks. Then, these mice were randomly divided into two groups: (1) high-fat/high-fructose (HF/HFr) group ($n = 6$) and (2) HF/HFr + 100 mg/kg BME (HF/HFr/BME) group ($n = 6$). Each group was orally administered either DMSO or BME (100 mg/kg) on every other day for 5 weeks under the HF/HFr diet. The body weight was measured before the sacrifice. For glucose tolerance tests (GTT), mice were fasted for 6 h and intraperitoneally injected with glucose solution (1 g/kg; Sigma-Aldrich) or insulin (1 unit/kg; Sigma-Aldrich). Blood samples were taken at different time points (0, 15, 60, and 120 min after insulin or glucose loading) from the tail vein. Plasma glucose levels were measured using an Accu-Chek glucometer (Roche, Basel, Switzerland). After GTT measurements, mice were sacrificed using carbon dioxide. Epididymal fat, perirenal fat, subcutaneous fat, and the liver of mice were removed and weighed. The liver was suspended in RIPA buffer for western blotting or homogenized in RNAiso Plus reagent for real-time PCR.

Measurement of triglyceride

Tissue triglyceride was extracted by using Folch extraction method and measured with commercially available kits (LabAssay™ triglyceride, Wako Diagnostics, Japan) using N-ethyl-N-(2-hydroxy-3-sulfopropyl)-3,5-dimethoxyaniline sodium salt (DAOS) as a blue pigment. For biochemical analysis of blood samples, blood was obtained from 6-h-fasted mouse and immediately centrifuged at 13,000 rpm for 1 min at 4°C . The upper plasma was then collected and stored at -80°C . Plasma glucose levels were measured using the glucose oxidase method. Plasma levels of total cholesterol, triglyceride, and alanine aminotransferase (ALT) were measured using an autochemical analyzer (Cobas c111, Roche, Germany).

Hematoxylin and eosin staining

The liver of each mouse was removed, fixed in 10% neutral-buffered formalin, embedded in paraffin, and sectioned to a thickness of $3\mu\text{m}$. Liver sections were then stained with hematoxylin and eosin (H&E).

Western blot analysis

RIPA buffer (150 mM NaCl, 1% NP-40, 0.5% deoxycholate, 0.1% sodium dodecyl sulfate [SDS], 50 mM Tris-HCl

pH 7.5, protease inhibitor cocktail; Roche Applied Science, Mannheim, Germany) was used to extract cellular proteins. Equivalent amounts of protein (10 μg each) in SDS sample buffer (50 mM Tris-HCl pH 6.8, 2% SDS, 100 mM DL-dithiothreitol, 10% glycerol) were separated by 8–15% SDS-polyacrylamide gel electrophoresis (SDS-PAGE) and then transferred to polyvinylidene difluoride (PVDF) membranes (Millipore, Bedford, MA, USA). Target antigens were reacted with primary antibodies after blocking membranes with 5% skim milk for 30 min. After binding with secondary antibodies (horseradish peroxidase [HRP]-conjugated anti-goat Immunoglobulin G (IgG), anti-mouse IgG, or anti-rabbit IgG), immunoreactive bands were detected using an enhanced chemiluminescence system (Pierce, Rockford, IL, USA). Band intensity was determined by densitometric analysis using Quantity One D image analysis system (Bio-Rad, Hercules, CA, USA).

DNA fragmentation assay

Cell death was determined by measuring fragmented DNA using Cell Death Detection enzyme-linked immunosorbent assay (ELISA) kit (Roche Applied Science, Mannheim, Germany). Briefly, cells were lysed by adding cell lysis buffer supplied with the kit. After centrifugation ($200 \times g$, 10 min), the supernatant was pipetted onto an anti-streptavidin-coated microplate. Anti-DNA monoclonal antibody conjugated with peroxidase (anti-DNA-POD) and anti-histone-biotin were added. After incubating at 25°C for 90 min, wells were rinsed with incubation buffer (supplied by the kit) three times. The color was developed by adding 2,20-azino-di-[3-ethylbenzthiazoline sulfonate] (ABTS) substrate solution and incubated at room temperature for 10–20 min with shaking (250 rpm). The amount of peroxidase retained in the nucleosome complex was determined by measuring absorbance at a wavelength of 405 nm.

DAPI staining

For nuclear staining, photosensitized cells were fixed with 4% paraformaldehyde (pH 7.4) for 10 min and then incubated with DAPI (1 $\mu\text{g}/\text{mL}$; Sigma-Aldrich) at 37°C for 10 min. After washing with PBS, stained cells were immediately observed under a fluorescence microscope (340 nm excitation and 388 nm emission). Cells exhibiting reduced nuclear size, chromatin condensation, intense fluorescence, and nuclear fragmentation were considered apoptotic.

Flow cytometric measurement of reactive oxygen species

HepG2 cells grown on a 12-well plate were treated with 300 μM PA and various concentrations of BME at the same time for 4 h. Cells were detached from culture plates by digesting with trypsin (Invitrogen, Carlsbad, CA, USA) and then sedimented by centrifugation at $500 \times g$ for 5 min.

To quantitatively analyze reactive oxygen species (ROS), cells were immediately incubated with dichlorofluorescein diacetate (DCFDA; Sigma-Aldrich) at 37°C for 10 min. After washing twice with PBS, fluorescence intensity of stained cells was analyzed on a FACSVantage SE cytometer (BD Biosciences, San Jose, CA, USA).

RNA isolation and quantitative real-time PCR

Total RNA was isolated from mouse liver tissues using RNAiso Plus reagent (TaKaRa Bio Inc., Tokyo, Japan) according to the manufacturer's instructions. Then, cDNA was synthesized from total RNA using cDNA synthesis kit and used as template in PCR using gene-specific primers for interleukin (IL)-6 [CCA TCC AGT TGC CTT GGG (F) and GCC GTG GTT GTC ACC AGC AT (R)], IL-1 β [TCT CGC AGC ACA TCA ACA (F) and CCT GGA AGG TCC ACG GGA AA (R)], and monocyte chemoattractant protein (MCP)-1 [CAG CCA GAT GCA GTT AAC GC (F) and GCC TAC TCA TTG GGA TCA TCT (R)]. Quantitative real-time PCR (qPCR) was performed using SYBR Green (TaKaRa Bio Inc.) on a TaKaRa TP-815 instrument. All expression values were normalized to levels of 36B4, an internal control.

Terminal deoxynucleotidyl transferase dUTP nick end labeling assay

Deparaffinized tissue sections were treated with proteinase K (20 μ g/mL) for 15 min. Endogenous peroxidase was then blocked using 3% hydrogen peroxide in PBS for 10 min. Samples were then washed three times in distilled water and incubated with terminal deoxynucleotidyl transferase buffer at room temperature for 10 min. Excess buffer was drained and samples were incubated with terminal transferase and biotin-16-dUTP at 37°C for 1 h. Samples were then rinsed four times with PBS and incubated with a 1:400 dilution of peroxidase-conjugated streptavidin at 37°C for 1 h. Slides were rinsed with PBS and incubated with 3,3-diaminobenzidine at room temperature for 5 min. Sections were then washed with PBS three times and counterstained with methyl green.

Statistical analysis

Data are presented as means \pm standard errors of the mean (SEMs) from at least three independent experiments. Statistical differences between groups were determined using Student's *t*-test and Fisher's exact test. *P*-values of less than 0.05 were considered statistically significant.

Results

BME inhibits PA-induced apoptosis in HepG2 cells

As a FFA, PA is cytotoxic to HepG2 cells. It can induce apoptotic cell death (15). To examine the protective effect of BME against PA-induced apoptosis, HepG2 cells were treated with 300 μ M PA and different concentrations

of BME. PA increased apoptosis marker such as cleaved caspase-3 (C-caspase-3) and cleaved PARP (C-PARP). However, it was noted that PA decreased the survival marker, P-Akt. Interestingly, it was noted that BME significantly prevented PA-induced C-PARP and C-caspase-3 in a dose-dependent manner. We also found that P-Akt gradually recovered as the BME concentration increased (Fig. 1a). We further investigated the effect of BME on PA-induced DNA fragmentation and nuclear condensation in HepG2 cells. Treatment with 300 μ M PA increased DNA fragmentation by fivefold. However, such an increase in DNA fragmentation was significantly and dose-dependently diminished by BME (Fig. 1b). Furthermore, in PA-treated HepG2 cells, DAPI staining demonstrated nuclear condensation, a typical characteristic of apoptosis. However, BME dose-dependently blocked PA-induced nuclear condensation, with a maximum effect observed at higher concentrations of BME (Fig. 1c). Taken together, these data demonstrated that PA-induced apoptosis in HepG2 cells and that BME definitely could inhibit such apoptotic effect of PA.

BME reduces PA-induced ER stress in HepG2 cells

ER stress is one of the major mechanisms leading to apoptosis and PA is an inducer of ER stress in HepG2 cells (16–18). When ER stress occurs, BiP is activated to restore ER function. If ER function fails to recover, ER stress-specific markers are activated and highly expressed (19). Therefore, we investigated whether BME could decrease PA-induced ER stress markers in HepG2 cells by western blot. Our results revealed that levels of ER stress markers were significantly enhanced by PA treatment compared with those in the control (Fig. 2). Expression level of cleaved calnexin (C-calnexin) was also increased by PA treatment. However, expression level of C-calnexin was reduced after BME treatment. Expression level of BiP was slightly increased after BME treatment (Fig. 2a). Furthermore, PA-induced P-eIF2 α and CHOP expression levels were decreased by BME in a dose-dependent manner (Fig. 2b). JNK and ROS are also involved in ER stress. Therefore, we examined the effect of BME on PA-induced JNK phosphorylation. As shown in Fig. 2c, BME suppressed PA-induced P-JNK and P-c-Jun levels. We also investigated the effect of BME on PA-induced ROS, a by-product of ER stress, in HepG2 cells. We found that BME inhibited PA-induced ROS production at concentrations ranging from 25 to 100 μ g/mL (Fig. 2d), indicating that BME had antioxidant activity in HepG2 cells. Collectively, our data revealed that BME could decrease PA-induced ER stress and ROS production.

BME inhibits HF-IHFr-induced hepatic injury

Since we found that BME efficiently reduced apoptosis and ER stress in PA-treated HepG2 cells, we further

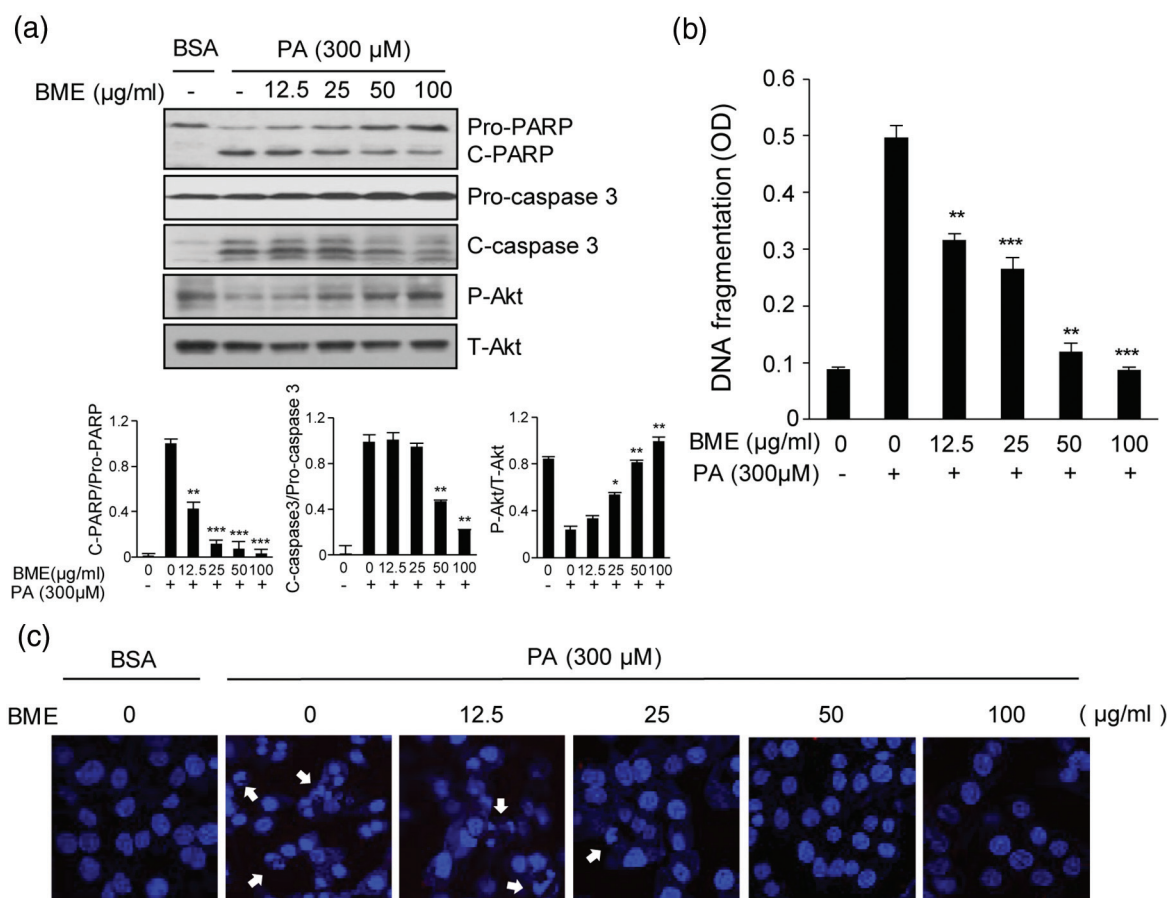


Fig. 1. Protective effects of BME on PA-induced HepG2 cell death. HepG2 cells were treated with different concentrations of BME and 300 μ M PA. DMSO was used as a vehicle. (a) HepG2 cells were collected at 12 h after treatment. Whole protein lysates were prepared using RIPA extraction buffer. PARP, cleaved caspase-3, and Akt were analyzed by western blot using anti-PARP, anti-cleaved caspase-3, and anti-Akt antibodies. Data are expressed as mean \pm SD of four independent experiments. * p < 0.05, ** p < 0.01, *** p < 0.001 versus PA-treated group. (b) HepG2 cells were treated with different concentrations of BME and 300 μ M PA for 12 h. Fragmented DNAs were then measured using a Cell Death Detection ELISA kit. Data are expressed as mean \pm SD of four independent experiments. ** p < 0.01, *** p < 0.001 versus PA-treated group. (c) Nuclear DNAs in BME-treated and PA-treated HepG2 cells were stained using DAPI and observed under a fluorescence microscope (388 nm emission). Arrows indicate condensed and fragmented nucleosomes.

examined the effect of BM on NAFLD *in vivo*. It has been reported that increased HF intake and HF consumption might contribute to NAFLD pathogenesis in mice (20–22). We have also previously reported that high fat and high fructose diet fed mice showed severe NAFLD phenotype such as impaired glucose tolerance, increased lipid synthesis, and inflammation compared to control mice (23). In this study, C57BL/6J mice were fed 60% HFD and 30% fructose water (HF/HFr) for 7 weeks. Then, the mice were randomly divided into two groups: an HF/HFr group and an HF/HFr plus BME group (HF/HFr/BME). Each group was orally administered either DMSO or BME (100 mg/kg) on every other day for 5 weeks under the HF/HFr diet. During this period, the food intake was randomly measured three times and averaged. There was no difference in

food intake between HF/HFr/BME group and HF/HFr group (Supplementary Fig. 2a), but BME significantly reduced body weight. Therefore, the effect of BME is not thought to have resulted from dietary control. We also measure the fat weight (Supplementary Fig. 2c). BME slightly reduced perirenal fat, but epididymal fat and subcutaneous fat did not change at all. Therefore, the effect of BME on body fat is considered to be negligible. As shown in Fig. 3a, GTT experiment revealed that HF/HFr/BME mice had significantly lower plasma glucose levels than HF/HFr mice. Interestingly, since BME significantly reduced liver weight (Supplementary Fig. 2c), we then performed H&E staining and Oil Red O staining to determine the effect of BME on the liver of mice. BME significantly prevented HF/HFr-induced fat accumulation in the liver (Fig. 3b). Liver TG

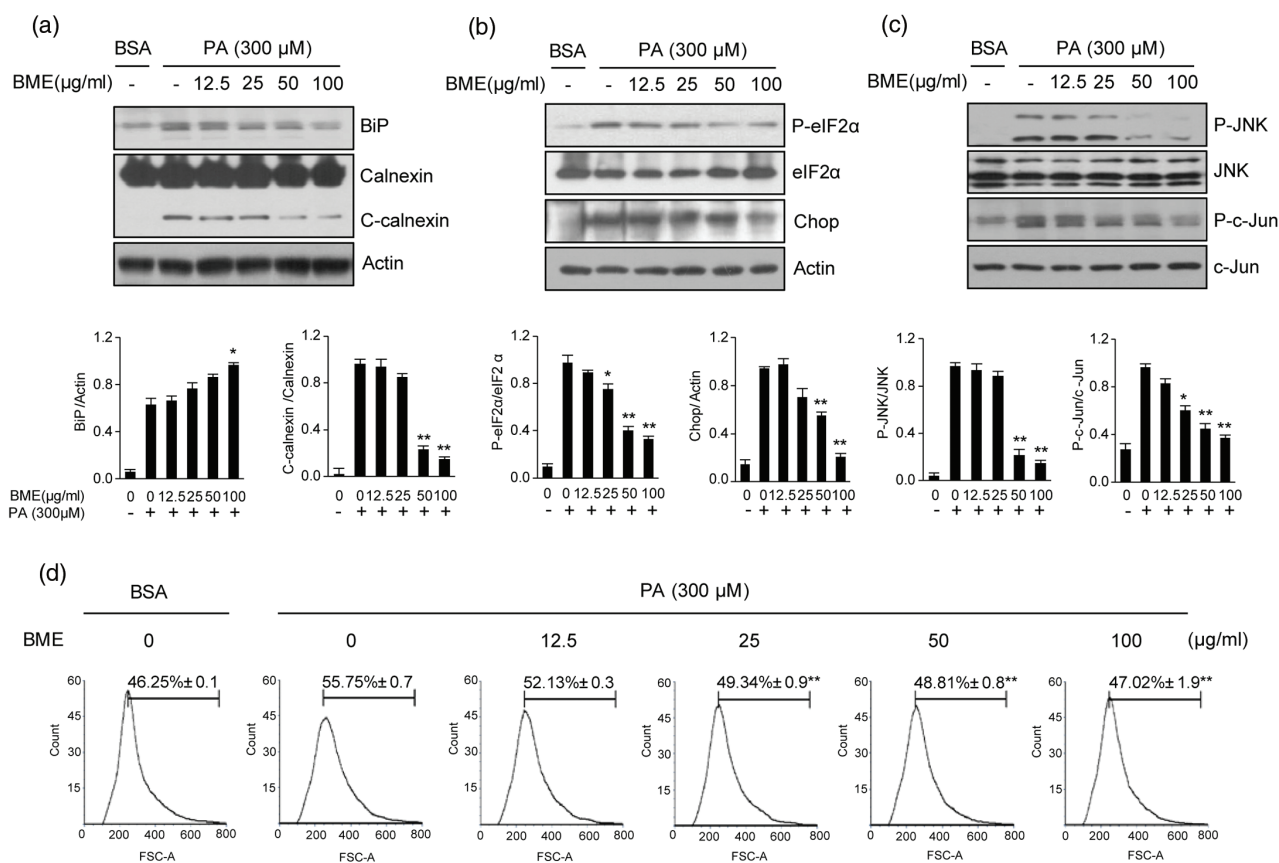


Fig. 2. Reduction of ER stress-related markers in BME-treated HepG2 cells. HepG2 cells were treated with different concentrations of BME and 300 μM PA for 12 h. DMSO was used as a vehicle. ER stress was analyzed by measuring levels of BiP, calnexin (a), P-eIF2α, CHOP (b), P-JNK and P-c-Jun (c). Data are expressed as mean ± SD of three independent experiments. * $p < 0.05$, ** $p < 0.01$ versus PA-treated group. (d) After treatment with BME and PA, cells were stained with DCFDA for 10 min. After washing twice with PBS, fluorescence intensity of DCFDA was determined by flow cytometry. Gated percentages are shown graphically. ** $p < 0.01$ versus PA-treated group.

in HF/HFr was reduced by 30% after BME administration (Fig. 3c). Furthermore, the HF/HFr/BME group showed significantly lower levels of ALT, TG, and FFA compared to the HF/HFr group. However, cholesterol level did not differ significantly between the two groups (Fig. 3d). Taken together, these data suggest that BME can improve glucose tolerance, serum lipid levels, and fatty liver.

BME reduces HF/HFr-induced stress/inflammatory proteins and apoptosis

We have previously reported that HF/HFr mice showed a higher inflammatory response than the control mice (23). Stress/inflammation-related signals such as JNK and nuclear factor kappa B (NF-κB) are known to be involved in the induction liver injury caused by Western diet (24, 25). To determine whether BME could decrease HF/HFr-induced activation of stress/inflammation-related genes and apoptosis, levels of proteins

and mRNAs extracted from the mice livers were examined by western blot and qPCR, respectively. Our results revealed that HF/HFr/BME livers showed significantly decreased inflammation-related genes, such as IL-1β, IL-6, and MCP-1 compared to HF/HFr livers (Fig. 4a). P-NF-κB levels also significantly reduced in BME-treated mice group (Fig. 4b). Based on results of our *in vitro* experiments, we next investigated the effect of BME on ER stress and apoptosis in HF/HFr and HF/HFr/BME groups of mice. As shown in Fig. 4c, a significant reduction in the expression level of ER stress markers like P-JNK, P-c-Jun, and CHOP was observed in HF/HFr/BME mice when compared to HF/HFr mice. The HF/HFr/BME mice showed lower C-caspase3 levels than HF/HFr mice (Fig. 4d). Terminal deoxynucleotidyl transferase dUTP nick and labeling (TUNEL) staining was then performed for liver tissues obtained from these two groups of mice. TUNEL-positive nuclei were observed in liver cells of HF/HFr mice. The number of

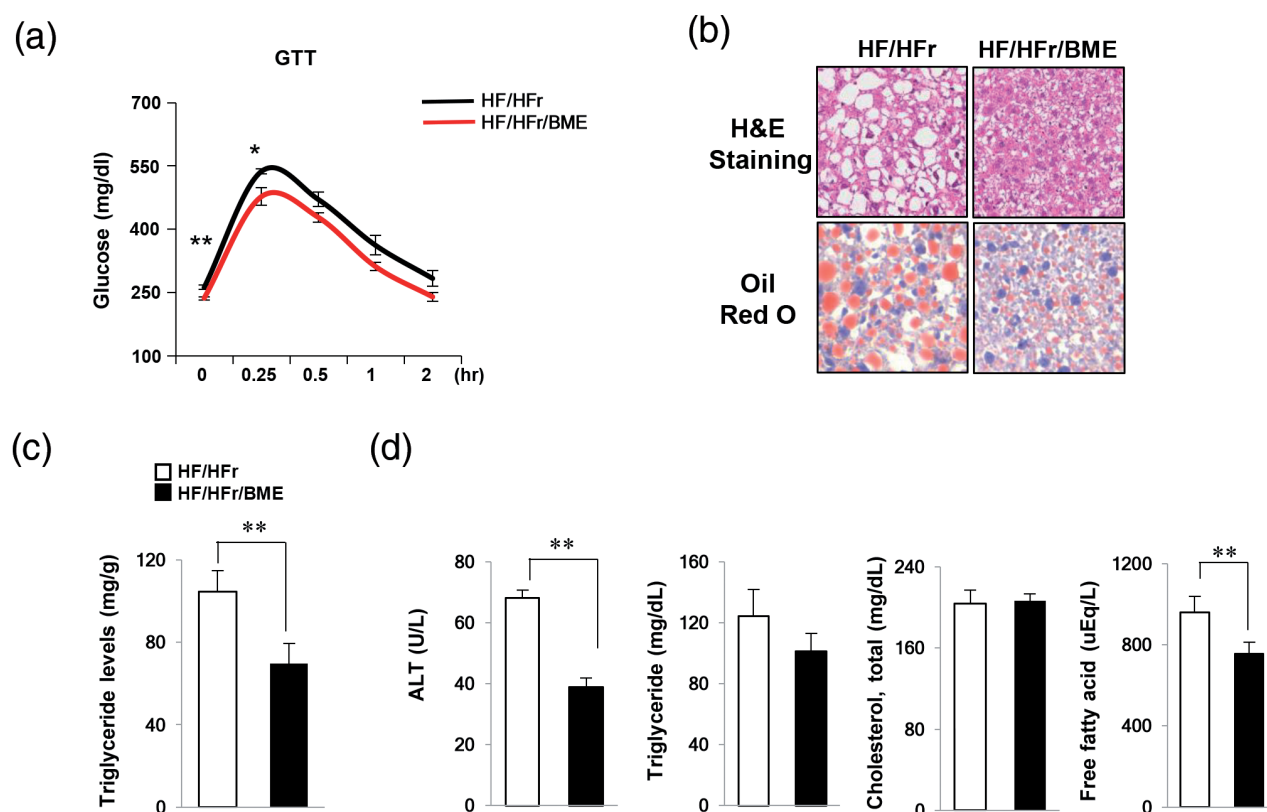


Fig. 3. Protection effects of BME on fatty liver induced by HF/HFrD. (a) HF (containing 60% fat)/HFr (containing 30% fructose) water was administered to C57BL/6J mice for 7 weeks. Subsequently, the mice were randomly divided into two groups ($n = 6$ mice/group). Each group was orally administered either DMSO or BME (100 mg/kg) on every other day for 5 weeks under the HF/HFr diet. (a) After 5 weeks, GTT was then carried out by measuring glucose levels at 0, 0.25, 0.5, 1, and 2 h after glucose injection (1 g/kg). Livers were isolated from HF/HFr and HF-/HFr-/BME-fed mice. Data are presented as mean \pm SEM ($n = 6$ per group). * $p < 0.05$, ** $p < 0.01$ versus HF/HFr group. (b) Liver sections stained with hematoxylin & eosin and Oil Red O. (c) Liver TG was extracted using the Folch extraction method and TG level was then measured with a TG assay kit. (d) Levels of plasma ALT, TG, cholesterol, and FFA were measured using an autochemical analyzer. Data are presented as mean \pm SEM ($n = 6$ per group). ** $p < 0.01$ versus HF/HFr group (c, d).

TUNEL-positive cells was also higher in HF/HFr group than that in HF/HFr/BME group (Fig. 4e). These results clearly revealed that BME treatment can prevent ER stress-mediated apoptosis induced by inflammatory signals in HF/HFr mice.

Discussion

Because BM has an effect on several diseases, BM has become a popular plant in the scientific community (10). Although effects of BM on numerous human diseases have been studied, studies on the effect of BM on NAFLD are insufficient. Therefore, this study focused on the effect of BME in ER stress-mediated apoptosis in PA-treated HepG2 cells as well as in an animal model of NAFLD.

NAFLD patients have increased delivery of FFA to the liver. Such elevated FFA can lead to serious diseases. It has been reported that PA belonging to FFA can increase

ER stress-related protein CHOP and induce apoptosis by activating caspase-3 in HepG2 cells (15). Based on this report, we induced ER stress and apoptosis using PA in this study. The severity of disease progression in NAFLD patients and animal models is the result of hepatocyte cell death due to apoptosis. Fructose has been used to study its effect on hepatic steatosis, oxidative stress, and inflammation in hepatocyte apoptosis in NAFLD animal models (26, 27). The apoptotic signaling network involves a cascade of ER stress, ROS production, and inflammation intermixed with each other. In the pathogenesis of NAFLD, apoptosis is further accelerated by persistent and excessive ER stress (28). To maintain ER homeostasis and prevent apoptosis by ER stress, expression of chaperone BiP is increased to bind to misfolded proteins and activate the UPR response. Overexpression of BiP is known to protect saturated fatty-acid-induced apoptosis in HepG2 cells (29). If excessive ER stress persists, BiP

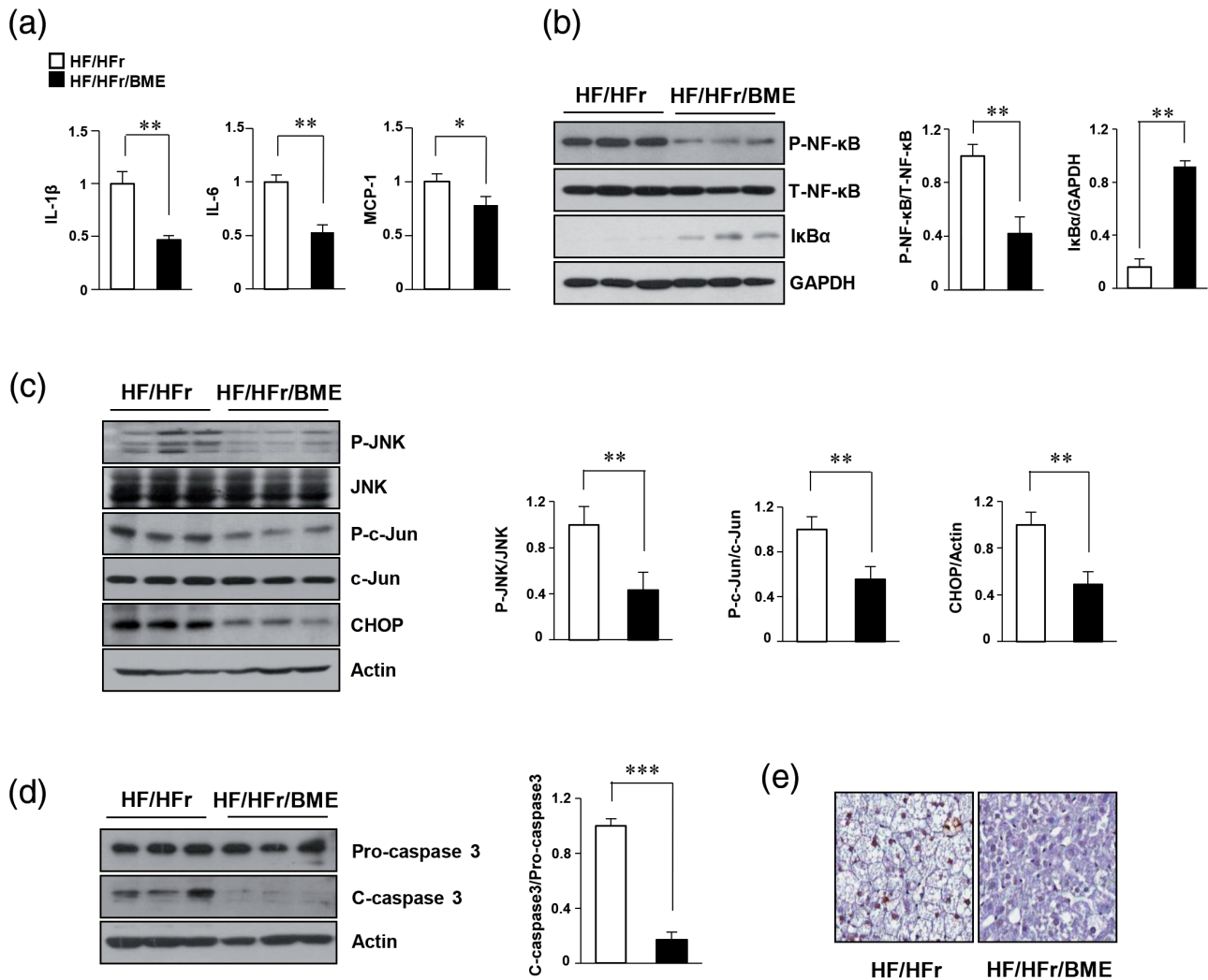


Fig. 4. Beneficial effects of BME on inflammation and ER stress-mediated apoptosis in HF-/HFfr-fed mice. Livers were isolated from HF/HFr and HF-/HFfr-/BME-fed mice. (a) Hepatic mRNA was isolated from mice livers, and levels of interleukin IL-1 β , IL-6, and MCP-1 mRNAs were quantified by real-time quantitative PCR. * p < 0.05, ** p < 0.01 versus HF/HFr group. (b) Proteins isolated from mice livers. NF- κ B protein levels were determined by western blot analysis. ** p < 0.01 versus HF/HFr group. (c, d) Expression levels of P-JNK, P-c-Jun, CHOP, and C-caspase-3 were detected by western blot analysis. * p < 0.05, ** p < 0.01, *** p < 0.001 versus HF/HFr group. (e) TUNEL staining of liver tissue sections showing DNA fragmentation.

will not be able to restore ER function. Therefore, other factors that cause apoptosis are activated. Calnexin is another ER chaperone known as an important marker in apoptosis triggered by ER stress. Proapoptotic function of calnexin can be regulated by BiP. It has been reported that overexpression of calnexin causes apoptotic death in *Schizosaccharomyces pombe* (30).

CHOP and caspase-3 are also prominent markers related to ER stress-mediated apoptosis. CHOP is activated by P-eIF2 α . It has been reported that CHOP is a key marker of ER stress-mediated apoptosis. Reduction of apoptosis in ER stress has been demonstrated in CHOP(-/-) mice (31). In addition, Oyadomari and Mori have found that

the reduction of CHOP in ER stress-mediated apoptosis is due to overexpression of BiP (32). Caspase-3 also promotes hepatocellular damage and pro-inflammatory signaling, leading to cell death. Caspase-3 inhibitors may be helpful for NAFLD progression (33, 34). Thus, targeting of BiP, calnexin, CHOP, and caspase-3 might be used as a potential strategy to treat NAFLD patients. Similar to previous reports, we also found that expression levels of CHOP, C-calnexin, and C-caspase-3 were efficiently decreased by BME, whereas BiP expression level was slightly increased in PA-treated HepG2 cells and animal model of NAFLD. These results suggest that BME can reduce apoptosis by inhibiting ER stress.

In fatty liver disease, excess supply of fatty acids and steatosis enhances ROS production due to ER dysfunction. ER stress signaling is associated with ROS formation and JNK activation. ROS produced by ER stress further promotes pro-inflammatory and pro-oncogenic signals (28). Oxidation of fatty acids activates inflammatory cytokines and produces ROS, leading to direct cell damage. Therefore, antioxidants are potentially therapeutic agents (29). In NAFLD, NF- κ B and JNK are known to regulate metabolism through cell survival, inflammation, and apoptosis (1). In mouse models, it has been shown that HFDs and obesity can activate hepatic NF- κ B which causes hepatic inflammation and increases the levels of IL-6, IL-1 β , and TNF- α . These cytokines may also further increase NF- κ B activation via a feed-forward mechanism (35). Interestingly, our results revealed that BME reduced ROS formation and levels of P-JNK and P-c-Jun. Furthermore, we found that NF- κ B protein level was decreased and mRNA levels of IL-6, IL-1 β , and MCP-1 were significantly lower in HF/HFr/BME mice than those in HF/HFr mice. Thus, BME might be able to alleviate PA-induced apoptosis by modulating ER stress–JNK signaling

HFD intake promotes hepatic steatosis and apoptosis. Guo et al. have reported that hepatic injury will occur when there is a lack of fat degradation or storage capacity due to excessive intake of fat and excess fatty acids in the liver. TG, a hallmark of NAFLD, is a major form of fat that accepts energy metabolism. It is accumulated in hepatocytes, causing steatosis. In mice fed with HFD, apoptosis is observed along with increased levels of ALT, cholesterol, glucose, and hepatocyte TG (36). It is well established that ALT levels are correlated with NAFLD severity and that reduction in serum ALT level is correlated with improvement of liver steatosis and inflammation (37). As expected, BME significantly reduced levels of glucose, TG, ALT, and FFA in HF/HFr mice sera. However, cholesterol levels were unchanged after BME treatment. Further studies are needed to clarify why BME could not affect cholesterol level.

In conclusion, this study demonstrated that BME could inhibit apoptosis by reducing ER stress in PA-treated HepG2 cells and an animal model of NAFLD. Our results suggest that BME might be useful for treating lifestyle-related diseases such as NAFLD.

Disclosure Statement

No potential conflict of interest was reported by the authors.

Conflict of interest and funding

All other authors declare that they have no competing interests. This project was supported by grant NRF-2016 R1D1A1B03930214 to KW Lee and NRF-2016R1A6

A3A11933787 to SE Choi from the National Research Foundation (NRF) of South Korea.

References

- Zhang XQ, Xu CF, Yu CH, Chen WX, Li YM. Role of endoplasmic reticulum stress in the pathogenesis of nonalcoholic fatty liver disease. *World J Gastroenterol* 2014; 20(7): 1768–76.
- Jeong HS, Kim KH, Lee IS, Park JY, Kim Y, Kim KS, et al. Ginkgolide A ameliorates non-alcoholic fatty liver diseases on high fat diet mice. *Biomed Pharmacother*. 2017; 88: 625–34.
- Patell R, Dosi R, Joshi H, Sheth S, Shah P, Jasdanwala S. Non-alcoholic fatty liver disease (NAFLD) in obesity. *J Clin Diagn Res* 2014; 8: 62–6.
- Takahara I, Akazawa Y, Tabuchi M, Matsuda K, Miyaaki H, Kido Y, et al. Toyocamycin attenuates free fatty acid-induced hepatic steatosis and apoptosis in cultured hepatocytes and ameliorates nonalcoholic fatty liver disease in mice. *PLoS One* 2017; 12(3): e0170591.
- Puri P, Mirshahi F, Cheung O, Natarajan R, Maher JW, Kellum JM, et al. Activation and dysregulation of the unfolded protein response in nonalcoholic fatty liver disease. *Gastroenterology* 2008; 134(2): 568–76.
- Xu C, Bailly-Maitre B, Reed JC. Endoplasmic reticulum stress: cell life and death decisions. *J Clin Invest* 2005; 115(10): 2656–64.
- Alkhoury N, Carter-Kent C, Feldstein AE. Apoptosis in nonalcoholic fatty liver disease: diagnostic and therapeutic implications. *Expert Rev Gastroenterol Hepatol* 2011; 5(2): 201–12.
- DeZwaan-McCabe D, Riordan JD, Arensdorf AM, Icardi MS, Dupuy AJ, Rutkowski DT. The stress-regulated transcription factor CHOP promotes hepatic inflammatory gene expression, fibrosis, and oncogenesis. *PLoS Genet* 2013; 9: e1003937.
- Momoi T. Caspases involved in ER stress-mediated cell death. *J Chem Neuroanat* 2014; 28: 101–5.
- Alam MA, Uddin R, Subhan N, Rahman MM, Jain P, Reza HM. Beneficial role of bitter melon supplementation in obesity and related complications in metabolic syndrome. *J Lipids* 2015; 2015: 496169. doi: 10.1155/2015/496169.
- Kunde DA, Chong WC, Nerurkar PV, Ahuja KD, Just J, Smith JA, et al. Bitter melon protects against ER stress in LS174T colonic epithelial cells. *BMC Complement Altern Med* 2017; 17: 2. doi: 10.1186/s12906-016-1522-1
- Krawinkel MB, Keding GB. Bitter gourd (*Momordica charantia*): a dietary approach to hyperglycemia. *Nutr Rev* 2006; 64: 331–7.
- Thenmozhi AJ, Subramanian P. Antioxidant potential of *Momordica charantia* in ammonium chloride-induced hyperammonemic rats. *Evid Based Complement Alternat Med* 2011; 2011: 612023.
- Jung IR, Choi SE, Jung JG, Lee SA, Han SJ, Kim HJ, et al. Involvement of iron depletion in palmitate-induced lipotoxicity of beta cells. *Mol Cell Endocrinol* 2015; 407: 74–84.
- Kim DS, Jeong SK, Kim HR, Kim DS, Chae SW, Chae HJ. Metformin regulates palmitate induced apoptosis and ER stress response in HepG2 liver cells. *Immunopharmacol Immunotoxicol* 2010; 32: 251–7.
- Leekumjorn S, Wu Y, Sum AK, Chan C. Experimental and computational studies investigating trehalose protection of HepG2 cells from palmitate-induced toxicity. *Biophys J* 2008; 94: 2869–2883.
- Zhang XQ, Pan Y, Yu CH, Xu CF, Xu L, Li YM, et al. PDIA3 knockdown exacerbates free fatty acid-induced hepatocyte steatosis and apoptosis. *PLoS One* 2015; 10: e0133882.

18. Li F, Yang Y, Yang L, Wang K, Zhang X, Zong Y, et al. Resveratrol alleviates FFA and CCl4 induced apoptosis in HepG2 cells via restoring endoplasmic reticulum stress. *Oncotarget* 2017; 8: 43799–809.
19. Higa A, Chevet E. Redox signaling loops in the unfolded protein response. *Cell Signal* 2012; 24: 1548–55.
20. Dhingra R, Sullivan L, Jacques PF, Wang TJ, Fox CS, Meigs JB, et al. Soft drink consumption and risk of developing cardiometabolic risk factors and the metabolic syndrome in middle-aged adults in the community. *Circulation* 2007; 116: 480–8.
21. Ouyang X, Cirillo P, Sautin Y, McCall S, Bruchette JL, Diehl AM, et al. Fructose consumption as a risk factor for non-alcoholic fatty liver disease. *J Hepatol* 2008; 48: 993–9.
22. Stanhope KL, Havel PJ. Endocrine and metabolic effects of consuming beverages sweetened with fructose, glucose, sucrose, or high-fructose corn syrup. *Am J Clin Nutr* 2008; 88: 1733s–7s.
23. Han SJ, Choi SE, Yi SA, Jung JG, Jung IR, Shin M, et al. Glutamate dehydrogenase activator BCH stimulating reductive amination prevents high fat/high fructose diet-induced steatohepatitis and hyperglycemia in C57BL/6J mice. *Sci Rep* 2016; 5: 37468.
24. Brenner C, Galluzzi L, Kepp O, Kroemer G. Decoding cell death signals in liver inflammation. *J Hepatol* 2013; 59: 583–94.
25. Takaki A, Kawai D, Yamamoto K. Molecular mechanisms and new treatment strategies for non-alcoholic steatohepatitis (NASH). *Int J Mol Sci* 2014; 15: 7352–79.
26. Choi Y, Abdelmegeed MA, Song BJ. Diet high in fructose promotes liver steatosis and hepatocyte apoptosis in C57BL/6J female mice. Role of disturbed lipid homeostasis and increased oxidative stress. *Food Chem Toxicol* 2017; 103: 111–21.
27. Federico A, Zulli C, Sio ID, Prete AD, Dallio M, Masarone M, et al. Focus on emerging drugs for the treatment of patients with non-alcoholic fatty liver disease. *World J Gastroenterol* 2014; 20: 16841–57.
28. Stickel F, Hellerbrand C. Non-alcoholic fatty liver disease as a risk factor for hepatocellular carcinoma: mechanisms and implications. *Gut* 2010; 59: 1303–7.
29. Gu X, Li K, Laybutt DR, He ML, Zhao HL, Chan JC, et al. Bip overexpression, but not CHOP inhibition, attenuates fatty-acid-induced endoplasmic reticulum stress and apoptosis in HepG2 liver cells. *Life Sci* 2010; 87: 724–32.
30. Guérin R, Arseneault G, Dumont S, Rokeach LA. Calnexin is involved in apoptosis induced by endoplasmic reticulum stress in the Fission Yeast. *Mol Biol Cell* 2008; 19(10): 4404–20.
31. Oyadomari S, Koizumi A, Takeda K, Gotoh T, Akira S, Araki E, et al. Targeted disruption of the Chop gene delays endoplasmic reticulum stress-mediated diabetes. *J Clin Invest* 2002; 109: 525–32.
32. Oyadomari S, Mori M. Roles of CHOP/GADD153 in endoplasmic reticulum stress. *Cell Death Differ* 2004; 11: 381–9.
33. Thapaliya S, Wree A, Povero D, Inzaugarat ME, Berk M, Dixon L, et al. Caspase 3 inactivation protects against hepatic cell death and ameliorates fibrogenesis in a diet-induced NASH model. *Dig Dis Sci* 2014; 59(6): 1197–1206.
34. Pagliassotti MJ. Endoplasmic reticulum stress in nonalcoholic fatty liver disease. *Annu Rev Nutr* 2012; 32: 17–33.
35. Cai D, Yuan M, Frantz DF, Melendez PA, Hansen L, Lee J, Shoelson SE. Local and systemic insulin resistance resulting from hepatic activation of IKK- β and NF- κ B. *Nat Med* 2005; 11: 183–190.
36. Guo R, Nair S, Zhang Y, Ren J. Adiponectin deficiency rescues high fat diet-induced hepatic injury, apoptosis and autophagy loss despite persistent steatosis. *Int J Obes (Lond)* 2017; 41(9): 1403–12.
37. Adams LA, Sanderson S, Lindor KD, Angulo P. The histological course of nonalcoholic fatty liver disease: a longitudinal study of 103 patients with sequential liver biopsies. *J Hepatol* 2005; 42: 132–8.

***Kwan-Woo Lee**

Department of Endocrinology and Metabolism
 Ajou University School of Medicine
 Suwon, Kyunggi-do 443-749, South Korea
 Email: LKW65@ajou.ac.kr

Assessment of nutritional status in the elderly: a proposed function-driven model

Stina Engelheart* and Robert Brummer

School of Medical Sciences, Örebro University, Örebro, Sweden

Abstract

Background: There is no accepted or standardized definition of ‘malnutrition’. Hence, there is also no definition of what constitutes an adequate nutritional status. In elderly people, assessment of nutritional status is complex and is complicated by multi-morbidity and disabilities combined with nutrition-related problems, such as dysphagia, decreased appetite, fatigue, and muscle weakness.

Objective: We propose a nutritional status model that presents nutritional status from a comprehensive functional perspective. This model visualizes the complexity of the nutritional status in elderly people.

Design and results: The presented model could be interpreted as the nutritional status is conditional to a person’s optimal function or situation. Another way of looking at it might be that a person’s nutritional status affects his or her optimal situation. The proposed model includes four domains: (1) physical function and capacity; (2) health and somatic disorders; (3) food and nutrition; and (4) cognitive, affective, and sensory function. Each domain has a major impact on nutritional status, which in turn has a major impact on the outcome of each domain.

Conclusions: Nutritional status is a multifaceted concept and there exist several knowledge gaps in the diagnosis, prevention, and optimization of treatment of inadequate nutritional status in elderly people. The nutritional status model may be useful in nutritional assessment research, as well as in the clinical setting.

Keywords: *nutritional status; nutritional assessment; elderly people; comprehensive geriatric assessment*

The prevalence of malnutrition is reported to be 18–30% in different populations of elderly people in need of health care services (1–6). As yet, there is no established or accepted definition of ‘malnutrition’ although several definitions have been used in the scientific literature (3, 7, 8) and several proposals have been presented (9–12). Hence, there is also no definition of what constitutes an adequate nutritional status.

This article will not attempt to define malnutrition but will elaborate on nutritional status, as a condition, from a comprehensive functional perspective. Impaired nutritional status (as in malnutrition) may not itself be a subjective problem or discomfort, unless it affects the persons’ capacities or contributes to their impairments or disease progression. We propose a function-driven nutritional status model in order to visualize the diversity of the situation and also to analyze and discuss nutritional status.

The proposed nutritional status model, as well as the associated nutritional assessment, is developed from questions concerning how nutritional status affects, and is affected by, health or disease. In a young or adult population, the

importance of an adequate nutritional status in supporting a long and healthy life is well established. But what about older people who are already in need of health care and social services? Is the aim still to lead a long and, depending on individual circumstances, relatively healthy life? Or is the aim to enable them to live an independent life? And how does the approach to nutritional status in old age affect practice in health care? Populations in geriatric care are heterogeneous, which further complicates the application of scientific research to individuals’ needs in health care.

Need for personalized nutritional care

There is a need for an effective, personalized, and scientifically based model for the assessment and evaluation of nutritional status in old people. Today, most countries and communities are facing a geriatric challenge (13), with an increasing proportion of older people in the population (14). A geriatric nutritional assessment is complicated by multi-morbidity, injuries, and disabilities in combination with nutrition-related problems such as dysphagia, decreased appetite, fatigue, and muscle weakness. Old age is the most

dominant risk factor for acute and chronic disease, as well as reduced physical, cognitive, affective, and social function. This functional decline may be the main reason for high risk of malnutrition (8, 15, 16), but the risk of malnutrition increases even further in the case of multi-morbidity, and such disease-related malnutrition is common in old people (17). The increased risk of malnutrition found in research may, however, be due to the method used for nutritional assessment, as some methods are based on parameters such as the number of drugs used, living arrangements (e.g. living at home vs. living in the nursing home), and diagnoses (e.g. dementia), indicating an increased risk of malnutrition according to the screening method. A minimum age, or definition of elderly people, for the proposed approach on nutritional status is not defined, as each individual situation has to be taken into concern. The concept of ‘frailty’ has been proposed to make a distinction between biological and chronological ages and is therefore applicable in this proposed model as it highlights the challenges of geriatric nutrition. Nutritional assessments require knowledge, qualified personnel, and scientifically based methods to evaluate and meet the nutritional needs of people at old age.

A comprehensive perspective is needed to adequately assess and interpret nutritional status in elderly people, as visualized in the proposed model for assessment of nutritional status (Fig. 1). The model takes account of the heterogeneity of the elderly population, with various symptoms,

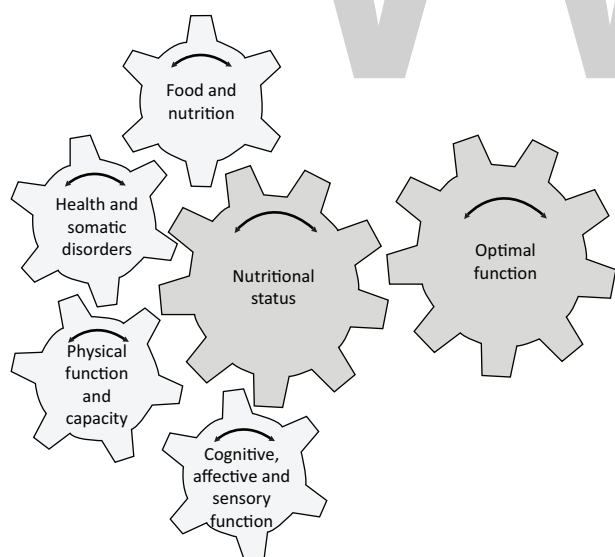


Fig. 1. Individualized model for assessment of nutritional status, including an obligatory examination of each of four domains, namely, (1) physical function and capacity; (2) health and somatic disorders; (3) food and nutrition; and (4) cognitive, affective, and sensory function. Each domain contributes to nutritional status. Optimal function (defined for each person) is the most important factor in analyzing nutritional status and at the same time is the overall goal of any actions and treatment.

disorders, and treatments affecting their nutritional status. Nutritional research, as well as the clinical methodology of nutritional assessment, has to explore associations between nutritional status and its predictors, exposures, and outcomes. In clinical practice and also in research we need a personalized approach, taking into account the heterogeneity of the population and the complex nature of nutritional status (18). Too often research including nutritional assessments ignores the complexity of nutritional status in elderly people and uses a single parameter such as low body mass index or low energy intake, or else it is based on simple screening methods such as the Mini Nutritional Assessment or Subjective Global Assessment. Also, most instruments aim to evaluate the presence of malnutrition rather than to adequately assess nutritional status.

In the proposed nutritional status model, the goal for actions and treatment in the clinical setting is to identify and achieve optimal function (and the optimal situation) for each person or patient. The model describes the complex interaction between four domains contributing to the overall goal – the optimal function.

Aim of the nutritional status model

The proposed model aims to visualize the interplay between the main components of nutritional status from an aging perspective. It is intended to be used in nutritional assessments in research as well as in clinical settings.

The four domains included in the proposed model of nutritional status were identified by two background questions: ‘What constitutes adequate nutritional status in old people?’ and ‘How do health care professionals perceive nutritional status in elderly people?’ The model should be applied flexibly, as the domains are interrelated and these interrelations are individually specific. The model may also require that in specific cases domains should be added or rebuilt.

The complexity of nutrition is highlighted within this research, as food has nutritional, social, biomedical, and functional implications. In the proposed model, we use four domains, overall categories or blocks in a comprehensive framework, to facilitate a fruitful discussion as part of the process of assessing nutritional status.

1. Physical function and capacity: comprising muscle strength, activities of daily living (ADL) functioning, physical activity, body composition, etc.
2. Health and somatic disorders: comprising prescribed pharmaceuticals, physical symptoms, current diseases, health-related quality of life, inflammation, etc.
3. Food and nutrition: comprising intake of energy and nutrients, mealtime habits, fluid intake, dietary patterns, etc.
4. Cognitive, affective, and sensory function: comprising cognitive decline, depression, mood, sense of taste and smell, etc.

In practical use, the model encourages transdisciplinary competence. No specific speciality has precedence of any area or domain, and no specific area or domain has precedence over any other area or domain, in the model.

The model could be interpreted as indicating that nutritional status is conditional to a person's optimal function (as defined by themselves), where each of the four domains contributes to the final goal (of optimal function). Also, the model could be interpreted as showing that nutritional status affects each domain and, consequently, the individual's optimal function. Each domain has a great impact on nutritional status, which has a great impact on the outcome of the domains, as explained below. In each individual case, each domain is more or less important for achieving optimal function, as the optimal function is defined by each person and each particular situation or setting.

In the following, the four domains are described and presented from this perspective.

Physical function and capacity

In the framework of this article, 'physical function' mainly comprises muscle, cardiovascular, and pulmonary function. Physical function is not necessarily related to physical capacity. The muscle function of leg muscles (measured using leg press) may be adequate, but when it comes to the capacity of performing household chores, the physical (i.e. muscle) function (e.g. strong legs) has to be transformed to physical capacity (e.g. walking, standing, bending, and keeping the balance). In general, loss of muscle mass is associated with loss of functional capacity and also with the risk of developing chronic metabolic disease (19).

Change in body weight is often used as a primary outcome measure in nutritional interventions in the elderly, in research, as well as in clinical practice. As an isolated biomarker, the individual's physical capacity will probably matter more than body weight. The ability to perform ADL is highly relevant in this context, as loss of muscle cell mass is related to loss of ADL function (20), and malnutrition is correlated with dependence on other people for ADLs (21). Nutritional interventions (dietary advice and nutritional supplementation) with the goal to improve ADL functions are most useful for people at risk of malnutrition (22).

Body composition is strongly related to nutritional status. Body fat mass and fat-free mass are associated with physical ability, morbidity, and mortality (23, 24). Body composition changes in old age, even in individuals with a stable body weight, and is characterized by increased fat mass and reduced fat-free mass (25). This change, probably due to hormonal changes, inadequate nutritional intake, increased morbidity, and less physical activity and exercise, among other reasons, causes sarcopenia and impaired physical function (7, 26).

Older people, especially those with multi-morbidity, have increased levels of systemic inflammatory markers, such as C-reactive protein (CRP) (26), and chronic inflammation also denoted as 'inflammaging'. Increased levels of inflammatory activity impair the anabolic processes in the body, as an anabolic block (27). The inflammatory condition may also decrease the intake of energy through loss of appetite, a condition also called 'anorexia of ageing' (28). Nutritional interventions in such a catabolic state are complicated and should not focus merely on achieving a positive energy balance, as this will result in increased body weight, meaning predominantly increased body fat. This may, in turn, stimulate the systemic inflammatory activity and hamper the anabolic processes even further (28).

In summary, physical function and capacity affect nutritional status in a bidirectional fashion. Changes in body weight as an indicator of a person's nutritional status have to be measured in terms of various body function indicators, as a complement. Physical function and capacity may be measured as muscle strength, ADL function, physical activity, body composition, etc.

Health and somatic disorders

Disease may negatively affect appetite, which can, in turn, lead to impairment of nutritional status and functional performance. As described previously in this article, old age is associated with chronic systemic inflammation (inflammaging), which substantially affects morbidity and mortality (29). Physical exercise has been discussed as preventive action (30), but its effect has not been clearly proven. The presence of this systemic inflammatory activity also disqualifies the use of serum albumin concentrations as a valid indicator of nutritional status. Because of its characteristic as a negative acute phase protein, it reflects inflammatory status rather than indicating adequate protein intake in particular, or nutritional status in general (31).

Acute or somatic disorders, and their treatment and the resulting functional impairments, may negatively affect the ability to ingest and/or digest a meal, as well as to absorb macro- and micronutrients, hence negatively affecting nutritional status. A poor nutritional status also impairs the immune function, increasing the risk of disease and contributing to a negative trend. Disease and multi-morbidity have traditionally been considered as a confounder (or just ignored) in the research on nutritional status and malnutrition. However, in the model presented here, this is an essential part of and contributor to nutritional status. Classification of disease status could not only be achieved by diagnosis or a combination of diagnoses, but also the number or category of pharmaceuticals can be an indicator of disease status.

The presence of physical or psychological symptoms, due to disorders, may affect not only dietary intake but also other components of lifestyle, such as physical activity and social interactions. Conversely, poor nutritional status may have an impact on physical capacity and social interaction and consequently will affect the quality of life.

In summary, the presence of disease and multi-morbidity, and the inflammation and symptoms they may cause, closely affect the nutritional status in a bidirectional fashion. The domain of health and somatic disorders may be measured as prescribed or used pharmaceuticals, physical symptoms, current diseases, health-related quality of life, inflammation, etc.

Food and nutrition

Old age *per se* does not cause reduced dietary intake. However, if functions required for habitual activities (such as shopping, cooking, and eating) are compromised due to disease or reduced capacity, then the intake of energy and nutrients will be decreased (32–35). The changes in food habits, in combination with the ongoing disease, challenge the health practitioners to provide individualized care and achieve a comprehensive view of the person's nutritional status.

The Nordic Nutrition Recommendations (NNR) (36) include dietary reference values for nutrients, foods, food patterns, physical activity, and sustainable food, with the aim to help prevent illnesses and chronic diseases. The reference values are adapted to different age groups, from infants to older adults, in good health. The use of reference values in frail elderly people, or those at immediate risk of frailty or malnutrition, is complicated and, hence, determining adequate nutritional intake on an individual basis in these elderly individuals is cumbersome and not evidence based. Therefore, more research is needed for this specific group of people. On an individual level, the care needs to be based on, among others, a comprehensive examination of energy need, body composition, physical function, and biomarkers.

The intake of fluids is rarely included in the analysis of dietary intake, although it is an essential contributor to optimal metabolic function and nutritional status. An impaired ability to achieve essential hydration status in combination with decreased fluid intake is common in old age (36, 37), and overt dehydration has been reported in old people in need of health and social care (38–40). However, the importance of fluid intake is probably underestimated in clinical practice (41). Low fluid intake is not synonymous with dehydration, as the risk of dehydration is also affected by the presence of diseases, and their treatment, as well as by the person's general physical condition. Unfortunately, the impact of dehydration and insufficient fluid intake in old age is insufficiently

studied, although confusion and cognitive impairment have been reported as symptoms (42, 43). Impaired cognitive performance may occur with dehydration matching only 2% of the person's body weight (44), and older people may reach this level of dehydration earlier than younger people, as body water volume decreases with age (45). The NNR (36) presents a guiding value of water and fluid intake (in addition to water from foods) at 1–1.5 L/day for adults. There is no specific recommendation for older people, but it is concluded that elderly people should have a broader safety margin due to less capacity to concentrate urine and often impaired feelings of thirst.

Food and nutrition is probably the domain most obviously associated with nutritional status, but it is complex as it comprises aspects such as adequate intake of macro- and micronutrients, dietary patterns, mealtime situation, mealtime habits, surrounding environment, and social interaction during meals. Food intake may be perceived as a pleasant event, but can also be a medical treatment, as well as a necessity for survival. Hence, the solution to an individual nutritional problem needs to be more than a recommendation of a specific dietary intake (8), and nutritional intervention studies should include a functional perspective in the nutritional assessments or outcomes.

In summary, food and nutrition, as the most obvious of the domains included, affect nutritional status in a bidirectional fashion. The food and nutrition domain should be analyzed from a broader perspective.

Cognitive, affective, and sensory function

Adequate cognitive function is crucial for most activities in daily living, including planning and preparing meals, food intake, physical exercise, and other factors contributing to adequate nutritional status. In the care of people with dementia, the importance of creating a dining environment based on each and every person has been emphasized (46), as the physical environment has a major impact on the food and meal experience and, hence, the person's nutritional status.

The definition of 'cognitive function' may comprise mood, regulation of anxiety, concentration, memory, and motivation or initiative. Most available scientific reports on the interaction between nutritional status and cognitive function deal with the hydration issue, or with the impact of dementia. Malnutrition is more common in people with dementia (47), with difficulties handling mealtimes during the progression of the disease (48). The identified increase in risk may also be due to the methods used for nutritional assessment.

An association between impaired nutritional status and depression has been observed, but the causal relationship is complex and it can be questioned whether

depression is the cause or consequence of impaired nutritional status (49).

Impairment of olfactory function worsens with age, and the prevalence is higher in malnourished and multi-morbid people (50). This may negatively affect dietary intake, and it may cause specific micronutrient deficiencies that may, in turn, deteriorate olfactory function. However, the association between malnutrition and olfactory function has not been widely investigated and can be questioned (51).

In summary, cognitive, affective, and sensory functions affect nutritional status in a bidirectional fashion. To assess this domain, measurements of cognitive function or decline, depression, mood, and sensory function such as taste and smell can be used.

Conclusion

A model for assessing nutritional status is presented. We argue that nutritional status is a multi-faceted concept and the presented model highlights the complexity. Several knowledge gaps exist in each domain, leading to uncertainty and lack of evidence on how to diagnose, prevent, and optimize nutritional status in an individual and personalized setting.

The proposed nutritional status model has been used in a research setting but not in regular clinical setting. The model should, therefore, be implemented in various settings in order to generate experience. In research setting, it has supported the understanding of the complex role of nutrition in the health and well-being of the elderly, at a group level as well as at an individual level, supporting comprehensive geriatric assessment.

Acknowledgement

S.E. is financially supported by the Foundation Olle Engkvist Byggmästare.

Conflict of interest and funding

The authors have not received any funding or benefits from industry or elsewhere to conduct this study.

References

- Johansson Y, Bachrach-Lindstrom M, Carstensen J, Ek AC. Malnutrition in a home-living older population: prevalence, incidence and risk factors. A prospective study. *J Clin Nurs* 2009; 18(9): 1354–64.
- Odlund Olin A, Koochek A, Cederholm T, Ljungqvist O. Minimal effect on energy intake by additional evening meal for frail elderly service flat residents – a pilot study. *J Nutr Health Aging* 2008; 12(5): 295–301.
- Meijers JM, van Bokhorst-de van der Schueren MA, Schols JM, Soeters PB, Halfens RJ. Defining malnutrition: mission or mission impossible? *Nutrition* 2010; 26(4): 432–40.
- Torma J, Winblad U, Cederholm T, Saletti A. Does undernutrition still prevail among nursing home residents? *Clin Nutr* 2013; 32(4): 562–8.
- Serrano-Urrea R, Garcia-Meseguer MJ. Malnutrition in an elderly population without cognitive impairment living in nursing homes in SpaIn: study of prevalence using the Mini Nutritional Assessment test. *Gerontology* 2013; 59(6): 490–8.
- van Nie-Visser NC, Meijers J, Schols J, Lohrmann C, Bartholomeyczik S, Spreeuwenberg M, et al. Which characteristics of nursing home residents influence differences in malnutrition prevalence? An international comparison of The Netherlands, Germany and Austria. *Br J Nutr* 2014; 111(6): 1129–36.
- Cruz-Jentoft AJ, Baeyens JP, Bauer JM, Boirie Y, Cederholm T, Landi F, et al. Sarcopenia: European consensus on definition and diagnosis: report of the European Working Group on Sarcopenia in Older People. *Age Ageing* 2010; 39(4): 412–23.
- Evans WJ, Morley JE, Argiles J, Bales C, Baracos V, Guttridge D, et al. Cachexia: a new definition. *Clin Nutr* 2008; 27(6): 793–9.
- White JV, Guenter P, Jensen G, Malone A, Schofield M, Academy of Nutrition and Dietetics Malnutrition Work Group, et al. Consensus statement of the Academy of Nutrition and Dietetics/American Society for Parenteral and Enteral Nutrition: characteristics recommended for the identification and documentation of adult malnutrition (undernutrition). *J Acad Nutr Diet* 2012; 112(5): 730–8.
- van Bokhorst-de van der Schueren MA, Guaitoli PR, Jansma EP, de Vet HC. A systematic review of malnutrition screening tools for the nursing home setting. *J Am Med Dir Assoc* 2014; 15(3): 171–84.
- Cederholm T, Jensen GL. To create a consensus on malnutrition diagnostic criteria: a report from the Global Leadership Initiative on Malnutrition (GLIM) meeting at the ESPEN Congress 2016. *Clin Nutr* 2017; 36(1): 7–10.
- Fischer M, JeVenn A, Hipskind P. Evaluation of muscle and fat loss as diagnostic criteria for malnutrition. *Nutr Clin Pract* 2015; 30(2): 239–48.
- Christensen K, Doblhammer G, Rau R, Vaupel JW. Ageing populations: the challenges ahead. *Lancet* 2009; 374(9696): 1196–208.
- European Commission. Eurostat. Your key to European statistics. European Union, Luxembourg 2014.
- Saragat B, Buffa R, Mereu E, Succa V, Cabras S, Mereu RM, et al. Nutritional and psycho-functional status in elderly patients with Alzheimer's disease. *J Nutr Health Aging* 2012; 16(3): 231–6.
- Donini LM, Savina C, Rosano A, Cannella C. Systematic review of nutritional status evaluation and screening tools in the elderly. *J Nutr Health Aging* 2007; 11(5): 421–32.
- Marengoni A, Winblad B, Karp A, Fratiglioni L. Prevalence of chronic diseases and multimorbidity among the elderly population in Sweden. *Am J Public Health* 2008; 98(7): 1198–200.
- Engelheart S, Akner G. Dietary intake of energy, nutrients and water in elderly people living at home or in nursing home. *J Nutr Health Aging* 2015; 19(3): 265–72.
- Koopman R, van Loon LJC. Aging, exercise, and muscle protein metabolism. *J Appl Physiol* 2009; 106(6): 2040–8.
- Zuliani G, Romagnoni F, Volpato S, Soattin L, Leoci V, Bollini MC, et al. Nutritional parameters, body composition, and progression of disability in older disabled residents living in nursing homes. *J Gerontol A Biol Sci Med Sci* 2001; 56(4): M212–16.
- van Bokhorst-de van der Schueren MA, Lonterman-Monasch S, de Vries OJ, Danner SA, Kramer MH, Muller M. Prevalence and determinants for malnutrition in geriatric outpatients. *Clin Nutr* 2013; 32(6): 1007–11.

22. Persson M, Hytter-Landahl A, Brismar K, Cederholm T. Nutritional supplementation and dietary advice in geriatric patients at risk of malnutrition. *Clin Nutr* 2007; 26(2): 216–24.
23. French SA, Folsom AR, Jeffery RW, Williamson DF. Prospective study of intentionality of weight loss and mortality in older women: the Iowa Women's Health Study. *Am J Epidemiol* 1999; 149(6): 504–14.
24. Allison DB, Zannolli R, Faith MS, Heo M, Pietrobella A, Van-Itallie TB, et al. Weight loss increases and fat loss decreases all-cause mortality rate: results from two independent cohort studies. *Int J Obes Relat Metab Disorders* 1999; 23(6): 603–11.
25. Beaufrère B, Morio B. Fat and protein redistribution with aging: metabolic considerations. *Eur J Clin Nutr* 2000; 54(Suppl 3): S48–53.
26. Vasto S, Candore G, Balistreri CR, Caruso M, Caruso C, Colonna-Romano G, et al. Inflammatory networks in ageing, age-related diseases and longevity. *Mech Ageing Dev* 2007; 128(1): 83–91.
27. Franceschi C. Inflammaging as a major characteristic of old people: can it be prevented or cured? *Nutr Rev* 2007; 65(12 Pt 2): S173–6.
28. Fernandez-Real JM, Ferri MJ, Vendrell J, Ricart W. Burden of infection and fat mass in healthy middle-aged men. *Obesity* 2007; 15(1): 245–52.
29. Franceschi C, Bonafe M, Valensin S, Olivieri F, De Luca M, Ottaviani E, et al. Inflamm-aging. An evolutionary perspective on immunosenescence. *Ann N Y Acad Sci* 2000; 908: 244–54.
30. de Araujo AL, Silva LC, Fernandes JR, Benard G. Preventing or reversing immunosenescence: can exercise be an immunotherapy? *Immunotherapy* 2013; 5(8): 879–93.
31. Sullivan DH, Johnson LE, Dennis RA, Roberson PK, Heif M, Garner KK, et al. The Interrelationships among albumin, nutrient intake, and inflammation in elderly recuperative care patients. *J Nutr Health Aging* 2011; 15(4): 311–15.
32. Lammes E, Akner G. Repeated assessment of energy and nutrient intake in 52 nursing home residents. *J Nutr Health Aging* 2006; 10(3): 222–30.
33. Suominen M, Laine T, Routasalo P, Pitkala KH, Rasanen L. Nutrient content of served food, nutrient intake and nutritional status of residents with dementia in a Finnish nursing home. *J Nutr Health Aging* 2004; 8(4): 234–8.
34. Akner G, Flöistrup H. Individual assessment of intake of energy, nutrients and water in 54 elderly multidiseased nursing-home residents. *J Nutr Health Aging* 2003; 7(1): 1–12.
35. Nowson CA, Sherwin AJ, McPhee JG, Wark JD, Flicker L. Energy, protein, calcium, vitamin D and fibre intakes from meals in residential care establishments in Australia. *Asia Pac J Clin Nutr* 2003; 12(2): 172–7.
36. Norden. Nordic nutrition recommendations 2012. Integrating nutrition and physical activity. Copenhagen: Nordic Council of Ministers; 2014.
37. Andreucci VE, Russo D, Cianciaruso B, Andreucci M. Some sodium, potassium and water changes in the elderly and their treatment. *Nephrol Dial Transplant* 1996; 11(Suppl 9): 9–17.
38. Buffa R, Mereu RM, Putzu PF, Floris G, Marini E. Bioelectrical impedance vector analysis detects low body cell mass and dehydration in patients with Alzheimer's disease. *J Nutr Health Aging* 2010; 14(10): 823–7.
39. Armstrong-Esther CA, Browne KD, Armstrong-Esther DC, Sander L. The institutionalized elderly: dry to the bone! *Int J Nurs Stud* 1996; 33(6): 619–28.
40. Montes JC. A typology of oral hydration problems exhibited by frail nursing home residents. *J Gerontol Nurs* 2006; 32(1): 13–19; quiz 20–1.
41. Popkin BM, D'Anci KE, Rosenberg IH. Water, hydration, and health. *Nutr Rev* 2010; 68(8): 439–58.
42. Benton D. Dehydration influences mood and cognition: a plausible hypothesis? *Nutrients* 2011; 3(5): 555–73.
43. Secher M, Ritz P. Hydration and cognitive performance. *J Nutr Health Aging* 2012; 16(4): 325–9.
44. Grandjean AC, Grandjean NR. Dehydration and cognitive performance. *J Am Coll Nutr* 2007; 26(5 Suppl): S49S–S54S.
45. Lieberman HR. Hydration and cognition: a critical review and recommendations for future research. *J Am Coll Nutr* 2007; 26(5 Suppl): 555–61.
46. Chaudhury H, Hung L, Badger M. The role of physical environment in supporting person-centered dining in long-term care: a review of the literature. *Am J Alzheimers Dis Other Demen* 2013; 28(5): 491–500.
47. Odlund Olin A, Koochek A, Ljungqvist O, Cederholm T. Nutritional status, well-being and functional ability in frail elderly service flat residents. *Eur J Clin Nutr* 2005; 59(2): 263–70.
48. Keller HH, Edward HG, Cook C. Mealtime experiences of families with dementia. *Am J Alzheimers Dis Other Demen* 2007; 21(6): 431–8.
49. Smoliner C, Norman K, Wagner K-H, Hartig W, Lochs H, Pirlich M. Malnutrition and depression in the institutionalised elderly. *Br J Nutr* 2009; 102(11): 1663–7.
50. Toffanello ED, Inelmen EM, Imoscopi A, Perissinotto E, Coin A, Miotto F, et al. Taste loss in hospitalized multimorbid elderly subjects. *Clin Interv Aging* 2013; 8: 167–74.
51. Smoliner C, Fischedick A, Sieber CC, Wirth R. Olfactory function and malnutrition in geriatric patients. *J Gerontol A Biol Sci Med Sci* 2013; 68(12): 1582–8.

***Stina Engelheart**

School of Medical Sciences
 Örebro University
 SE-701 82 Örebro, Sweden
 Email: stina.engelheart@oru.se

Antioxidant effects of compound walnut oil capsule in mice aging model induced by D-galactose

Huandong Zhao^{1,2}, Jian Li^{3*}, Juan Zhao⁴, Yang Chen³, Caiping Ren⁵ and Yuxiang Chen^{2*}

¹Key Laboratory of Nanobiological Technology of Chinese Ministry of Health, Xiangya Hospital, Central South University, Changsha, China; ²School of Pharmaceutical Sciences, Central South University, Changsha, China; ³Institute of Biomedical Engineering, Xiangya Hospital, Central South University, Changsha, China; ⁴Department of Clinical Laboratory, Xiangya Hospital, Central South University, Changsha, China; ⁵Cancer Research Institute, Collaborative Innovation Center for Cancer Medicine, Key Laboratory for Carcinogenesis of Chinese Ministry of Health, School of Basic Medical Science, Central South University, Changsha, China

Abstract

Background: Many plant original foods have been shown beneficial effects in humans. In the previous work, we have developed a compound capsule which contains major constituents of walnut oil and grape seed extract.

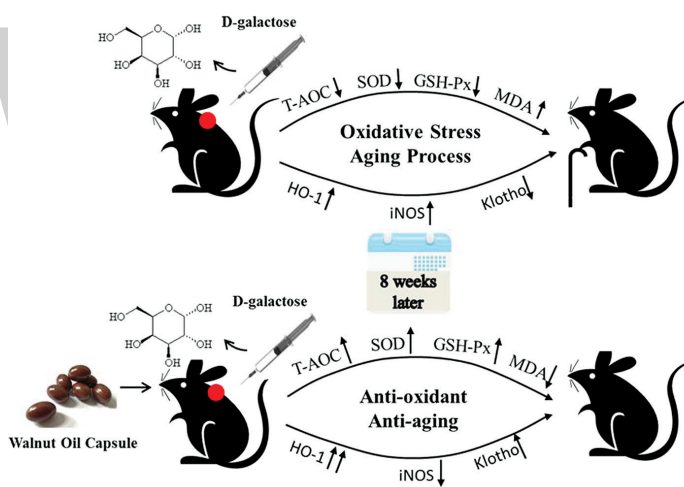
Objective: To investigate the antioxidant effects of the Compound Walnut Oil Capsule (WOC) in aging model induced by D-gal.

Design: 70 C57BL/6J mice were randomly divided into seven groups. Mice in normal group received daily subcutaneous injection of saline while the control group, WOC groups, Vitamin C (VC) group and pure walnut oil group received daily subcutaneous injection of D-galactose (D-gal) for 8 weeks. Total antioxidant capacity (T-AOC), super dismutase (SOD), glutathione peroxidase (GSH-Px) and malondialdehyde (MDA) in serum, liver and brain were determined. The expression of Heme Oxygenase (HO-1), iNOS and Klotho in liver and brain were obtained.

Results: WOC could improve the pathologic lesions caused by oxidative stress and significantly enhance the T-AOC, increase the activities of SOD, GSH-Px and decrease the contents of MDA in serum, liver and brain. Also, the WOC could obviously up-regulate the expression of HO-1 and Klotho and down-regulate the expression of iNOS.

Conclusion: WOC can be used as an anti-aging food for its effectively eliminating free radicals, enhancing the antioxidant capacity and alleviating the damages of oxidative stress.

Keywords: walnut oil capsule; oxidative stress; antioxidant; D-galactose; aging model



Aging is a complex natural process closely related to oxidative stress and free radicals, which has become a hot topic nowadays (1, 2). Accumulation of free radicals can affect the functions and

abilities of human body such as lung, heart, and brain (3, 4). It is important to select appropriate scavengers to protect body from the damage of free radicals and improve the quality of life.

Natural drugs for their low toxicity and low side-effects are widely used in the field of medicine. It is reported that many plant original foods and medicines have potential antioxidant capacity *in vitro* and *in vivo*, such as *Asparagus cochinchinensis* (Lour.), (5) *Trollius chinensis* Bunge (6), and *Cinnamomum verum* (7). In the research, we have developed a compound capsule which contains major constituents of walnut oil and grape seed extract. Walnut oil is rich in linolenic acid and linoleic acid; previous studies showed that it has several health benefits including anti-inflammatory and antioxidant effects (8, 9). Many researches indicated that the main ingredients of grape seed extract are anthocyanin and procyanidin, which have strong anti-inflammatory and anti-lipid peroxidation effects (10–12).

Nowadays, the aging model induced by D-galactose (D-gal) is widely used in the field of oxidative stress and antioxidant research for its easy operation, cheapness, and short periods, which was first reported by Gong et al. in 1997 (13). Long-time injection of high dosage of D-gal can cause massive production of free radicals, neurotoxicity, tissue injury, and inflammation, followed by senescence (14, 15). The inbred C57BL/6J mice were widely used in the brain aging research for its lower growth rate and smaller individual difference (16). In our work, we used walnut oil capsule (WOC) to investigate its antioxidant effects in C57BL/6J mice aging model established by D-gal. Not only did we detect the activities of oxidative stress-related enzymes but also discussed the expression of some free radicals and aging-related enzymes at the molecular level. The histopathologic examination was also observed to see the effects of WOC on liver and brain. The research aimed to develop the WOC as an antioxidant health food for elderly people.

Materials and methods

Drugs and reagents

WOC was prepared by us according to designed prescription and the China patent (No:201410564056.x). Pure walnut oil was purchased from Valder Fields CO., Ltd (Yuxi, China), and Vitamin C (VC) from Solarbio Science & Technology CO., Ltd (Beijing, China). D-gal was purchased from Sigma-Aldrich (St Louis, MO, USA). 1,1-diphenyl-2-picrylhydrazyl (DPPH) was purchased from TCI (Shanghai) Development Co., Ltd (Shanghai, China). Total antioxidant capacity (T-AOC), superoxide dismutase (SOD), glutathione peroxidase (GSH-PX) and malondialdehyde (MDA) kits were purchased from Jiancheng Bioengineering Institute (Nanjing, China). BCA protein assay kit and SDS-PAGE kits were purchased from Multi Sciences Biotech CO., Ltd (Hangzhou, China). Anti-Heme Oxygenase-1 (HO-1) antibody and anti-Klotho antibody were purchased from Abcam (Shanghai, China).

Anti-iNOS antibody and anti- β -actin antibody were purchased from cell signaling technology (Danvers, USA).

Measurement of radical scavenging *in vitro*

DPPH free radicals scavenging test has been effectively used to evaluate the free radical scavenging capacity of antioxidant drugs *in vitro* (17). Briefly, 20 μ L of sample was quickly mixed with 180 μ L 0.1 mmol/L DPPH and placed in the dark for 0 min, 10 min, 20 min, and 30 min. Then the absorbance at 517 nm was measured. Absolute alcohol was used as negative control. The DPPH scavenging rate was determined using $K\% = [1-(A_i-A_j)/A_o] \times 100\%$ (A_i , the absorbance of sample mixed with DPPH; A_j , the absorbance of sample mixed with absolute alcohol; A_o , the absorbance of negative control).

Treatment of animals

Seventy 3-month-old C57BL/6J male mice, weighing about 20 ± 2 g, were obtained from CAVENS Laboratory Animal Co., Ltd (Changzhou, China; certification No. SCXK (Su) 2016-0010). The mice were housed in an SPF environment at 25°C and 60% relative humidity under 12-/12-h dark/light cycle with free access to food and water. The protocols were conducted in accordance with the Guidance Suggestions for the Care and Use of Laboratory Animals, formulated by the Ministry of Science and Technology of China. After a week of acclimation, the mice were randomly divided into seven groups (10 mice/group), including a normal group; an aging model group as control; WOC low, medium, and high groups; a VC group; and a pure walnut oil group as positive control. For the control group, WOC groups, positive control groups, all mice received daily subcutaneous injection of 1,000 mg/kg D-gal for 8 weeks. For mice in normal group, 0.2 mL physiological saline was injected for 8 weeks. From the second week, mice in the WOC, positive control groups received daily intragastric administration of WOC at doses of 6 mL/kg, 12 mL/kg, 18 mL/kg; VC at a dose of 200 mg/kg; pure walnut oil at a dose of 12 mL/kg, while the normal and control groups received intragastric administration of distilled water at a dose of 12 mL/kg. Twenty-four hours after final administration, the mice were anaesthetized by intraperitoneal injection of 10 mL/kg 5% chloral hydrate; 0.5 mL blood samples were extracted from peri-orbital sinus and the serum was collected after being centrifuged at 3,000 r/min for 10 min. Mice were sacrificed, followed by rapid isolation of liver and brain.

Histomorphological observation of liver and brain

Tissues were fixed in 10% formalin at room temperature for 48 h, then desiccated and embedded in paraffin. After that, tissues were sliced into 5 μ m slices for hematoxylin-eosin (H&E) staining. Specimens were scanned and

pathological changes were observed using Case Viewer 2.0 (3D HISTECH, Ltd, Budapest, Hungary).

Western blotting

Western blot analysis was performed as described previously (18). Briefly, tissues were lysed into homogenate using RIPA lysis buffer and PMSF, and total proteins were separated by SDS-PAGE and then transferred to PVDF membranes at 300 mA for 1 h. After being transferred, the membranes were placed in blocking buffer (5% non-fat milk in Tris-buffered saline containing Tween-20 [TBST]) for 1 h, and the blots were incubated with an appropriate primary antibody (anti-Klotho antibody [1:1,000], anti-HO-1 antibody [1:20,000], anti-iNOS antibody [1:1,000], anti- β -actin antibody [1:1,000]) at 4°C overnight, and then treated with secondary antibody (1:5,000) at room temperature for 1 h. Then the chemiluminescent indicator was applied to membranes and specific proteins were detected by fluorchem device.

Statistical analysis

All data were expressed as mean \pm SD and analyzed using SPSS 18.0 software (SPSS Inc., Chicago, IL, USA). The significance of difference among groups was tested by one-way analysis of variance (ANOVA) test, and inter-group differences were compared using least-significant difference *t*-test.

Results

In vitro radical scavenging of WOC

The scavenging rate of WOC and pure walnut showed concentration dependence and time dependence. The WOC results showed that when the concentration was higher than 1%, the changes of scavenging rate was not obvious with the decrease of concentration, while when the concentration was lower than 1%, the scavenging rate decreased obviously. On the contrary, when the concentration was above 1%, pure walnut oil showed that the scavenging rate decreased sharply with the decrease of concentration, but it flattened out below 1%. As regards

the result of VC, there was no obvious concentration dependence and time independence. Instead, the scavenging rate remained almost unchanged with the decrease in concentration, and as time went on, the scavenging rate was almost constant, which indicated the scavenging rate of VC reached the maximum in a short time after reaction. In other words, the DPPH scavenging rate followed VC > WOC > pure walnut oil *in vitro* (Fig. 1).

General condition of mice

Mice were weighed daily and the weight changes were recorded in order to observe the effects of different drugs on mice body weight. Result showed that there were no significant differences among groups in body weight both on the first day and the last day (Table 1). But the growth rate in the normal group was higher than that in other groups ($p < 0.05$ or $p < 0.01$). It indicated that not only D-gal but also WOC, VC, and pure walnut oil could affect body weight in mice.

There were also differences in appearance among different groups (Fig. 2). Mice in the normal group had smooth hair and active spirit (A), but in the control group, mice were curled up and had coarse hair, severe hair loss, and poor spirit (B). Mice treated with WOC, VC, and pure walnut oil exhibited improvements in their hair color and spirit (C D E F G).

Table 1. The weight changes in mice

Group	First day (g)	Last day (g)	Growth rate (%)
Normal	25.21 \pm 1.28	30.07 \pm 1.35	19.80 \pm 2.94
Control	25.53 \pm 1.07	28.74 \pm 1.81	12.51 \pm 3.10**
WOC low	25.72 \pm 1.19	29.49 \pm 1.67	14.68 \pm 4.18*
WOC medium	24.88 \pm 1.61	28.43 \pm 1.52	14.43 \pm 4.68*
WOC high	25.19 \pm 1.04	28.39 \pm 1.70	12.44 \pm 3.47**
VC	25.03 \pm 1.76	28.57 \pm 2.79	14.13 \pm 7.81*
Pure walnut oil	25.12 \pm 1.21	28.35 \pm 1.90	12.78 \pm 2.13*

The body weight change in C57BL/6J mice on the first and last day. * $p < 0.05$, ** $p < 0.01$ versus normal group ($n = 10$ in each group).

WOC, walnut oil capsule; VC, Vitamin C.

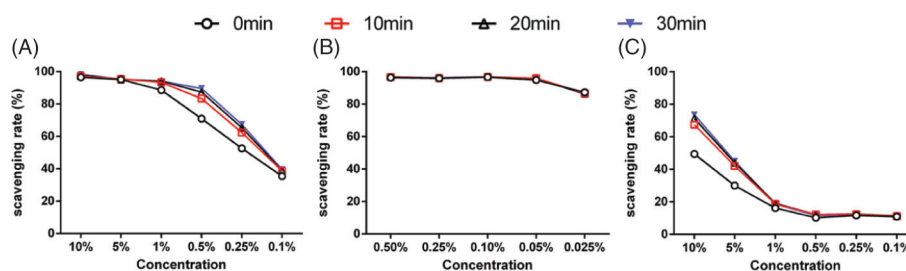


Fig. 1. DPPH scavenging rates of WOC, VC, and pure walnut oil at different time points. (A) WOC; (B) VC; (C) Pure walnut oil.

The effects of WOC on histological changes in liver and brain

The pathological changes in liver were shown in Fig. 3. In the normal group, the shape of cell nucleus was large and round. Hepatic cords were neatly arranged and there were no cell necrosis and degeneration. There were spotty necrosis, hydropic degeneration, vacuolar degeneration and lymphocytic infiltration in the control group. And the hepatic cords were disarranged. Mice treated with WOC, VC, and pure walnut oil had exhibited improvements in these situations. And as the dose of WOC increased, the improvements got better.

The pathological changes in hippocampus dentate gyrus were observed (Fig. 4). Compared with the normal group, the granular cells in the control group were smaller, fewer, and disarranged. Furthermore, cells with

hyperchromatism, changes of nuclear shape, and karyopyknosis were also observed, which indicated cell aging (19, 20). Groups treated with WOC, VC, and pure walnut oil showed improvements in the cells number and arrangement.

The effects of WOC on T-AOC, SOD, GSH-Px, and MDA

In the result of serum (Fig. 5), decreased levels of T-AOC, SOD, and GSH-Px, and increased contents of MDA were found in the control group compared with the normal group ($p < 0.05$ or $p < 0.001$). Mice treated with WOC, VC, and pure walnut oil showed improvements in T-AOC, SOD, GSH-Px, and MDA compared with the control group ($p < 0.05$ or $p < 0.01$ or $p < 0.001$), and there were significant differences

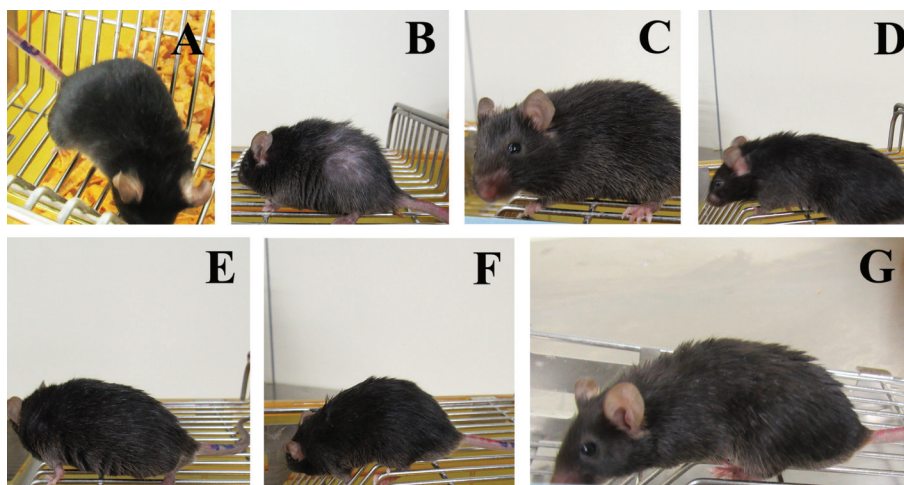


Fig. 2. The appearance changes in different groups. (A) Normal group; (B) Control group; (C) WOC low group; (D) WOC medium group; (E) WOC high group; (F) VC group; (G) Pure walnut oil.

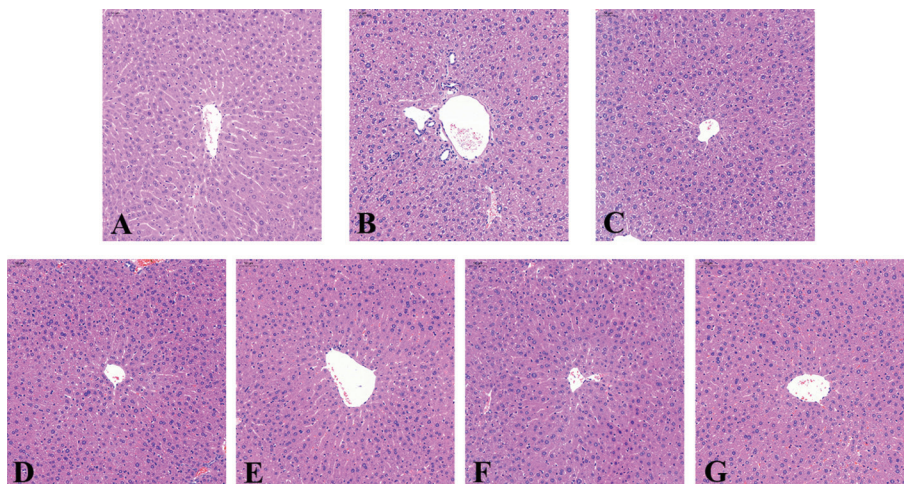


Fig. 3. Pathological changes in liver. (A) Normal group; (B) Control group; (C) WOC low group; (D) WOC medium group; (E) WOC high group; (F) VC group; (G) Pure walnut oil.

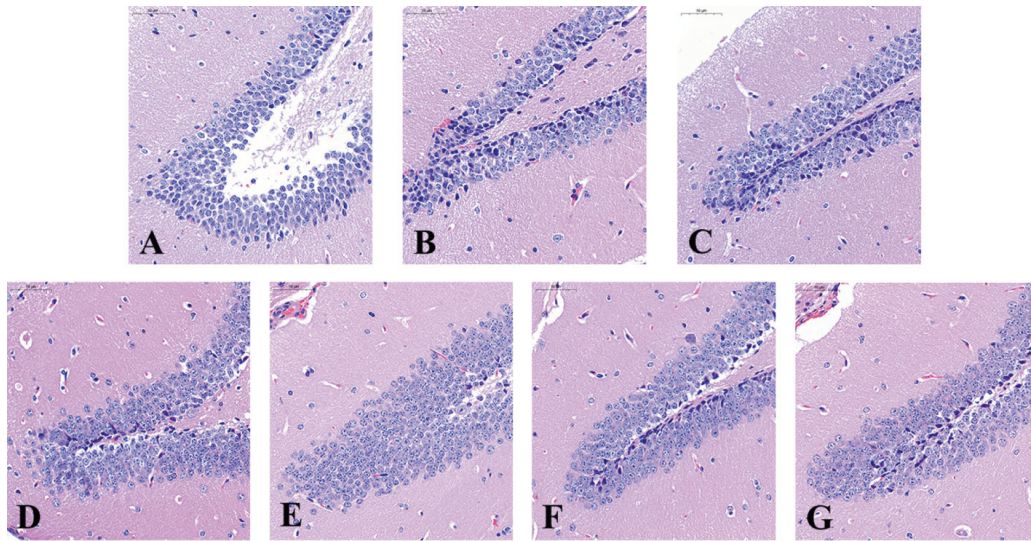


Fig. 4. Pathological changes in brain (H&E staining, ×500). (A) Normal group; (B) Control group; (C) WOC low group; (D) WOC medium group; (E) WOC high group; (F) VC group; (G) Pure walnut oil.

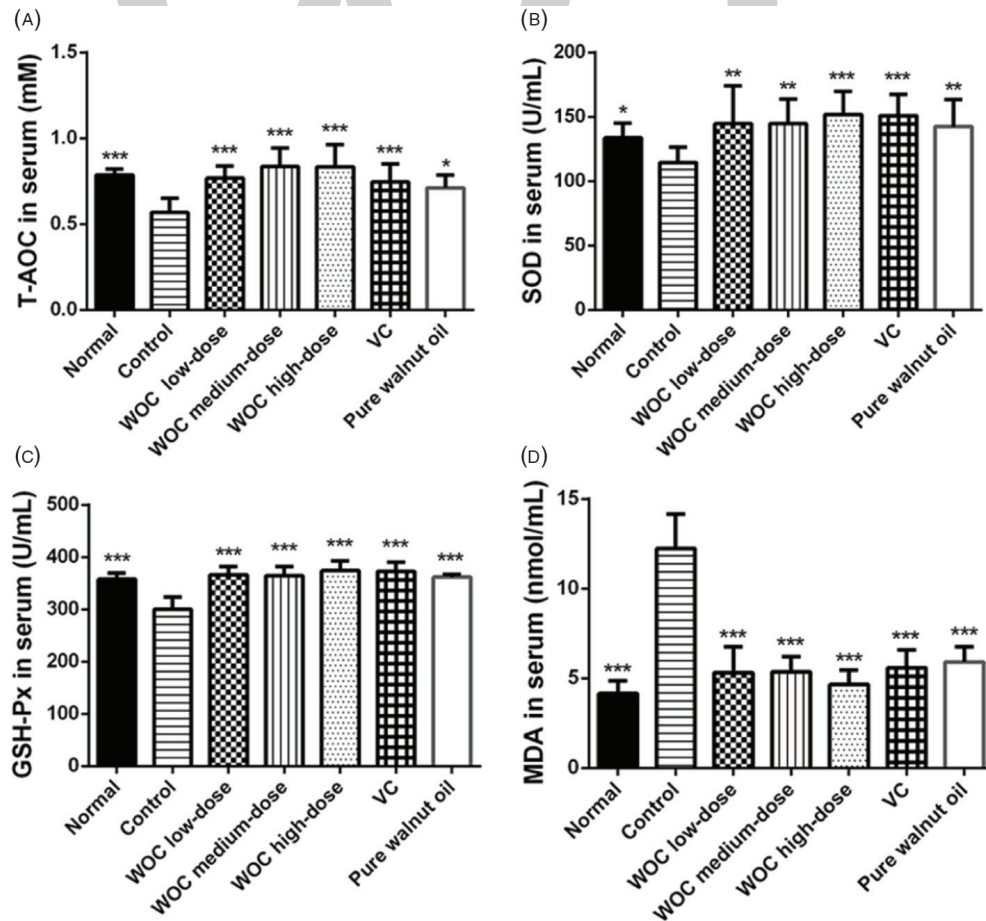


Fig. 5. Biochemical indicators in serum. (A) Effects of WOC on T-AOC; (B) Effects of WOC on the activities of SOD; (C) Effects of WOC on the activities of GSH-Px; (D) Effects of WOC on the contents of MDA. * $p < 0.05$, ** $p < 0.01$, *** $p < 0.001$ versus the control group.

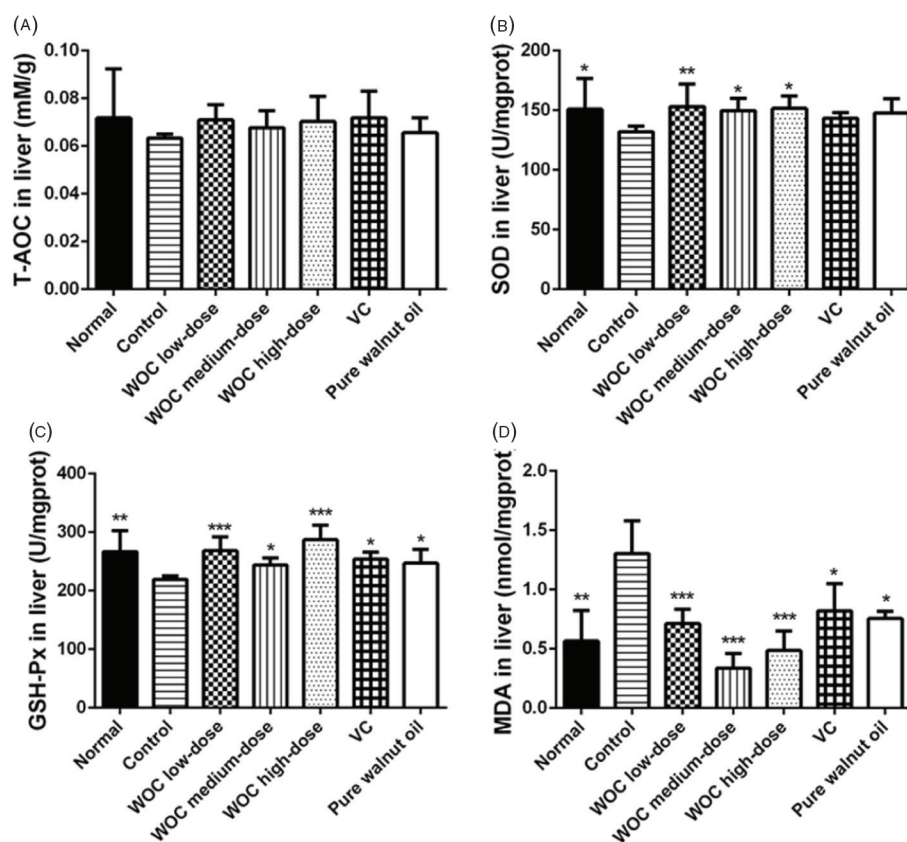


Fig. 6. Biochemical indicators in liver. (A) Effects of WOC on T-AOC; (B) Effects of WOC on the activities of SOD; (C) Effects of WOC on the activities of GSH-Px; (D) Effects of WOC on the contents of MDA. * $p < 0.05$, ** $p < 0.01$, *** $p < 0.001$ versus the control group.

between WOC high group and pure walnut oil group ($p < 0.05$) in MDA result. But there were no significant differences found among WOC, VC, and pure walnut oil groups in other results.

As shown in the result of liver (Fig. 6), there were no significant differences among groups in T-AOC. In WOC groups, the SOD and GSH-Px were significantly higher than the control group and the MDA lower than that in the control group ($p < 0.05$ or $p < 0.01$ or $p < 0.001$). There were also significant differences between the control group and the positive control groups in the results of GSH-Px and MDA ($p < 0.05$) but not in the SOD result. Moreover, the improvement levels of a high dose of WOC was higher than VC and pure walnut oil in GSH-Px ($p < 0.05$), also the MDA level in WOC medium group was lower than positive control groups ($p < 0.05$ or $p < 0.01$).

For the result of brain (Fig. 7), the T-AOC levels and the activities of SOD and GSH-Px in WOC groups were significantly higher than that in the control group. The contents of MDA decreased significantly in WOC groups compared with the control group ($p < 0.01$ or $p < 0.001$). Moreover, the T-AOC levels in the WOC medium group were significantly higher than that in the positive control groups ($p < 0.001$).

Expression of HO-1, iNOS, and Klotho in liver and brain

In the results of western blotting (Fig. 8), the expression of HO-1 in D-gal-induced aging mice was significantly increased compared with the normal group. Mice treated with WOC, VC, and pure walnut oil all exhibited the higher upregulation of HO-1 than the control group and the enhancements of WOC were higher than VC and pure walnut oil. iNOS found high expression in the control group. WOC, VC, and pure walnut oil could obviously downregulate the expression of iNOS both in liver and brain. Mice in the control group showed extremely low expression of Klotho, but WOC, VC, and pure walnut oil differently upregulated the expression of Klotho in liver and brain.

Discussion

Aging is an inevitable process which can lead to oxidative stress and affect the function of kidney, brain, liver, and so on (21–24). In recent years, discovery of many antioxidant ingredients has made it possible to delay senescence, and finding effective anti-aging foods or drugs has become a hot topic. Many plants and plant extracts are rich in bioactive constituents and have been widely used in pharmaceutical application and research; thus, they are potential in the screening of antioxidant drugs.

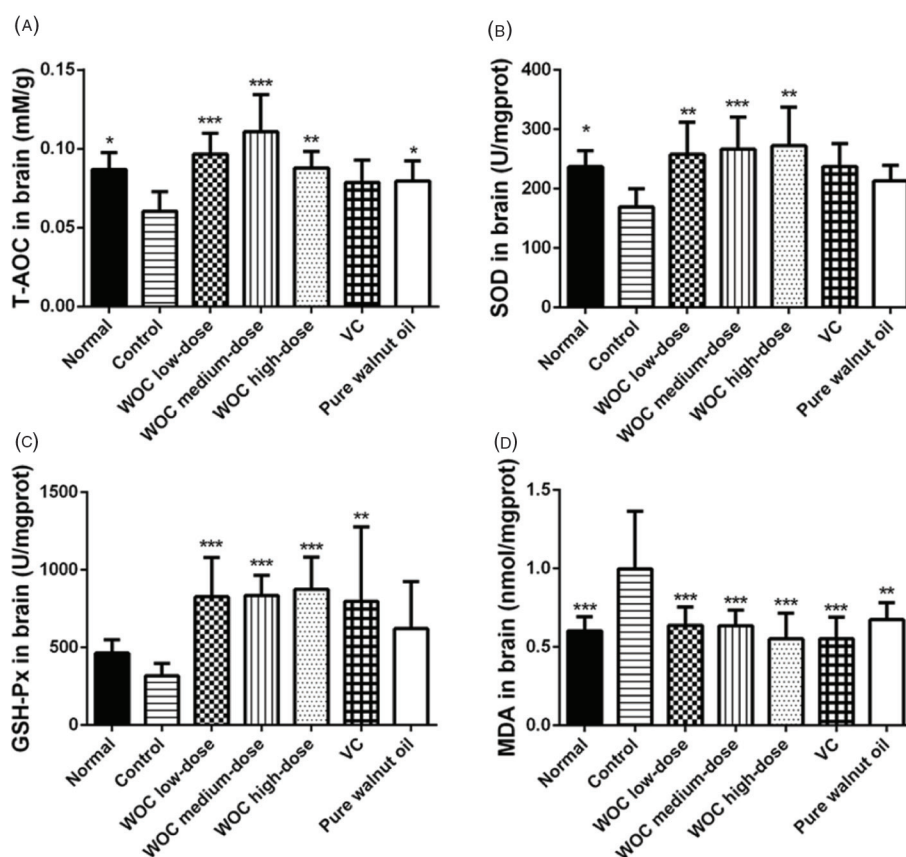


Fig. 7. Biochemical indicators in brain. (A) Effects of WOC on T-AOC; (B) Effects of WOC on the activities of SOD; (C) Effects of WOC on the activities of GSH-Px; (D) Effects of WOC on the contents of MDA. * $p < 0.05$, ** $p < 0.01$, *** $p < 0.001$ versus the control group.

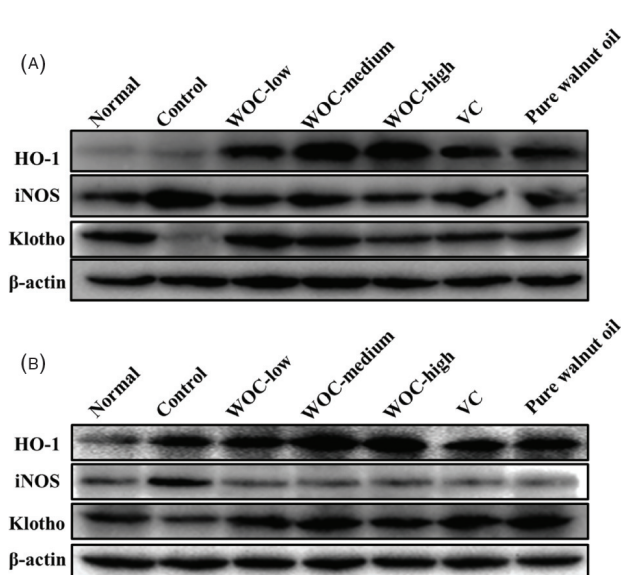


Fig. 8. Western blotting assays of HO-1, iNOS, and Klotho. (A) The expression of HO-1, iNOS, and Klotho in liver; (B) The expression of HO-1, iNOS, and Klotho in brain.

In this study, we investigated the compound capsule of walnut oil and grape seed extract to verify its antioxidant capacity and lay basis for its daily use by elderly people.

Generally, in this study, we investigated the antioxidant effects of WOC *in vitro* and *in vivo*. The DPPH scavenging test was selected to explore the antioxidant capacity of WOC *in vitro*. The biochemical indicators such as T-AOC, SOD, GSH-Px and MDA in serum, liver and brain were detected to evaluate the antioxidant of WOC *in vivo*. Also, the western blotting assays were employed to detect some proteins which were closely related to oxidative stress and aging. Moreover, the histopathologic examination was observed to discuss the effects of WOC on tissues.

The DPPH scavenging test showed that the scavenging rate of VC was much higher than WOC, but it was the opposite in *in vivo* research. The reason might be that the instability of VC led to the low bioavailability *in vivo*. Instead, the bioactive ingredients of WOC might have higher bioavailability.

The dose of D-gal covered a wide range wherein the minimal dose could be 50 mg/kg (25), while the higher

dose could be 1,250 mg/kg (26). The modeling period usually ranges from 6 to 8 weeks. In this research, the aging model was established by 1,000 mg/kg D-gal for 8 weeks. Different indicators were selected to evaluate the antioxidant effects of WOC *in vivo*. T-AOC could reflect the T-AOC of the body. The activity of SOD and GSH-Px and the content of MDA are closely related to aging process and oxidative stress (27–29). Enzymes of SOD and GSH-Px are important antioxidases with strong ability of eliminating free radicals (27, 30). The MDA can reflect the extent of lipid peroxidation and attacks from free radicals to tissues and cells (31). In the results, WOC could obviously increase the levels of T-AOC and the activities of SOD and GSH-Px. It could also decrease the contents of MDA.

HO-1 is an oxidative, stress-induced enzyme belonging to the HO family, which has strong antioxidant capacity (32, 33). Normally, the expression of HO-1 is low in normal organs, such as brain, and high only in the spleen and liver (34). However, the expression of HO-1 will be upregulated under the condition of oxidative stress (35). In the results, the expression of HO-1 in the aging model group was higher than the normal group. WOC, VC, and pure walnut could obviously upregulate the expression of HO-1 and thus enhance the antioxidant capacity.

iNOS belongs to a family of enzymes called nitric oxide synthase (NOS), which is closely related to the production of nitric oxide (NO) (36). NO plays contrasting roles in living organism. It is an important host defense effector in the immune system. It is also a free radical that plays an important role in pathological processes, especially in inflammatory disorders (37–39). In many systems, the oxidative stress could increase cytokine-mediated iNOS expression (40), which is accompanied by increasing production of NO, and the NO could react with superoxide to produce the strong oxidant peroxynitrite, which in turn can increase lipid peroxidation (41). In our results, WOC could alleviate the oxidative stress by obviously decreasing the expression of iNOS.

Klotho is an anti-aging gene that was first discovered in mice by Kuro-o et al. in 1997. Deficiency of Klotho leads to a syndrome resembling aging, including a short lifespan; stunted growth and kyphosis; vascular calcification and atherosclerosis; osteoporosis; pulmonary emphysema; cognitive impairment; deafness; and atrophy of skin, muscles, gonads, and many other organs (42). Conversely, an overexpression of klotho could extend life span (43). Moreover, studies also indicated that Klotho worked as an important factor in the regulation of oxidative stress, cell proliferation, and apoptosis (44, 45). Our results showed that WOC could upregulate the expression of Klotho and protect against the damages of oxidative stress.

All results showed WOC could enhance the antioxidant capacity of the body, but the improvements did not exhibit a dose-dependent behavior. We inferred that there might be two reasons: (1) The dose gradient we designed was small and so there were no obvious differences among WOC groups; (2) The improvements reached a maximum at a low dose of WOC, but the effects did not enhance with an increase in dose. The expression of proteins HO-1, iNOS, and Klotho were related to many factors and could be regulated through different pathways (41, 46–47). So the mechanism of how WOC regulates the expression of these proteins needs further studies. And, the data of weight changes in mice showed that the growth rate in the WOC group was lower than that in the normal group, leading to the inference that WOC might have a weight-loss function.

Conclusion

In conclusion, WOC could improve the antioxidant capacity in aging mice induced by D-gal through increasing the activities of antioxidant enzymes, decreasing the contents of MDA, and regulating the expression of oxidative stress-related proteins. Our study suggests that WOC can be used as a promising anti-aging and weight-loss food.

Authors' contributions

Huandong, Zhao, postgraduate student of Xiangya Hospital, majored in Biomedical Engineering; Jian, Li, professor of surgery in Xiangya hospital; Juan, Zhao, postgraduate student of Xiangya hospital, majored in Clinical Laboratory Diagnostics; Yang, Chen, postgraduate student of Xiangya hospital, majored in Biomedical Engineering; Caiping, Ren, professor of Oncology in School of Basic Medical Science, Central South University; Yuxiang, Chen, professor of pharmacy in School of Pharmaceutical Sciences, Central South University.

Conflict of interest and funding

All authors declared no conflict of interest.

Funding

This work was supported by the Development and Research of Compound Walnut Oil Soft Capsule (2014.10–2018.09), National Basic Research Program of China (2010CB833605), and Hunan Provincial Science Department Program (2014FJ6006).

References

1. Dillin A, Gottschling DE, Nystrom T. The good and the bad of being connected: the integrons of aging. *Curr Opin Cell Biol* 2014; 26: 107–12.
2. Diamanti-Kandarakis E, Dattilo M, Macut D, Duntas L, Gonos E, Goulis DG, et al. Mechanisms in endocrinology: aging and anti-aging: a combo-endocrinology overview. *Eur J Endocrinol* 2017; 176: R283–308.

3. Forman HJ. Redox signaling: an evolution from free radicals to aging. *Free Radic Biol Med* 2016; 97: 398–407.
4. Jyoti A, Mishra N, Dhas Y. Ageing: consequences of excessive free radicals and inflammation. *Curr Sci India* 2016; 111: 1787–93.
5. Lei L, Ou L, Yu X. The antioxidant effect of *Asparagus cochinchinensis* (Lour.) Merr. shoot in D-galactose induced mice aging model and in vitro. *J Chin Med Assoc* 2016; 79: 205–11.
6. An F, Yang GD, Tian JM, Wang SH. Antioxidant effects of the orientin and vitexin in *Trollius chinensis* Bunge in D-galactose-aged mice. *Neural Regen Res* 2012; 7: 2565–75.
7. Mathew S, Abraham TE. In vitro antioxidant activity and scavenging effects of *Cinnamomum verum* leaf extract assayed by different methodologies. *Food Chem Toxicol* 2006; 44: 198–206.
8. Laubertova L, Konarikova K, Gbelcova H, Ďuračková Z, Žitňanová I. Effect of walnut oil on hyperglycemia-induced oxidative stress and pro-inflammatory cytokines production. *Eur J Nutr* 2015; 54: 291–9.
9. Arranz S, Perez-Jimenez J, Saura-Calixto F. Antioxidant capacity of walnut (*Juglans regia* L.): contribution of oil and defatted matter. *Eur Food Res Technol* 2008; 227: 425–31.
10. Jayaprakasha GK, Singh RP, Sakariah KK. Antioxidant activity of grape seed (*Vitis vinifera*) extracts on peroxidation models in vitro. *Food Chem* 2001; 73: 285–90.
11. Park M, Cho H, Jung H, Lee H, Hwang KT. Antioxidant and anti-inflammatory activities of tannin fraction of the extract from black raspberry seeds compared to grape seeds. *J Food Biochem* 2014; 38: 259–70.
12. Szeto YT, Lee KY, Kalle W, Pak SC. Protective effect of grape seed extracts on human lymphocytes: a preliminary study. *Appl Physiol Nutr Metab* 2013; 38: 275–9.
13. Gong G, Xu F. Study of aging model in mice. *J China Pharmaceut Univ* 1991; 2: 101–3.
14. Zhu Y. Establishment and measurement of D-galactose induced aging model. *Fudan Univ J Med Sci* 2007; 34: 617–19.
15. St-Pierre J, Buckingham JA, Roebuck SJ, Brand MD. Topology of superoxide production from different sites in the mitochondrial electron transport chain. *J Biol Chem* 2002; 277: 44784–90.
16. Wei H, Li L, Song Q, Ai H, Chu J, Li W. Behavioural study of the D-galactose induced aging model in C57BL/6J mice. *Behav Brain Res* 2005; 157: 245–51.
17. Sharma OP, Bhat TK. DPPH antioxidant assay revisited. *Food Chem* 2009; 113: 1202–5.
18. Chen J, Li Y, Zhu Q, Li T, Lu H, Wei N, et al. Anti-skin-aging effect of epigallocatechin gallate by regulating epidermal growth factor receptor pathway on aging mouse model induced by d-Galactose. *Mech Ageing Dev* 2017; 164: 1–7.
19. Martin GM. Aging and cell structure. *Hum Pathol* 1981; 14: 96.
20. Pannese E. Neuroglial cells: morphological changes during normal aging. *Rend Lincei Sci Fis* 2013; 24: 101–106.
21. Go Y, Jones DP. Redox theory of aging: implications for health and disease. *Clin Sci* 2017; 131: 1669–1688.
22. Glasscock RJ, Denic A, Rule AD. The conundrums of chronic kidney disease and aging. *J Nephrol* 2017; 30: 477–83.
23. Bickford PC, Flowers A, Grimmig B. Aging leads to altered microglial function that reduces brain resiliency increasing vulnerability to neurodegenerative diseases. *Exp Gerontol* 2017; 94: 4–8.
24. Tian L, Hui CW, Bisht K, Tan Y, Sharma K, Chen S, et al. Microglia under psychosocial stressors along the aging trajectory: consequences on neuronal circuits, behavior, and brain diseases. *Prog Neuro Psychoph* 2017; 79: 27–39.
25. Yu X, Li S, Yang D, Qiu L, Wu Y, Wang D, et al. A novel strain of *Lactobacillus mucosae* isolated from a Gaotian villager improves in vitro and in vivo antioxidant as well as biological properties in D-galactose-induced aging mice. *J Dairy Sci* 2016; 99: 903–14.
26. Wang PP, Sun HX, Liu CJ, Hu MH, He XQ, Yue S, et al. Racemic oleracein E increases the survival rate and attenuates memory impairment in D-galactose/NaNO₂-induced senescent mice. *Phytomedicine* 2016; 23: 460–7.
27. Selvaratnam JS, Robaire B. Effects of aging and oxidative stress on spermatozoa of superoxide-dismutase 1- and catalase-null mice. *Biol Reprod* 2016; 95: 60.
28. Thiab NR, King N, McMillan M, Almashhadany A, Jones GL. Age-related protein and mRNA expression of glutathione peroxidases (GPx) and Hsp-70 in different regions of rat kidney with and without stressor. *Aims Mol Sci* 2016; 3: 125–37.
29. Li G, Chen Y, Hu H, Liu L, Hu X, Wang J, et al. Association between age-related decline of kidney function and plasma malondialdehyde. *Rejuven Res* 2012; 15: 257–64.
30. Mari M, Morales A, Colell A, Garcia-Ruiz C, Fernández-Checa JC. Mitochondrial glutathione, a key survival antioxidant. *Antioxid Redox Sign* 2009; 11: 2685–700.
31. Yonny ME, Garcia EM, Lopez A, Arroquy JI, Nazareno MA. Measurement of malondialdehyde as oxidative stress biomarker in goat plasma by HPLC-DAD. *Microchem J* 2016; 129: 281–5.
32. Tenhunen R, Marver HS, Schmid R. The enzymatic conversion of heme to bilirubin by microsomal heme oxygenase. *Proc Natl Acad Sci U S A* 1968; 61: 748–55.
33. Maher J, Yamamoto M. The rise of antioxidant signaling – the evolution and hormetic actions of Nrf2. *Toxicol Appl Pharmacol* 2010; 244: 4–15.
34. Maines MD. The heme oxygenase system and its functions in the brain. *Cell Mol Biol* 2000; 46: 573–85.
35. Ryter SW, Alam J, Choi A. Heme oxygenase-1/carbon monoxide: from basic science to therapeutic applications. *Physiol Rev* 2006; 86: 583–650.
36. Aktan F. iNOS-mediated nitric oxide production and its regulation. *Life Sci* 2004; 75: 639–53.
37. Alderton WK, Cooper CE, Knowles RG. Nitric oxide synthases: structure, function and inhibition. *Biochem J* 2001; 357: 593–615.
38. Da Cunha NV, Cortegoso Lopes FN, Panis C, Cecchini R, Pinge-Filho P, Martins-Pinge MC. iNOS inhibition improves autonomic dysfunction and oxidative status in hypertensive obese rats. *Clin Exp Hypertens* 2017; 39: 50–7.
39. Bogdan C. Nitric oxide and the immune response. *Nat Immunol* 2001; 2: 907–16.
40. Kuo PC, Abe KY, Schroeder RA. Oxidative stress increases hepatocyte iNOS gene transcription and promoter activity. *Biochem Biophys Res Commun* 1997; 234: 289–92.
41. Dias AS, Porawski M, Alonso M, Marroni N, Collado PS, González-Gallego J. Quercetin decreases oxidative stress, NF-kappaB activation, and iNOS overexpression in liver of streptozotocin-induced diabetic rats. *J Nutr* 2005; 135: 2299–304.
42. Kuro-o M, Matsumura Y, Aizawa H, Kawaguchi H, Suga T, Utsugi T, et al. Mutation of the mouse *klotho* gene leads to a syndrome resembling ageing. *Nature* 1997; 390: 45–51.
43. Kurosu H, Yamamoto M, Clark JD, Pastor JV, Nandi A, Gurnani P, et al. Suppression of aging in mice by the hormone Klotho. *Science* 2005; 309: 1829–33.
44. Kokkinaki M, Abu-Asab M, Gunawardena N, Ahern G, Javidnia M, Young J, et al. Klotho regulates retinal pigment epithelial functions and protects against oxidative stress. *J Neurosci* 2013; 33: 16346–59.

45. Yao Y, Wang Y, Zhang Y, Liu C. Klotho ameliorates oxidized low density lipoprotein (ox-LDL)-induced oxidative stress via regulating LOX-1 and PI3K/Akt/eNOS pathways. *Lipids Health Dis* 2017; 16: 77.
46. Luo Y, Lu S, Dong X, Xu L, Sun G, Sun X. Dihydromyricetin protects human umbilical vein endothelial cells from injury through ERK and Akt mediated Nrf2/HO-1 signaling pathway. *Apoptosis* 2017; 22: 1013–24.
47. Wang Y, Kuro-o M, Sun Z. Klotho gene delivery suppresses Nox2 expression and attenuates oxidative stress in rat aortic smooth muscle cells via the cAMP-PKA pathway. *Aging Cell* 2012; 11: 410–17.

***Jian Li**

87 Xiangya Road
Changsha 410008, China.
Email: lijian869@126.com

***Yuxiang Chen**

172 Tongzipo Road
Changsha, 410013, China
Email: Yuxiangchen@csu.edu.cn

WWT

Efficacy and safety of *Eurycoma longifolia* (Physta[®]) water extract plus multivitamins on quality of life, mood and stress

Annie George^{1,2}, Jay Udani³, Nurhayati Zainal Abidin¹ and Ashril Yusof^{4*}

¹Institute of Biological Sciences, Faculty of Science, University of Malaya, Kuala Lumpur, Malaysia; ²Biotropics Malaysia Berhad, Lot 21, Jalan UI/19, Section UI, Hicom-Glenmarie Industrial Park, 40150 Shah Alam, Malaysia; ³Agoura Hills, CA, USA; ⁴Exercise Science, Sports Centre, University of Malaya, 50603 Kuala Lumpur, Malaysia

Abstract

Background: The use of alternative and complementary medicines to alleviate stress has increased to avoid the negative effects of pharmaceutical drugs.

Objective: This study investigated the safety and efficacy of *Eurycoma longifolia* in combination with multivitamins (EL+MV) versus placebo on improving quality of life (QoL), mood and stress in moderately stressed healthy participants.

Methods: This randomised, double-blind, placebo-controlled 24-week study enrolled 93 participants aged 25–65 years, with a body mass index of 18–30 kg/m², scoring ≤18 in tension and ≤14 in fatigue subscale of Profiles of Mood Scores (POMS) questionnaire and supplemented with EL+MV or placebo. The primary endpoints were QoL measured by 12-Item Short Form Health Survey (SF-12) questionnaire and mood measured by POMS. The secondary endpoint was stress measured by Multi-Modal Stress Questionnaire (MMSQ). The safety of the intervention product was measured by complete metabolic panel, lipid and renal analysis including several immune parameters.

Results: While there were no significant between-group differences, within-group improvements were observed in the SF-12 QoL, POMS and MMSQ domains. In the SF-12 domain, improvements were seen in role limitation due to emotional health ($P = 0.05$), mental component domain ($P < 0.001$), emotional well-being ($P < 0.001$), social functioning ($P = 0.002$) as well as vitality ($P = 0.001$) at week 12. An increasing trend in POMS-vigour domain was also observed in the EL+MV group at week 12. A 15% decrease in physical stress domain ($P < 0.05$) compared with 0.7% in the placebo group was also observed in MMSQ. When the subjects were subgrouped according to age, 25–45 and 46–65 years of age, for primary outcomes, between-group significance was observed in the 25–45 year group in the social functioning domain of SF-12 ($P = 0.021$) and POMS-vigour ($P = 0.036$) in the 46–65 year group. No significant changes were observed in vital signs and complete metabolic panel. Regarding immune parameters, the lymphocytes increased significantly in the active group ($P \leq 0.05$). In total, 13 adverse events were reported: six on placebo and seven on EL+MV.

Conclusion: EL+MV may support the QoL, mood, stress and immune parameters in healthy participants.

Trial registration: This study has been registered at clinicaltrials.gov (NCT02865863).

Key words: *Eurycoma longifolia*; multivitamins; quality of life; mood; stress

Unresolved stress greatly increases the risk of developing depression, consequently becoming a topic of public health awareness and therapeutic interventions. Depression afflicts approximately 20–25% of women and 10–17% of men during their lifetime (1). While certain drugs like fluoxetine (Prozac) and sertraline (Zoloft) have been used to treat stress and anxiety disorders and, in recent years, the anti-depressant setraline,

there is a concern that one can be addicted to and dependent on drug usage (2). Alternative and complementary medicines, such as herbal supplements, have emerged as substitutes to conventional therapeutics for ameliorating depression and maintaining mental well-being (3–5).

In South East Asia, where traditional/herbal medicine is popular, supplementation with *Eurycoma longifolia* Jack, Simaroubaceae (*Tongkat Ali* or Malaysian ginseng), has

been shown to be efficacious for alleviating stress (6), as well as many other ailments including fever, arthritis, high blood pressure, diabetes, low energy or libido, bacterial infections and cancer (7–9). *Eurycoma longifolia* (EL) is a slender evergreen tree mainly found in Malaysia, Indonesia and the Philippines. Derivatives of this plant have been used to restore and enhance energy levels, to improve physical and mental performance, endurance and stamina (9) and quality of life (QoL), as evidenced by a decrease in aging males symptoms score and an increase in serum testosterone levels (10). Another related study showed improvement in QoL and sexual well-being in men, specifically in the domains of ‘physical function’ and ‘vitality’ (11). The roots of EL are largely responsible for its biological activity due to the presence of alkaloids, quassinoids, quassinoid diterpenoids, eurycomacocide, eurycolactone, laurylcolactone or eurycomalactone and pasakbumin-B (7) and peptides (12). It has been demonstrated to reduce stress through the reduction of cortisol (6) with a concurrent increase in lymphocytes and natural killer cells (13). These active ingredients in EL and in other plants, such as mountain ginseng (*Panax ginseng*), may be responsible for improving QoL, as well as combating stress without adverse effects (11, 14–16). A recent 4-week, randomised clinical study on moderately stressed participants consuming water extract from EL reported significant improvements in mood, tension, anger and confusion (6). This was accompanied by a reduction in cortisol and increased testosterone levels. Another study investigated the effect of EL on the immune status of moderately stressed subjects (13), whereby a 1-month supplementation of 200 mg EL extract per day nearly significantly improved vigour measured by Profile of Mood States (POMS) while scores for immunological vigour also improved.

Micronutrient deficiencies contribute to stress and depression (5). Indeed, low levels of folic acid may be correlated with depressive symptomatology (16) that can be ameliorated by mineral supplementation (17). Multinutrient formulations have a significantly greater effect in reducing stress and anxiety in subjects than single interventions alone (18). In addition, a recent study demonstrated that a formulation consisting of multivitamins, minerals and herbal extracts was more effective than placebo in significantly reducing the overall score on a depression, anxiety and stress scale, as well as improving alertness and general daily functioning in healthy older men (19). Furthermore, a high dose of vitamin B complex with vitamin C and minerals led to significant improvements in ratings on Perceived Stress Scales, General Health Questionnaire and the ‘vigour’ subscale of POMS in healthy males (20).

While preclinical and clinical studies lend credence to the ability of EL to improve mood which was possibly linked to hormonal balance favouring elevated mood (21), efficacy studies of EL in combination with micronutrients and

conducted in accordance with established standards are currently lacking. The objective of this study was to investigate the safety and efficacy of a multivitamin mix in combination with EL water extract on QoL, mood and stress of moderately stressed but healthy participants.

Materials and methods

This study was conducted in accordance with the Guidelines for Good Clinical Practice (ICH-6) and the Declaration of Helsinki. Institutional Review Board (IRB) approval was obtained from IntegReview Ethical Review Board, an independent IRB located in Austin, TX, USA, comprising scientific and non-scientific members of mostly medical doctors, on 17 January 2014 prior to initiation of any study-related activities. The IRB reviewed the protocol, medical ethics, informed consent, advertisement, stipend and compliance to protocol. The study was conducted at Medicus Research LLC, a clinical research site located at Agoura Hills, CA, USA. Written informed consent was obtained from volunteers prior to all study procedures. The recruitment and follow-up took place from 7 February 2014 to 13 March 2015.

Study design

This was a randomised, double-blind, placebo-controlled parallel study with a 12-week efficacy and a 24-week safety period. The allocation *ratio* of participants in each of the comparison groups was 1:1. Efficacy was measured at 6 and 12 weeks, with safety and adverse events at 6, 12 and 24 weeks. The participants were required to make a total of four visits to the clinical trial site at Medicus Research LLC, Agoura Hills, CA.

At screening/baseline (week 0), inclusion/exclusion criteria, medical history and concomitant therapies were reviewed; baseline demographic data were collected; heart rate, respiratory rate, blood pressure and oral temperature were measured; and body mass index (BMI) was calculated. Fasting blood samples were obtained for assessment of complete blood count (CBC), comprehensive metabolic panel (CMP) including kidney function (estimated glomerular filtration rate, blood urine nitrogen [BUN], creatinine and bilirubin), liver function (aspartate aminotransferase, alanine transaminase), lipid panel (total cholesterol [TC], high-density lipoprotein-cholesterol [HDL-C], low-density lipoprotein-cholesterol [LDL-C], and triglycerides), testosterone (free and total) and urinalysis (leukocyte esterase, amorphous and calcium oxalate crystals). A urine pregnancy test was conducted on females with child-bearing potential. Electrocardiogram (EKG) was performed and POMS (22), SF-12 QoL (23), and Multi-Modal Stress Questionnaire (MMSQ) (24) were administered. Participants were dispensed a 6-week supply of the investigational product, a daily dosing diary and a 3-day food recall. Subjects who met all the

study inclusion criteria and none of the exclusion criteria were enrolled in the study. After eligibility was confirmed, all volunteers received a randomisation number.

Participants returned to the clinic at weeks 6, 12 and 24 after having fasted for 10 h for assessment of medical and concomitant medication history. Vital signs and anthropometric measures, compliance and adverse events, and current medical history were reviewed. Fasting blood was collected for CBC, CMP, lipid panel, testosterone (free and total) measurements and urinalysis was performed. EKG was performed at baseline and at week 24.

POMS, SF-12 and MMSQ questionnaires were administered and a daily dosing diary and a 3-day food recall were dispensed at baseline, week 6 and week 12 only. At week 6, participants were dispensed a 6-week supply of the investigational product and at week 12, a 12-week supply of the investigational product. Participants maintained their daily diary for the duration of the study period and were required to record concomitant therapies and adverse events.

Participants

Study participants were recruited from the general population by online advertising, recruiting and available clinical trial databases. Inclusion criteria were as follows: healthy volunteers between 25 and 65 years of age, BMI 18–30 kg/m² and having self-reported moderate stress. Moderate stress was defined as a measure of both the tension and fatigue subscale of the POMS questionnaire. Participants who scored ≤18 in the tension subscale and ≤14 in the fatigue subscale were considered as having moderate stress. The tension subscale items are tense, on edge, uneasy, restless, nervous and helpless. A highest score (4 = extremely) for each of these items will give a total subscale score of ≤24 in tension and ≤20 in fatigue. An upper cut-off limit was determined, that is, a scoring of ≤18 in the tension subscale and ≤14 in the fatigue subscale, to exclude subjects who might fall within extremely stressed and possibly depressed category that will require medication and possibly cannot be addressed with health supplementation of multinutrients. The subjects were furthermore required to answer a Yes/No questionnaire in the inclusion/exclusion criteria as to whether they perceived themselves to having mid-level stress at work as a result of employment and life balance.

Exclusion criteria: participants were excluded if they were pregnant, lactating, planning to become pregnant or unwilling to use adequate contraception during the duration of the study, or had a history of immune system disorders, neurological disorders, temporal arthritis, ulcerative colitis, history of cancer within 2 years prior to enrolment, any active infection, or infection requiring antibiotics within 30 days of enrolment, significant gastrointestinal conditions including, but not limited to,

inflammatory bowel disease, eating disorders, untreated hypothyroidism and use of herbal products containing androgenic/anxiolytic activity within 30 days prior to enrolment.

Investigational product

The investigational product (50 mg per tablet) was a proprietary water extract of EL root (Physta® also known as LJ100 in the USA). The multivitamin mix consisted of ascorbic acid (50 mg), retinyl acetate (4,000 IU), cholecalciferol (200 IU), D1-alpha tocopherol acetate (15 IU), thiamine mononitrate (1.5 mg), riboflavin (1.7 mg), pyridoxine hydrochloride (2 mg), cyanocobalamin (0.001 mg), folic acid (0.2 mg), niacinamide (20 mg), D-biotin (0.15 mg), copper (2 mg), iron (10 mg), magnesium (10 mg), manganese (2.5 mg), selenium (0.005 mg), zinc (5 mg) and calcium (100 mg). The placebo contained microcrystalline cellulose, polyvinylpyrrolidone, sodium starch glycolate, colloidal silicon dioxide and magnesium stearate. The investigational product was produced under good manufacturing practices (GMP) requirements by Unison Nutraceutical Sdn Bhd and stored in a dry place at room temperature. Participants were instructed to consume either EL+MV or the placebo starting the day following the baseline visit, one tablet daily in the morning with water for 24 weeks.

Outcome measures

The primary and secondary outcomes measures were assessed by questionnaires at week 0 (Visit 0), week 6 (Visit 1) and 12 (Visit 2). The primary outcome measure for this study was the assessment of the efficacy of EL+MV versus placebo on mood and QoL. Mood state was assessed using the POMS questionnaire, which consisted of the following: total mood disturbance and its subscales, tension, depression, anger, fatigue, confusion and vigour. The POMS rated emotional and physical aspects of mood as ranging from 'not at all (1 point)' to 'extremely (5 points)'. A lower score, except for vigour, indicates better mood.

The POMS Iceberg profile, designed for assessing active/healthy individuals (25), was also analysed. QoL was assessed by the SF-12 questionnaire which measured the following domains: physical component summary, mental component summary, physical functioning, role limitations due to physical health, role limitations due to emotional health, energy/fatigue ratio (vitality), emotional well-being, social functioning, pain and general health. Scores on the SF-12 scales ranged from 0 to 100, with higher scores indicating better health.

The secondary objective was to assess stress using MMSQ, which measured the following subscales: total, behavioural, cognitive and physical. The MMSQ rated emotional and physical aspects of stress as ranging from 'never (1 point)' to 'constantly (5 points)'.

Safety and tolerability of the investigational product were assessed through changes in CBC, CMP, lipid panel, total and free testosterone, urinalysis and vital signs at all visits. The study would be temporarily stopped for any of the following: if WHO Grade 3 toxicity is experienced by four or more patients or WHO Grade 4 toxicity is experienced by two or more patient(s).

Compliance

The dispensed study product compliance diaries were returned to the clinic and participants who were non-compliant with their diaries were reminded of their obligations regarding appropriate study compliance.

Sample size

The sample size was calculated using the G*Power 3.0.10 software based on a reference value proposed by Perazzo et al. (26), which assessed QoL (SF-12) following treatment of Gerovital (a multivitamin and mineral combined with Panax ginseng extract) and placebo. In addition, a between-factor repeated-measure analysis of variance (ANOVA) with a level of significance (α) of 0.05 (two sided) and power of 80% was considered, while the ratio between trial and control group was set at 1, resulting in 36 subjects per group. A 20% loss to follow-up was considered relevant, thus resulting in 45 subjects per group.

Randomisation

Stratified randomisation sequences were created with computer-generated random numbers, which allocated subjects based on sex (male/female) into two groups. Demographic stratifications based on gender were set and crossed. Patients were randomly assigned to order of treatment (placebo or active) using simple randomisation based on the atmospheric noise method and sequential assignment was used to determine group allocation (GraphPad Prism 6). A computer-generated list of random numbers was used in order to allocate participants. The results of these two randomisations were combined and assigned as the final randomisation sequence for this trial. Allocation, enrolment and assignment of participants to products were performed by the staff of Medicus Research LLC who did not perform any analyses or clinical procedures. The allocation information was disclosed to the investigator, subjects and a statistician after all measurements were completed. The investigational product was stored in a sequentially numbered Study Product Container in a locked cabinet with limited access.

Statistical analysis

The modified per-protocol analysis included subjects with at least one post-dose completed visit and participants who completed all visits of the 24-week study and

consumed the product. Subgroup analysis was performed based on gender for testosterone measurements, domains within questionnaires and age groups. The safety analysis was based on all randomised participants known to have taken at least one dose of the investigational or placebo products. Subgroup analysis of primary endpoints was performed for the age groups, 25–45 and 46–65 years, due to perceived stress from increased responsibilities in the older age group and potential hormonal variances which affect QoL in these subgroups.

All evaluations were performed using the software package R 3.2.2 (R Core Team, 2015). Descriptive statistics were calculated for each group and statistical comparisons were performed using the analysis of covariance (ANCOVA) adjusting for baseline values. Numerical endpoints that are intractably non-normal were assessed by the Mann-Whitney U test; in these instances, only the comparisons of the changes from baseline were considered in the formal testing between groups. Statistical comparisons for baseline characteristics, lipid and testosterone levels, and measures of safety (haematology, blood chemistry, anthropometrics and vital signs) were performed using ANOVA. For categorical endpoints, the differences in proportions between groups were formally tested by the Fisher's exact test. The Shapiro–Wilk normality test was carried out to determine data normality when $P > 0.05$. Within-group comparisons on numeric endpoints were made using Student's paired t -test or, in the case of intractable non-normality, the Wilcoxon signed rank test. Differences were considered significant at $P \leq 0.05$. Subgroup analysis based on gender differences was conducted for testosterone measurements only.

Results

Participant baseline characteristics

A total of 120 participants were screened and a total of 93 subjects were enrolled, of which 7 were lost to follow-up due to the long enrolment period of 6 months (Fig.1). There were 28 females and 19 males in the EL + multivitamins group (EL+MV), and 20 females and 19 males in the placebo group. The demographic characteristics of participants were not significantly different in terms of age, BMI, employment and relationship status between groups at baseline (Table 1).

More than 94% of participants in both groups were employed and were predominantly Caucasian in ethnicity. There were no significant differences in CBC, CMP and urinalysis, anthropometric measures and vital signs between groups at baseline (Table 2). Analysis of POMS-Tension-Anxiety mood state subscale showed participants to be moderately stressed.

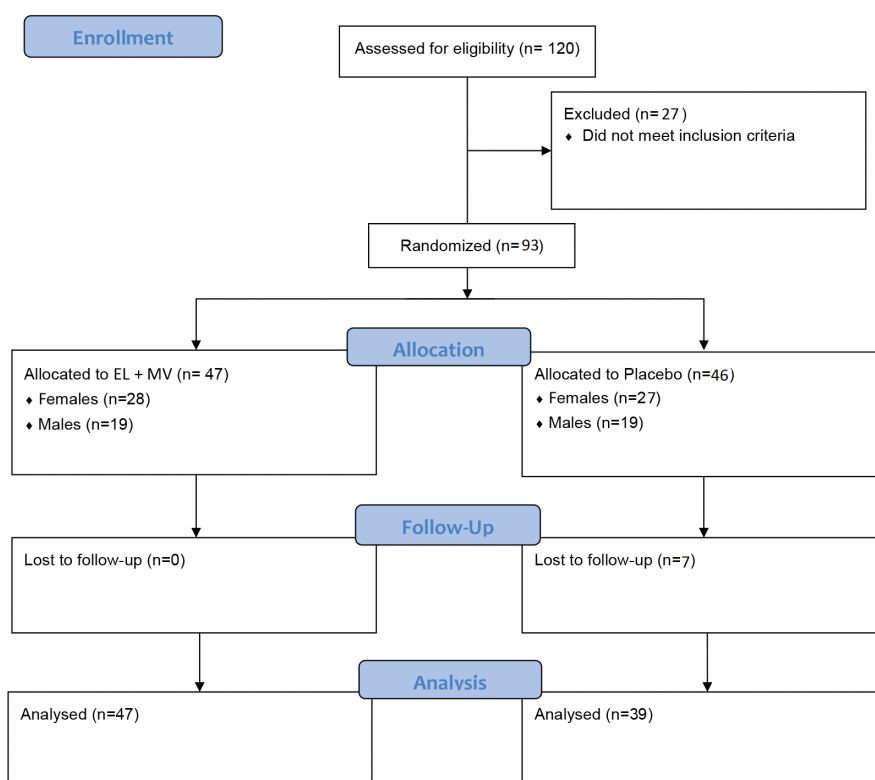


Fig. 1. Study flowchart. A total of 120 participants were screened, of which 93 were randomised in the study, with 47 in the EL+MV group and 39 in the placebo group enrolled as the modified per-protocol population in the final analysis. EL+MV, *E. longifolia* + multivitamin.

Primary endpoints

SF-12 questionnaire on QoL

POMS, SF-12 and MMSQ scores obtained by all participants in the study before and after supplementation with EL+MV group or placebo are presented in Table 3. There were no significant between-group differences reported in physical component, mental component, physical functioning, role limitations due to physical health, role limitations due to emotional health, vitality, emotional well-being, social functioning, pain and general health domains as assessed by the SF-12 questionnaire, but several within-group significant findings were observed (Table 3).

Participants supplemented with EL+MV reported significant improvements from baseline, with 9.7% improvement in role limitation due to emotional health at week 6 ($P = 0.003$) and 9.2% at week 12 ($P = 0.05$) (Fig. 2a) and a further 11.3% improvement in vitality (energy/fatigue ratio) at week 12 ($P = 0.001$) (Fig. 2b). Similar improvements from baseline were not reported by participants in the placebo group.

Participants supplemented with EL+MV reported a significant increase in the mental component domain at weeks 6 ($P = 0.001$) and 12 ($P < 0.001$), with an increase of

24.6% in the EL+MV compared to 12.7% in the placebo group at week 12. The placebo group only had significant improvements at week 6 ($P = 0.007$). In the emotional well-being domain, significant improvements were observed in both groups, with a 23% ($P < 0.001$) and 6.9% ($P < 0.01$) improvement observed at week 12, respectively, in the EL+MV and placebo groups. The social functioning domain for participants supplemented with EL+MV significantly improved by 11.3% at week 12 ($P = 0.002$) but only by 7.5% at week 6 ($P = 0.01$) in the placebo group.

A subgroup analysis of subjects based on age group 25–45 years had $n = 29$ on treatment and $n = 24$ on placebo, while age subgroup 46–65 years had $n = 18$ on treatment and $n = 12$ on placebo. Primary and secondary outcome measures of POMS, SF-12 and MMSQ revealed a 14.4% increase in the social functioning score within the SF-12 questionnaire in the 25–45-year subgroup of the EL+MV group, achieving a between-group significance ($P = 0.021$). Changes in other domains remained non-significant.

Profile of mood states questionnaire on mood

There were no significant between-group differences reported in total mood disturbance, tension, depression, anger, fatigue, confusion and vigour assessed by POMS

Table 1. Demographics and anthropometric measures of all 86 participants enrolled in the study.

	EL+MV (n = 47)	Placebo (n = 36)	P-value [§]
Age (years)			
Mean ± SD	40.6 ± 12.3	41.0 ± 9.9	0.744 [¶]
Median (min – max)	36 (25 – 62)	39.5 (25 – 62)	
Gender (n[%])			
Female	28 (60%)	18 (50%)	0.504
Male	19 (40%)	18 (50%)	
BMI (kg/m ²)			
Mean ± SD (n)	23.9 ± 3.20	25.0 ± 3.24	0.124
Median (min – max)	23.4 (18.1 – 35)	24.8 (18.3 – 31.8)	
Tobacco use (n[%])			
Current smoker	7 (16%)	4 (11%)	0.505
Non-smoker	31 (69%)	29 (81%)	
Past smoker	7 (16%)	3 (8%)	
Alcohol use (n[%])			
Current consumer	31 (67%)	22 (61%)	0.739
Non-drinker	11 (24%)	12 (33%)	
Past drinker	4 (9%)	2 (6%)	
Ethnicity (n[%])			
African-American	5 (11%)	4 (11%)	0.384
Asian	3 (6%)	2 (6%)	
Caucasian	32 (68%)	18 (51%)	
Latino/Hispanic	3 (6%)	7 (20%)	
Other	4 (9%)	4 (11%)	
Current employment (n[%])			
Employed	44 (96%)	33 (94%)	1.000
Not employed	2 (4%)	2 (6%)	
Relationship status (n[%])			
Divorced	4 (9%)	3 (8%)	0.318
Domestic partnership	1 (2%)	1 (3%)	
Married	12 (26%)	8 (22%)	
Separated	0 (0%)	4 (11%)	
Single	28 (60%)	19 (53%)	
Widowed	2 (4%)	1 (3%)	
Have children (n[%])			
No	32 (71%)	18 (50%)	0.067
Yes	13 (29%)	18 (50%)	
Systolic blood pressure (mmHg)			
Mean ± SD (n)	117.7 ± 14.3	118.4 ± 13.5	0.819
Median (min – max)	117 (91 – 154)	119 (91 – 150)	
Diastolic blood pressure (mmHg)			
Mean ± SD (n)	74.5 ± 10.6	77.0 ± 10.9	0.296
Median (min – max)	73 (50 – 105)	75 (60 – 99)	
Heart Rate (beats per minute)			
Mean ± SD (n)	66.2 ± 10.7	64.5 ± 9.5	0.468
Median (min – max)	66 (42 – 94)	65 (41 – 84)	
Body temperature (°F)			
Mean ± SD (n)	98.14 ± 0.44	98.16 ± 0.64	0.868
Median (min – max)	98.2 (97.2 – 99.8)	98.1 (96.4 – 99.6)	
Respiratory rate (per minute)			
Mean ± SD (n)	14.57 ± 1.96	14.95 ± 1.60	0.354
Median (min – max)	15 (12 – 20)	15 (12 – 18)	

[¶]Between-group comparison was made using the independent Student's *t*-test.

[§]Between-group comparisons were performed using Fisher's exact test. The variable *n* indicates the number of subjects analysed. Demographics data were not available for three participants.

Table 2. CBC and CMP safety parameters assessed in participants at all visits.

Item	Reference value	Group	Screening (Week 0)	Week 6	Week 12	Week 24
AST	7 – ≤70 U/L	EL + MV	24.8 ± 10.1	23.9 ± 7.8	29.3 ± 27.1	21.5 ± 7.9
		Placebo	25.2 ± 9.0	23.7 ± 10.2	24.3 ± 11.1	29.1 ± 36.1
ALT	12 – <90 U/L	EL + MV	21.5 ± 13.4	21.5 ± 9.4	22.9 ± 14.5	21.2 ± 16.7*
		Placebo	23.5 ± 14.9	21.1 ± 12.4*#	22.0 ± 13.5**	22.3 ± 16.2
ALP	39–117 IU/L	EL + MV	64.5 ± 19.2	63.7 ± 19.8	63.8 ± 19.1	59.2 ± 20.3
		Placebo	66.9 ± 18.9	67.1 ± 18.4	67.5 ± 17.1	66.1 ± 19.7
Total bilirubin	≤25 µmol/L	EL + MV	0.62 ± 0.36	0.53 ± 0.32	0.454 ± 0.284	0.463 ± 0.213
		Placebo	0.62 ± 0.36	0.53 ± 0.33	0.450 ± 0.244	0.474 ± 0.350
Sodium	133–148 mmol/L	EL + MV	141.18 ± 1.85	141.30 ± 2.47	140.8 ± 4.7	138.9 ± 6.5
		Placebo	141.17 ± 2.50	141.08 ± 2.20	140.8 ± 4.9	141.0 ± 2.8
Potassium	3.3–5.7 mmol/L	EL + MV	4.21 ± 0.35	4.39 ± 1.25	4.24 ± 0.37	4.20 ± 0.37
		Placebo	4.17 ± 0.27	4.24 ± 0.32	4.61 ± 1.74*	4.36 ± 0.39*
Chloride	98–115 mmol/L	EL + MV	102.48 ± 1.97	102.42 ± 2.29	101.5 ± 3.9	99.2 ± 5.7***
		Placebo	103.17 ± 2.66	102.73 ± 1.79	101.9 ± 4.1*	100.9 ± 2.8***
Carbon dioxide	18–29 mmol/L	EL + MV	26.98 ± 1.99	28.6 ± 11.3	25.4 ± 3.4*	23.43 ± 2.93***
		Placebo	26.64 ± 2.26	24.9 ± 3.9*	24.8 ± 2.8*	23.97 ± 2.65***
Anion gap	3–11 mEq/L	EL + MV	12.3 ± 3.5	13.3 ± 5.0	16.6 ± 5.6***	20.0 ± 3.3***
		Placebo	11.7 ± 3.2	14.8 ± 5.7*	17.0 ± 5.3***	19.8 ± 4.2***
Calcium	8.4–10.4 mg/dL	EL + MV	9.61 ± 0.40	9.60 ± 0.40	9.26 ± 1.58	9.04 ± 0.67***
		Placebo	9.56 ± 0.41	9.51 ± 0.41	9.47 ± 0.59	9.19 ± 0.45**
Glucose	70–109 mg/dL	EL + MV	94.9 ± 8.6	93.5 ± 9.6	95.2 ± 11.4	89.0 ± 11.6**
		Placebo	92.2 ± 10.2	93.3 ± 6.4	91.6 ± 10.5	88.5 ± 16.3
Blood urea nitrogen	8.0–20.0 mg/dL	EL + MV	13.2 ± 3.1	13.4 ± 4.4	12.8 ± 3.1	14.7 ± 11.3
		Placebo	13.4 ± 3.7	12.9 ± 4.0	12.9 ± 5.2	13.1 ± 4.1
Creatinine	0.47–0.79 mg/dL	EL + MV	0.795 ± 0.152	0.782 ± 0.147	0.777 ± 0.172	0.770 ± 0.204
		Placebo	0.794 ± 0.200	0.768 ± 0.220	0.812 ± 0.247	0.774 ± 0.192
Blood urea nitrogen: creatinine ratio	10:1 –20:1	EL + MV	17.1 ± 4.7	17.8 ± 5.3	17.1 ± 4.2	17.8 ± 4.8
		Placebo	17.6 ± 5.3	17.6 ± 5.9	16.3 ± 5.0	17.4 ± 4.9
Estimated glomerular filtration rate	50–≥120 mL/min/1.73 m ²	EL + MV	64.6 ± 13.1	69.2 ± 19.5	78.2 ± 23.2***	92.1 ± 28.2***
		Placebo	62.6 ± 9.5	74.9 ± 32.4*#	83.5 ± 30.9**	93.1 ± 23.6***
Total serum protein	6.7–8.3 g/dL	EL + MV	7.13 ± 0.37	7.09 ± 0.41	8.0 ± 6.2	6.72 ± 0.56***#
		Placebo	7.13 ± 0.47	7.02 ± 0.45	7.0 ± 0.6	7.09 ± 0.48
Serum albumin	3.5 to 5.5 g/dL	EL + MV	4.63 ± 0.29	4.60 ± 0.30	4.59 ± 0.43	4.42 ± 0.48*#
		Placebo	4.54 ± 0.34	4.56 ± 0.33	4.56 ± 0.38	4.55 ± 0.31
Globulin	2.6–4.6 g/dL	EL + MV	2.493 ± 0.277	2.49 ± 0.30	2.36 ± 0.29*	2.31 ± 0.51***#
		Placebo	2.586 ± 0.304	2.46 ± 0.35*	2.45 ± 0.33	2.53 ± 0.32
Albumin : globulin ratio	0.8–2.0	EL + MV	1.877 ± 0.251	1.875 ± 0.260	1.958 ± 0.205	1.99 ± 0.35*
		Placebo	1.778 ± 0.251	1.897 ± 0.320*#	1.894 ± 0.269*	1.83 ± 0.30
Total cholesterol	120–219 mg/dL	EL + MV	195 ± 46	194 ± 43	192 ± 43	180 ± 36*
		Placebo	184 ± 34	184 ± 41	184 ± 40	177 ± 40
Triglycerides	30–149 mg/dL	EL + MV	89 ± 52	104 ± 99	111 ± 90	91 ± 54
		Placebo	98 ± 75	111 ± 171	118 ± 110	97 ± 53
HDL cholesterol	40–95 mg/dL	EL + MV	74.8 ± 22.6	73.7 ± 23.2	72.7 ± 24.9	61.5 ± 17.9***
		Placebo	69.3 ± 20.5	67.5 ± 24.3	63.0 ± 20.9**	61.3 ± 18.7**
LDL cholesterol	65–139 mg/dL	EL + MV	102 ± 38	100 ± 41	99 ± 34	103 ± 33
		Placebo	95 ± 28	95 ± 29	97 ± 31	99 ± 28
Coronary risk factor (cholesterol : HDL)	<3.3	EL + MV	2.79 ± 0.99	2.87 ± 1.07	4.3 ± 8.6*	3.26 ± 1.18***
		Placebo	2.87 ± 1.03	3.07 ± 1.71	3.1 ± 1.1**	3.15 ± 1.06**

Table 2. Continued

Item	Reference value	Group	Screening (Week 0)	Week 6	Week 12	Week 24
VLDL cholesterol	2 to 30 mg/dL	EL + MV	17.9 ± 10.4	20.9 ± 19.7	22.1 ± 18.1	18.2 ± 10.9
		Placebo	19.5 ± 14.9	22.3 ± 34.3	23.6 ± 22.0	19.4 ± 10.6
White blood cell	3,300–9,000/ μ L	EL + MV	6.06 ± 1.65	5.60 ± 1.55*	5.57 ± 1.47*	5.88 ± 1.41
		Placebo	5.93 ± 1.86	6.10 ± 2.07	5.86 ± 1.58	5.43 ± 1.34
Red blood cell	430–570 10^4 /mL	EL + MV	4.71 ± 0.44	4.69 ± 0.49	4.64 ± 0.42*	4.63 ± 0.45*
		Placebo	4.79 ± 0.47	4.70 ± 0.46	4.70 ± 0.42	4.60 ± 0.40***
Haemoglobin	M: 13.5–17.5 g/dL	EL + MV	14.69 ± 1.29	14.58 ± 1.44	14.38 ± 1.32**	14.30 ± 1.42**
	F: 11.5–15.0 g/dL	Placebo	14.61 ± 1.45	14.40 ± 1.49	14.44 ± 1.53	13.98 ± 1.36***
Haematocrit	M: 39.7–52.4%	EL + MV	43.2 ± 3.5	43.3 ± 3.7	43.1 ± 3.4	43.0 ± 3.7
	F: 34.8–45.0%	Placebo	43.3 ± 3.6	42.8 ± 3.3	43.4 ± 3.8	42.3 ± 3.4*
Blood platelet	14.0–34.0 $\times 10^3$ /mm ³	EL + MV	248 ± 57	255 ± 61#	256 ± 80	277 ± 76**
		Placebo	227 ± 57	223 ± 50	239 ± 49*	245 ± 81*
Mean corpuscular volume	85–102 fl	EL + MV	92.1 ± 3.9	92.6 ± 4.4	92.9 ± 4.3*	93.0 ± 4.1*
		Placebo	90.7 ± 5.4	91.4 ± 5.2	92.3 ± 4.9*	90.7 ± 11.6
Mean corpuscular haemoglobin	28.0–34.0 pg	EL + MV	31.22 ± 1.38	31.11 ± 1.47	31.00 ± 1.50	30.91 ± 1.14*
		Placebo	30.57 ± 2.13	30.67 ± 2.13	30.72 ± 2.10	30.42 ± 2.02*
Mean corpuscular haemoglobin concentration	30.2–35.1%	EL + MV	33.95 ± 0.92	33.61 ± 1.12	33.39 ± 1.22*	33.24 ± 0.99***
		Placebo	33.74 ± 1.15	33.57 ± 1.43	33.26 ± 1.24*	33.01 ± 1.19***
Neutrophil count	1.6–8.0 $\times 10^9$ /L	EL + MV	55.5 ± 10.8	53.5 ± 10.9#	52.2 ± 10.6*	54.9 ± 9.5
		Placebo	56.1 ± 10.1	57.3 ± 9.8	55.8 ± 9.0	56.8 ± 7.7
Lymphocyte count	0.8–3.0 $\times 10^9$ /L	EL + MV	32.5 ± 9.2	34.6 ± 9.8	35.4 ± 9.1**	33.2 ± 8.4
		Placebo	32.6 ± 8.6	32.4 ± 9.5	32.4 ± 6.9	32.9 ± 6.6
Monocyte count	0.1–1.5 $\times 10^9$ /L	EL + MV	7.33 ± 2.01	8.00 ± 2.32	7.93 ± 1.94	8.09 ± 2.47
		Placebo	7.42 ± 1.67	7.27 ± 1.90	8.19 ± 2.72	7.65 ± 1.91
Eosinophil count	0.0–0.7 $\times 10^9$ /L	EL + MV	3.2 ± 4.0	3.08 ± 2.20	3.28 ± 2.47	3.22 ± 2.35
		Placebo	2.8 ± 3.3	2.40 ± 1.93	2.45 ± 1.97	2.25 ± 1.20
Basophil count	0.0–0.2 $\times 10^9$ /L	EL + MV	1.56 ± 0.89	1.42 ± 1.32	1.23 ± 1.76**	0.60 ± 0.54***
		Placebo	1.29 ± 0.56	1.08 ± 0.59	1.17 ± 2.30**	0.48 ± 0.46***

* $P < 0.05$, ** $P < 0.01$, *** $P < 0.001$, significant within-group differences and #significant between-group differences in *E. longifolia* + multivitamins (EL+MV) group ($n = 44$ – 47) and the placebo group ($n = 34$ – 36).

questionnaire. Within group, participants supplemented with EL+MV and placebo reported significant improvements in several of the POMS domains. An increasing trend was observed in the vigour domain of the EL+MV group at week 12.

The POMS Iceberg profile was applied to the POMS raw scores of healthy, moderately stressed population of participants in this study. Average baseline profiles showed that participants in both groups had the expected normal profiles. A normal profile consists of a peak in vigour with tension, depression, anger, fatigue and confusion making up the trough of the profile (Fig. 3). In the subgroup analysis of the POMS scores, participants between the ages of 46 and 65 years showed significant between-group improvement in vigour ($P = 0.036$) by 14.1% in the EL+MV group, observed by the mean change from weeks 0 to 12.

Secondary outcomes

Multi-modal stress questionnaire on stress

There were no significant between-group differences in self-reported total, behavioural, cognitive and physical stress by participants, as assessed by the MMSQ questionnaire (Table 3).

Significant within-group effects were observed in several domains in both groups, but only for the EL+MV group, significant reduction in physical stress was observed at week 12 ($P < 0.05$), as evidenced by a reduction of 15% compared to 0.7% in the placebo group only at week 6 ($P < 0.05$). The decrease in cognitive stress and total stress in the EL+MV group was significant ($P < 0.001$) compared to the placebo group ($P < 0.01$) at week 12.

Table 3. POMS and SF-12 MMSQ scores in all participants in the study.

	Before supplementation		P-value	After supplementation—week 6		P-value	After supplementation – week 12		P-value
	EL+MV	Placebo		EL+MV	Placebo		EL+MV	Placebo	
POMS [†]									
Tension-anxiety	8.3 ± 4.4	9.8 ± 5.7	0.289	6.6 ± 4.0**	6.8 ± 4.2***	0.909	5.4 ± 2.9 ***	6.4 ± 4.0***	0.489
Depression-dejection	8.7 ± 9.5	10.6 ± 11.5	0.892	5.7 ± 9.1**	5.6 ± 8.0**	0.821	3.5 ± 5.4***	5.2 ± 7.7*	0.427
Anger-hostility	5.1 ± 5.1	7.2 ± 8.5	0.682	3.9 ± 6.3	4.5 ± 6.3*	0.976	2.4 ± 3.5**	4.2 ± 5.8	0.162
Vigour-activity	15.0 ± 6.1	16.6 ± 6.1	0.237	15.1 ± 6.6	16.4 ± 6.1	0.453	16.3 ± 5.4	16.5 ± 5.8	0.974
Fatigue-inertia	6.2 ± 5.7	6.7 ± 5.5	0.673	5.2 ± 5.4	5.5 ± 4.7	0.634	4.2 ± 4.6*	3.2 ± 3.9***	0.268
Confusion-bewilderment	6.0 ± 4.0	7.9 ± 4.9	0.108	4.96 ± 2.88	5.19 ± 2.72**	0.521	4.63 ± 2.03	5.31 ± 3.01*	0.576
Overall mood	19 ± 27	25 ± 36	0.651	11.2 ± 27.3*	11.1 ± 25.3**	0.962	3.8 ± 18.6***	7.9 ± 23.8**	0.485
SF-12 [†]									
Physical component	56.2 ± 5.5	54.9 ± 4.8	0.294	54.1 ± 5.8*	55.1 ± 3.2	0.332	53.8 ± 4.6**	53.7 ± 5.3	0.930
Mental component	28.4 ± 11.2	32.0 ± 10.8	0.148	33.4 ± 9.9**	35.8 ± 8.6**	0.266	35.4 ± 9.4***	36.0 ± 8.9	0.749
Physical functioning	53.4 ± 7.6	52.5 ± 9.4	0.781	52.7 ± 9.3	54.7 ± 5.4	0.413	53.7 ± 6.3	54.0 ± 7.7	0.391
Role limitations-physical	28.43 ± 2.60	28.88 ± 1.98	0.444	28.84 ± 1.93	29.14 ± 1.31	0.517	28.74 ± 2.01	28.62 ± 2.18	0.817
Role limitations-emotional	18.5 ± 4.7	20.5 ± 3.9	0.044	20.3 ± 3.6**	20.9 ± 3.5	0.341	20.2 ± 4.2*	21.6 ± 2.9	0.101
Energy/fatigue	44.7 ± 11.6	48.3 ± 11.7	0.158	47.3 ± 10.6	51.2 ± 10.0	0.081	49.7 ± 10.1**	51.2 ± 10.6	0.465
Emotional well-being	34.6 ± 13.0	40.7 ± 11.6	0.274	37.5 ± 12.7**	42.8 ± 11.7*	0.429	42.7 ± 10.8***	43.5 ± 11.6**	0.797
Social functioning	46.7 ± 9.9	49.1 ± 8.9	0.284	49.5 ± 8.5	52.8 ± 6.5*	0.066	52.0 ± 6.3**	50.2 ± 8.2	0.446
Pain	54.3 ± 5.2	54.2 ± 5.4	0.966	53.2 ± 7.6	55.4 ± 4.8	0.207	53.0 ± 7.0	54.5 ± 5.3	0.404
General health	56.6 ± 5.6	56.1 ± 5.1	0.487	56.5 ± 5.5	56.1 ± 6.0	0.843	55.9 ± 5.2	54.7 ± 7.9	0.888
MMSQ [†]									
Physical stress	47.6 ± 13.6	43.8 ± 13.0	0.198	45.2 ± 13.1	43.5 ± 11.2*	0.071	40.4 ± 9.1*	40.3 ± 9.5	0.277
Behavioural stress	22.1 ± 5.5	21.6 ± 5.0	0.700	20.6 ± 5.2*	19.6 ± 3.4**	0.323	19.6 ± 4.7***	19.2 ± 4.5***	0.673
Cognitive stress	16.5 ± 6.0	14.2 ± 5.8	0.094	14.0 ± 5.4***	12.2 ± 3.9**	0.091	12.4 ± 3.7***	11.8 ± 4.2**	0.520
Overall stress	86.1 ± 23.0	79.7 ± 21.3	0.209	79.8 ± 21.4*	72.2 ± 14.6**	0.064	75.5 ± 18.0***	71.3 ± 15.7**	0.181

POMS, SF-12 and MMSQ scores are depicted as mean ± SD.

* $P \leq 0.05$, ** $P \leq 0.01$, *** $P \leq 0.001$, significant within-group difference in *E. longifolia* + multivitamins (EL+MV) ($n = 47$) and placebo group ($n = 36$).

[†]Between-group comparisons were made using ANCOVA.

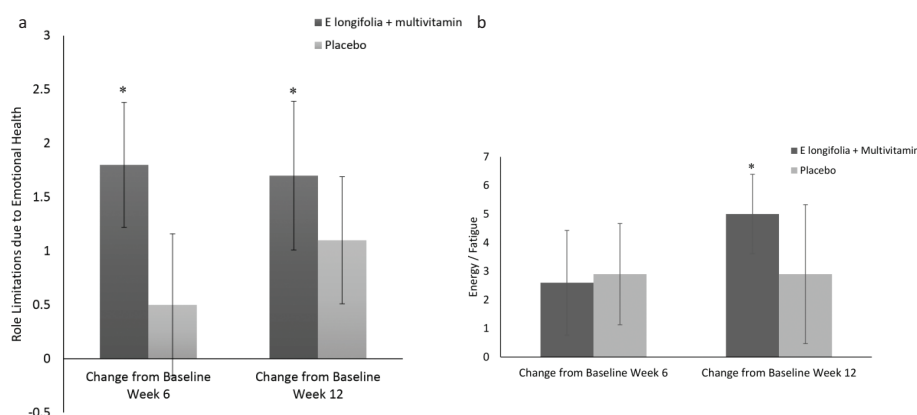


Fig. 2. (a) Changes in role limitation due to emotional health in EL+MV ($n = 46$) and placebo ($n = 35$) groups. Participants consuming *E. longifolia* + multivitamins displayed a significant improvement in role limitation due to emotional health at week 6 (9.7%; $P = 0.003$) and week 12 (9.2%; $P = 0.05$) when compared to baseline. Axes represent change in scores that numerically capture domains in the SF-12 questionnaire. Within-group comparisons were made using the paired *t*-test. Mean ± SE values. * $P \leq 0.05$. (b) Energy/fatigue ratio in EL+MV ($n = 46$) and placebo ($n = 35$) groups. Only participants consuming *E. longifolia* + multivitamins showed a significant increase (11.2%, $P = 0.001$) in their energy/fatigue ratio at week 12 when compared to baseline. Axes represent change in scores that numerically capture domains in the SF-12 questionnaire. Within-group comparisons were made using the paired *t*-test. Mean ± SE values. * $P \leq 0.05$.

Compliance

Compliance, which was assessed by counting the returned unused test product at each visit, was calculated by determining the number of dosage units taken divided by the number of dosages expected to have been taken multiplied by 100. The overall mean compliance was greater than 99% in both EL+MV and placebo groups.

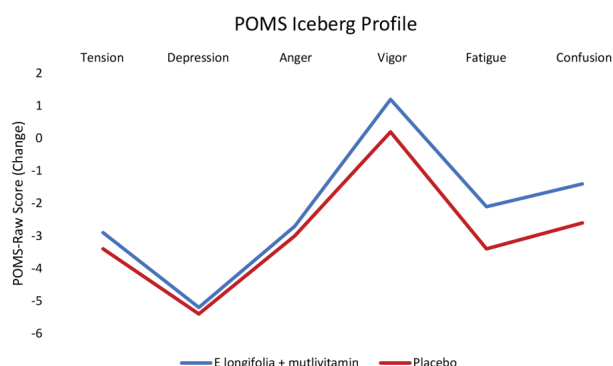


Fig. 3. Changes in POMS Iceberg profiles in EL+MV ($n = 46$) and placebo ($n = 36$) groups. Changes in POMS Iceberg profiles based on the raw POMS mood state subscales were consistent with that of healthy and active individuals in tension, depression, anger, vigour, fatigue and confusion in *E. longifolia* + multivitamins and placebo groups. Vigour activity in placebo group was reduced compared to an increase in the supplemented group. Axes represent change in scores that numerically capture domains in POMS Iceberg profile.

No participants were removed from the study due to low compliance (less than 80%).

Safety parameters

Anthropometric measures and vital signs (systolic and diastolic blood pressure, body temperature, respiratory rate and heart rate) were similar between EL+MV and placebo groups after 24 weeks of supplementation. Participants consuming EL+MV showed incidental differences in their respiratory rate at week 12 ($P = 0.03$) and mean diastolic blood pressure at week 6 ($P = 0.02$) compared to the placebo, but not at other time points (Table 1). However, all excursions were within a normal clinical reference range for the duration of the study.

Reduction in neutrophil count at week 6 ($P = 0.03$) and an increase in lymphocyte count at week 12 ($P = 0.01$) versus placebo were observed (Table 2). Mean platelet volume increased in the EL+MV at weeks 12 ($P < 0.001$) and 24 ($P < 0.001$) and in the placebo group at weeks 6 ($P = 0.03$), 12 ($P < 0.001$) and 24 ($P < 0.001$) compared to baseline, but all values remained within their normal laboratory range (Table 2).

Participants in the EL+MV group showed a decrease in glucose concentration ($P = 0.005$) and TC ($P = 0.03$) at 24 weeks compared to baseline (Table 2). Urinalysis revealed a difference in the presence of leukocyte esterase at week 6 ($P = 0.008$), with 25% of participants in the EL+MV group testing negative (Table 4). Nine per cent more participants in the placebo group tested positive

Table 4. Urinalysis of all participants in the study based on the number of subjects (n).

		Presence of leukocyte esterase (n)				Presence of calcium oxalate crystals (n)		
		EL+MV	Placebo	P-value [§]		EL+MV	Placebo	P-value [§]
Week 0 (screening)	1+	5 (11%)	1 (3%)	0.121	Few None	0 (0%)	3 (9%)	0.079
	2+	2 (4%)	0 (0%)			44	31	
	3+	1 (2%)	1 (3%)			(100%)	(91%)	
	Negative	34 (74%)	32 (94%)					
	Trace	4 (9%)	0 (0%)					
Week 6	1+	2 (5%)	0 (0%)	0.008	Few None	3 (9%)	7 (27%)	0.085
	2+	0 (0%)	2 (6%)			31	19	
	3+	2 (5%)	0 (0%)			(91%)	(73%)	
	Negative	38 (88%)	25 (76%)					
	Trace	1 (2%)	6 (18%)					
Week 12	1+	3 (7%)	2 (6%)	0.108	Few None	1 (6%)	2 (17%)	0.548
	2+	1 (2%)	1 (3%)			17	10	
	3+	1 (2%)	1 (3%)			(94%)	(83%)	
	Negative	35 (85%)	21 (66%)					
	Trace	1 (2%)	7 (22%)					
Week 24	1+	2 (5%)	0 (0%)	0.744	Few None	2 (25%)	2 (50%)	0.547
	2+	3 (7%)	2 (6%)			6	2 (50%)	
	3+	0 (0%)	0 (0%)			(75%)		
	Negative	35 (80%)	28 (88%)					
	Trace	4 (9%)	2 (6%)					

[§]Between-group analysis was made using the Fisher's exact test. $P \leq 0.05$ is statistically significant.

for the presence of calcium oxalate crystals in the urine compared to EL+MV group (Table 4).

Testosterone levels

There was no between-group significance; however, a significant time effect within group changes in testosterone levels was observed. Serum total testosterone decreased in the placebo group at week 6 compared to during screening ($P = 0.009$) (Fig. 4a). This decrease continued till weeks 12 and 24, but was not observed in the EL+MV group. In contrast, free serum testosterone levels increased in both groups ($P < 0.001$) (Fig.4b).

However, there was an increase in free testosterone levels in males supplemented with EL+MV from 1.67 ± 2.35 ng/dL at baseline to 11.4 ± 24.9 ng/dL, double the increase seen in the placebo group, from 1.4 ± 12.7 ng/dL to 6.4 ± 2.9 ng/dL (Table 5). An increase in free testosterone levels from 0.15 ± 0.3 ng/dL in the EL+MV and 0.12 ± 0.4 ng/dL in the placebo group at baseline to 1.05 ± 0.9 ng/dL and 1.3 ± 1.3 ng/dL, respectively, at week 24 was observed in female participants. There were no significant between-group differences in free testosterone levels in both genders.

Adverse events

In this clinical study, there were a total of 13 adverse events reported by 13 participants: six (urinary tract infection, blood in urine, nasal congestion, nasopharyngitis [$n = 2$] and migraine) of which were in the placebo group and 7 (food poisoning, kidney infection, fracture, influenza, vomiting, nausea and urinary tract infection) were in the EL+MV group.

Discussion

This study evaluated the efficacy and safety of EL+MV in healthy males and females with moderate stress. The

demographics of the population studied were middle class and lower middle class individuals who worked hard to sustain their families and maintain their lifestyles while juggling work-related requirements. The participants were employed and experienced self-reported job-related stress due to work responsibilities, particularly when responsibility and authority were mismatched (27).

Participants on EL+MV reported a significant improvement in their mental component domain, suggesting they felt 'calm and peaceful', emotional well-being and improvement in energy/fatigue profile after the 12-week supplementation. This supports the results of the POMS analysis with regard to the vigour activity domain, which reported an increasing trend in the EL+MV group. These results were further supported by the POMS Iceberg profiles that showed optimal peaks of vigour activity and a decrease in the negative mood clusters, contributing to the trough values of the profile in both EL+MV and placebo groups. This concept has previously been applied to assess physical activity and mood among healthy individuals (28, 29). After the 12-week supplementation, the POMS Iceberg profiles favoured an improvement in vigour among participants in the EL+MV group. Previous studies with nutritionally enriched coffee (28) and adaptation to competitive sports (30) have reported a similar shift to healthy POMS Iceberg profiles, akin to positive mood states associated with the use of multivitamins and protein supplements in other stressed populations (31). In another study, a significant improvement in mood by a reduction in tension and anxiety domain of the POMS was found ($P = 0.054$) in stressed subjects with EL supplementation (13).

Participants on EL+MV reported significant improvement in role limitation due to emotional health and in social functioning domains, suggesting an enhancement in their QoL, social interactions and related activities.

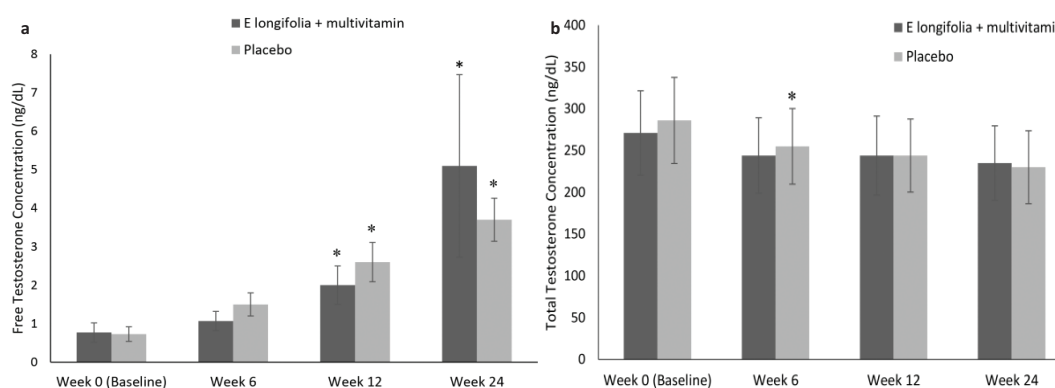


Fig. 4. (a) Serum total testosterone levels in EL+MV ($n = 44$) and placebo groups ($n = 36$). Serum total testosterone decreased significantly ($P = 0.009$) in the placebo group at week 6 compared to baseline. Within-group comparisons were made using the paired t -test. Mean \pm SE values. * $P \leq 0.05$. (b) Serum free testosterone levels in EL+MV ($n = 44$) and placebo ($n = 36$) groups. Serum free testosterone increased significantly in both groups ($P < 0.001$). Larger percentage increases were observed in the *E. longifolia* + multivitamins group. Within-group comparisons were made using the paired t -test. Mean \pm SE values. * $P \leq 0.05$.

Table 5. Mean concentrations of testosterone in female and male participants.

	EL+MV		P-value (t-test) [†]	EL+MV		P-value (t-test) [†]
	Female			Male		
	Mean ± SD (n) Within Group P-value	Mean ± SD (n) Within Group P-value		Mean ±SD (n) Within Group P-value	Mean ± SD (n) Within Group P-value	
Total testosterone concentration (ng/dL)						
Week 0 (baseline)	15.9 ± 12.7 (26)	20.5 ± 12.6 (19)	0.270	641 ± 198 (18)	582 ± 177 (17)	0.269
Week 6	18.3 ± 14.2 (26)	17.8 ± 9.6 (20)	0.723	570 ± 193 (18)	468 ± 230 (17)	0.184
	21.6 ± 22.0 (23)	29.4 ± 28.6 (17)	0.155	563 ± 189 (16)	458 ± 188 (17)	0.118
Week 24	18.6 ± 13.2 (28)	20.0 ± 13.1 (19)	0.737	573 ± 208 (18)	434 ± 154 (16)	0.070
Change from weeks 0 to 6	1.9 ± 6.5 (24) P = 0.223 [‡]	-2.9 ± 10.2 (19) P = 0.556 [‡]	0.271	-64 ± 125 (17) P = 0.058 [‡]	-124 ± 156 (15) P = 0.003 [‡]	0.246
Change from weeks 0 to 12	5.3 ± 14.0 (21) P = 0.203 [‡]	8.6 ± 33.3 (16) P = 0.660 [‡]	0.530	-74 ± 153 (16) P = 0.094 [‡]	-130 ± 152 (15) P = 0.005 [‡]	0.401
Change from weeks 0 to 24	1.9 ± 8.1 (26) P = 0.115 [‡]	± 8.5 (18) P = 0.433 [‡]	0.839	-79 ± 155 (17) P = 0.049 [‡]	-127 ± 185 (14) P = 0.017 [‡]	0.710
Free testosterone concentration (ng/dL)						
Week-0 (baseline)	0.15 ± 0.30 (26)	0.12 ± 0.44 (19)	0.239	1.67 ± 2.35 (18)	1.40 ± 1.27 (17)	0.298
Week-6	0.39 ± 0.62 (26)	0.27 ± 0.50 (20)	0.456	2.04 ± 2.19 (18)	2.95 ± 2.53 (17)	0.276
Week-12	0.85 ± 0.78 (23)	0.68 ± 1.04 (17)	0.175	3.7 ± 4.2 (16)	4.6 ± 3.1 (17)	0.231
Week-24	1.05 ± 0.89 (28)	1.36 ± 1.37 (19)	0.931	11.4 ± 24.9 (18)	6.4 ± 2.9 (16)	0.506
Change from week-0 to -6	0.16 ± 0.43 (24) P = 0.132 [‡]	0.09 ± 0.31 (19) P = 0.888 [‡]	0.304	-0.04 ± 1.72 (17) P = 0.678 [‡]	1.72 ± 2.51 (15) P = 0.030 [‡]	0.086
Change from week-0 to 12	0.62 ± 0.76 (21) P < 0.001 [‡]	0.53 ± 0.99 (16) P = 0.025 [‡]	0.249	2.0 ± 4.4 (16) P = 0.130 [‡]	3.4 ± 3.0 (15) P = 0.002 [‡]	0.151
Change from week-0 to-24	0.86 ± 0.93 (26) P < 0.001 [‡]	1.26 ± 1.34 (18) P < 0.001 [‡]	0.519	9.7 ± 25.9 (17) P = 0.005 [‡]	5.3 ± 2.9 (14) P < 0.001 [‡]	0.218

[‡]Within-group analysis was made using the Wilcoxon signed rank test. Significant within-group difference in *E. longifolia* + multivitamins (EL+MV) and placebo groups;

[†]Between-group analysis was made using the t-test. Probability values $P \leq 0.05$ are statistically significant; n = number of subjects.

A significant between-group improvement in the 25–45 years subgroup in the social functioning domain could be explained by the higher occurrence of mood and anxiety disorder generally increasing with age (30), hence the extract at a low dosage of 50 mg EL/day, not showing an intervention effect in the older subgroup, instead having an effect in the younger subgroup. In another study, EL with a dosage of 200 mg/day was reported to improve the QoL demonstrated by a reduction of 38% in aging males score (QoL) after 1-month supplementation (10). A higher dosage of EL therefore may be required to affect an older and otherwise healthy population.

The results of this study indicate that the consumption of EL+MV formulation affected the emotional health (SF-12) and vigour (POMS) of the participants. Significant between-group differences favouring the EL group in the vigour activity domain of POMS for the 46–65 years age group could be due to the physical fitness since the reduction in muscle strength in the upper and lower limbs, changes in body fat percentages and endurance increase with age and poor nutrition (31). Hence, an intervention

effect may have probably arisen from muscle and strength improvement (32, 33), anti-ageing and enhancement of vigour (13) properties of EL. In addition, participants consuming EL+MV showed a significant decrease in glucose concentrations from baseline to the end of the study, supporting its previously reported anti-hyperglycaemic properties *in vivo* (34, 35) which overall may contribute to well-being of subjects.

Improvement in mood with the highest decrease in cognitive stress subscale in the MMSQ – which is made up of several questions that include a participant's perception of 'feeling out of control', 'inability to concentrate', 'feeling no good' and a general sense of things being 'really bad' and a desire to 'run away and hide' – in participants supplemented with EL+MV is possibly due to the previously reported calming effect of EL (6), which is corroborated by animal studies demonstrating the anti-anxiolytic effects of EL (22). It was observed that there were more parents with children in the placebo group. It is surprising however that the mean for MMSQ (stress) at baseline was lower in all four domains in the placebo group in

spite of them having more children. The POMS, however, had higher baseline means in individual domains. The SF-12 had mixed baseline values where either placebo or treatment group had higher baseline values. There were no between-group differences in all domains at baseline. There were also more women in the treatment group, which may have contributed to higher mean at baseline in MMSQ compared to placebo since stress was more prevalent among women (36).

A large placebo effect as well as large standard deviations in POMS total mood disturbance and its subscales, however, perhaps contributed to the absence of between-group significance in the questionnaires tested. Furthermore, it is also plausible that the lower dose of EL (50 mg/day) used in the current formulation may not have provided the clinical benefits achieved with the higher dose (200 mg/day) used in previous studies which showed improvements in tension, anger and confusion with EL supplementation (6). A reduction in negative mood states mediated by phytochemicals has been demonstrated in numerous studies, with placebo effects ranging from 1 to 50% (37–41); therefore, the 10–12% placebo effect seen with SF-12 and MMSQ and nearly 70% in POMS in the current study is not surprising. Thus, the lower dose of EL and a substantial placebo effect exacerbated by the large statistical deviations observed in the current study may have obscured the efficacy of EL+MV. This is a challenge in clinical trials conducted on a healthy population as the effects of nutrition interventions are subtle, whereas drug trials compare exposure with no exposure, and nutrition trials compare higher and lower exposures. Everyone consumes nutrients in their diet; therefore, subtle differences may be difficult to detect and have long latency periods. Taken together, these limitations and considerations mean that it is difficult to demonstrate statistically significant benefit between groups (42). In addition, due to the lack of significant difference between groups in primary and secondary outcomes, a comparison was made in both outcomes across groups and within groups at multiple time points, and also in subgroup analyses by sex and age. This could contribute to type II error, lack of between-group statistical significance and false positives. The problem of multiple comparisons to be counteracted by, for example, Bonferroni analysis, may be considered.

Within the safety parameters, significant increase in lymphocytes similar to earlier reports (15, 43, 44) was observed. Furthermore, micronutrients contribute to the body's natural defences by supporting physical barriers (skin/mucosa), cellular immunity and antibody production. Vitamins A, B6, B12, C, D, E and folic acid and the trace elements iron, zinc, copper and selenium work in synergy to support the protective activities of the immune cells, whereby vitamins A, C, E and zinc assist in

enhancing the skin barrier function (45). Combining EL with micronutrients thus is anticipated to provide health benefits through hormonal balance and optimal nutritional requirements.

Participants in this study showed a significant decrease in neutrophils that degranulate to release proteases during pathogenesis and psychological stress (46). Stress also enhances neutrophilia and neutrophil counts (47) without concurrent increase in eosinophils or monocytes (48), which was also noted in this study. Plant extracts are known to reduce leukocyte esterase (49) and calcium oxalate crystals (50) in urine, similar to observations made in this study, which suggests fewer urinary abnormalities associated with EL+MV. It can be speculated that EL is a nutritional adaptogen (51), an agent that rejuvenates the body through restoration, which may regulate neutrophils and leukocyte esterase release. It is plausible that the EL+MV-mediated improvement in emotional health and vitality may be associated with changes in these immune parameters.

Importantly, serum total testosterone levels in the EL+MV group did not alter, while it decreased in the placebo group. The stress hormone cortisol increases under stressed states and as a result, the opposite effect is that the testosterone levels dip. It is possible through the absence of the hormone modulating effect of EL and multinutrients, the cortisol levels as a result of stress may have increased, hence causing the reduction in testosterone levels (52). However, there was an increase in free testosterone levels in males in the EL+MV group. Increase in free testosterone levels is a measure of bioavailable testosterone (53). Our results are in agreement with other studies showing a 10.3% increase in free testosterone with EL in combination of *Polygonum minus* supplementation compared to 4.3% with the placebo (54), and EL-mediated enhancement of free testosterone levels by 46.8% in subjects suffering from hypogonadism (10). A supplementation with testosterone improves mood, energy, friendliness and decreased negative mood (55). Eurypeptides, a bioactive peptide of 4.3 kDa with testosterone-modulating properties identified in EL (10), may restore normal testosterone levels by influencing the release of free testosterone from its binding hormone, sex-hormone-binding globulin, which results in improvement in QoL (10, 55). Eurypeptides enhance metabolism of pregnenolone and progesterone to yield more dehydroepiandrosterone and androstenedione (10, 44, 56) by activating the CYP17 (17 α -hydroxylase and 17,20lyase) enzyme (10). In addition, even though levels of free testosterone increased significantly from baseline in females in both groups, the increase was higher in the placebo group compared to EL+MV group, rendering it non-significant between groups. Therefore, EL+MV and the adaptogenic nature of EL may be considered safe in

women, preventing an increase in free testosterone, which is related to conditions such as hirsutism and polycystic ovary syndrome (57).

There were no significant and sustained changes from baseline or against placebo in relevant blood, liver and kidney laboratory tests. This product was well-tolerated and safe in the population studied, with no serious adverse events reported, which corroborates findings from previous randomised and controlled clinical trials evaluating EL (11). This study did not measure cortisol levels, which perhaps may have provided valuable information to understand the efficacy of EL+MV on various stress indicators and immunological parameters. This is a limitation of the study and should be considered when conducting future clinical studies.

Observational studies and clinical trials evaluating the efficacy of EL on mood, stress and testosterone levels have consistently shown favourable changes in these parameters, thereby providing a rationale for its incorporation into new formulations of multivitamins. Multivitamin supplementation enhanced mood by 15% and energy levels by 17% (58) and reduced depressive symptoms since inadequacy of key micronutrients has been associated with poor mood states (19). Therefore, it is reasonable to speculate that EL synergises health benefits exerted by multivitamins through improvement in mood states, vigour and a reduction in stress. The effect of intervention on depressed subjects could be evaluated in the future since the subjects used in this study were healthy subjects with only mid-level stress and not in a depressed state. There are differences and similarities in the way drugs affect a depressed mental state compared to the product. For example, fluoxetine (Prozac) and sertraline (Zoloft) are newer medicines that act as selective serotonin reuptake inhibitors (SSRIs). The product in this study appears to affect energy and mood levels most likely via hormonal modulation (testosterone) and nutritional supplementation, for example, vitamins B complex and C, which also affect mood (20). Vitamin B complex is involved in the metabolism of S-adenosylmethionine (SAM), a donor of methyl groups, which plays a decisive role in the functioning of the nervous system and in the formation of neurotransmitters (e.g. serotonin) (59). The target of the vitamins is similar, whereas the target of EL is different for this study. There could be a lack of intervention effect in subjects with chronic stress or depressed state; hence, one needs to be open to a more prescription-based therapy than nutritional supplementation for beyond everyday moderate stress. With unrealistic expectations to treat depression or stress related to suffering from, for example, advanced disease, there is a risk of dropping traditional medication exacerbated with a fear of potential interactions between EL and other medications. It is however noteworthy that recent research on herb-drug interaction of EL was weak and inconclusive due to

the dissimilarities between investigated solvent extract and aqueous extract of EL (60).

Conclusions

This study reports significant within-group improvements in QoL, mood and stress of moderately stressed participants supplemented with EL+MV for 12 weeks. Despite the placebo effects, participants supplemented with EL+MV reported improvements in vigour, mental component, emotional well-being, cognition and testosterone levels possibly through hormonal balance and nutritional supplementation. The stress-related changes in neutrophils and leukocyte esterase suggest the counteracting effect of EL+MV supplementation; hence, further research is warranted. Significant between-group improvements in the social functioning domain of SF-12 observed in the 25–45 years age group and vigour domain of POMS in the 46–65 years age group supplemented with EL+MV indicate the efficacy of the supplement in particular spheres of influence, particularly relating to age. EL+MV was found to be safe and well-tolerated in this 24-week supplementation study on moderately stressed participants.

Acknowledgements

The authors would like to thank the volunteers for their time and participation in the study; Ms. Sasikala Chinnappan for assisting in the data management and Dr. Joseph Antony for the statistics and editing of the manuscript.

Conflict of interest and funding

The study was funded by NKEA Research Grant Scheme (NRGS) EPP#1 under the Ministry of Agriculture and Agro Based Industry, Malaysia. Annie George is an employee of Biotropics Malaysia Berhad. The authors have no potential conflict of interest.

References

1. Liu RT, Alloy LB. Stress generation in depression: a systematic review of the empirical literature and recommendations for future study. *Clin Psychol Rev* 2010; 30(5): 582–93. doi: 10.1016/j.cpr.2010.04.010

2. Fernandes AC, Chandran D, Khondoker M, Dewey M, Shetty H, Dutta R, et al. Demographic and clinical factors associated with different antidepressant treatments: a retrospective cohort study design in a UK psychiatric healthcare setting. *BMJ Open* 2018; 8(9): e022170. doi: 10.1136/bmjopen-2018-022170
3. Schrader E. Equivalence of St John's wort extract (Ze 117) and fluoxetine: a randomized, controlled study in mild-moderate depression. *Int Clin Psychopharmacol* 2000; 15(2): 61–8. doi: 10.1097/00004850-200015020-00001
4. Edwards D, Heufelder A, Zimmermann A. Therapeutic effects and safety of *Rhodiolarosea* extract WS® 1375 in subjects with life-stress symptoms – results of an open-label study. *Phytother Res* 2012; 26(8): 1220–5. doi: 10.1002/ptr.3712
5. Kaplan BJ, Crawford SG, Field CJ, Simpson JS. Vitamins, minerals, and mood. *Psychol Bull* 2007; 133(5): 747–60. doi: 10.1037/0033-2909.133.5.747
6. Talbott SM, Talbott JA, George A, Pugh M. Effect of Tongkat Ali on stress hormones and psychological mood state in moderately stressed subjects. *J Int Soc Sports Nutr* 2013; 10(1): 28. doi: 10.1186/1550-2783-10-28
7. Wizneh FM, Asmawi MZ. *Eurycoma longifolia* jack (simarubaceae); advances in its medicinal potentials. *Pharmacognosy J* 2014; 6(4): 1–9. doi: 10.5530/pj.2014.4.1
8. Bhat R, Karim AA. Tongkat Ali (*Eurycoma longifolia* Jack): a review on its ethnobotany and pharmacological importance. *Fitoterapia* 2010; 81(7): 669–79. doi: 10.1016/j.fitote.2010.04.006
9. Goreja WG. Tongkat Ali: The tree that cures a hundred diseases. Vol. 2. New York: Amazing Herb Press, TNC International Inc.; 2004, pp. 10–11.
10. Tambi MI, Imran MK, Henkel RR. Standardised water-soluble extract of *Eurycoma longifolia*, Tongkat Ali, as testosterone booster for managing men with late-onset hypogonadism. *Andrologia* 2012; 44(Suppl 1): 226–30. doi: 10.1111/j.1439-0272.2011.01168.x
11. Ismail SB, Wan Mohammad WM, George A, Nik Hussain NH, Musthapa Kamal ZM, Liske E. Randomized clinical trial on the use of PHYSTA freeze-dried water extract of *Eurycoma longifolia* for the improvement of quality of life and sexual well-being in men. *Evid Based Complement Alternat Med* 2012; 2012: 429268. doi: 10.1155/2012/429268
12. Sambandan TG, Rha CK, Kadir AA, Aminudim N, Saad J, Mohammed M. Bioactive fraction of *Eurycoma longifolia*. [7132117 B2.]. United States Patent; 2006. <https://patents.google.com/patent/US20040087493A1/en>.
13. George A, Suzuki N, Abas AB, Mohri K, Utsuyama M, Hirokawa K, et al. Immunomodulation in middle-aged humans via the ingestion of Physta® standardized root water extract of *Eurycoma longifolia* Jack-arandomized, double-blind, placebo-controlled, parallel study. *Phytother Res* 2016; 30(4): 627–35. doi:10.1002/ptr.5571
14. Coleman CI, Hebert JH, Reddy P. The effects of Panax ginseng on quality of life. *J Clin Pharm Ther* 2003; 28(1): 5–15. <https://doi.org/10.1046/j.1365-2710.2003.00467.x>.
15. Kaneko H, Nakanishi K. Proof of the mysterious efficacy of ginseng: basic and clinical trials: clinical effects of medical ginseng, Korean red ginseng: specifically, its anti-stress action for prevention of disease. *J Pharmacol Sci* 2004; 95(2): 158–62. <https://doi.org/10.1254/jphs.FMJ04001X5>.
16. Fava M, Abraham M, Clancy-Colecchi K, Pava JA, Matthews J, Rosenbaum JF. Eating disorder symptomatology in major depression. *J Nerv Ment Dis* 1997; 185: 140–4.
17. Benton D, Cook R. The impact of selenium supplementation on mood. *Biol Psychiatry* 1991; 29(11): 1092–8. [http://dx.doi.org/10.1016/0006-3223\(91\)90251-G](http://dx.doi.org/10.1016/0006-3223(91)90251-G).
18. Kaplan BJ, Rucklidge JJ, Romijn AR, Dolph M. A randomised trial of nutrient supplements to minimise psychological stress after a natural disaster. *Psychiatry Res* 2015; 228: 373–9. doi: 10.1016/j.psychres.2015.05.080
19. Harris E, Kirk J, Rowsell R, Vitetta L, Sali A, Scholey AB, et al. The effect of multivitamin supplementation on mood and stress in healthy older men. *Hum Psychopharmacol* 2011; 26(8): 560–7. doi: 10.1002/hup.1245
20. Kennedy DO, Veasey R, Watson A, Dodd F, Jones E, Maggini S, et al. Effects of high-dose B vitamin complex with vitamin C and minerals on subjective mood and performance in healthy males. *Psychopharmacology (Berl)* 2010; 211(1): 55–68. doi: 10.1007/s00213-010-1870-3
21. Ang HH, Cheang HS. Studies on the anxiolytic activity of *Eurycoma longifolia* Jack roots in mice. *Jpn J Pharmacol* 1999; 79(4): 497–500.
22. McNair D, Lorr M, Droppleman L. Profile of Mood States (POMS). San Diego, California: Multi-Health Systems Inc.; 1992.
23. Jenkinson C, Layte R, Jenkinson D, Lawrence K, Petersen S, Paice C, et al. A shorter form health survey: can the SF-12, replicate results from the SF-36 in longitudinal studies? *J Public Health Med* 1997; 19(2): 179–86.
24. Lefebvre RC, Sandford SL. A multi-modal questionnaire for stress. *J Hum Stress* 1985; 11(2): 69–75.
25. Morgan WP, Brown DR, Raglin JS, O'Connor PJ, Ellickson KA. Psychological monitoring of overtraining and staleness. *Br J Sports Med* 1987; 21(3): 107–14.
26. Perazzo FF, Fonseca FLA, Souza GHB, Maistro EL, Rodrigues M, Jose CT, Carvalho. Double-blind clinical study of a multivitamin and polymineral complex associated with Panax ginseng extract (Gerovital®). *Open Complement Med J* 2010; 2: 100–4. doi: 10.2174/1876391X01002010100
27. Dewe PJ, O'Driscoll MP, Cooper CL. Theories of psychological stress at work. In: Gatchel RJ, Schultz IZ eds. *Handbook of occupational health and wellness*. New York: Springer Science; 2012, pp. 23–38.
28. Hoffman JR, Kang J, Ratamess NA, Jennings PF, Mangine G, Faigenbaum AD. Thermogenic effect from nutritionally enriched coffee consumption. *J Int Soc Sports Nutr* 2006; 3: 35–41. doi: 10.1186/1550-2783-3-1-35
29. Casanova N, Palmeira-de-Oliveira A, Pereira A, Crisostomo LD, Travassos B, Costa AM. Cortisol, testosterone and mood state variation during an official female football competition. *J Sports Med Phys Fitness* 2016; 56(6): 775–81.
30. Byers AL, Yaffe K, Covinsky KE, Friedman MB, Bruce ML. High occurrence of mood and anxiety disorders among older adults: The National Comorbidity Survey Replication. *Arch Gen Psychiatry* 2010; 67(5): 489–96. doi: 10.1001/archgenpsychiatry.2010.35
31. Milanović Z, Pantelić S, Trajković N, Sporiš G, Kostić R, James N. Age-related decrease in physical activity and functional fitness among elderly men and women. *Clin Interv Aging* 2013; 8: 549–56. doi:10.2147/CIA.S44112
32. Henkel RR, Wang R, Bassett SH, Chen T, Liu N, Zhu Y, et al. Tongkat Ali as a potential herbal supplement for physically active male and female seniors – a pilot study. *Phytother Res* 2014; 28(4): 544–50. doi: 10.1002/ptr.5017
33. Hamzah S, Yusof A. The ergogenic effects of *Eurycoma longifolia* Jack: a pilot study. *Br J Sports Med* 2003; 37: 465–6.

34. Husen R, Pihie AH, Nallappan M. Screening for antihyperglycaemic activity in several local herbs of Malaysia. *J Ethnopharmacol* 2004; 95(2-3): 205-8. doi: 10.1016/j.jep.2004.07.004
35. Li CH, Liao JW, Liao PL, Huang WK, Tse LS, Lin CH, et al. Evaluation of acute 13-week subchronic toxicity and genotoxicity of the powdered root of Tongkat Ali (*Eurycoma longifolia* Jack). *Evid Based Complement Alternat Med* 2013; 2013: 102987. doi: 10.1155/2013/102987
36. Chaplin TM, Hong K, Bergquist K, Sinha R. Gender differences in response to emotional stress: an assessment across subjective, behavioral, and physiological domains and relations to alcohol craving. *Alcohol Clin Exp Res* 2008; 32(7): 1242-50. doi:10.1111/j.1530-0277.2008.00679
37. Bradwejn J, Zhou Y, Koszycki D, Shlik J. A double-blind, placebo-controlled study on the effects of Gotu Kola (*Centella asiatica*) on acoustic startle response in healthy subjects. *J Clin Psychopharmacol* 2000; 20(6): 680-4.
38. Jana U, Sur TK, Maity LN, Debnath PK, Bhattacharyya D. A clinical study on the management of generalized anxiety disorder with *Centella asiatica*. *Nepal Med Coll J* 2010; 12(1): 8-11.
39. Lopresti AL, Maes M, Maker GL, Hood SD, Drummond PD. Curcumin for the treatment of major depression: a randomised, double-blind, placebo controlled study. *J Affect Disord* 2014; 167: 368-75. doi: 10.1016/j.jad.2014.06.001
40. Stojanovska L, Law C, Lai B, Chung T, Nelson K, Day S, et al. Maca reduces blood pressure and depression, in a pilot study in postmenopausal women. *Climacteric* 2015; 18(1): 69-78. doi: 10.3109/13697137.2014.929649
41. Terauchi M, Horiguchi N, Kajiyama A, Akiyoshi M, Owa Y, Kato K, et al. Effects of grape seed proanthocyanidin extract on menopausal symptoms, body composition, and cardiovascular parameters in middle-aged women: a randomized, double-blind, placebo-controlled pilot study. *Menopause* 2014; 21(9): 990-6. doi: 10.1097/GME.0000000000000200
42. Moyer MW. Nutrition: vitamins on trial. *Nature* 2014; 510(7506): 462-4. doi: 10.1038/510462a
43. Muhamad AS, Ooi FK, Chen CK. Effects of *Eurycoma longifolia* on natural killer cells and endurance running performance. *Int J Sports Sci Coach* 2015; 5(3): 93-8. doi: 10.5923/j.sports.20150503.01
44. Tambi MI. Standardized water soluble extract of *Eurycoma longifolia* maintains healthy aging in man. *Aging Male* 2007; 10: 77-87. doi: 10.1111/j.1439-0272.2011.01168.x
45. Maggini S, Wintergerst ES, Beveridge S, Hornig DH. Selected vitamins and trace elements support immune function by strengthening epithelial barriers and cellular and humoral immune responses. *Br J Nutr* 2007; 98(1): S29-35. doi: 10.1017/S0007114507832971
46. Hwang TI, Juang GD, Yeh CH, Chang YH, Chou KY, Chen HE. Hormone levels in middle-aged and elderly men with and without erectile dysfunction in Taiwan. *Int J Impot Res* 2006; 18(2): 160-3. doi: 10.1038/sj.ijir.3901382.
47. Nishitani N, Sakakibara H. Association of psychological stress response of fatigue with white blood cell count in male daytime workers. *Ind Health* 2014; 52(6): 531-4. doi: 10.2486/indhealth.2013-0045
48. Darko DF, Rose J, Gillin JC, Golshan S, Baird SM. Neutrophilia and lymphopenia in major mood disorders. *Psychiatry Res* 1988; 25(3): 243-51.
49. Vicariotto F. Effectiveness of an association of a cranberry dry extract, D-mannose, and the two microorganisms *Lactobacillus plantarum* LP01 and *Lactobacillus paracasei* LPC09 in women affected by cystitis: a pilot study. *J Clin Gastroenterol* 2014; 48(Suppl 1): S96-101. doi: 10.1097/MCG.0000000000000224
50. Bashir S, Gilani AH. Antiuro lithic effect of *Berberis ligulata* rhizome: an explanation of the underlying mechanisms. *J Ethnopharmacol* 2009; 122(1): 106-16. doi: 10.1016/j.jep.2008.12.004
51. Thu HE, Mohamed IN, Hussain Z, Jayusman PA, Shuid AN. *Eurycoma longifolia* as a potential adoptogen of male sexual health: a systematic review on clinical studies. *Chin J Nat Med* 2017; 15(1): 0071-80. doi: 10.1016/S1875-5364(17)30010-9
52. Sherman GD, Lerner JS, Josephs RA, Renshon J, Gross JJ. The interaction of testosterone and cortisol is associated with attained status in male executives. *J Pers Soc Psychol* 2016; 110(6): 921-9. doi: 10.1037/pspp0000063
53. Speroff L, Glass RH, Kase NG. Clinical gynecologic endocrinology and infertility. 5th edn. Baltimore, MD: Lippincott, Williams and Wilkins; 1994.
54. Udani JK, George AA, Musthapa M, Pakdaman MN, Abas A. Effects of a proprietary freeze-dried water extract of *Eurycoma longifolia* (Physta) and *Polygonum minus* on sexual performance and well-being in men: arandomized, double-blind, placebo-controlled study. *Evid Based Complement Alternat Med* 2014; 2014: 179529. doi: 10.1155/2014/179529
55. Bain J. The many faces of testosterone. *Clin Interv Aging* 2007; 2(4): 567-76.
56. Tambi MI, Imran MK. *Eurycoma longifolia* Jack in managing idiopathic male infertility. *Asian J Androl* 2010; 12(3): 376-80. doi: 10.1038/aja.2010.7
57. Manni A, Pardridge WM, Cefalu W, Nisula BC, Bardin CW, Santner SJ, et al. Bioavailability of albumin-bound testosterone. *J Clin Endocrinol Metab* 1985; 61(4): 705-10. doi: 10.1210/jcem-61-4-705
58. Sarris J, Cox KH, Camfield DA, Scholey A, Stough C, Fogg E, et al. Participant experiences from chronic administration of a multivitamin versus placebo on subjective health and wellbeing: a double-blind qualitative analysis of a randomised controlled trial. *Nutr J* 2012; 11: 110. doi: 10.1186/1475-2891-11-110
59. Karakuła H, Opolska A, Kowal A, Domański M, Płotka A, Perzyński J. [Does diet affect our mood? The significance of folic acid and homocysteine]. *Pol Merkur Lekarski* 2009; 26(152): 136-41.
60. Young MH, In SK, Rehman SU, Choe K, Yoo HH. *In vitro* evaluation of the effects of *Eurycoma longifolia* extract on CYP-mediated drug metabolism. *Evid Based Complement Alternat Med* 2015; 2015: 631329. doi: 10.1155/2015/631329

***Dr. Ashril Yusof**

Exercise Science, Sports Centre, University of Malaya,
50603 Kuala Lumpur, Malaysia.
Email: ashрил@um.edu.my

Rice bran triterpenoids improve postprandial hyperglycemia in healthy male adults

Koichi Misawa^{1*}, Hiroko Jokura² and Akira Shimotoyodome³

¹Biological Science Laboratories, Kao Corporation, Ichikai-machi, Haga-gun, Tochigi, Japan; ²Lifestyle Research Center, Kao Corporation, Tokyo, Japan; ³Health Care Food Research Laboratories, Kao Corporation, Tokyo, Japan

Abstract

Background: Compared to white rice, brown rice induces a lower glyceic response in healthy and diabetic humans. This effect is partly attributed to the higher amounts of water- or oil-soluble bran components and dietary fiber in brown rice. We hypothesized that dietary supplementation with oil-soluble rice bran triterpenoids (RBTs; triterpene alcohol and sterol prepared from rice bran) might reduce the incidence of postprandial hyperglycemia in healthy humans.

Objective: We examined the acute effects of a single RBT-supplemented meal on the postprandial blood glucose responses of healthy male adults in a double-blind, randomized, placebo-controlled, crossover trial.

Design: Nineteen subjects consumed a test meal containing either placebo- or RBT-supplemented olive oil. Blood biomarkers were evaluated in a fasting state and up to 240 min postprandially.

Results: Compared to the placebo-supplemented meal, the RBT-supplemented meal significantly suppressed the increase in postprandial blood glucose level. A subclass analysis revealed that RBT-supplemented oil significantly reduced blood glucose increases in subjects with higher postprandial blood glucose elevations. Postprandial increases in blood insulin, glucose-dependent insulinotropic peptide (GIP), and glucagon-like peptide-1 (GLP-1) levels did not differ between the groups.

Conclusion: These results suggest that RBT consumption improves postprandial hyperglycemia in healthy humans, especially those with higher postprandial glucose increases.

Keywords: *blood glucose; GIP; GLP-1; insulin; metabolism*

Diabetes, a condition that results from impaired insulin secretion or insulin resistance, is currently a health problem worldwide. Global statistics suggest that 425 million people were living with diabetes in 2017 and predict that this number will exceed 629 million by 2045 (1). Hyperglycemia is a major risk factor for both microvascular and macrovascular complications (2, 3). Recent epidemiological studies indicated an association between isolated postprandial hyperglycemia and increased cardiovascular mortality (4–6). Therefore, lifestyle changes that ameliorate/prevent postprandial hyperglycemia, and particularly dietary changes, are recommended as primary preventive and treatment measures. Accordingly, the demand for food components that can prevent/mitigate postprandial hyperglycemia in diabetic, pre-diabetic, and healthy humans has increased.

For thousands of years, rice has been consumed as a staple food in Asian countries. Unpolished brown rice

contains various nutrients in the germ and bran layers, which are removed during the production of white rice. Recent increases in the incidence rates of diabetes and other relevant diseases have led to increased interest in brown rice and its components as natural foods with significant health benefits. Rice bran contains nutrients such as minerals, fiber, fatty acids, and oil-soluble nutraceuticals (7). Triterpene alcohols, plant sterols, and their ferulic acid esters (γ -oryzanol), which exhibit hypocholesterolemic (8), antioxidant (9), anti-inflammatory (10), anti-carcinogenic (11), and other effects, are characteristic components of rice bran oil.

We previously demonstrated that rice bran triterpenoids (RBTs; triterpene alcohol and sterol prepared from rice bran) lowered postprandial blood glucose (12) and increased glucose-dependent insulinotropic peptide (GIP) (13) levels in mice. GIP is a gut hormone secreted from enteroendocrine K cells into the bloodstream after

food consumption (14). Dietary carbohydrates and fats are major secretagogues for postprandial blood GIP responses (14). Our previous study suggested that cycloartenol, a major triterpene alcohol derived from RBTs, reduced postprandial intestinal glucose absorption by suppressing the translocation of sodium-glucose cotransporter-1 (SGLT1) to the apical plasma membranes of intestinal epithelial cells (12).

Compared to milled rice, brown rice induces lower glycemic responses in healthy and diabetic humans. This effect is partly attributed to the relatively higher amounts of water-soluble rice bran components (phytic acid and polyphenols), dietary fiber, and oil in brown rice (15). However, the acute effects of rice bran-derived oil-soluble components on postprandial blood glucose response remain to be clarified.

Against this background, we hypothesized that dietary supplementation with RBTs might reduce postprandial hyperglycemia in healthy humans. To test this hypothesis, we examined the acute effects of a single RBT-supplemented meal on the postprandial blood glucose responses of healthy male adults in a double-blind, randomized, placebo-controlled, crossover trial.

Materials and methods

Materials

Commercially available food-grade RBTs (Oryza triterpenoid – PK) were purchased from the Oryza Oil & Fat Chemical Company (Aichi, Japan). The triterpenoid composition was determined using gas chromatography (Agilent 6890N series GC System; Agilent Technologies Inc., Santa Clara, CA, USA). This composition included cycloartenol, 24-methylene cycloartenol, β -sitosterol, and campesterol in mass ratios of 57/38/1/2% (w/w) (Lot Q-404). Rice (Sato No Gohan®; energy 294 kcal, carbohydrate 67.8 g, protein 4.2 g, fat 0 g) was obtained from Sato Foods (Niigata, Japan).

Subjects

Twenty of the 56 men initially recruited for eligibility screening were enrolled and 19 subjects aged 37–56 years were analyzed in this study (Fig. 1). The subjects were required to meet the following inclusion criteria: male sex, body mass index (BMI) between 20 and 28 kg/m², systolic blood pressure \leq 139 mmHg and diastolic blood pressure \leq 89 mmHg, and blood triglyceride (TG) concentration between 50 and 149 mg/dL. The main exclusion criteria were as follows: chronic pharmaceutical intake; diagnosed heart, liver, kidney, gastrointestinal, or infectious disease; diagnosed food allergy; smoking habit; alcohol abuse; and simultaneous participation in another study. The study interventions were conducted at the Osaki Hospital Tokyo Heart Center (Tokyo, Japan).

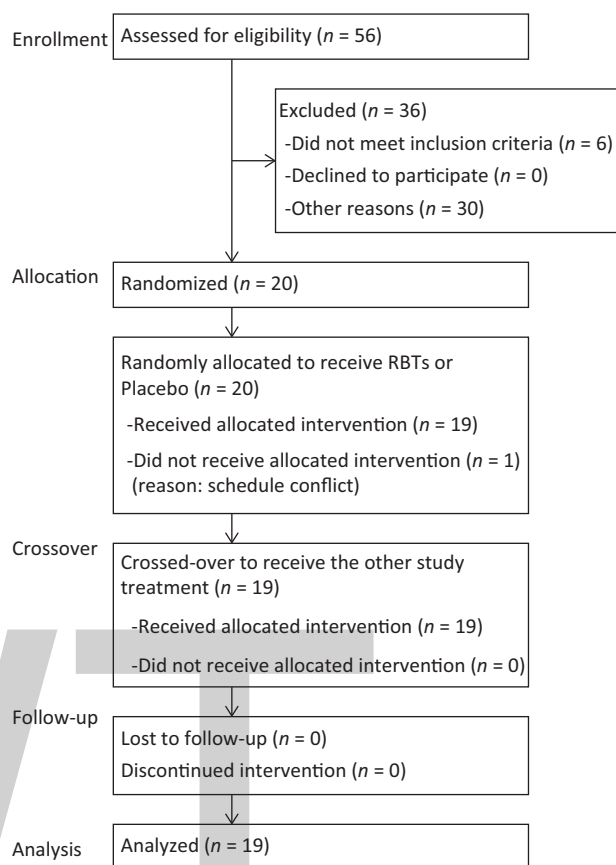


Fig. 1. Flow chart of the study and numbers of study participants from screening to study completion. RBTs, rice bran triterpenoids.

We calculated the sample size based on data from a preliminary pilot study. The previous data indicated that the differences in the responses of matched pairs were normally distributed, with a standard deviation of 15. Accordingly, if the true difference in the mean responses of matched pairs was 10, we would need to study 20 pairs of subjects to be able to reject the null hypothesis of a response difference of zero, with a probability (power) of 0.8. A 0.05 probability of a type I error was associated with the test of this null hypothesis.

The Human Ethics Committee of Kao Corporation approved the study protocol. All subjects provided written informed consent. The study was conducted under the supervision of the chief investigator in accordance with the tenets of the Declaration of Helsinki. The trial was registered at UMIN Clinical Trials Registry (UMIN000017447; preregistered on May 7, 2015).

Methods

Study design and diet

We examined the acute effects of the ingestion of a single meal containing RBT-supplemented olive oil on

blood glucose levels in a double-blind, randomized, placebo-controlled, crossover trial with a washout period of 7 days. After an overnight fasting period of at least 10 h, fasting blood samples (baseline) were collected. Subsequently, the subjects were requested to consume the assigned meals. Blood samples were also collected at 0.5, 1, 2, 3, and 4 h after the beginning of the meal consumption. The subjects were not allowed to consume any food or beverages for 4 h after meal intake, except for 200 mL of mineral water at the 2-h time point. The subjects consumed one of the following two meals: 1) placebo (200 g of cooked rice containing 11 g of olive oil) or 2) RBTs (200 g of cooked rice containing 11 g of olive oil supplemented with 16.5 mg of RBTs).

Blood sampling and analysis

Blood samples were obtained from the antecubital vein. Blood glucose levels were measured using a self-monitoring device (ACCU-CHEK COMFORT, Roche Diagnostics, Basel, Switzerland) immediately. At each time point, approximately 5 mL of blood was collected into Venoject® II vacuum tubes (Terumo, Tokyo, Japan) and centrifuged at 3,000 g for 15 min at ambient temperature. Serum samples were collected and stored at -80°C until analysis. In addition, 2 mL of blood was collected into BD Vacutainer™ plastic blood collection tubes containing EDTA 2K (Becton, Dickinson and Company, Franklin Lakes, NJ, USA) for plasma preparation. After adding a protease inhibitor (Protease Inhibitor Cocktail powder, P2714-1BTL, Sigma, St. Louis, MO, USA) and serine protease inhibitor (Pefabloc, Roche Diagnostics, Basel, Switzerland), the blood samples were centrifuged at 2,900 g for 10 min at ambient temperature. The resulting plasma samples were stored at -80°C until analysis. The blood concentrations of TG, total cholesterol, high-density and low-density lipoprotein cholesterol, aspartate transaminase (AST), alanine transaminase (ALT), and lactate dehydrogenase (LD) were measured using an automatic blood analyzer (ACCUTE TBA-40FR, Toshiba Co., Tokyo, Japan) and compatible reagents (Nittobo, Tokyo, Japan). Enzyme-linked immunosorbent assays were used to measure the blood concentrations of insulin (Merckodia, Sweden), active glucagon-like peptide-1 (GLP-1) (Millipore, Bedford, MA, USA), and GIP (Millipore). The homeostatic model assessment of insulin resistance (HOMA-IR) was calculated as the product of the fasting serum insulin concentration (in mU/L) and glucose concentration (in mg/dL), divided by 405.

Statistical analysis

Numerical data are expressed as means and standard deviations. A preliminary *F*-test of within-group variance homogeneity followed by Student's *t*-test or a paired *t*-test was used when comparing values between the groups. A

two-way repeated analysis of variance (ANOVA), followed by Bonferroni's post hoc test, was used to compare changes over time and between the groups. Differences were considered significant when the error probability was <0.05 . All statistical analyses were performed using GraphPad Prism 6 (GraphPad Software, La Jolla, CA, USA).

Results

Subject characteristics

The study participants were all male, with a mean age of 48.6 (standard deviation, SD: 5.8) years and a mean BMI of 25.4 (SD: 2.3) kg/m^2 (Table 1). The concentrations of the blood parameters before each meal (in the fasting state) are presented in Table 2. There were no significant differences in these parameters between the test meal groups.

Effects of RBTs on postprandial blood glucose levels

The overall postprandial blood glucose responses tended to be lower ($P = 0.087$) after the RBT-supplemented meal relative to the placebo meal (Fig. 2a). The postprandial increases in blood glucose levels (area under the curve, AUC 0–1 h [$P = 0.042$], AUC 0–2 h [$P = 0.014$], or AUC 0–3 h [$P = 0.012$]) were significantly lower in subjects who consumed the RBT-supplemented meal, compared to the placebo meal (Table 3). No significant differences were observed in the postprandial blood insulin (Fig. 2b), GLP-1 (Fig. 2c), and GIP responses (Fig. 2d).

A subclass analysis of subjects ($n = 8$) with higher postprandial incremental blood glucose levels at 2 h after placebo meal ingestion (>32.8 mg/dL, the average of all subjects) showed significantly lower overall postprandial blood glucose levels ($P = 0.003$; Fig. 3a) and postprandial increases in blood glucose levels (AUC 0–1 h [$P = 0.014$], AUC 0–2 h [$P = 0.002$], AUC 0–3 h [$P < 0.001$], or AUC 0–4 h [$P < 0.001$]; Table 4) after consumption of the RBT-supplemented meal relative to the placebo meal. The fasting concentrations of blood variables did not differ between the placebo and RBT groups or between subjects with higher and lower postprandial glucose levels (Table 5).

Table 1. Baseline demographic and anthropometric characteristics of the study subjects (mean values and standard deviation)

Index	Subjects ($n = 19$)	
	Mean	Standard deviation
Age (years)	48.6	5.8
Height (m)	1.71	0.05
Weight (kg)	74.9	8.5
Body mass index (kg/m^2)	25.4	2.3
% Body fat	22.1	3.6

Table 2. Concentrations of blood biomarkers obtained in the fasting state among the study subjects (mean values and standard deviation)

Index	Placebo (n = 19)		Rice bran triterpenoids (n = 19)	
	Mean	Standard deviation	Mean	Standard deviation
Glucose (mg/dL)	95.9	15.5	96.1	12.0
Insulin (mU/L)	5.95	3.06	5.76	2.80
Homeostasis model assessment of insulin resistance	1.39	0.74	1.37	0.69
Glucagon-like peptide I (pM)	3.48	11.43	1.40	3.19
Glucose-dependent insulinotropic polypeptide, (pg/mL)	64.8	34.5	55.9	26.0
Triglyceride (mg/dL)	145.7	78.2	154.2	75.5
Total cholesterol (mg/dL)	196.9	24.2	201.6	27.7
LDL-cholesterol (mg/dL)	118.2	17.5	126.1	17.6
HDL-cholesterol (mg/dL)	49.8	8.3	49.7	8.0
Aspartate aminotransferase (U/L)	23.5	9.4	23.5	10.3
Alanine aminotransferase (U/L)	29.8	19.1	31.1	21.1
Lactate dehydrogenase (U/L)	185.8	23.5	182.6	23.7

Note: There were no significant differences in the baseline variables between the test meal groups.

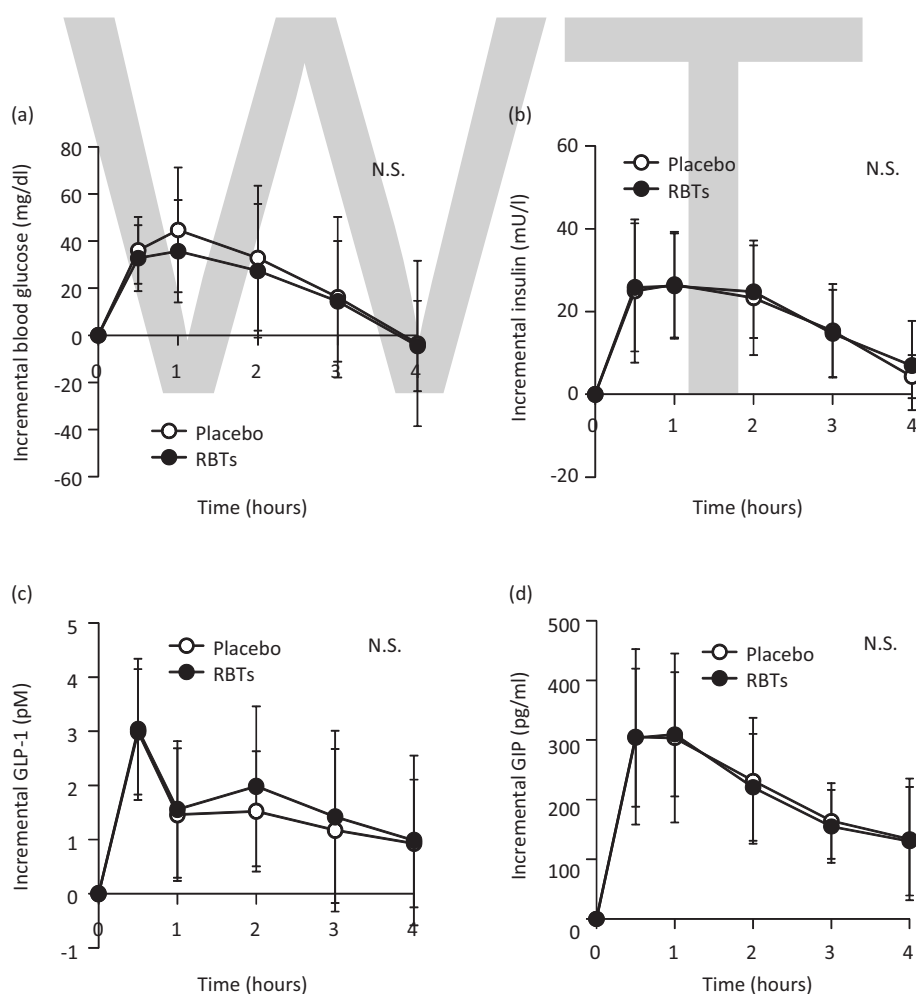


Fig. 2. Postprandial changes in blood variables after the consumption of rice bran triterpenoids (RBTs). Blood glucose (a), insulin (b), active glucagon-like peptide-1 (GLP-1) (c), and total glucose-dependent insulinotropic polypeptide (GIP) (d) after the consumption of placebo (\circ , $n = 19$) and RBTs (\bullet , $n = 19$). Data are expressed as means and standard deviations, which are represented by vertical bars. A two-way repeated analysis of variance was used to compare changes over time and between the groups.

Table 3. Postprandial area under the curves for blood glucose concentration (mean values and standard deviations)

	Placebo (n = 19)		Rice bran triterpenoids (n = 19)		P
	Mean	Standard deviation	Mean	Standard deviation	
AUC _{0-1 h}	29.2	11.9	25.3	10.4	0.042
AUC _{0-2 h}	68.0	38.2	56.8	32.8	0.014
AUC _{0-3 h}	92.4	66.3	77.7	57.8	0.012
AUC _{0-4 h}	98.8	92.5	82.6	75.7	0.059

No significant differences were observed in the blood insulin (Fig. 3b), GLP-1 (Fig. 3c), and GIP responses (Fig. 3d). Among subjects ($n = 11$) with lower postprandial incremental blood glucose levels, all blood variables remained similar between the meal groups (Fig. 3e-h; Table 4).

Discussion

This study indicates that the consumption of RBT-supplemented oil significantly decreases the postprandial increase in blood glucose levels in healthy male subjects,

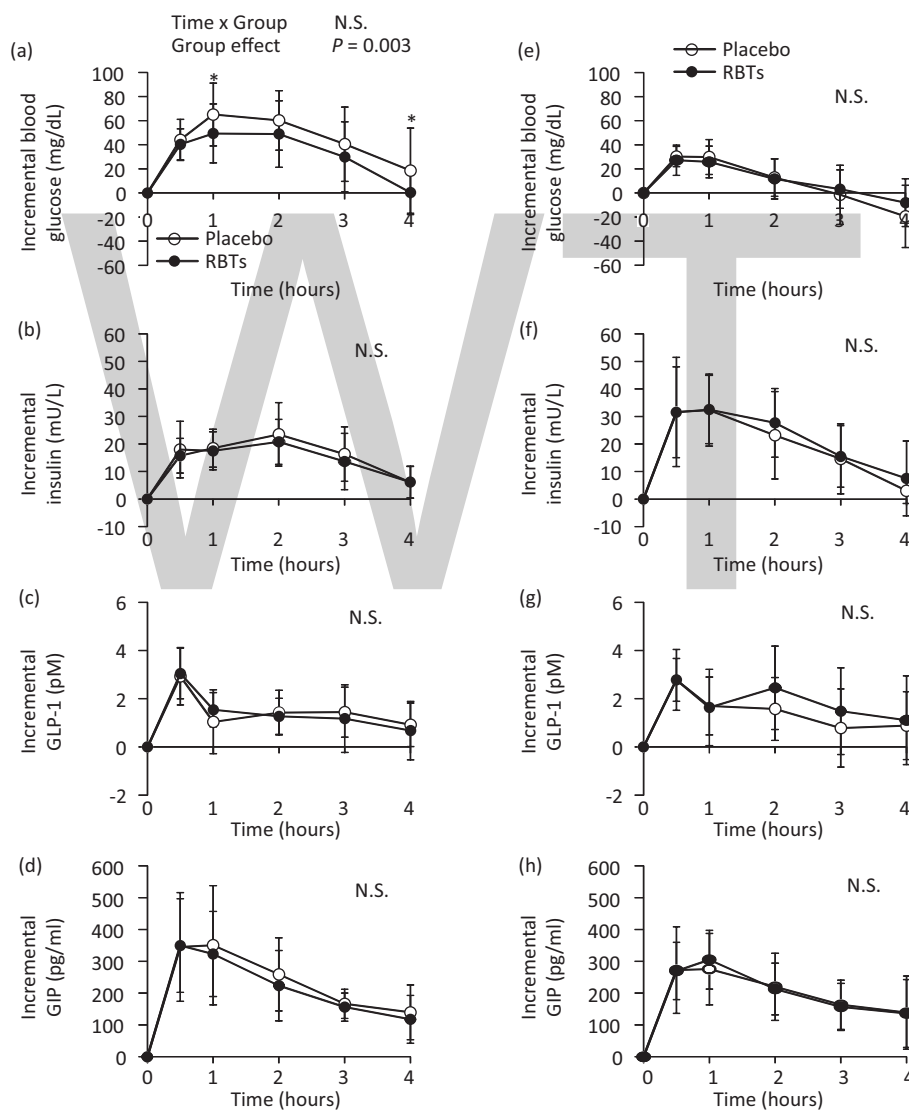


Fig. 3. Postprandial changes in blood variables after rice bran triterpenoid (RBT) consumption in subjects with higher (a-d, $n = 8$) and lower (e-h, $n = 11$) postprandial incremental blood glucose levels at 2 h. Blood glucose (a, e), insulin (b, f), active glucagon-like peptide-1 (GLP-1) (c, g), and glucose-dependent insulinotropic polypeptide (GIP) (d, h) after the consumption of placebo (○) and RBTs (●) in subgroups comprising subjects with higher (>32.8 mg/dL; i.e. average of all subjects) or lower (<32.8 mg/dL) postprandial incremental blood glucose levels at 2 h after the placebo meal. Data are expressed as means and standard deviations, which are represented by vertical bars. A two-way repeated analysis of variance was used to compare changes over time and between the groups. Asterisks indicate the probability of random differences between groups: * $P < 0.05$ indicates a significant difference between groups (Bonferroni test).

Table 4. Postprandial area under the curves for blood glucose concentration in subjects with higher and lower postprandial glucose levels (mean values and standard deviations)

	Higher glucose level group (n = 8)					Lower glucose level group (n = 11)				
	Placebo		Rice bran triterpenoids		P	Placebo		Rice bran triterpenoids		P
	Mean	Standard deviation	Mean	Standard deviation		Mean	Standard deviation	Mean	Standard deviation	
AUC _{0-1 h}	38.3	11.2	32.5	10.9	0.014	22.6	7.4	20.0	6.1	NS
AUC _{0-2 h}	101.0	33.0	81.7	35.3	0.002	43.9	19.0	38.8	14.4	NS
AUC _{0-3 h}	151.4	56.4	121.1	60.7	<0.001	49.6	29.9	46.2	28.8	NS
AUC _{0-4 h}	180.9	72.1	136.2	78.8	<0.001	39.1	49.6	43.7	44.7	NS

NS, not significant.

Table 5. Concentrations of blood variables obtained in the fasting state among subjects with higher and lower postprandial glucose levels (mean values and standard deviation)

	Higher glucose level group (n = 8)				Lower glucose level group (n = 11)			
	Placebo		Rice bran triterpenoids		Placebo		Rice bran triterpenoids	
	Mean	Standard deviation	Mean	Standard deviation	Mean	Standard deviation	Mean	Standard deviation
Glucose (mg/dL)	96.0	9.9	97.5	12.2	95.7	19.0	95.1	12.3
Insulin (U/L)	5.23	1.97	4.96	1.24	6.47	3.67	6.34	3.49
Homeostasis model assessment of insulin resistance	1.21	0.43	1.18	0.31	1.52	0.90	1.51	0.86
Glucagon-like peptide I (pM)	0.67	0.79	0.52	0.59	5.51	14.97	2.04	4.13
Glucose-dependent insulinotropic polypeptide (pg/mL)	60.1	23.5	57.8	24.3	68.3	41.6	54.5	28.2
Triglyceride (mg/dL)	200.4	92.1	201.5	77.3	106.0	30.6	119.8	54.6
Total cholesterol (mg/dL)	214.9	16.6	217.5	26.2	183.8	20.3	190.1	23.4
LDL-cholesterol (mg/dL)	126.6	13.2	132.9	16.3	112.0	18.1	121.1	17.5
HDL-cholesterol (mg/dL)	51.7	9.8	51.7	10.3	48.4	7.1	48.2	6.0
Aspartate aminotransferase (U/L)	23.4	10.0	25.6	9.5	23.6	9.5	21.9	11.0
Alanine aminotransferase (U/L)	29.1	16.5	32.6	20.2	30.3	21.5	30.0	22.7
Lactate dehydrogenase (U/L)	191.4	22.6	188.0	21.0	181.7	24.3	178.6	25.8

Note: There were no significant differences in baseline variables between the test meal groups.

especially those with elevated postprandial hyperglycemia. Thirteen of the 19 subjects exhibited mitigated blood glucose increases after consuming RBT-supplemented oil, compared with the placebo. This finding supports our hypothesis that dietary RBT supplementation reduces postprandial hyperglycemia in healthy humans.

To our knowledge, this study is the first to report that the consumption of dietary oil supplemented with RBTs (16.5 mg, equivalent to approximately 3.7 g of rice bran) reduced the postprandial increase in the blood glucose level by >15%, compared with the control group, during a 240-min period after meal consumption; however, both groups maintained similar postprandial insulin responses. Our results, therefore, contradict the general perception that a decreased blood glucose response leads

to a decreased postprandial insulin response. This contradiction might be explained by the finding that RBTs did not decrease the magnitude of the initial blood glucose increase, which may determine the initial release of insulin from pancreatic β cells. In fact, the increases in blood glucose levels during the first 30 min after meal ingestion were similar between the RBT and control groups. Accordingly, the consumption of RBTs is likely to reduce glucose levels beginning at 60 min after ingestion.

Our subclass analysis of subjects with elevated postprandial blood glucose responses also showed that the postprandial blood glucose response was significantly reduced by RBT consumption. Accordingly, dietary RBTs are likely to be effective even in subjects with impaired glucose tolerance or patients with diabetes.

Although RBT consumption significantly improved postprandial hyperglycemia, the postprandial GIP response was not affected. These results were inconsistent with our previous finding that RBTs reduced the high-fat diet-induced GIP response in mice (13). The reason for this difference remains unclear, but may be related to differences in the macronutrient compositions of the test meals. The carbohydrate:fat ratio of the test meal was 2:1 in our previous study (13), but was 20:1.1 (200 g of cooked rice with 11 g of olive oil) in the present study. Dietary fat is a more potent GIP secretagogue, compared to dietary carbohydrates. However, further studies are needed to clarify the discrepant findings that RBTs reduced the postprandial blood glucose response but not the GIP response after consuming a high-carbohydrate meal.

The major weakness of this study was the small sample size, particularly regarding subjects with higher postprandial blood glucose responses. Accordingly, it remains unclear whether consumption of the RBT-supplemented oil improved postprandial hyperglycemia. Further studies with larger sample sizes are warranted to clarify whether the consumption of RBT-supplemented oil could improve impaired glucose tolerance.

Conclusion

In conclusion, the consumption of RBT-supplemented oil improved postprandial hyperglycemia in healthy human male subjects, especially those with higher postprandial increases in glucose levels. The consumption of oil-soluble RBTs might, therefore, benefit postprandial glycemic control. Further studies are needed to clarify the beneficial actions of RBTs in subjects with impaired glucose tolerance or patients with diabetes.

Acknowledgements

We are very grateful to Kentaro Okamoto, MD, of Dokkyo Medical University for supervising this clinical study. All the authors are employees of the Kao Corporation. The present study was supported financially by the Kao Corporation.

Conflict of interest and funding

The authors declare that they have no conflicts of interest. The authors have not received any funding or benefits from industry or elsewhere to conduct this study.

References

- International Diabetes Federation. IDF Diabetes Atlas –8th edn. 2017. Available from: <http://www.diabetesatlas.org/>
- Brown A, Reynolds LR, Bruemmer D. Intensive glycemic control and cardiovascular disease: an update. *Nat Rev Cardiol* 2010;7:369–75. doi: 10.1038/nrcardio.2010.35
- Mannucci E, Monami M, Lamanna C, Adalsteinsson JE. Post-prandial glucose and diabetic complications: systematic review of observational studies. *Acta Diabetol* 2012;49:307–14. doi: 10.1007/s00592-011-0355-0
- Pillarsetti S. Potential drug combinations to reduce cardiovascular disease burden in diabetes. *Trends Pharmacol Sci* 2016;37:207–19. doi: 10.1016/j.tips.2015.11.009
- Takao T, Suka M, Yanagisawa H, Iwamoto Y. Impact of postprandial hyperglycemia at clinic visits on the incidence of cardiovascular events and all-cause mortality in patients with type 2 diabetes. *J Diabetes Investig* 2017;8:600–8. doi: 10.1111/jdi.12610
- Suades R, Cosentino F, Badimon L. Glucose-lowering treatment in cardiovascular and peripheral artery disease. *Curr Opin Pharmacol* 2018;39:86–98. doi: 10.1016/j.coph.2018.03.001
- Cicero AFG, Derosa G. Rice bran and its main components: potential role in the management of coronary risk factors. *Curr Top Nutraceutical Res* 2005;3:29–46. Available from: <http://www.nchpjournals.com/journals/manuscript.php?msid=880>
- Rong N, Ausman LM, Nicolosi RJ. Oryzanol decreases cholesterol absorption and aortic fatty streaks in hamsters. *Lipids* 1997;32:303–9. doi: 10.1007/s11745-997-0037-9
- Son MJ, Rico CW, Nam HS, Kang MY. Influence of oryzanol and ferulic acid on the lipid metabolism and antioxidative status in high fat-fed mice. *J Clin Biochem Nutr* 2010;46:150–6. doi: 10.3164/jcfn.09-98
- Akihisa T, Yasukawa K, Yamaura M, Ukiya M, Kimura Y, Shimizu N, et al. Triterpene alcohol and sterol ferulates from rice bran and their anti-inflammatory effects. *J Agric Food Chem* 2000;48:2313–19. doi: 10.1021/jf000135o
- Yasukawa K, Akihisa T, Kimura Y, Tamura T, Takido M. Inhibitory effect of cycloartenolferulate, a component of rice bran, on tumor promotion in two-stage carcinogenesis in mouse skin. *Biol Pharm Bull* 1998;21:1072–6. doi: 10.1248/bpb.21.1072
- Okahara F, Suzuki J, Hashizume K, Osaki N, Shimotoyodome A. Triterpene alcohols and sterols from rice bran reduce postprandial hyperglycemia in rodents and humans. *Mol Nutr Food Res* 2016;60:1521–31. doi: 10.1002/mnfr.201500897
- Fukuoka D, Okahara F, Hashizume K, Yanagawa K, Osaki N, Shimotoyodome A. Triterpene alcohols and sterols from rice bran lower postprandial glucose-dependent insulinotropic polypeptide release and prevent diet-induced obesity in mice. *J Appl Physiol* 2014;117:1337–48. doi: 10.1152/jappphysiol.00268.2014
- Yabe D, Seino Y. Two incretin hormones GLP-1 and GIP: comparison of their actions in insulin secretion and beta cell preservation. *Prog Biophys Mol Biol* 2011;107:248–56. doi: 10.1016/j.pbiomolbio.2011.07.010
- Panlasigui LN, Thompson LU. Blood glucose lowering effects of brown rice in normal and diabetic subjects. *Int J Food Sci Nutr* 2006;57:151–8. doi: 10.1080/09637480500410879

*Koichi Misawa

Biological Science Laboratories
Kao Corporation, 2606 Akabane, Ichikai-machi
Haga-gun, Tochigi 321-3497, Japan
Email: misawa.koichi@kao.com

Grape seed proanthocyanidin extract supplementation affects exhaustive exercise-induced fatigue in mice

Liu Xianchu^{1,2}, Liu Ming^{1,2*}, Liu Xiangbin² and Zheng Lan²

¹Institute of Physical Education, Hunan University of Arts and Science, Hunan Province, Changde, China; ²Key Laboratory of Physical Fitness and Exercise Rehabilitation of Hunan Province, Hunan Normal University, Changsha, China

Abstract

Background: Grape seed proanthocyanidin extract (GSPE) has been extensively reported to possess a wide range of beneficial properties in multiple tissue damage. Previous studies have shown that exhaustive exercise-induced fatigue associates with oxidative stress injury, inflammatory response, and mitochondrial dysfunction.

Objective: The aim of this study is to investigate the anti-fatigue effects of GSPE in mice and explore its possible underlying mechanism.

Design: The mouse model of exhaustive exercise-induced fatigue was established by using the forced swimming test, and GSPE was orally treated for successive 28 days at 0, 1, 50 and 100 mg/kg/day of body weight, designated the control, GSPE-L, GSPE-M and GSPE-H groups, respectively.

Results: The presented results showed that treatment of GSPE at a dose of 50 and 100 mg/kg/day of body weight significantly relieved exhaustive exercise-induced fatigue, indicated by increasing the forced swimming time. In addition, treatment of GSPE significantly improved the creatine phosphokinase and lactic dehydrogenase, as well as lactic acid level in exhaustive swimming. For underlying mechanisms, treatment of GSPE had anti-fatigue effects by promoting antioxidant ability and resisting oxidative effect, as represented by increased total antioxidative capability levels, enhanced superoxide dismutase and catalase activities, and ameliorated malondialdehyde levels. Furthermore, treatment of GSPE significantly inhibited the activity of tumor necrosis factor- α and interleukin-1 β , which suggested that its protective effects on exhaustive exercise-induced fatigue may be attributed to inhibition of inflammatory response. Last but not the least, treatment of GSPE significantly improved succinate dehydrogenase and Na⁺-K⁺-ATPase levels to enhance mitochondrial function during exhaustive swimming-induced fatigue.

Conclusions: These results proved that treatment of GSPE possessed the beneficial properties of anti-inflammatory, antioxidant, and mitochondrial protection to improve exhaustive exercise, which suggested that GSPE could be used as an effective functional food to delay fatigue.

Keywords: *GSPE; exhaustive exercise; fatigue; anti-inflammatory; antioxidant; mitochondria*

Exercise involves human physiological changes (1, 2). Regular exercise has been widely demonstrated to have a function of lowering the risk of human chronic diseases, such as metabolic syndrome, cardiovascular disease, obesity, hypertension, type 2 diabetes, and even some types of cancers (3–5). However, exhaustive exercise is harmful, as it can cause muscle damage and also induce fatigue, which can be considered as extreme tiredness physically. Therefore, fatigue is a sub-health status and is closely associated with reducing the quality of life, which can result in fatigue syndrome and even lead to physical and mental unfitness (6, 7). Nowadays, fatigue as a complicated physiological phenomenon has become

a serious phenomenon because of the huge pressures of life and work in the rapid development of society (8). So it is necessary and significant to seek effective measures to prevent and ease fatigue.

There are multiple reasons on the etiology of fatigue, such as exhaustion theory, homeostasis disturbance theory, and catastrophe theory (9). Among these, oxidative stress injury, inflammatory response, and mitochondrial dysfunction are widely known to play a critical role in the development of fatigue (10, 11). Nowadays, the development of natural products with the ability of reducing muscle injury and possessing anti-fatigue effects is becoming a major research focus (12). Previous studies have showed

that *Dendrobium officinale* extract delays fatigue effects through enhancing glutathione peroxidase (GSH-Px) level and inhibiting malondialdehyde (MDA) content in serum (13). In the single exhaustive swimming test, dietary tea polyphenols can effectively protect against fatigue by inhibiting serum levels of tumor necrosis factor- α (TNF- α), interleukin-1 β (IL-1 β), and IL-6, improving IL 10/TNF- α ratio in serum and reducing IL-1 β mRNA expression in liver (14). In addition, dietary nucleotides possess the function of improving mitochondrial biogenesis, including succinate dehydrogenase (SDH), Na⁺-K⁺-ATPase, and Ca²⁺-Mg²⁺-ATPase, in skeletal muscles, to exert anti-fatigue effects (15). Therefore, nutritional intervention on antioxidant and anti-inflammatory, as well as mitochondrial protection is a valuable approach to fight against fatigue.

Grape is one of the most popular fruits in the world, and proanthocyanidin is the main component of grape seed with various pharmacological effects (16, 17). More and more researches have showed that grape seed proanthocyanidin extract (GSPE) has been used for the treatment of numerous diseases because of its therapeutic activities, such as anti-inflammatory and antioxidant properties (18). Previous studies have showed that natural proanthocyanidin-rich extracts from grape seed exhibits an antioxidant effect in the gastrointestinal tract, as represented by reduced intestinal ROS in fasted animals (19, 20). On the subchronic immune injury, intervention of GSPE could significantly decrease the expression of TNF- α , IL-1 β , IL-6, and IFN- γ to restrain inflammatory reaction (21). Moreover, GSPE can significantly improve indoxyl sulfate-induced HUVEC (human umbilical vein endothelial cells) injury by ameliorating mitochondrial dysfunction (22). Although previous studies have demonstrated that grape seed extract is involved in regulating oxidative stress on the treadmill running performance (23), there is no prior report on the protective effects of proanthocyanidins from grape seed on exhaustive exercise. Furthermore, the anti-fatigue mechanism of GSPE remains to be observed deeply. The purpose of this study was to study the relationship between GSPE and exhaustive exercise, and further clarify the possible protective effects of GSPE on fatigue.

Materials and methods

Animals

Male ICR mice (about 8 weeks old, 25 ± 2 g) were obtained from the Animal Center of Hunan Normal University (Changsha, China). All mice were grown at a standard laboratory condition ($23 \pm 2^\circ\text{C}$, 50–60% humidity, 12-h light/12-h dark cycle). The mice were randomly divided and housed in groups of four animals per cage. They were provided with free access to standard diet and

distilled water. In this study, all animal experiments were inspected according to the Animal Care Committee of Hunan Normal University.

GSPE was purchased from Tianjin Jianfeng Natural Product R&D Co., LTD (purity: $\geq 95\%$, Tianjin, China). Thirty-two male ICR mice were randomly assigned to four experimental groups (8 mice per group) for GSPE treatment: (1) control group, (2) low-dose group (GSPE-L), (3) medium-dose group (GSPE-M), and (4) high-dose group (GSPE-H). Three GSPE intervention groups were treated with GSPE at a dose of 1, 50 and 100 mg/kg/day of body weight, respectively. The control group mice were administered at the same dosage volume of physiological saline equivalent to individual body weight. GSPE supplementation was given by oral gavages once a day for 28 successive days.

Forced swimming test

The mice were challenged by the forced swimming test to establish exhaustive exercise-induced fatigue. One hour after the final dosing, all mice underwent weight-loaded swimming test with a lead (approximately 5% of each mouse's body weight), which was attached to their tails root. All mice were trained individually in the same condition ($25 \pm 1^\circ\text{C}$, 30 cm depth) (25). Before being subjected to the forced swimming test, all mice were also drilled to adapt to swimming without any loads for 3 days (20 min/day). The time to exhaustion (TTE), which was defined by failure to rise to the above water within 10 s and a lack of apparent coordinated movements, was recorded immediately. After the exhaustive swimming, the mice were killed by an intraperitoneal injection of anesthetic. Then blood and skeletal muscle tissues were collected and removed for further experiments.

Biochemical assay

Blood samples were obtained and centrifuged at $1,200 \times g$ and 4°C for 15 min to separate serum after the swimming exercise. The serum biochemical variables related to fatigue (Catalog number: A019 for lactic acid [LA], A020 for lactic dehydrogenase [LDH], A032 for creatine phosphokinase [CK], Nanjing Jiancheng Biotechnology Institute, Nanjing, China) were measured according to the manufacturer's protocol.

Determination of oxidative stress

After the swimming exercise, skeletal muscle tissues were immediately acquired and stored at -80°C . In our research, skeletal muscle tissues were carefully grounded and centrifuged. Then the serum and supernatant in skeletal muscle were used for oxidative stress assay. Furthermore, the level of antioxidant enzymes and oxidative indicators (Catalog number: A001 for superoxide

dismutase [SOD], A003 for MDA, A007 for catalase [CAT], A015 for total antioxidative capability [T-AOC], Nanjing Jiancheng Biotechnology Institute, Nanjing, China) were determined by spectrophotometer according to the manufacturer's protocol.

Examination of inflammatory response

The level of inflammatory cytokines (Catalog number: EK0527 for TNF- α , EK0411 EK0394 for IL-1 β , BOSTER Biological Technology, Wuhan, China) were examined to assess inflammatory responses in the serum and supernatant of skeletal muscle by ELISA. The absorbance value was measured at 450 nm to analyze inflammatory parameters according to the manufacturer's instructions.

Measurements of energy metabolism

The energy metabolism parameters SDH and Na+K+-ATPase (Catalog number: A022 for SDH, A016 for Na+K+-ATPase, Nanjing Jiancheng Biotechnology Institute, Nanjing, China) in skeletal muscles were determined to assess mitochondrial function by detection kits according to the manufacturer's protocol.

Statistics

All results were displayed as mean \pm standard deviation (SD). The data was statistically analyzed using SPSS 16.0 software. Statistical significance between groups was demonstrated with one-way analysis of variance (ANOVA). A *p* value of less than 0.05 was considered statistically significant.

Results

Effects of GSPE on body weight of mice

The body weight of mice in our experiment is presented in Table 1. The general condition of all mice was normal and the survival rate was 100% during the whole experimental process. There were no remarkable differences among the groups on the initial body weight. After GSPE supplementation for 28 successive days, the terminal weight in mice showed that the control, GSPE-L, GSPE-M, and GSPE-H groups were 38.82 ± 1.70 , 37.66 ± 1.81 , 36.91 ± 2.11 , and 38.30 ± 1.80 g, respectively, which displayed that there were no remarkable differences in final body weight in the control and GSPE groups.

Effects of GSPE in the weight-loaded swimming test

The effects of GSPE on the weight-loaded swimming time are presented in Table 1. Our results displayed that the TTE of the control, GSPE-L, GSPE-M, and GSPE-H groups was 8.60 ± 1.46 , 10.29 ± 2.24 , 13.03 ± 3.50 , and 16.63 ± 2.98 , respectively. When compared to the control group, the TTE in GSPE groups increased by 19.65, 51.51, and 93.37%, respectively, and the difference was markedly significant in the GSPE-M and GSPE-H groups.

Effects of GSPE on LA, CK, and LDH in serum

The effects of GSPE on the blood biochemical parameters are presented in Table 2. In comparison with the control group, the LA levels in serum were significantly increased in GSPE-M and GSPE-H groups after exhaustive swimming.

Table 1. Effects of grape seed proanthocyanidin extract on the body weight and time to exhaustion in mice

Parameters	Control		GSPE-L		GSPE-M		GSPE-H	
	Mean	SD	Mean	SD	Mean	SD	Mean	SD
Initial body weight (g)	25.56	0.70	25.14	0.90	25.25	1.36	25.29	1.28
Final weight (g)	38.82	1.70	37.66	1.81	36.91	2.11	38.30	1.80
Exhaustive time (min)	8.60	1.46	9.79	1.90	13.03**	3.50	16.63**	2.98

Note: Data were displayed as means \pm SD. ***p* < 0.01, versus control group. GPSE-L, dietary grape seed proanthocyanidin extract low-dose group; GPSE-M, dietary grape seed proanthocyanidin extract medium-dose group; GPSE-H, dietary grape seed proanthocyanidin extract high-dose group; SD, standard deviation.

Table 2. Effects of grape seed proanthocyanidin extract on biochemical indexes in serum of mice

Parameters	Control		GSPE-L		GSPE-M		GSPE-H	
	Mean	SD	Mean	SD	Mean	SD	Mean	SD
LA (mmol/L)	12.44	2.75	10.80	1.51	9.51*	1.19	8.74**	1.35
CK(U/mL)	1.42	0.15	1.29	0.14	1.06**	0.23	0.85**	0.17
LDH(U/mL)	5.33	0.19	5.09	0.26	4.74**	0.47	4.24**	0.40

Note: Data were displayed as means \pm SD. **p* < 0.05, ***p* < 0.01, versus control group. GPSE-L, dietary grape seed proanthocyanidin extract low-dose group; GPSE-M, dietary grape seed proanthocyanidin extract medium-dose group; GPSE-H, dietary grape seed proanthocyanidin extract high-dose group; SD, standard deviation.

Moreover, the CK and LDH activity in serum was also measured to evaluate the protective effects of GSPE on the tissue damage induced by exhaustive swimming. In this study, the serum CK and LDH activities in GSPE-M and GSPE-H groups were significantly lower than those in the control group.

Effects of GSPE on parameters of oxidative stress in serum and skeletal muscles of mice

The effects of GSPE on oxidative stress in both serum and skeletal muscles of mice are presented in Table 3. In the comparison with the control group, the activities of SOD and CAT were significantly increased in GSPE-M and GSPE-H groups. In addition, T-AOC levels were significantly enhanced, while MDA levels were significantly improved, in GSPE-M and GSPE-H groups compared with the control group.

Effects of GSPE on activities of inflammatory response in serum and skeletal muscles of mice

Inflammatory cytokines, including TNF- α and IL-1 β , in both serum and skeletal muscles of mice were measured to evaluate the effects of GSPE on inflammatory response.

As shown in Table 4, the TNF- α and IL-1 β levels of mice were improved in GSPE-M and GSPE-H groups with remarkable differences in comparison with the control group after exhaustive exercise.

Effect of GSPE on activities of mitochondrial function in skeletal muscles

The SDH and Na⁺-K⁺-ATPase activity were measured to evaluate the effects of GSPE on mitochondrial function in skeletal muscles. As shown in Table 5, when compared with the control group, the SDH and Na⁺-K⁺-ATPase activities in skeletal muscle were markedly increased in the GSPE-M and GSPE-H groups.

Discussion

Grape is a popular fruit throughout the world. Nowadays, proanthocyanidin, as major flavonoids in grape seed, is used as a nutritional supplementation worldwide for its medicinal and health effects (26, 27). It has been suggested that grape seed extract supplementation improves oxidative stress by preventing MDA levels and increasing antioxidant enzyme activities to prevent exercise-induced oxidative damage (23, 28). In this study, proanthocyanidin

Table 3. Effects of grape seed proanthocyanidin extract on oxidative stress parameters in serum and skeletal muscles of mice

Parameters	Control		GSPE-L		GSPE-M		GSPE-H		
	Mean	SD	Mean	SD	Mean	SD	Mean	SD	
Serum	T-AOC (U/mL)	117.75	12.14	121.62	9.66	139.76**	10.68	139.49**	9.07
	SOD (U/mL)	71.82	12.02	76.86	6.17	84.49**	7.67	88.11**	6.32
	CAT (U/mL)	24.63	3.34	27.71	2.58	27.97*	2.83	28.97**	2.30
	MDA (nmol/mL)	8.36	0.68	7.93	0.82	7.19*	1.24	6.77**	0.95
Skeletal muscle	T-AOC (U/mg pro)	4.08	0.50	4.39	0.52	5.01**	0.54	5.04**	0.64
	SOD (U/mg pro)	7.19	0.72	7.95	0.98	8.12*	0.65	9.83**	1.00
	CAT (U/mg pro)	3.50	0.78	4.08	0.60	4.71**	0.45	4.74**	0.49
	MDA (nmol/mg pro)	4.74	0.44	4.39	0.36	4.29*	0.39	3.75**	0.76

Note: Data are displayed as means \pm SD. * $p < 0.05$, ** $p < 0.01$, versus control group. GSPE-L, dietary grape seed proanthocyanidin extract low-dose group; GSPE-M, dietary grape seed proanthocyanidin extract medium-dose group; GSPE-H, dietary grape seed proanthocyanidin extract high-dose group; SD, standard deviation.

Table 4. Effects of grape seed proanthocyanidin extract on inflammatory response in serum and skeletal muscles of mice

Parameters	Control		GSPE-L		GSPE-M		GSPE-H		
	Mean	SD	Mean	SD	Mean	SD	Mean	SD	
Serum	TNF- α (pg/mL)	153.88	7.98	146.71	10.24	143.89*	9.60	140.41**	7.91
	IL-1 β (pg/mL)	75.70	3.42	72.48	4.15	70.06*	4.46	69.57**	3.19
Skeletal muscle	TNF- α (pg/mg pro)	73.72	4.02	70.98	3.90	67.12**	3.06	65.12**	3.92
	IL-1 β (pg/mg pro)	27.39	1.62	25.94	1.29	24.85**	1.28	24.65**	2.02

Note: Data are displayed as means \pm SD. * $p < 0.05$, ** $p < 0.01$, versus control group. GSPE-L, dietary grape seed proanthocyanidin extract low-dose group; GSPE-M, dietary grape seed proanthocyanidin extract medium-dose group; GSPE-H, dietary grape seed proanthocyanidin extract high-dose group; SD, standard deviation.

Table 5. Effects of grape seed proanthocyanidin extract on mitochondrial function in skeletal muscles of mice

Parameters	Control		GSPE-L		GSPE-M		GSPE-H	
	Mean	SD	Mean	SD	Mean	SD	Mean	SD
SDH (U/mg pro)	2.52	0.28	2.70	0.34	2.91*	0.38	2.91*	0.27
Na+K+-ATPase (U/mg pro)	0.83	0.11	0.94	0.10	1.03**	0.12	1.06**	0.13

Note: Data are displayed as means \pm SD. * $p < 0.05$, ** $p < 0.01$, versus control group. GSPE-L, dietary grape seed proanthocyanidin extract low-dose group; GSPE-M, dietary grape seed proanthocyanidin extract medium-dose group; GSPE-H, dietary grape seed proanthocyanidin extract high-dose group; SD, standard deviation.

from grape seed was hypothesized to bring beneficial health effects against exhaustive exercise-induced fatigue because of its notable effects of inhibiting oxidative stress and inflammatory response, as well as potentiating mitochondrial function. The mouse model of exhaustive exercise was established to assess the anti-fatigue effects of GSPE by forced swimming test and to illuminate its potential mechanism. In general, the ability of delaying fatigue is positively correlated with the TTE in forced swimming test (29). In this study, our results showed that treatment with GSPE improved the fatigue. GSPE supplementation prolonged the TTE, particularly at 19.65, 51.51, and 93.37% in GSPE-treated groups, which may indicate that GSPE is capable of delaying fatigue. Furthermore, our results showed that GSPE supplementation did not significantly cause body weight changes in either the control group or the GSPE group, which was consistent with the previous reports (30). In summary, there was no abnormality and no death occurred in this study, which indicates that GSPE does not have any toxicity and is an anti-fatigue natural agent.

LA is formed as a metabolic by-product in skeletal muscles and released into the bloodstream. However, excess LA is harmful for skeletal muscles during intense exercise, which may result in fatigue (31). Therefore, LA is identified as a biochemical index relevant to fatigue in blood. CK and LDH are muscle injury indicators clinically (32, 33). There is a prominent positive correlation between the activity of CK and LDH and the process of fatigue. To further evaluate the protective effect of GSPE on exhaustive swimming-induced fatigue, the fatigue indicators, including LA, CK, and LDH, were tested in our study. GSPE could lower the contents of LA and decrease the activity of LDH and CK in serum, which indicates that GSPE is capable of protecting skeletal muscles from damage and delaying fatigue in exhaustive exercise.

Exhaustive exercise leads to oxidative stress, which can destabilize the balance between oxidation and antioxidation systems and play an important role in fatigue-related disorders (34, 35). It is also believed that antioxidant enzymes play an important role in defending

against oxidative stress. SOD and CAT belong to antioxidant enzymes, while MDA is a part of oxidative indicators and aggravates oxidative damage. The anomaly between oxidation and antioxidation is associated with the development of fatigue progress. Previous literature has showed that okra seeds promote antioxidant ability through increasing SOD and GSH-PX levels and lowering MDA level to possess anti-fatigue effects (9). In addition, GSPE significantly improved oxidative stress by enhancing SOD and CAT levels and reducing MDA contents in spontaneously hypertensive rats (36). In this study, our results showed that GSPE increased the activity of SOD and CAT and inhibited MDA contents in exhaustive exercise, indicating that anti-fatigue mechanism of GSPE was at least partly associated with its antioxidant effects.

Exhaustive exercise has been reported to cause inflammatory response which can contribute to fatigue. TNF- α , IL-6, and IL-1 β are often used as an index to evaluate the inflammatory response. Glycine-leucine and leucine-glycine dipeptides, as primary peptides of fermented porcine placenta, significantly decreased IL-6 and IL-1 β serum levels to display an anti-fatigue effect (37). Furthermore, oxidative stress is recognized as a primary mediator of inflammatory response. Hence, anti-inflammatory effect as a part of nutritional intervention is an indispensable part of prevention and improvement of fatigue. Thus far, relatively few studies have demonstrated whether GSPE can possess anti-fatigue function through affecting inflammatory cytokine activities during exhaustive exercise, although its anti-inflammatory function has been reported on multiple diseases in animal experiments and clinical studies. In this study, the elevated inflammatory cytokine activity induced by exhaustive exercise in blood, which was represented by increasing the level of TNF- α and IL-1 β , was noticeably alleviated by GSPE pretreatment. Moreover, excess inflammatory cytokine in skeletal muscle can induce tissue injury and further accelerate fatigue. Our results also showed that GSPE decreased the activity of TNF- α and IL-1 β in the skeletal muscle. These data well suggested that anti-fatigue effects of GSPE might be related to its anti-inflammatory function.

Mitochondrion is the place of adenosine triphosphate (ATP) generation. The human body needs more ATP to maintain muscle contraction and movement during exercise. However, exhaustive exercise can lead to damaged mitochondria that further cause skeletal muscles damage and fatigue (38). SDH plays an important role in ATP synthesis, while Na⁺-K⁺-ATPase can reflect ATP hydrolysis during energy supply to maintain normal physiologic function (39, 40). Therefore, SDH and Na⁺-K⁺-ATPase are the primary factors responsible for energy metabolism in mitochondria, the disorder activity of which contributes to exhaustive swimming-induced fatigue. Previous findings indicate that GSPE promotes mitochondrial oxygen consumption and the enzyme activity of citric acid cycle and electron transport chain (ETC) to affect the mitochondrial function and energy metabolism (41). To elucidate the anti-fatigue effect of GSPE after exhaustive swimming, the activities of SDH and Na⁺-K⁺-ATPase in skeletal muscles were measured to assess mitochondrial function. Our results showed that GSPE could improve mitochondrial function for energy supplementation, as represented by enhancing levels of SDH and Na⁺-K⁺-ATPase, to delay fatigue during exhaustive swimming.

Conclusion

To our knowledge, this research is the first to investigate the effect of GSPE supplementation on exhaustive swimming-induced fatigue in mice. Treatment with GSPE improved the fatigue by prolonging the TTE in the forced swimming test. Furthermore, several biochemical markers for fatigue, including LA, LDH, and CK, were significantly alleviated by the administration of GSPE. The anti-fatigue property may be associated with the amelioration of inflammatory response, suppression of oxidative stress, and improvement of mitochondrial function. According to the data, these findings indicate that GSPE is a natural and safe ingredient and dietary agent in excessive exercise-induced fatigue.

Conflict of interest and funding

No potential conflict of interest was reported by the authors. This study was supported in part by the Postdoctoral Science Foundation of China (2016M592430), the Innovative Projects for College Students in Hunan Province (1021-0001-017-062), and the Innovative Projects for College Students in Hunan Normal University (2017113).

Acknowledgements

The authors greatly acknowledge the funding support provided by the Postdoctoral Science Foundation of China, the Innovative Projects for College Students in

Hunan Province, and the Innovative Projects for College Students in Hunan Normal University.

References

- Mitchell J H, Blomqvist G. Maximal Oxygen Uptake. *The New England Journal of Medicine*. 1971; 284(18): 1018-1022.
- Martínez-Sánchez A, Ramos-Campo DJ, Fernández-Lobato B, Rubio-Arias JA, Alacid F, Aguayo E. Biochemical, physiological, and performance response of a burdensome watermelon juice enriched in L-citrulline during a half-marathon race. *Food & Nutrition Research*. 2017; 61(1):1330098.
- Roberts CK, Barnard RJ. Effects of exercise and diet on chronic disease. *J Appl Physiol*. 2005; 98(1):3-30.
- Lee I-M, Shiroma EJ, Lobelo F, Puska P, Blair SN, Katzmarzyk PT, et al. Effect of physical inactivity on major non-communicable diseases worldwide: an analysis of burden of disease and life expectancy. *Lancet*. 2012; 380(9838):219-229.
- Pedersen L, Idorn M, Olofsson GH, Lauenborg B, Nookaew I, Hansen RH, et al. Voluntary Running Suppresses Tumor Growth through Epinephrine- and IL-6-Dependent NK Cell Mobilization and Redistribution. *Cell Metabolism*. 2016; 23(3): 554-562.
- Kim KM, Yu KW, Kang DH, Koh JH, Hong BS, Suh HJ. Anti-stress and anti-fatigue effects of fermented rice bran. *Bioscience, Biotechnology, and Biochemistry*. 2001; 65(10): 2294-2296.
- Uehata T. Karoshi, death by overwork. *Nihon Rinsho*. 2005; 63, 1249-1253.
- Chaudhuri A, Behan PO. Fatigue in neurological disorders. *The Lancet*. 2004; 363(9413): 978-988.
- Xia F, Zhong Y, Li M, Chang Q, Liao Y, Liu X, et al. Antioxidant and Anti-Fatigue Constituents of Okra. *Nutrients*. 2015; 7(10): 8846-8858.
- Finsterer J, Mahjoub SZ. Fatigue in Healthy and Diseased Individuals. *American Journal of Hospice and Palliative Medicine*. 2014; 31(5): 562-575.
- Glaister M. Multiple Sprint Work: Physiological Responses, Mechanisms of Fatigue and the Influence of Aerobic Fitness. *Sports Medicine*. 2005; 35(9): 757-777.
- Herrlinger KA, Chirouzes DM, Ceddia MA. Supplementation with a polyphenolic blend improves post-exercise strength recovery and muscle soreness. *Food & Nutrition Research*. 2015; 59:30034.
- Wei W, Li ZP, Zhu T. Anti-Fatigue Effects of the Unique Polysaccharide Marker of *Dendrobium officinale* on BALB/c Mice. *Molecules*. 2017; 22(1).
- Lixia Liu, Xiuqin Wu, Bingchen Zhang, Yang W, Li D, Dong Y, et al. Protective effects of tea polyphenols on exhaustive exercise-induced fatigue, inflammation and tissue damage. *Food & Nutrition Research*. 2017; 61:1, 1333390.
- Meihong Xu, Rui Liang, Yong Li, Wang J. Anti-fatigue effects of dietary nucleotides in mice. *Food & Nutrition Research*. 2017; 61:1, 1334485.
- Shi J, Yu J, Pohorly J E, Kakuda Y. Polyphenolics in grape seeds-biochemistry and functionality. *Journal of Medicinal Food*. 2003; 6(4):291-299.
- Han F, Ju Y, Ruan X. Color, anthocyanin, and antioxidant characteristics of young wines produced from spine grapes (*Vitis davidii* Foex) in China. *Food & Nutrition Research*. 2017; 61(1):1339552.
- Bagchi D, Sen CK, Ray SD, Das DK, Bagchi M, Preuss HG, et al. Molecular mechanisms of cardioprotection by a novel grape seed proanthocyanidin extract. *Mutation Research*. 2003; 523-524(2):87-97.

19. Pinent M, Castell-Auví A, Inés GM, Serrano J, Casanova A, Blay M, et al. Antioxidant effects of proanthocyanidin-rich natural extracts from Grape seed and Cupuassu on gastrointestinal mucosa. *Journal of the Science of Food & Agriculture*. 2016; 96(1):178-182.
20. Àngela CasanovaMartí, Serrano J, Blay MT, Terra X, Ardévol A, Pinent M. Acute selective bioactivity of grape seed proanthocyanidins on enteroendocrine secretions in the gastrointestinal tract. *Food & Nutrition Research*. 2017; 61(1):1321347.
21. Long M, Zhang Y, Li P, Yang SH, Zhang WK, Han JX, et al. Intervention of Grape Seed Proanthocyanidin Extract on the Subchronic Immune Injury in Mice Induced by Aflatoxin B1. *International Journal of Molecular Sciences*. 2016; 17(4):516.
22. Lu Z, Lu F, Zheng Y, Zeng Y, Zou C, Liu X. Grape seed proanthocyanidin extract protects human umbilical vein endothelial cells from indoxyl sulfate-induced injury via ameliorating mitochondrial dysfunction. *Renal Failure*. 2016; 38(1):100-8.
23. Belviranlı M, Gökbel H, Okudan N, Başaralı K. Effects of grape seed extract supplementation on exercise-induced oxidative stress in rats. *British Journal of Nutrition*. 2012; 108(2):249-56.
24. Chen S, Zhu Y, Liu Z, Gao Z, Li B, Zhang D, et al. Grape Seed Proanthocyanidin Extract Ameliorates Diabetic Bladder Dysfunction via the Activation of the Nrf2 Pathway. *Plos One*. 2015; 10(5):e0126457.
25. Tan W, Yu KQ, Liu YY, Ouyang MZ, Yan MH, Luo R, et al. Anti-fatigue activity of polysaccharides extract from *Radix Rehmanniae Preparata*. *Int J Biol Macromol*. 2012; 50(1):59-62.
26. Meltzer HM, Malterud KE. Can dietary flavonoids influence the development of coronary heart disease?. *Food & Nutrition Research*. 1997; 41:50-57.
27. Ma Y, Gao W, Wu K, Bao Y. Flavonoid intake and the risk of age-related cataract in China's Heilongjiang Province. *Food & Nutrition Research*. 2015; 59:29564.
28. Belviranlı M, Gökbel H, Okudan N, Büyükbaş S. Effects of Grape Seed Polyphenols on Oxidative Damage in Liver Tissue of Acutely and Chronically Exercised Rats. *Phytotherapy Research*. 2013; 27(5):672-7.
29. Xin F, Rong J, Dam J. Antifatigue effect of coenzyme Q10 in mice. *Journal of Medicinal Food*. 2010; 13(1):211-215.
30. Yamakoshi J, Saito M, Kataoka S, Kikuchi M. Safety evaluation of proanthocyanidin-rich extract from grape seeds. *Food & Chemical Toxicology*. 2002; 40(5):599-607.
31. Gibson H, Edwards RH. Muscular exercise and fatigue. *Sports Medicine*. 1985; 2(2):120-132.
32. Kim H, Park S, Han DS, Park T. Octacosanol supplementation increases running endurance time and improves biochemical parameters after exhaustion in trained rats. *J Med Food*. 2003; 6(4):345-351.
33. Coombes JS, McNaughton LR. Effects of branched-chain amino acid supplementation on serum creatine kinase and lactate dehydrogenase after prolonged exercise. *J Sports Med Phys Fitness*. 2000; 40(3):240-246.
34. Barclay JK, Hansel M. Free radicals may contribute to oxidative skeletal muscle fatigue. *Canadian Journal of Physiology & Pharmacology*. 1991; 69(2):279-84.
35. Bagis S, Tamer L, Sahin G, Bilgin R, Guler H, Ercan B, et al. Free radicals and antioxidants in primary fibromyalgia: an oxidative stress disorder? *Rheumatology International*. 2005; 25(3):188-190.
36. Liang Y, Wang J, Gao H, Wang Q, Zhang J, Qiu J. Beneficial effects of grape seed proanthocyanidin extract on arterial remodeling in spontaneously hypertensive rats via protecting against oxidative stress. *Molecular Medicine Reports*. 2016; 14(4):3711-8.
37. Nam SY, Kim HM, Jeong HJ. Anti-fatigue effect by active dipeptides of fermented porcine placenta through inhibiting the inflammatory and oxidative reactions. *Biomedicine & Pharmacotherapy*. 2016; 84:51-59.
38. Echtay KS, Roussel D, St-Pierre J, Jekabsons MB, Cadenas S, Stuart JA, et al. Superoxide activates mitochondrial uncoupling proteins. *Nature*. 2002; 415(6867):96-99.
39. Nkandeu D S, Mqoco TV, Visagie MH, Stander BA, Wolmarans E, Cronje MJ, et al. In vitro changes in mitochondrial potential, aggresome formation and caspase activity by a novel 17- β -estradiol analogue in breast adenocarcinoma cells. *Cell Biochemistry & Function*. 2013; 31(7):566-574.
40. Huang XP, Tan H, Chen BY, Deng CQ. Astragalus extract alleviates nerve injury after cerebral ischemia by improving energy metabolism and inhibiting apoptosis. *Biological & Pharmaceutical Bulletin*. 2012; 35(4):449-454.
41. Pajuelo D, Diaz S, Quesada H. Acute Administration of Grape Seed Proanthocyanidin Extract Modulates Energetic Metabolism in Skeletal Muscle and BAT Mitochondria. *Journal of Agricultural & Food Chemistry*. 2011; 59(8):4279-87.

***Liu Ming**

No. 3150 Dongting Avenue,
 Changde, 415003, Institute of Physical Education,
 Hunan University of Arts and Science,
 Hunan Province, Changde, China
 E-mail: liuminghappy36@163.com

Sufficient iodine status among Norwegian toddlers 18 months of age – cross-sectional data from the Little in Norway study

Inger Aakre^{1*}, Maria Wik Markhus¹, Marian Kjellevold¹, Vibeke Moe², Lars Smith² and Lisbeth Dahl¹

¹Food Security and Nutrition, Institute of Marine Research, Bergen, Norway; ²Department of Psychology, University of Oslo, Oslo, Norway

Abstract

Background: Inadequate iodine intake has been identified in several population groups in the Nordic countries over the past years; however, studies of iodine status in infants and toddlers are scarce.

Objective: The aim of this study is to evaluate the iodine status and dietary iodine sources among 18-month-old toddlers from Norway.

Methods: Cross-sectional and country representative data from the Little in Norway study were used. All children who had given a spot urine sample at 18 months age were included ($n = 416$). Urinary iodine concentration (UIC) was determined by inductively coupled plasma mass-spectrometry. Dietary habits and supplement use were measured by a food frequency questionnaire.

Results: Median (25th–75th percentiles [p25–p75]) UIC was 129 (81–190) $\mu\text{g/L}$ while estimated median (p25–p75) habitual iodine intake was 109 (101–117) $\mu\text{g/day}$. None of the children were below the estimated average requirement (EAR) of 65 $\mu\text{g/day}$ or above the upper intake level of 180 $\mu\text{g/day}$. There were no differences in either UIC or estimated habitual iodine intake between different geographic areas in Norway. Milk was the most important iodine source, contributing an estimated 70% to the total iodine intake, while other foods rich in iodine such as seafood and enriched baby porridge contributed about 30%.

Conclusions: The iodine status among 18-month-old toddlers from different geographic areas in Norway was sufficient, indicated by a median UIC above the WHO cutoff of 100 $\mu\text{g/L}$. This was further supported by the estimated habitual iodine intake, where none of the participants were below the EAR. Milk was an important iodine source in this age group; thus children with a low intake might be at risk of insufficient iodine intake.

Keywords: *Iodine; Urinary iodine concentration; Iodine intake; Dietary iodine intake; Toddlers*

Infants and toddlers are particularly vulnerable to inadequate iodine nutrition, as iodine is crucial for optimal child growth and development (1, 2) through the many functions of the thyroid hormones (3, 4). Thus, iodine deficiency has been pointed out as one of the main factors that prevent children from achieving their developmental potential (5). Even though the global work towards eliminating iodine deficiency disorders has been successful (6, 7), iodine deficiency has been reemerging in Europe (8); and inadequate iodine status has been reported in several European countries during recent years (9–12).

Iodine is present in relatively few food groups, and iodized salt is the most important source globally (13). In Norway, the permitted iodine level of 5 $\mu\text{g/g}$ in table salt

is too low to be considered a significant iodine source in the population (9). However, animal feed is enriched with iodine in Norway; therefore milk, dairy products, and eggs have significant levels of iodine. Marine fish, especially lean fish such as cod, haddock, and saithe, and fish products also have high levels of iodine (14, 15). Industry-manufactured baby food is enriched with iodine; thus among toddlers this is an important iodine source as well as breast milk or formula (16). Dietary surveys among Norwegian toddlers revealed that only 35% and 4% were still breastfed at 12 (17) and 24 months of age (18), respectively. Young children in the weaning period are therefore dependent on iodine-rich complementary foods in order to reach an intake of 50–70 $\mu\text{g/day}$ as recommended in the Nordic countries (19).

As the consumption of milk, yoghurt, and lean fish has been declining in Norway, recent studies have reported insufficient iodine status among pregnant and lactating women (20–23). An association between insufficient iodine intake in pregnant Norwegian women and poorer developmental status in children at 3 years of age has also been found (24). Infants and young children have therefore been identified as a vulnerable group regarding insufficient iodine intake. Recently published data among 5-year-old preschool children ($n = 220$) and 3–9-year-old children ($n = 47$) showed iodine sufficiency in these groups, with a median urinary iodine concentration (UIC) of 132 and 148 $\mu\text{g/L}$, respectively (25, 26). Studies among infants and toddlers remain scarce; however, iodine status was measured in a study of Norwegian toddlers under the age of 2 with cow's milk protein allergy. This study found a median UIC of 159 $\mu\text{g/L}$, indicating sufficient iodine status (27). The main objective of this paper is to assess iodine status in toddlers 18 months of age participating in the Little in Norway study (LiN). To our knowledge, this is the first paper from Norway to present data on iodine status and its relation to dietary habits among healthy children less than 2 years of age.

Subjects and methods

Study design and subjects

This paper is based on data from the LiN project (ISRCTN registry number 66710572), a prospective population-based cohort study conducted between September 2011 and November 2014. The study was established to investigate pre- and postnatal risk factors influencing child development from pregnancy to 18 months of age. Pregnant women at nine primary health clinics across all four Norwegian health regions were recruited. The data collection included questionnaires completed by the mothers and biological samples of mother and child. In total, 1,036 pregnant women consented to participate in the LiN cohort. In this paper, cross-sectional data from toddlers 18 months of age were used, as well as background characteristics of their mothers at study enrollment. Of the 1,036 participating pregnant women, 777 children were still participating at 18 months age. Not all toddlers were able to give a urine sample at the time of data collection and some failed due to technical issues. Thus, the final sample size consisted of 416 toddlers 18 months of age, along with their mothers. Further details regarding study attrition for the participants have been described elsewhere (28).

Urinary iodine concentration

UIC was assessed in spot urine samples from the children using Uricol collection pack (Sterisets International B.V., SteriSets GP Supplies, Newcastle Urine Collection

Pack, UK). The urine was extracted from the pad with a syringe and transferred to CryoTubes (CryoTubes™ Vials, Nunc A/S, Roskilde, Denmark) for storage at -18°C pending analysis. Content of iodine in urine was determined by inductively coupled plasma mass-spectrometry at the Institute of Marine Research in Norway. Further description of the analytic method and accuracy has been published elsewhere (23).

Estimated habitual iodine intake

The children's habitual food intake was mapped by the mothers of the children answering questions about average intake of selected food items and dishes through an online questionnaire. There were 13 questions concerning the general diet, of which nine questions concerned iodine-containing food items, where intake of yoghurt, porridge, fish, and fish products was assessed. Frequency responses were recorded as never/rarely to seven times per week or more. There was one question assessing intake of eggs, where the frequency responses ranged from less than one egg per week to eight or more per week. There were nine questions assessing intake of fats and oils, of which questions regarding margarine and butter were relevant for iodine intake. The frequency responses ranged from never to daily. There was one question regarding breast milk intake at 18 months of age, where the frequency responses ranged from once in the last 24 h to 10 times or more. However, there were no data available from Norway regarding the amount of breast milk consumed among 18-month-old children. Nor has data regarding breast milk intake been registered in the national dietary surveys for 1- and 2-year-old children in Norway (17, 18). Therefore, children still breastfed at 18 months were excluded from the iodine intake estimations. The intake frequencies related to yoghurt, porridge, fish/fish products, eggs, and butter/margarine were converted to daily amounts using data from a national nutrition survey among children 2 years of age (18) and multiplied with the iodine concentration for each food item or dish. In all calculations, iodine content reported in the Norwegian Food Composition Table (29) was used. The questionnaire did not contain intake of milk and cheese, which are important dietary iodine sources in Norway. Mean intake of milk, white cheese/cheese spread and brown cheese/whey cheese spread among Norwegian 2-year-olds, both users and non-users of the food, was used to calculate the iodine contribution from these foods. In total, milk and cheese were estimated to contribute 79 $\mu\text{g/day}$, which was applied in the estimation of daily iodine intake among all non-breastfed children.

The frequency responses of the major iodine-contributing foods – fish, yoghurt, and porridge – were divided into low/medium consumption and high consumption using the following criteria: high consumption of fish: lean fish or fish products for dinner at least two to three

times per week and fish (fatty and lean) as bread topping at least four to six times per week; high consumption of yoghurt: at least four to six times per week; high consumption of fish and yoghurt: both intake of fish and yoghurt was high; high consumption of porridge: (home-made or industry manufactured) at least four to six times per week.

Definitions of iodine status and iodine intake

The epidemiological criteria for assessing iodine nutrition based on median UIC for children were used in this study (13). For children less than 2 years of age a median UIC $<100 \mu\text{g/L}$ indicates insufficient iodine status, while a median UIC ≥ 100 indicates adequate iodine status. In the Nordic Nutrition Recommendations, an iodine intake of $50\text{--}70 \mu\text{g/day}$ is estimated to be sufficient for infants and children <2 years of age (19). However, as the Nordic Nutrition Recommendations does not have an average requirement for young children, the estimated average requirement (EAR) from the US Institute of Medicine of $65 \mu\text{g/day}$ was used for evaluating the habitual iodine intake from food (30). To assess excessive iodine intakes, the World Health Organization's (WHO) upper intake level (UL) of $180 \mu\text{g/day}$ for children under 2 years was used (31).

Background characteristics and anthropometry

The mothers answered a precoded questionnaire concerning background variables for themselves and their children. The WHO body mass index (BMI) (kg/m^2) was used to classify underweight, normal weight, overweight, and obesity, defined by BMI $< 18.5 \text{ kg/m}^2$, BMI = $18.5\text{--}24.9 \text{ kg/m}^2$, BMI = $25.0\text{--}29.9 \text{ kg/m}^2$, and BMI $\geq 30 \text{ kg/m}^2$, respectively (32). The children's height and weight were registered at the primary health clinic by trained health personnel. The gender-specific z -scores height-for-age, weight-for-age, weight-for-height (WHZ), and BMI-for-age (BMI z) were calculated using the WHO macro for SPSS (33, 34). A child was categorized as undernourished if WHZ or BMI z , was < -2 , and overweight if WHZ or BMI z was above 2.

Ethics

Ethics approval for the survey was given by the Regional Committees for Medical Research Ethics (2011/560 REK Sør-Øst). Written informed consent was provided by the mothers on behalf of themselves and their children. All aspects of the study agreed with the latest version of the Helsinki Declaration.

Statistics

Normally distributed data were presented as mean \pm SD. Non-normally distributed data were presented as median and 25th–75th percentiles (p25–p75). Due to the skewed distribution, non-parametric tests were used for two-sided

tests of differences between groups (Mann–Whitney U test). The UIC among children was used as dependent variable in linear regression analyses. Because of skewed distribution, UIC was log₂-transformed. Background characteristics (from Table 1) and dietary variables (from Table 4) were assessed for associations in simple linear models. All variables with an association ($p < 0.20$) were selected for the preliminary multiple model, which included the following: iodine supplements during pregnancy, high consumption of fish, high consumption of fish and yoghurt, high consumption of porridge. By backwards stepwise selection conducted manually, variables with a significant association at $p \leq 0.05$ were included in the final model. Analysis of the residuals was performed to examine the fit of the model.

Results

Background characteristics of mothers and toddlers are presented in Table 1. The distribution of participants between different geographic regions in Norway was quite even. Mean age among the mothers was 30 years, and 82% had higher education at university level. The gender distribution among the toddlers was even, with 52% boys and 48% girls. Almost 10% of the toddlers were still breastfed, 67% had received breast milk previously, while 4.6% had never been breastfed. Only 0.7 and 5.3% were wasted and overweight, respectively, according to weight-for-length z -scores. In total, 60.8% of the toddlers received dietary supplements, and cod liver oil was the most commonly used supplement.

Table 2 presents the UIC among the toddlers in different geographical regions of Norway and across all areas. The median UIC (p25–p75) was 129 (81–190) $\mu\text{g/L}$. As indicated by Fig. 1, 34% had UIC below $100 \mu\text{g/L}$, 59% had UIC between 100 and $200 \mu\text{g/L}$ and 7% had UIC above $300 \mu\text{g/L}$. There were no significant or substantial differences in UIC between different geographical regions or genders. The children who had never been breastfed had higher median UIC ($149 \mu\text{g/L}$) than children who were no longer breastfed. The children who were still breastfed had a median UIC of $117 \mu\text{g/L}$; however the differences in UIC between breastfeeding statuses were not statistically significant. Children who were attending kindergarten had similar median UIC as children who were not attending kindergarten.

Intake frequencies of iodine-rich foods are shown in Table 3. Yoghurt was commonly consumed among the toddlers; however, 22% were given yoghurt ≤ 1 time/week. About two-thirds of the children were given porridge, either industry manufactured or homemade ≤ 1 time/week. About 80, 70, and 80% of the children were given fatty fish, lean fish, or fish products for dinner ≤ 1 time/week, respectively. Baby food with fish was not commonly consumed, with 95% in the category of less than or equal to

Table 1. Characteristics of Norwegian mothers and toddlers 18 months of age

Characteristics of mothers	(n = 416)	Characteristics of toddlers	(n = 416)
Age, years	30.3 ± 4.7	Boy	217 (52.2)
BMI, kg/m ^{2a}	23.8 ± 4.5	Girl	198 (47.6)
<18.5	15 (3.6)	Never been breastfed	19 (4.6)
18.5–24.9	233 (56.9)	Stopped breastfeeding	279 (67.1)
≥25	101 (24.3)	Still breastfed	41 (9.9)
Education level		Breastfeeding frequency per 24 h ^c	
Primary and secondary school	7 (1.7)	1 time	6 (14.6)
High school	67 (16.2)	2–3 times	25 (61.0)
<4 years of university ^b	167 (40.1)	≥4 times	10 (24.4)
≥4 years of university ^b	174 (41.8)	Weight-for-length/height, z-score	0.6 ± 1.0
Work situation		<-2 (wasted)	3 (0.7)
Work full-time	319 (76.7)	>2 (overweight)	22 (5.3)
Work part-time	29 (7.0)	BMI-for-age, z-score	0.5 ± 1.01
Student	58 (13.9)	<-2 (underweight)	5 (1.2)
Unemployed	9 (2.2)	>2 (overweight)	21 (5.0)
Geographic region		Supplement use (all types) weekly	253 (60.8)
Mid-Norway	134 (32.2)	Cod liver oil	151 (36.3)
North Norway	80 (19.2)	Vitamin D drops	84 (20.2)
Western Norway	89 (21.4)	Omega-3	19 (4.6)
Eastern Norway	112 (26.9)	Multivitamin mixture	40 (9.6)
Use medication for thyroid disorder	15 (3.6)	Iron	1 (0.2)
Used iodine supplements during pregnancy	91 (21.9)	Other	14 (3.4)

Values are presented as mean ± SD and n (%).

^aBody mass index before pregnancy.

^bUniversity or university college.

^cBreastfeeding frequency among children still breastfed (n = 41). Missing values: 67 missing from women's BMI; 1 missing from mother's education; 1 missing from geographic area; 1 missing from use of medication for thyroid disorder; 93 missing from iodine supplements during pregnancy; 1 missing from tobacco use in pregnancy; 1 missing from work situation; 1 missing from gender of child; 77 missing from breastfeeding status; 21 missing from anthropometric measures of children; 90 missing from supplement use in children.

Table 2. Urinary iodine concentration (UIC) among Norwegian toddlers 18 months of age by different geographical regions and characteristics (n = 416)

	UIC (µg/L)				Min	Max
	Median	p25–p75	Mean	SD		
Total (n = 416)	129	81–190	148	97	8	688
Gender						
Boys (n = 217)	139	83–258	147	95	12	687
Girls (n = 198)	128	75–199	150	100	8	688
Geographic region						
Mid-Norway (n = 134)	125	69–186	138	83	8	426
North Norway (n = 80)	136	94–195	149	83	17	349
Western Norway (n = 89)	144	88–220	170	125	14	688
Eastern Norway (n = 112)	125	75–182	143	95	14	515
Breastfeeding status						
Never been breastfed (n = 19)	149	76–212	169	126	24	515
Stopped breastfeeding (n = 279)	130	74–201	146	91	8	539
Still breastfed (n = 41)	117	85–188	144	87	19	422
Kindergarten attendance						
Yes (n = 332)	131	81–190	148	94	8	687
No (n = 68)	126	73–195	148	114	16	688

There were no significant differences in UIC between gender ($p = 0.461$), geographic areas ($p = 0.321$), breastfeeding status ($p = 0.854$), or kindergarten attendance ($p = 0.311$) tested by Kruskal–Wallis test/Mann–Whitney U test.

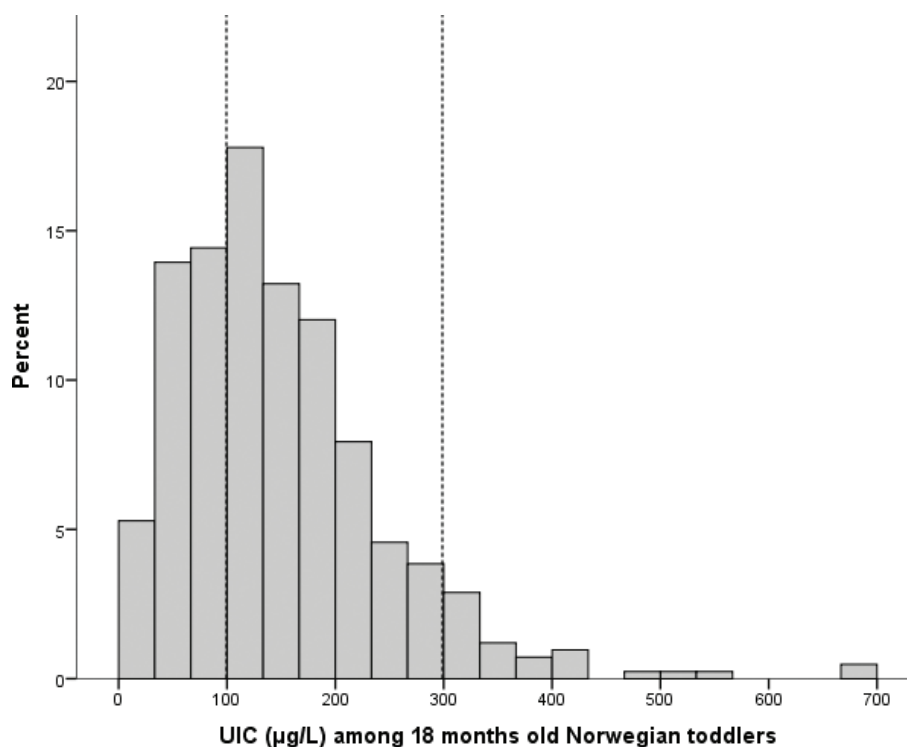


Fig. 1. Distribution of urinary iodine concentration (UIC) among Norwegian children 18 months of age: 33% had UIC below 100 µg/L, 59% had UIC between 100 and 299 µg/L, and 7% had UIC above 300 µg/L ($n = 416$).

Table 3. Frequency of intake (times/week) of iodine-rich foods among Norwegian toddlers 18 months of age ($n = 340^a$)

Iodine-rich foods	Never/rarely	1 time per week	2–3 times per week	≥4 times per week
	<i>n</i> (%)	<i>n</i> (%)	<i>n</i> (%)	<i>n</i> (%)
Yoghurt	41 (12)	35 (10)	95 (28)	169 (50)
Porridge (industry manufactured)	193 (57)	28 (8)	37 (11)	82 (24)
Porridge (homemade)	147 (43)	85 (25)	62 (18)	46 (14)
Fatty fish, dinner	69 (20)	202 (59)	67 (20)	2 (1)
Lean fish, dinner	80 (19)	221 (53)	39 (12)	0
Fish products, dinner	55 (16)	225 (66)	55 (16)	5 (2)
Baby food with fish (industry manufactured)	296 (87)	28 (8)	15 (4)	1 (0.3)
Fatty fish, spread	171 (50)	64 (19)	64 (19)	41 (12)
Lean fish, spread	141 (42)	78 (23)	87 (26)	34 (10)
Eggs	86 (32)	96 (36)	63 (24)	22 (8)

Values given in *n* (%) within participants with dietary intake category.

^a $n = 340$ for all foods except eggs where $n = 267$.

once a week. Lean fish products such as caviar and fishcakes and fatty fish products such as mackerel or salmon were consumed as bread spread among 31 and 36% 2–3 times/week or more frequently, respectively, while the rest consumed fish as bread topping ≤ 1 time/week. Sixty-eight percent consumed eggs less than or equal to once a week.

UIC according to low/medium and high consumption frequencies of iodine-rich foods is shown in Table 4. There

were no substantially or statistically significant differences in UIC between the different consumption categories for any of the foods. There were quite a few children with a high consumption frequency of fish (20%). Yoghurt was more frequently consumed, and 50% had a high intake. Only 12% had a high frequency in intake of both fish and yoghurt. Industry-manufactured porridge is enriched with iodine in Norway; nevertheless, there were no difference in

Table 4. Urinary iodine concentration (UIC) among Norwegian toddlers 18 months of age with low/medium consumption frequency and high consumption frequency of iodine-rich foods ($n = 340$)

	UIC ($\mu\text{g/L}$)			
	Low/medium consumption		High consumption ^a	
	Median (p25–p75)	n	Median (p25–p75)	n
Fish	134 (83–200)	271	117 (56–200)	69
Yoghurt	123 (79–200)	171	132 (75–200)	169
Fish and yoghurt	131 (81–200)	298	117 (55–198)	42
Porridge, industry-manufactured	129 (81–193)	258	123 (55–208)	82
Porridge, homemade	129 (76–205)	294	119 (73–185)	46

Values given as median (p25–p75).

^aFish: Lean fish or fish products for dinner at least 2–3 times/week, and lean fish or fatty fish as bread topping at least 4–6 times/week. Yoghurt: at least 4–6 times/week. Fish and yoghurt: both intake of fish and yoghurt was high. Porridge (homemade or industry-manufactured): at least 4–6 times/week. Differences in UIC between consumption frequencies were tested by Mann–Whitney U test for each of the food groups. None were statistically significant.

Table 5. Estimated habitual iodine intake among non-breastfed Norwegian toddlers 18 months of age in different geographical regions of Norway ($n = 232^a$)

	Estimated habitual iodine intake ($\mu\text{g/day}$)					
	Median	p25–p75	Mean	SD	Min	Max
Total ($n = 232$)	109	101–117	110	13	82	157
Geographic region						
Mid-Norway ($n = 76$)	110	101–116	109	11	90	157
North Norway ($n = 44$)	105	97–120	105	12	84	149
Western Norway ($n = 51$)	107	101–118	109	13	82	138
Eastern Norway ($n = 61$)	113	102–124	114	14	88	145

^a149 missing from dietary data and 35 excluded as they were still breastfed. Iodine intake from milk and cheese have been estimated based on data from 2-year-old children (18) and were estimated to contribute 79 μg iodine/day.

median UIC between the group who received homemade porridge and those who received industry-manufactured porridge.

All the dietary variables among children included in Table 4, as well as background characteristics of the mothers and children, were tested for associations in linear regression models. None of the food consumption variables or background characteristics for mothers or children had a significant association with the children's UIC. Table 5 shows the estimated habitual iodine intake from the main dietary iodine sources (yoghurt, milk, cheese, fish/fish products, porridge, eggs, butter/margarine) among non-breastfed children 18 months of age in Norway. Estimated median (p25–p75) habitual iodine intake was 109 (101–117) $\mu\text{g/day}$ for all children across geographic regions (where the estimated iodine contribution from milk and cheese is included). There was no substantial difference in estimated habitual iodine intake between the different geographic regions. None of the children were below the EAR (65 $\mu\text{g/day}$) or above the UL (180 $\mu\text{g/day}$). Estimated iodine intake from milk and

cheese contributed about 72% of the total iodine mean intake, while fish contributed about 12% and other foods about 16%.

Discussion

The Norwegian toddlers in this study had adequate iodine status, as indicated by a median UIC of 129 $\mu\text{g/L}$, which is above the WHO cutoff of 100 $\mu\text{g/L}$. This finding was supported by the estimated habitual iodine intake, which was 109 $\mu\text{g/day}$. None of the children had an estimated habitual iodine intake below the EAR of 65 $\mu\text{g/day}$ or above the UL of 180 $\mu\text{g/day}$. There were no substantial differences in either UIC or iodine intake between different geographic areas of Norway. These findings are in line with the local small-scale Norwegian studies among toddlers with cow's milk protein allergy and young children presented in the introduction (25–27).

Infant formula is enriched with iodine in Norway, and the average iodine content of several products of prepared formula intended for consumption from 6 months age, using data from the food composition

table, is 15 µg/100 g (29). A recent study among lactating Norwegian women found that the median iodine concentration in breast milk was 68 µg/L (7 µg/100 g) (20), about half of the iodine content found in formula. The children who were never breastfed might still receive formula at 18 months of age, which could explain why the median UIC was highest in this group. A correlation with UIC and use of infant formula has been reported by others (35, 36). Similar results to ours were also found in the mentioned study of 57 infants under the age of 2 with cow's milk protein allergy, where the breastfed children had lower UIC than the children who received formula or were weaned (27).

Intake of milk, formula, and cheese was not recorded in this study, which is a major limitation to the dietary data, as milk is an important component in the diet of young Norwegian children (17, 18). In our study, yoghurt was the most frequently consumed iodine-rich food. Fish and fish products were not as frequently consumed and about 52% consumed fish or fish products (all types) for dinner no more than once a week and 42% as bread spread no more than once a week (data not shown). Similar results were found in a Norwegian study among preschool children (4–6 years of age); however, the consumption of fish as bread spread was higher than in our study (26). Portion sizes were not registered in this study; however data from all the Nordic countries suggest that fish consumption is generally low among preschool children, including Norway (37). This is in line with our findings, where the majority had an intake below the recommendation for 2-year-old children (38). We did not find any substantial difference in UIC between different consumption frequencies of yoghurt, fish, porridge, or eggs, which was in line with the findings from the regression model where none of the dietary intake variables were associated with UIC. This suggests that milk probably made a large contribution to the total iodine intake among the children in this study. Milk as an important contributor to young children's iodine status in Norway has also been found by others (25). Recent studies suggest that pregnant and lactating women in Norway have mild to moderate iodine deficiency (20–23). Others have also found adequate iodine status among children, while mothers from the same population were iodine deficient (39–41). In line with our findings, this has been suggested to be caused by a relatively higher consumption of milk among children (25, 39). On the other hand, as pointed out by Trøan et al., children with a high milk consumption may be at risk of excessive iodine intakes in Norway as the iodine content of milk is relatively high (42).

The median estimated habitual iodine intake was lower than the median UIC. There are several challenges related

to dietary assessment, in addition to the mentioned limitation of using extrapolated intake values for milk and cheese. Only the main dietary iodine-containing food items were included in the estimated habitual intake, and missed sources (e.g. vegetables, meat, and bread) cannot be ruled out. Portion sizes from a national survey among 2-year-old children were used. As dietary habits rapidly change in the weaning period (43), the portion sizes may not be accurate for toddlers 18 months of age. Also, most toddlers in this study were attending kindergarten (79.8%, data not shown), which may further complicate dietary assessment as the parents have less control of food consumption. Nevertheless, the estimated habitual iodine intake indicated sufficient iodine status in this age group, which was in line with the WHO epidemiological criteria for assessing iodine nutrition by median UIC. Further, the estimated habitual iodine intake allows one to assess the iodine status at an individual level, as opposed to the UIC, which provides valuable information. None of the children had an estimated iodine intake below the EAR or above the UL.

Conclusion

Iodine is a crucial nutrient during the first 1,000 days of life (44), and children under 2 years of age have been identified as a particularly vulnerable group for inadequate iodine intake by the WHO (31). Thus, the iodine status among young children should be carefully monitored. This study showed that the iodine status among 18-month-old toddlers was sufficient. Further, milk seemed to be the major iodine-contributing food item among these children, and the intake of fish and enriched porridge was low. Children with low intake of milk could therefore potentially be at risk of insufficient iodine intake in Norway.

Acknowledgements

We are grateful to all the families that participated in the Little in Norway study and all research assistants at the public health clinics. A special warm thanks to Unni Tranaas Vannebo for her positive and enthusiastic engagement in organizing the project data collection. Thanks to Anne Karin Syversen for taking care of all the collected biological samples and to Tonja Lill Eidsvik and Berit Solli for technical assistance with the laboratory work. The Research Council of Norway (grant number 196156) and the Norwegian Seafood Research Fund, FHF (grant number 900842) supported the work.

Conflict of interest and funding

The authors declare no conflict of interest. The Research Council of Norway (grant number 196156) and the Norwegian Seafood Research Fund, Fiskeri og Havbruksnæringens Forskningsfond (grant number 900842) supported the work.

References

- Zimmermann MB, Jooste PL, Pandav CS. Iodine-deficiency disorders. *Lancet* 2008; 372(9645): 1251–62. [https://doi.org/10.1016/S0140-6736\(08\)61005-3](https://doi.org/10.1016/S0140-6736(08)61005-3).
- Zimmermann BM. The role of iodine in human growth and development. *Semin Cell Dev Biol* 2011; 22(6): 645–52. <https://doi.org/10.1016/j.semcdb.2011.07.009>.
- Brent GA. Mechanisms of thyroid hormone action. *J Clin Invest* 2012; 122(9): 3035–43. <https://doi.org/10.1172/JCI60047>.
- Bernal J. Thyroid hormones and brain development. *Vitam Horm* 2005; 71: 95–122. [https://doi.org/10.1016/S0083-6729\(05\)71004-9](https://doi.org/10.1016/S0083-6729(05)71004-9).
- Walker SP, Wachs TD, Grantham-McGregor S, Black MM, Nelson CA, Huffman SL, et al. Inequality in early childhood: risk and protective factors for early child development. *Lancet* 2011; 378(9799): 1325–38. [https://doi.org/10.1016/S0140-6736\(11\)60555-2](https://doi.org/10.1016/S0140-6736(11)60555-2).
- Andersson M, Karumbunathan V, Zimmermann MB. Global iodine status in 2011 and trends over the past decade. *J Nutr* 2012; 142(4): 744–50. <https://doi.org/10.3945/jn.111.149393>.
- IGN. Iodine Global Network, 2016. Annual Report. Zürich, Switzerland: Iodine Global Network; 2016.
- Lazarus JH. Iodine status in Europe in 2014. *Eur Thyroid J* 2014; 3(1): 3–6. <https://doi.org/10.1159/000358873>.
- Nyström HF, Brantsæter AL, Erlund I, Gunnarsdóttir I, Hulthén L, Laurberg P, et al. Iodine status in the Nordic countries – past and present. *Food Nutr Res* 2016; 60(1): 31969. <https://doi.org/10.3402/fnr.v60.31969>.
- Bath SC, Steer CD, Golding J, Emmett P, Rayman MP. Effect of inadequate iodine status in UK pregnant women on cognitive outcomes in their children: results from the Avon Longitudinal Study of Parents and Children (ALSPAC). *Lancet* 2013; 382(9889): 331–7. [https://doi.org/10.1016/S0140-6736\(13\)60436-5](https://doi.org/10.1016/S0140-6736(13)60436-5).
- Manousou S, Dahl L, Heinsbaek Thuesen B, Hulthén L, Nystrom Filipsson H. Iodine deficiency and nutrition in Scandinavia. *Minerva Med* 2017; 108(2): 147–58. <https://doi.org/10.23736/S0026-4806.16.04849-7>.
- Torlinska B, Bath S, Janjua A, Boelaert K, Chan S-Y. Iodine status during pregnancy in a region of mild-to-moderate iodine deficiency is not associated with adverse obstetric outcomes: Results from the Avon Longitudinal Study of Parents and Children (ALSPAC). *Nutrients* 2018; 10(3): 291. <http://dx.doi.org/10.3390/nu10030291>.
- WHO. Assessment of iodine deficiency disorders and monitoring their elimination. A guide for programme managers. Geneva, Switzerland: World Health Organization, International Council for Control of Iodine Deficiency Disorders, United Nations Children's Fund; 2007.
- Dahl L, Meltzer HM. The iodine content of foods and diets: Norwegian perspectives. In: Preedy VR, Burrow GN, Watson RR, eds. *Comprehensive handbook of iodine. Nutritional, biochemical, pathological and therapeutic aspects*. London: Academic Press; 2009, pp. 345–52.
- Nerhus I, Wik Markhus M, Nilsen BM, Øyen J, Maage A, Ødegård ER, et al. Iodine content of six fish species, Norwegian dairy products and hen's egg. 2018; p. 62. Available from: <https://dx.doi.org/10.29219/fnr.v62.1291> [cited 25 May 2018].
- Meltzer HM, Torheim LE, Brandsæter AL, Madar A, Abel MH, Dahl L. Risiko for jodmangel i Norge. Identifisering av et akutt behov for tiltak. Oslo, Norway: Nasjonalt råd for ernæring; 2016.
- Lande B, Helleve A. Amming og spedbarns kosthold. Landsomfattende undersøkelse 2013. Oslo: The Norwegian Directorate of Health; 2013.
- Kristiansen AL, Frost AL, Lande B. Diet among 2 year olds. National dietary survey – Småbarnskost. Oslo, Norway: The Norwegian Directorate of Health; 2009.
- Nordic Council of Ministers. *Nordic Nutrition Recommendations 2012: integrating nutrition and physical activity*. 5 ed. Copenhagen: Nordisk Ministerråd; 2014, 627 p. <http://dx.doi.org/10.6027/Nord2014-002>.
- Henjum S, Lilleengen AM, Aakre I, Dudareva A, Gjengedal ELF, Meltzer HM, et al. Suboptimal iodine concentration in breastmilk and inadequate iodine intake among lactating women in Norway. *Nutrients* 2017; 9(7): 643. <https://doi.org/10.3390/nu9070643>.
- Brantsæter AL, Abel MH, Haugen M, Meltzer HM. Risk of suboptimal iodine intake in pregnant Norwegian women. *Nutrients* 2013; 5(2): 424–40. <http://dx.doi.org/10.3390/nu5020424>.
- Henjum S, Aakre I, Lilleengen A, Garnweidner-Holme L, Borthne S, Pajalic Z, et al. Suboptimal iodine status among pregnant women in the Oslo Area, Norway. *Nutrients* 2018; 10(3): 280. <http://dx.doi.org/10.3390/nu10030280>.
- Dahl L, Wik Markhus M, Sanchez P, Moe V, Smith L, Meltzer H, et al. Iodine Deficiency in a study population of Norwegian pregnant women – results from the little in Norway Study (LiN). *Nutrients* 2018; 10(4): 513. <https://doi.org/10.3390/nu10040513>.
- Abel MH, Caspersen IH, Meltzer HM, Haugen M, Brandlistuen RE, Aase H, et al. Suboptimal maternal iodine intake is associated with impaired child neurodevelopment at 3 years of age in the Norwegian Mother and Child Cohort Study. *J Nutr* 2017; 147(7): 1314–24. <https://doi.org/10.3945/jn.117.250456>.
- Brantsæter A, Knutsen H, Johansen N, Nyheim K, Erlund I, Meltzer H, et al. Inadequate iodine intake in population groups defined by age, life stage and vegetarian dietary practice in a Norwegian convenience sample. *Nutrients* 2018; 10(2): 230. <https://doi.org/10.3390/nu10020230>.
- Nerhus I, Odland M, Kjelleveid M, Midtbø LK, Markhus MK, Graff IE, et al. Iodine status in Norwegian preschool children and associations with dietary sources of iodine – FINS-KIDS study. *Eur J Nutr* 2018; 1–9. <https://doi.org/10.1007/s00394-018-1768-0>.
- Thomassen RA, Kvammen JA, Eskerud MB, Júlíusson PB, Henriksen C, Rugtveit J. Iodine status and growth in 0–2-year-old infants with cow's milk protein allergy. *J Pediatr Gastroenterol Nutr* 2017; 64(5): 806–11. doi: 10.1097/MPG.0000000000001434.
- Fredriksen E, von Soest T, Smith L, Moe V. Parenting stress plays a mediating role in the prediction of early child development from both parents' perinatal depressive symptoms. *J Abnorm Child Psychol* 2018; 1–6. <https://doi.org/10.1007/s10802-018-0428-4>.
- Norwegian Food Safety Authority, The Norwegian Directorate of Health, University of Oslo. *The Norwegian food composition table*. Oslo, Norway: Norwegian Food Safety Authority, The Norwegian Directorate of Health, University of Oslo; 2011.
- IOM. Reference intakes for vitamin A, vitamin k, arsenic, boron, chromium, copper, iodine, iron, manganese, molybdenum, nickel, silicon, vanadium and zinc: a report of the Panel on Micronutrients, Subcommittees on Upper Reference Levels of Nutrients and Interpretation and Uses of Dietary Reference Intakes, and the Standing Committee on the Scientific Evaluation of Dietary Reference Intakes. Washington, DC: Institute of Medicine; 2001.
- Andersson M, De Benoist B, Delange F, Zupan J, Secretariat W. Prevention and control of iodine deficiency in pregnant

- and lactating women and in children less than 2-years-old: conclusions and recommendations of the technical consultation. *Public Health Nutr* 2007; 10(12): 1606. <https://doi.org/10.1017/S1368980007361004>.
32. WHO. Global database on body mass index. BMI classification: World Health Organization; 2004. Available from: http://apps.who.int/bmi/index.jsp?introPage=intro_3.html [cited 29 May 2018].
 33. WHO. WHO Anthro (version 3.2.2, January 2011) and macros 2011. Available from: <http://www.who.int/childgrowth/software/en/> [cited 20 May 2018].
 34. WHO. WHO Child Growth Standards. Length/height-for-age, weight-for-age, weight-for-length, weight-for-height and body mass index-for-age. Methods and development. Geneva, Switzerland: World Health Organization; 2006.
 35. Skeaff SA, Ferguson EL, McKenzie JE, Valeix P, Gibson RS, Thomson CD. Are breast-fed infants and toddlers in New Zealand at risk of iodine deficiency? *Nutrition* 2005; 21(3): 325–31. <https://doi.org/10.1016/j.nut.2004.07.004>.
 36. Andersson M, Aeberli I, Wüst N, Piacenza AM, Bucher T, Henschen I, et al. The Swiss iodized salt program provides adequate iodine for school children and pregnant women, but weaning infants not receiving iodine-containing complementary foods as well as their mothers are iodine deficient. *J Clin Endocrinol Metab* 2010; 95(12): 5217–24. <https://doi.org/10.1210/jc.2010-0975>.
 37. Fagt S, Gunnarsdottir I, Hallas-Møller T, Helldán A, Ingi Halldorsson T, Knutsen H, et al. Nordic dietary surveys: study designs, methods, results and use in food-based risk assessments. Copenhagen: Nordic Council of Ministers; 2012.
 38. Norwegian Directorate of Health. Norwegian guidelines on diet, nutrition and physical activity. Oslo, Norway: Norwegian Directorate of Health; 2014.
 39. Vandevijvere S, Mourri AB, Amsalkhir S, Avni F, Oyen HV, Moreno-Reyes R. Fortification of bread with iodized salt corrected iodine deficiency in school-aged children, but not in their mothers: a national cross-sectional survey in Belgium. *Thyroid* 2012; 22(10): 1046–53. <https://doi.org/10.1089/thy.2012.0016>.
 40. Andersson M, Berg G, Eggertsen R, Filipsson H, Gramatkovski E, Hansson M, et al. Adequate iodine nutrition in Sweden: a cross-sectional national study of urinary iodine concentration in school-age children. *Eur J Clin Nutr* 2009; 63(7): 828–34. doi: 10.1038/ejcn.2008.46.
 41. Granfors M, Andersson M, Stinca S, Akerud H, Skalkidou A, Poromaa IS, et al. Iodine deficiency in a study population of pregnant women in Sweden. *Acta Obstet Gynecol Scand* 2015; 94(11): 1168–74. <https://doi.org/10.1111/aogs.12713>.
 42. Trøan G, Dahl L, Margrete Meltzer H, Hope Abel M, Geir Indahl U, Haug A, et al. A model to secure a stable iodine concentration in milk. *Food Nutr Res* 2015; 59(1): 29829. <https://doi.org/10.3402/fnr.v59.29829>.
 43. WHO. Guiding principles for complementary feeding of the breastfed child. Geneva, Switzerland: World Health Organization; 2003.
 44. Velasco I, Bath S, Rayman M. Iodine as essential nutrient during the first 1000 days of life. *Nutrients* 2018; 10(3): 290. <http://dx.doi.org/10.3390/nu10030290>.
-
- *Inger Aakre**
Institute of Marine Research
PO. Box 2029 Nordnes
NO-5817 Bergen, Norway
Email: inger.aakre@hi.no

Cholesterol-lowering effects and potential mechanisms of chitooligosaccharide capsules in hyperlipidemic rats

Yao Jiang^{1,2}, Chuhan Fu^{1,2}, Guihua Liu³, Jiao Guo^{2*}, and Zhengquan Su^{1,2*}

¹Guangdong Engineering Research Center of Natural Products and New Drugs, Guangdong Pharmaceutical University, Guangzhou, China; ²Guangdong Metabolic Diseases Research Center of Integrated Chinese and Western Medicine, Key Unit of Modulating Liver to Treat Hyperlipemia SATCM (State Administration of Traditional Chinese Medicine), Guangdong Pharmaceutical University, Guangzhou, China; ³Shenzhen Center for Disease Control and Prevention, Shenzhen, China.

Abstract

Background: Chitooligosaccharide (COS) has shown potential antihyperlipidemic activity in a few studies as a functional food.

Method: We investigated the cholesterol-lowering effect and potential mechanisms of chitooligosaccharide capsules (COSTC) in male SD rats fed a high-fat diet.

Results: COSTC could ameliorate serum lipid levels. Simultaneously, the cholesterol-lowering effect is probably attributed to its role in two pathways: upregulating the gene expression and activity of cholesterol 7 α -hydroxylase (CYP7A1), liver X receptor alpha (LXRA), and peroxisome proliferation activated receptor- α (PPAR α), which facilitates the conversion of cholesterol into bile acid; downregulating the gene expression and activity of enzymes including 3-hydroxy-3-methylglutaryl-coenzyme A reductase (HMGCR) and sterol-responsive element binding protein-2 (SREBP2) and upregulating the low-density lipoprotein receptor (LDLR) to reduce the denovo synthesis of cholesterol.

Conclusion: Studies have suggested that COSTC has potential usefulness as a natural supplement or functional food for preventing and treating hyperlipidemia.

Keywords: *chitosan oligosaccharide; antihyperlipidemic; gene difference expression; high-fat diet; CYP7A1; HMGCR*

With the rapid development of the economy, many people have experienced improvements in living standards, and thus, the proportion of high-fat diet increases with each passing day. The long-term intake of high-fat food disrupts internal lipid metabolism, appearing as a decrease in high-density lipoprotein cholesterol (HDL-C) and an increase in total cholesterol (TC), triglyceride (TG), and low-density lipoprotein cholesterol (LDL-C), eventually resulting in fat accumulation, obesity, and hyperlipidemia (1). Hyperlipidemia is an important risk factor for the development and progression of atherosclerosis and subsequent cardiovascular disease, which is one of the most serious diseases of mankind (2).

In recent decades, seek for new drugs for ameliorating serum lipid profiles (reducing TG and TC levels) and/or targeting lipid metabolic-related factors (3–8), such as CYP7A1, HMGCR, proprotein convertase subtilisin/kexin type 9 (PCSK9), and LDLR, has received

increasing attention. Although lipid-lowering medicines are primarily chemical drugs with good effects on the market, the adverse effects of these chemicals are problematic (9, 10). Given the side effects of the current antihyperlipidemic drugs, the development of natural products as alternative sources of antihyperlipidemic functional foods or agents remains an urgent necessity. Accumulating studies have indicated the significant cholesterol-lowering activities of natural agents, particularly polysaccharides, which have been used in preventing obesity and improving plasma lipids (11–13).

COS is an oligosaccharide easily obtained through acid hydrolysis or enzymatic hydrolysis from chitosan (14, 15). The family of COS compounds which contains between 2 and 10 glucosamine residues that are attached through β -d-(1–4) glycoside linkages have received much attention because of their small molecular weight, good aqueous solubility, and diverse biological activity (16–19). Previous studies have shown that chitosan oligosaccharide with a molecular weight ≤ 1000 Da

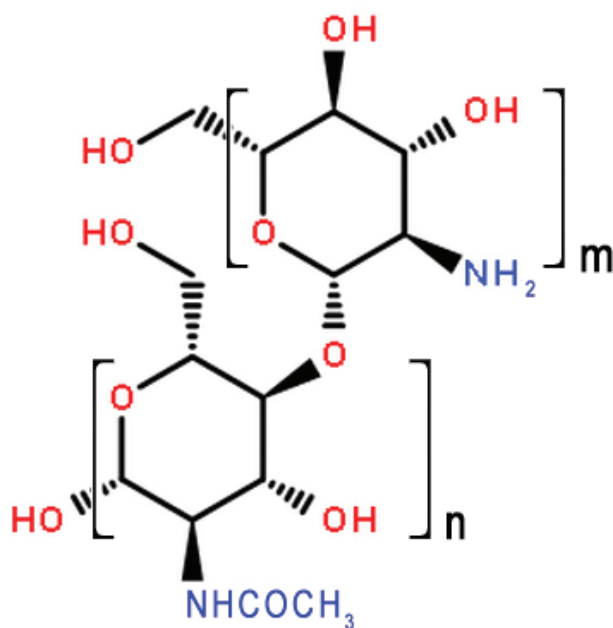


Fig. 1. The molecular structures of COST ($n = 2-10$).

(COST, Fig. 1) shows improvements in lipids and total bile acids (TBA) levels in hyperlipidemic rats (20). Previous studies have also shown that COST has effects on the inhibition of 3T3-L1 preadipocyte differentiation and enhancement of hepatic function (21–24). However, until recently, the in-depth mechanisms of cholesterol-lowering and hepato-protective activities of COST remain unclear. Digital gene expression (DGE) tag profiling is a powerful method for evaluating differences in gene expression with high repeatability in a chosen cell, tissue, organism, or condition. Gene ontology is an internationally accepted gene function analysis that represents the molecular function of the gene, including the biological processes involved and cell location (25).

In this study, we investigated COST capsules (COSTC), prepared according to a previous study (26), which have several advantages: (1) enhancing the stability of COST, which shows strong hygroscopicity and oxidability; (2) boosting the action rate of COST, because the capsule is rapidly dissolved, dispersed, and assimilated in the gastrointestinal tract; and (3) these molecules are easy to identify and administer to most people. Based on the analysis of differential gene expression in the liver tissues of hyperlipidemic rats, which was closely related to the hepatic hyperlipidemic response, we investigated the antihyperlipidemic effects of COSTC using high-fat diet-induced rats, and the results demonstrated that COSTC can ameliorate lipid metabolism and its related complications. However, fewer studies have been reported on the aspect of the antihyperlipidemic mechanism of COSTC in the liver. Therefore, in this study, we demonstrated that COSTC improved lipid metabolism via the upregulation of the gene expression and

activity of CYP7A1, LXRA, and PPAR α , which promotes the conversion of cholesterol into bile acid, downregulating the gene expression and activity of enzymes, including HMGCR and SREBP2, and upregulating LDLR to reduce the *de novo* synthesis of cholesterol. Thus, these results show that COSTC may be a prospective functional food and agent for antihyperlipidemic prevention or treatment.

Materials and Methods

Materials

Commercial samples of COST (Mw \leq 1,000 Da; degree of deacetylation, 95.6%; lot: 160926C) used in this study were obtained from Aokang (Shandong, China). Atorvastatin calcium tablets were supplied from Pfizer Pharmaceutical Company Limited (Daolian, Liaoning, China). Povidone and carboxymethylcellulose sodium were obtained from Tianjin Kernel Chemical Reagent Co., Ltd. (Tianjin, China). TC, TG, HDL-C, LDL-C, aspartate aminotransferase (AST), and alanine aminotransferase (ALT) kits were purchased from BioSino Biotechnology and Science, Inc. (Beijing, China). The COSTC used in this study were prepared in the laboratory.

Animals and Diets

Eighty healthy male Specific Pathogen Free (SPF) Sprague-Dawley rats (weight, 200 ± 20 g; age, 8 weeks; No.44007200034526) were used for the animal experiments and were obtained from the Guangdong Medical Laboratory Animal Center (GMLAC, Guangzhou, China). The animals were fed in an SPF room (temperature: 22–25°C; related humidity: 50–70%; differential pressure: ≥ 10 Pa; 12:12 h light/dark cycle). All animal experimental protocols were approved through the Institutional Animal Care and Use Committee of Guangdong Pharmaceutical University (Guangzhou, China). Water was *arbitrarily* provided throughout the experiments. All animals were fed a normal diet (Guangdong Pharmaceutical University Laboratory Animal Center, Guangzhou, China) for 1 week of adaptive feeding. Subsequently, 10 rats continued to be fed the normal diet as a control group (NF), and the remaining rats were fed high-fat diets to achieve the hyperlipidemia model.

The basic diet was composed of crude protein (20.0%), crude fiber (4.8%), total crude fat (4.3%), moisture (9.7%), calcium (1.19%), phosphorus (0.77%), $Ca^{2+}/P^5 = 1.55$, and crude ash (6.6%). The test results showed that total bacterial count (B10 cfu/g), total molds and yeasts (B10 cfu/g), the *Escherichia coli* count (B3.0 MPN/100 g), and *Salmonella* (not detected) all met the stipulated standards. The high-fat diet included basic feed (52.6%), sucrose (20.0%), lard (15.0%), cholesterol (1.2%), bile salts (0.2%), casein (10%), calcium hydrophosphate (0.6%), and mountain flour (0.4%) in SPF packaging (provided by GMLAC, No. 20160939). After 2 weeks, blood samples were collected from the

orbital vein using a capillary under ether anesthesia. The blood samples were centrifuged (4°C ; $3,500 \text{ r} \times \text{min}^{-1}$; 15 min) to obtain plasma samples to determine serum TG, TC, and LDL-C levels, and in the model group versus control group, the differences in the TC, TG, or LDL-C levels were significant, thereby establishing a judgment model.

Fifty rats were divided into 5 stochastically selected groups ($n = 10$ rats per group): (1) high-fat diet feeding group (HF); (2) high-fat diet feeding administered with atorvastatin ($7 \text{ mg/kg}\cdot\text{day}$) (AVT); (3) high-fat diet feeding administered with a low dose of COSTC ($150 \text{ mg/kg}\cdot\text{day}$) (COSTC-L); (4) high-fat diet feeding administered with an intermediate dose of COSTC ($300 \text{ mg/kg}\cdot\text{day}$) (COSTC-M); and (5) high-fat diet feeding administered with a high dose of COSTC ($600 \text{ mg/kg}\cdot\text{day}$) (COSTC-H) according to a previous study (27). The test samples, dissolved in water, were treated orally through gavage with a simultaneous dose of $1 \text{ mL}/100 \text{ g}$ per day for 6 weeks. The rats in the NF and HF groups were administered an equal capacity of solvent.

Experimental Design

Determination of Food Intake, Weight Gain and Parameters of Viscera

A record of the food intake levels for all rats was maintained daily, and the body weight was measured weekly during the experimental period. All rats obtained food and water *ad libitum*. At the end of experimental period, the rats were fasted for 24 h and subsequently subjected to 1% sodium pentobarbital ($0.5 \text{ mL}/100 \text{ g BW}$) anesthesia, and the blood samples were assembled from the abdominal aorta. Then, the heart, liver, kidneys, epididymal white adipose tissue, and perirenal white adipose tissue of rats were quickly harvested and the samples weighed on electronic scales. The total wet weight of the epididymal and perirenal fat samples was used to measure the body fat ratio. The wet weight of the liver was analyzed to determine the visceral index. The tissues were promptly stored at -80°C until further analysis.

Serum Biochemical Analysis

Blood samples were collected by cardiac puncture and subsequently centrifuged; the serum was stored at 20°C . The concentrations of TG, TC, LDL-C, and HDL-C in the serum were analyzed using commercial assay kits and an automated biochemistry analyzer BC200 instrument (BC200, Beijing Precil Instrument Co. Ltd., Beijing, China) according to the manufacturer's instructions. The activities of plasma ALT and AST were analyzed using ALT and AST assay kits, respectively, and a Mithras LB 940 Multimode Microplate Reader (Berthold Technologies GmbH & Co. KG, Germany).

Histological Staining

The liver, kidney, white epididymal, perirenal, and subcutaneous adipose tissues samples (about 0.5 cm^3) were taken,

washed with pre-cooling saline, placed in the embedding box, labeled with a pencil on the embedding box, and then placed in 12% formaldehyde solution. After immobilization, the ethanol was gradually dehydrated at a concentration of 30–100%. After impregnation, the paraffin was embedded and then sliced on a slicer, and subsequently cut into 3–5- μm -thick sections using a microtome (Leica RM2235; Leica, Heidelberg, Germany). The tissues were stained with hematoxylin and eosin (H&E) and observed under a microscope at $200\times$ magnification.

Digital Gene Expression Tag Profiling

The liver RNA in HF and COSTC groups was extracted using Agilent RNA 6000 Pico kits (Agilent Technologies, Santa Clara, CA, USA). The concentration and quality were detected using an Agilent 2100 instrument (Agilent Technologies, Santa Clara, CA, USA). The Beijing Genomics Institution conducted the DGE. The experiment pipeline is described in Fig. 2. Briefly, the rRNA was

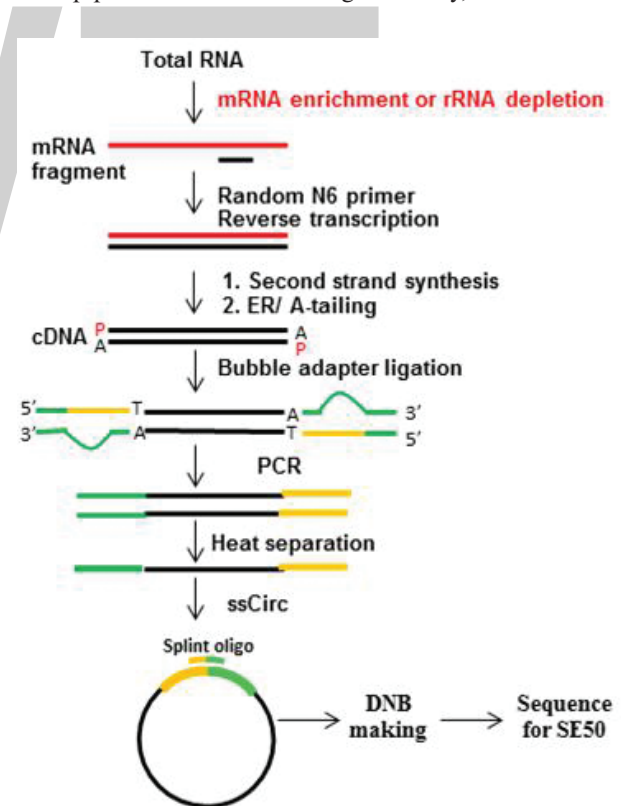


Fig. 2. RNA-Seq experimental process. Hybridize the rRNA with the DNA probe and subsequently digest the DNA/RNA hybrid strand, followed by DNase I digestion to remove the DNA probe. Obtain the target RNA through purification. Fragment the target RNA and perform reverse transcription to double-stranded cDNA (dscDNA) using the N6 random primer. End repair the dscDNA with phosphate at the 5'-end, and add a sticky 'A' tail at the 3'-end. Subsequently, ligate the adaptor at the 3'-end of the dscDNA using a sticky 'T' tail. Amplify the ligation product using two specific primers. Denature the PCR product by heating, and cyclize the single-stranded DNA using a splint oligo and DNA ligase.

hybridized with DNA probe, and the DNA/RNA hybrid strand was digested, followed by a DNase I reaction to remove DNA probe. Subsequently, the target RNA was obtained after purification. The target RNA was fragmented and reverse transcribed to double-stranded cDNA (ds-cDNA) using an N6 random primer. The PCR product was denatured using heat, and the single-stranded DNA was cyclized using a splint oligo and DNA ligase. The prepared library was sequenced, and subsequently, the differentially expressed genes were screened using the NOISeq method and clustering analysis of differentially expressed genes, Gene Ontology.

Quantitative RT-PCR

Total RNA was isolated from the liver tissues of rats using TRIzol reagent (Invitrogen, Inc., USA). Single-stranded cDNA was generated using the PrimeScript™ RT Reagent kit with gDNA Eraser (TaKaRa, Lot: D413KA5332, Shiga, Otsu, Japan) and stored at -20°C. The cDNA products were amplified using real-time RT-PCR and the TaKaRa SYBR Premix Ex Taq™ kit (TaKaRa, Lot: AK7103, Shiga, Otsu, Japan) as well as the Bio-Rad IQ5 real-time PCR system and analysis software (Applied Biosystems, Carlsbad, CA, USA). After initial denaturation at 95°C for 30 s, PCR amplification was performed using 40 cycles at 95°C for 3 s, 60°C for 20 s, and 65°C for 15 s. The nucleotide sequences used for PCR were designed and synthesized at Sangon Biotech Co. Ltd. (Shanghai, China). Beta-actin (β -actin) was used as the internal control (housekeeping gene). The relative quantification of mRNA expression was analyzed using the delta CT method. The following primer pairs were used for PCR: 5'-ACCTGCCGGTACTAGACAGC-3' and 3'-CAGGACATATTGTCGCGCCT-5' for CYP7A1; 5'-CTGCAACGGAGTTGTGGAAG-3' and 3'-TCGCAGCTCAGCA CATTGTA-5' for LXRA; 5'-GCCGACCTGACGAA TTCCAG-3' and 3'-ATCCGACCAGTCACGACAGT-5' for LDLR; 5'-GGAGACCATGGAGACCCTCAC-3' and 3'-AGACAATGGGACCTGGCTGAA-5' for SREBP2; 5'-CCTCCATTGAGATCCGGAGGA-3' and 3'-ACA AAGAGGCCATGCATACGG-5' for HMGCR; and 5'-TCTGAACATTGGCGTTCGCA-3' and 3'-TCCCTCAAGGGGACAACCAG-5' for PPAR α .

Western Blotting

Total proteins were isolated from liver tissues (50 mg) using 1.0 mL of cold RIPA lysis buffer (50 mM Tris, pH 7.4, 150 mM NaCl, 1% Triton X-100, 1% sodium deoxycholate, 0.1% SDS, and protease and phosphatase inhibitor), followed by centrifugation twice at 12,000 \times g for 20 min at 4°C, and the protein concentration was measured using the BCA Protein Assay Kit (Beyotime, Lot: 0907A16, Shanghai, China). The isolated proteins were diluted to the same protein concentrations. The extracted

proteins were diluted to the same protein concentrations. Equal amounts of each protein lysate were electrophoresed via sodium dodecyl sulfate-polyacrylamide gel electrophoresis (SDS-PAGE) and electrophoretically transferred onto polyvinylidene difluoride (PVDF) membranes (Millipore Corp., Billerica, MA, USA). After sealing with 5% bovine serum albumin (BSA) or skim milk powder in TBST buffer (25 mM Tris, 150 mM NaCl, and 0.05% Tween 20, pH 7.2–7.5), the membranes were hatched with primary antibodies, including HMGCR, CYP7A1, SREBP2, LDLR, LXRA, and PPAR α polyclonal antibodies (Proteintech, Inc., Wuhan, China), and rabbit anti- β -actin (Biosynthesis Biotechnology Co., Ltd., Beijing, China), followed by the secondary antibody, goat anti-rabbit immunoglobulin G/horseradish peroxidase (Goat Anti-rabbit IgG/HRP, Biosynthesis Biotechnology Co., Ltd., Beijing, China). Subsequently, the protein bands were visualized using enhanced chemiluminescence (ECL, Millipore Corp., Billerica, MA, USA) and detected using a chemiluminescence imaging system (Sage Creation, Beijing, China). Lane 1D gel image software (Sage Creation, Beijing, China) was used to quantify the gray scale of protein bands using the value of the β -actin band as a reference.

Statistical Analysis

All data are expressed as the means \pm standard deviation (SD). Differences between groups were compared using a one-way ANOVA test followed by Duncan's multiple comparison test using SPSS software (SPSS Inc., Chicago, IL, USA).

Results

Food Intake, Body Weight Gain, Body Fat Ratio, and Liver Index

To evaluate the effect of COSTC on cholesterol lowering, the 6-week food intake and body weight gain of rats were analyzed, and the results are shown in Fig. 3. As shown in Fig. 3a, there was no significant difference among the HF, AVT and COSTC groups, indicating that COSTC exerted no influence on the appetite of rats. The result of COSTC on weight gain is revealed in Fig. 3b. In contrast to the HF group, rats administered COSTC-H ($p < 0.01$), COSTC-M, and COSTC-L ($p < 0.05$) showed significantly decreased body weight gains in a dose-dependent manner.

The body fat ratio (Fig. 3c) in the HF group was significantly higher than that for the rats in the NF group ($p < 0.01$), demonstrating that the content of white adipose tissue in HF group was high. COSTC dose-dependently inhibited the high lipid diet-induced elevation of fat pad and body fat ratio, particularly in the COSTC-H and COSTC-M groups ($p < 0.01$), showing effects slightly superior to the AVT group.

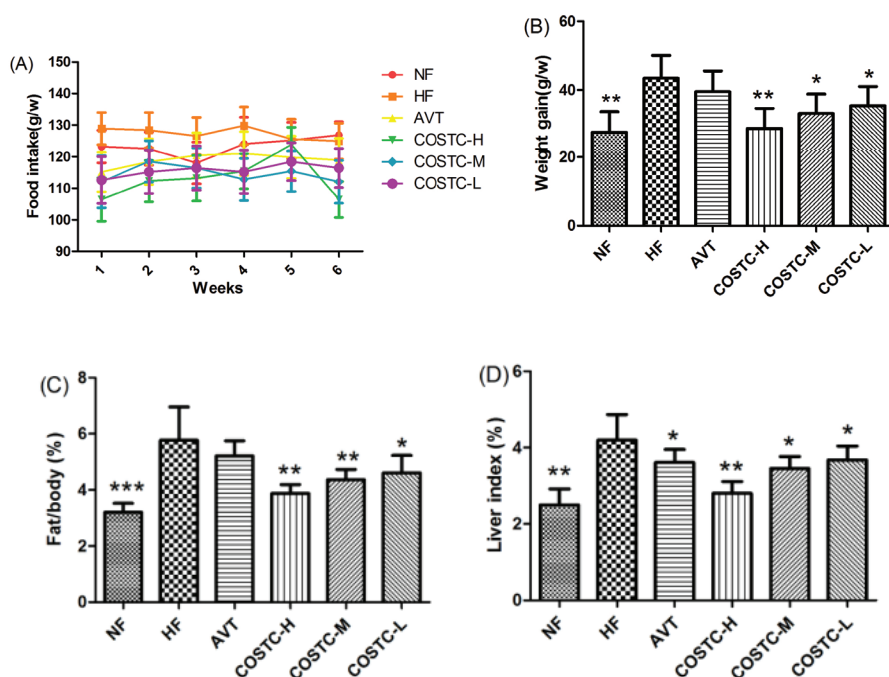


Fig. 3. The main index of COSTC. Changes in the food intake (a), body weight gain (b), body fat ratio (c), and liver index (d) after 6 weeks of treatment. The data are presented as the means \pm SD ($n = 10$). Note: Compared with HF, * $p < 0.05$; ** $p < 0.01$.

The effects of COSTC on liver fat deposition were detected, and the liver indices (liver mass \times 100/body mass) are revealed in Fig. 3d. The liver index of the NF group was markedly lower than that of the HF group ($p < 0.01$), indicating that the livers of the HF group possess a high fat content. The liver index was decreased in a dose-dependent manner after administering different doses of COSTC, and the difference of COSTC-H was significant ($p < 0.01$) compared to the HF group. These results demonstrate that COSTC effectively decreased the body weight gain in high-fat-diet-fed rats via preventing the high-fat diet from enhancing the body fat.

Effect of COSTC on Serum Lipid Levels in Rats

The serum lipid levels of high-fat-diet-fed rats were determined using an automatic biochemical analyzer, and the results are displayed in Fig. 4 and Table 1. In this study, the serum and liver TG, TC, and LDL-C levels in the HF group were significantly higher than those in the NF group ($p < 0.01$, Fig. 4a–d), showing that the rat experimental hyperlipidemic model was successful. Compared to the HF group, the serum levels for COSTC-H, COSTC-M, and COSTC-L treatment groups were significantly decreased by 30.50%, 15.85%, and 13.41% for TC, by 26.26%, 19.55%, and 12.85% for TG and by 24.37%, 15.19%, and 7.91% for LDL-C ($p < 0.05$), respectively. However, treatment did not significantly improve the effect on HDL-C.

The atherogenic index (AI), an indicator of coronary heart disease risk (28), was significantly reduced in the serum of rats fed COSTC-H (67.00%), COSTC-M (58.80%), and COSTC-L (31.20%) than in that of rats fed HF ($p < 0.05$, Fig. 4E). In addition, the treatment group exhibited a markedly reduced AI value than the HF group in a dose-dependent manner ($p < 0.05$), showing that although COSTC did not significantly ameliorate the effect on LDL-C and HDL-C, it did significantly ameliorate their proportion.

Liver injury, or hepatotoxicity, is the main relative factor of hyperlipidemia (29). Additionally, the increased serum activities of AST and ALT, which were specific toxicological indices for liver function test, are observed in the case of liver injury (30). This study revealed that AST and ALT activities in serum were significantly lower in the COSTC group at a dose of 600 and 300 mg/kg/d than in rats in the HF group ($p < 0.05$, Fig. 4f–g), suggesting that COSTC has no toxicity to the liver function and minimizes the damage resulting from high-fat diet. Thus, that COSTC administration had liver protective activity.

Effect of COSTC on Fecal TC, TG, and TBA

The positive charge in the structure of chitosan and COS can vigorously absorb fat, fatty acids (FA), and bile acids (BA), containing a negative charge, which contributes to lowering serum TC and TG (31). Nonetheless, several

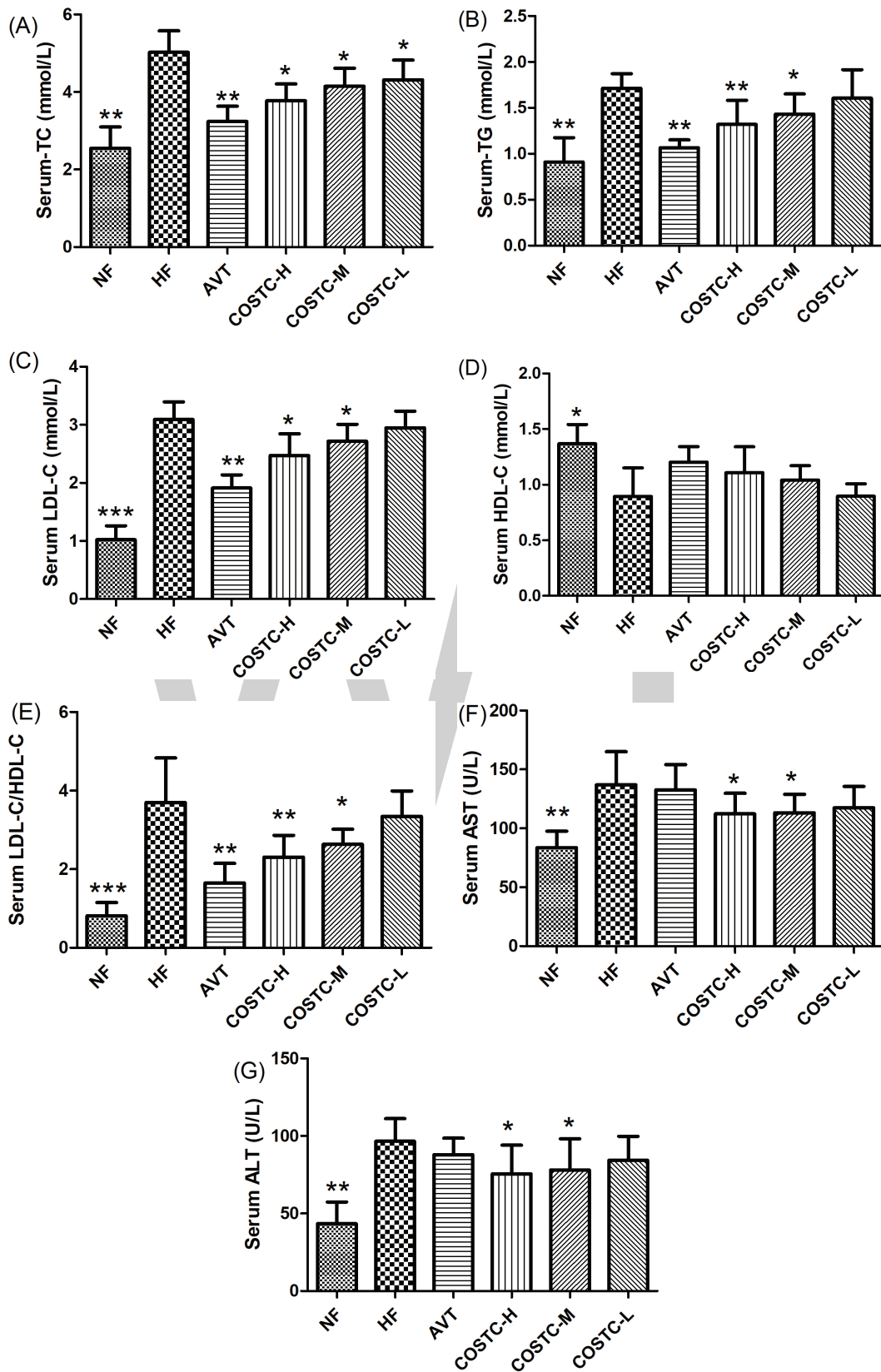


Fig. 4. The serum and liver lipid levels in high-fat diet rats. The effect of COSTC on lipid levels in the serum (a-d), AI in the serum (e), and AST activity and ALT activity in the serum (f-g) after 6 weeks of treatment. The data are presented as the means \pm SD ($n = 10$). Note: Compared with HF, * $p < 0.05$; ** $p < 0.01$.

Table 1. The serum, liver, and fetal lipid levels in high-fat diet rats

Groups	NF	HF	AVT	COSTC-H	COSTC-M	COSTC-L
Serum (mmol/L)						
TC	2.55 ± 0.52**	4.92 ± 0.63	3.24 ± 0.37**	3.77 ± 0.41*	4.14 ± 0.44*	4.26 ± 0.48*
TG	0.91 ± 0.27**	1.79 ± 0.15	1.06 ± 0.08**	1.32 ± 0.6**	1.44 ± 0.22*	1.56 ± 0.29*
HDL-C	1.42 ± 0.26*	0.82 ± 0.28	1.06 ± 0.32	1.56 ± 0.35	1.06 ± 0.29	0.96 ± 0.45
LDL-C	1.03 ± 0.24***	3.16 ± 0.25	1.89 ± 0.22*	2.39 ± 0.32*	2.68 ± 0.28*	2.91 ± 0.28*
AI	0.80 ± 0.53***	5.00 ± 0.83	1.56 ± 0.42**	1.65 ± 0.62**	2.06 ± 0.53*	3.44 ± 0.81*
AST (U/L)	83.06 ± 13.86**	138.22 ± 27.98	134.02 ± 21.13	114.20 ± 16.78*	115.10 ± 15.1*	117.88 ± 18.16*
ALT (U/L)	44.88 ± 13.56**	92.88 ± 11.35	85.52 ± 8.76	74.32 ± 18.16*	77.00 ± 20.14*	79.60 ± 15.59*
Fetal (mg/g)						
TC	5.53 ± 1.01**	10.46 ± 1.48	11.67 ± 0.83	15.63 ± 1.76**	14.38 ± 1.56**	12.75 ± 1.80*
TG	5.40 ± 1.42**	12.58 ± 0.96	13.68 ± 1.11	16.16 ± 2.04*	15.48 ± 2.02*	14.63 ± 2.74*
TBA	1.83 ± 0.53**	3.20 ± 0.91	2.90 ± 0.67	5.55 ± 1.53**	5.13 ± 1.51*	4.68 ± 0.143*

TG, triglyceride; HDL-C, high-density lipoprotein cholesterol; LDL-C, low-density lipoprotein cholesterol; NF, control group; HF, feeding group; TC, total cholesterol; TBA, total bile acids; AVT, atorvastatin. Data are expressed as means ± SD ($n = 10$ per group). Note: Compared with HF; * $p < 0.05$, ** $p < 0.01$, and *** $p < 0.001$.

studies have reported that the mechanism through which COSTC reduces lipid levels is related to change and the regulation of liver lipid metabolism (32). In order to remove excess cholesterol, it must be transported from the peripheral tissue to the liver and intestine, and finally through the feces to the form of BA discharge. Traditionally, the metabolic pathway is thought to be the reverse of the cholesterol transporter or centripetal cholesterol pathway. To determine the effect of the three compounds on the reverse cholesterol transport process, we investigated changes in fecal lipid and BA levels after COSTC administration.

The fecal TC, TG, and TBA levels of tested rats are shown in Fig. 5 and Table 1. TC and TG concentrations in rats fed different doses of COSTC increased in a dose-dependently manner compared with that in the HF groups. The results indicated that COSTC effectually reduces the lipid concentration by promoting the excretion of cholesterol via feces.

Histological Analysis of Different Tissues

The whole liver and the slices of liver sections are displayed in Fig. 6a–b, respectively. The livers in the NF group were bright red in color, smooth in the tunica of tissues, and characterized by sharp edges, supple texture, and small volume. However, the rats' livers in the HF group were intumescent and slightly soft; they became pale, the edges were hypertrophic, and the white fat granules in the surface of the liver were readily observed, suggesting that severe fatty-liver-like illness was developed via consuming high-fat diets in rats. The groups administered COSTC improved the steatosis in hepatocytes for which the color was between bright red and dull pale, and the white fat granules were reduced. For further observation, the

morphology of liver sections in different groups showed no histological abnormalities in the hepatocytes of the NF group with fewer fat droplets, whereas the hepatocytes in the HF group possessed serious fat vacuoles and partly infiltrated the inflammatory cells, further indicating that the rats developed a high degree of steatosis induced by high-fat diet. Different doses of COSTC groups markedly decreased fat vacuoles in hepatocytes with varying degrees, and the infiltration of inflammation was alleviated, particularly the effects observed in the COSTC-H group, whose cell morphology was similar to that in the NF group, which exerted the hepatoprotective effect via efficiently relieving the fatty liver.

The slices of the heart and kidney pathology tissue were displayed in Fig. 6c–d, respectively. The heart striated muscles and myocardial cells in slices from rats in the HF group (Fig. 6c) were disarrayed with the infiltration of inflammatory cells. However, the heart slices showed aligned myocardial cells without enlargement, clear stripes and muscle space, and have no cardiac hypertrophy in the NF and COSTC-treated groups. In Fig. 6d, the kidney slices from rats treated with different doses of COSTC showed an intact glomerular structure. Additionally, the renal capsule, mesangial cells and matrix, capillary basement membrane, and Sertoli cells of rats in the COSTC groups showed no pathological changes, similar to the NF group. These results demonstrated that the COSTC in different doses were not injurious and were nontoxic in heart and kidney samples.

The images of white adipose pathology tissues sections, including perirenal and subcutaneous fatty tissues, were exhibited in Fig. 6e–f, respectively. The perirenal and subcutaneous adipocytes in the HF group are distinctly hypertrophic compared to the NF group. The sizes of adipocytes

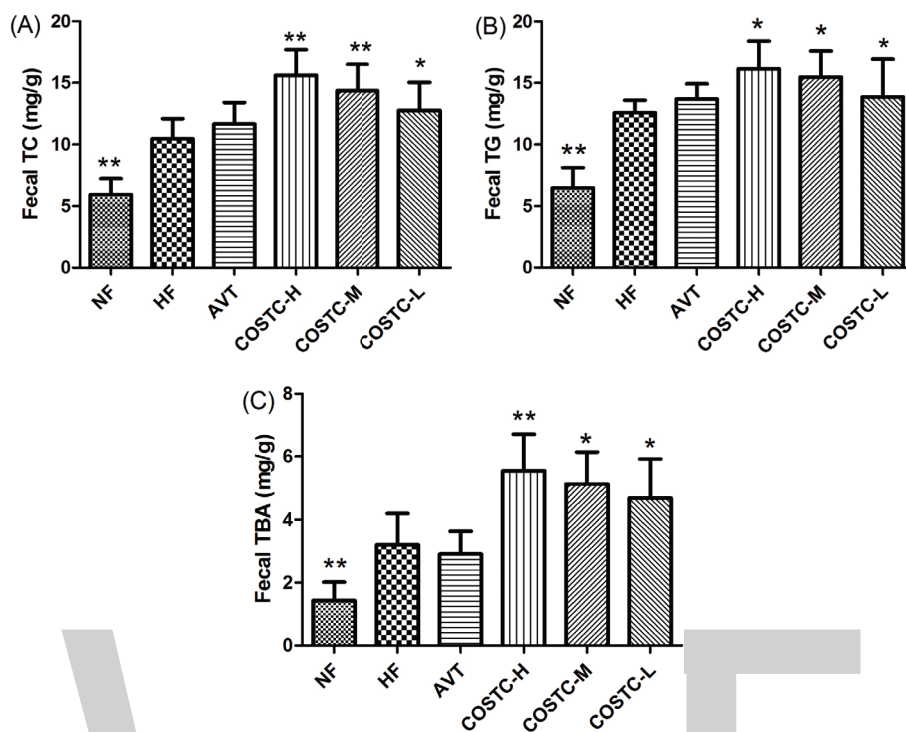


Fig. 5. The fecal levels TC, TG, and TBA fetal in high-fat diet rats. The effect of COSTC on fecal levels of TC (a), TG (b), and TBA (c) after 6 weeks of treatment. The data are presented as the means \pm SD ($n = 10$). Note: Compared with HF, * $p < 0.05$; ** $p < 0.01$.

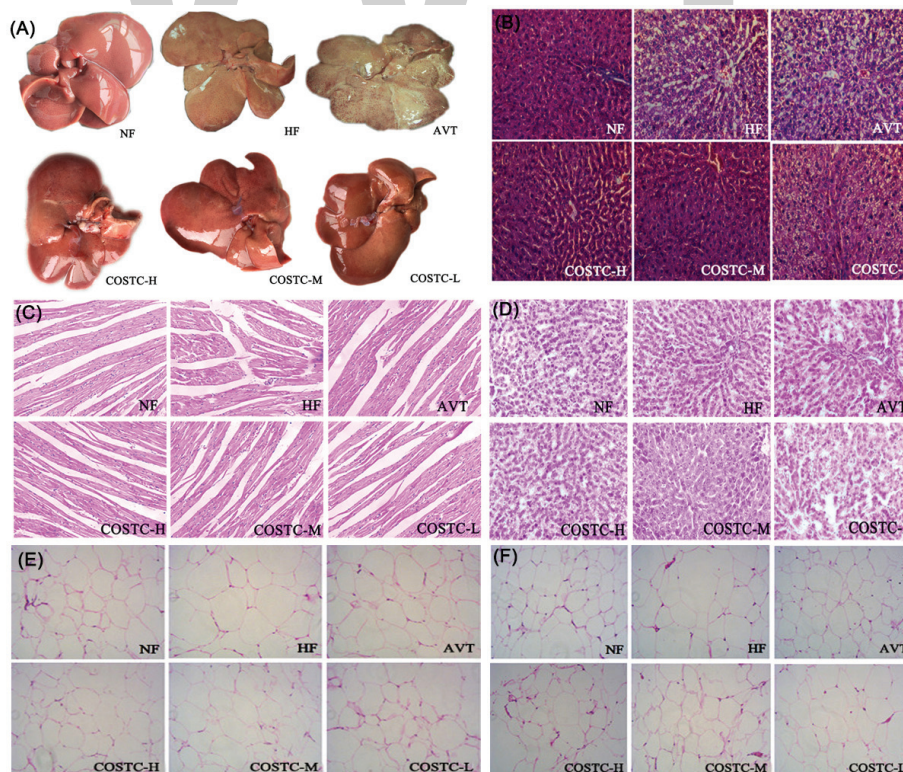


Fig. 6. The whole liver (a), slices of liver (b), heart (c), kidney (d), perirenal adipose tissues (e), and subcutaneous adipose tissues (f) from different groups of rats (200 \times) after 6 weeks of treatment. Tissue sections were stained with hematoxylin and eosin (H&E).

were prominently diminished to different degrees after administering different doses of COSTC, suggesting that COSTC can effectively suppress the growth of white adipose tissues to exert the hyperlipidemia effect.

Differential Gene Expression

RNA quality test results showed that the value of 28S/18S was close to 2, indicating that good RNA integrity was consistent with the requirement to construct a sequencing library. The integrity of each RNA sample (RIN) is satisfactory (date not shown). In Fig. 7a–b, the statistical results of differential gene expression analysis were exhibited. Six hundred and thirty genes were differentially expressed in the COSTC group compared to the HF group. Five hundred and seventeen genes were downregulated, while one hundred and thirteen genes were upregulated. The GO enrichment analysis shown in Fig. 7c–d suggested that differentially expressed genes in the COSTC group compared to the HF group were primarily associated with biological regulation and cellular progress, such as organelle membrane, minute bodies, mitochondria and cytoplasm. Among others, the main molecular functions were steroid dehydrogenation activity, oxidoreductase activity, catalytic activity, ion binding, NADH or NADPH as a donor, and purine nucleotide binding. The enriched genes were primarily involved in biological processes, including fatty acid metabolism, lipid metabolism, steroid metabolism, and small molecule metabolites. The genes expressed of large differences (HF vs. COSTC) are shown in Table 2. Based on data analysis, we selected the critical factors involved in fatty acid and lipid metabolism to explore the lipid-lowering activities of COSTC.

COSTC Inhibits Hepatic Cholesterol Synthesis

The first few genes showing differential expression in fatty acid and lipid metabolism were selected for verification, including HMGCR, SREBP2, and LDLR, which are involved in the regulation of hepatic cholesterol synthesis. Therefore, we next investigated these activities using RT-PCR and western blotting. The experimental results presented in Fig. 8a–g showed that the activity of HMGCR and SREBP2 in livers of hyperlipidemic rats was dramatically lower in hyperlipidemic rats following COSTC administration. In contrast, the activity of LDLR in the livers of hyperlipidemic rats administered COSTC was upregulated compared with the HF group ($p \leq 0.05$). The AVT group showed a similar regulation effect on HMGCR gene expression. Real-time PCR data showed that the gene expression of these modulators in the liver was the same as that of the liver.

COSTC Promotes Hepatic Cholesterol Excretion

The first few genes showing differential expression in fatty acid and lipid metabolism were selected for verification,

including CYP7A1, LXRA, and PPAR α , which are involved in the regulation of hepatic cholesterol excretion. Therefore, we next investigated these activities using RT-PCR and western blotting. The experimental results presented in Fig. 9a–g revealed that the activity of CYP7A1, LXRA, and PPAR α in the liver of high-fat diet rats was upregulated following the administration of COSTC compared with in the HF group ($p \leq 0.05$), although COSTC-L did not show significance. The AVT group did not show similar regulatory effect on the gene expression of CYP7A1, as AVT primarily inhibited HMGCR, playing a role in lipid lowering. Real-time PCR data showed that the gene expression of these modulators in the liver was the same as that of the liver.

Discussion

Previous studies have reported that COS are beneficial in improving plasma lipids and diminishing atherosclerotic risks; as the molecular weight of COS decreases, the biological activity increases (33, 34). In this study, we showed that COSTC administration did not only significantly decrease the serum AST and ALT levels but also reduce the serum TC, TG, and LDLC levels. In addition, we demonstrated that COSTC improved lipid metabolism via upregulating the gene expression and activity of CYP7A1, LXRA, and PPAR α , which promote the conversion of cholesterol into bile acid, downregulating the gene expression and activity of enzymes, including HMGCR and SREBP2, and upregulating the gene expression and activity of LDLR to reduce the *de novo* synthesis of cholesterol.

Hyperlipidemia refers to a condition characterized by high levels of cholesterol in the blood (2). These indicators for the clinical diagnostic criteria of hyperlipidemia were examined in this study. An obvious increase in serum TC, TG, and LDL-C levels and a decrease in HDL-C level were observed in hyperlipidemic rats. The regular administration of different doses of COSTC modified the disorders of serum lipid metabolism in 6 weeks, similar to AVT. It is reported that liver injury, or hepatotoxicity, is the main relative factor of hyperlipidemia. Additionally, increased AST and ALT serum activities, which were specific toxicological indices for liver function test, are observed in liver injury. This study showed that serum AST and ALT activities were obviously decreased in the COSTC group at a dose of 600 mg/kg/d than those in the HDF group ($p < 0.05$), suggesting that COSTC has no toxicity to liver function and minimizes the damage induced by high-fat diet. Thus, COSTC administration showed liver protective activity.

Bile acids are synthesized in the liver and secreted into the small intestine where they promote absorption of cholesterol and fat (35). Apart from reabsorbed bile acids, the residue is excreted into the feces (36, 37). In this study,

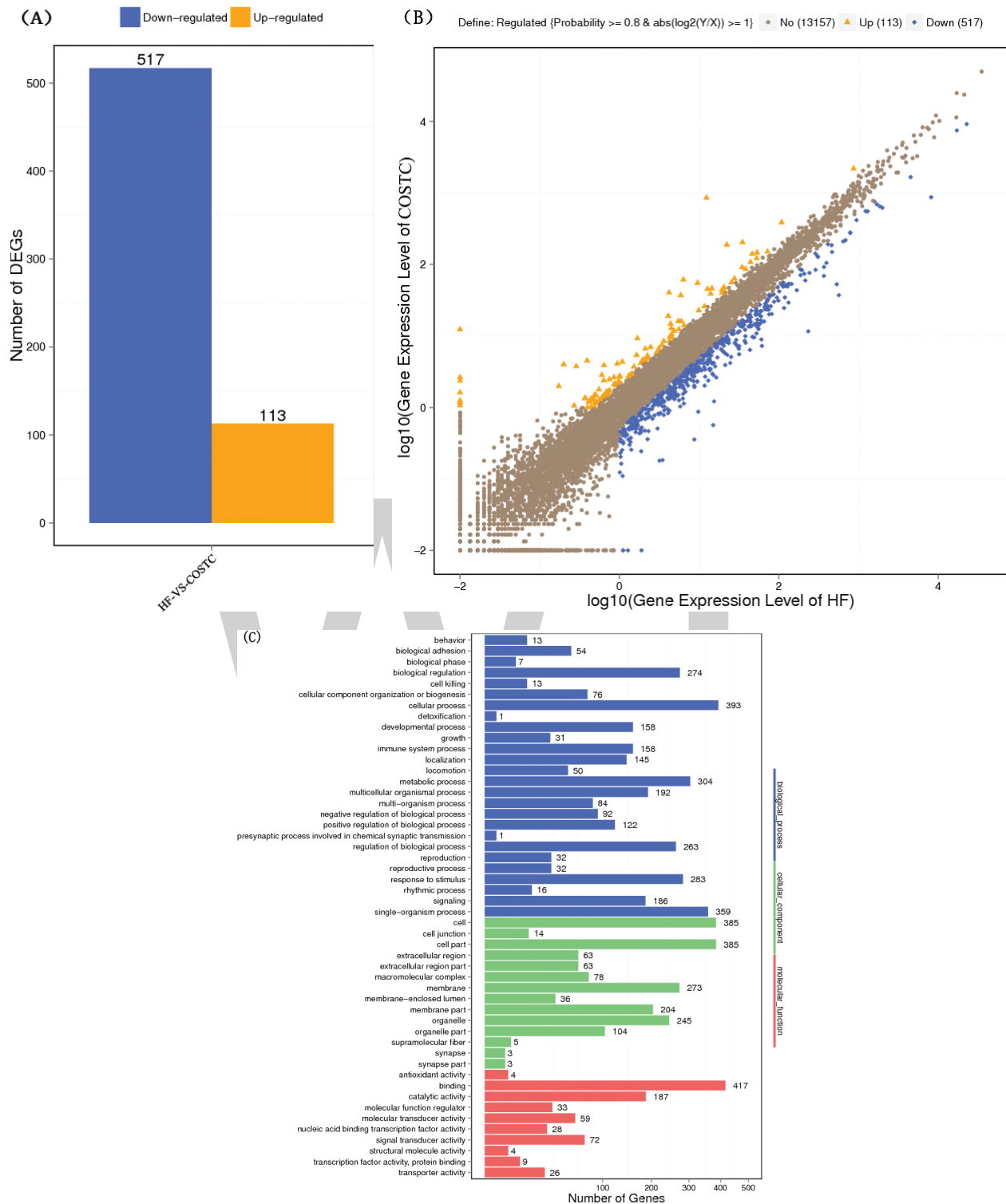


Fig. 7. Differential gene expression analysis (HF vs. COSTC).

the fecal output of total bile acids was increased in groups administrated with COSTC compared to the HF group, indicating the potential of COSTC to promote the conversion of cholesterol into bile acids in the liver and entrap bile acids in the small intestine, which further increases the

excretion of bile acids from feces in addition to the fecal loss of steroids due to reduced enterohepatic recycling. These findings might reflect the potential mechanisms of the cholesterol-lowering effect of COSTC on high-fat-diet-induced hyperlipidemic rats.



Fig. 7. Continued Differential gene expression analysis (HF vs. COSTC).

Table 2. The genes expressed of large differences (HF vs. COSTC)

GeneID	log2 ratio (COSTC/HF)	Upregulation–downregulation (COSTC/HF)	Symbol	GO function or process
25675	0.2244909	Down	HMGCR	GO:0006732;GO:0006694//steroid biosynthetic process;GO:0008203//cholesterol metabolic process;GO:0016114//terpenoid biosynthetic process
691312	10.26795	Up	CYP7A1	GO:0008395//steroid hydroxylase activity; GO:0055092//sterol homeostasis;GO:0050810//regulation of steroid biosynthetic process
100134871	1.8314004	Up	PPAR α	GO:0030492//hemoglobin binding; GO:0022892//substrate-specific transporter activity; GO:0016209//antioxidant activity
100314100	8.0407463	Up	LXR α	GO:0005126//cytokine receptor binding; GO:0033764//steroid dehydrogenase activity, acting on the CH-OH group of donors, NAD or NADP as acceptor; GO:0008203//cholesterol metabolic process
500564	5.163333	Up	LDLR	GO:0004871//signal transducer activity; GO:0060090//binding, bridging;GO:0070325//lipoprotein particle receptor binding;GO:0045309//protein phosphorylated amino acid binding
79451	0.176667	Down	SREBP2	GO:0015248//sterol transporter activity; GO:0046983//protein dimerization activity; GO:0055092//sterol homeostasis;GO:0050810//regulation of cholesterol synthesis process

HMGCR, 3-Hydroxy-3-Methylglutaryl-Coenzyme A Reductase; HMGCR: 3-Hydroxy-3-Methylglutaryl-Coenzyme A Reductase; PPAR α , Peroxisome Proliferation Activated Receptor- α ; LXR α , Liver X Receptor Alpha; LDLR, low-density lipoprotein receptor; SREBP-2, Sterol-Responsive Element Binding Protein-2.

The DGE analysis showed that 630 genes were differentially expressed in the COSTC group compared to the HF group, including 517 downregulated genes and 113 upregulated genes. The GO enrichment analysis showed that the enriched genes were primarily involved in biological processes, including bile acids, inflammation, steroid

metabolism, and β -oxidation of fatty acids. Based on the analysis of differential expression in fatty acid and lipid metabolism, critical differential gene expressions were selected for verification. CYP7A1, a rate-determining enzyme in the conversion of cholesterol to primary bile acids, catalyzes the initial step in cholesterol catabolism

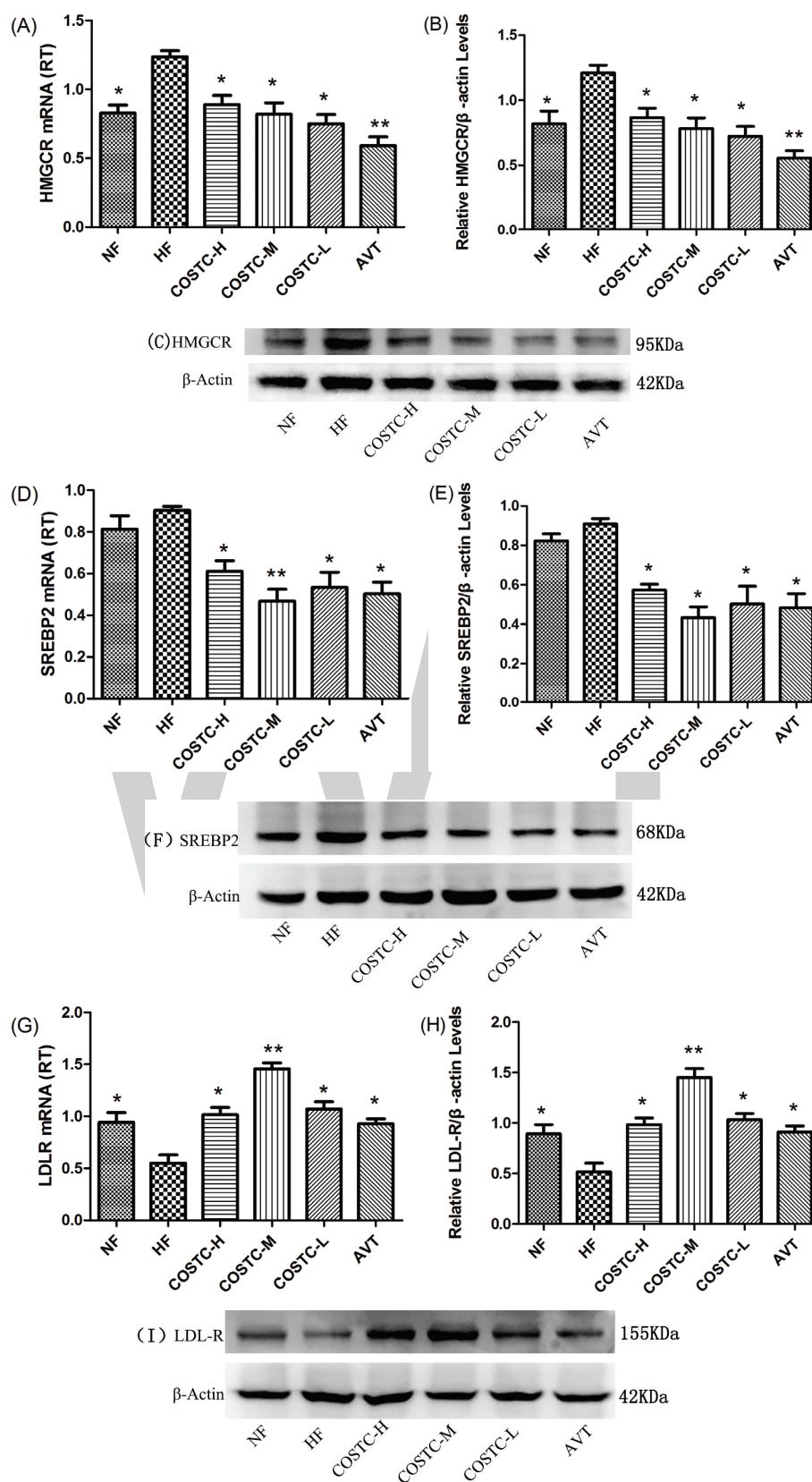


Fig. 8. Effect of COSTC on the mRNA and protein expression of hepatic HMGCR genes (a–c); effect of COSTC on the mRNA and protein expression of hepatic SREBP2 genes (d–f); and effect of COSTC on the mRNA and protein expression of hepatic LDLR genes (g–i). The data are the presented as the means \pm SD ($n = 3$). Note: Compared with HF, * $p < 0.05$; ** $p < 0.01$.

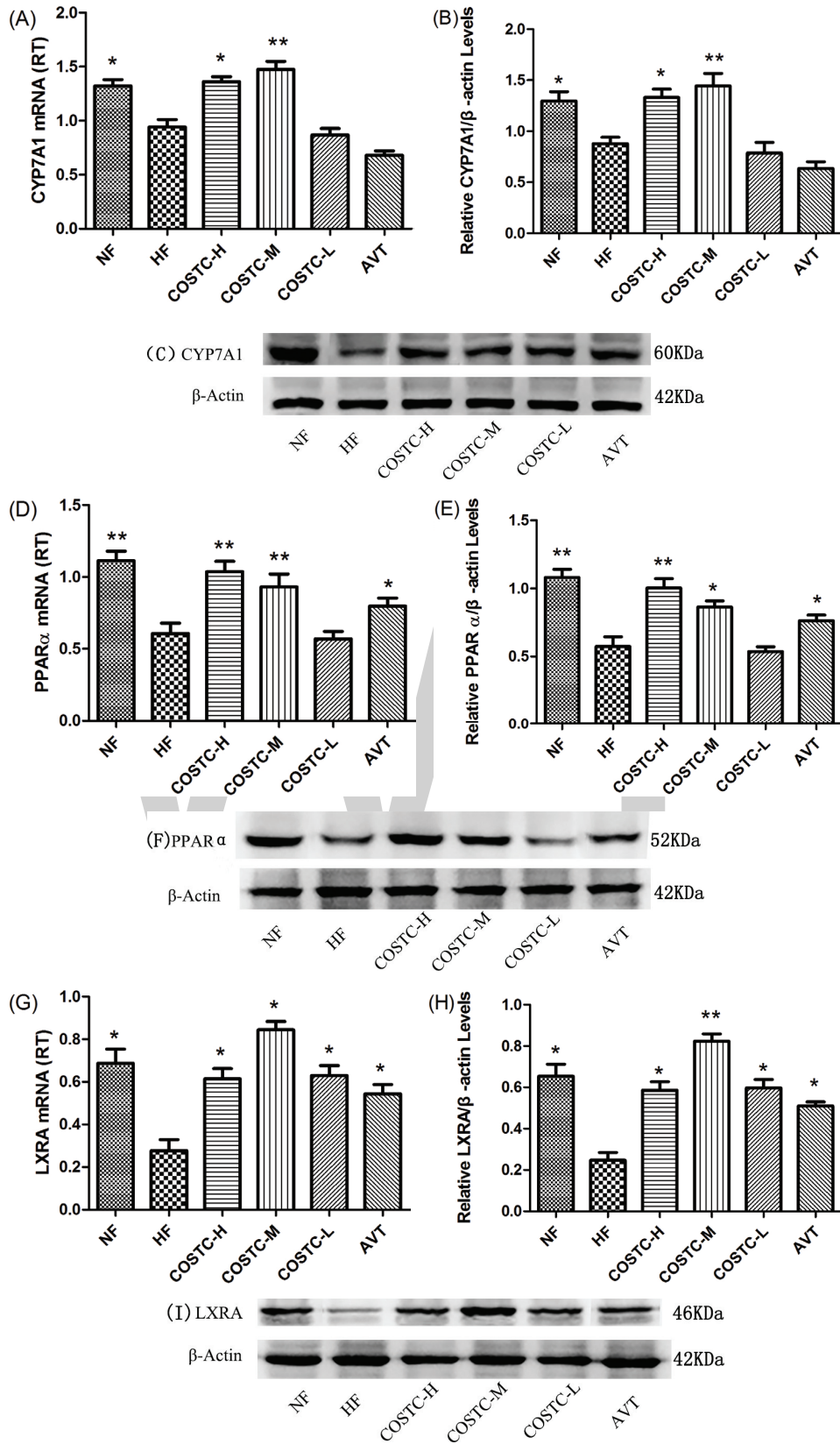


Fig 9. Effect of COSTC on the mRNA and protein expression of hepatic CYP7A1 genes (a-c); effect of COSTC on the mRNA and protein expression of hepatic PPAR α genes (d-f); and effect of COSTC on the mRNA and protein expression of hepatic LXRA genes (g-i). The data are presented as the means \pm SD ($n = 3$). Note: Compared with HF, * $p < 0.05$; ** $p < 0.01$.

and bile acid synthesis (38). Increased bile acid excretion activates CYP7A1, increasing liver cholesterol into bile acid excretion. This leads to a decrease in free cholesterol levels in the liver, which may in turn stimulate LDLR expression. LXRA is a master regulator maintaining the homeostasis of bile acids (39). PPAR α is a nutritional sensor that allows the adaptation of the rates of fatty acid catabolism and lipogenesis (40). SREBP2 is primarily responsible for cholesterol-related gene expression (7). HMGCR is the rate-limiting enzyme of hepatic cholesterol biosynthesis (3). The downregulation of HMGCR and SREBP2 activity will inhibit cholesterol *de novo* synthesis in the liver and thus reduce serum cholesterol levels.

Therefore, in this study, we demonstrated that COSTC improved lipid metabolism via the upregulation of gene expression and activity of CYP7A1, LXRA, and PPAR α , which promote the conversion of cholesterol into bile acid, downregulating the gene expression and activity of enzymes including HMG-CoA reductase and SREBP2 and upregulating LDLR to reduce the *de novo* synthesis of cholesterol. Thus, the results of this study indicate that COSTC may be a prospective functional food or supplement for antihyperlipidemic prevention or treatment.

Conclusions

In summary, this study was the first to provide evidence that COSTC favorably alters lipid metabolism partly through decreased cholesterol biosynthesis and increased cholesterol conversion into bile acids in high-fat-diet-induced hyperlipidemic rats. The potential cholesterol-lowering mechanisms of COSTC could promote the activity of CYP7A1 to increase the cholesterol conversion into bile acids and inhibit the activity of HMGCR to reduce the *de novo* synthesis of cholesterol. Thus, these promising findings indicated that COSTC has potential usefulness as a natural supplement or functional food for preventing and treating hyperlipidemia. Although the in-depth mechanisms need further illumination, these findings will be helpful for designing new therapeutic strategies to prevent the occurrence of hyperlipidemia.

Acknowledgement

This project was financially supported by the Industry University Research Collaborative Innovation Major Projects of Guangzhou Science Technology Innovation Commission (no.201604020164), China; the Science and Technology Planning Project of Yunfu (no.201702-9), Guangdong, China; the Science and Technology Planning Project of Guangdong (no.2013B021100018), China; and the National Science Foundation of China, China (no. 81173107).

Conflicts of interest

The authors declare no conflicts of interest.

References

- Schonfeld WPG, Rudel LL, Nelson C, Epstein M, Olson RE. Effects of dietary cholesterol and fatty acids on plasma lipoproteins. *J Clin Invest* 1982; 69: 1072–80.
- Ross R, Harker L. Hyperlipidemia and atherosclerosis. *Science* 1976; 193: 1094–100.
- Di Croce GBL, Trentalance A. Independent behavior of rat liver LDL receptor and HMGCoA Reductase under estrogen treatment. *Biochem Bioph Res Co* 1996; 224: 345–50.
- Horie T, Nishino T, Baba O, Kuwabara Y, Nakao T, Nishiga M, et al. Ono, MicroRNA-33 regulates sterol regulatory element-binding protein 1 expression in mice. *Nat Commun* 2013; 4: 2883.
- Zhu Z, Lin Z, Jiang H, Jiang Y, Zhao M, Liu X. Hypolipidemic effect of Youcha in hyperlipidemia rats induced by high-fat diet. *Food Funct* 2017; 8: 1680–7.
- Dossi CG, Cadagan C, San Martin M, Espinosa A, Gonzalez-Manan A, Silva D, et al. Effects of rosa mosqueta oil supplementation in lipogenic markers associated with prevention of liver steatosis. *Food Funct* 2017; 8: 832–41.
- He K, Li X, Xiao Y, Yong Y, Zhang Z, Li S, et al. Hypolipidemic effects of *Myrica rubra* extracts and main compounds in C57BL/6j mice. *Food Funct* 2016; 7: 3505–15.
- Miceli N, Modello MR, Monforte MT, Sdrafkakis V, Dugo P, Crupi ML, et al. Hypolipidemic effects of citrus bergamia Risso et Poiteau Juice in rats fed a hypercholesterolemic diet. *J Agric Food Chem* 2007; 55: 10671–7.
- Campins L, Camps M, Riera A, Pleguezuelos E, Yebenes JC, Serra-Prat M. Oral drugs related with muscle wasting and sarcopenia. A review. *Pharmacology* 2017; 99: 1–8.
- Wiggers JK, van Golen RF, Verheij J, Dekker AM, van Gulik TM, Heger M. Atorvastatin does not protect against ischemia-reperfusion damage in cholestatic rat livers. *BMC Surg* 2017; 17: 35.
- Fu C, Jiang Y, Guo Y, Su Z. Natural products with anti-obesity effects and different mechanisms of action. *J Agric Food Chem* 2016; 64: 9571–85.
- Lai YS, Lee WC, Lin YE, Ho CT, Lu KH, Lin SH, et al. Ginger essential oil ameliorates hepatic injury and lipid accumulation in high fat diet-induced nonalcoholic fatty liver disease. *J Agric Food Chem* 2016; 64: 2062–71.
- Jiang C, Wang Q, Wei Y, Yao N, Wu Z, Ma Y. Cholesterol-lowering effects and potential mechanisms of different polar extracts from *Cyclocarya paliurus* leave in hyperlipidemic mice. *J Ethnopharmacol* 2015; 176: 17–26.
- Hamer SN, Cord-Landwehr S, Biarnes X, Planas A, Waegeman H, Moerschbacher BM, et al. Enzymatic production of defined chitosan oligomers with a specific pattern of acetylation using a combination of chitin oligosaccharide deacetylases. *Sci Rep* 2015; 5: 8716.
- Huang J, Xie H, Hu S, Xie T, Gong J, Jiang C, et al. Preparation, characterization, and biochemical activities of N-(2-Carboxyethyl) chitosan from squid pens. *J Agric Food Chem* 2015; 63: 2464–71.
- Zou P, Yang X, Wang J, Li Y, Yu H, Zhang Y, et al. Advances in characterisation and biological activities of chitosan and chitosan oligosaccharides. *Food Chem* 2016; 190: 1174–81.
- Muanprasat C, Chatsudthipong V. Chitosan oligosaccharide: biological activities and potential therapeutic applications. *Pharmacol Ther* 2017; 170: 80–97.
- Ngo D.-H, Ngo T.-S, Kang D.-N, Je K.-H, Pham J.-Y, Byun HN.-D, et al. Biological effects of chitosan and its derivatives. *Food Hydrocolloid* 2015; 51: 200–16.

19. Chatchai VC. Muanprasat chitosan oligosaccharide: biological activities and potential therapeutic applications. *Pharmacol Therapeut* 2017; 170: 80–97.
20. Pan H, Yang Q, Huang G, Ding C, Cao P, Huang L, et al. Hypolipidemic effects of chitosan and its derivatives in hyperlipidemic rats induced by a high-fat diet. *Food Nutr Res* 2016; 60: 31137.
21. Cao P, Huang G, Yang Q, Guo J, Su Z. The effect of chitooligosaccharides on oleic acid-induced lipid accumulation in HepG2 cells. *Saudi pharm J: SPJ* 2016; 24: 292–8.
22. Cho EJ, Rahman A, Kim SW, Baek YM, Hwang HJ, Oh JY, et al. Chitosan oligosaccharides inhibit adipogenesis in 3T3-L1 adipocytes. *J Microbiol Biotechnol* 2008; 18: 80–7.
23. Choi CR, Kim EK, Kim YS, Je JY, An SH, Lee JD, et al. Chitooligosaccharides decreases plasma lipid levels in healthy men. *Int J Food Sci Nutr* 2012; 63: 103–6.
24. Wang D, Han J, Yu Y, Li X, Wang Y, Tian H, et al. Chitosan oligosaccharide decreases very-low-density lipoprotein triglyceride and increases high-density lipoprotein cholesterol in high-fat-diet-fed rats. *Exp Biol Med (Maywood)* 2011; 236: 1064–9.
25. Tarazona S, Garcia-Alcalde F, Dopazo J, Ferrer A, Conesa A. Differential expression in RNA-seq: a matter of depth. *Genome Res.* 2011; 21: 2213–23.
26. Zhengquan JG, Lanlan Huang SU. A method for preparation of COS capsule. Patent No.CN201510988017.7, 2015.12.24.
27. Huang L, Chen J, Cao P, Pan H, Ding C, Xiao T, et al. Anti-obese effect of glucosamine and chitosan oligosaccharide in high-fat diet-induced obese rats. *Mar Drugs.* 2015; 13: 2732–56.
28. Buzzetti E, Pinzani M, Tsochatzis EA. The multiple-hit pathogenesis of non-alcoholic fatty liver disease (NAFLD). *Metabolism* 2016; 65: 1038–48.
29. Mota M, Banini BA, Cazanave SC, Sanyal AJ. Molecular mechanisms of lipotoxicity and glucotoxicity in nonalcoholic fatty liver disease. *Metabolism* 2016; 65: 1049–61.
30. Brown GT, Kleiner DE. Histopathology of nonalcoholic fatty liver disease and nonalcoholic steatohepatitis. *Metabolism* 2016; 65: 1080–6.
31. Kiyoshiebihara A, Schneeman O. Interaction of bile acids, phospholipids, cholesterol and triglyceride with dietary fibers in the small intestine of rats. *Carbohydr Fibers* 1989; 119: 1100–6.
32. Liu X, Xia W, Jiang Q, Xu Y, Yu P. Synthesis, characterization, and antimicrobial activity of kojic acid grafted chitosan oligosaccharide. *J Agric Food Chem* 2014; 62: 297–303.
33. Qinna NA, Karwi QG, Al-Jbour N, Al-Remawi MA, Alhussainy TM, Al-So'ud KA, et al. Influence of molecular weight and degree of deacetylation of low molecular weight chitosan on the bioactivity of oral insulin preparations. *Mar Drugs* 2015; 13: 1710–25.
34. Dong W, Han B, Shao K, Yang Z, Peng Y, Yang Y, et al. Effects of molecular weights on the absorption, distribution and urinary excretion of intraperitoneally administrated carboxymethyl chitosan in rats. *J Mater Sci* 2012; 23: 2945–52.
35. Siow H.-L, Choi S.-B, Gan C.-Y. Structure–activity studies of protease activating, lipase inhibiting, bile acid binding and cholesterol-lowering effects of pre-screened cummin seed bioactive peptides. *J Funct Foods* 2016; 27: 600–11.
36. He K, Hu Y, Ma H, Zou Z, Xiao Y, Yang Y, et al. Rhizoma coptidis alkaloids alleviate hyperlipidemia in B6 mice by modulating gut microbiota and bile acid pathways. *Biochim Biophys Acta* 2016; 1862: 1696–709.
37. Kong B, Wang L, Chiang JY, Zhang Y, Klaassen CD, Guo GL. Mechanism of tissue-specific farnesoid X receptor in suppressing the expression of genes in bile-acid synthesis in mice. *Hepatology* 2012; 56: 1034–43.
38. Zong C, Yu Y, Song G, Luo T, Li L, Wang X, Qin S. Chitosan oligosaccharides promote reverse cholesterol transport and expression of scavenger receptor BI and CYP7A1 in mice. *Exp Biol Med (Maywood)* 2012; 237: 194–200.
39. Ducheix S, Lobaccaro JM, Martin PG, Guillou H. Liver X Receptor: an oxysterol sensor and a major player in the control of lipogenesis. *Chem Phys Lipids* 2011; 164: 500–14.
40. Pawlak M, Lefebvre P, Staels B. Molecular mechanism of PPAR- α action and its impact on lipid metabolism, inflammation and fibrosis in non-alcoholic fatty liver disease. *J Hepatol* 2015; 62: 720–33.

***Jiao Guo**

Guangdong Pharmaceutical University
280 East Wai-huan Road
Guangzhou Higher Education Mega Centre
Guangzhou 510006, China
Email: gyguoyz@163.com.

***Zhengquan Su**

Guangdong Pharmaceutical University,
280 East Wai-huan Road,
Guangzhou Higher Education Mega Centre
Guangzhou 510006, China
Email: suzhq@scnu.edu.cn.

Mulberry leaf extract displays antidiabetic activity in *db/db* mice via Akt and AMP-activated protein kinase phosphorylation

Ui-Jin Bae^{1,2†}, Eun-Soo Jung^{2†}, Su-Jin Jung², Soo-Wan Chae^{2,3*} and Byung-Hyun Park^{1*}

¹Department of Biochemistry, Chonbuk National University Medical School, Jeonju, Jeonbuk, Republic of Korea;

²Clinical Trial Center for Functional Foods, Chonbuk National University Hospital, Jeonju, Jeonbuk, Republic of Korea;

³Department of Pharmacology, Chonbuk National University Medical School, Jeonju, Jeonbuk, Republic of Korea

Abstract

Background: Augmenting glucose utilization in skeletal muscle via the phosphatidylinositol-3 kinase (PI3 kinase)/protein kinase B (Akt) pathway or the adenosine monophosphate (AMP)-activated protein kinase (AMPK) pathway is necessary to regulate hyperglycemia in patients with type 2 diabetes mellitus.

Objective: We investigated the effect of mulberry leaf extract (MLE) on glucose uptake in skeletal muscle cells and explored its *in vivo* antidiabetic potential.

Design: Male *db/db* mice were treated with either MLE (50 mg/kg, 100 mg/kg, and 250 mg/kg) or metformin (100 mg/kg) for 8 weeks.

Results: MLE treatment stimulated glucose uptake, driven by enhanced translocation of glucose transporter 4 to cell membranes in L6 myotubes. These effects of MLE were synergistic with those of insulin and were abolished in the presence of PI3K inhibitor or AMPK inhibitor. In *db/db* mice, supplementation with MLE decreased fasting blood glucose and insulin levels and enhanced insulin sensitivity, with increases of p-Akt and p-AMPK in skeletal muscle. Moreover, MLE improved blood lipid parameters and attenuated hepatic steatosis in diabetic *db/db* mice.

Discussion: These findings suggest that MLE exerts antidiabetic activity through stimulating glucose disposal in skeletal muscle cells via the PI3K/Akt and AMPK pathways.

Conclusions: MLE can potentially improve hyperglycemia and hepatic steatosis in patients with type 2 diabetes.

Keywords: glucose uptake; muscle; steatosis; insulin; hypertriglyceridemia

Type 2 diabetes mellitus (T2DM) is characterized by insulin resistance (IR), hyperglycemia, and hyperinsulinemia. Skeletal muscle accounts for approximately 70–80% of insulin-stimulated glucose uptake in the postprandial state and plays a key role in maintaining glucose homeostasis (1). Two distinct pathways are responsible for glucose transport in skeletal muscle: phosphatidylinositol-3 kinase (PI3 kinase)/protein kinase B (Akt) and AMP-activated protein kinase (AMPK). Insulin facilitates glucose uptake by increasing the translocation of glucose transporter 4 (GLUT4) from an intracellular pool to the plasma membrane through the activation of the PI3K/Akt pathway (2). Skeletal muscle contraction or metformin treatment activates AMPK and stimulates GLUT4 translocation in an insulin-independent manner (3). Impairment of GLUT4 translocation or decreased GLUT4 activity results in systemic IR (4, 5).

Mulberry (*Morus alba* L.), a member of the Moraceae family, has been cultivated worldwide for sericulture from ancient times and has been used in Chinese medicine to prevent and cure T2DM (6). Results from animal studies show that mulberry leaf extract (MLE) reduces postprandial blood glucose levels in rats with high fat diet- and streptozotocin-induced diabetes (7, 8). Similarly, long-term administration of MLE in subjects with impaired glucose tolerance or T2DM produces a dose-dependent decrease in postprandial blood glucose levels (9, 10). A number of studies have revealed that 1-deoxynojirimycin (DNJ), a potent α -glucosidase inhibitor, is the main component responsible for these activities (11, 12). MLE activates the PI3K/Akt pathway and stimulates glucose uptake in rat adipocytes (13, 14). It increases adipogenesis and stimulates adiponectin secretion from murine 3T3-L1

[†]These authors contributed equally to this work.

adipocytes: both activities are associated with decreased blood glucose levels (15). Anthocyanins isolated from MLE maintain the PI3K/Akt pathway and suppress hepatic gluconeogenesis in HepG2 cells, a human hepatocellular carcinoma cell line (14). Given that skeletal muscle is a major site of whole-body glucose uptake and utilization, MLE might also act as a direct stimulant of glucose transport in skeletal muscle in addition to its role in adipocytes and hepatocytes. However, the effects of MLE on skeletal muscle are poorly understood. In this study, using *db/db* mice, we carried out an 8-week supplementation study to ascertain the antidiabetic efficacy of MLE. We also explored the underlying mechanism of action of MLE, with a particular focus on the AMPK and PI3K/Akt signaling pathways, in L6 myotubes.

Materials and methods

Preparation of MLE

Dried mulberry leaves were obtained from the Buan Agricultural Development & Technology Center (Buan, Korea) in 2016. Dried mulberry leaf extract was prepared with 15 volumes of water at 50°C for 4 h, using a DH-M03 accelerated solvent extractor (DM Engineering Co., Siheung, Korea). The extracts were filtered using filter cartridges (1 μ m), concentrated using a vacuum evaporator (DH-M07, Vacuum Engineering Co., Seoul, Korea) at 60°C, and spray dried with 20% dextrin.

High-performance liquid chromatography analysis of MLE

The components of MLE were analyzed using an Agilent 1260 Infinity HPLC system (Agilent, Santa Clara, CA, USA) with an MG C₁₈ column (4.6 mm \times 250 mm, 5 μ m, Shiseido Co., Tokyo, Japan). The mobile phase was composed of 0.1% acetic acid in water (A) and acetonitrile (B). The gradient program (A:B) was as follows: 70:30 for 0–16 min, 20:80 for 17–27 min, and 70:30 for 28–35 min. The flow rate was 1 mL/min, the injection volume was 10 μ L, and the column temperature was maintained at 35°C. Signals were detected at the wavelengths of excitation (254 nm) and emission (322 nm) using a fluorescence detector. The standard (DNJ) for HPLC analysis was obtained from Sigma-Aldrich (St Louis, MO, USA). The DNJ content was determined using a validation method established using dilutions of each standard at concentrations ranging from 1.03 to 32.90 ppb injected into the HPLC system (correlation coefficient 0.999).

Liquid chromatography mass spectrometry (LC-MS) analysis of MLE

Unbiased metabolomics analysis was performed using an ultra-performance liquid chromatography (UPLC) system (Waters, Milford, CT, USA). Chromatographic separation was carried out using an ACQUITY UPLC HSS

T3 column (100 mm \times 2.1 mm, 1.8 μ m, Waters) with a column temperature of 40°C and a flow rate of 0.5 mL/min, where the mobile phase contained solvent A (0.1% formic acid in distilled water [DW]) and solvent B (0.1% formic acid in acetonitrile). Metabolites were eluted using the following gradient elution conditions: 97% solvent A for 0–5 min, 3–100% linear gradient solvent B for 5–16 min, 100% solvent B for 16–17 min, 100–3% reverse linear gradient solvent B for 17–19 min; and 97% solvent A for 19–25 min. The loading volume of each sample was 5 μ L. The metabolites eluted from the column were detected by a high-resolution tandem mass spectrometer SYNAPT G2 Si HDMS QTOF (Waters) in positive and negative ion modes. For positive ion mode, the capillary voltage and the cone voltage were set at 2 kV and 40 V, respectively. For negative ion mode, they were set at 1 kV and 40 V, respectively. Centroid MSE mode was used to collect the mass spectrometry data. The primary scan ranged from 50 to 1,200 Da and the scanning time was 0.2 sec. All the parent ions were fragmented using 20–40 eV. Information for all fragments was collected, and the time was 0.2 sec. In the data acquisition process, the LE signal was gained every 3 sec for real-time quality correction. For accurate mass acquisition, leucine enkephalin at a flow rate of 10 μ L/min was used as a lock mass by a lock spray interface to monitor the positive ($[M + H]^+ = 556.2771$) and the negative ($[M - H]^- = 554.2615$) ion modes. Data acquisition and analysis were controlled using the Waters UNIFI V1.71 software. The scan ranges in MS and MS/MS modes were each 50–1,200 m/z.

Cell culture and differentiation

Rat myoblast cells (L6) were obtained from the American Type Culture Collection (Manassas, VA, USA). Cells were grown in Dulbecco's modified Eagle's medium containing 10% fetal bovine serum, 10 units/mL penicillin, and 10 μ g/mL streptomycin, at 37°C and air containing 5% CO₂. L6 myoblasts were seeded at the density of 2×10^4 cells/cm² in 96-well plates one day before the start of the differentiation. The differentiation of myoblasts into myotubes was induced by switching the media to alpha minimum essential medium (α -MEM) supplemented with 2% fetal bovine serum and antibiotics. Cells were allowed to differentiate into myotubes for 5 days. Fresh medium was added on day 2. The myotubes were then cultured in α -MEM containing 0.2% BSA and antibiotics for 12 h and then used for glucose uptake experiments. Cell viability was assessed using the 3-(4,5-dimethylthiazol-2-yl)-2,5-diphenyltetrazolium bromide (MTT) assay.

Muscle glucose uptake

L6 myotubes were treated with phosphate buffered saline (PBS), 0.1 μ M human insulin (Sigma-Aldrich), and MLE in 0.2% BSA and antibiotics at 37°C in a CO₂ incubator

for 4 h. The cells were washed with PBS and starved for 1 h in glucose-free 4-(2-hydroxyethyl)-1-piperazineethanesulfonic acid (HEPES)-buffered saline (20 mM HEPES, 140 mM NaCl, 5 mM KCl, 2.5 mM MgSO₄, 1 mM CaCl₂; pH 7.4) while maintaining the same concentrations of test compounds and insulin. Finally, HEPES-buffered saline containing 10 μM 2-deoxy-D-glucose (2DOG, Sigma-Aldrich) and 0.5 μCi/μL [³H]2-deoxy-D-glucose (Perkin-Elmer, Turku, Finland) was added to the myotubes, and the uptake reaction was allowed to proceed for 15 min at room temperature. The uptake reaction was stopped by washing the cells three times with ice-cold PBS. The cells were lysed in 0.5 M NaOH, and the radioactivity in the lysates was counted by liquid scintillation (PerkinElmer).

Animals and experimental design

All mice were purchased from The Jackson Laboratory (Bar Harbor, ME, USA). The mice were housed in standard laboratory conditions (23±1°C, 40–60% relative humidity, and a 12 h light–dark cycle) in a barrier facility with laminar flow cabinets in the Laboratory Animal Care facilities of Chonbuk National University Hospital. All mice were allowed free access to a normal chow diet and tap water. After 1 week of acclimatization, 7-week-old male *db/db* mice (C57BLK-*lepr*^{db}/*lepr*^{db}) and non-diabetic *db/m* mice (C57BLK-*lepr*^{db}/+) were randomly divided into six groups (*n* = 7 per group): normal control (*db/m*, non-treated), negative control (*db/db*, PBS), positive control (*db/db*, 100 mg/kg of metformin), and three test groups (*db/db*, MLE). MLE was administered at doses of 50 mg/kg (low dose), 100 mg/kg (middle dose), and 250 mg/kg (high dose) to the three test groups for 8 weeks. All reagents (PBS, metformin, and MLE) were administered by oral gavage once daily. Food consumption, body weight, and fasting blood glucose (FBG) were measured every week. At the end of the 7th week, the mice underwent an oral glucose tolerance test (OGTT) and an insulin tolerance test (ITT). The animals were sacrificed on the 8th week. Blood sample was collected from the truncal vein. After the mice were anesthetized using ketamine and xylazine, liver and skeletal muscle tissues were harvested. This protocol was approved by the Institutional Animal Care and Use Committee of Chonbuk National University Hospital (permit no. cuh-IACUC-2017-5-1), and all work was performed in accordance with the *Guide for the Care and Use of Laboratory Animals* (National Institutes of Health Publication no. 85-23, revised 2011).

Biochemical assays

Whole blood glucose levels were measured using Accu-Chek Aviva glucose monitors (Roche Diagnostics, Indianapolis, IN, USA), with blood drawn from the tail vein. Serum insulin and adiponectin levels were measured

using an enzyme-linked immunosorbent assay (ELISA) kit (Millipore, Bedford, MA, USA), with blood drawn from the truncal vein. To assess IR, the homeostasis model assessment (HOMA) index scores were calculated as follows: HOMA-IR = (fasting insulin concentration × fasting glucose concentration)/22.5. Serum levels of total cholesterol (TC), triglyceride (TG), and high-density lipoprotein cholesterol (HDL-C) were measured using commercially available kits (Asan Pharmaceuticals Co., Ltd., Seoul, Korea). For quantification of liver TG contents, the liver tissue was homogenized and extracted in chloroform, methanol, and DW (2/1/1 ratio). All procedures were performed according to the manufacturer's instructions.

Glucose and insulin tolerance tests

For the OGTT, glucose (1 g/kg body weight) was administered by oral gavage after overnight fasting. The ITT was performed with an intraperitoneal injection of insulin (0.75 U/kg body weight) after 6 h of fasting. These two tests were performed at a 3-day interval and had the same sampling times: 0 (baseline), 15, 30, 60, 120, and 180 min postglucose (or postinsulin) challenge. The glucose levels were measured in the blood drawn from the tail vein. Insulin responsiveness was also assessed in the liver and skeletal muscle. Briefly, insulin (0.75 U/kg body weight) was first administered *via* the truncal vein. Tissue samples were then collected from the liver 5 min later and from the skeletal muscle 10 min later. The levels of total and phosphorylated Akt in each sample were then assessed.

Histological assay

Liver specimens were immediately fixed in 10% formalin, embedded in paraffin, and cut into 5-μm sections. The specimens were stained with hematoxylin and eosin and examined on a light microscope (Eclipse E600 polarizing microscope, Nikon, Tokyo, Japan).

Western blotting

Protein samples (20 μg) from L6 myotubes, liver or skeletal muscle tissue extracts were resolved by sodium dodecyl sulfate–polyacrylamide gel electrophoresis and then transferred to nitrocellulose membranes (Millipore). The membranes were probed with primary antibodies against AMPK, p-AMPK, Akt, p-Akt (Cell Signaling Technology, Beverly, MA, USA), GLUT4, and β-actin (Santa Cruz Biotechnology, Dallas, TX, USA) overnight at 4°C. After washing, the membranes were incubated with horseradish peroxidase-conjugated anti-IgG secondary antibodies (Zymed, South San Francisco, CA, USA) for 1 h at room temperature. Immunoreactive bands were detected using an LAS-4000 imager (GE Healthcare Life Science, Pittsburgh, PA, USA), and band density was normalized to that of the β-actin loading control.

Statistical analysis

Data are expressed as the mean \pm SEM. Statistical comparisons were made using one-way analysis of variance followed by Fisher's post hoc analysis using GraphPad Prism 5.02 (San Diego, CA, USA). *P*-values < 0.05 were considered statistically significant.

Results

Chromatography analysis of MLE

A typical HPLC chromatographic profile of MLE is shown in Fig. 1a. DNJ was adequately resolved from other unknown compounds and could be clearly identified by retention time. The content of DNJ in the extracts was calculated from the relevant peak area by using an external standard method, and quantified as 0.2%.

The constituents of the MLE were further analyzed by LC-MS. MLE contained several polyphenols, including caffeoylquinic acid derivatives and flavonoid glycosides (Fig. 1b).

MLE increases glucose uptake in L6 myotubes

To investigate whether MLE has direct effects on muscle cell glucose uptake, L6 myotubes were treated with various concentrations of MLE. The cell viability observed after treatment with ≤ 60 $\mu\text{g}/\text{mL}$ of MLE was similar to that of the control (Fig. 2a). MLE (60 $\mu\text{g}/\text{mL}$) treatment increased [^3H]-2-deoxy-D-glucose uptake into myotubes (Fig. 2b). Interestingly, glucose uptake was not dependent on the insulin action. To elucidate the mechanism behind this increase in glucose uptake, the levels of p-Akt, p-AMPK, and GLUT4 were measured by western

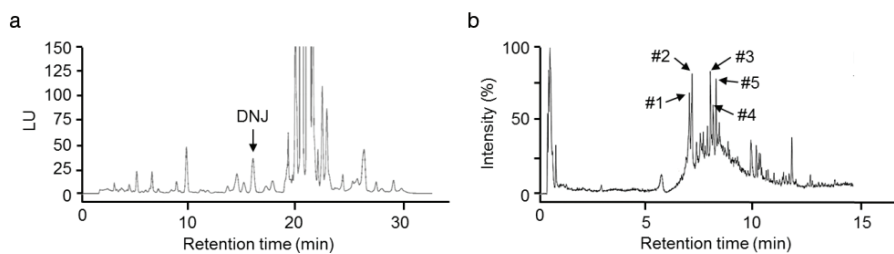


Fig. 1. Representative chromatograms of MLE. (a) HPLC analysis of DNJ in MLE. (b) LC-MS analysis of phenolic compounds in MLE. Numbers refer to the main peaks identified: #1, 4-O-caffeoylquinic acid; #2, 1-O-caffeoylquinic acid; #3, kaempferol-3,7-diglucoside; #4, 6-hydroxykaempferol-3-O-glucoside; #5, genistein-7,4'-di-O- β -D-glucoside.

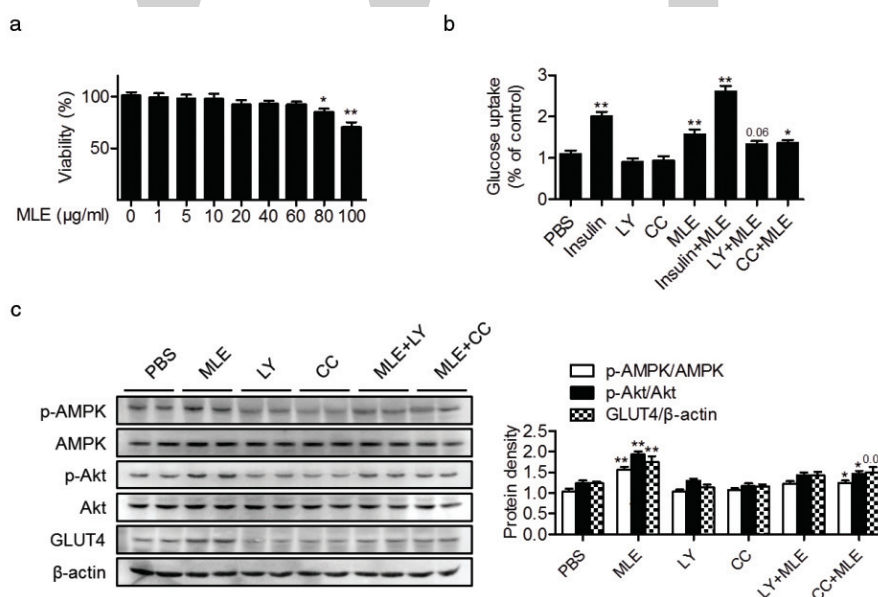


Fig. 2. Effects of MLE on glucose uptake in L6 myotubes. (a) L6 myotubes were treated with the indicated concentrations of MLE, and cell viability was determined by MTT assay ($n = 5$). (b) L6 myotubes were treated with MLE (60 $\mu\text{g}/\text{mL}$), 0.1 μM insulin, 25 μM LY294002 (LY), or 10 μM compound C (CC) as indicated. After 6 h, [^3H]2DOG uptake was measured ($n = 7$ /each group). (c) L6 myotubes were treated with MLE (60 $\mu\text{g}/\text{mL}$), 25 μM LY294002, or 10 μM compound C (CC) for 5 min, and protein levels of p-Akt, Akt, p-AMPK, AMPK, and GLUT4 were analyzed by western blotting. The band intensities of each protein were quantitated ($n = 5$). Values are expressed as mean \pm SEM. MLE, mulberry leaf extract; CC, compound C; LY, LY294002.

blotting. A significant increase of p-Akt/Akt, p-AMPK/AMPK, and GLUT4 was observed after MLE treatment (Fig. 2c). Using the PI3-K inhibitor LY294002 and the AMPK inhibitor compound C, we further confirmed the activation of the PI3K/Akt and AMPK pathways in the MLE-stimulated glucose uptake (Figs. 2b and 2c).

MLE decreases blood glucose concentration in db/db mice

To investigate glucose homeostasis and insulin sensitivity after MLE treatment *in vivo*, we used diabetic *db/db* mice treated with PBS or various concentrations of MLE. Metformin was used as a positive control. All *db/db* mice were confirmed to be diabetic when the experiment began, as indicated by the high mean FBG level (150.10±32.3 mg/dL). After 5 weeks of metformin treatment, the mice exhibited significantly reduced FBG levels compared with the control mice (Fig. 3a). Mice that received 5 weeks of MLE supplementation (250 mg/kg) also exhibited reduced FBG levels; this effect persisted until the end of the study. The glucose-lowering effect of MLE was concentration dependent, and the efficacy of 250 mg/kg MLE supplementation was similar to that of metformin treatment. The average weekly weight gains (Fig. 3b) and food intakes (Fig. 3c) were not different among groups. At the end of the study, the FBG levels, insulin levels, and HOMA-IR scores were significantly decreased in the MLE (100 and 250 mg/kg)-treated *db/db* mice compared with the PBS-treated *db/db* mice (Figs. 3d–3f). Consistent with the changes in FBG levels, MLE supplementation (100 and 250 mg/kg) significantly increased serum adiponectin levels (Fig. 3g).

Mice with MLE supplementation (100 and 250 mg/kg) also exhibited improvements in post-bolus glucose clearance

compared with PBS-treated *db/db* mice at all time points of the OGTT (Fig. 4a). Significant decreases in blood glucose levels during the ITT were also observed in the MLE (50, 100, and 250 mg/kg)-supplemented mice (Fig. 4b). To identify the tissue that contributes to this MLE-mediated increase in insulin sensitivity, the levels of insulin-stimulated Akt phosphorylation were compared in the liver and skeletal muscle tissues. Insulin-injected *db/+* mice showed Akt phosphorylation (Ser473) in the liver and skeletal muscle; however, only weak effects were observed in PBS-treated *db/db* mice (Fig. 4c). In contrast, both MLE (250 mg/kg)- and metformin-treated mice showed significantly increased Akt phosphorylation compared with PBS-treated mice. These results suggest that MLE supplementation improves systemic and peripheral IR in *db/db* mice.

MLE supplementation ameliorates hepatic steatosis and hypertriglyceridemia in db/db mice

At the end of the study, supplementation with MLE and supplementation with metformin both resulted in significantly lower serum TG and TC levels in *db/db* mice (Figs. 5a and 5b). However, no significant differences in HDL-C levels were observed with MLE supplementation (Fig. 5c).

Morphological analysis of the livers also indicated that lipid accumulation was most pronounced in the control *db/db* mice. However, supplementation with MLE (250 mg/kg) and metformin both resulted in reduced liver sizes and reduced numbers of lipid droplets compared with *db/db* mice (Fig. 5d). Liver wet weight (Fig. 5e), liver TG content (Fig. 5f), and serum levels of aspartate aminotransferase (AST) and alanine aminotransferase (ALT) (Fig. 5g) were well correlated with the degree of lipid accumulation.

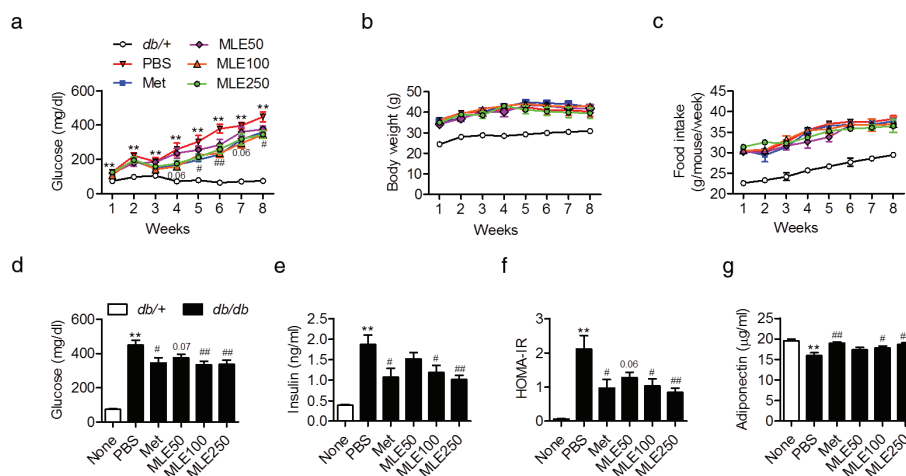


Fig. 3. Effects of MLE supplementation on glycemic control in *db/db* mice. Male *db/db* mice received PBS, metformin (100 mg/kg), or MLE (50, 100, and 250 mg/kg) once daily for 8 weeks by oral gavage. (a) Fasting blood glucose, (b) body weight, and (c) food intake changes were recorded at the indicated times. (d–g) At the end of the study, glucose, insulin, and adiponectin concentrations were analyzed and the HOMA-IR scores were calculated. Values are expressed as mean±SEM (*n* = 7/each group). ***p* < 0.01 versus *db/+*, #*p* < 0.05 and ###*p* < 0.01 versus *db/db*+PBS. Met, metformin; MLE50, MLE 50 mg/kg; MLE100, MLE 100 mg/kg; MLE250, MLE 250 mg/kg.

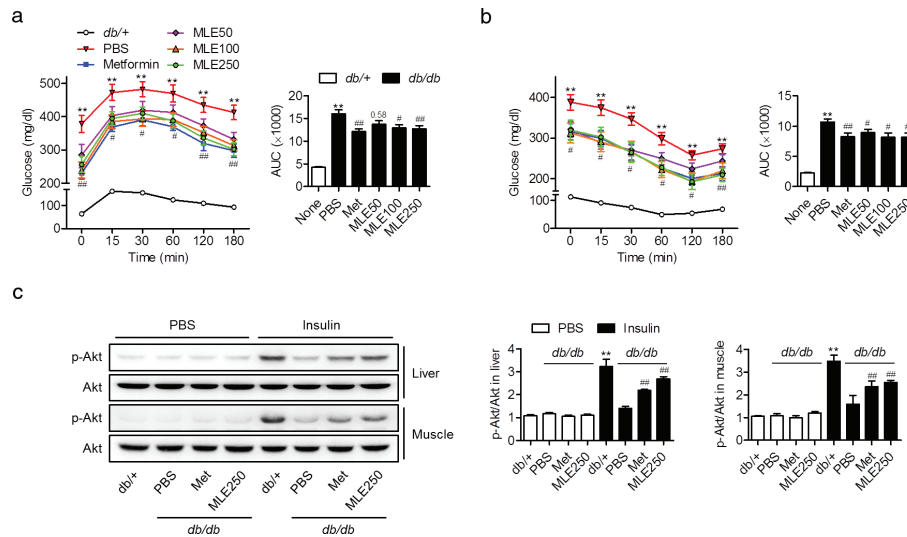


Fig. 4. Effects of MLE supplementation on insulin sensitivity in *db/db* mice. At the 7th week, glucose concentrations during oral glucose tolerance tests (a) and insulin tolerance tests (b) were measured. Areas under the curve were compared ($n = 7$ /each group). (c) At the end of the study, insulin-stimulated Akt phosphorylation was measured in the liver and skeletal muscle. The band intensities of p-Akt and Akt were quantitated ($n = 3$ /each group). Values are expressed as mean \pm SEM. ** $p < 0.01$ versus *db/+* or *db/+* with PBS, # $p < 0.05$ and ### $p < 0.01$ versus *db/db*+PBS or *db/+* with insulin.

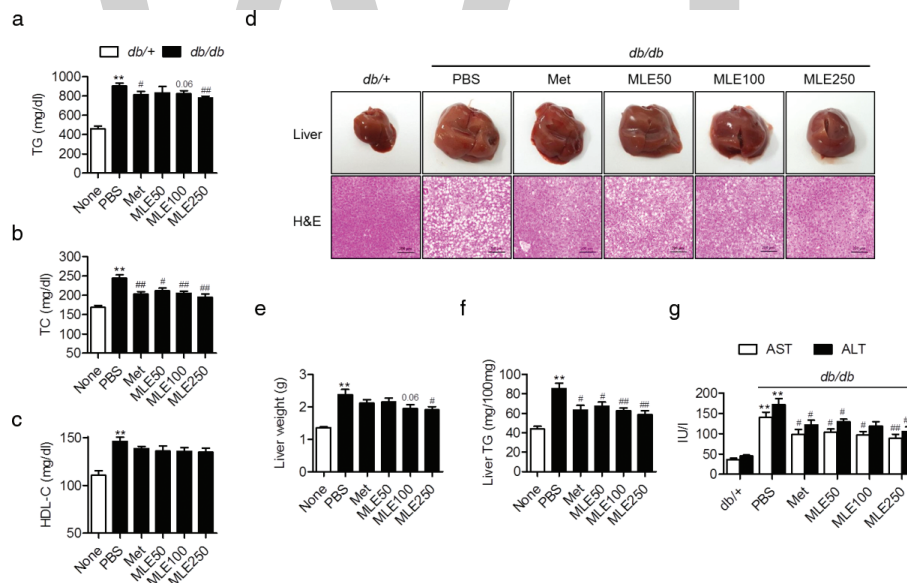


Fig. 5. Effects of MLE supplementation on hepatic steatosis and serum lipid profiles in *db/db* mice. (a–c) At the end of the study, serum levels of triglyceride (TG), total cholesterol (TC), and high-density lipoprotein cholesterol (HDL-C) were analyzed. (d) Macroscopic and microscopic images of liver sections. Liver sections were stained with H&E. Bar = 100 μ m. (e, f) Liver wet weight and hepatic TG content were determined. (g) Serum levels of AST and ALT were measured as an index of liver injury. Values are expressed as mean \pm SEM ($n = 7$ /each group). ** $p < 0.01$ versus *db/+*, # $p < 0.05$ and ### $p < 0.01$ versus *db/db*+PBS.

MLE supplementation activates PI3K/Akt in skeletal muscle
Because we observed an increased glucose uptake in L6 myotubes with MLE (Fig. 2), we further verified the improvement of MLE-mediated glucose metabolism in

skeletal muscle, the major tissue for glucose disposal. As shown in Fig. 6, phosphorylated forms of Akt and AMPK were significantly decreased in the muscles of PBS-treated *db/db* mice compared with the *db/+* mice.

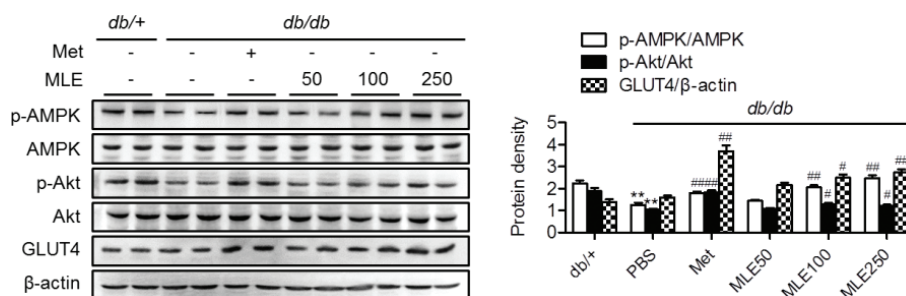


Fig. 6. Activation of PI3K/Akt signaling pathways by MLE in muscle. At the end of the study, the total and phosphorylated forms of Akt and AMPK, and GLUT4 were measured in skeletal muscle tissues. The band intensities of each form were quantitated. Values are expressed as mean±SEM (*n* = 7/each group). ***p* < 0.01 versus *db/+* and #*p* < 0.05, ##*p* < 0.01 versus *db/db*+PBS.

However, supplementation of MLE (100 and 250 mg/kg) significantly increased the phosphorylated forms of these proteins as well as that of GLUT4 protein. These results indicate that MLE likely increases glucose disposal in skeletal muscle by increasing both insulin sensitivity and GLUT4 expression *via* the Akt- and AMPK-dependent pathways.

Discussion

MLE is rich in the iminosugar DNJ, and therefore much attention has been focused on MLE-dependent suppression of the postprandial elevation of blood glucose levels by delaying glucose absorption in the small intestine. Our LC-MS analysis shows that in addition to DNJ, MLE contains genistein glycoside, kaempferol glycosides, and caffeoylquinic acid derivatives. Previous studies have shown that genistein is responsible for suppressed hepatic gluconeogenesis and increased insulin secretion (16, 17), kaempferol stimulates insulin secretion and exerts insulinotropic effects (18, 19), and caffeoylquinic acid is effective in stimulating glucose transport in muscle cells by activating AMPK and Akt (20). These results suggest that the antidiabetic effects of MLE in *db/db* mice may be mediated by not only DNJ but also a combination of several constituents of MLE.

To determine whether MLE can decrease blood glucose levels in an *in vivo* diabetes model, we treated *db/db* mice with MLE for 8 weeks. Remarkably, MLE supplementation sufficiently lowered FBG levels, and this effect was relatively stable, as with metformin, from 5 weeks after treatment. Because there were decreases in serum insulin levels and HOMA-IR values with MLE supplementation, the insulin sensitization in peripheral tissues is likely the main mechanism by which MLE regulates blood glucose levels. Indeed, our results provide evidence of insulin sensitization with MLE. First, we observed an increase of insulin signaling in the liver and skeletal

muscle, as evidenced by the increase of p-Akt/Akt. Second, there was an increase of glucose disposal as shown by an ITT. Third, high levels of adiponectin were detected, which can predict enhanced insulin sensitivity. Finally, GLUT4 expression in skeletal muscle and glucose uptake into L6 myotubes both increased. All of these results indicate that the favorable antidiabetic effects of MLE arise from enhancement of insulin sensitivity in skeletal muscle.

Adipose tissue accounts for a small fraction of glucose disposal after a meal, whereas skeletal muscle is proposed to be the primary site of whole-body insulin-mediated glucose uptake (1). GLUT1 is predominantly responsible for transporting glucose during basal conditions, while GLUT4 becomes the major glucose transporter in skeletal muscle cells in response to insulin (21). Therefore, this study investigated the glucose uptake through GLUT4 in myotubes. Results showed that MLE treatment stimulated glucose uptake independent of insulin action, which was paralleled by increased GLUT4 translocation to the cell surface. The glucose uptake into skeletal muscle is mediated by two pathways: insulin-dependent Akt phosphorylation and contraction-stimulated AMPK activation (2, 3). Studies using the PI3K inhibitor LY294002 and the AMPK inhibitor compound C revealed that both PI3K and AMPK were essential for MLE-enhanced muscular glucose uptake. In agreement with our study, MLE activated AMPK phosphorylation in isolated rat muscle (22); however, in contrast to our results, MLE inhibited Akt signaling in the smooth muscle cell line A7r5 (23). The latter discrepancy is most likely due to using different cell types (skeletal muscle cells in our study vs. smooth muscle cells in their study), as well as visualizing Akt activity at a different MLE concentration (60 µg/mL in our study vs. > 500 µg/mL in their study).

Mice in the MLE treatment group showed decreased serum levels of TG and TC and recovery of fatty liver.

Excess glucose enters the liver and is metabolized to acetyl-CoA, which is used for TG synthesis through *de novo* lipogenesis. Insulin and glucose activate SREBP-1c and ChREBP, respectively, and these transcription factors are involved in the induction of lipogenic genes (24). Therefore, downregulation of glucose and insulin levels by MLE may, at least in part, be responsible for the improvement of dyslipidemia and fatty liver in *db/db* mice.

In summary, MLE-supplemented *db/db* mice had not only lowered blood glucose and insulin but also decreased TG and TC levels, and improvements in IR and fatty liver. The mechanism of MLE action involves activation of AMPK and Akt signaling for muscular glucose uptake. Our findings manifest that MLE has a favorable therapeutic potential for the management of type 2 diabetes.

Acknowledgements

This research was supported by the Ministry of Agriculture, Food and Rural Affairs (MAFRA), through the 2016 Healthy Local Food Branding Project of the Rural Resources Complex Industrialization Support Program.

Conflict of interest and funding

The authors have no conflicts of interest to declare. The authors have not received any funding or benefits from industry to conduct this study.

References

- Carnagarin R, Dharmarajan AM, Dass CR. Molecular aspects of glucose homeostasis in skeletal muscle – A focus on the molecular mechanisms of insulin resistance. *Mol Cell Endocrinol* 2015; 417: 52–62. doi: 10.1016/j.mce.2015.09.004
- Saltiel AR, Kahn CR. Insulin signalling and the regulation of glucose and lipid metabolism. *Nature* 2001; 414(6865): 799–806. doi: 10.1038/414799a
- Lund S, Holman GD, Schmitz O, O Pedersen. Contraction stimulates translocation of glucose transporter GLUT4 in skeletal muscle through a mechanism distinct from that of insulin. *Proc Natl Acad Sci U S A* 1995; 92(13): 5817–5821.
- Wang HY, Ducommun S, Quan C, Xie B, Li M, Wasserman DH, et al. AS160 deficiency causes whole-body insulin resistance via composite effects in multiple tissues. *Biochem J* 2013; 449(2): 479–489. doi: 10.1042/BJ20120702
- Xiong W, Jordens I, Gonzalez E, McGraw TE. GLUT4 is sorted to vesicles whose accumulation beneath and insertion into the plasma membrane are differentially regulated by insulin and selectively affected by insulin resistance. *Mol Biol Cell* 2010; 21(8): 1375–1386. doi: 10.1091/mbc
- Chan EW, Lye PY, Wong SK. Phytochemistry, pharmacology, and clinical trials of *Morus alba*. *Chin J Nat Med* 2016; 14(1): 17–30. doi: 10.3724/SP.J.1009.2016.00017
- Sheng Y, Zheng S, Ma T, Zhang C, Ou X, He X, et al. Mulberry leaf alleviates streptozotocin-induced diabetic rats by attenuating NEFA signaling and modulating intestinal microflora. *Sci Rep* 2017; 7(1): 12041. doi: 10.1038/s41598-017-12245-2
- Jiao Y, Wang X, Jiang X, Kong F, Wang S, Yan C. Antidiabetic effects of *Morus alba* fruit polysaccharides on high-fat diet- and streptozotocin-induced type 2 diabetes in rats. *J Ethnopharmacol* 2017; 199: 119–127. doi: 10.1016/j.jep.2017.02.003
- Asai A, Nakagawa K, Higuchi O, Kimura T, Kojima Y, Kariya J, et al. Effect of mulberry leaf extract with enriched 1-deoxynojirimycin content on postprandial glycemic control in subjects with impaired glucose metabolism. *J Diabetes Investig* 2011; 2(4): 318–323. doi: 10.1111/j.2040-1124.2011.00101.x
- Riche DM, Riche KD, East HE, Barrett EK, May WL. Impact of mulberry leaf extract on type 2 diabetes (Mul-DM): a randomized, placebo-controlled pilot study. *Complement Ther Med* 2017; 32: 105–108. doi: 10.1016/j.ctim.2017.04.006
- Liu Y, Li X, Xie C, Luo X, Bao Y, Wu B, et al. Prevention effects and possible molecular mechanism of mulberry leaf extract and its formulation on rats with insulin-insensitivity. *PLoS One* 2016; 11(4): e0152728. doi: 10.1371/journal.pone.0152728
- Liu Q, Li X, Li C, Zheng Y, Peng G. 1-Deoxynojirimycin alleviates insulin resistance via activation of insulin signaling PI3K/AKT pathway in skeletal muscle of *db/db* mice. *Molecules* 2015; 20(12): 21700–21714. doi: 10.3390/molecules201219794
- Naowaboot J, Pannangpetch P, Kukongviriyapan V, Prawan A, Kukongviriyapan U, Itharat A. Mulberry leaf extract stimulates glucose uptake and GLUT4 translocation in rat adipocytes. *Am J Chin Med* 2012; 40(1): 163–175. doi: 10.1142/S0192415X12500139
- Yan F, Dai G, Zheng X. Mulberry anthocyanin extract ameliorates insulin resistance by regulating PI3K/AKT pathway in HepG2 cells and *db/db* mice. *J Nutr Biochem* 2016; 36: 68–80. doi: 10.1016/j.jnutbio.2016.07.004
- Naowaboot J, Chung CH, Pannangpetch P, Choi R, Kim BH, Lee MY, et al. Mulberry leaf extract increases adiponectin in murine 3T3-L1 adipocytes. *Nutr Res* 2012; 32(1): 39–44. doi: 10.1016/j.nutres.2011.12.003
- Dkhar B, Khongsti K, Thabab D, Syiem D, Satyamoorthy K, Das B. Genistein represses PEPCK-C expression in an insulin-independent manner in HepG2 cells and in alloxan-induced diabetic mice. *J Cell Biochem* 2018; 119(2): 1953–1970. doi: 10.1002/jcb.26356
- Kim EK, Kwon KB, Song MY, Seo SW, Park SJ, Ka SO, et al. Genistein protects pancreatic β cells against cytokine-mediated toxicity. *Mol Cell Endocrinol* 2007; 278(1–2): 18–28. doi: 10.1016/j.mce.2007.08.003
- Zhang Y, Zhen W, Maechler P, Liu D. Small molecule kaempferol modulates PDX-1 protein expression and subsequently promotes pancreatic β -cell survival and function via CREB. *J Nutr Biochem* 2013; 24(4): 638–646. doi: 10.1016/j.jnutbio.2012.03.008
- Alkhalidy H, Moore W, Zhang Y, McMillan R, Wang A, Ali M, et al. Small molecule kaempferol promotes insulin sensitivity and preserved pancreatic β -cell mass in middle-aged obese diabetic mice. *J Diabetes Res* 2015; 2015: 532984. doi: 10.1155/2015/532984
- Wu C, Zhang X, Zhang X, Luan H, Sun G, Sun X, et al. The caffeoylquinic acid-rich *Pandanus tectorius* fruit extract increases insulin sensitivity and regulates hepatic glucose and lipid

- metabolism in diabetic *db/db* mice. *J Nutr Biochem* 2014; 25(4): 412–419. doi: 10.1016/j.jnutbio.2013.12.002
21. Zhao FQ, Keating AF. Functional properties and genomics of glucose transporters. *Curr Genomics* 2007; 8(2): 113–128.
 22. Ma X, Iwanaka N, Masuda S, Karaike K, Egawa T, Hamada T, et al. *Morus alba* leaf extract stimulates 5'-AMP-activated protein kinase in isolated rat skeletal muscle. *J Ethnopharmacol* 2009; 122(1): 54–59. doi: 10.1016/j.jep.2008.11.022
 23. Chan KC, Ho HH, Huang CN, Lin MC, Chen HM, Wang CJ. Mulberry leaf extract inhibits vascular smooth muscle cell migration involving a block of small GTPase and Akt/NF- κ B signals. *J Agric Food Chem* 2009; 57(19): 9147–9153. doi: 10.1021/jf902507k
 24. Wong RH, Sul HS. Insulin signaling in fatty acid and fat synthesis: a transcriptional perspective. *Curr Opin Pharmacol* 2010; 10(6): 684–691. doi: 10.1016/j.coph.2010.08.004

***Byung-Hyun Park**

Chonbuk National University Medical School
567 Baekje-daero, Deokjin-gu
Jeonju, Jeonbuk 54896
Republic of Korea
Email: bhpark@jbnu.ac.kr

***Soo-Wan Chae**

Department of Pharmacology
Chonbuk National University Medical School
567 Baekje-daero, Deokjin-gu
Jeonju, Jeonbuk 54896
Republic of Korea
Email: soowan@jbnu.ac.kr

The image shows a large, light gray logo consisting of the letters 'WWT'. The 'W' is formed by two overlapping 'V' shapes, and the 'T' is a simple vertical bar with a horizontal top bar. The logo is centered on the page.

Green tea (*Camellia sinensis*) aqueous extract alleviates postmenopausal osteoporosis in ovariectomized rats and prevents RANKL-induced osteoclastogenesis *in vitro*

Xin Wu^{1,2†}, Chuan-qi Xie^{1,2†}, Qiang-qiang Zhu^{1,2†}, Ming-yue Wang^{1,2}, Bin Sun^{1,2}, Yan-ping Huang^{1,2}, Chang Shen^{1,2}, Meng-fei An^{1,2}, Yun-li Zhao^{1,2,3*}, Xuan-jun Wang^{1,4,5*} and Jun Sheng^{1,4,5*}

¹Key Laboratory of Pu-erh Tea Science, Ministry of Education, Yunnan Agricultural University, Kunming, China; ²College of Food Science and Technology, Yunnan Agricultural University, Kunming, China; ³State Key Laboratory of Phytochemistry and Plant Resources in West China, Kunming Institute of Botany, Chinese Academy of Sciences, Kunming, China; ⁴College of Science, Yunnan Agricultural University, Kunming, China; ⁵State Key Laboratory for Conservation and Utilization of Bio-Resources in Yunnan, Kunming, China

Abstract

Background: Green tea (*Camelliasinensis* [L.] Kuntze) belongs to the plant family Theaceae and is mainly distributed in East Asia, the Indian subcontinent and Southeast Asia. This plant has been proven to be beneficial to human health, and green tea is the second most consumed beverage in the world after water. However, until now, the effect of green tea aqueous extract (GTE) upon postmenopausal osteoporosis has remained unclear. In this study, we investigated the therapeutic effects of GTE on estrogen deficiency-induced osteoporosis and explored the possible mechanisms *in vivo* and *in vitro*.

Materials and methods: Ovariectomized (OVX) female rats were orally administered with GTE at doses of 60, 120, and 370 mg kg⁻¹ for 13 consecutive weeks. The biochemical parameters, bone gla protein, alkaline phosphatase, acid phosphatase, estrogen, interleukin-1 β , and interleukin-6 in blood samples were detected, and histological change in bones was analyzed by hematoxylin and eosin staining. Meanwhile, the mechanisms of GTE on osteoclast formation were explored in RAW 264.7 cells induced by receptor activation of the nuclear factor kappa B ligand (RANKL).

Results: The results showed that GTE could increase bone mass and inhibit trabecular bone loss in OVX rats. Furthermore, real-time quantitative reverse transcription polymerase chain reaction analysis from *in vitro* experiments also showed that GTE reduced the mRNA expression of osteoclast-associated genes such as *cathepsin K* (cath-K), *c-Fos*, *matrix metalloproteinase 9*, *nuclear factor of activated T cells cytoplasmic 1* (NFATc1) and *tartrate-resistant acid phosphatase*. In addition, GTE caused a reduction in the protein levels of NFATc1, c-Fos, c-src and cath-K.

Conclusion: Evidence from both animal models and *in vitro* experiments suggested that GTE might effectively ameliorate the symptoms of osteoporosis in OVX rats and inhibit RANKL-induced osteoclast-specific gene and protein expression.

Keywords: *green tea aqueous extract; osteoporosis; ovariectomy; receptor activator of the nuclear factor kappa B ligand; osteoclast*

Osteoporosis is a systemic metabolic bone disease characterized by low bone mass, damaged microstructure, highly fragile bone, and greater vulnerability to fracture (1). The factors underlying osteoporosis are very complex and involve aging, endocrine disorders, calcium malabsorption, and limb disuse, as well as immune, nutritional, and genetic factors (2). There are two

types of osteoporosis: primary and secondary. Postmenopausal osteoporosis (PMOP) is the most prevalent of the primary forms of osteoporosis (3). Bone metabolism is a process of dynamic equilibrium, in which osteoblasts and osteoclasts work together to maintain homeostasis. However, the dynamic equilibrium of bone metabolism can be disrupted in response to the reduced level of estrogen (4).

[†]These authors contributed equally to this work.

Postmenopausal women are at high risk of developing osteoporosis because of the significant alterations in bone metabolism associated with estrogen deficiency (5). Approximately half of women over the age of 50 years are expected to suffer an osteoporosis-related fracture over their remaining lifetime (6, 7). Some individuals may develop osteopenia, a condition characterized by low bone density (8). The rapid bone loss and higher bone fragility that take place during menopause lead to an increased incidence of spine, hip, and wrist fractures in postmenopausal women. Estrogen replacement therapy (9), which represents the most common therapy for the prevention and treatment of PMOP, has been reported to be associated with an increased risk of breast cancer, ovarian cancer, endometrial cancer, and cardiovascular disease in postmenopausal women (10). Therefore, estrogen therapy is no longer recommended for the prevention of fractures in postmenopausal women, and developing alternative treatment strategies is needed (11).

Thousands of years of human experimentation has led to a significant belief in the safety of 'natural' products and this has contributed to the fairly widespread use of complementary therapies to relieve postmenopausal symptoms (12). Since ancient times, green tea, a Chinese traditional beverage, has been held to be beneficial to human health. The pharmacological effects and safety of this plant have been confirmed, particularly in respect of catechins, which make up 30% of the dry weight of tea leaves (13). Water extracts from green tea contain abundant bioactive constituents and have shown various biological activities, including antioxidant (14), anti-obesity (15), hypolipidemic, antidiabetic (16), anti-inflammatory, and anticancer (17) properties. Tea drinking is closely associated with bone health and may provide protection against osteoporosis and osteoporotic fracture; these effects have been verified both *in vitro* and *in vivo* (13, 18–20). Previous studies also showed that some chemical compositions of tea could improve bone loss *in vivo* (15, 21). Green tea polyphenols could improve bone loss in middle-aged female rats (21). (-)-Epigallocatechin-3-gallate, a main active ingredient in green tea, also showed a protective effect on bone microarchitecture in ovariectomized (OVX) rats (15). However, until now, the effect of green tea aqueous extract (GTE) upon PMOP has not been specifically investigated.

In the present study, we demonstrate that GTE had an ameliorative effect in OVX-induced osteoporosis rats, and that GTE could inhibit osteoclastic activities *in vitro*. Collectively, these data provide a theoretical foundation relating to the molecular mechanisms of GTE against osteoporosis.

Materials and methods

Reagents and antibodies

Escherichia coli (*E. coli*)-derived recombinant mouse receptor activation of the nuclear factor kappa B ligand (RANKL) was purchased from R&D Systems (Minneapolis, MN, USA) and dissolved in 1% bovine serum albumin in phosphate-buffered saline. Xian-Ling-Gu-Bao (XLGB) capsules were obtained from Guizhou Tongjitang Pharmaceutical Co., Ltd. (Guizhou, China). Alkaline phosphatase (ALP), calcium (Ca), and phosphorus (P) assay kits were purchased from Zhong-Sheng BeiKong Bio-Technology and Science (Beijing, China). Bone gla protein (BGP) and estrogen (E_2) radioimmunoassay kits were obtained from the Beijing North Institute of Biological Technology (Beijing, China). Rat interleukin-1 β (IL-1 β) and IL-6 enzyme-linked immunosorbent assay kits (R111102-07a; R111102-06a) were purchased from NeoBioscience Biological Technology Co., Ltd. (Shenzhen, China). tartrate-resistant acid phosphatase (TRAP) staining kits and acid phosphatase (ACP) assay kits were obtained from Nanjing Jiancheng Bioengineering Institute (Nanjing, China). Anti-nuclear factor of activated T cells cytoplasmic 1 (anti-NFATc1), anti-c-Src, anti-cathepsin K, and anti-c-Fos antibodies were purchased from Santa Cruz Biotechnology (Santa Cruz, CA, USA). Anti- β -tubulin and horseradish peroxidase-conjugated secondary antibodies were purchased from Proteintech Group, Inc. (Rosemont, IL, USA) and Thermo Fisher Scientific (Waltham, MA, USA), respectively.

Preparation of GTE

The green tea from a variety named Yunnan Daye (*Camellia sinensis* [Linn.] var. *assamica* [Masters] Kitamura) (22) were collected in 2015 in Yunnan Province and identified by Prof. Kaicong Fu of the Pu'er National Institute of Traditional Medicine, and a voucher specimen (2015-DPE-5) was deposited in the Key Laboratory of Pu-erh Tea Science of Yunnan Agricultural University. In each case, 100 g of green tea was extracted twice using 1200 mL of water each time (1.5 hours) under reflux. The extract was then decanted, filtered, and vacuum freeze-dried to obtain a 20 g crude water extract. GTE powder was dissolved in distilled water to a concentration of 50 mg/mL and the solution was kept at 4°C.

Animals

Healthy specific-pathogen-free female Wistar rats (12 weeks of age) were provided by the Laboratory Animal Center of Jilin University and were used for all animal experiments. All rats were raised in polypropylene cages with sterile paddy husk and kept under a controlled environment (humidity 50–60%; ambient temperature $24 \pm 1^\circ\text{C}$; light–dark cycle: 12L:12D). Experimental maintenance rat

chow (XieTong Organism, JiangSu, China) based upon the mean weekly food consumption of the sham group was used for feeding OVX rats. The calcium content of our rat chow is about 10–18 g/kg; the phosphorus content is about 6–12 g/kg. All experimental procedures were performed according to the guidelines of the Yunnan Agricultural University Committee for Care and Use of Laboratory Animals and were approved by the Animal Experiments Ethics Committee of Yunnan Agricultural University.

Group designations and treatment administration

After the rats were allowed to acclimate for 1 week, they were anesthetized with chloral hydrate and underwent resection of the bilateral ovaries (OVX). A further 12 rats (the sham group) were also anesthetized but only underwent resection of a small sample of fat, rather than the bilateral ovaries. All rats were monitored for 15 days before initiating the therapeutic regimen, to allow them to recover from the operation. We randomly divided the OVX rats ($n = 70$) into five groups: model group, XLGB capsule group (240 mg·kg⁻¹), low-dose GTE group (low dose, 60 mg kg kg⁻¹), medium-dose GTE group (medium dose, 120 mg kg⁻¹), and a high-dose GTE group (high dose, 370 mg kg⁻¹). Each group contained 14 rats. The animals were continuously administered with their respective treatments via gavage (10 mL/kg) every day for 13 weeks, and an equal volume of distilled water was intragastrically administered to the sham and model groups. XLGB capsules are widely used for the treatment of osteoporosis as a traditional Chinese medicine (3). The dosage of XLGB capsules for rats in our present study was based on the dosage used in clinical trials and calculated by a dose conversion table between human and rats. Furthermore, in the present study, the different dosage levels of GTE were determined and calculated based on previous research (23) and slightly modified to adapt to the current experimental conditions.

We weighed rats weekly during the treatment period. After the treatment period end, we euthanized rats by deep ether anesthesia and obtained blood samples for biochemical analyses. The uterus, left–right femur, and vagina were collected, and the samples for histological analysis were fixed in 10% neutral formaldehyde and then stored at room temperature for subsequent use.

Analysis of biochemical parameters in blood samples

Blood samples were incubated at room temperature for 2 h and centrifuged at 1,200 g for 10 min at 4°C, then serum was collected and stored at –20°C to await subsequent biochemical analysis. ALP, ACP, BGP, and E₂ levels were detected in rat serum according to the kit manufacturer's instructions. In addition, IL-1β and IL-6 levels were detected in the rat plasma.

Determination of organ coefficients

We completely removed and weighed the left femur and uterus. Then, organ coefficients were calculated as follows: organ coefficient = wet weight of organs/body weight.

Detection of bone mass and biomechanical testing

The intact left femur of each rat was removed with the muscle and connective tissue was peeled off before analysis. Femoral bone mineral density (BMD) was detected using dual-energy X-ray absorptiometry (LUNAR® Expert #1170, Lunar Prodigy Advance DEXA, GE Healthcare, Madison, WI, USA), in accordance with the manufacturer's instructions (24). Briefly speaking, the left femur was scanned, and the femoral BMD value was measured automatically. The maximum deflection of the left femur in OVX rats was also evaluated by using the three-point bending flexural test method (24). Therefore, the femur was placed in a biomechanical testing instrument (Changchun Research Institute for Mechanical Science Co., Ltd., Changchun, China) programmed with a stride distance of 20 mm and a loading velocity of 5 mm/s. The data were recorded on a computer, then the maximum deflection was calculated.

Histological analysis of the uterus and femur

The location of structural analysis of cortical thickness was 1/3 near-end of the right femurs. Fresh femur tissue was collected and fixed in 10% neutral formaldehyde for 72 h, decalcified in ethylenediaminetetraacetic acid (Sigma, St. Louis, Missouri, USA) pH 7.4 for 1 week, and then embedded in paraffin to perform sections following the longitudinal axis. Embedded tissues were cut into 4 μm sections and then were stained with hematoxylin and eosin (H&E) in accordance with a standard technique described previously (25). For analysis of the trabecular bone, consecutive slices (4 μm) were selected as the region of interest beginning 3.5 mm away from the distal femur growth plate. Static structural images of the cortical and trabecular bone were acquired using a medical image analysis system (BI-2000, Taimeng, Chengdu Technology 1 & Market Co., Ltd., Chengdu, China). Cortical bone thickness and trabecular bone area were measured using computer-aided software.

Cell culture and maintenance

RAW 264.7 murine macrophages (ATCC, Manassas, VA, USA) were used in this study as a cell model. Cells were cultured in Dulbecco's Modified Eagle's Medium (DMEM) supplemented with 10% fetal bovine serum (FBS) at 37°C in a humidified atmosphere with 5% CO₂. DMEM and FBS were purchased from Thermo Fisher Scientific and Biological Industries (Israel BeitHaemek Ltd.), respectively.

In vitro osteoclastogenesis assay

To induce osteoclasts, RAW 264.7 cells (ATCC®TIB-71TM, macrophage, Abelson murine leukemia virus transformed, 2×10^3 cells/well) were cultured in the presence of RANKL (50 ng/mL) (26). After 6 days, cells were fixed and then stained for TRAP activity in accordance with the kit manufacturer's protocol. Cells were defined as mature osteoclasts if light microscopy showed that they were TRAP-positive multinucleated cells with more than five nuclei.

Quantitative real-time reverse transcription PCR analysis

RAW 264.7 cells (1.2×10^5 cells/well) were inoculated in a 12-well plate and then treated with RANKL (50 ng/mL) in the absence or presence of XLGB (10 µg/mL) or GTE (25, 50, 100 µg/mL) for 48 h. Total RNA was extracted using TransZol Up (TransGen Biotech, Beijing, China) according to the manufacturer's protocol. Reverse transcription was performed using the PrimeScript RT Reagent Kit with gDNA Eraser (TaKaRa Bio, Otsu, Japan) in accordance with the manufacturer's protocol. Quantitative real-time reverse transcription PCR (qRT-PCR) was performed using SYBR® Premix Ex Taq™II (TliRNaseH Plus, TaKaRa Bio), and results were determined using a 7900HT Fast Real-Time PCR system (Applied Biosystems, Foster City, CA, USA). Data were calculated using the comparative $2^{-\Delta\Delta CT}$ method, and all values were normalized to the mRNA level of the endogenous *GAPDH* gene (25). The primer sequences (Generay Biotech, Shanghai, China) are provided in Table 1.

Protein preparation and Western blot analysis

RAW 264.7 cells (4×10^5 cells/well) were inoculated in 60-mm plates and incubated overnight. Then, the cells were treated with RANKL (50 ng/mL) in the absence or presence of XLGB (10 µg/mL) or GTE (25, 50, or 100 µg/mL) for 48 h. Western blot analysis was then performed as previously described (27). In brief, whole cell lysates were prepared from cultured cells using RIPA buffer (Solarbio, Beijing, China) according to the manufacturer's protocol. Cell lysates were normalized to calculate

protein concentration by using the bicinchoninic acid (BCA) method. Then proteins were separated by SDS-PAGE and transferred to polyvinylidene fluoride (PVDF) membranes (EMD Millipore Corporation, Merck Life Sciences, KGaA, Darmstadt, Germany). After washing, blocking, and hatching with the primary antibody, the membrane was hatched with a proper horseradish peroxidase-conjugated secondary antibody, and the resultant bands were detected using a Pro-light HRP Chemiluminescent Kit (Tiangen Biotech, Beijing, China). The representative images were finally acquired using a FluorChem E System (ProteinSimple, Santa Clara, CA).

Statistical analyses

We presented all data as the mean and standard deviations of the mean (SD). Differences within groups were analyzed statistically using one-way ANOVA and $p < 0.05$ was considered to be statistically significant. All analyses were performed using SPSS 17.0 (Chicago, IL, USA) and GraphPad Prism 5 (GraphPad Software, Inc., La Jolla, CA, USA).

Results

GTE influenced the body weight of OVX rats

As shown in Table 2, body weight increased with advancing age. The body weight of the model group increased significantly when compared with the sham group ($p < 0.01$), although the same amount of food was provided to both groups.

Body weight did not increase in the XLGB group compared with the model group and there were no significant differences between the GTE groups and the model group during the first 7 weeks of treatment. However, OVX rats treated with high-dose GTE showed a reduction in body weight at Week 8, compared with the model group ($p < 0.05$).

GTE influenced the serology indicators of PMOP in OVX rats

In order to examine the effect of GTE upon serology indicators of PMOP in OVX rats, serum BGP, ALP, ACP, E_2 , and plasma IL-1 β and IL-6 levels were determined using appropriate assay kits (Fig. 1).

Table 1. Primers used in the qRT-PCR study

Genes	Forward (5'–3')	Reverse (5'–3')
<i>GADPH</i>	AACTTTGGCATTGTGGAAGG	ACACATTGGGGGTAGGAACA
<i>TRAP</i>	GCTGGAAACCATGATCACCT	GAGTTGCCACACAGCATCAC
<i>c-Fos</i>	CAAGCGGAGACAGATCAACTTG	TTTCCTTCTTTTCAGCAGATTGG
<i>cathepsin K</i>	CTTCCAATACGTGCAGCAGA	TCTTCAGGGCTTTCTCGTTC
<i>MMP-9</i>	CGTCGTGATCCCCACTTACT	AACACACAGGGTTTGCCCTTC
<i>NFATc1</i>	TGGAGAAGCAGAGCACAGAC	GCGGAAAGGTGGTATCTCAA

Notes: qRT-PCR, quantitative reverse transcription polymerase chain reaction; TRAP, tartrate-resistant acid phosphatase; NFATc1, activated T cells cytoplasmic 1; MMP, metalloproteinase 9.

Table 2. Effect of green tea extract on body weight (g) in OVX rats

Time (week)	Sham	Model	XLGB	Low-dose	Medium-dose	High-dose
0	254.0 ± 17.54 (12) ^b	278.3 ± 22.23 (14)	279.9 ± 19.89 (14)	282.4 ± 21.02 (14)	280.4 ± 28.78 (14)	278.8 ± 24.08 (14)
1	260.3 ± 18.66 (12) ^b	290.0 ± 32.50 (14)	298.0 ± 25.57 (14)	297.4 ± 25.78 (14)	298.9 ± 30.16 (13)	290.1 ± 24.30 (14)
2	263.3 ± 18.87 (12) ^c	295.8 ± 21.21 (13)	304.4 ± 29.58 (14)	304.5 ± 22.50 (13)	300.7 ± 37.19 (13)	282.1 ± 27.16 (14)
3	268.6 ± 17.64 (12) ^c	311.5 ± 23.63 (13)	318.0 ± 27.90 (14)	311.3 ± 26.61 (13)	304.2 ± 47.19 (13)	306.7 ± 33.83 (14)
4	271.8 ± 17.85 (12) ^c	317.5 ± 22.61 (13)	322.2 ± 27.30 (14)	310.8 ± 25.07 (13)	316.5 ± 33.96 (12)	311.4 ± 34.23 (14)
5	275.1 ± 16.08(12) ^c	327.5 ± 17.22 (13)	331.9 ± 29.08 (14)	328.6 ± 24.56 (13)	326.0 ± 33.76 (12)	320.6 ± 33.46 (14)
6	270.3 ± 14.25 (12) ^c	335.9 ± 14.82 (13)	331.0 ± 29.62 (14)	330.6 ± 25.41 (13)	323.9 ± 31.68 (12)	319.4 ± 31.91 (14)
7	278.6 ± 15.59 (12) ^c	343.7 ± 15.16 (13)	336.4 ± 26.45 (14)	340.6 ± 26.86 (13)	328.6 ± 34.67 (12)	328.9 ± 30.44 (14)
8	283.1 ± 24.27 (12) ^c	353.1 ± 16.61 (13)	338.7 ± 31.11 (14)	347.6 ± 37.28 (13)	336.5 ± 36.32 (12)	332.2 ± 32.19 (14) ^a
9	281.0 ± 24.27 (12) ^c	353.6 ± 15.27 (13)	349.9 ± 28.27 (14)	355.2 ± 31.13 (13)	338.5 ± 33.60 (12)	340.5 ± 33.24 (14)
10	284.9 ± 15.5 (12) ^c	351.3 ± 18.25 (13)	351.4 ± 28.41 (14)	352.0 ± 31.73 (11)	344.2 ± 35.40 (12)	342.9 ± 31.00 (14)
11	298.6 ± 16.29 (12) ^c	352.8 ± 32.74 (13)	362.5 ± 30.81 (13)	359.2 ± 32.91 (11)	354.3 ± 35.41 (12)	353.9 ± 32.12 (14)
12	296.5 ± 19.67 (12) ^c	365.9 ± 19.23 (13)	366.1 ± 30.79 (13)	369.2 ± 33.62 (11)	365.2 ± 34.60 (12)	365.4 ± 33.35 (14)
13	303.0 ± 20.85 (12) ^c	367.0 ± 17.68 (13)	366.7 ± 31.14 (13)	365.9 ± 33.67 (11)	367.3 ± 36.38 (12)	364.3 ± 33.16 (13)

Notes: All data are presented as mean ± SD (n = 12–14). ^ap < 0.05, ^bp < 0.01, and ^cp < 0.001 versus the model group. OVX, ovariectomized; XLGB, Xian-Ling-Gu-Bao.

Serum BGP, ALP, and ACP were evaluated as biomarkers of bone formation and bone resorption (Fig. 1A–C). In the model group, these parameters were significantly increased compared with those in the sham group ($p < 0.01$). In OVX rats treated with low-dose GTE, the serum BGP and ALP levels were lower than those of the model group (Fig. 1A and B). OVX rats treated with low-dose and medium-dose GTE showed lower serum ACP levels compared with the model group (Fig. 1C).

The level of serum E_2 in the model group was significantly lower than that in the sham group ($p < 0.01$, Fig. 1D). Compared with the model group, OVX rats treated with XLGB showed moderately increased E_2 levels. GTE showed no significant influence on serum E_2 level in OVX rats.

Many cytokines are associated with bone resorption, including IL-1 β and IL-6. There were significant differences in IL-1 β and IL-6 when comparing levels between the model and sham groups ($p < 0.05$; Fig. 1E and F). The plasma levels of IL-1 β and IL-6 in OVX rats treated with XLGB and GTE (at any dose) were lower than in the model group. These results revealed that GTE could improve bone homeostasis in OVX rats.

Organ coefficients of the femur and uterus in OVX rats

PMOP can lead to a variety of problems with vital organs. For example, we found that following ovariectomy, the uterus of female rats became atrophied and this could also lead to vaginal atrophy. To further investigate the influence of GTE on OVA rats' organs, we determined the organ coefficients for the femur and uterus of OVX rats.

The organ coefficients of the femur and uterus in the model group were all significantly smaller than those of the sham group ($p < 0.01$, Fig. 2A and B). However, compared with the model group, the OVX rats treated with GTE had no obvious effect on either the femur or uterus organ coefficient. These results showed that GTE did not improve the organ coefficients in OVX rats to any extent.

GTE improved femoral BMD, biomechanical properties, and bone microarchitecture in OVX rats

We determined the BMD and maximum deflection of the femur in OVX rats to further investigate the protective effects of GTE upon bone (Fig. 3). The femoral BMD of OVX rats decreased significantly to 0.297 ± 0.013 g/cm², compared with 0.312 ± 0.025 g/cm² in the sham rats ($p < 0.05$), and the femoral BMD increased significantly in the high-dose GTE ($p < 0.05$); the positive control (XLGB) showed the same effect (Fig. 3A).

Next, we analyzed the femoral biomechanical properties by determining the maximum deflection. We revealed that the maximum deflection of the medium-dose GTE was significantly increased compared with the model group ($p < 0.05$, Fig. 3B).

These results suggested that treatment with GTE could improve femoral BMD and biomechanical properties in OVX rats. Furthermore, the trabecular bone microarchitectures in the femur were analyzed. As expected, the thickness of the cortical bone and the trabecular bone in the model group was significantly reduced compared to that in the sham group (Fig. 3C and E). Treatment with GTE could increase the thickness of the cortical bone slightly,

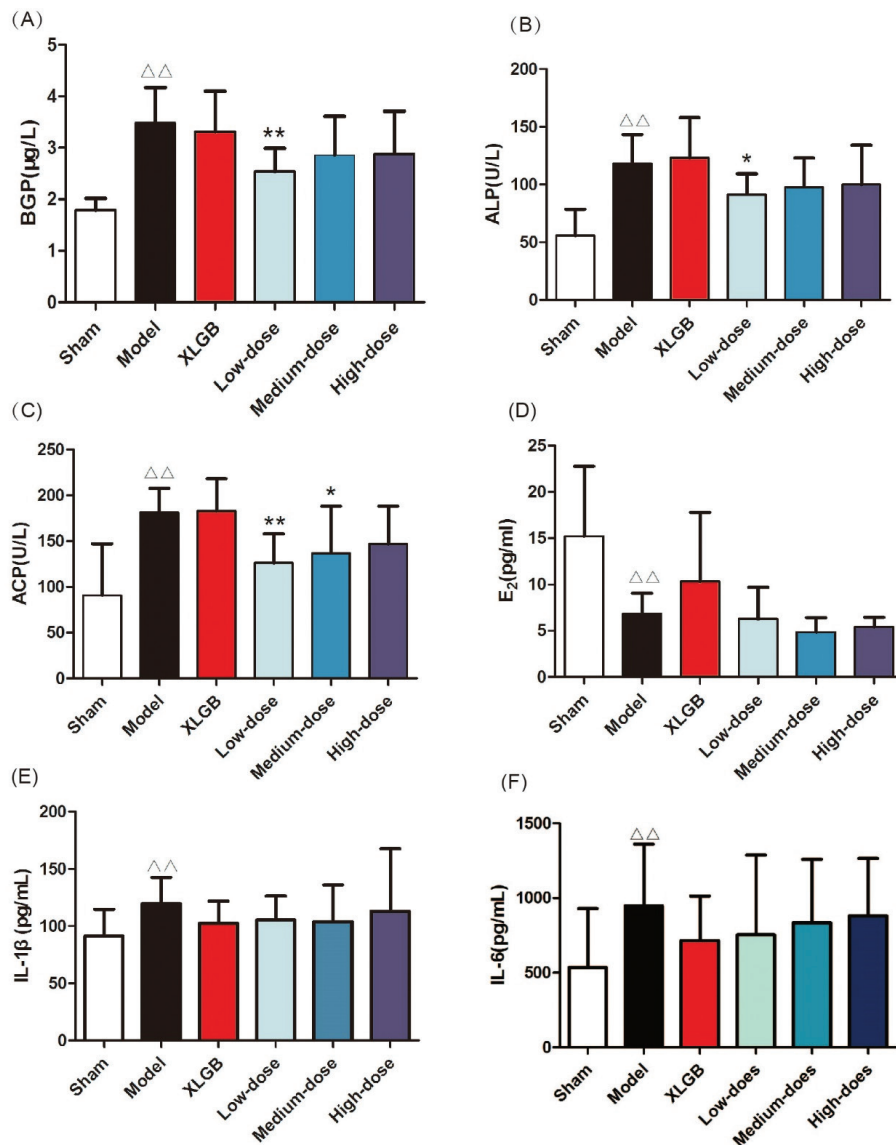


Fig. 1. GTE treatment attenuated the serology indicators of postmenopausal osteoporosis (PMOP) in ovariectomized (OVX) rats. (A) Serum bone gla protein (BGP); (B) alkaline phosphatase (ALP) acid; (C) phosphatase (ACP); (D) estrogen (E₂); (E) interleukin-1 β (IL-1 β); (F) interleukin-6 (IL-6). All data are presented as mean \pm SD ($n = 10$). $\Delta p < 0.05$ and $\Delta\Delta p < 0.01$ versus the sham group; and * $p < 0.05$ and ** $p < 0.01$ versus the model group.

Sham: underwent resection of a small sample of fat
 Model: underwent resection of the bilateral ovaries
 XLGB: Xian-Ling-Gu-Bao capsule group (XLGB, 240 mg kg⁻¹)
 Low-dose: administered GTE (60 mg kg⁻¹)
 Medium-dose: administered GTE (120 mg kg⁻¹)
 High-dose: administered GTE (370 mg kg⁻¹)

but these changes had no statistical significance (Fig. 3D). However, treatment with XLGB or GTE led to a significant improvement in the trabecular bone area ($p < 0.05$ or $p < 0.01$; Fig. 3F). In particular, it was evident that the increase in trabecular bone area in the GTE groups occurred in a dose-dependent manner. These results suggested that GTE has a protective effect on bone quality in OVX rats.

Furthermore, an osteoclast formation induced by RANKL in RAW 264.7 cells was successfully established (Fig. 4A and 4B). To determine whether GTE had cytotoxicity to RAW 264.7 cells, we further examined the cytotoxicity of GTE in RAW 264.7 cells using the 3-(4,5-Dimethylthiazol-2-yl)-2,5-diphenyltetrazolium bromide (MTT) assay (Fig. 4C). As expected, GTE did not have a cytotoxic

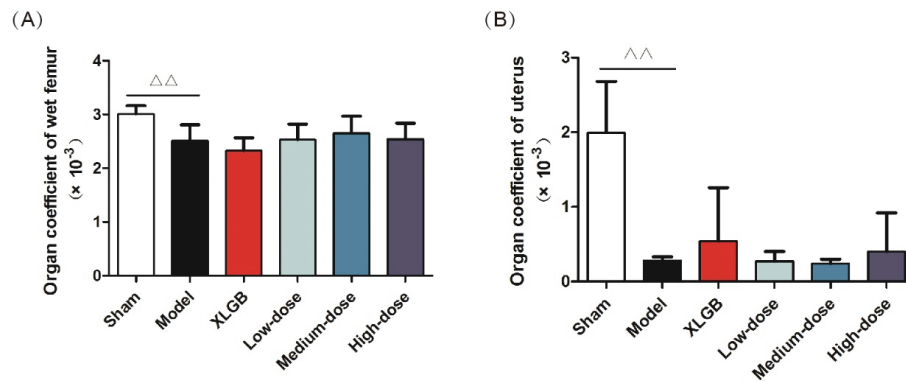


Fig. 2. Organ coefficients. (A) Femur and (B) uterus. All data are presented as mean \pm SD ($n = 10$). $\Delta p < 0.05$ and $\Delta\Delta p < 0.01$ versus the sham group, and $*p < 0.05$ and $**p < 0.01$ versus the model group.

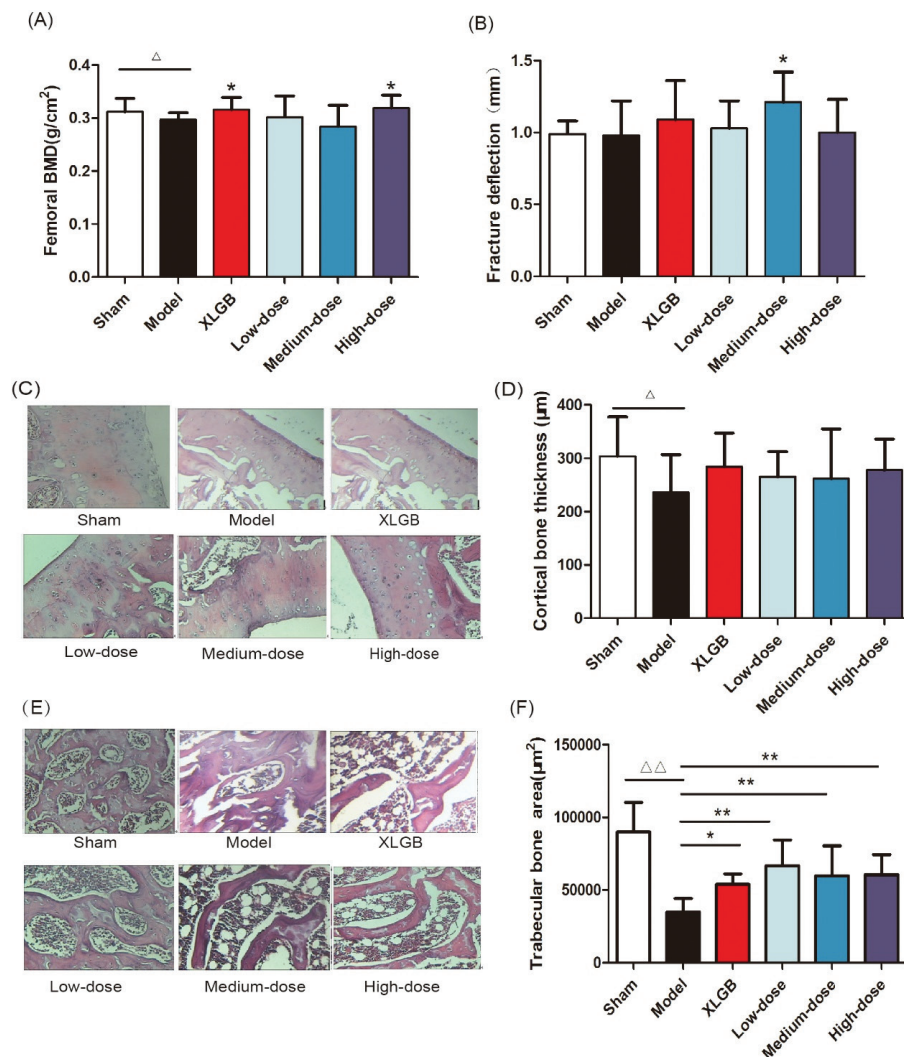


Fig. 3. GTE treatment improved femoral bone mineral density (BMD) (A) and fracture deflection (B) in OVX rats. Cortical bone tissue (C) and trabecular bone tissue (E) were stained with H&E; furthermore, the cortical bone thickness (D) and trabecular bone area (F) was calculated. Representative images were acquired using a medical image analysis system, and the original magnification was $\times 400$. All data are presented as the mean \pm SD ($n = 10$). $\Delta p < 0.05$ and $\Delta\Delta p < 0.01$ versus the sham group, and $*p < 0.05$ and $**p < 0.01$ versus the model group. Scale bar = 40 μm .

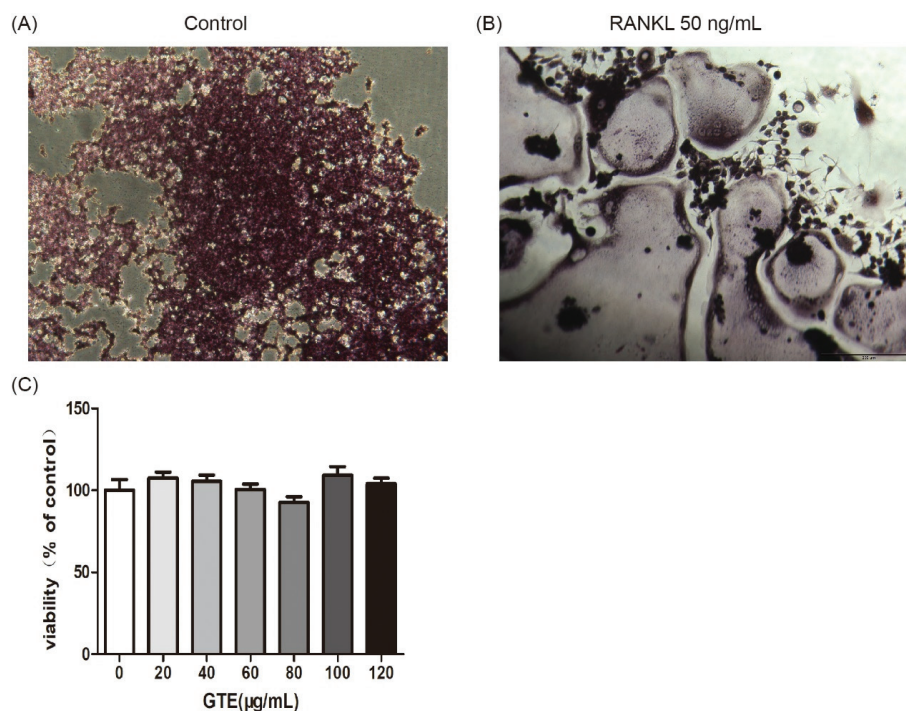


Fig. 4. Osteoclast differentiation was induced by receptor activator for nuclear factor- κ B ligand (RANKL) in RAW 264.7 cells (2×10^3 cells/well). After 6 days, cells were fixed and then stained for TRAP activity according to the manufacturer's protocol (A,B). The effect of GTE treated 48 h on the viability of RAW 264.7 cells as determined by the MTT assay (C). All data are presented as the mean \pm SD. * $p < 0.05$ and ** $p < 0.01$ versus the control group.

effect on osteoclast precursor cells. The qRT-PCR analysis showed that the osteoclastogenesis of *NFATc1*, *c-Fos*, *c-Src*, and *cathepsin K* genes were all inhibited by GTE treatment (Fig. 5). Collectively, Western blotting results indicated that GTE downregulated the expressions of the NFATc1, c-Fos, c-src and cathepsin K protein (Fig. 6).

Discussion and conclusions

Green tea, a popular well-known beverage worldwide, has captured considerable attention for its scientifically demonstrated beneficial effects on human health (25). Most of these positive and significant effects are attributed to its polyphenolic flavonoids, such as catechins (epicatechin, epigallocatechin, and epicatechin-3-gallate, as well as the major flavonoid (–)-epigallocatechin-3-gallate) (28). The most commonly recognized property of green tea is its potent antioxidant activity, which arises from an ability to scavenge reactive oxygen species (16).

In this study, we used OVX rats to induce a model of PMOP. The primary roles of 17- β estradiol and other estrogens are as regulators of reproductive function (29), although it is now appreciated that these steroid hormones play important activities in other processes that are unrelated to reproduction. Notably, the cessation of ovarian estrogen production that occurs at menopause is associated with an increased risk of osteoporosis, cardiovascular

disease, and vasomotor instability (30). Consequently, the OVX model is a highly useful and relevant model for postmenopausal women. Postmenopausal women are commonly linked with weight gain (31). According to previous study, body fat mass is negatively correlated with bone mass when the mechanical loading effect of body weight is statistically removed, suggested that interventions or treatments reducing obesity might increase bone mass and thus protect against osteoporosis (32). In our study, body weight, serum indexes, organ coefficients, and biomechanical parameters were significantly altered compared to the sham group. Collectively, these results showed that the OVX rats represented a useful model of PMOP.

Animal weight was observed throughout the study; high-dose GTE (370 mg kg^{-1}) could decrease the body weight at Week 8 compared with model group, which was probably due to the error of measurement or the decrease in food intake. Our data therefore showed that GTE had no obvious effect on weight gain induced by estrogen deficiency. Bone is a complex tissue; its fundamental function is to resist mechanical injury and absorb pressure (33). However, bone strength depends upon the quantity and quality of bone tissue, which is defined by the geometry and shape of the bone, the microarchitecture of the trabecular bone morphology, cortical thickness, and porosity. Bone strength is also characterized by the intrinsic

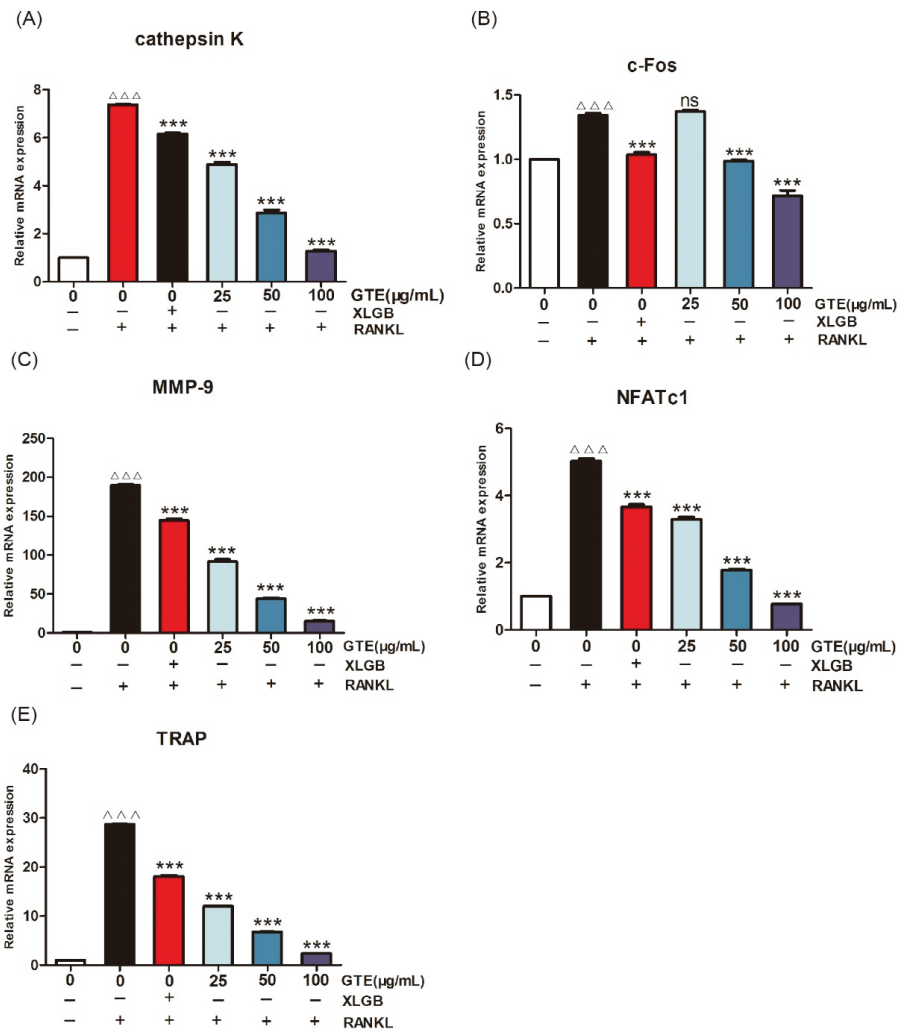


Fig. 5. GTE treatment suppressed RANKL-induced osteoclast-specific gene expression. The mRNA expression levels of *cathepsin K* (A), *c-Fos* (B), *matrix metalloproteinase-9* (MMP-9) (C), *NFATc1* (D), and *TRAP* (E). ^{^^^}*p* < 0.001 compared with control; ^{***}*p* < 0.001 compared with RANKL treatment only.

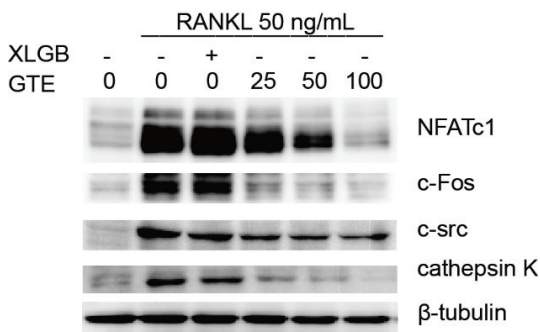


Fig. 6. The RANKL-induced osteoclast-specific protein expression of NFATc1, c-Fos, c-Src, and cathepsin K were downregulated by GTE.

BMD, biomechanical properties, and bone microarchitecture of OVX rats (Fig. 3A–E), implying that GTE could be of significant benefit to patients with PMOP.

Our *in vitro* studies showed that GTE could inhibit RANKL-induced osteoclast-specific gene and protein expression (Figs. 5 and 6). It is well known that osteoclast differentiation is directed by the expression of a range of marker genes, such as *NFATc1*, *TRAP*, *c-Fos*, *c-Src*, *cathepsin K*, and *MMP-9*. Most of these markers are regulated by *NFATc1* (34), a member of the NFAT (nuclear factor of activated T cells) family of transcription factor genes. *NFATc1* is the most strongly induced transcription factor gene following stimulation by RANKL, and it has been heavily implicated in the bone remodeling process in which RANKL-induced osteoclast differentiation plays a central role; if the expression of *c-Fos* increases, then the levels of *NFATc1* are upregulated (35, 36). Furthermore, data derived from our experiments with RAW 264.7 cells

properties of bone tissue such as turnover, mineral composition, and collagen. Furthermore, our present work revealed that GTE treatment could improve the femoral

showed that *NFATc1* levels could be upregulated by RANKL, while treatment with GTE led to a notable reduction in the expression of RANKL-induced *NFATc1*. The downregulation of *NFATc1* implied that the ability of RAW 264.7 cells to turn into osteoclasts had been suppressed by GTE treatment (Fig. 4B). Cathepsin K is a cysteine proteinase expressed predominantly by osteoclasts; this enzyme cleaves key bone matrix proteins and is believed to play an important role in degrading the organic phase of bone during bone resorption (37). Studies have shown that the overexpression of cathepsin K can perturb bone metabolism and thus cause bone loss. GTE also could reduce the expression of cathepsin K induced by RANKL, meaning that GTE could reduce bone loss by suppressing the expression of cathepsin K (Fig. 4B). C-Fos and MMP-9 are other examples of transcription factors involved in the formation of osteoclasts induced by RANKL. According to our current data, the expression of c-Fos and MMP-9 was also reduced in response to GTE treatment. In general, our study showed that GTE treatment suppressed the expression of osteoclast-specific genes and proteins.

In summary, our data demonstrated that GTE could improve a series of health problems induced by menopause, such as weight gain and organ pathology. Serum tests also showed that GTE could relieve bone loss. We also demonstrated that GTE could improve osteoporosis by suppressing osteoclast-specific gene and protein expression.

It has been reported that green tea aqueous extract consists of many chemical components, including green tea polyphenols (38), caffeine, aromatic oils, pigments and amino acids. Because of the extraordinary complexity of its components, the precise bioactive ingredient(s) responsible for the effect upon postmenopausal osteoporosis remains unidentified. Therefore, further research is urgently required in order to investigate the bioactive components responsible for the anti-osteoporotic effect of green tea. Our current results provided a theoretical basis for the subsequent exploration of the specific chemical constituents contained in green tea extract, which could act up on osteoporosis.

Acknowledgements

This work was supported by research grants from the Scholarship for Talent Academic Leader of Yunnan Province (2017HA015), the Scholarship for Young Academic and Technological Leaders of Yunnan Province (2015HB037), and the Science and Technology Major Project of Yunnan Province (2017ZF003).

Author contributions

JS, XW, and YZ conceived and designed the study. XW, CX, and MW performed the *in vivo* experiments. QZ and BS performed the *in vitro* experiments and analyzed the

data. YH, MFA, and CS performed the data analysis. XW, CX, MW, QZ, BS, YZ, and YH wrote the paper. All authors discussed the results and reviewed the manuscript.

Conflict of interest and funding

There are no conflicts of interest to declare.

References

1. Nelson ER, Wardell SE, McDonnell DP. The molecular mechanisms underlying the pharmacological actions of estrogens, SERMs and oxysterols: implications for the treatment and prevention of osteoporosis. *Bone* 2013; 53(1): 42–50.
2. Sharma C, Mansoori MN, Dixit M, Shukla P, Kumari T, Bhandari SP, et al. Ethanolic extract of *Coelogyne cristata* Lindley (Orchidaceae) and its compound coelogen promote osteoprotective activity in ovariectomized estrogen deficient mice. *Phytomedicine* 2014; 21(12): 1702–7.
3. Li Y, Lü SS, Tang GY, Hou M, Tang Q, Zhang XN, et al. Effect of *Morinda officinalis* capsule on osteoporosis in ovariectomized rats. *Chinese J Nat Med* 2014; 12(3): 204–12.
4. Casarrubios L, Matesanz MC, Sanchez-Salcedo S, Arcos D, Vallet-Regi M, Portoles MT. Nanocrystallinity effects on osteoblast and osteoclast response to silicon substituted hydroxyapatite. *J Colloid Interface Sci* 2016; 482: 112–20.
5. Andersen CY, Kristensen SG. Novel use of the ovarian follicular pool to postpone menopause and delay osteoporosis. *Reprod Biomed Online* 2015; 31(2): 128–31.
6. Xu F, Ding Y, Guo Y, Liu B, Kou Z, Xiao W, et al. Anti-osteoporosis effect of *Epimedium* via an estrogen-like mechanism based on a system-level approach. *J Ethnopharmacol* 2016; 177: 148–60.
7. Rossouw JE, Prentice RL, Manson JE, Wu L, Barad D, Barnabei VM, et al. Postmenopausal hormone therapy and risk of cardiovascular disease by age and years since menopause. *JAMA* 2007; 297(13): 1465–77.
8. Al-Anazi AF, Qureshi VF, Javaid K, Qureshi S. Preventive effects of phytoestrogens against postmenopausal osteoporosis as compared to the available therapeutic choices: an overview. *J Nat Sci Biol Med* 2011; 2(2): 154–63.
9. Wang C, Yu C, Gu Y, Zhang L. Research progress of drugs for osteoporosis treatment. *Chinese Sci Bull* 2014; 59(13): 1209–14.
10. Khosla S. Update on estrogens and the skeleton. *J Clin Endocrinol Metab* 2010; 95(8): 3569–77.
11. Karvande A, Khedgikar V, Kushwaha P, Ahmad N, Kothari P, Verma A, et al. Heartwood extract from *Dalbergia sissoo* promotes fracture healing and its application in ovariectomy-induced osteoporotic rats. *J Pharm Pharmacol* 2017; 69(10): 1381–97.
12. Zhang R, Pan YL, Hu SJ, Kong XH, Juan W, Mei QB. Effects of total lignans from *Eucommia ulmoides* barks prevent bone loss in vivo and in vitro. *J Ethnopharmacol* 2014; 155(1): 104–12.
13. Byun MR, Sung MK, Kim AR, Lee CH, Jang EJ, Jeong MG, et al. (-)-Epicatechin gallate (ECG) stimulates osteoblast differentiation via Runt-related transcription factor 2 (RUNX2) and transcriptional coactivator with PDZ-binding motif (TAZ)-mediated transcriptional activation. *J Biol Chem* 2014; 289(14): 9926–35.
14. Tsai CF, Hsu YW, Ting HC, Huang CF, Yen CC. The in vivo antioxidant and antifibrotic properties of green tea (*Camellia sinensis*, Theaceae). *Food Chem* 2013; 136(3–4): 1337–44.
15. Chen CH, Kang L, Lin RW, Fu YC, Lin YS, Chang JK, et al. (-)-Epigallocatechin-3-gallate improves bone microarchitecture in ovariectomized rats. *Menopause J North Am Menopause Soc* 2013; 20(6): 687–94.

16. Suliburska J, Bogdanski P, Szulinska M, Stepien M, Pupek-Musialik D, Jablecka A. Effects of green tea supplementation on elements, total antioxidants, lipids, and glucose values in the serum of obese patients. *Biol Trace Elem Res* 2012; 149(3): 315–22.
17. Matoušková P, Bártíková H, Boušová I, Szotáková B, Martin J, Skorkovská J, et al. Effect of defined green tea extract in various dosage schemes on drug-metabolizing enzymes in mice in vivo. *J Funct Foods* 2014; 10: 327–35.
18. Shen CL, Yeh JK, Cao JJ, Wang JS. Green tea and bone metabolism. *Nutr Res* 2009; 29(7): 437–56.
19. Shen CL, Yeh JK, Cao JJ, Chyu MC, Wang JS. Green tea and bone health: evidence from laboratory studies. *Pharmacol Res* 2011; 64(2): 155–61.
20. Oka Y, Iwai S, Amano H, Irie Y, Yatomi K, Ryu K, et al. Tea polyphenols inhibit rat osteoclast formation and differentiation. *J Pharmacol Sci* 2012; 118(1): 55–64.
21. Shen CL, Wang P, Guerrieri J, Yeh JK, Wang JS. Protective effect of green tea polyphenols on bone loss in middle-aged female rats. *Osteoporos Int* 2008; 19(7): 979–90.
22. Zhengyi PHR, Eds Wu, Peter H, Wu Z. *Flora of China*. Bei Jing: Science Press; 2000.
23. Henning SM, Niu Y, Liu Y, Lee NH, Hara Y, Thames GD, et al. Bioavailability and antioxidant effect of epigallocatechin gallate administered in purified form versus as green tea extract in healthy individuals. *J Nutr Biochem* 2005; 16(10): 610–16.
24. Chunxiao W, Chengying G, Liang J, Xiaoming S, Feng G, Junting Y, et al. Pharmacological effects of a recombinant hPTH(1-34) derived peptide on ovariectomized rats. *Eur J Pharmacol* 2017; 794: 193–200.
25. Wang S, Huang Y, Xu H, Zhu Q, Lu H, Zhang M, et al. Oxidized tea polyphenols prevent lipid accumulation in liver and visceral white adipose tissue in rats. *Eur J Nutr* 2016; 56(6): 2037–48.
26. Garcia Palacios V, Robinson LJ, Borysenko CW, Lehmann T, Kalla SE, Blair HC. Negative regulation of RANKL-induced osteoclastic differentiation in RAW264.7 cells by estrogen and phytoestrogens. *J Biol Chem* 2005; 280(14): 13720–7.
27. Cai X, Fang C, Hayashi S, Hao S, Zhao M, Tsutsui H, et al. Pu-erh tea extract ameliorates high-fat diet-induced nonalcoholic steatohepatitis and insulin resistance by modulating hepatic IL-6/STAT3 signaling in mice. *J Gastroenterol* 2016; 51(8): 819–29.
28. Badr El Dine FMM, Nabil IM, Dwedat FI. The effect of tributylin on thyroid follicular cells of adult male albino rats and the possible protective role of green tea: a toxicological, histological and biochemical study. *Egypt J Forensic Sci* 2017; 7(1): 7.
29. Wang C, Yu C, Gu Y, Zhang L. Research progress of drugs for osteoporosis treatment. *Chinese Sci Bull* 2014; 59(13): 49–54.
30. Khaw KT. Epidemiology of coronary heart disease in women. *Heart* 2006; 92(Suppl_3): iii2–iii4.
31. Davis SR, Castelo-Branco C, Chedraui P, Lumsden MA, Nappi RE, Shah D, et al. Understanding weight gain at menopause. *Climacteric* 2012; 15(5): 419–29.
32. Zhao LJ, Liu YJ, Liu PY, Hamilton J, Recker RR, Deng HW. Relationship of obesity with osteoporosis. *J Clin Endocrinol Metab* 2007; 92(5): 1640–6.
33. Goldberg G. Nutrition and bone. *Womens Health Med* 2004; 1(1): 25–9.
34. Kum CJ, Kim EY, Kim JH, Lee B, Min JH, Heo J, et al. Cyperus Rotundus L. extract suppresses RANKL-induced osteoclastogenesis through NFATc1/c-fos downregulation and prevent bone loss in OVX-induced osteoporosis rat. *J Ethnopharmacol* 2017; 205: 186–94.
35. Asagiri M, Sato K, Usami T, Ochi S, Nishina H, Yoshida H, et al. Autoamplification of NFATc1 expression determines its essential role in bone homeostasis. *J Exp Med* 2005; 202(9): 1261–9.
36. Takayanagi H, Kim S, Koga T, Nishina H, Isshiki M, Yoshida H, et al. Induction and activation of the transcription factor NFATc1 (NFAT2) integrate RANKL signaling in terminal differentiation of osteoclasts. *Dev Cell* 2002; 3: 889–901.
37. Saftig P, Hunziker E, Everts V, Jones S, Boyde A, Wehmeyer O, et al. Functions of Cathepsin K in bone resorption. *Adv Exp Med Biol* 2000; 477: 293–303.
38. Khan SA, Priyamvada S, Farooq N, Khan S, Khan MW, Yusufi AN. Protective effect of green tea extract on gentamicin-induced nephrotoxicity and oxidative damage in rat kidney. *Pharmacol Res* 2009; 59(4): 254–62.

*Jun Sheng

Key laboratory of Pu-er Tea Science,
Ministry of Education (Yunnan Agricultural University),
Kunming, 650201, P. R. China
Email: shengj@ynau.edu.cn

*Xuan-jun Wang

Key laboratory of Pu-er Tea Science,
Ministry of Education (Yunnan Agricultural University),
Kunming, 650201, P. R. China
Email: wangxuanjun@gmail.com

*Yun-li Zhao

Kunming Institute of Botany,
Chinese Academy of Sciences,
Kunming, 650201, P. R. China
Email: zhaoyunli@mail.kib.ac.cn.

TLR2/4-mediated NF- κ B pathway combined with the histone modification regulates β - defensins and interleukins expression by sodium phenyl butyrate in porcine intestinal epithelial cells

Xiujing Dou, Junlan Han, Qiuyuan Ma, Baojing Cheng, Anshan Shan*, Nan Gao and Yu Yang

Institute of Animal Nutrition, Northeast Agricultural University, Harbin, China

Abstract

Background: Host defense peptides (HDPs) possess direct antibacterial, antineoplastic, and immunomodulatory abilities, playing a vital role in innate immunity. Dietary-regulated HDP holds immense potential as a novel pathway for preventing infection.

Objective: In this study, we examined the regulation mechanism of HDPs (pEP2C, pBD-1, and pBD-3) and cytokines (IL-8 and IL-18) expression by sodium phenylbutyrate (PBA).

Design: The effects of PBA on HDP induction and the mechanism involved were studied in porcine intestinal epithelial cell lines (IPEC J2).

Results: In this study, the results showed that HDPs (pEP2C, pBD-1, and pBD-3) and cytokines (IL-8 and IL-18) expression was increased significantly upon stimulation with PBA in IPEC J2 cells. Furthermore, toll-like receptor 2 (TLR2) and TLR4 were required for the PBA-mediated upregulation of the HDPs. This process occurred and further activated the NF- κ B pathway via the phosphorylation of p65 and an I κ B α synthesis delay. Meanwhile, histone deacetylase (HDAC) inhibition and an increased phosphorylation of histone H3 on serine S10 also occurred in PBA-induced HDP expression independently with TLR2 and TLR4. Furthermore, p38-MAPK suppressed PBA-induced pEP2C, pBD-1 pBD-3, IL-8, and IL-18 expression, but ERK1/2 failed to abolish the regulation of pBD-3, IL-8, and IL-18. Moreover, epidermal growth factor receptor (EGFR) is involved in PBA-mediated HDP regulation.

Conclusions: We concluded that PBA induced HDP and cytokine increases but did not cause an excessive pro-inflammatory response, which proceeded through the TLR2 and TLR4-NF- κ B pathway and histone modification in IPEC J2 cells.

Keywords: *sodium phenylbutyrate; β -defensins; inflammatory cytokines; signaling pathway*

There are now global voices calling for solutions to the antibiotic resistance problem to guarantee the quality and safety of livestock products and human health. It is projected that 10 million people could die of infectious diseases caused by bacteria, viruses, or fungi by 2050 if effective measures are not taken (1). Such a devastating event should never occur. Therefore, efforts are now urgently needed to formulate a proper strategy for developing new range of antibiotics.

In multicellular animals, plants and insects, Host defense peptides (HDPs) are not only naturally produced but also involved in immunomodulatory and adjuvant functions in the immune cells to boost immune response of the organisms (2); HDPs are also expressed by the host as an antibiotic to protect against potential invading pathogenic microbes via their unique physical properties

and membrane-permeabilizing antibacterial mechanisms of action, making drug resistance difficult (3). Recently, the role of HDPs in innate and adaptive immunity is being increasingly appreciated. As an important first line of defense, HDPs are mostly expressed in the epithelial cells of the digestive, respiratory, or urogenital tracts. More than 30 HDPs, including the β -defensin and cathelicidin genes, have been reported to date in pigs (4, 5); indeed, these HDPs include, but are not limited to, β -defensin 1 (pBD1), pBD2, pBD3, pBD129, and epididymis protein 2 splicing variant C (pEP2C), which are present in a wide range of porcine tissues (6).

The hypothesis that HDPs synthesis are induced by some small molecules or dietary compounds which not alter an excessive inflammatory response, this fact will be a promise of preventing and controlling inflammatory

response and related infective diseases (7). Butyrate is a short-chain fatty acid (SCFA) naturally produced by colonic bacteria fermentation, and sodium butyrate is capable of inducing HDP expression without affecting the expression of IL-6 enhancing disease resistance in piglets via HDAC inhibition (8). This mechanism is supported by an increased phosphorylation of histone H3 on serine S10 and the activation of the I κ B kinase complex, which also leads to the activation of NF- κ B. Moreover, both NF- κ B and histone acetyltransferase p300 support the enhanced induction of hBD2 expression (9). However, due to the special cheese-like, rancid odor of sodium butyrate, the use is limited among some animals.

Sodium 4-phenylbutyrate (PBA), an aromatic SCFA, is a HDAC inhibitor known for inducing favorable effects on many pathologies, including cancer and pulmonary tuberculosis (10, 11). Indeed, PBA plays an immunomodulatory or anti-inflammatory role. Some studies have focused on cathelicidin antimicrobial peptide (CAMP)-inducing gene expression by PBA in various tissues, and the underlying molecular mechanism of CAMP gene expression has been resolved; interest in this research area is steadily increasing. Previous studies have focused on cathelicidin antimicrobial peptide (CAMP) gene expression induced by PBA in various tissues, however, current research trend focused on induce CAMP expression depends on the vitamin D receptor (VDR) pathway (12) and mitogen activated protein kinase (MAPK) signaling, coupled with PBA-regulated HDP expression displays the gene specific regulation and tissue specificity (13). To date, there is no data regarding how PBA controls HDP expression and exerts its immune defense ability on porcine cells. Herein, we initially show that HDP genes are expressed in porcine intestinal epithelial cells and are enhanced by PBA, but we also show that there is no effect on IL-6 levels. Our results demonstrate that PBA induces HDP expression via the toll-like receptor (TLR) pathway. This process is supported by the phosphorylation of NF- κ B p65 independent of myeloid differentiation primary response gene (MyD88) and an I κ B α synthesis delay process; this phosphorylation leads to NF- κ B activation. PBA possesses a strong ability to inhibit HDAC and enhance the phosphorylation modification of histone H3 on serine S10 in IPEC J2 cells. Thus, we provide novel insights into the regulation of HDP gene expression and evaluate the role of PBA in the innate and adaptive immunity of IPEC J2 cells.

Materials and methods

Reagents and antibodies

Sodium phenylbutyrate (purity above 98%) was purchased from Sigma (St. Louis, MO, USA). SB203580 (p38 MAPK inhibitor) and PD98059 (MAPKK inhibitor)

were both purchased from Beyotime (Shanghai, China). Gefitinib was purchased from MedChem Express (Trenton, New Jersey, USA). We used rabbit mAb phospho-NF- κ B p65 (Ser536, Cell Signaling Technology, Beverly, MA, USA), anti-I κ B (SC-371, Santa Cruz Biotechnology, Dallas, TX, USA), anti- β -actin (13E5, Cell Signaling Technology), and secondary horseradish peroxidase (HRP)-conjugated anti-rabbit IgG (4970, 7077, Cell Signaling Technology, Beverly, MA, USA). Dimethylsulfoxide (DMSO) was purchased from Sigma (St. Louis, MO, USA).

Cell culture

The IPEC J2 cell lines, porcine intestinal epithelial cell lines originally derived from the jejunal crypt of a neonatal piglet, were cultured in DMEM/F12 medium (Gibco, Carlsbad, CA, USA) supplemented with 8% (vol/vol) fetal bovine serum (FBS, Bioid), 5 μ g/L ITS (Sciencell, Carlsbad, CA, USA, Cat: 0803), 5 μ g/L epidermal growth factor (Sciencell, Carlsbad, CA, USA, Cat: 10504), and 1% penicillin/streptomycin (100 U/mL and 100 mg/mL) (V900929, Sigma, St. Louis, MO, USA) at 37°C with 5% CO₂.

Cytotoxicity measurement

The MTT dye reduction assay was used to determine the cytotoxicity of PBA on the IPEC J2 cell lines. Briefly, the IPEC J2 cells were seeded into a 96-well cell culture plate (Corning, NY, USA) with complete DMEM/F12 medium and were grown overnight at 37°C in 5% CO₂ in a humidified incubator. The cells were washed twice with phosphate buffer solution (PBS), and then fresh DMEM/F12 medium containing different concentrations of PBA was added and incubated for 24 h. Next, 10 μ L of MTT (0.5 mg/mL) was added and then the cells were incubated for another 4 h at 37°C. Subsequently, 100 μ L of DMSO was added to dissolve the formazan crystals that formed. Finally, the Optical Density (OD) was measured using a microplate reader (TECAN GENios F129004, Austria) at 490 nm.

RNA isolation and quantitative real-time PCR

Total RNA was isolated with the TRIzol reagent (Ambion Life Technologies, Carlsbad, CA, USA), and almost immediately the cDNA was synthesized using a reverse transcription kit (RR037A, Takara, Ostu, Japan) according to the manufacturer's instructions. PCR was performed using a SYBR® Premix Ex Taq™ (Tli RnaseH Plus) (RR420A, Takara, Ostu, Japan) on a 7,500 real-time PCR system (Applied Biosystems, Carlsbad, CA, USA). Each sample reaction was run in duplicate on the same plate. The gene-specific primers are presented in Table 1 (14–16). The mRNA expression levels were determined using the 2^{- $\Delta\Delta$ Ct} method with β -actin as a reference.

Table 1. List of primers used for qRT-PCR

Target gene	Sequence (5'-3')	Reference/accession
pBD-3	Forward: GAAGTCTACAGAAGCCAAAT Reverse: GGTAACAAATAGCACCATAA	a
pEP2C	Forward: GTTGACCTGGGAGCCAAAG Reverse: GCACAGATGACAAAGCCTCA	c
pBD-1	Forward: CCGCCTCCTCCTTGATT Reverse: GGTGCCGATCTGTTTCAT	MF925344.1
IL-6	Forward: TGGCTACTGCCTTCCCTACC Reverse: CAGAGATTTTGCCGAGGATG	b
IL-8	Forward: CTGGCTGTTGCCTTCTTG Reverse: TCGTGGAAATGCGTATTATG	b
IL-18	Forward: ACTTTACTTTGTAGCTGAAAACGATG Reverse: TTTAGGTTCAAGCTTGCCAAA	b
TLR2	Forward: TCACTTGTCTAACTTATCATCCTCTTG Reverse: TCAGCGAAGGTGTCATTATTGC	b
TLR3	Forward: AGTAAATGAATCACCTGCCTAGCA Reverse: GCCGTTGACAAAACACATAAGGACT	b
TLR4	Forward: GCCATCGCTGCTAACATCATC Reverse: CTCATACTCAAAGATACACCATCGG	b
NF- κ B1 (p50)	Forward: CTCGCACAAGGAGACATGAA Reverse: ACTCAGCCGGAAGGCATTAT	b
NF- κ B3 (p65)	Forward: TGTGTAAGAAGCGGGACCT Reverse: CACTGTCACCTGGAAGCAGA	c
β -actin	Forward: GGCTCAGAGCAAGAGAGGTATCC Reverse: GGTCTCAAACATGATCTGAGTCATCT	c

a (14); b (15); c (17); The sequences of pBD-1 in Table 1 are available through GenBank (<http://www.ncbi.nlm.nih.gov/nucore/>) under the accession numbers listed above.

HDAC activity detection

The HDAC activity assay was performed using the amplite™ fluorometric HDAC activity assay kit (AAT Bioquest®, Sunnyvale, CA, USA) according to manufacturer's protocol. Briefly, the IPEC J2 cells were cultured in a 12-well tissue culture plate overnight at a density of 1×10^5 cells/wells. The cells were treated in duplicate with increasing concentrations of PBA (0–8 mM). A well-characterized HDAC inhibitor, trichostatin A (TSA), was used as a positive control. The cell pellets were harvested after 24 h and homogenized in ice-cold RIPA lysis buffer (P0013B, Beyotime, Shanghai, China) containing the complete protease inhibitor, phenylmethylsulfonyl fluoride (PMSF) (ST506, Beyotime, Shanghai, China). The protein concentration of cell lysates was measured using the trace nucleic acid protein analyzer (Implen, Germany), and the cell lysates were diluted into an appropriate range, which containing equivalent amount of the protein in the assay buffer. Then, 50 μ L of the HDAC Green™ substrate working solution was added to each well, and the plate was incubated at room temperature for 45 min. The fluorescence intensity at Ex/Em = 490/525 nm was monitored.

The fluorescence was detected in the blank wells with buffer only, which was used as the background and was subtracted from the values determined for the wells subjected to the HDAC Green™ reactions. All the fluorescence readings are expressed in the relative fluorescence units (RFU), and each experiment was performed in triplicate.

Western blot analysis

For the immunoblot analyses, the total protein was extracted from the cytoplasm of the IPEC J2 cells, and the samples were denatured in 4 \times SDS-PAGE loading buffer (40 mM Tris-HCl, PH 8.0, 200 mM DTT, 4% (v/v) SDS, 40% (v/v) Glycerol and 0.032% (v/v) Bromophenol Blue) (No. 7173 Takara, Ostu, Japan) and boiled for 10 min. The denatured proteins were separated using 12% SDS-PAGE and were transferred onto a PVDF membrane (0.45 μ M) (Millipore, Boston, Massachusetts, USA). The membrane was blocked in Tris Buffered Saline with Tween (TBST) (10 mM Tris, 100 mM NaCl, 0.1% Tween 20) with 5% (w/v) nonfat milk powder for 1.5 h. After washing with TBST for three times, the blocked membranes were incubated with the primary antibodies overnight at

4°C in TBST and were then washed three times followed by incubation with the corresponding HRP-linked secondary antibodies (1:2500) for 1 h at room temperature. The membranes were washed three times, and bound antibodies were detected using an ECL plus detection system (P1010, Applygen, Beijing, China). The expression of each protein was normalized to that of β -actin.

siRNA and transfections

The IPEC J2 cells were cultured to approximately 80% confluence in DMEM/F12 medium supplemented with 8% (v/v) FBS in 24-well plates. The cells were then transfected with 160 nM siRNA using Lipofectamine 2000 (Invitrogen) in Opti-MEM media (Gibco) according to the manufacturer's instructions. After 6 h, the transfection medium was replaced with DMEM/F12 medium. Then the IPEC J2 cells were cultured with 8 mM PBA for 24 h. The cell lysates were harvested and analyzed by qRT-PCR. The small interfering RNA (siRNA) molecules targeting TLR2, TLR4, and a scrambled control were obtained from Shanghai Gene Pharma, and the sequences are presented in Table 2 (15).

Plasmids transfections and luciferase reporter assays

The NF- κ B p65 luciferase reporter plasmid (pNF- κ B-Luc) and the internal-control plasmid-encoding Renilla luciferase (pRL-TK) were kindly provided by Prof. Guangxing Li (Northeast Agricultural University, Harbin, P. R. China). The IPEC J2 cells were co-transfected with 0.3 μ g of pNF- κ B-Luc and 0.1 μ g of pRL-TK using the Lipofectamine 2,000 (Invitrogen) reagent in 24-well plates overnight at a density of 1×10^5 cells/wells. After 6 h, the cells were treated with PBA at 8 mM and were cultured for 24 h continually. The cells stimulated by lipopolysaccharide (LPS) were used as a positive control, which usually activates the NF- κ B pathway. The cell lysates were harvested and analyzed using the Dual-Luciferase[®] Reporter Assay Kit (Promega, Madison, WI, USA). The luciferase activities were detected using a Promega GloMax 20/20 Luminous detector (Promega, China).

Immunofluorescence assays

The IPEC J2 cells were seeded into 24-well plates and were treated with PBA (8 mM) and TSA (1 μ M) for 24 h,

washed with PBS, fixed with 200 μ L 4% paraformaldehyde for 10 min, and quenched with 0.1 M glycine for 5 min at room temperature. Subsequently, the cells were permeabilized with 1% Triton X-100, and diluted into PBS for 10 min. After washing with PBS three times, the cells were then incubated at 37°C with a histone H3 mouse monoclonal antibody (1:200) for 45 min, washed three times, and were subsequently incubated with a TRITC-conjugated AffiniPure goat anti-mouse IgG(H+L) (1:200) for 30 min. Thereafter, the cells were washed with PBS and then stained with DAPI at 37°C for 10 min to detect the nuclei, and washed with PBS three times again. The fluorescence signals were visualized using a fluorescence microscope (Leica).

Statistical analysis

All the results were expressed as the means \pm SD. Differences between the groups were compared using an unpaired Student's *t*-test or GLM (General Linear Model of Statistical Analysis System, SAS 9.4.2, 2000). Differences between the treatments were considered significant for $P < 0.01$.

Results

PBA facilitates endogenous HDP gene expression but does not enhance IL-6 production in IPEC J2 cells

Recent studies show that sodium 4-phenylbutyrate (PBA), an odorless derivative of butyrate sodium, is an even more potent inducer of cathelicidins in vitro than butyrate sodium (13). We investigated the expression of inducible genes encoding HDPs (pEP2C, pBD-1, pBD-3) and cytokines (IL-6, IL-8, IL-18) in the innate immune response by PBA. Our real-time PCR analyses indicated that HDP expression was markedly increased in a dose-dependent manner following a 24-h treatment with PBA in IPEC J2 cells (Fig. 1a). Similarly, the expression levels of IL-8 and IL-18 were dose-dependently induced by PBA (Fig. 1b). However, the mRNA level of the IL-6 gene was not affected. Furthermore, an obvious time-dependent induction of pEP2C, pBD-1, pBD-3, IL-8, and IL-18 was observed in the IPEC J2 cells, and the IL-6 expression was still not affected (Fig. 1c, 1d). Herein, the cytotoxicity was not significantly altered by PBA at concentrations \leq 8 mM in the IPEC J2 cells, as assessed by the MTT assay (Fig. 1e). The concentration and time of PBA were selected at 8 mM and 24 hour respectively in the following trials.

PBA-induced HDP gene expression via TLR2 in IPEC J2 cells

TLRs mediate diverse signaling pathways, which recognize molecular-associated patterns of microorganisms. Intestinal epithelial cells express TLRs, and their activation leads to the production of anti- or pro-inflammatory

Table 2. The sequences of siRNA

Names	Sequences(5'-3')	Reference
TLR2	CCA GAU CUU UGA GCU CCA UTT AUG GAG CUC AAA GAU CUG GTT	a
TLR4	GCA UGG AGC UGA AUU UCU ATT UAG AAA UUC AGC UCC AUG CTT	a
NC	UUC UCC GAA CGU GUC ACG UTT ACG UGA CAC GUU CGG AGA ATT	a

The sequences of siRNA. a (15).

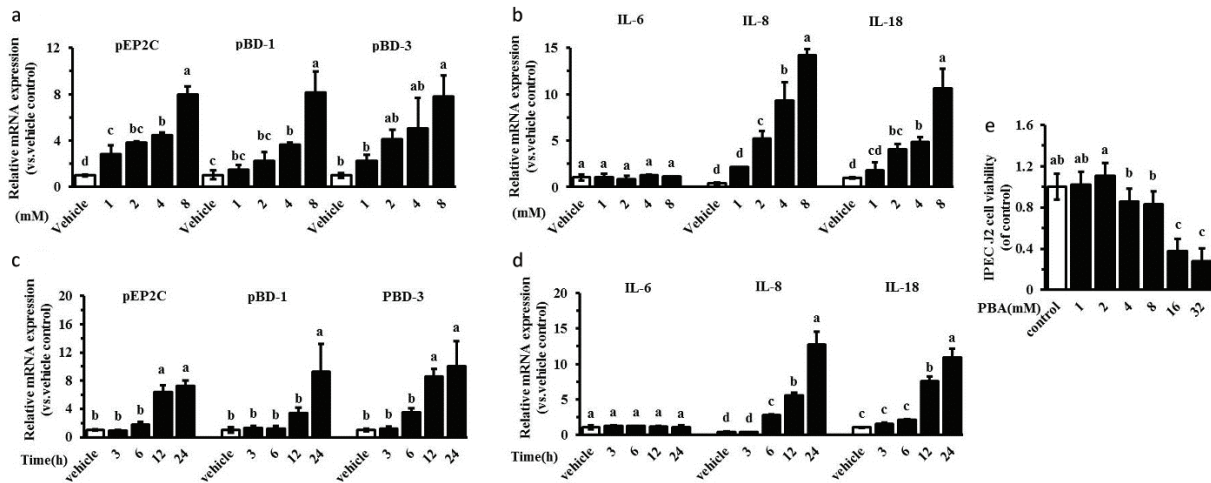


Fig. 1. PBA upregulates endogenous HDPs gene expression. IPEC J2 cells were stimulated with 0 mM, 1 mM, 2 mM, 4 mM, and 8 mM PBA for 24 h (a, b) or 8 mM of PBA for 3 h, 6 h, 12 h, and 24 h (c, d). HDPs (pEP2C, pBD-1, pBD-3) and cytokines (IL-6, IL-8, IL-18) were analyzed by qRT-PCR. (e) IPEC J2 cells in a broad range of concentrations (0–32 mM) for 24 h, we used the MTT dye reduction assay to examine their toxicity. All data are expressed as the means \pm SD. Letters with different superscripts are significantly different at $P < 0.01$, compared with vehicle.

cytokines contributing to inflammatory responses (17). Previous studies have shown that sodium butyrate activate TLR2 and then mediate HDP gene expression (16). In our studies, the expression of TLR2 was enhanced 10-fold by PBA, and the expression of TLR4 showed an increasing tendency but was not significant. However, the expression of TLR3 was significantly decreased by quantitative real-time PCR (Fig. 2a). We further evaluated the role of TLR2 or TLR4 in the gene regulation of encoding HDPs and cytokines by PBA. The IPEC J2 cells were transfected with a siRNA-targeting TLR2 or TLR4 to silence TLR2 or TLR4, respectively. Compared with the control siRNA, the results showed that TLR2 or TLR4 expression were reduced markedly following the transfection of TLR2/4 siRNA by qRT-PCR (Fig. 2b and 2c). Thereafter, we further analyzed the regulation changes of HDP expression by PBA after silencing TLR2 or TLR4. The results showed that even though the expression of pEP2C was still increased significantly by PBA, it was remarkably reduced in the cells treated with TLR2/4 siRNA, compared with the control siRNA by PBA (Fig. 2d). Most clearly, pBD-1, induced by PBA, was dramatically and completely destroyed under the condition of silencing both TLR2 and TLR4 (Fig. 2d). Distinguishingly, TLR4 silencing did not effect pBD-3 mRNA expression, compared with the cells transfected with the negative control siRNA (Fig. 2f). Taken together, these data indicate that TLR2 silencing stopped or interfered with the upregulation of HDPs expression by PBA in IPEC J2 cells. Interestingly, TLR4 silencing had no effect on the pBD-3 induction by PBA, but the role of TLR4

signaling was similar to TLR2 with respect to the regulation of pEP2C and pBD-1 expression by PBA. Furthermore, the results further showed that the induction of IL-8 exhibited an obvious difference with the pBD-1, pBD-3, or pEP2C genes regulated by PBA, and the expression regulation of IL-8 by PBA was not altered after knocking down TLR2 or TLR4 completely (Fig. 2g). While the expression of IL-18 significantly declined in the IPEC J2 cells treated with TLR2 or 4 siRNA, the IL-18 expression was still elevated by PBA; this result was similar to when expression of the pEP2C induced by PBA was blocked by TLR2 or 4 silencing (Fig. 2h). The myeloid differentiation primary response gene adaptor molecule (MyD88) was involved in the TLR signaling pathways (18). Our results showed that PBA did not influence MyD88 mRNA levels (Fig. 2i), suggesting that PBA influenced signaling effectors during TLR activation but not MyD88.

PBA activates the NF- κ B signaling pathway in IPEC J2 cells and induces HDP gene expression

Cytokine production mediated by TLR recognition and activation is usually dependent on the NF- κ B pathway and MAPKs, and thus, we evaluated both signaling pathways after PBA stimulation in IPEC J2 cells. First, we took a luciferase reporter approach using a luciferase vector containing the NF- κ B p65 initiation factor sequences, as previously reported by others. The IPEC J2 cells were co-transfected with the pNF- κ B-Luc plasmid and the internal-control pRL-TK plasmid, and were then treated with PBA or LPS to address the effect on

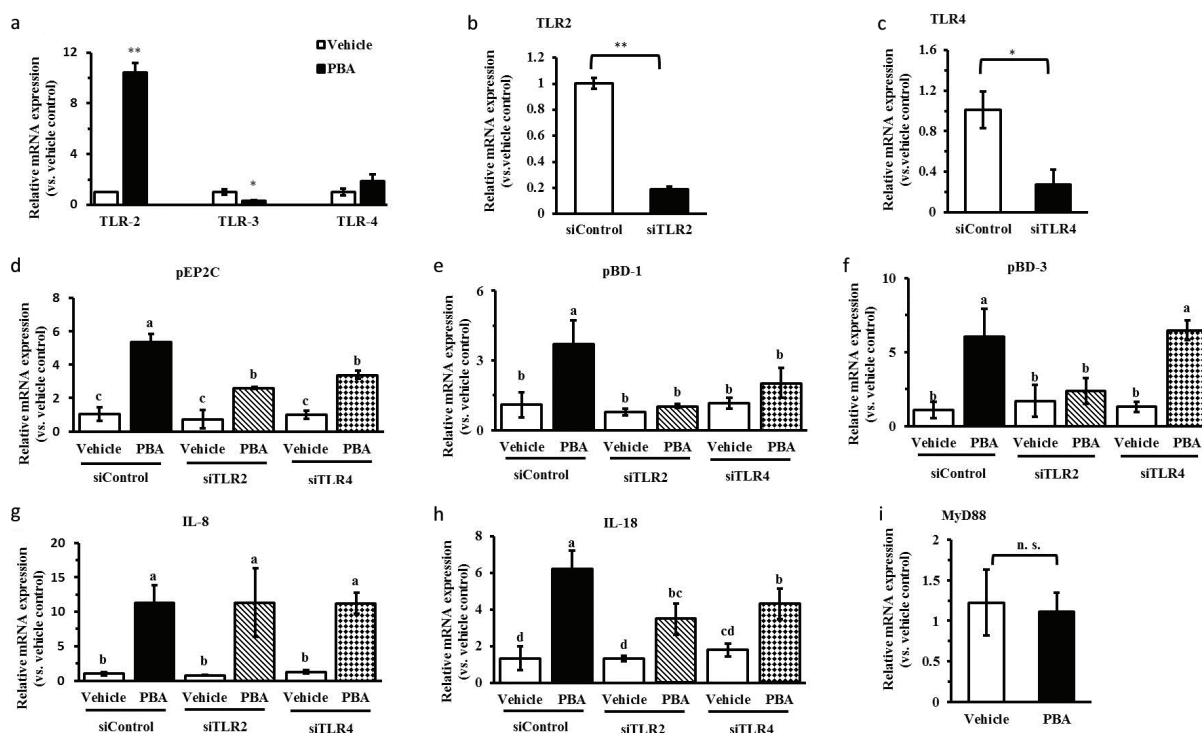


Fig. 2. PBA-induced HDPs gene expression via TLR2. (a) Expressions of TLRs were determined by quantitative real-time PCR. (b, c) IPEC J2 cells were transfected with TLR2/4 siRNA to specifically silence TLR2/4 and then treated with PBA. TLR2/4(b, c), HDPs (pEP2C, pBD-1, pBD-3) (d, e, f), and cytokines (IL-8, IL-18) (g, h) gene expressions were analyzed by qRT-PCR. (i) IPEC J2 cells were treated with PBA for 24 h, by qRT-PCR to detect the expression of MyD88 mRNA. Letters with different superscripts are significantly different at $P < 0.01$, compared with vehicle.

NF- κ B translational activity. LPS is known as a positive stimulus of NF- κ B. In agreement, we observed a strong expression of the NF- κ B-regulated luciferase following PBA pretreatment compared to expression without treatment by the stimulant, and similar results were obtained in the IPEC J2 cells after stimulation with LPS (Fig. 3a). The classic NF- κ B activation pathway is a multi-step process that involves several key proteins in inflammatory and immune responses and cellular proliferation. The most abundant form of NF- κ B is a heterodimer of p50 and p65 (19). Our results showed a markedly reduced p50 expression but not p65 by qRT-PCR (Fig. 3b). Next, we observed a clear increase of NF- κ B p65 phosphorylation in a time-dependent manner following PBA pretreatment (Fig. 3c). A crucial negative regulator that controls NF- κ B activation is the inhibitor of κ B (I κ B); this inhibitor binds to p65 in the cytosol to block the nuclear translocation of the p65/p50 complex. Based on the I κ B- α protein assays, we found that PBA eventually facilitated the proteasomal degradation of I κ B- α in response to PBA treatment for 24 h, which freed p65/p50, allowing the entry of p65/p50 to the nucleus to activate gene expression. There was degradation at 24 h compared

with the vehicle without pretreatment; however, it is interesting that an increased expression of I κ B- α protein from 6 h to 24 h under the internal reference calibration were observed (Fig. 3c). Collectively, our results establish that PBA upregulates HDP expression and activates the NF- κ B pathway.

To identify whether TLR2/4 mediated the activation of the NF- κ B signaling pathway by PBA, the IPEC J2 cells were transfected with a siRNA-targeted TLR2/4 to specifically silence TLR2/4 and were then challenged with PBA, and the protein levels of I κ B- α and phospho-p65 were assessed. The data showed that both TLR2 and TLR4 silencing still markedly facilitated the degradation of I κ B- α protein compared with the non-silencing control after PBA treatment in the IPEC J2 cells. However, interestingly, I κ B- α protein synthesis increased significantly when both TLR2 and TLR4 were silenced alone without treatment by PBA. It was observed that TLR4 silencing slightly influenced p65 phosphorylation induced by PBA, but no effect by TLR2 (Fig. 3d). The above results indicate that TLR2 and TLR4 silencing did not inhibit the I κ B- α degradation induced by PBA indirectly. However, TLR4 silencing decreased the phosphorylation of p65 but not completely.

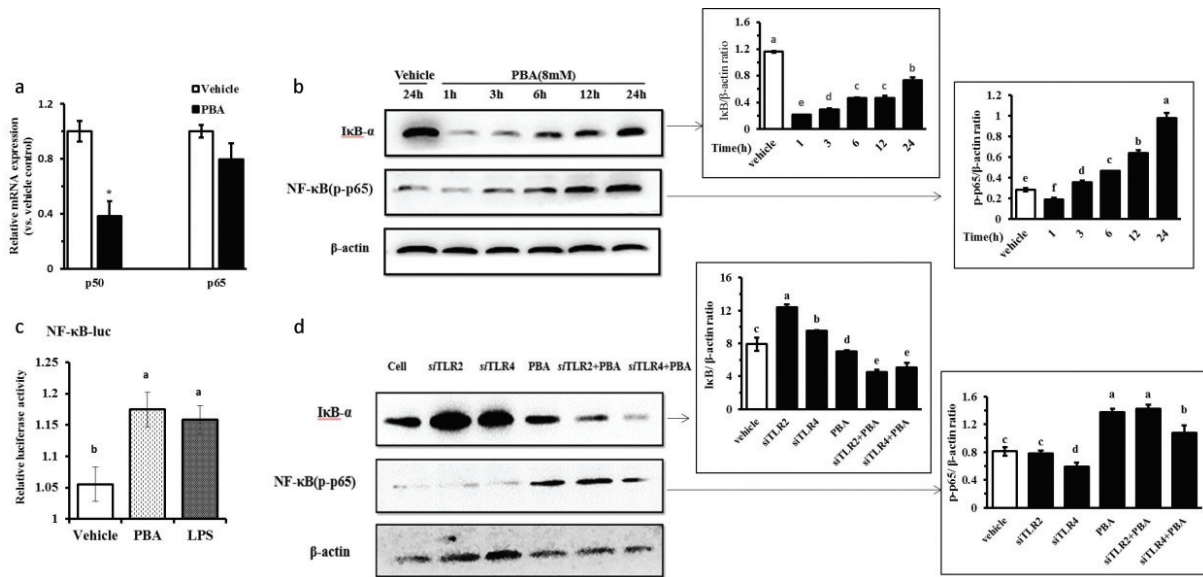


Fig. 3. PBA-induced HDPs gene expression activates the NF- κ B signaling pathway. (a) qRT-PCR analysis of p50 and p65 transcription in cells treated with 8 mM PBA for 24 h. (b) Immunoblot analysis of the phospho-NF- κ B p65 protein and the I κ B- α protein in cells pretreated or not for 0–24 h with 8 mM PBA. (c) IPEC J2 cells were co-transfected with the pNF- κ B-Luc and the internal-control phRL-TK plasmids for 6 h, and were treated with PBA or LPS for 24 h. The cells were then harvested and analyzed by luciferase reporter assays. (d) The IPEC J2 cells were transfected with TLR2/4 siRNA to specifically silence TLR2/4 for 6 h and were then challenged with PBA at 8 mM for 24 h, and a Western blot was used to assess the protein levels of I κ B- α and phospho-p65. A densitometric analysis of the I κ B- α and phospho-p65 protein levels is represented as the mean \pm SD from six independent experiments. Letters with different superscripts are significantly different at $P < 0.01$, compared with the vehicle.

Histone modification occurs while PBA induces the HDP gene expression increase in IPEC J2 cells

Phenylbutyrate is known as a reversible inhibitor of class I and II HDACs. It is considered a first generation HDAC inhibitor due to its non-specific inhibitory effect. Moreover, PBA exerts its effects in relatively high, millimolar working concentrations, and the effects are pleiotropic. Several studies suggest that the HDAC inhibitor TSA or butyrate significantly impacts the induction of antimicrobial peptide gene expression and requires the acetylation of histones H3 at several lysine residues (8, 9). We therefore investigated whether PBA behaves as an HDAC inhibitor in IPEC J2 cells. By HDAC activity detection, we identified a significant dose-dependent manner of HDAC activity inhibition efficiency with PBA in the IPEC J2 cells, and TSA (1 μ M) was a positive control of the HDAC inhibition (Fig. 4a). In addition, the histone H3 phosphorylation levels were observed by immunofluorescence. There was a strong increase in the fluorescence intensity of the phosphorylation marker following PBA and TSA pretreatment for 24 h compared with the control, which was without treatment in the IPEC J2 cells. Together, these results indicate that PBA regulated histone modification including deacetylation and phosphorylation in IPEC J2 cells, as well as upregulated HDP expression and

has no effect on IL-6 expression (Fig. 4b); these results are a reminder that epigenetic pharmacology should be achieved to induce epithelial host defense.

In addition, as the above results show, TLR2 and TLR4 silencing affected I κ B- α protein and p65 phosphorylation levels and regulated HDP gene expression induced by PBA. It is interesting whether TLR2 or TLR4 influences HDAC activity with or without PBA treatment. First, IPEC J2 cells were transfected with an siRNA-targeted TLR2 or TLR4 for 6 h to specifically silence TLR2 or TLR4, and then, the cells were treated with PBA for 24 h. As revealed by HDAC activity detection assay, our results indicated that HDAC activity inhibition by PBA was not slow down after TLR2 or TLR4 silencing, interestingly, TLR2 and TLR4 silencing alone significantly enhanced HDAC activation which had the opposite effect on HDAC activation with PBA (Fig. 4c). Taken together, these results suggest that PBA improved HDP gene expression upon histone modification.

Activation of the MAPK pathway is necessary for PBA-mediated HDP upregulation

Previous studies indicate that PBA-induced CAMP gene expression is attenuated by MAPK inhibitors (13).

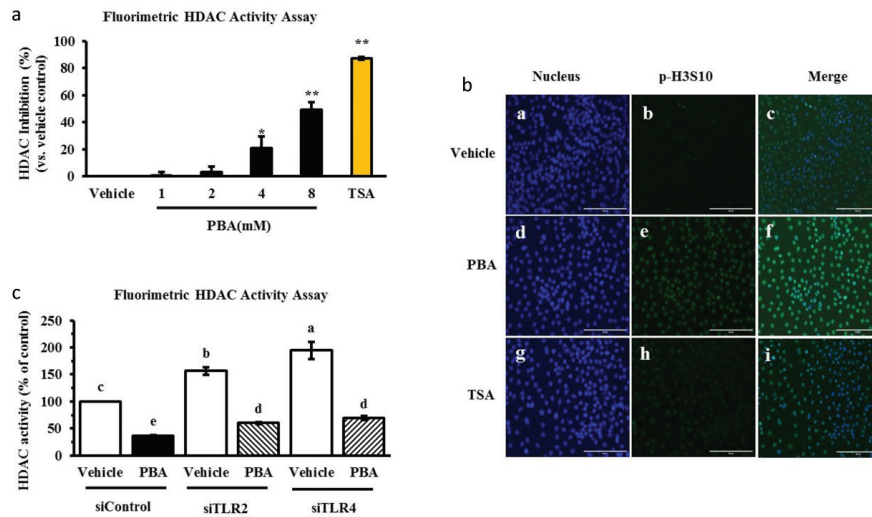


Fig. 4. PBA induces HDP gene expression upon histone modification. (a) HDAC activity was determined. The cells were incubated with increasing concentrations of PBA, and TSA was used as a reference. (b) An immunofluorescence analysis of phospho-histone H3 in the IPEC J2 cells, which were treated with PBA and TSA for 24 h. (c) The IPEC J2 cells were transfected with TLR2/4 siRNA before a treatment with PBA, and then HDAC activity was detected. Letters with different superscripts are significantly different at $P < 0.01$ compared with the vehicle.

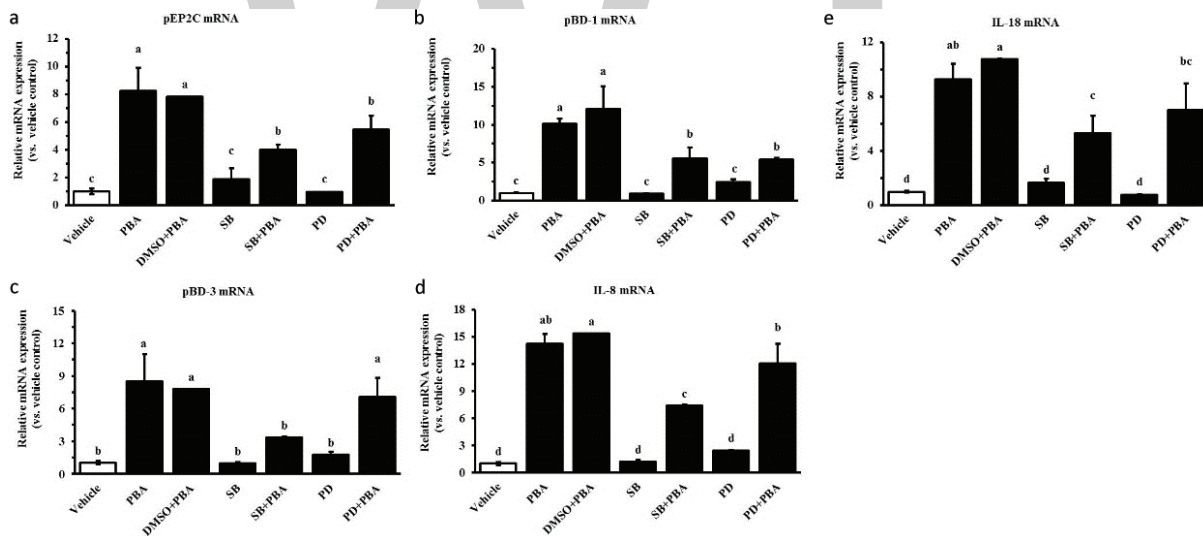


Fig. 5. The effect of MAPK inhibitors on the upregulation of PBA-mediated HDP expression. IPEC J2 cells were pretreated with the p38 MAPK inhibitor SB203580 and the ERK1/2 inhibitor PD98059 for 6 h before incubation with PBA at 8 mM for 24 h. qRT-PCR was used to detect the gene expression of (a) pEP2C, (b) pBD-1, (c) pBD-3, (d) IL-8, and (e) IL-18. Letters with different superscripts are significantly different at $P < 0.01$ compared with the vehicle.

We therefore analyzed HDP expression in IPEC J2 cells treated with the specific inhibitors of the MAPK pathways by qRT-PCR. The IPEC J2 cells were pretreated with the p38 MAPK inhibitor SB203580 and the ERK1/2 inhibitor PD98059 for 6 h before incubation with PBA at 8 mM for 24 h. DMSO was the solvent of the reagent. As shown in Fig. 5a, Fig. 5b, and Fig. 5c, the inhibitors

SB203580 and PD98059 significantly reduced PBA-induced pEP2C and pBD1 gene expressions but they were not inhibited completely. However, PD98059 failed to inhibit the pBD-3 induction by PBA determined at the mRNA level. The MAPK pathway also plays a critical role in intracellular cytokine production. In addition, PBA influences the activation of the cytokines IL-8 and

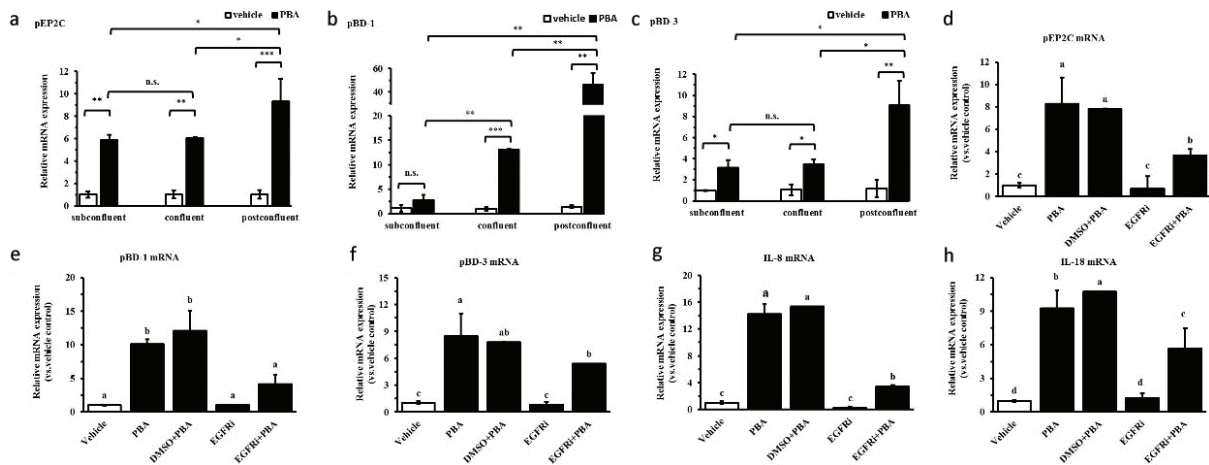


Fig. 6. The effect of cell density or EGFR on the upregulation of PBA-mediated HDP expression. (a–c) qRT-PCR analysis of pEP2C, pBD-1, and pBD-3 transcription at different cell densities treated with 8 mM PBA. (d–h) The IPEC J2 cells were pre-treated with the EGFR inhibitor Gefitinib and were then treated with PBA. Letters with different superscripts are significantly different at $P < 0.01$, compared with the vehicle.

IL-18 in IPEC J2 cells. To test whether the MAPK pathway is involved in the induction of cytokines by PBA in the IPEC J2 cells, further studies were performed to detect the effects of the inhibitors SB203580 and PD98059 on IL-8 and IL-18 mRNA expression before PBA treatment. Interestingly, SB203580 markedly suppressed the production of IL-8 and IL-18 induced by PBA. In contrast, there was no significant change in the IL-8 and IL-18 mRNA levels after a pretreatment with PD98059 compared with a treatment with PBA alone (Fig. 5d, 5e). Overall, the data from the above experiment demonstrate the relevance of host defense cytokines and the MAPK pathway in innate host defense. The p38 MAPK and ERK1/2 pathway may have partially contributed to the upregulation of the HDPs pEP2C, pBD-1, and pBD-3 mediated by PBA, but the ERK1/2 pathway did not influence pBD-3 upregulation induced by PBA in the IPEC J2 cells.

EGFR is a critical factor for PBA-mediated HDP upregulation

IPEC J2 cells possess the typical feature of growth polarity and form tight junctions during cell growth, differentiation, survival, and movement in response to different degrees of confluence. Previous studies report that differences in the EGFR transcript expression levels at different degrees of confluence affect the production of antimicrobial peptides (20). Therefore, different degrees of confluence were mimicked by culturing the cells at different cell densities, including subconfluent, confluent, and post-confluent; at a subconfluent cell density and at a confluent cell density, there was relatively little inducible pEP2C, pBD-1, and pBD-3 mRNA expression compared with the post-confluent cell density, although the HDPs were markedly increased at any confluences;

pEP2C, pBD-1, and pBD-3 mRNA increased 10-, 50-, and 10-fold, respectively, for cells stimulated with PBA at a post-confluent density (Fig. 6a, 6b, 6c). It is reported that EGFR is expressed at dramatically higher levels in post-confluent density than in subconfluent and confluent conditions, and the signaling pathways showed a switch in the post-confluent cells (20). To understand the correlation of EGFR in the intestinal epithelial cells, IPEC J2 cells were pretreated with the gefitinib, an EGFR inhibitor, for 6 h and were treated with 8 mM PBA. DMSO was in control of the solvent of the gefitinib. The results showed that the increased mRNA expression of pEP2C, pBD-1, and pBD-3 by PBA were downregulated in the presence of gefitinib compared with the PBA treatment alone by qRT-PCR assay (Fig. 6d, 6e, 6f). In addition, gefitinib caused a significant reduction in IL-8 or IL-18 expression compared to the PBA treatment alone (Fig. 6g, 6h). The above results show that EGFR is a critical factor governing the regulation of HDP expression by PBA; this regulation is consistent with the trends of HDP expression regulation by the PBA between the different degrees of confluence, as expected.

Discussion

The establishment and maintenance of epithelial homeostasis were contributed to various actors in the intestinal tract. HDPs, as an essential component of innate immunity, have the potential to regulate and improve intestinal barrier function in animal health and productivity (21, 22). Oral supplementation of HDPs-induced compounds show promise in preventing and controlling infections in humans and several animal species (7). HDPs and cytokine genes are generally considered to be

synchronously expressed in innate immune response to diverse pathogenic microorganism stimuli. *Staphylococcus aureus* or lipopolysaccharide (LPS) induces the expression of several HDPs including bovine β -defensin 1 and bovine neutrophil β -defensin 4, after infection (23). In our studies, PBA, which is an odorless derivative of butyric acid naturally produced by colonic bacteria fermentation, increased the endogenous HDP gene expression of pEP2C, pBD-1, and pBD-3 and the cytokine IL-8 and IL-18 production in IPEC J2 cells. However, PBA had no effect on the expression level of pro-inflammatory IL-6. This result is exactly what the difference between nutrients and pathogenic microorganisms exposed to the surface of host cells is shown to be on innate immunity. This work suggests that PBA may be a potential functional feed additive to achieve the induction of epithelial antimicrobial defenses while limiting the deleterious risk of an inflammatory response.

As we know, this mechanism occurring in jejunum epithelial cells is orchestrated between HDP gene expression regulation and exogenous stimulus mainly through signaling pathways, which result in the recognition of a receptor, chromatin histone modification, the activation of key signaling factors, and so on. Therefore, it is indispensable to further investigate the mechanism between HDP gene expression and PBA in jejunum epithelial cells. TLRs are generally activated in response to a diverse array of microbial products. Human corneal epithelial cells (HCECs) express TLR2, which responds to *Staphylococcus aureus* infection through the expression and secretion of pro-inflammatory cytokines and β -defensin-2 (hBD2) (24). In addition, human tracheobronchial epithelial cells respond to bacterial lipopeptide in a TLR2-dependent manner with the induction of mRNA and protein of the antimicrobial peptide human defensin-2 (25). In our studies, PBA also activated the TLR2 and inhibited TLR3 expression in IPEC J2 cells. Moreover, TLR2 silencing weakened the ability of HDPs expression induction by PBA; this outcome was similar to the result of sodium butyrate in porcine kidney cells, but the activation ability of PBA in IPEC J2 cells was less than sodium butyrate in porcine kidney cells (16). The production of pEP2C, pBD-1, and pBD-3 in IPEC J2 cells stimulated with PBA also occurred in a TLR4-dependent pathway although TLR4 was not markedly activated. PBA possesses the ability to regulate HDP expression and PEP2C, pBD-1, and pBD-3 are well-known as HDPs for their antimicrobial activity against a broad range of bacterial, fungal, and viral pathogens; TLRs are the viral recognition receptors of pathogenic microorganisms (4), however, in our results, which showed a regulatory role in the HDPs expression regulation by PBA.

Intestinal epithelial cells have long been known to provide a source of inflammatory cytokines and chemokines

(26), and they also gather different kinds of HDPs. Recent studies demonstrate that HDPs function as immunomodulatory mediators and antimicrobial agents through either direct chemotactic activity or the upregulation of several cytokines and chemokines in various cell types. Cathelicidin LL-37 not only favorably induces IL-8 expression and secretion in human gingival epithelial cells (27) but also increases IL-18 mRNA expression in keratinocytes (28). Likewise, we found that PBA upregulated endogenous HDPs and cytokine production in IPEC J2 cells. We hypothesized that HDPs and cytokines were not synchronously expressed with different regulatory rules; however, a TLR2/4-dependent activation of epithelial cells induced cytokine IL-18 gene expression, and HDPs. In addition, IL-8 gene expression was not affected by TLR2/4. It remains to be determined which signaling pathways are responsible for TLR2/4-dependent HDP and cytokine production and which other signaling pathways are activated.

The NF- κ B pathway, as a hub of regulation in the host immune defense between many exogenous stimuli, activates host immunity, particularly the expression of regulatory cytokines. In our studies, PBA modulates NF- κ B signaling in IPEC J2 cells; this modulation is dependent on the enhancement of NF- κ B p65 phosphorylation and I κ B α degradation. Furthermore, we found that TLR2 or TLR4 silencing did not affect PBA-induced NF- κ B p65 phosphorylation and I κ B degradation. MyD88, a primary adaptor molecule of TLRs, was not affected by PBA, indicating that the PBA effect on HDP production was different than the pathogen-associated molecular pattern (PAMPs). In this case, the results indicated that PBA-induced HDP increase was related to the TLR2/4 and NF- κ B signaling pathway; p65 (NF- κ B3) and p50 (NF- κ B1) are two key subunits of the NF- κ B pathway, and p50 lacks a transcriptional activation domain, which induces its downstream target gene expression by interacting with other transcription factors or transcription co-activators (19, 29). In our studies, a dramatic decrease in p50 expression was present after PBA treatment, which suggests the NF- κ B pathway activation in the IPEC J2 cells. In agreement, lower p50 levels were beneficial for HDP expression. The increase in both p65 phosphorylation in a time-dependent manner and the NF- κ B luciferase activity following PBA pretreatment together suggested that NF- κ B was activated by PBA in the IPEC J2 cells. Interestingly, an apparent increase in I κ B α protein levels was observed in a time-dependent manner after PBA treatment, but there was significant degradation compared with the untreated control cells. Previous studies show that trichostatin A potentiates tumor necrosis factor (TNF) α -elicited NF- κ B activation by histone deacetylase inhibitor (HDACi) and delays I κ B α cytoplasmic reappearance (19, 30). PBA is also a HDAC inhibitor,

which suggested to us that PBA induced HDP gene expression via delaying I κ B α synthesis and then activating the NF- κ B pathway.

Acetylation is a pivotal post-translational modification of numerous proteins, such as histones and transcription factors, including NF- κ B. Histone acetylation and deacetylation modifications play a crucial role in the chromatin structure, cellular function, and transcriptional regulation of gene expression (30, 31). Two enzyme families with opposite activities are crucial regulators of gene expression. Histone acetyltransferase (HAT) acts in a positive manner and HDAC acts in a negative manner. NF- κ B functions are regulated by post-translational modifications, including phosphorylation and acetylation (32). Several studies show that HDAC 3 induces the NF- κ B p65 subunit deacetylation, leading to the repression of its transcriptional activity (33). In addition, we addressed HDAC inhibitors as an approach to attenuate inflammatory responses and their potential as novel therapeutics (33). In our study, a significant dose-dependent inhibition of HDAC activity was detected after PBA incubation. Furthermore, PBA-mediated HDAC inhibition activated an alternative pathway, inducing H3S10 phosphorylation. The phosphorylation of H3S10, as well as the acetylation of histone H3 lysines, is highlighted in the current model as discrete modifications promoting chromatin remodeling at the promoter of specific innate immune genes, allowing the precise recruitment of NF- κ B (9, 34). Herein, the delay of I κ B α protein synthesis seems to be due to impairing of the recruitments of p65 phosphorylation, but not histone H3 on Ser10 phosphorylation (30). PBA could also be an HDACi, as it enhances HDPs and then attenuates inflammatory responses in IPEC J2 cells. Interestingly, TLR2 and TLR4 silencing did not reverse adjust the inhibition of HDAC activity by PBA. Moreover, both TLR2 and TLR4 silencing alone increased the HDAC ability in IPEC J2 cells; this result was consistent with the control of PBA increasing TLR2 and TLR4 expression and then the inhibition of the HDAC activity, as in the results above from our studies.

In a previous study, the canonical phosphorylation of histone H3 occurred through the activation of the MAPK signaling pathway, and both ERK and p38 kinases induced the phosphorylation of H3S10 at the promoter of the activated genes (35). In addition, ERK and MAPK signaling pathways are involved in cathelicidin gene expression induced by PBA (13). In this study, we observed that both the p38 MAPK inhibitor SB203580 and the ERK1/2 inhibitor PD98059 weakened the pEP2C and pBD-1 expression induced by PBA; this result had a distinct effect on blocking the induction of pBD-3. In addition, ERK1/2 signal blockade had no effect on the induction of pBD-3, IL-8, and IL-18 by PBA; this outcome indicated to us that the signaling pathway of both the p38

and ERK1/2 signaling pathways participated in the regulatory mechanism of pEP2C, pBD-1, and pBD-3, but were not identical. In addition, unexpectedly, the degree of confluence significantly improved the regulatory ability of PBA on HDP expression in the IPEC J2 cells. In a previous report, the degree of confluence also changed the regulatory ability of sodium butyrate on HDP expression in sodium butyrate in porcine kidney cells, but the trend was just in contrast with this study. As reported, epidermal growth factor receptor (EGFR) expression levels increased as the degree of confluence increased (20). EGFR was also critical in the regulation of cathelicidin expression (12). Presumably, EGFR may play a role in the process of PBA-regulated HDP expression in IPEC J2 cells. As expected, inhibition of EGFR with a specific inhibitor significantly reduced PBA-increased HDPs gene expression. Moreover, in porcine Intestinal epithelial cells, host defense peptides regulation maybe utilized different signal transduction pathways or a switch in signaling pathways with the altered degrees of confluence, including sub confluent, confluent, and post-confluent (20).

To conclude, as shown in Figure 7, PBA regulated HDPs and interleukins expression closely via a complex route system.

Funding

This work was financially supported by the National Natural Science Foundation of China (31472104, 31672434), Natural Science Foundation of Heilongjiang Province (C2018028), the China Postdoctoral Science Foundation (2017M621237), Postdoctoral Foundation in Heilongjiang Province (LBH-Z17013), and the China Agriculture Research System (CARS-35).

Disclosure statement

No authors have conflicting financial, professional, or personal interests.

Authors' Contributions

X.J.D. and J.L.H. contributed equally to this work, and they are co-first authors. X.J.D. and J.L.H. participated in the design of this study and performed most of the experiments. Q.Y.M. performed the cell culture and the real-time PCR experiments. B.J.C., Y.Y., and N.G. were the assistants during all of the experiments. X.J.D. and J.L.H. performed the statistical analysis and drafted the main manuscript. A.S.S. supervised the work. A.S.S. revised the final version of the manuscript. All authors have read and approved the final version of the manuscript.

Acknowledgements

This work was financially supported by the National Natural Science Foundation of China (31472104, 31672434), and Natural Science Foundation of Heilongjiang Province

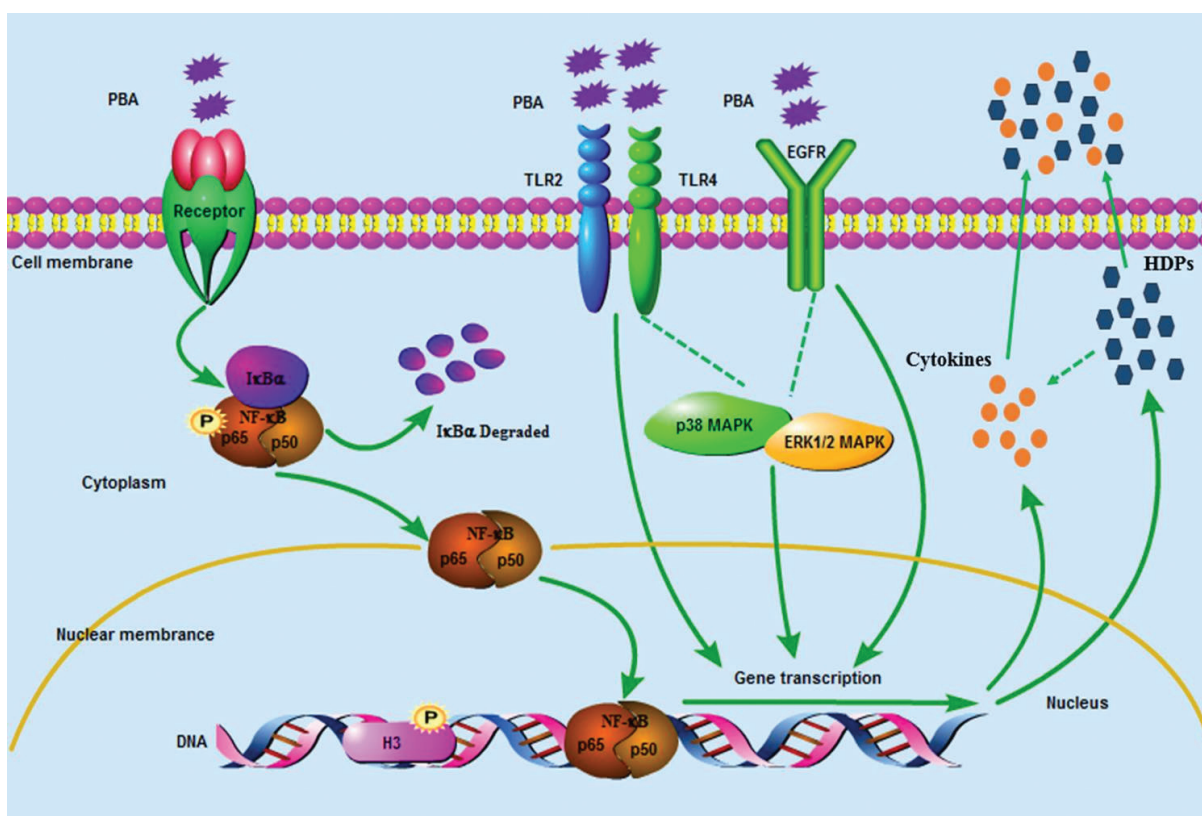


Fig. 7. The signaling pathway of defensins and interleukins gene expression is regulated by PBA in porcine intestinal epithelial cells. Sodium phenyl butyrate (PBA) activated the NF- κ B pathway via the phosphorylation of p65 and I κ B α synthesis delayed and degraded. TLR2, TLR4, and EGFR were required for the PBA-mediated up-regulation of the HDPs. Meanwhile, histone deacetylase (HDAC) inhibition and an increased phosphorylation of histone H3 on serine S10 also occurred in PBA-induced HDP expression independently on TLR2 and TLR4. Furthermore, p38-MAPK suppressed PBA-induced pEP2C, pBD-1, pBD-3, IL-8, and IL-18 expression, and ERK1/2 abolished the regulation of pEP2C and pBD-1. In conclusion, HDPs and interleukins expression were regulated by PBA via a complex route system.

(C2018028), the China Postdoctoral Science Foundation (2017M621237), Postdoctoral Foundation in Heilongjiang Province (LBH-Z17013), the China Agriculture Research System (CARS-35).

References

- O'Neill J. The review on antimicrobial resistance: tracking drug resistant infections globally. Wellcome Trust and the Department of Health of UK Government 2016.
- Hancock REW, Haney EF, Gill EE. The immunology of host defence peptides: beyond antimicrobial activity. *Nat Rev Immunol* 2016; 16: 321.
- Zhang LJ, Gallo RL. Antimicrobial peptides. *Curr Biol Cb* 2016; 26: R14.
- Sang Y, Blecha F. Porcine host defense peptides: expanding repertoire and functions. *Dev Comp Immunol* 2009; 33: 334–43.
- Choi MK, Le MT, Nguyen DT, Choi H, Kim W, Kim JH, et al. Genome-level identification, gene expression, and comparative analysis of porcine β -defensin genes. *Bmc Genet* 2012; 13: 98.
- Zeng X, Sunkara LT, Jiang W, Bible M, Carter S, Ma X, et al. Induction of porcine host defense peptide gene expression by short-chain fatty acids and their analogs. *Plos One* 2013; 8: e72922.
- Lyu W, Curtis AR, Sunkara LT, Zhang G. Transcriptional regulation of antimicrobial host defense peptides. *Curr Protein Pept Sci* 2015; 16: 672–9.
- Xiong H, Guo B, Gan Z, Song D, Lu Z, Yi H, et al. Butyrate upregulates endogenous host defense peptides to enhance disease resistance in piglets via histone deacetylase inhibition. *Sci Rep* 2016; 6: 27070.
- Fischer N, Sechet E, Friedman R, Aurélien Amiot, Sobhani I, Nigro G, et al. Histone deacetylase inhibition enhances antimicrobial peptide but not inflammatory cytokine expression upon bacterial challenge. *P Natl Acad Sci USA* 2016; 113: 201605997.
- Coussens AK, Wilkinson RJ, Martineau AR. Phenylbutyrate is bacteriostatic against mycobacterium tuberculosis and regulates the macrophage response to infection, synergistically with 25-Hydroxy-Vitamin D₃. *Plos Pathogens* 2015; 11: e1005007.
- Merzviniskyte R, Treigyte G, Savickiene J, Magnusson KE, Navakauskiene R. Effects of histone deacetylase inhibitors, sodium phenyl butyrate and vitamin B₃, in combination with retinoic acid on granulocytic differentiation of human promyelocytic leukemia HL-60 cells. *Ann Ny Acad Sci* 2006; 1091: 356–67.

12. Kulkarni NN, Yi Z, Huehnken C, Agerberth B, Gudmundsson GH. Phenylbutyrate induces cathelicidin expression via the vitamin D receptor: Linkage to inflammatory and growth factor cytokines pathways. *Mol Immunol* 2014; 63: 530–39.
13. Kulkarni NN, Yi Z, Huehnken C, Agerberth B, Gudmundsson GH. Phenylbutyrate induces antimicrobial peptide expression. *Antimicrob Agents Chemother* 2009; 53: 5127.
14. Mariani V, Palermo S, Fiorentini S, Lanubile A, Giuffra E. Gene expression study of two widely used pig intestinal epithelial cell lines: IPEC-J2 and IPI-2I. *Vet Immunol Immunopathol* 2009; 131: 278–84.
15. Cao L, Ge X, Gao Y, Ren Y, Ren X, Li G. Porcine epidemic diarrhea virus infection induces NF- κ B activation through the TLR2, TLR3 and TLR9 pathways in porcine intestinal epithelial cells. *J Gen Virol* 2015; 96: 1757.
16. Dou X, Han J, Song W, Dong N, Xu X, Zhang W, et al. Sodium butyrate improves porcine host defense peptide expression and relieves the inflammatory response upon toll-like receptor 2 activation and histone deacetylase inhibition in porcine kidney cells. *Oncotarget* 2017; 8: 26532.
17. Fukata M, Vamadevan AS, Abreu MT. Toll-like receptors (TLRs) and Nod-like receptors (NLRs) in inflammatory disorders. *Semin Immunol* 2009; 21: 242–53.
18. Kamdar K, Nguyen V, Depaolo RW. Toll-like receptor signaling and regulation of intestinal immunity. *Virulence* 2013; 4: 207–12.
19. Quivy V, Van LC. Regulation at multiple levels of NF- κ B-mediated transactivation by protein acetylation. *Biochem Pharmacol* 2004; 68: 1221.
20. Johnston A, Gudjonsson JE, Aphale A, Guzman AM, Stoll SW, Elder JT. EGFR and IL-1 signaling synergistically promote keratinocyte antimicrobial defenses in a differentiation-dependent manner. *J Invest Dermatol* 2011; 131: 329–37.
21. Robinson K, Deng Z, Hou Y, Zhang G. Regulation of the intestinal barrier function by host defense peptides. *Front Vet Sci* 2015; 2: 57.
22. Peterson LW, Artis D. Intestinal epithelial cells: regulators of barrier function and immune homeostasis. *Nat Rev Immunol* 2014; 14: 141.
23. Alva-Murillo N, Téllez-Pérez AD, Sagrero-Cisneros E, López-Meza JE, Ochoa-Zarzosa A. Expression of antimicrobial peptides by bovine endothelial cells. *Cell Immunol* 2012; 280: 108–12.
24. Kumar A, Zhang J, Yu FX. Toll-like receptor 2-mediated expression of β -defensin-2 in human corneal epithelial cells. *Microb Infect* 2006; 8: 380–9.
25. Hertz CJ, Wu Q, Porter EM, Zhang YJ, Weismüller KH, Godowski PJ, et al. Activation of Toll-like receptor 2 on human tracheobronchial epithelial cells induces the antimicrobial peptide human beta defensin-2. *J Immunol* 2003; 171: 6820–6.
26. Stadnyk AW. Intestinal epithelial cells as a source of inflammatory cytokines and chemokines. *J Canadien de Gastroenterologie* 2002; 16: 241–6.
27. Montreekachon P, Nongparn S, Sastraruji T, Khongkhunthian S, Chruewkamlow N, Kasinrerker W, et al. Favorable interleukin-8 induction in human gingival epithelial cells by the antimicrobial peptide LL-37. *Asian Pacific Journal of Allergy & Immunology* 2014; 32: 251–60.
28. François Niyonsaba, Ushio H, Nagaoka I, Okumura K, Ogawa H. The human beta-defensins (-1, -2, -3, -4) and cathelicidin LL-37 induce IL-18 secretion through p38 and ERK MAPK activation in primary human keratinocytes. *J Immunol* 2005; 175: 1776.
29. Luo MC, Zhou SY, Feng DY, Xiao J, Li WY, Xu CD, et al. Runt-related transcription factor 1 (RUNX1) binds to p50 in macrophages and enhances TLR4-triggered inflammation and septic shock. *J Biol Chem* 2016; 291: 22011.
30. Horion J, Gloire G, El Mjijad N, Quivy V, Vermeulen L, Vandenberghe W, et al. Histone deacetylase inhibitor trichostatin A sustains sodium pervanadate-induced NF- κ B activation by delaying ikappaB α mRNA resynthesis: comparison with tumor necrosis factor alpha. *J Biol Chem* 2007; 282: 15383–93.
31. Furumai R, Ito A, Ogawa K, Maeda S, Saito A, Nishino N, et al. Histone deacetylase inhibitors block nuclear factor- κ B-dependent transcription by interfering with RNA polymerase II recruitment. *Cancer Science* 2011; 102: 1081.
32. Wollebo HS, Bellizzi A, Cossari DH, Safak M, Khalili K, White MK. Epigenetic regulation of polyomavirus JC involves acetylation of specific lysine residues in NF- κ B p65. *J Neurovirol* 2015; 21: 679–87.
33. Leus NGJ, Zwinderman MRH, Dekker FJ. Histone deacetylase 3 (HDAC 3) as emerging drug target in NF- κ B-mediated inflammation. *Curr Opin Chem Biol* 2016; 33: 160–8.
34. Sacconi S, Pantano S, Natoli G. p38-dependent marking of inflammatory genes for increased NF- κ B recruitment. *Nat Immunol* 2002; 3: 69.
35. Clayton AL, Mahadevan LC. MAP kinase-mediated phosphoacetylation of histone H3 and inducible gene regulation. *FEBS Lett* 2003; 546: 51–8.

***Anshan Shan**

Institute of Animal Nutrition
Northeast Agricultural University
Harbin 150030
P. R. China
Email: asshan@neau.edu.cn

Phoenix Dan Cong Tea: An Oolong Tea variety with promising antioxidant and *in vitro* anticancer activity

Xiaobin Zhang^{1†}, Zhenhuan Song^{1†}, Yuanyuan You¹, Xiaoling Li^{2*} and Tianfeng Chen^{1*}

¹The First Affiliated Hospital, and Department of Chemistry, Jinan University, Guangzhou 510632, China; ²Institute of Food Safety and Nutrition, Jinan University, Guangzhou 510632, China.

Abstract

Background: Phoenix Dan Cong tea is an Oolong tea produced in Chaozhou, China. Nowadays, the experimental studies on the beneficial effects of the Phoenix Dan Cong tea are rare.

Objective: The objective of this study was to comprehensively evaluate the activity of Phoenix Dan Cong tea aqueous extract (PDCE).

Methods: We used a series of evaluation methods in the present study to achieve an in-depth understanding and evaluation of the antioxidant and antitumor activity of PDCE.

Results: High-performance liquid chromatography (HPLC) studies have indicated that PDCE is rich in catechins such as gallic acid (GA), epigallocatechin (EGCG) and epicatechin gallate (ECG), with sparse amounts of theaflavins. We discovered that PDCE scavenges ABTS^{•+} and DPPH[•] free radicals in a dose-dependent manner. In addition, PDCE can significantly induce apoptosis of MDA-MB231 cells, mainly through the death-receptor-mediated extrinsic apoptotic pathway. Internalized PDCE can not only downregulate intracellular reactive oxygen species levels but also induce oxidative damage to mitochondria in MDA-MB231 cells.

Conclusions: Phoenix Dan Cong tea may act as a substitute for natural antioxidants and as a promising anticancer agent due to its protective effect on human health.

Keywords: *Dan Cong tea; aqueous extract; cell apoptosis; protective effect; free radical scavenging; oxidative damage*

Various degenerative and chronic diseases are frequently attributed to oxidative stress, which is often caused by free radicals (1). Free radicals can easily react with the cellular molecules because of their highly reactive and unstable nature, and can oxidize nucleic acids, proteins, and fats, thus promoting degenerative diseases (2). Essential biochemical reactions in the human body as well as external exposure may generate free radicals (3). In general, antioxidants can react with free radicals producing relatively stable substances. The human body does not need to replenish antioxidants under normal circumstances because it continues to synthesize and secrete endogenous antioxidants. However, exogenous antioxidants are needed when free radicals are produced in large quantities (4). It is necessary to maintain a balance between free radicals and antioxidants for normal physiological function of the human body. Natural antioxidants can not only protect the human body from damage caused by reactive oxygen species (ROS) but also inhibit

lipid peroxidase activity and thus prevent the degenerative diseases (5). Most importantly, natural antioxidants, such as tea polyphenols, have low toxicity and cause no harm to humans even if used chronically.

Tea has been consumed for thousands of years as a daily health drink in China. Tea has been traditionally used as a medication based on experience, and biological activities including antioxidant and antitumor activities of the active ingredients of tea have been extensively described in China and Japan. The major ingredients in the extract of tea, flavonols and polyphenols, have been proven to be beneficial to the human body (6–8). Active components playing crucial roles in most of the biological activities of tea are known to be catechins (also known as polyphenols) (9, 10). Tea polyphenols are considered responsible for antimutagenic and anticarcinogenic activity, and protection against cardiovascular diseases (11). Teas are mainly classified into green tea (unfermented), Oolong tea (semi-fermented), and black tea (fully fermented) depending on the degree

[†]These authors contributed equally to this work.

of fermentation in manufacture, where the term fermentation refers to the natural browning reactions resulting from oxidative enzymes in the cells of tea leaves (12). Oolong tea has been the most favored choice among Taiwanese over the past few decades owing to its special taste and flavor (13, 14). Phoenix Dan Cong tea, a variety of Oolong tea, is one of the six tea categories in China. It has a long history and reputation of more than 900 years. The Chaozhou Phoenix mountains are one of the three major Oolong tea producing areas in China and the 'Phoenix narcissus variety' of tea owes its origin to these mountains. The Phoenix Dan Cong tea used in the present study has been screened out from the Phoenix narcissus variety by generations of tea farmers. It is one of the most tasty and fragrant varieties of tea in China. Phoenix Dan Cong tea has many health benefits, for example, vitamin C is known to play an important role in skin growth but easily reacts with ROS in the human body; however, the antioxidant effect of tea polyphenols in Phoenix Dan Cong tea is able to eliminate ROS and inhibit the elimination of vitamin C, protecting the skin and enabling its whitening (15–17).

Based on the fact that different varieties of tea are used as health care products worldwide, but experimental studies on the beneficial effects of teas such as the Phoenix Dan Cong tea are rare, the present investigation was aimed to comprehensively evaluate the activity of Phoenix Dan Cong tea aqueous extract (PDCe), assessing ABTS•+ and DPPH• levels and antitumor activity using the human tumor cell lines MDA-MB231 (human breast cancer cells) and SW480 (human colon cancer cells). The possible mechanisms involved that were studied were induction of cell cycle arrest and apoptosis.

The MDA-MB231 human breast cancer cell line and SW480 human colon cancer cells were selected as cellular models to evaluate *in vitro* antitumor effects of PDCe, while ABTS•+ and DPPH• free radicals were used to evaluate its antioxidant effects. As shown in Fig. 1A, PDCe not only had an excellent anticancer effect against MDA-MB231 cells but also protected against damage caused by ROS. Our results provide evidence that PDCe may act as a substitute for natural antioxidants and as a promising anticancer agent.

Materials and methods

Materials and reagents

Reference standards for caffeine, EC, ECG, CG, C, CA, EGC, and EGCG ($\geq 98\%$) and those for TF1, TF2, TF3, and TF4 ($\geq 90\%$) were purchased from Chen du purify Co. (Chen du, China). Folin-Ciocalteu's phenol reagent was purchased from Sigma (St. Louis, MO). Methanol (HPLC grade), 85% phosphoric acid, acetonitrile (HPLC grade), and Milli-Q water were filtered through a 0.45 μm membrane before use. 6-hydroxy-2,5,7,8-tetramethylchromane-2-carboxylic acid (Trolox), 2,2'-

azinobis-3-ethylbenzothiazolin-6-sulfonic acid (ABTS•+), 1,1-diphenyl-2-picrylhydrazyl (DPPH•), propidium iodide (PI), thiazolyl blue tetrazolium bromide (MTT), glutathione (GSH), 4',6-diamidino-2-phenylindole (DAPI), bicinchoninic acid (BCA), sodium selenite, and all other chemicals were obtained from Sigma-Aldrich (St. Louis, MO, USA). Fetal bovine serum (FBS) and antibiotic mixture (penicillin-streptomycin) were purchased from Invitrogen (Carlsbad, CA, USA). Caspase-3, caspase-8, and caspase-9 were purchased from Cell Signaling Technology (Beverly, MA, USA). Caspase-3, caspase-8, and caspase-9 substrates were obtained from Biomol (Germany).

Preparation of PDCe

A dry fine powder of Phoenix Dan Cong tea was purchased from the local tea processing plant. The powder was stored at 4 °C, and when necessary, it was dissolved in phosphate-buffered saline (PBS) to make a 10 mg/mL working solution.

Measurement of total polyphenol content

Total polyphenol content (TPC) was measured using spectrophotometric detection of gallic acid (GA) per the Folin-Ciocalteu method (18, 19). Each sample was measured in triplicate under the same conditions. The procedures were repeated for standard solutions. The absorbance of the mixture was measured at 765 nm with water as blank using a spectrophotometer (Genesys5, Spectronic Instruments, Rochester, NY). The TPC was expressed as gallic acid equivalents (GAE) in milligram of GA per gram of tea extract.

HPLC analysis of catechins and theaflavins in PDCe

High-performance liquid chromatography (HPLC) (20–22) was used to measure the catechin and theaflavin content of PDCe. HPLC was performed using a 1260 infinity II chromatography system from Agilent Technologies. PDCe was injected onto a SiO_2 column (250×4.6 mm), previously equilibrated with a solution composed of solvent A (acetonitrile) and solvent B (0.4% aqueous phosphoric acid, v/v). Compounds were eluted from the column using the following program: 7–15% A in 0–13 min, 15–20% A in 13–35 min, 20–50% A in 35–70 min, 50–80% A in 70–90 min, 80–87% A in 90–115 min. The flow-rate of the chromatographic mobile phase was set as 1.0 mL/min and the effluent was detected at 278 nm for acquiring chromatograms.

ABTS•+ scavenging assay

The ABTS•+ scavenging assay as previously described (23) was applied to evaluate the antioxidant activity of PDCe. The absorbance of the solution was measured at 734 nm after the initiation of mixing for 1 min. The antioxidant capacity of PDCe was evaluated by calculating half maximal inhibitory concentration (IC_{50}). The scavenging assay was

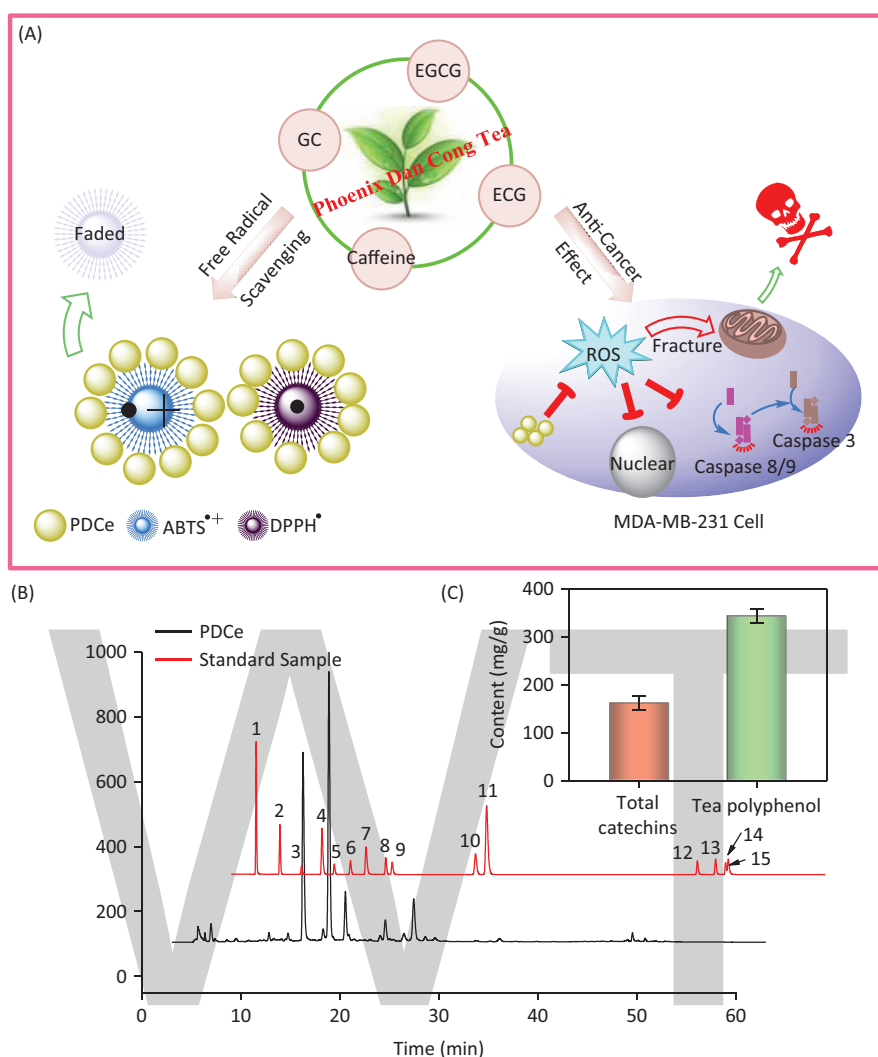


Fig. 1. The antioxidant and anti-breast cancer behavior *in vitro* and HPLC analysis of the active ingredients in Phoenix Dan Cong Tea. (A) The anticancer mechanism and the free radical scavenging behavior of PDCe. (B) Representative HPLC-UV chromatogram acquired at 278 nm of 15 standard samples and PDCe. (C) The total catechins and total phenolic contents (TPC) (as GAE) in PDCe. 1: A; 2: GA; 3: GC; 4: theophylline; 5: EGC; 6: C; 7: Caffeine; 8: EC; 9: EGCG; 10: ECG; 11: CG; 12: TF1; 13: TF2; 14: TF3; 15: TF4.

performed using a spectrophotometer (Genesys 5, Spintronic Instruments, Rochester, NY).

DPPH[•] scavenging assay

The DPPH[•] scavenging activity of PDCe was evaluated using a spectrophotometer (Genesys5, Spectronic Instruments, Rochester, NY) following the method described by Chen and Wong (2008a) (23). The change in absorbance of a mixture that was left to stand for 5 min at 515 nm was measured. Half maximal inhibitory concentration (IC₅₀) was calculated to evaluate the antioxidant capacity of PDCe.

Cell culture

Human cell lines used in this study included HeLa cervical cancer cells, SW480 human colon cancer cells,

MDA-MB231 human breast cancer cells, HepG2 hepatocellular carcinoma cells, WI38 human lung cells, and L02 human normal liver cells, and they were purchased from the American Type Culture Collection (ATCC, Manassas, Virginia). The cell lines were cultured in DMEM media, with penicillin (100 units/mL), streptomycin (50 units/mL), and FBS (10%) at 37°C in a humidified incubator under 5% CO₂.

Cell viability assay

Changes in cell viability induced by the PDCe was determined using MTT assay, based on a previous study (24). In short, the cell viability (2 × 10⁴ cells per mL for cancer cells and 4 × 10⁴ cells per mL for normal cells) after treatment with different concentrations of PDCe for 72 h was

determined using an MTT assay. A micro-plate spectrophotometer (Spectro Amax TM 250) was used to measure the color intensity of the formazan solution at 570 nm which reflected the growth of the cells (25).

Flow cytometric analysis

Cell cycle distribution was analyzed via flow cytometry as previously described (26, 27). In short, MDA-MB-231 cells treated with PDCe were washed with PBS and then treated with 5% trypsin, then fixed in 75% ethanol overnight at -20°C . Subsequently, the fixed cells were stained with PI in darkness. The stained cells were analyzed using an FC-500 flow cytometer (Beckman Coulter, Miami, FL). Cell cycle distribution was analyzed using the software Multi-Cycle (Phoenix Flow Systems, San Diego, CA). The proportion of cells in G0/G1, S, and G2/M phases was represented in the DNA histogram. Apoptotic cells with hypodiploid DNA content were measured by quantifying the sub-G1 peak in the cell cycle pattern. A total of 10,000 events were recorded in each experimental sample.

Caspase activity assay

Caspase activity was determined via fluorescence intensity measurement using specific caspase-3, caspase-8, and caspase-9 substrates as reported (28). Specifically, harvested cells pellets were suspended in cell lysis buffer (Beyotime) and incubated on ice for 1 h. After centrifugation at 11,000 g for 30 min, the BCA assay was immediately performed to measure protein concentration in the supernatants. Thereafter, the cell lysates and specific caspases substrates (Ac-DEVD-AMC for caspase-3, Ac-IETD-AMC for caspase-8, and Ac-LEHD-AMC for caspase-9) were mixed at specific ratios in 96-well plates and incubated at 37°C for 2 h. The fluorescence intensity of the mixtures which reflected the caspase activity was detected at excitation and emission wavelengths of 380 nm and 460 nm, respectively.

Measurement of intracellular ROS generation

The relative levels of ROS were determined using fluorometric assays (DHE and DCFH-DA assay) (29, 30). The generation of ROS was determined via fluorescence intensity measurement using a multifunction spectrometer (Bio-Tek®, ELX 800, American) at excitation and emission wavelengths of 300 nm and 600 nm, respectively. Relative DHE and DCFH-DA fluorescence intensity of the treated cells was expressed as a percentage of control (as 100%).

Mitochondrial fragmentation analysis

Mitochondrial fragmentation analysis was carried out as reported (31). Briefly, mitochondria and nuclei of the MDA-MB231 cells were stained with Mito Tracker Red CMXRos and H33342, respectively. Prior to that, the cells

were treated with PDCe (30 $\mu\text{g}/\text{mL}$) for 0, 6, or 12 h, and following straining, photographed using a monochromatic Cool SNAPFX camera (Roper Scientific, USA).

Statistical analysis

Results were expressed as mean \pm SD, which were obtained from at least three independent experimental results. The difference between the two groups was analyzed using a two-tailed Student's *t*-test. Differences with $P < 0.05$ (*) or $P < 0.01$ (**) were considered statistically significant. One-way analysis of variance (ANOVA) was used to compare multiple groups.

Results and discussion

Measurement of the active ingredients in PDCe

Because several tea extracts are now available, the concentrations of components are known and standard solutions with suitable concentration ranges are available for analysis; these would reduce error and enable reproducibility and credibility of the results. Therefore, the concentrations of different components in the extract was calculated using a calibration curve method. Fig. 1B shows the typical HPLC-UV chromatogram at 278 nm of the PDCe and standard samples mixture including catechins and theaflavins. The retention times and spectra were compared with those of commercially available catechins and theaflavins. The peaks and retention times of PDCe components were compared to those of the standard compounds, and 15 active compounds were identified in the PDCe (Table 1). Compounds such as GC, GA, and ECG, and especially EGCG and caffeine, were abundant, while ingredients such as EC, theophylline, and CG

Table 1. Chemical composition analysis of PDCe by HPLC analysis

Peak	Retention Time (min)	Compound	Contents (%)
1	2.436	A	0.31
2	4.375	GA	1.55
3	6.467	GC	3.89
4	8.771	Theophylline	0.04
5	9.890	EGC	0.82
6	11.56	C	0.80
7	13.36	Caffeine	5.21
8	15.34	EC	0.76
9	15.97	EGCG	6.15
10	24.52	ECG	1.58
11	25.66	CG	0.63
12	47.14	TF1	0.09
13	48.97	TF2	0.21
14	49.98	TF3	0.06
15	50.24	TF4	0.06

were low. It is worth mentioning that there were almost no theaflavins in the PDCe. In addition, as shown in Fig. 1C, the TPC of PDCe was 343.6 mg/g and the total catechin content was 161.9 mg/g, which accounted for approximately 47.1% of the TPC. Taken together, our data allow us to conclude that GC, EGCG, ECG, and caffeine are the major catechins in PDCe, while theaflavins are rare. These tea polyphenols or caffeine in the PDCe may play an important role in its antioxidant activity and *in vitro* antitumor activity.

Determination of the optimum wavelength

ABTS^{•+} and DPPH[•] free radical scavenging has been widely used in the measurement of total antioxidant capacity of test samples (25). In the test, the ABTS^{•+} and DPPH[•] solution were subjected to UV-Vis spectral scanning. As shown in Fig. 2A, the ABTS^{•+} solution showed characteristic absorption peaks at 734 nm and 415 nm, while the characteristic absorption peak of the DPPH[•] solution was at 515 nm. We discovered that the PDCe had no UV absorption at 515 nm or 734 nm, but there was slight ultraviolet UV absorption at 415 nm. Further, the absorption peak at 734 nm (ABTS^{•+}) and 515 nm (DPPH[•]) showed dose-dependent inhibition and excellent linearity correlation after the addition of PDCe (Fig. 2B and C). The results above indicated that the change in absorption peaks at 734 nm and 515 nm reflect scavenging

of ABTS^{•+} and DPPH[•] free radicals by PDCe to some extent. Therefore, we selected 734 nm and 515 nm as the detection wavelengths in the two free radical scavenging experiments, the ABTS and DPPH assays, respectively.

Antioxidant activity evaluation

Determination of the response time of the system is known to be a very important factor in evaluating different antioxidants using the ABTS^{•+} and DPPH[•] radical scavenging assays. To understand the reaction kinetic characteristics of the ABTS^{•+} and DPPH[•] free radical systems, we measured absorbance change kinetics of the ABTS^{•+} and DPPH[•] solutions after treating with PDCe or Trolox (as positive control). According to the results of UV spectral scanning shown in Fig. 3A and B, when different concentrations of PDCe and Trolox was added to the ABTS^{•+} system, the characteristic absorption peaks (A734) of the ABTS^{•+} system decreased significantly in 60 sec, and tended to be steady after 6 min. As illustrated in Fig. 3C and D, the characteristic absorption peaks (A515) of the DPPH[•] system decreased significantly in 120 sec and tended to be steady after 12 min following treatment with PDCe or Trolox.

The ABTS and DPPH assays were used in the present study to evaluate the free radical scavenging activity of the PDCe because they can accommodate many experimental samples and also have sufficient sensitivity to detect

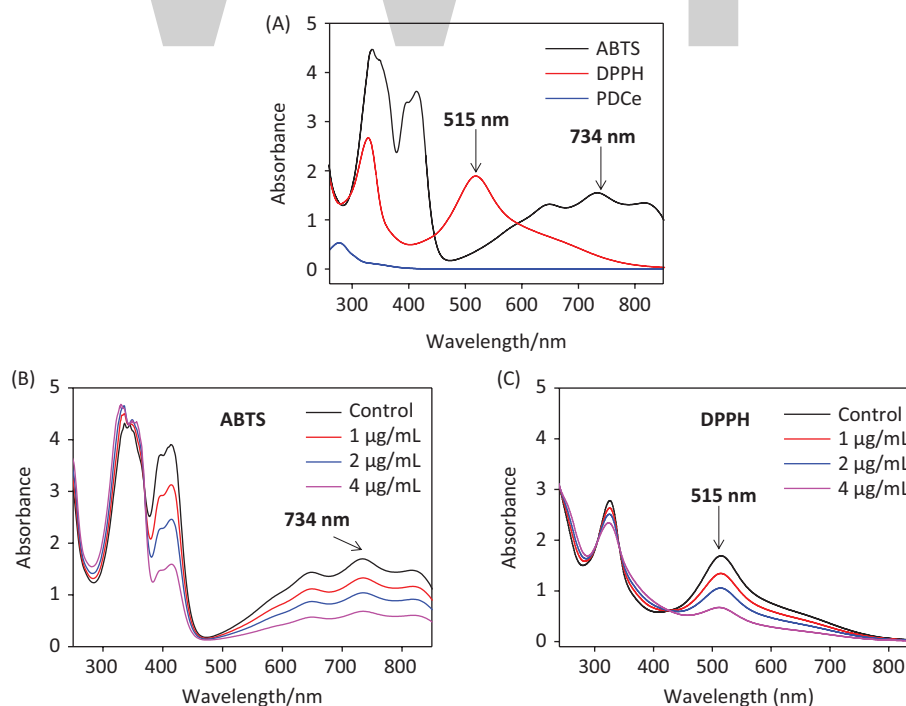


Fig. 2. Ultraviolet absorbance spectra. (A) Absorbance spectra of PDCe and the ABTS^{•+} and DPPH[•] solutions. (B) Changes in absorbance spectra of ABTS^{•+} solution with the addition of PDCe. (C) Changes in absorbance spectra of DPPH[•] solution with the addition of PDCe.

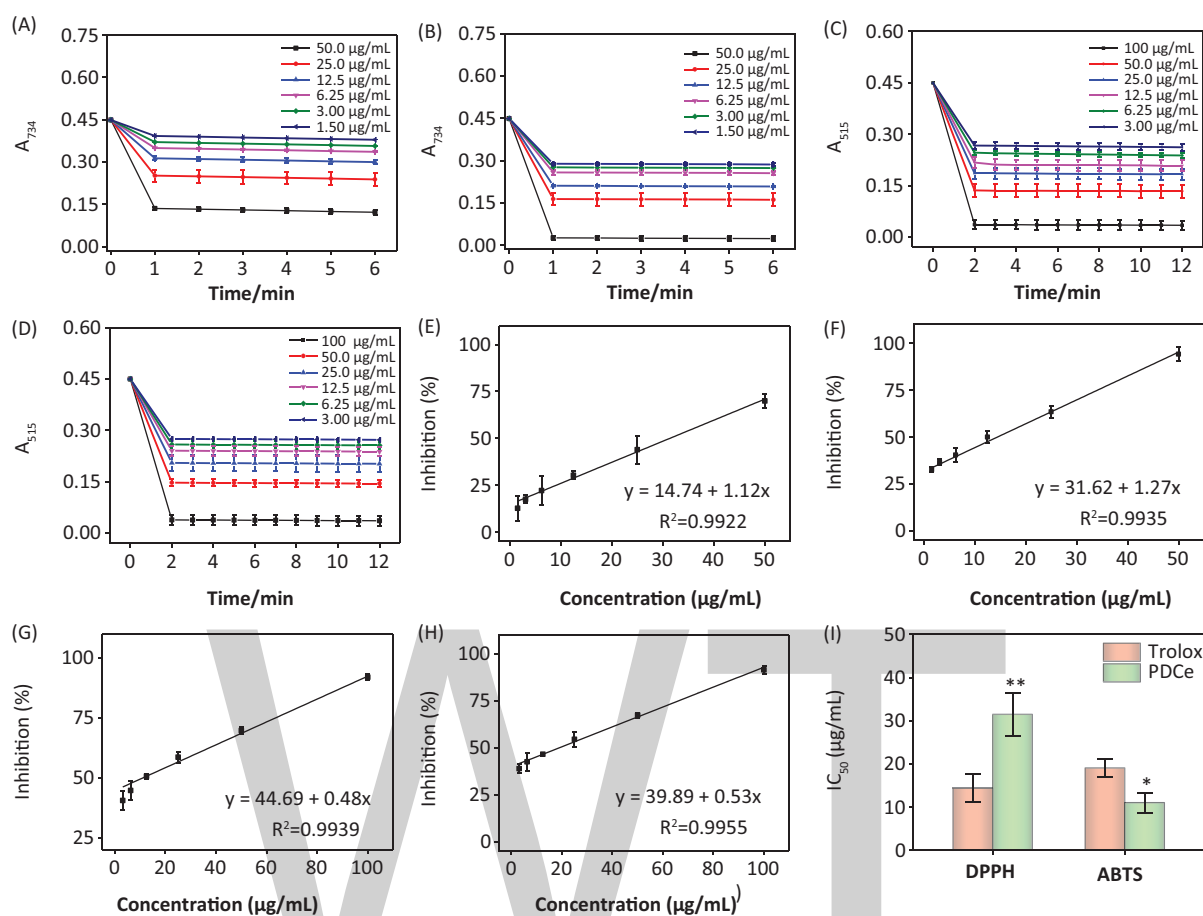


Fig. 3. Effect of PDCe and Trolox in free radicals scavenging. (A) Changes in absorbance spectra of ABTS•+ solution with the addition of PDCe. (B) Changes in absorbance spectra of ABTS•+ solution with the addition of Trolox. (C) Changes in absorbance spectra of DPPH• solution with the addition of PDCe. (D) Changes in absorbance spectra of DPPH• solution with the addition of Trolox. (E) Dose-dependent inhibitions of PDCe on ABTS•+ and its linearity correlation. (F) Dose-dependent inhibitions of Trolox on ABTS•+ and its linearity correlation. (G) Dose-dependent inhibitions of PDCe on DPPH• free radicals and its linearity correlation. (H) Dose-dependent inhibitions of PDCe on DPPH• free radicals and its linearity correlation. (I) The inhibitions of the antioxidants on ABTS•+ and DPPH• free radicals. The IC₅₀ values of PDCe and the standard antioxidant Trolox determined by ABTS•+ and DPPH• assays. * and ** indicate statistical difference at $P < 0.05$ and $P < 0.01$, respectively, by comparing with the Trolox group.

antioxidant activity at low concentrations. For ABTS•+, the IC₅₀ values of the corresponding antioxidants (PDCe or Trolox) were calculated based on free radical scavenging at the optimum wavelengths (734 nm) and reaction times (60 sec). The same method was applied to DPPH•. In the range of 1.50–50.0 μg/mL, PDCe and Trolox had excellent linear relationships to ABTS•+ scavenging (Fig. 3E and F) and the IC₅₀ values could be calculated; the IC₅₀ values of PDCe and the standard antioxidant Trolox (as positive control) were 11.06 ± 2.32 and 19.08 ± 1.98 μg/mL, respectively (Fig. 3I). In the DPPH• free radical system, PDCe and Trolox also showed good linear relationships to free radical scavenging in the range of 3.00–100 μg/mL (Fig. 3G and H). As shown in Fig. 3I, the IC₅₀ values of PDCe and Trolox in DPPH• scavenging were 31.48 ± 4.96 and 14.47 ± 3.28 μg/mL, respectively;

this suggested that PDCe also has an excellent scavenging effect on lipophilic free radicals (DPPH•), although its free radical scavenging ability is not as good as Trolox. Based on the results discussed above, it is clear that PDCe has good antioxidant activity. We can also conclude that PDCe has an excellent inhibitory effect on water-soluble free radicals (ABTS•+) and a lesser effect on lipid soluble free radicals (DPPH•).

Cytotoxicity of PDCe

The anticancer effect of PDCe was evaluated using various human cancer and normal cell lines via MTT assay. The IC₅₀ values obtained in the cytotoxicity assays are shown in Table 2. As shown in Fig. 4A, we found that PDCe had significant cytotoxicity towards MDA-MB-231 cells and SW480 cells with IC₅₀ values

of 30.90 ± 5.55 and 79.33 ± 0.06 $\mu\text{g/mL}$, respectively. However, the PDCe demonstrated relatively low cytotoxicity against L02 and WI38 cells, with IC_{50} values of 198.3 ± 3.48 and 94.1 ± 3.98 $\mu\text{g/mL}$ strongly indicating that PDCe is more cytotoxic to cancer cells (MDA-MB-231, SW480, HeLa) than normal cells (L02 and WI38). It is worth mentioning that the IC_{50} of PDCe against liver cancer cells (HepG2) was 142.4 ± 2.96 $\mu\text{g/mL}$, which was higher than that against normal human lung cells (WI38). Further, as shown in Fig. 4B, the PDCe had a dose-dependent effect on MDA-MB-231 cell death. Cell death at PDCe concentrations above 40 $\mu\text{g/mL}$ can be clearly seen. Therefore, MDA-MB231 breast cancer cells and SW480 colon cancer cells, which showed the most sensitivity to PDCe, were selected to investigate the specific mechanisms involved in the anticancer activity of PDCe based on the results of the MTT assay.

Flow cytometry analysis of cellular apoptosis or arrest

Cell cycle arrest and apoptosis are known to be two major routes causing cell death (32–34). In different biological phenomena or systems including cell division, embryonic development, the immune system, chemically induced cell death, and morphological changes, apoptosis is indispensable (35). It has also been shown that cellular apoptosis

Table 2. Cytotoxicity Effects of PDCe

Cell Name	IC_{50} ($\mu\text{g/mL}$)
L02	198.3 ± 4.48
WI38	94.1 ± 3.98
MDA-MB231	30.9 ± 5.55
SW480	79.3 ± 6.06
HepG2	142.4 ± 5.96
HeLa	65.5 ± 6.53

is an important mechanism in the antitumor activity of natural extracts (36). We performed flow cytometry to analyze the effect of PDCe on the cell cycle distribution of MDA-MB231 breast cancer cells. As shown in Fig. 5A, it is clear that the proportion of sub-G1 peaks of MDA-MB231 cells were significantly dose-dependently increased after PDCe treatment for 72 h, the proportion of sub-G1 peaks was only 8.2% when the concentration of PDCe was 30 $\mu\text{g/mL}$. However, when the concentration of PDCe was doubled, the proportion of sub-G1 peaks was increased to 71.3%, indicating that more than two-thirds of the MDA-MB231 cells were dead. Moreover, there was a slight dose-dependent increase in the proportion of MDA-MB231 cells in the G0/G1 phases due to PDCe (Fig. 5C). It is worth mentioning that when SW480 cells were treated identically (Fig. 5B), only 0.2% of them were found to be dead at 60 $\mu\text{g/mL}$ PDCe concentration, but the proportion of cells in the G2/M phase showed a significant dose-dependent increase after PDCe treatment (Fig. 5D), which further indicated that the mechanism of PDCe-induced SW480 cell death involved a G2/M phase block rather than apoptosis.

Caspase activation induced by PDCe

Caspases, cysteine-containing aspartic acid proteolytic enzymes, are a group of cytoplasmic proteases. Caspases are closely associated with cellular apoptosis (37). Caspase-3 plays a key role in apoptosis; it acts as a central regulator, while caspase-8 and caspase-9 act as the initiators of the exogenous death receptor-mediated and endogenous mitochondria-mediated apoptotic pathways, respectively (38). To assess caspase activity in MDA-MB231 cells during PDCe-induced apoptosis, we measured the fluorescence intensity of substrates of caspase-3, -8, and -9, which indicate the activation of the corresponding enzymes after treatment with PDCe at 7.5,

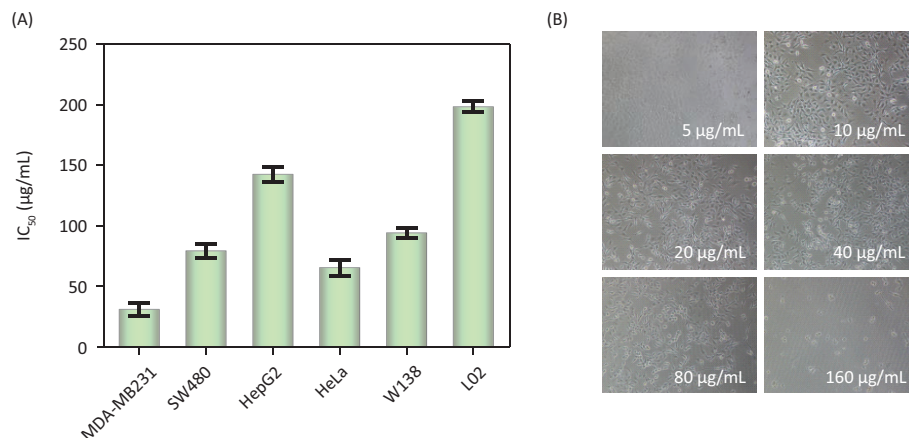


Fig. 4. Cytotoxic effects of the PDCe. (A) Antitumor activity of PDCe on various tumor and normal cells. Each value represents means \pm SD ($n = 3$). (B) Effect of the PDCe on the MDA-MB231 breast cancer cells *in vitro*. The cells' pictures were taken after treating with PDCe for 72 h. Original magnification: 10 \times .

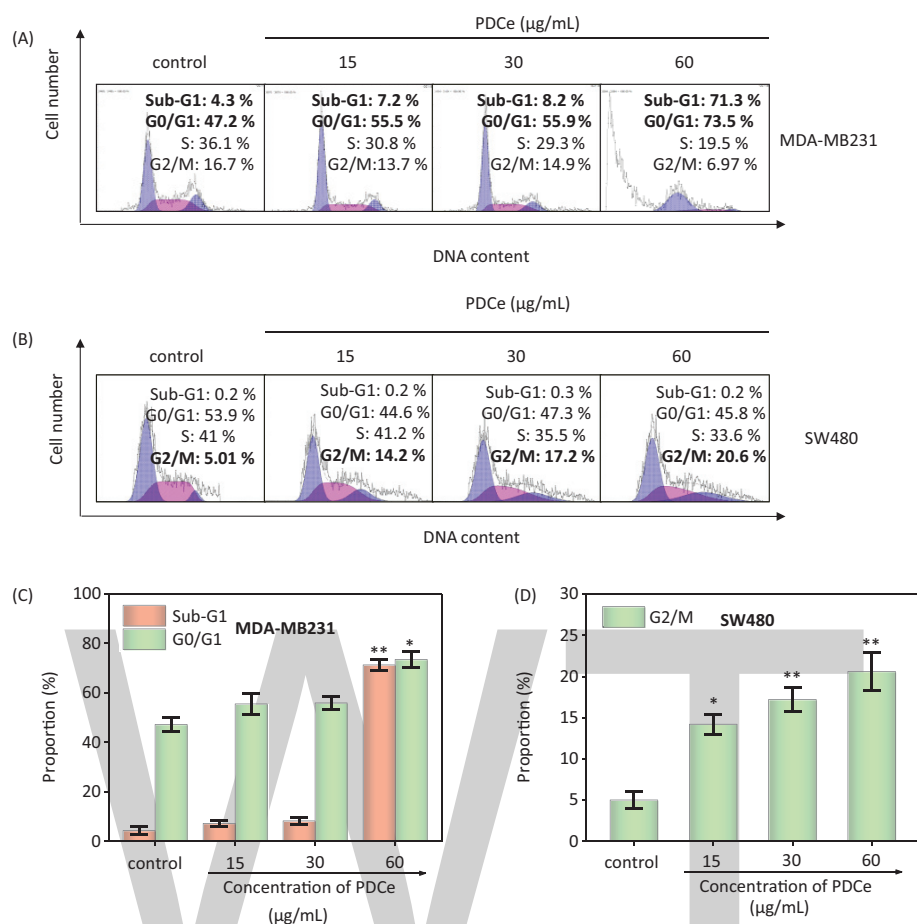


Fig. 5. Flow cytometric analysis of MDA-MB231 cells and SW480 cells after treatment of PDCe for 72 h. (A) Cell cycle changes of MDA-MB231 cells treated with PDCe for 72 h by flow cytometry analysis. (B) Cell cycle changes of SW480 cells treated with PDCe for 72 h by flow cytometry analysis. (C) Quantitative analysis of sub-G1 and G0/G1 proportion by PDCe in MDA-MB231 cells. (D) Quantitative analysis of G2/M proportion by PDCe in SW480 cells. Each value represents means \pm SD (n = 3). * and ** indicate statistical difference at $P < 0.05$ and $P < 0.01$, respectively, by comparing with the control group.

15, or 30 $\mu\text{g/mL}$. The results shown in Fig. 6A–C indicate that PDCe could activate caspase-3, caspase-8, as well as caspase-9 in MDA-MB231 cells at different PDCe concentrations, including at the highest concentration of 30 $\mu\text{g/mL}$. This suggested that both the death receptor-mediated and the mitochondria-mediated pathways are involved in PDCe-induced apoptosis. The activation level of caspase-8 was clearly higher than that of caspase-9 in MDA-MB231 cells after PDCe treatment.

PDCe-induced intracellular mitochondrial fragmentation

Mitochondria are known to play a key role in cellular activities, but some factors can damage the structure and function of mitochondria and further induce cell apoptosis (39). Fluorescence microscopy-based imaging was used to monitor changes in mitochondrial morphology after PDCe treatment. In the test, two special fluorescence trackers including Mito Tracker (red) and DAPI (blue) were used to label mitochondria and nuclei of

cancer cells (Fig. 6D). Initially, the mitochondria were present as red thread-like filaments, and we observed mitochondrial fragmentation and aggregation over time; the morphology was not significantly altered at 6 h, but the mitochondria were fragmented into small particles at 12 h after the addition of PDCe. These results suggested that PDCe had a clear impact on mitochondria, specifically causing mitochondrial fragmentation.

PDCe-induced downregulation of intracellular ROS generation

It has been found that ROS and RNS generation play a key role in the oxidative damage to islet cells. Several DNA components can be subject to attack due to excess ROS in cells, thus causing DNA damage (40, 41). In addition, an intermediate ROS level is a key factor in several cell signaling pathways (42, 43). We assessed intracellular ROS level via measurement of DHE fluorescence intensity after treatment with different concentrations of PDCe. As shown in Fig. 7A, ROS generation in MDA-MB231 cells

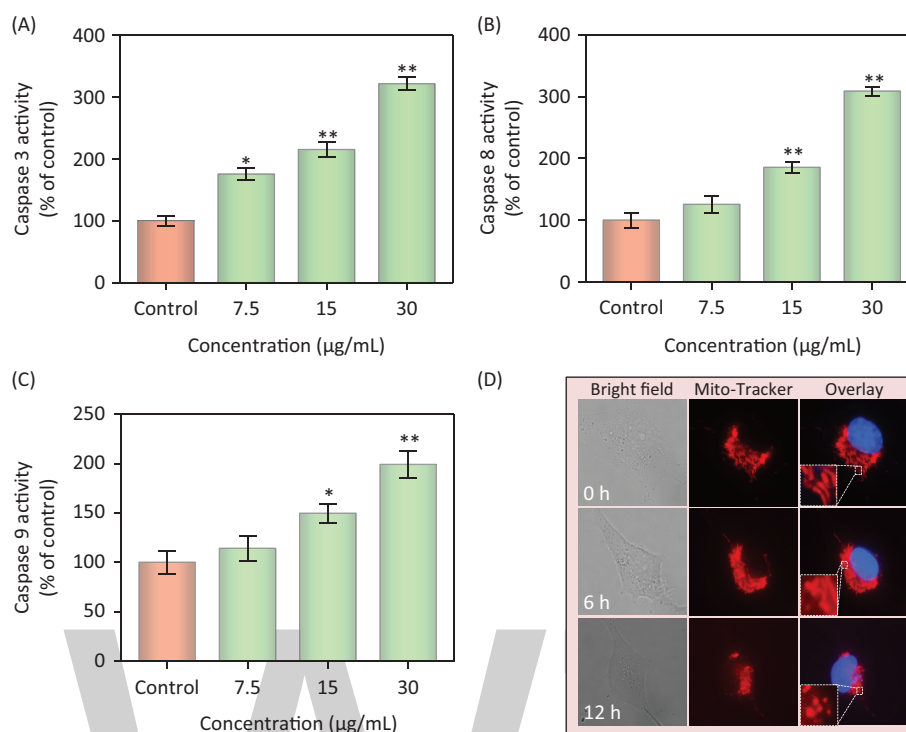


Fig. 6. Activation of extrinsic and intrinsic apoptotic pathway by PDCe. (A–C) Quantitative analysis of caspase activation triggered by PDCe. MDA-MB231 cells were treated with PDCe for 48 h. Significant difference between treatment and control groups is indicated at * $P < 0.05$, ** $P < 0.01$ level. (D) PDCe inhibits mitochondrial fragmentation: representative images of mitochondrial fragmentation in MDA-MB231 cells after treatment with 30 µg/mL PDCe for 12 h. Mitochondria fragmentation was measured by using a fluorescence microscope. Original magnification: 100×.

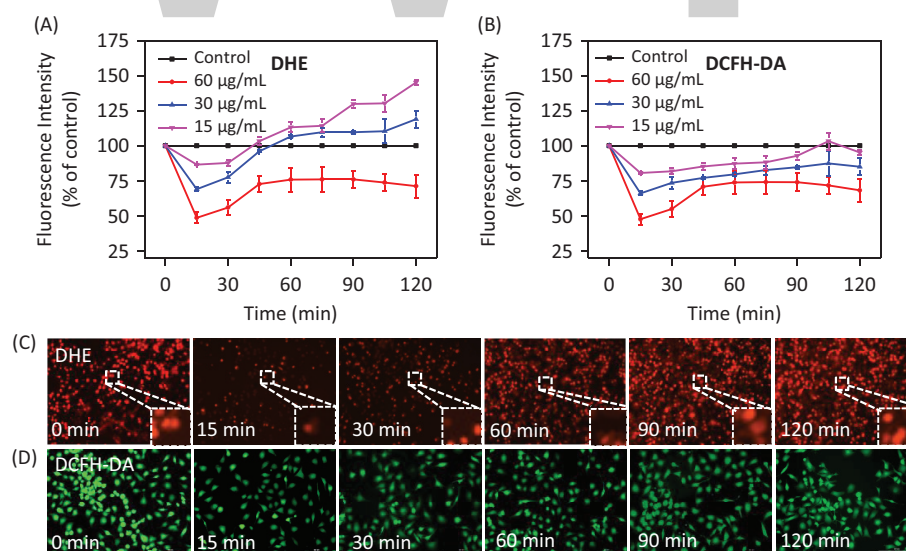


Fig. 7. Changes in ROS generation induced by PDCe. (A) The change of the intracellular ROS levels (DHE) in MDA-MB231 cells after being treated with PDCe. All experiments were performed in triplicate. (B) The change of the intracellular ROS levels (DCFH-DA) in MDA-MB231 cells after being treated with PDCe. All experiments were performed in triplicate. Fluorescence imaging of ROS generation in MDA-MB231 cells after the incubation of PDCe (30 µg/mL) for indicated times using a DHE (C) and DCFH-DA (D) probe, respectively. Original magnification: 10×.

declined rapidly after treatment with PDCe at different concentrations for 15 min, and increased slowly after 15 min showing a significant dose-dependence. To visually verify that PDCe could downregulate ROS, we imaged red fluorescence of DHE in MDA-MB231 cells using microscopy. As shown in Fig. 7C, it is clear that the fluorescence intensity was weakest at 15min, and weaker than that at 0 min at all other times, consistent with the ROS curve shown in Fig. 7A. Further, we found the same phenomenon using the DCFH-DA Test (Fig. 7B and D), with the fluorescence intensity being the weakest at 15 min and subsequently increasing. Taken together, our results show a significant change in ROS generation in MDA-MB231 cells due to the actions of PDCe, which finally induced cell apoptosis. This indicates that PDCe can not only significantly scavenge ABTS•+ and DPPH• free radicals but also cause remarkable clearance of ROS in MDA-MB231 cells.

Conclusions

In conclusion, the results of the experiments above strongly suggest that PDCe has excellent antioxidant activity, effectively scavenging DPPH• and ABTS•+ free radicals *in vitro*. Further, the inhibition of water-soluble free radicals (ABTS•+) was significantly higher than that of fat-soluble radicals (DPPH•). In addition, PDCe has excellent cytotoxicity against cancer cells, inducing cancer cell death via apoptosis and cell cycle arrest at the G2/M phase. In breast cancer cells, PDCe could not only downregulate intracellular ROS level significantly, causing mitochondrial rupture, but could also induce apoptosis by activating the mitochondria-mediated apoptotic pathway. Overall, our study provides valuable information regarding the beneficial effects of Phoenix Dan Cong tea on human health, and that it can act as a natural antioxidant and a promising anticancer agent.

Funding

This work was supported by Natural Science Foundation of China (21877049), National Program for Support of Top-notch Young Professionals (W02070191), YangFan Innovative & Entrepreneurial Research Team Project (201312H05) and Fundamental Research Funds for the Central Universities.

References

1. Widowati W, Herlina T, Ratnawati H, Constantia G, Deva IDGS, Maesaroh M. Antioxidant potential of black, green and Oolong Tea Methanol Extracts. *Biol Med & Nat Prod. Chem* 2015;4:35–39.
2. Venkatalakshmi P, Brindha P, Vellingiri V. In vitro antioxidant and anti-inflammatory studies on bark, wood and fruits of *Terminalia catappa* L. *Int J Phytomed* 2015;7:246–253.
3. Bagchi K, Puri S. Free radicals and antioxidants in health and disease. *Cell mol biol (Noisy-le-Grand, France)*. 1998;53:1–2.
4. Johnson P. Antioxidant enzyme expression in health and disease: effects of exercise and hypertension. *Comp Biochem Physiol C Toxicol Pharmacol* 2002;133:493–505.
5. Wiseman SA, Balentine DA, Frei B. Antioxidants in tea. *Crit Rev Food Sci* 1997;37:705–718.
6. Hara Y. Elucidation of physiological functions of Tea Catechins and their practical applications. *J Food Drug Anal* 2012;20:296–300.
7. Yang CS, Jin HY, Guan F, Chen YK, Wang H. Cancer preventive activities of Tea Polyphenols. *J Food Drug Anal* 2012;20:318–322.
8. Nakayama T, Ishii T, Uekusa Y, Kato K, Kumazawa S. Interaction of tea catechins with phospholipids - Roles in their tastes and biological activities. *J Food Drug Anal* 2012;20:305–308.
9. Hossain MS, Nibir YM, Zerín S, Ahsan N. Antibacterial activities of the Methanolic extract of Bangladeshi Black tea against various human pathogens. *Dhaka Univ J Pharm Sci* 2015;13:97–103.
10. Zhao C, Li C, Liu S, Yang L. The galloyl catechins contributing to main antioxidant capacity of tea made from *Camellia sinensis* in China. *Sci World J* 2014;2014:1–11.
11. Tijburg LB, Mattern T, Folts JD, Weisgerber UM, Katan MB. Tea flavonoids and cardiovascular disease: a review. *Crit Rev Food Sci* 1997;37:771–785.
12. Haslam E. Thoughts on thearubigins. *Phytochemistry* 2003;64:61–73.
13. Chen GH, Yang CY, Lee SJ, Wu CC, Tzen JTC. Catechin content and the degree of its galloylation in oolong tea are inversely correlated with cultivation altitude. *J Food Drug Anal* 2014;22:303–309.
14. Chung TY, Kuo PC, Liao ZH, Shih YE, Cheng ML, Wu CC, et al. Analysis of lipophilic compounds of tea coated on the surface of clay teapots. *J Food Drug Anal* 2015;23:71–81.
15. Grinberg LN, Newmark H, Kitrossky N, Rahamim E, Chevion M, Rachmilewitz EA. Protective effects of Tea Polyphenols against oxidative damage to Red Blood Cells. *Biochem Pharmacol* 1997;54:973–978.
16. Barbosa NS, Kalaaji AN. CAM use in dermatology. Is there a potential role for honey, green tea, and vitamin C? *Complement Ther Clin* 2014;20:11–15.
17. Lykkesfeldt J, Michels AJ, Frei B. Vitamin C. *Adv Nutr* 2014;5:16–18.
18. Lamuela-Raventós RM, Singleton VL, Orthofer R. Analysis of total phenols and other oxidation substrates and antioxidants by means of Folin-Ciocalteu reagent. *J Wiley & sons* 1999;299:152–178.
19. Ballus CA, Meinhart AD, Campos FADS, Godoy HT. Total phenolics of virgin olive oils highly correlate with the Hydrogen Atom Transfer Mechanism of Antioxidant Capacity. *J Am Oil Chem Soc* 2015;92:843–851.
20. Russo A, Cardile V, Lombardo L, Vanella L, Vanella A, Garbarino JA. Antioxidant activity and antiproliferative action of methanolic extract of *Geum quellyon* Sweet roots in human tumor cell lines. *J Ethnopharmacol* 2005;100:323–332.
21. Schoenmakers P. Practical HPLC method development. *J Chromatogr* 1988;16:338–338.
22. Taylor T. The LCGC blog: practical HPLC method development screening; *LC GC N. Am* 2016, 1–2.
23. Miller NJ, Sampson J, Candeias LP, Bramley PM, Rice-Evans CA. Antioxidant activities of carotenes and xanthophylls. *Febs Lett* 1996;384:240.
24. Xie L, Luo Z, Zhao Z, Chen T. Anticancer and Antiangiogenic Iron(II) complexes that target thioredoxin reductase to trigger cancer cell apoptosis. *J Med Chem* 2017;60:202–214.

25. Liu C, Fu Y, Li CE, Chen T, Li X. Phycocyanin-functionalized selenium nanoparticles reverse palmitic acid-Induced pancreatic beta cell apoptosis by enhancing cellular uptake and blocking Reactive Oxygen Species (ROS)-Mediated Mitochondria Dysfunction. *J Agric Food Chem* 2017;65:4405–4413.
26. Chen J, Luo Z, Zhao Z, Xie L, Zheng W, Chen T. Cellular localization of iron(II) polypyridyl complexes determines their anti-cancer action mechanisms. *Biomaterials* 2015;71:168–177.
27. Deng Z, Yu L, Cao W, Zheng W, Chen T. A selenium-containing ruthenium complex as a cancer radiosensitizer, rational design and the important role of ROS-mediated signalling. *Chem Commun (Camb)* 2015;51:2637–2640.
28. Fu X, Yang Y, Li X, Lai H, Huang Y, He L, et al. RGD peptide-conjugated selenium nanoparticles: antiangiogenesis by suppressing VEGF-VEGFR2-ERK/AKT pathway. *Nanomed: Nanotechnol* 2016;12:1627–1639.
29. Fan C, Zheng W, Fu X, Li X, Wong YS, Chen T. Enhancement of auranofin-induced lung cancer cell apoptosis by selenocystine, a natural inhibitor of TrxR1 in vitro and in vivo. *Cell Death Dis* 2014;5:e1191.
30. Huang Y, He L, Liu W, Fan C, Zheng W, Wong YS, et al. Selective cellular uptake and induction of apoptosis of cancer-targeted selenium nanoparticles. *Biomaterials* 2013;34:7106–7116.
31. Jiang W, Fu Y, Yang F, Yang Y, Liu T, Zheng W, et al. Gracilaria lemaneiformis polysaccharide as integrin-targeting surface decorator of selenium nanoparticles to achieve enhanced anticancer efficacy. *ACS Appl Mater Inter* 2014;6:13738–13748.
32. Sinha R, Elbayoumy K. Apoptosis is a critical cellular event in cancer chemoprevention and chemotherapy by selenium compounds. *Curr Cancer Drug Tar* 2004;4:13–28.
33. Li XL, Wong YS, Xu G, Chan JCN. Selenium-enriched Spirulina protects INS-1E pancreatic beta cells from human islet amyloid polypeptide-induced apoptosis through suppression of ROS-mediated mitochondrial dysfunction and PI3/AKT pathway. *Eur J Nutr* 2015;54:509–522.
34. Yu Z, Ying-Xin G, Jia-Ji M, Jun-Yu S, Shi-Chong Q, Hong-Chang L. N-acetyl cysteine protects human oral keratinocytes from Bis-GMA-induced apoptosis and cell cycle arrest by inhibiting reactive oxygen species-mediated mitochondrial dysfunction and the PI3K/Akt pathway. *Toxicol in Vitro* 2015;29:2089–2101.
35. Kim GJ, Kim W, Kim KT, Lee JK. DNA damage and mitochondria dysfunction in cell apoptosis induced by nonthermal air plasma. *Appl Phys Lett* 2010;96:1721.
36. Agarwal C, Veluri R, Kaur M, Chou SC, Thompson JA, Agarwal R. Fractionation of high molecular weight tannins in grape seed extract and identification of procyanidin B2-3,3'-di-O-gallate as a major active constituent causing growth inhibition and apoptotic death of DU145 human prostate carcinoma cells. *Carcinogenesis* 2007;28:1478–1484.
37. Kumar S. Caspase function in programmed cell death. *Cell Death Differ* 2007;14:32–43.
38. Zhang X, Dai C, You Y, He L, Chen T. Tea regimen, a comprehensive assessment of antioxidant and antitumor activities of tea extract produced by Tie Guanyin hybridization. *RSC Adv* 2018;8:11305–11315.
39. Ni HM, Williams JA, Ding WX. Mitochondrial dynamics and mitochondrial quality control. *Redox Biol* 2015;4:6.
40. Wang C, Zhang H, Xue Z, Yin H, Niu Q, Chen H. The relation between doses or post-plasma time points and apoptosis of leukemia cells induced by dielectric barrier discharge plasma. *Aip Adv* 2015;5:143702–143129.
41. Klaunig JE, Wang Z, Pu X, Zhou S. Oxidative stress and oxidative damage in chemical carcinogenesis. *Toxicol Pathol* 2011;38:96–109.
42. Held P. Tech Resources-app guides. *Biotek Com*; 1970.
43. Ma E, Sasazuki S, Shimazu T, Sawada N, Yamaji T, Iwasaki M, et al. Reactive oxygen species and gastric cancer risk: a large nested case-control study in Japan. *Eur J Epidemiol* 2015;30:589–594.

***Xiaoling Li**

Institute of Food Safety and Nutrition
Jinan University
Guangzhou 510632
China
Email: tlxlli@jnu.edu.cn

***Tianfeng Chen**

The First Affiliated Hospital
Department of Chemistry
Jinan University
Guangzhou 510632
China
Email: tchentf@jnu.edu.cn

Nutritional, biochemical and sensory properties of instant beverage powder made from two different varieties of pearl millet

Anthony O. Obilana^{1*}, Barathi Odhav² and Victoria A. Jideani¹

¹Food Technology Department, Cape Peninsula University of Technology, Bellville Campus, Cape Town, South Africa;

²Biotechnology and Food Technology Department, Durban University of Technology, Durban, South Africa

Abstract

Introduction: The traditional method of producing instant foods involves producing a gelatinised paste from the preferred grain flour and proceeding to dry it using a drum drier. This produced a flaked product, which can be used as is or ground and sieved to obtain the desired particle size. With the advent of extrusion cooking technology and diverse production processes associated with the technology, food products including instant foods from cereals were developed.

Objectives: The primary objective of this study was to produce a nutritious and acceptable pearl millet instant beverage powder (PMIBP) using combination processing.

Methods: The effect of different processing methods (malting, extrusion, and a combination of both processes) on the nutritional, biochemical, and sensory characteristics of beverage powders and beverages made from two varieties of pearl millet (*Pennisetum glaucum*) were evaluated.

Results: Combination processing led to a significant ($p \leq 0.05$) decrease in total fat and total dietary fibre (TDF) (3.85 and 22.99 g/100 g, respectively) of AgriGreen (AgG) extruded malted pearl millet (EMPM) and extruded raw pearl millet–malted pearl millet mix (ERPMMPM). Combination processing also led to a decrease in the ash, total fat, TDF, Fe and Zn content (1.76, 3.48, 14.26 g/100 g, 7.78 and 4.74 mg/100 g, respectively) of Babala (Ba) EMPM and Ba ERPMMPM (1.88, 4.22, 21.71 g/100 g, 7.24 and 4.14 mg/100 g, respectively). Beverages of 10% total solids were prepared from the samples and offered to an untrained consumer panel. The beverages were rated on appearance, colour, aroma, flavour, texture and overall acceptability on a nine-point hedonic scale. In general, Ba raw pearl millet was rated 4 (like slightly), AgG malted pearl millet was rated 6 (dislike slightly), and all other pearl millet samples from both varieties were rated 5 (neither like nor dislike).

Conclusion: Although combination processing led to an increase in carbohydrates, Ca, energy, Fe content, and 12 of the 15 amino acids measured as well as protein and starch digestibility and no change in the other nutrients measured, this did not significantly impact on the acceptability of the beverages.

Keywords: *Instant beverage powder, pearl millet, combination processing, malting, extrusion, Instant beverage powder*

Combination processing (hurdle technology) is the use of two or more processing methods in the manufacture and preservation of a food product. It was initially developed in order to ensure microbiological food safety. However, this concept is proving successful as an intelligent combination of hurdles secures microbial stability and safety as well as the sensory quality of foods, provides convenience and freshness of foods to the consumers, and might be cost-efficient for the producers because it demands less energy during production and storage (1).

Babala (Ba) is the most widely used variety of pearl millet in the world. It has been developed to adapt to

the specific climates in which it grows. It is a nutrient-dense grain with a variety of food and beverage applications. Hybrids of Ba are developed for various other climatic and weather conditions and, ideally, developed hybrids are required to have similar characteristics to Ba under various processing conditions. The objective of this study was to evaluate the effect of malting, extrusion, and a combination of both methods on the nutritional and biochemical properties and sensory characteristics of flours and their beverages made from two varieties of pearl millet (Ba and AgriGreen [AgG] – a hybrid of Ba).

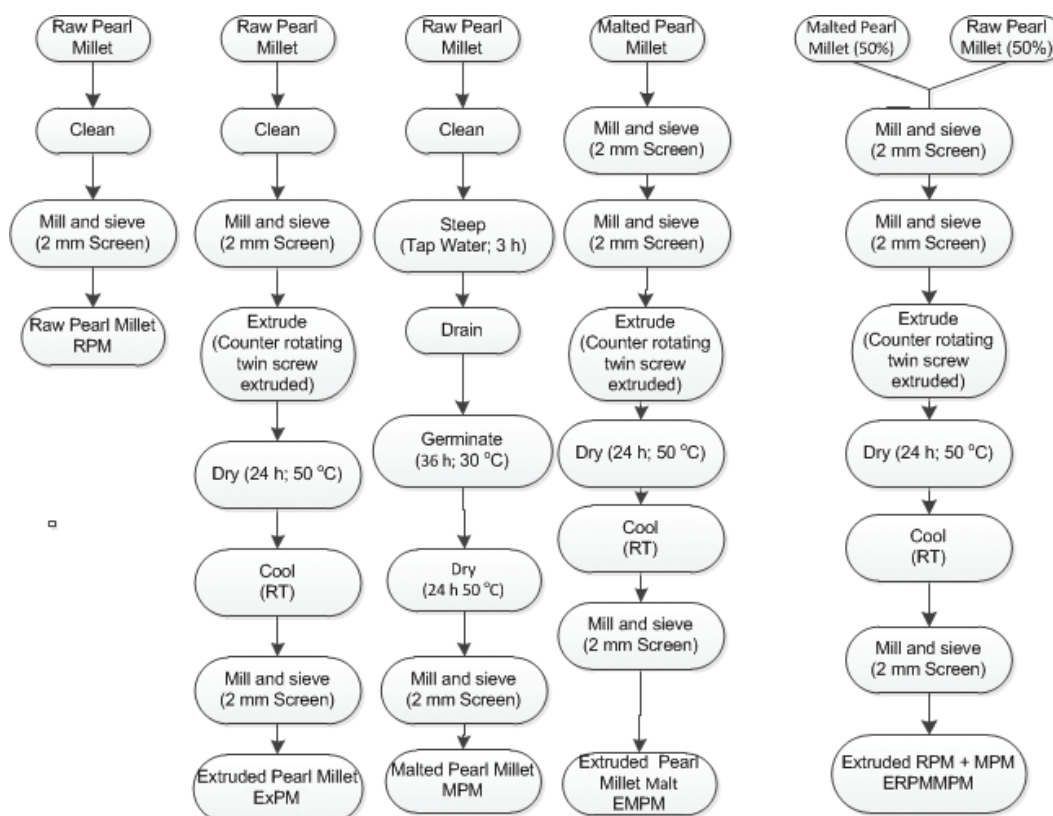


Fig. 1. Processing steps of pearl millet into beverage. RPM = raw pearl millet, MPM = malted pearl millet, ERPMPMPM = extruded mix of raw and malted pearl millet, RT = Room Temperature, EMPM = extruded pearl millet malt, ExPM = Extruded pearl millet.

Materials and methods

Source of materials

Two different varieties of pearl millet (*Pennisetum glaucum*), Ba and AgG, a hybrid of Babala, were obtained from Agricol Pty. Ltd., Cape Town, South Africa. All chemical reagents were obtained from Sigma-Aldrich South Africa. All equipment used was located in the Department of Food Technology, Cape Peninsula University of Technology (CPUT), Bellville, South Africa, and The Council for Scientific and Industrial Research (CSIR), Pretoria, South Africa.

Processing of pearl millet into beverage powder

The pearl millet (Ba and AgG) was cleaned by placing it in a tray and removing the chaff and damaged grains as well as stones or pebbles, together with all other extraneous matter, by a combination of winnowing and picking. The cleaned grains were further processed (Fig. 1).

Determination of the proximate composition of pearl millet flours made from two different varieties

The moisture, protein, total ash, crude fibre contents, total fat, saturated, monounsaturated, and polyunsaturated fat content of the samples were determined according to the

methods of the Association of Official Agricultural Chemists (AOAC) (2).

Biochemical assay of beverage powder from two varieties of pearl millet

The amino acid content of the millet-based instant beverage powder was determined according to the methods of Benson and Patterson (3) and Klapper (4), with slight modifications. Calcium, iron, and zinc were analysed using the inductively coupled plasma (ICP) spectrometer (Perkin Elmer, model nr, Rodgau, Germany). Prior to analysis, samples were digested in a microwave digester (Milestone Microwave Laboratory Systems, Sorisole, Italy). The concentrations of minerals were calculated using the concentrations from the ICP analysis reports, using the following formula:

$$\text{Mineral concentration (mg 100g}^{-1}\text{)} = \frac{\text{Instrument concentration (ppm)} \times \text{Volume (ml)} \times 100}{\text{Mass of sample (mg)}}$$

Sample solutions were quantified against standard solutions of known concentrations that were analysed concurrently (5).

The determination of *in vitro* protein and starch digestibility was carried out according to the method of Saunders et al. (6). Digestibility was calculated using the following formula (7):

$$\text{Protein digestibility (\%)} = \frac{\text{Nitrogen in supernatant} \times 100}{\text{Nitrogen in sample}}$$

In vitro carbohydrate digestibility was determined using a method described by the authors of Ref. (8). Microsoft Excel (2010) was used to plot the standard curve and to calculate the concentration of starch digestion products in test solutions. The values were expressed as mg maltose/g starch.

The total amount of phenolic compounds in the pearl millet whole meal flour and product extract was determined using the method described by Silvia et al. (9) with modifications for use with a 96-well plate reader. The concentration of phenolic compounds in the extracts was calculated from a calibration curve of the standard and expressed as gallic acid equivalents.

The antioxidant activity (by free radical scavenging) of the pearl millet whole meal flour and products were determined using the Trolox (6-Hydroxy-2,5,7,8-tetramethylchroman-2-carboxylic acid) equivalent antioxidant capacity (TEAC) assay as described by the authors of Ref. (10) with modifications for a 96-well plate reader.

Beverage preparation and sensory evaluation

The sensory evaluation of the beverages was exploratory in nature in order to determine if any one of the samples warranted further development. The flour (80 g) of each sample (raw pearl millet [RPM], extruded pearl millet [ExPM], malted pearl millet [MPM], extruded pearl millet malt [EMPM], and extruded mix of raw and malted pearl millet [ERPMPM]) were individually weighed into separate 3 L stainless steel pots with 200 ml of tap water ($25 \pm 3^\circ\text{C}$) and mixed to form a paste. Boiling water (700 ml) was then added slowly whilst stirring to prevent the formation of lumps. Two 900 ml pots of each sample beverage were prepared to give a total of 1800 ml of beverage for each sample. The mixture was brought to a rolling boil. The prepared beverages were allowed to cool to between 50 and 60°C and then transferred into appropriately labelled 18/8 stainless steel double-walled vacuum thermal flasks.

The consumer panel assessments were conducted at the CPUT Department of Food Science and Technology sensory facilities using an untrained panel consisting of a mix of staff and students of the department (78).

For each sample, 78 randomly generated three-digit numbers were used to code samples presented to the consumer. Freshly prepared beverages of each sample

(15–25 ml) were poured into 30 ml polystyrene cups to retain temperature (50–60°C) and consistency during the evaluation. Each consumer was presented with five cups of beverages on a polystyrene tray representing the five samples at between 40 and 45°C. The consumers were provided with water and an empty polystyrene cup to use as a spittoon and were instructed to rinse their mouths between samples. They were given written instructions together with a nine-point hedonic scale (1 = like extremely to 9 = dislike extremely), on which they were required to rate each sample's flavour, texture, taste, colour, and overall acceptability.

Data analyses

All data were collected in triplicate. The data were subjected to multivariate analysis of variance to establish mean differences ($p \leq 0.05$) between treatments. Duncan multiple range tests were used to separate means where differences existed. All data analyses were carried out using IBM SPSS Statistics version 21 (2012).

Results and discussion

Effect of malting, extrusion, and their combination on the proximate content of beverage powders made from two varieties of pearl millet

Malting, extrusion, and the combination of both had varying effects on the nutritional values of RPM, ExPM, MPM, EMPM, and ERPMPM produced from both varieties of pearl millet (Table 1). The effect of extrusion on nutritional values (Table 1) include the following: a significant ($p \leq 0.05$) increase in the total fats (3.98 to 4.61 g/100 g); ash (1.75 to 2.03 g/100 g); carbohydrates (81.64 to 83.56 g/100 g); energy (1723.80 to 1789.44 KJ/100 g); and the minerals (Table 2) Ca (35.05 to 36.23 mg/100 g) and Fe (7.10 to 9.63 mg/100 g).

These changes depend on temperature, moisture, pH, shear rate, residence time, their interactions, the nature of the proteins themselves, and the presence of materials such as carbohydrates and lipids (11). The time-temperature conditions to which foods are exposed during extrusion are comparable to other high-temperature, short-time processes, which is considered preferable in terms of nutrient retention and safety of foods since antinutritional factors and contaminating microorganisms are more effectively destroyed (12).

According to Bjork and Asp (12), extrusion processing affects the nutritional value of lipids through different mechanisms such as oxidation, cis-trans isomerisation, or hydrogenation. A decrease in the fat content of extruded products has been reported by several authors. Fabriani et al. (13) interpreted the decrease in the extractable-fat content of extruded products as the result of the formation of complexes with other compounds present in the

Table 1. Effect of processing on the proximate composition (g/100 g) and energy (KJ/100 g) of pearl millet (AgriGreen and Babala) (d.b.)^{1,2}

	Nutrient	RPM	ExPM	MPM	EMPM	ERPMMPM
AgriGreen	Moisture	12.56 ± 0.25 ^a	9.68 ± 0.21 ^b	9.60 ± 0.03 ^b	8.41 ± 0.15 ^c	9.47 ± 0.07 ^b
	Protein	12.46 ± 0.22 ^a	12.30 ± 0.28 ^a	12.73 ± 0.64 ^a	12.51 ± 0.16 ^a	12.47 ± 0.09 ^a
	Ash	1.75 ± 0.11 ^a	2.03 ± 0.14 ^b	1.54 ± 0.32 ^a	1.67 ± 0.09 ^a	1.75 ± 0.02 ^a
	Total fat	3.98 ± 0.41 ^a	4.61 ± 0.30 ^b	2.93 ± 0.29 ^c	3.85 ± 0.19 ^a	4.21 ± 0.08 ^a
	TDF	26.59 ± 3.15 ^a	17.11 ± 0.75 ^b	19.33 ± 1.99 ^c	22.99 ± 2.90 ^c	18.12 ± 2.62 ^b
	Carbohydrates	81.64 ± 0.34 ^a	83.56 ± 0.90 ^b	85.41 ± 0.64 ^c	85.68 ± 0.35 ^c	84.27 ± 0.06 ^b
	Energy	1723.80 ± 5.48 ^a	1789.44 ± 3.14 ^b	1763.19 ± 11.53 ^c	1804.34 ± 2.78 ^d	1789.83 ± 3.48 ^b
Babala	Moisture (g/100 g)	11.91 ± 0.06 ^a	6.88 ± 0.04 ^b	10.69 ± 0.11 ^c	8.18 ± 0.06 ^d	7.76 ± 0.19 ^e
	Protein (g/100 g)	12.03 ± 0.18 ^a	12.06 ± 0.08 ^a	12.75 ± 0.04 ^b	12.36 ± 0.26 ^c	12.46 ± 0.11 ^c
	Ash (100/g)	1.98 ± 0.04 ^a	1.97 ± 0.03 ^a	1.83 ± 0.07 ^b	1.76 ± 0.07 ^b	1.88 ± 0.12 ^b
	Total fat (g/100 g)	4.79 ± 0.17 ^a	4.25 ± 0.50 ^b	2.84 ± 0.56 ^c	3.48 ± 0.37 ^c	4.22 ± 0.55 ^b
	TDF (g/100 g)	26.69 ± 4.58 ^a	16.51 ± 0.53 ^b	25.17 ± 7.82 ^c	14.26 ± 2.15 ^b	21.71 ± 5.89 ^c
	Carb (g/100 g)	81.64 ± 0.09 ^a	86.85 ± 0.48 ^b	84.17 ± 0.62 ^c	86.35 ± 0.63 ^d	85.73 ± 0.41 ^d
	Energy (KJ/100 g)	1750.11 ± 1.99 ^a	1838.08 ± 12.42 ^b	1735.04 ± 10.60 ^a	1799.15 ± 8.42 ^c	1821.70 ± 13.71 ^d

¹Values are mean ± standard deviation. Different superscripts in rows differ significantly ($p \leq 0.05$).

²RPM = raw pearl millet; ExPM = extruded pearl millet; MPM = malted pearl millet; EMPM = extruded pearl millet malt; ERPMMPM = extruded raw pearl millet–malted pearl millet mix; TDF = total dietary fibre.

Table 2. Effect of processing on the mineral (mg/100 g) composition of pearl millet (AgriGreen and Babala) (d.b.)^{1,2}

	Nutrient	RPM	ExPM	MPM	EMPM	ERPMMPM
AgriGreen	Ca	35.05 ± 0.25 ^a	36.23 ± 0.04 ^b	38.78 ± 0.45 ^c	40.32 ± 0.25 ^d	36.90 ± 0.14 ^e
	Fe	7.10 ± 0.29 ^a	9.63 ± 0.29 ^b	7.01 ± 0.16 ^a	8.56 ± 0.28 ^c	10.57 ± 0.31 ^d
	Zn	3.43 ± 0.13 ^a	3.30 ± 0.08 ^a	4.18 ± 0.09 ^b	3.19 ± 0.11 ^a	3.16 ± 0.50 ^a
Babala	Ca	30.74 ± 0.25 ^a	27.43 ± 0.20 ^b	34.15 ± 0.13 ^c	32.56 ± 0.24 ^d	33.66 ± 0.28 ^d
	Fe	9.60 ± 0.43 ^a	9.51 ± 0.09 ^a	7.08 ± 0.45 ^b	7.78 ± 0.13 ^c	7.24 ± 0.33 ^b
	Zn	5.36 ± 0.54 ^a	5.51 ± 0.37 ^a	3.97 ± 0.45 ^b	4.74 ± 0.05 ^c	4.14 ± 0.08 ^b

¹Values are mean ± standard deviation. Different superscripts in rows differ significantly ($p \leq 0.05$).

²RPM = raw pearl millet; ExPM = extruded pearl millet; MPM = malted pearl millet; EMPM = extruded pearl millet malt; ERPMMPM = extruded raw pearl millet–malted pearl millet mix.

food matrix and/or shear damage caused by the action of the screws and subsequent pressures generated. These could explain the decrease in fat content observed in Babala. However, the increase in the extractable fat content of AgG (Table 1) could have been a result of the exact opposite happening, that is, no complexes being formed with other compounds in the food matrix during the processes and/or little or no shear damaged caused by the actions of the screws and subsequent pressures generated.

Malting led to a significant ($p \leq 0.05$) increase in the carbohydrates, energy (Table 1), Ca, and Zn (Table 2) (81.64 to 85.41 g/100 g, 1723.8 to 1763.2 KJ/100 g, 35.05 to 38.78 mg/100 g and 3.43 to 4.18 mg/100 g, respectively). A significant ($p \leq 0.05$) decrease in the TDF and total fat (26.59 to 19.33 and 3.98 to 2.93 g/100 g respectively) was observed, but no effect on the protein, ash, and Fe content of AgG MPM (Table 1). These are in contrast to observations of slightly increased protein content (11, 7, and 2%, respectively) for red sorghum, millet, and maize made by

Traoré et al. (14). Shayo et al. (15) also observed an increase in protein content of 5% after 48 h of germination at 30°C in two varieties of millet from Tanzania. Whilst the increase in protein content in these experiments was attributed to a passive variation resulting from a decrease in the carbohydrate compounds used for respiration (16), the lack of change in protein content in this particular experiment could be attributed to the shorter germination time (36 h as opposed to 48 h). According to Chavan and Kadam (17), a considerable portion of endosperm carbohydrates decrease during germination, causing apparent increase in the protein and fibre contents of cereals; this could be the reason for no marked changes in the endosperm protein content of sorghum and pearl millet, although the rootlets separated from them contained substantial levels of protein.

The decreases in fat content are in agreement with observations made by other authors (14, 16–18). This decrease could be explained by the fact that lipids are used

to produce the necessary energy for the biochemical and physiological modifications that occur in the seed during germination (18). Combination processing (malting and extrusion) led to a significant ($p \leq 0.05$) increase in carbohydrates, energy (Table 1), Ca, and Fe (Table 2) (81.64 to 85.68 g/100 g, 1723.8 to 1804.3 KJ/100 g, 35.05 to 40.32 and 7.10 to 8.56 mg/100 g, respectively); a significant ($p \leq 0.05$) decrease in TDF (26.59 to 22.99 g/100 g); and no effect on the protein and ash content of AgG EMPM.

Combination processing of the ERPMPM led to a significant ($p \leq 0.05$) increase in carbohydrates, energy (Table 1), Ca, and Fe (Table 2) (81.64 to 84.27 g/100 g, 1723.8 to 1789.8 KJ/100 g, 35.05 to 36.90 and 7.10 to 10.57 mg/100 g, respectively); a significant ($p \leq 0.05$) decrease in TDF (26.59 to 18.12 g/100 g); and no effect on ash, total fat, and Zn content of AgG ERPMPM.

The extrusion process led to a significant ($p \leq 0.05$) increase in carbohydrates and energy (81.64 to 86.85 g/100 g and 1750.11 to 1838.08 KJ/100 g, respectively); a significant ($p \leq 0.05$) decrease in total fat, TDF (Table 1), and Ca (Table 2) (4.79 to 4.25, 26.69 to 16.51 g/100 g and 30.74 to 27.43 mg/100 g, respectively); but had no effect on the protein, ash, Fe, and Zn content of Ba ExPM (Table 1).

The observations on the effect of malting on proximate composition, mineral (Ca, Fe, and Zn) and fibre content of both AgG and Ba were in agreement with observations made by several authors (19–21) but differed from observations made by Opoku et al. (16) and Suma and Urooj (22). According to Malleshi and Klopfenstein (21), during germination several biochemical, textural, and physiological transformations occur in the seeds. The growing root and shoot mainly derive nutrients from the embryo, scutellum, and the endosperm and this result in loss of protein, carbohydrates, and minerals from the seed. Consequently, the proportion of some of these nutrients in the malt will be altered.

Leaching of water-soluble compounds and metabolism of carbohydrates during germination also contribute to dry matter loss of seeds. This could explain the varying changes in the nutritional properties of the pearl millet after malting.

Malleshi and Klopfenstein (21) observed that raw sorghum and pearl millet contained 11.8 and 16.1% protein, respectively, which did not change appreciably on malting and is in agreement with the observations made for the protein content of AgG but differed for that of Ba. They also observed a slight increase in the dietary fibre content of their samples after malting.

This was in contradiction to observations made in this experiment. Also, dietary fibre levels reported in their works were markedly lower than those reported in this work. Combination processing (malting and extrusion) led to a significant ($p \leq 0.05$) increase in protein content, carbohydrates, energy (Table 1), and Ca (Table 2) (12.03

to 12.36, 81.64 to 86.35 g/100 g, 1750.11 to 1799.2 KJ/100 g and 30.74 to 32.56 mg/100 g, respectively) and a significant ($p \leq 0.05$) decrease in the ash, total fat, TDF (Table 1), Fe, and Zn (Table 2) (1.98 to 1.76, 4.79 to 3.48, 26.69 to 14.26 g/100 g, 9.60 to 7.78 and 5.36 to 7.74 mg/100 g, respectively) content of the EMPM. Combination processing of the ERPMPM led to a significant ($p \leq 0.05$) increase in the protein, carbohydrates, energy (Table 1), and Ca (Table 2) (12.03 to 12.46, 81.64 to 85.73 g/100 g, 1750.11 to 1821.70 KJ/100 g and 30.74 to 33.66 mg/100 g) and a significant ($p \leq 0.05$) decrease in the ash, total fat, TDF (Table 1), Fe, and Zn (Table 2) (1.98 to 1.88, 4.79 to 4.22, 26.69 to 21.71 g/100 g, 9.60 to 7.24 and 5.36 to 4.14 mg/100 g, respectively) content of Ba ERPMPM. These variations in values observed could be attributed to several factors such as differences in the pearl millet varieties experimented with as well as extrinsic factors including growth region, climate, and soil type, to name a few. The decrease in moisture content of both AgG and Ba was the result of the kilning of germinated grains. The information observed is a summary and a reinforcement of earlier discussions on the effect of the processing methods on the two varieties of pearl during the production of the Pearl Millet Instant Beverage Powder (PMIBP).

Extrusion, malting, and a combination of both processes significantly ($p \leq 0.05$) reduced the fat constituents (saturated, monounsaturated, and polyunsaturated) of Ba-bala (Table 3). However, extrusion significantly ($p \leq 0.05$) increased the content of polyunsaturated fat of AgG, but the combination process did not affect the fat constituents of AgG significantly ($p \leq 0.05$) (Table 3). The reduction in fat content could be as a result of conversion or utilisation for energy during germination or through different mechanisms such as oxidation, cis–trans isomerisation, or hydrogenation during extrusion processing (12).

Effect of malting, extrusion, and their combination on the amino acid content of beverage powders made from two varieties of pearl millet

The effects of malting, extrusion, and a combination of both methods on the amino acid content of the PMIBP made from the two different varieties of pearl millet, AgG and Ba, are shown in Table 4. For the AgG variety, extrusion led to a significant ($p \leq 0.05$) increase in the concentration of the amino acids in the AgG ExPM.

Malting led to a significant ($p \leq 0.05$) increase in all amino acids, except for glutamic acid, leucine, and methionine, which remained unchanged in the AgG MPM. The combination of malting and extrusion significantly ($p \leq 0.05$) increased all amino acids except for glutamic acid, leucine, and arginine in the AgG EMPM. Similar results were obtained for the AgG ERPMPM, with glutamic acid, leucine, lysine, and arginine remaining unchanged by the process. None of the treatments led to a

Table 3. Effect of processing on the fat constituents (g/100 g) of pearl millet (AgriGreen and Babala) (d.b.)^{1,2}

	Nutrient	RPM	ExPM	MPM	EMPM	ERPMMMPM
AgriGreen	Total fat (g/100 g)	3.98 ± 0.41 ^a	4.61 ± 0.30 ^b	2.93 ± 0.29 ^c	3.85 ± 0.19 ^a	4.21 ± 0.08 ^a
	Saturated fat (g/100 g)	1.11 ± 0.10 ^a	1.27 ± 0.06 ^b	0.83 ± 0.07 ^c	1.07 ± 0.05 ^a	1.16 ± 0.03 ^a
	Monounsaturated fat (g/100 g)	1.14 ± 0.13 ^a	1.33 ± 0.10 ^b	0.82 ± 0.09 ^c	1.09 ± 0.07 ^a	1.23 ± 0.02 ^a
	Polyunsaturated fat (g/100 g)	1.72 ± 0.18 ^a	2.01 ± 0.14 ^b	1.28 ± 0.13 ^c	1.69 ± 0.08 ^a	1.82 ± 0.05 ^a
Babala	Total fat (g/100 g)	4.79 ± 0.17 ^a	4.25 ± 0.50 ^b	2.84 ± 0.56 ^c	3.48 ± 0.37 ^c	4.22 ± 0.55 ^b
	Saturated fat (g/100 g)	1.24 ± 0.06 ^a	1.16 ± 0.14 ^b	0.78 ± 0.15 ^c	0.96 ± 0.11 ^c	1.15 ± 0.16 ^b
	Monounsaturated fat (g/100 g)	1.28 ± 0.04 ^a	1.18 ± 0.20 ^b	0.76 ± 0.20 ^c	0.95 ± 0.15 ^c	1.16 ± 0.22 ^b
	Polyunsaturated fat (g/100 g)	2.27 ± 0.11 ^a	1.92 ± 0.16 ^b	1.29 ± 0.21 ^c	1.57 ± 0.10 ^c	1.92 ± 0.17 ^b

¹Values are mean ± standard deviation. Different superscripts in columns differ significantly ($p \leq 0.05$).

²RPM = raw pearl millet; ExPM = extruded pearl millet; MPM = malted pearl millet; EMPM = extruded pearl millet malt; ERPMMMPM = extruded raw pearl millet–malted pearl millet mix.

Table 4. Effect of processing on the amino acid content (mg/100 g) of pearl millet (Babala and AgriGreen)^{1,2}

	AA	RPM	ExPM	MPM	EMPM	ERPMMMPM	
AgriGreen	Asp	0.43 ± 0.03 ^a	0.72 ± 0.03 ^b	0.68 ± 0.04 ^b	0.64 ± 0.03 ^b	0.57 ± 0.06 ^c	
	Thr	0.22 ± 0.00 ^a	0.33 ± 0.02 ^b	0.29 ± 0.00 ^c	0.26 ± 0.00 ^d	0.25 ± 0.03 ^d	
	Ser	0.27 ± 0.00 ^a	0.43 ± 0.03 ^b	0.36 ± 0.02 ^c	0.35 ± 0.04 ^c	0.33 ± 0.02 ^c	
	Glu	1.12 ± 0.05 ^a	1.61 ± 0.16 ^b	1.23 ± 0.04 ^a	1.30 ± 0.14 ^a	1.29 ± 0.14 ^a	
	Gly	0.19 ± 0.00 ^a	0.29 ± 0.02 ^b	0.25 ± 0.01 ^c	0.23 ± 0.01 ^c	0.23 ± 0.02 ^c	
	Ala	0.40 ± 0.01 ^a	0.59 ± 0.05 ^b	0.51 ± 0.01 ^c	0.51 ± 0.04 ^c	0.48 ± 0.03 ^c	
	Val	0.28 ± 0.03 ^a	0.46 ± 0.03 ^b	0.39 ± 0.03 ^c	0.39 ± 0.01 ^c	0.38 ± 0.01 ^c	
	Met	0.06 ± 0.00 ^a	0.11 ± 0.01 ^b	0.05 ± 0.03 ^a	0.10 ± 0.04 ^c	0.09 ± 0.01 ^c	
	Ile	0.23 ± 0.00 ^a	0.34 ± 0.02 ^b	0.27 ± 0.00 ^c	0.29 ± 0.03 ^c	0.27 ± 0.02 ^c	
	Leu	0.53 ± 0.01 ^a	0.79 ± 0.08 ^b	0.59 ± 0.01 ^a	0.63 ± 0.06 ^a	0.63 ± 0.06 ^a	
	Tyr	0.21 ± 0.01 ^a	0.32 ± 0.04 ^b	0.27 ± 0.01 ^c	0.28 ± 0.01 ^c	0.25 ± 0.02 ^c	
	Phe	0.28 ± 0.01 ^a	0.42 ± 0.04 ^b	0.35 ± 0.02 ^c	0.35 ± 0.04 ^c	0.32 ± 0.02 ^c	
	His	0.17 ± 0.00 ^a	0.28 ± 0.04 ^b	0.26 ± 0.01 ^b	0.26 ± 0.04 ^b	0.23 ± 0.02 ^b	
	Lys	0.19 ± 0.00 ^a	0.32 ± 0.02 ^b	0.32 ± 0.01 ^b	0.31 ± 0.09 ^b	0.24 ± 0.03 ^a	
	Arg	0.23 ± 0.01 ^a	0.48 ± 0.06 ^b	0.44 ± 0.13 ^b	0.37 ± 0.08 ^a	0.38 ± 0.02 ^a	
	Babala	Asp	0.46 ± 0.05 ^a	0.61 ± 0.04 ^b	0.79 ± 0.00 ^c	0.68 ± 0.03 ^c	0.69 ± 0.02 ^c
		Thr	0.23 ± 0.04 ^a	0.27 ± 0.01 ^b	0.27 ± 0.00 ^b	0.29 ± 0.00 ^b	0.28 ± 0.04 ^b
Ser		0.33 ± 0.04 ^a	0.36 ± 0.01 ^a	0.35 ± 0.00 ^a	0.38 ± 0.01 ^a	0.35 ± 0.00 ^a	
Glu		1.23 ± 0.21 ^a	1.45 ± 0.09 ^b	1.11 ± 0.00 ^a	1.42 ± 0.08 ^b	1.43 ± 0.16 ^b	
Gly		0.20 ± 0.03 ^a	0.25 ± 0.02 ^b	0.28 ± 0.00 ^b	0.24 ± 0.00 ^b	0.24 ± 0.00 ^b	
Ala		0.47 ± 0.07 ^a	0.54 ± 0.03 ^b	0.44 ± 0.00 ^a	0.54 ± 0.03 ^b	0.53 ± 0.03 ^c	
Val		0.36 ± 0.07 ^a	0.40 ± 0.03 ^a	0.38 ± 0.00 ^a	0.42 ± 0.03 ^a	0.40 ± 0.02 ^a	
Met		0.09 ± 0.02 ^a	0.08 ± 0.02 ^b	0.05 ± 0.00 ^a	0.12 ± 0.01 ^b	0.12 ± 0.05 ^c	
Ile		0.27 ± 0.04 ^a	0.29 ± 0.01 ^b	0.26 ± 0.00 ^a	0.33 ± 0.02 ^b	0.33 ± 0.02 ^b	
Leu		0.62 ± 0.11 ^a	0.71 ± 0.03 ^b	0.55 ± 0.00 ^a	0.72 ± 0.03 ^b	0.69 ± 0.04 ^b	
Tyr		0.24 ± 0.02 ^a	0.28 ± 0.02 ^b	0.25 ± 0.00 ^a	0.32 ± 0.01 ^b	0.28 ± 0.01 ^b	
Phe		0.33 ± 0.04 ^a	0.39 ± 0.02 ^a	0.33 ± 0.00 ^a	0.39 ± 0.01 ^a	0.38 ± 0.07 ^a	
His		0.29 ± 0.06 ^a	0.24 ± 0.00 ^a	0.29 ± 0.00 ^a	0.26 ± 0.01 ^a	0.36 ± 0.08 ^b	
Lys		0.22 ± 0.02 ^a	0.29 ± 0.09 ^a	0.32 ± 0.00 ^a	0.30 ± 0.09 ^a	0.28 ± 0.03 ^a	
Arg		0.35 ± 0.06 ^a	0.35 ± 0.04 ^a	0.36 ± 0.00 ^a	0.83 ± 0.37 ^b	0.39 ± 0.17 ^a	

¹Values are mean ± standard deviation. Different superscripts in columns differ significantly ($p \leq 0.05$).

²RPM = raw pearl millet; ExPM = extruded pearl millet; MPM = malted pearl millet; EMPM = extruded pearl millet malt; ERPMMMPM = extruded raw pearl millet–malted pearl millet mix; AA = Amino Acid.

decrease in the amino acid content of AgG. Similar results were obtained for Ba with a different set of amino acids remaining unchanged in the RMF and extruded samples.

Germination of cereals is known to increase their lysine and tryptophan contents. The subject has been reviewed exhaustively by the authors of Refs. (17) and (23). However, Malleshi and Klopfenstein (21) only observed similar trends in finger millet as its lysine content increased on malting, but no appreciable changes in the lysine content were observed during sorghum and pearl millet germination. Elmalik et al. (24) reported an increase in most of the amino acid contents of sorghum cultivars of varying endosperm texture on germination and the increase being higher in corneous cultivars than the floury cultivars.

According to Malleshi and Klopfenstein (21), malting of sorghum and millets marginally enhances some of their essential amino acids but substantially improves their riboflavin, niacin, and ascorbic acid contents. Malting in combination with extrusion led to either a significant ($p \leq 0.05$) increase or no change in the amino acid content.

This is promising as it means that there would not be a need for replacement fortification of the finished product with the lost amino acids. Of the nine essential amino acids required by humans, seven were identified in the ERPMMMPM of both varieties of pearl millet; valine and tryptophan were not identified in the various samples.

The amino acid content of pearl millet was lower than the Nutrient Reference Values (NRV). This was observed by other researchers and informed the decision to composite millet especially with legumes in order to increase their content in the resultant complementary food, and hence its protein quality, *viz.* protein digestibility corrected amino acid score. The NRVs are based on Recommended Dietary Allowances (RDAs), which will meet the needs of nearly all (97 to 98%) healthy individuals to prevent nutrient deficiencies. RDA values are not necessarily enough to maintain optimum nutritional status and prevent chronic disease. These values are therefore considered the minimum amounts necessary to achieve and

maintain optimum nutritional status, which will assist in the reduction of disease, specifically degenerative diseases of lifestyle (25). This could be happening for several reasons, including the degradation of antinutritional properties, the presence of which could prevent quantification of amino acids in the RPM. According to El-Hady et al. (26), soaking reduced phytic content (known antinutrients) in all tested legumes in their experiment. Their data were in agreement with the findings of Alonso et al. (27) and these reductions may be ascribed to the activation of the endogenous phytase during the long soaking treatment and possible enzyme action continued during the germination and drying steps of malting. They also observed a further decrease in the phytic content on extruding their samples at high (180°C) temperatures.

Effect of malting, extrusion, and their combination on the in vitro protein and starch digestibility of beverage powders made from two varieties of pearl millet

Table 5 summarises the *in vitro* protein and starch digestibility for RPM, ExPM, MPM, EMPM, and ERPMMMPM from both AgG and Ba. Malting significantly ($p \leq 0.05$) decreased the *in vitro* protein (69.4%) and starch (33.24 mg maltose/100 g starch) digestibility of AgG, whilst extrusion had no effect on protein (73.18%) digestibility but significantly ($p \leq 0.05$) increased the starch (66.90 mg maltose/100 g starch) digestibility of AgG.

Combination processing led to a significant ($p \leq 0.05$) decrease in protein digestibility of products from both AgG and Ba, a significant ($p \leq 0.05$) increase in the starch digestibility of EMPM from AgG, and no change in the starch digestibility of EMPM from Ba.

Heat treatment of foods may enhance *in vitro* protein digestibility of food products by altering and breakdown of high molecular weight protein or by destroying the heat labile protease inhibitors. The increase in protein digestibility on malting could also be attributed to the degradation of storage protein (28), which may be more easily available to pepsin attack.

Table 5. Digestibility of beverage powder produced from two varieties of pearl millet by malting, extrusion, and a combination of both processes^{1,2}

	AgriGreen		Babala	
	Protein digestibility (%)	Starch digestibility (mg maltose/100 g starch)	Protein digestibility (%)	Starch digestibility (mg maltose/100 g starch)
RPM	87.20 ± 6.96 ^a	40.01 ± 2.42 ^a	96.61 ± 1.18 ^a	35.44 ± 11.24 ^a
ExPM	73.18 ± 10.90 ^a	66.90 ± 18.37 ^b	67.89 ± 5.10 ^b	74.47 ± 9.55 ^b
MPM	69.94 ± 5.16 ^b	33.24 ± 6.13 ^a	79.70 ± 4.66 ^c	41.93 ± 2.54 ^a
EMPM	70.04 ± 7.68 ^b	65.70 ± 11.45 ^b	69.45 ± 1.38 ^b	41.56 ± 18.03 ^a
ERPMMMPM	61.81 ± 9.02 ^b	65.85 ± 12.76 ^b	78.29 ± 0.96 ^c	37.95 ± 6.85 ^a

¹Values are mean ± standard deviation. Different superscripts in columns differ significantly ($p \leq 0.05$).

²RPM = raw pearl millet; ExPM = extruded pearl millet; MPM = malted pearl millet; EMPM = extruded pearl millet malt; ERPMMMPM = extruded raw pearl millet–malted pearl millet mix.

The proteins present in the feed material may undergo structural unfolding and/or aggregation when subjected to heat or shear during extrusion. Intact protein structures represent a significant barrier to digestive enzymes; and the combination of heat and shear is a very efficient way of disrupting such structures. In general, denaturation of protein to random configurations improves nutritional quality by making the molecules more accessible to proteases and thus more digestible. This is especially important in legume-based foods that contain active enzyme inhibitors in the raw state (11).

Disulphide bonds are involved in stabilising the native tertiary configurations of most proteins. Their disruption and shearing can contribute to the breaking of these bonds, aiding in protein unfolding and thus digestibility (11).

Partial hydrolysis of proteins during extrusion increases their digestibility by producing more open configurations and increasing the number of exopeptidase-susceptible sites. Conversely, production of an extensively isopeptide cross-linked network could interfere with protease action, reducing the digestibility (29).

The inherent property of sprouting seeds to increase the hydrolytic activity of enzymes may cause the mobilisation of protein, leading to the formation of polypeptides, dipeptides, and free amino acids. Further, during malting, the polyphenols and phytic acids are catabolised, and in addition, their leftover amount was removed as malting loss. This may be responsible for increasing the protein digestibility during malting (30).

Considering that most investigators observed an increase in protein digestibility with processing, it is unclear what may have caused the opposite in these experiments, but there are some possible explanations that would need further investigation; the difference in types and varieties of raw materials (grains used) could be a factor in the difference in observations, as well as the processing (exact parameters) conditions for the experiments. It is possible

that the combination of malting and extrusion, led to the formation of complexes between protein and other compounds thus lowering its digestibility. The decrease in *in vitro* protein digestibility for both AgG and Ba could be a direct result of an increase in total phenolic content after malting (Table 6).

The *in vitro* starch digestibility for both AgG and Ba (Table 5) was improved significantly ($p \leq 0.05$) by extrusion cooking, whilst malting only increased starch digestibility for Ba, with no effect on AgG; this is in agreement with the authors of Ref. 31, who also observed an increase in *in vitro* starch digestibility of pearl millet. This increase they attributed to malting loss, which may represent the removal of antinutrients present in sprouts. According to Holm et al. (32), other factors that have been shown to affect the starch digestion of food included degree of gelatinisation, granule particle size, amylose–mylopectin ratio, starch–protein interaction, amylase–lipid complexes, percentages of resistant or retrograded starch, and presence of other non-starch carbohydrates. In seeds, factors such as amylase inhibitors, phytic acid, and polyphenols have been reported to inhibit α -amylase (33, 34), hence decreasing *in vitro* starch digestibility. The levels of these compounds in pearl millet decreases during malting as a result of leaching and enzymatic breakdown; this in turn results in increased starch digestibility of malted pearl millet (31). During malting, amylase and phosphorylase might become active and catalyse amylolysis. The resulting increased concentration of oligosaccharides may contribute towards better starch digestibility of pearl millet malt (30).

Effect of malting, extrusion, and their combination on the total phenolic content and antioxidant activity of beverage powders made from two varieties of pearl millet

The effects of extrusion and malting on the total phenolic content and antioxidant activity of AgrG and Ba are

Table 6. TPC and antioxidant activity of beverage powder from two varieties of pearl millet processed by malting, extrusion, and a combination of both processing methods^{1,2}

	AgriGreen		Babala	
	Total phenolics ($\mu\text{g/g}$)	TEAC ($\mu\text{mole TE/g}$)	Total phenolics ($\mu\text{g/g}$)	TEAC ($\mu\text{mole TE/g}$)
RPM	2.67 \pm 0.05 ^a	1.80 \pm 0.18 ^a	3.04 \pm 0.20 ^a	1.73 \pm 0.07 ^a
ExPM	1.78 \pm 0.06 ^b	1.73 \pm 0.18 ^b	0.93 \pm 0.05 ^b	1.74 \pm 0.18 ^b
MPM	3.68 \pm 0.04 ^c	6.41 \pm 0.30 ^b	4.55 \pm 0.12 ^c	7.70 \pm 0.10 ^b
EMPM	1.34 \pm 0.01 ^d	2.14 \pm 0.16 ^c	1.30 \pm 0.06 ^d	1.78 \pm 0.25 ^a
ERPMPM	1.59 \pm 0.08 ^e	2.59 \pm 0.09 ^c	1.62 \pm 0.01 ^e	3.34 \pm 0.04 ^c
OTE	2.34 \pm 0.97	3.25 \pm 2.06	2.28 \pm 1.41	2.94 \pm 2.15

¹Values are mean \pm standard deviation. Different superscripts in columns differ significantly ($p \leq 0.05$).

²RPM = raw pearl millet; ExPM = extruded pearl millet; MPM = malted pearl millet; EMPM = extruded pearl millet malt; ERPMPM = extruded raw pearl millet–malted pearl millet mix; OTE = overall treatment effect; TEAC = Trolox (6-Hydroxy-2,5,7,8-tetramethylchroman-2-carboxylic acid) equivalent antioxidant capacity; TE = Trolox Equivalent; TPC = Total phenolic content.

summarised in Table 6. Extrusion significantly ($p \leq 0.05$) reduced total phenolic content of both AgG ($1.78 \mu\text{g/g}$) and Ba ($0.93 \mu\text{g/g}$), whilst malting significantly ($p \leq 0.05$) increased total phenolic content of both AgG ($3.68 \mu\text{g/g}$) and Ba ($4.55 \mu\text{g/g}$). Extrusion had no effect on the antioxidant activity (TEAC) of AgG ($1.73 \mu\text{mole TE/g}$) and Ba ($1.74 \mu\text{mole TE/g}$), whilst malting significantly increased antioxidant activity (TEAC) of both AgG ($6.41 \mu\text{mole TE/g}$) and Babala ($7.70 \mu\text{mole TE/g}$).

Contrary to observations of the effect of malting on total phenolics (increase), Archana and Kawatra (31) reported polyphenol content in untreated (raw) pearl millet grains of 764.45 mg/100 g and observed a significant ($p < 0.05$) destruction of polyphenols by malting; the level of destruction was dependent on germination time.

It is speculated that leaching of polyphenols during steeping may account for some of this loss. Loss of polyphenols during malting may be attributed to the presence of polyphenol oxidase (25) and to the hydrolysis of tannin-protein and tannin-enzyme complexes, which results in the removal of tannins or polyphenols (37). Contrary to the present study, germination has been reported to reduce the polyphenol content in pearl millet (30, 38). The increase in total phenolics could be attributed to a possible increase in lignin (16).

Sensory acceptability of the pearl millet-based instant beverage prepared from beverage powders made from two varieties of pearl millet

Figs. 2 and 3 summarise the sensory acceptability of RPM, ExPM, MPM, EMPM, and ERPMMPM beverages made from two varieties of pearl millet (AgG and Ba, respectively). The average overall acceptance rating for RPM, ExPM, MPM, EMPM, and ERPMMPM from Ba and AgG ranged from 4.71 ± 0.22 (like slightly) (AgG-RPM) to 6.15 ± 0.23 (dislike slightly) (AgG-RPM). In general, the different sensory attributes rated by the panellists ranged from 'like slightly' (=4) to 'dislike slightly' (=6).

The majority of the panellists neither liked nor disliked the different beverages. Significant differences ($p \leq 0.05$) existed in all the panellists' acceptability scores for the sensory attributes for the different products rated. The different backgrounds and possible prior exposure to similar products would affect the ratings of the different products (RPM, ExPM, MPM, EMPM, and ERPMMPM from pearl millet) by the panellists.

An improvement in the attributes of the beverages is required in order to improve and increase its overall acceptability. This can be achieved with significantly increased protein content and quality over the unsupplemented

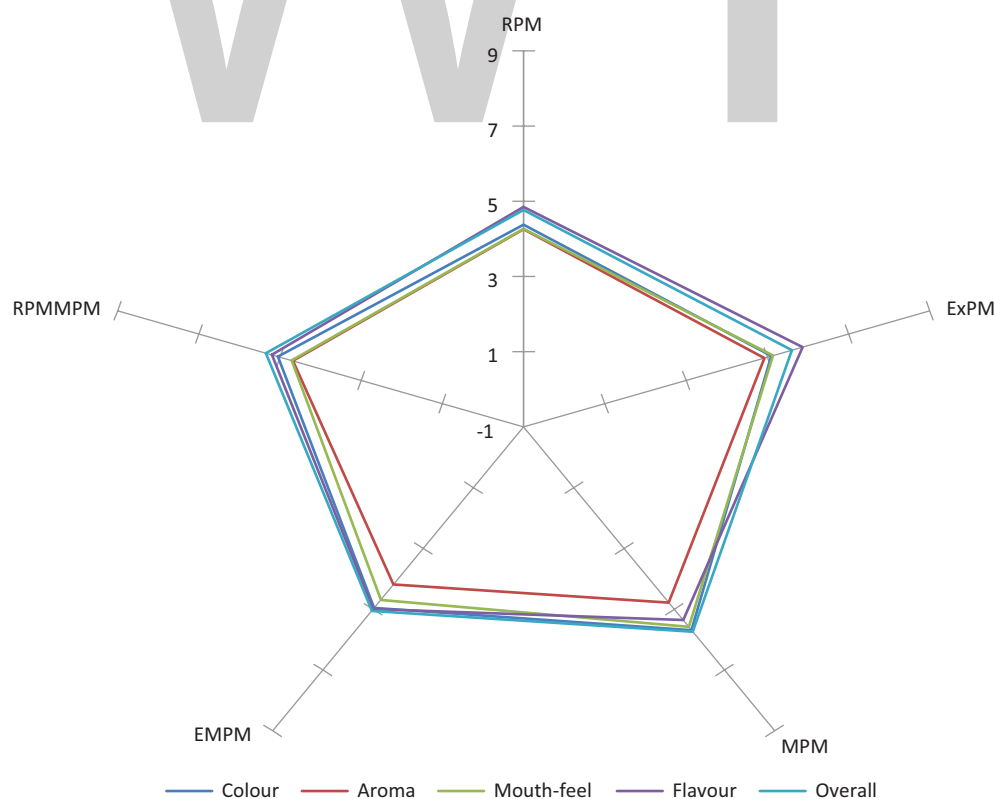


Fig. 2. Spider sensory plot for Babala. RPM = raw pearl millet; ExPM = extruded pearl millet; MPM = malted pearl millet; EMPM = extruded pearl millet malt; ERPMMPM = extruded raw pearl millet-malted pearl millet mix.

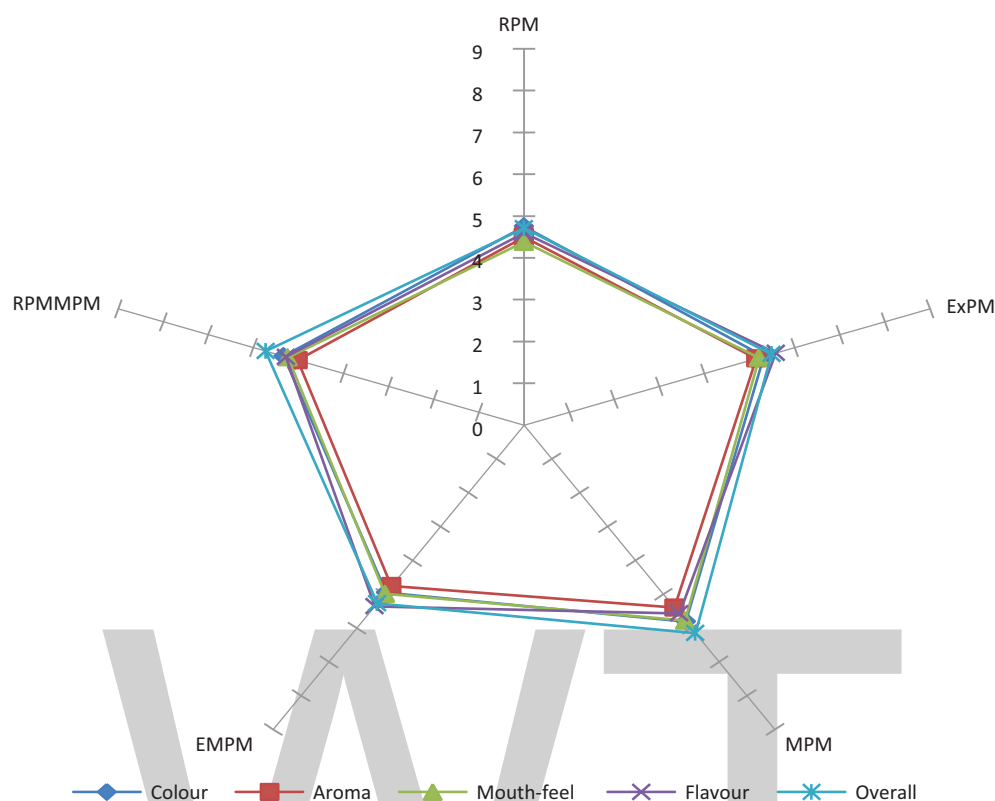


Fig. 3. Spider sensory plot for AgriGreen. RPM = raw pearl millet; ExPM = extruded pearl millet; MPM = malted pearl millet; EMPM = extruded pearl millet malt, ERPMMMPM = extruded raw pearl millet–malted pearl millet mix.

pearl millet by the addition of any of the following: soybean, morama bean, or Bambara groundnut. These would also act as functional ingredients supplying taste, texture, colour, and other properties to variety of foods (35). The percentage inclusion of the suggested legumes will have to be determined so as not to adversely affect the flavour and colour of the final product.

The colour difference calculated from the data collected (36) gives an indication of both the perception of a colour difference between ExPM, MPM, EMPM, ERPMMMPM, and RPM and the effect of processing methods used for the preparation of the beverage powders.

The perception (visual) of a colour difference between samples could also be an influencing factor in rating of the other attributes of the beverages and hence the overall acceptability of the beverage.

Conclusions

Beverages produced from both varieties of millet, though not unacceptable, were not acceptable to the panellists. Improving the colour or rather decreasing the colour difference (ΔE) as well as improving the flavour of the beverages could inevitably lead to better or increased overall acceptance of the beverages. These could be achieved by increasing the kilning temperature during malting, to affect

the development of a more intense flavour profile as well as a roasted or toasted colour in the grains. Addition of suitable adjuncts could further boost the nutritional value of the products and, more importantly, increase the overall acceptability of beverages from pearl millet (AgG and Ba).

Acknowledgements

I would like to thank the Durban University of Technology and Cape Peninsula University of Technology for funding this project.

References

1. Leistner L. Combined methods for food preservation. In: Rahman MS, ed. Handbook of food preservation. Boca Raton, FL: CRC Press; 2007, pp. 867–93. DOI: 10.1201/9781420017373
2. AOAC. Official methods of analysis. 17th ed. Horwitz VW, ed. The Association of Official Analytical Chemists International. Washington, DC: Association of Official Analytical Chemists; 2003.
3. Benson JV, Patterson JA. Accelerated automatic chromatographic analysis of amino acids on spherical resin. Anal Chem 1965; 37: 1108–10. DOI: 10.1016/j.jup.2018.07.002
4. Klapper DG. A new low-cost, fully automated amino acid analyser using a gradient HPLC. In: Elzinga M, ed. Methods in protein sequence analysis. Clifton, NJ: Humana Press; 1982, pp. 509–15.
5. Perkin-Elmer. Plasma 400: users manual. Hamburg, Germany; 1996.

6. Saunders RM, Connor MA, Booth AN, Bickoff EM, Kohler GO. Measurement of digestibility of Alfalfa protein concentrates by in vivo and in vitro methods. *J Nutr* 1973; 103: 530–5. DOI: 10.1093/jn/103.4.530
7. Ali MAM, El Tinay AH, Abdalla AH. Effect of fermentation on the *in vitro* protein digestibility of pearl millet. *Food Chem* 2003; 80(1): 51–4. DOI: 10.1016/S0308-8146(02)00234-0
8. Onyango C, Noetzold H, Bley T, Henle T. Proximate composition and digestibility of fermented and extruded uji from maize–finger millet blend. *LWT. Food Sci Technol* 2004; 37: 827–32. DOI: 10.1016/j.lwt.2004.03.008
9. Silvia MT, Miller EE, Pratt DE. Chia seeds as a source of natural lipid antioxidants. *J Am Oil Chem Soc* 1984; 61: 928–31. DOI: 10.1007/BF02542169
10. Awika JM, Rooney LW, Wu X, Prior RL, Cisneros-Zevallos L. Screening methods to measure antioxidant activity of sorghum (*Sorghum bicolor*) and sorghum products. *J Agric Food Chem* 2003; 51(23): 6657–62. DOI: 10.1021/jf034790i
11. Dobraszczyk BJ, Ainsworth P, Ibanoglu S, Bouchon P. Baking, extrusion and frying. In: Brennan JG, ed. *Food processing handbook*. Weinheim, Germany: Wiley-VCH Verlag GmbH & Co. KGaA; 2006, pp. 237–90.
12. Bjork I, Asp N-G. The effects of extrusion cooking on nutritional value – a literature review. *J Food Eng* 1983; 2: 281–308. DOI: 10.1016/0260-8774(83)90016-X
13. Fabriani G, Lintas C, Quaglia GB. Chemistry of lipids in processing and technology of pasta products. *Cereal Chem* 1968; 45: 454–63.
14. Traoré T, Mouquet C, Icard-Vernière C, Traoré AS, Trèche S. Changes in nutrient composition, phytate and cyanide contents and α -amylase activity during cereal malting in small production units in Ouagadougou (Burkina Faso). *Food Chem* 2004; 88(1): 105–14. DOI: 10.1016/j.foodchem.2004.01.032
15. Shayo NB, Nnko SAM, Gidamis AB, Dillon VM. Assessment of cyanogenic glucoside (cyanide) residues in Mbege: an opaque traditional Tanzanian beer. *Int J Food Sci Nutr* 1998; 49: 333–8. DOI: 10.3109/09637489809089407
16. Opoku AR, Ohenhen SO, Ejiogor N. Nutrient composition of millet (*Pennisetum typhoides*) grains and malt. *J Agric Food Chem* 1981; 29: 1247–8. DOI: 10.1021/jf00108a036
17. Chavan JK, Kadam SS. Nutritional improvement of cereals by sprouting. *Crit Rev Food Sci Nutr* 1989; 28: 401–37. DOI: 10.1080/10408398909527508
18. Elmaki HB, Babiker EE, ElTinay AH. Changes in chemical composition, grain malting, starch and tannin contents and protein digestibility during germination of sorghum cultivars. *Food Chem* 1999; 64: 331–6. DOI: 10.1016/S0308-8146(98)00118-6
19. Abdalla AA, ElTinay AH, Mohamed BE, Abdalla AH. Effect of traditional processes on phytate and mineral content of pearl millet. *Food Chem* 1998; 63(1): 79–84. DOI: 10.1016/S0308-8146(97)00194-5
20. Adeola O, Orban JI. Chemical composition and nutrient digestibility of pearl millet (*Pennisetum glaucum*) fed to growing pigs. *J Cereal Sci* 1995; 22: 177–84. DOI: 10.1016/0733-5210(95)90048-9
21. Malleshi NG, Klopfenstein CF. Nutrient composition, amino acid and vitamin contents of malted sorghum, pearl millet, finger millet and their rootlets. *Int J Food Sci Nutr* 1998; 49: 415–22. DOI: 10.3109/09637489809086420
22. Suma PF, Urooj A. Nutrients, antinutrients & bioaccessible mineral content (*in vitro*) of pearl millet as influenced by milling. *J Food Sci Technol* 2014; 51(4): 756–61. DOI: 10.1007/s13197-011-0541-7
23. Lorenz K. Cereal sprouts: composition, nutritive value, food application. *CRC Crit Rev Food Sci Nutr* 1980; 13: 353–85. DOI: 10.1080/10408398009527295
24. Elmalik M, Klopfenstein CF, Hosney RC, Bates LS. Effects of germination on the nutritional quality of sorghum grain with contrasting kernel characteristics. *Nutr Rep Int* 1986; 34: 941–50.
25. Rao PU, Deosthale YG. Tannin content of pulses: varietal differences and effects of germination and cooking. *J Sci Food Agric* 1982; 33: 1013–16. DOI: 10.1002/jfsa.2740331012
26. El-Hady EAA, Habiba RAA. Effect of soaking and extrusion conditions on antinutrients and protein digestibility of legume seeds. *LWT – Food Sci Technol* 2003; 36(3): 285–93. DOI: 10.1016/S0023-6438(02)00217-7
27. Alonso R, Orue E, Marzo F. Effects of extrusion and conventional processing methods on protein and antinutritional factor contents in pea seeds. *Food Chem* 1998; 63(4): 505–12. DOI: 10.1016/S0308-8146(98)00037-5
28. Bhise V, Chavan J, Kadam S. Effects of malting on proximate composition and in vitro protein and starch digestibilities of grain sorghum. *J Food Sci Technol* 1988; 25(6): 327–9.
29. Phillips RD. Effect of extrusion cooking on the nutritional quality of plant proteins. In: Phillips RD, Finley JW, eds. *Protein quality and the effect of processing*. New York: Marcel Dekker; 1989, pp. 219–46.
30. Pawar VS, Pawar VD. Malting characteristics and biochemical changes of foxtail millet. *J Food Sci Technol* 1997; 34: 416–18.
31. Archana SS, Kawatra A. In vitro protein and starch digestibility of pearl millet (*Pennisetum glaucum* L.) as affected by processing techniques. *Nahrung – Food* 2001; 45(1): 25–7. DOI: 10.1002/1521-3803(20010101)45:1<25::AID-FOOD25>3.0.CO;2-W
32. Holm, J., Asp, N.G. & Björck, I. Factors affecting enzymatic degradation of cereal starches in vitro and in vivo. In: *Cereals in a European context* (edited by MORTON, J.D.), 1987. Pp. 169–187. Chichester: Ellis Horwood.
33. Deshpande SS, Cheryan M. Effects of phytic acid, divalent cations and their interactions on α -amylase activity. *J Food Sci* 1984; 49: 516–9.
34. Thompson LV, Yoon JH. Starch digestibility as affected by polyphenols and phytic acid. *J Food Sci* 1984; 49: 1228–9.
35. Ali, MaM., Tinay, AHE., Mohamed, IA. & Babiker, EE. Supplementation and cooking of pearl millet: Changes in protein fractions and sensory quality. *World Journal of Dairy & Food Sciences*. 2009; 4: 41–45.
36. Obilana AO., Odhav, B., Jideani, VA. Functional and Physical Properties of Instant Beverage Powder Made From Two Different Varieties of Pearl Millet. *Journal of Food and Nutrition Research*. 2.2014; 5: 250-257. DOI: 10.12691/jfnr-2-5-7
37. Farhangi M, Valadon LRG. Effect of acidified processing and storage on carotenoids (Pro vitamin A) and vitamin C in moongbean sprouts. *J Food Sci* 1981; 46: 1464. DOI: 10.1111/j.1365-2621.1981.tb04199.x
38. Osuntogun BA, Adewusi SRA, Ogundiwin JO, Nwasike CC. Effect of cultivar, steeping, and malting on tannin, total polyphenol, and cyanide content of Nigerian sorghum. *Cereal Chem* 1989; 66: 87–9.

***Dr. Anthony “Tony” O. Obilana (Lecturer)**

Cape Peninsula University of Technology
 Department of Food Science and Technology
 PO Box 1906, Bellville, 7535
 Email: obilanaa@cput.ac.za

Oolong tea polysaccharide and polyphenols prevent obesity development in Sprague–Dawley rats

Tao Wu^{1,2,3#}, Jinling Xu^{2#}, Yijun Chen², Rui Liu² and Min Zhang^{1,2,3*}

¹Beijing Advanced Innovation Center for Food Nutrition and Human Health, Beijing Technology and Business University, Beijing, China; ²State Key Laboratory of Food Nutrition and Safety, Tianjin University of Science and Technology, Tianjin, China; ³Tianjin Food Safety & Low Carbon Manufacturing Collaborative Innovation Center, Tianjin, China

Abstract

Background: Several studies have evaluated the effects of oolong tea extracts on obesity. However, only few studies focused on the anti-obesity effect of specific components of oolong tea.

Objective: This study investigated the specific anti-obesity capabilities of oolong tea polysaccharide (TPS) and tea polyphenols (TPP) in high-fat diet-induced Sprague–Dawley rats.

Methods: Oolong tea water extract, TPS, TPP, and polysaccharide mixed with polyphenol (TPSM) given at doses of 400 or 800 mg/kg were administered to rats fed with high-fat diet for 6 weeks to explore the anti-obesity effects of the treatments.

Results: TPS and TPP were responsible for the suppressive effect on body fat accumulation. TPSM exhibited the highest effect on body weight reduction, and TPS and TPP effectively reduced serum leptin levels and significantly improved blood lipid and antioxidant levels. Moreover, microarray analysis of hepatic and adipose gene expression profiles revealed that TPP and TPS inhibited obesity through effects on the pathways of fatty acid biosynthesis, steroid hormone biosynthesis, unsaturated fatty acid biosynthesis, fatty acid elongation, glycerolipid metabolism, and glycerophospholipid metabolism.

Conclusions: TPSM might be a potential therapy for the treatment of obesity.

Keywords: *oolong tea; anti-obesity; polysaccharide; polyphenols*

The incidence of obesity has increased dramatically in recent years and has become a serious health medical problem in the world (1). Epidemiological studies have shown that obesity is a complex metabolic disorder caused by the imbalance between energy intake and energy expenditure and boosts the risk of various chronic diseases, such as hypertension, type II diabetes, coronary artery disease, and cancers (2, 3). Currently, the available therapy for obesity causes a number of side effects (4–6). Therefore, the prevention of obesity is an urgent matter, and the use of food to suppress the accumulation of body weight and body fat may be a safe solution (7, 8).

As a traditional type of Chinese tea (*Camellia sinensis*), oolong tea has been a popular beverage worldwide because of its health benefits including anti-oxidation, anti-microbial, cholesterol-lowering effect, and reducing the risks of cancer (9–11). Oolong tea polysaccharide,

caffeine, and polyphenols contribute to these health benefits (12, 13). The polyphenols found in semi-fermented oolong tea mainly comprise epigallocatechin, epigallocatechin gallate (EGCG), epicatechin, and epicatechin gallate (14–16). Given the ever-growing obesity pandemic, the anti-obesity effects of oolong tea have been the focus of considerable attention (17). However, the strength of such anti-obesity effects differs depending on the variety and functional components. Rumpler et al. observed that oolong tea extract intake significantly increased the energy expenditure in a group of young males (18). Since then, clinical trials have reported the effects of tea preparations on increasing energy expenditure, fat oxidation, weight loss, fat mass, and weight maintenance after weight loss (19–21). Oolong tea extracts decreased weight and body fat gain in rodent models in several studies (18, 22). Kuo et al. reported that body weight suppression occurs

[#]The first two authors contributed to the work equally and should be regarded as co-first authors.

in tea-leaf-fed groups in the following order: oolong tea > pu-erh tea > black tea > green tea (23).

Several studies have evaluated the effects of oolong tea extracts on obesity (24–26). However, only few studies have focused on the anti-obesity effect of specific components of oolong tea. Therefore, this study aimed to isolate polyphenols and polysaccharides from oolong tea and investigated their influence on the development of obesity.

Materials and methods

Chemicals and animals

The coarse old oolong tea employed in the study was produced in Fujian, China. A total of 145 male Sprague–Dawley rats (~200 g) were purchased from PLA Military Academy of Medical Sciences Laboratory Animal Center (license number SCXK [Beijing] 2012–0004).

Extraction of tea polyphenols and polysaccharides from oolong tea

Crude oolong tea leaves (JinFuDe, Fujian Province, China) were ground into powder by a grinder. Water extracts were obtained three times at 85°C at a solid–liquid ratio of 1:15 once an hour. The extracts were filtered using a nine-layer gauze and concentrated under reduced pressure. One part of the concentrate was lyophilized as the total water extract. The other part of the concentrate was extracted by chloroform, and the aqueous layer was extracted with ethyl acetate. Finally, the organic layer was lyophilized to tea polyphenols (TPP), and the aqueous layer was precipitated with ethanol and lyophilized to tea polysaccharides (TPS) after protein removal. The obtained oolong TPP was analyzed through high-performance liquid chromatography (HPLC; Shimadzu, Kyoto, Japan) equipped with an ultraviolet (UV) detector. The oolong TPP is composed of EGC (59.09%), EGCG (12.83), EC (13.47%), and ECG (14.61%). The oolong TPS comprised 4.06 mol% rhamnose, 2.58 mol% fucose, 27.19 mol% arabinose, 1.26 mol% xylose, 5.68 mol% mannose, 4.66 mol% galactose, and 54.57 mol% glucose.

Animals and experimental protocols

All of the experimental procedures employed in the study followed the guidelines of the Committee on the Ethics of Animal Experiments of Tianjin University of Science and Technology (TUST20131015) and were based on the National Institutes of Health Guide for the Care and Use of Laboratory Animals. All efforts were exerted to minimize suffering.

Rats were kept in a room maintained under standard conditions of 20°C to 25°C, 12 h/12 h light/dark cycle, and relative humidity of 45 to 65%. After 7 days of adaptation, the rats were randomly divided into two groups (Group I = 10 and Group II = 135) by weight. Rats in Group I were

given free access to distilled water and normal diet. Group II rats were orally administered with distilled water and a high-fat diet consisting of 79% basal feed, 10% lard, 10% egg yolk powder, 0.5% cholesterol, and 0.5% cholate. After a 2-week high-fat diet, the Group II rats were sorted by weight gain, and one-third of the rats with a slower speed of gaining weight (obesity-resistant rats, body weight gain less than 20%) were eliminated from the study. The 90 screened out obesity-sensitive rats were randomly divided into different groups as follows: model control, the group given 40 mg/kg orlistat, the group given 400 or 800 mg/kg total water extract, the group given 400 or 800 mg/kg TPP, the group given 400 or 800 mg/kg TPS, and the group given a combination of TPS and TPP at 400 mg/kg. All rats used in the experiment were given oolong tea functional materials via oral gavage. These groups were given high-fat diet and designated as normal control group (NC), model control group (MC), positive control group, orlistat (OC), high dose of total water extract group (TWH), low dose of total water extract group (TWL), high dose of tea polyphenols group (TPPH), low dose of tea polyphenols group (TPPL), high dose of tea polysaccharides group (TPSH), low dose of tea polysaccharides group (TPSL), and the complex of tea polysaccharides and polyphenols group (TPSM), respectively. During the experiment, food intake was recorded daily, and body weight and length were measured once every 3 days.

After 6 weeks of experimentation, all rats were fasted overnight, blood sample was collected from the abdominal femoral arteries of the rats, and the rats were sacrificed by cervical vertebral dislocation. The liver, heart, kidney, perinephric fat pads, epididymal adipose tissues, and mesenteric adipose tissues were quickly removed and weighed. Then, the tissues were stored at –80°C.

Blood and liver biochemical analysis

The rat serum parameters, including triglyceride (TG), total cholesterol (TC), high-density lipoprotein cholesterol (HDLC), low-density lipoprotein cholesterol (LDLC), malondialdehyde (MDA) levels, and total superoxide dismutase (T-SOD) activities, were determined using commercially available kits (BioSino, Beijing, China). The serum leptin was characterized by immunoassay using rat/mouse ELISA kit (R&D Systems, Minneapolis, USA). Hepatic TG, TC, MDA, and T-SOD concentrations were estimated using the same kit for serum analysis. All measurements performed were in accordance with the manufacturers' instructions.

Adipose and liver histopathology

Suitable rat epididymal adipose and hepatic tissues were selected and fixed in 10% formalin for 16 h. Then, all of the tissues were dehydrated in graded ethanol (70% ethanol for 10 min, 80% ethanol for 10 min, 95% ethanol for

10 min thrice, and 100% ethanol for 15 min thrice). Xylene was used to clear the tissues (15 min twice). Then, the tissues were dipped in wax twice at 60°C, 1 h to 2 h each time, and paraffin embedded at the same temperature. Fat and liver tissue blocks were cut into five microsections and stained with hematoxylin and eosin.

Gene chip analysis, reverse transcription polymerase chain reaction (RT-PCR) verification, and metabolic pathway analysis

Differentially expressed genes were screened for the NC, TPP, TPS, and TPSM groups using the gene expression profile array (GeneChip Rat Genome 230 2.0 Array, Affymetrix, Santa Clara, CA, USA). In addition, the differentially expressed genes screened by gene chip arrays were verified through RT-PCR. Specific primers for the genes were designed, synthesized, and diluted with sterile water in accordance with the manufacturer's manual. The total RNA in the liver and epididymal adipose tissues served as raw material, whereas the rat Glyceraldehyde-3-phosphate dehydrogenase (GADPH) genes were used as housekeeping genes. The One-Step SYBR PrimeScript PLUS RT-PCR Kit (TaKaRa, Shiga, Japan) was used for PCR. The differentially expressed genes screened through gene chip arrays and verified via RT-PCR were used to determine the related metabolic pathways with the GenBank ID in the national center for biotechnology information (NCBI) gene database and Kyoto Encyclopedia of Genes and Genomes (KEGG) metabolic pathway database. The effects of the resulting genes on the fat metabolic pathway were also explored.

Statistical analysis

The results are presented as means with their standard errors. Statistical analysis was performed using the Statistical Product and Service Solutions (SPSS) program. Data were analyzed by one-way analysis of variance (ANOVA). Differences between the groups were established using the least significant difference test, and the criterion for statistical significance was set at $p < 0.05$.

Results

Changes in rat body weight, food utilization, and Lee's index

Table 1 shows the changes in body weight, food utilization (body weight gain/food intake $\times 100\%$), and Lee's index ($3\sqrt{\text{body weight} \times 1000/\text{body length}}$). The final body weight of rats in the MC group was significantly higher than that of the NC group. By contrast, all of the treated groups, except for TPSL, exhibited a significant reduction in body weight gain compared with the MC group. Moreover, TPSM group showed the highest anti-obesity effects when compared with the other groups. These results indicate that polysaccharides and polyphenols were synergistic in reducing body weight gain. Meanwhile, all of the groups, except for TPSH, exhibited a significant decrease in Lee's index compared with the MC group.

Body fat weight

At the end of the experiment, the perinephric fat pads, epididymal adipose tissues, and mesenteric adipose tissues of each group were collected and measured. MC group exhibited a significantly higher weight of the three fat parts than that of the NC group. Meanwhile, tea water extract, TPP, TPS, and TPSM decreased in adipose tissue.

Blood and liver biochemical profiles

Hepatic lipid and antioxidant profiles are shown in Fig. 1 and Table 2. The triglyceride and cholesterol levels of rats in the MC group increased significantly compared with the NC group. Meanwhile, the serum triglyceride and cholesterol levels lowered significantly in the TWH, TPPH, TPPL, and TPSM groups. Moreover, the serum MDA and T-SOD levels reduced significantly in the TPSM, TWH, and TPPL groups; similar results were also observed in the hepatic MDA and T-SOD levels. However, the serum LDL-C levels in TWL, TPPH, TPPL, TPSH, TPSL, and TPSM groups were significantly lower

Table 1. Body weight and other characters of rats in each group

Groups	Initial BW(g)	Final BW(g)	Lee's index	Food utilization (%)
NC	228.58 \pm 14.03	459.31 \pm 27.19	311.21 \pm 11.83	18.73% \pm 2.02%
MC	348.74 \pm 22.35	548.74 \pm 51.74	339.55 \pm 8.06	26.87% \pm 0.98%
OC	351.33 \pm 17.90	511.86 \pm 43.54 ^{***}	322.31 \pm 9.66 ^{***}	24.35% \pm 1.76%
TWH	346.51 \pm 19.37 ^{**}	466.78 \pm 34.21 ^{###&}	316.08 \pm 9.64 ^{###}	19.78% \pm 2.16% [#]
TWL	352.16 \pm 21.12 ^{**}	478.61 \pm 45.36 ^{###}	318.45 \pm 12.83 ^{###}	20.56% \pm 2.29% [#]
TPPH	348.44 \pm 16.09 ^{**}	473.26 \pm 32.75 ^{###&}	315.34 \pm 5.85 ^{###}	20.37% \pm 3.12% [#]
TPPL	347.89 \pm 13.16 ^{**}	485.57 \pm 34.27 ^{###}	324.27 \pm 9.03 ^{###}	21.51% \pm 2.29% [#]
TPSH	349.89 \pm 18.27 ^{**}	522.72 \pm 42.43 ^{**}	328.56 \pm 5.68 ^{**#}	22.67% \pm 2.03%
TPSL	343.06 \pm 16.62 ^{**}	505.92 \pm 32.48 ^{**#}	325.73 \pm 7.79 ^{**#}	21.67% \pm 1.97% [#]
TPSM	345.73 \pm 12.75 ^{**}	447.67 \pm 33.80 ^{###&}	318.49 \pm 10.14 ^{###}	19.04% \pm 2.14% [#]

All values are means \pm SD ($n = 10$). Values with different superscripts are significantly different among the groups by ANOVA with Duncan's multiple range test from NC at * $P < 0.05$, ** $P < 0.01$; MC at # $P < 0.05$, ## $P < 0.01$; OC, & $P < 0.05$, && $P < 0.01$.

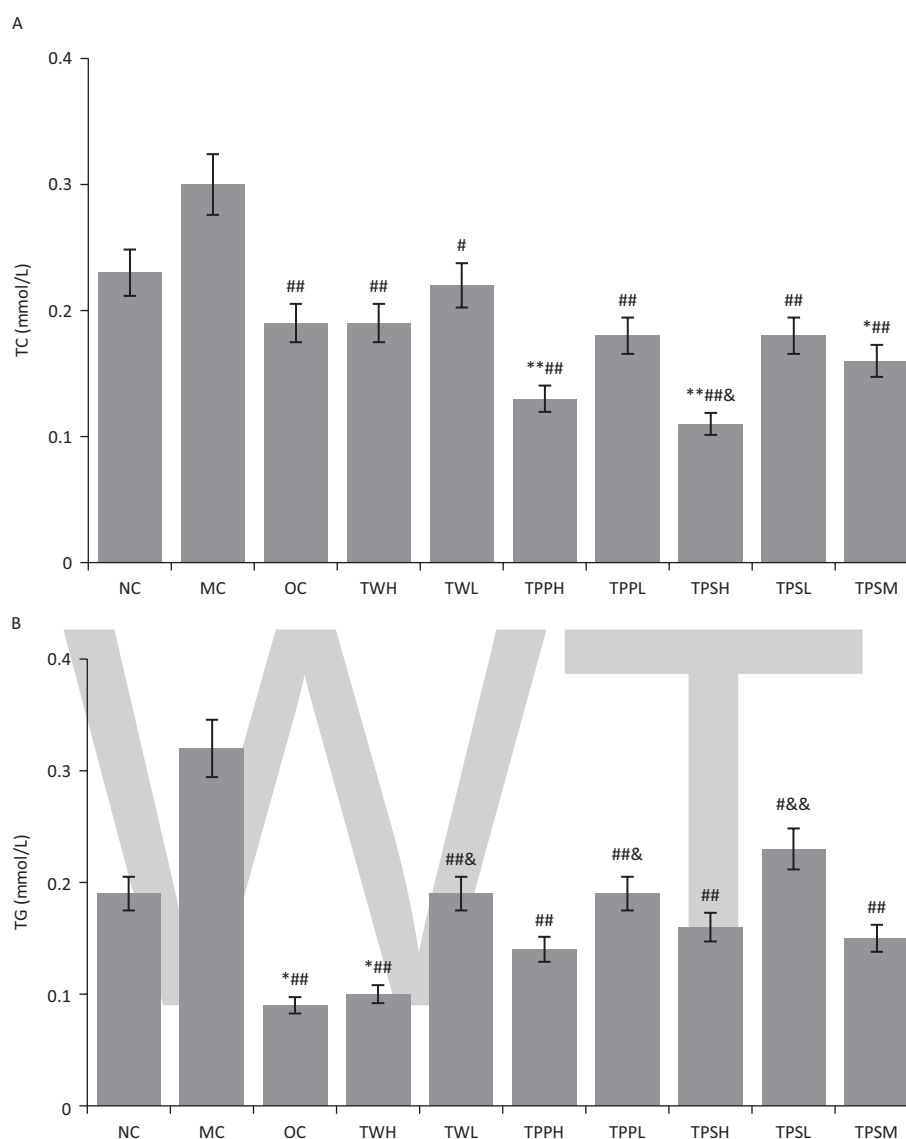


Fig. 1. The effect of oolong tea extracts on rat hepatic lipid profile and antioxidants. (a) Hepatic contents of TG and TC. (b) Hepatic contents of TG and TC. (c) Hepatic MDA content. (d) Hepatic total SOD content. Values with different superscripts are significantly different among the groups by ANOVA with Duncan's multiple range test from NC at $*P < 0.05$, $**P < 0.01$; MC at $\#P < 0.05$, $\#\#P < 0.01$; OC, $\&P < 0.05$, $\&\&P < 0.01$.

than that of the MC group. TPSL and TPSM groups also exhibited significantly lower leptin levels than the other groups.

Histological analysis of liver and epididymal white adipose tissue

Changes in the degree of infiltration of lipid droplets in the liver are shown in Supplementary Fig. 1. The representative liver section of the MC group showed increased infiltration of lipid droplets, leading to a hepatic steatotic condition. Meanwhile, the infiltration of lipid droplets in the representative liver section of the other groups was markedly reduced; even the liver histological section of the TPSM group was free from lipid droplets. The histology

of the rat epididymal white adipose tissue is shown in Supplementary Fig. 2, and the numbers of adipocytes within the same field are presented in Supplementary Table 1. The adipocyte size of the MC group was significantly larger than that of the NC group, and the numbers of fat cells in the MC group were significantly less than that of the NC group. In all of the medicated groups, adipocyte sizes were significantly smaller, and the number of fat cells was significantly lower than those of the MC group.

Result of cDNA microarray

The Affymetrix GeneChip® Rat Genome 230 2.0 Array includes approximately 31,000 probe sets representing

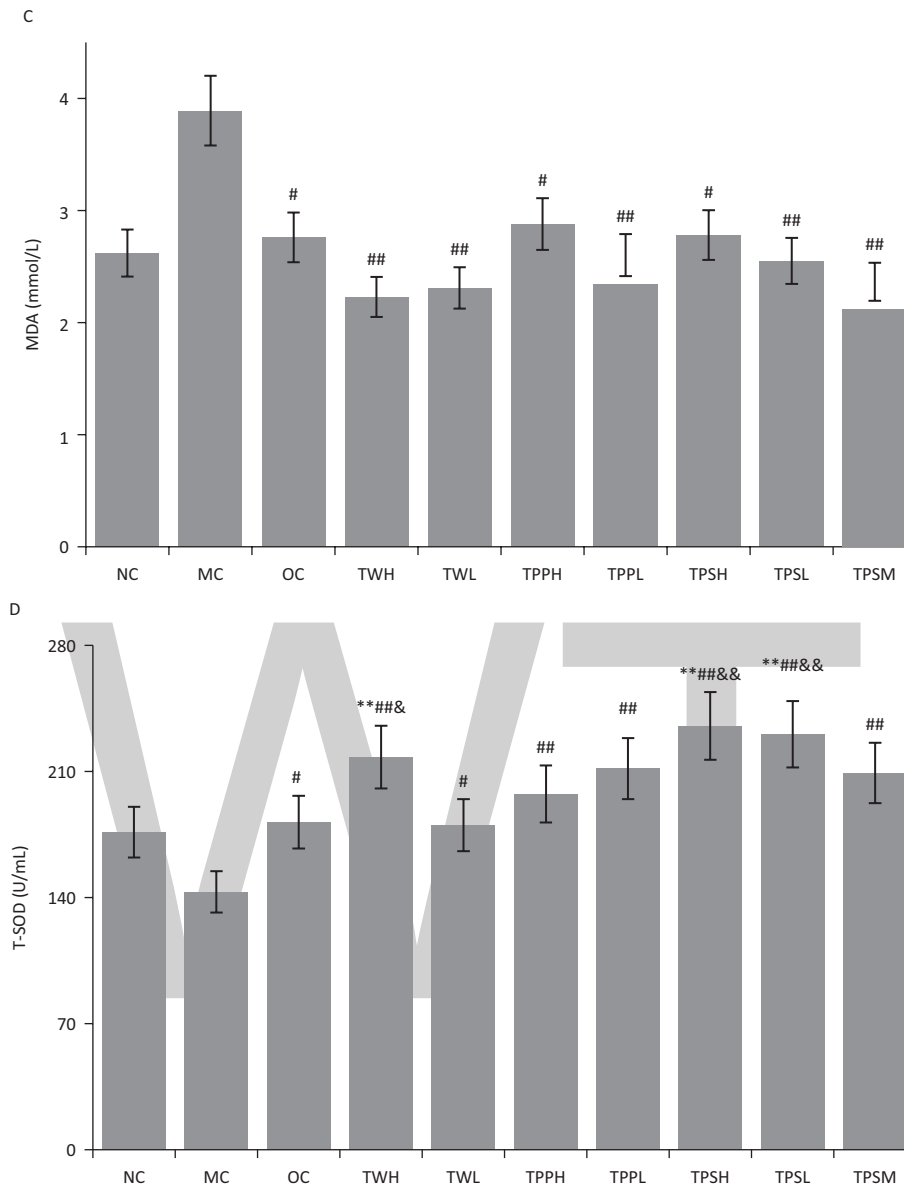


Fig. 1. Continued The effect of oolong tea extracts on rat hepatic lipid profile and antioxidants. (a) Hepatic contents of TG and TC. (b) Hepatic contents of TG and TC. (c) Hepatic MDA content. (d) Hepatic total SOD content. Values with different superscripts are significantly different among the groups by ANOVA with Duncan's multiple range test from NC at $*P < 0.05$, $**P < 0.01$; MC at $\#P < 0.05$, $\#\#P < 0.01$; OC, $\&P < 0.05$, $\&\&P < 0.01$.

28,000 specific genes. According to the results provided by the Tianjin Biochip Corporation, we screened out the differentially expressed genes related to lipid metabolism in the liver and epididymal adipose tissues. Under the premise of greater than twofold difference relative to that of the MC group, we detected 11 differentially co-expressed genes in the liver of the NC, TPPL, TPSL, and TPSM groups. Among the 11 genes, 2 genes were significantly upregulated and 9 genes were significantly downregulated. In the same circumstance, we detected 13 differentially co-expressed genes in the epididymal

adipose tissues of the NC, TPPL, TPSL, and TPSM groups. Among the 13 genes, 6 genes were significantly upregulated and 7 genes were significantly downregulated (Table 3). Then, these genes were searched on the KEGG website to determine their lipid metabolism pathways (Supplementary Figs. 3–8). Microarray analysis revealed that TPP and TPS inhibited obesity through effects on the pathways of fatty acid biosynthesis, steroid hormone biosynthesis, unsaturated fatty acid biosynthesis, fatty acid elongation, glycerolipid metabolism, and glycerophospholipid metabolism.

Table 2. Serum figures of rats in each group

Groups	TC (mmol/l)	TG (mmol/L)	HDLC (mmol/L)	LDLC (mmol/L)	MDA (mmol/L)	T-SOD (U/mL)	LEP (pg/mL)
NC	1.57 ± 0.25	0.86 ± 0.42	2.22 ± 1.64	0.94 ± 0.23	0.12 ± 0.09	157.03 ± 20.24	179.73 ± 12.12
MC	2.58 ± 0.43	1.23 ± 0.26	1.14 ± 0.16	1.52 ± 0.56	0.27 ± 0.03	122.99 ± 17.16	198.82 ± 27.41*
OC	1.56 ± 0.32 ^{###}	0.76 ± 0.26 ^{###}	1.71 ± 0.55	0.40 ± 0.48	0.21 ± 0.15*	184.48 ± 15.27 ^{###}	178.82 ± 25.42 [#]
TWH	1.99 ± 0.43 ^{###&}	0.61 ± 0.28 ^{###}	1.98 ± 0.53 ^{###}	0.91 ± 0.31 ^{#&}	0.15 ± 0.07 ^{###}	187.06 ± 18.00 ^{###}	182.91 ± 22.67
TWL	1.80 ± 0.77 ^{###}	0.64 ± 0.33 ^{###}	1.74 ± 0.42 [#]	0.67 ± 0.78 ^{###}	0.13 ± 0.07 ^{###}	154.45 ± 18.70 ^{###&}	185.64 ± 29.16
TPPH	1.97 ± 0.41 ^{###&}	0.77 ± 0.20 ^{###}	2.26 ± 0.40 ^{###}	0.73 ± 0.46 ^{###}	0.17 ± 0.08 ^{###}	97.82 ± 24.34 ^{###&}	175.18 ± 19.78 [#]
TPPL	1.75 ± 0.48 ^{###}	0.68 ± 0.16 ^{###}	1.75 ± 0.43 ^{###}	0.43 ± 0.64 ^{###}	0.10 ± 0.04 ^{###&}	163.03 ± 18.09 ^{###&}	178.67 ± 21.07 [#]
TPSH	1.86 ± 0.43 ^{###}	1.11 ± 0.34 ^{&}	1.65 ± 0.31	0.67 ± 0.34 ^{###}	0.17 ± 0.11 [#]	174.83 ± 23.80 ^{###}	179.86 ± 16.80
TPSL	1.58 ± 0.27 ^{###}	1.22 ± 0.53 ^{###&}	1.41 ± 0.34 ^{**}	0.36 ± 0.78 ^{###}	0.21 ± 0.11*	192.21 ± 11.58 ^{###}	166.50 ± 15.71 ^{###}
TPSM	1.55 ± 0.25 ^{###}	0.69 ± 0.31 ^{###}	1.73 ± 0.58 [#]	0.27 ± 0.43 ^{###}	0.13 ± 0.04 ^{###&}	146.94 ± 19.69 ^{###&}	170.50 ± 19.16 ^{###}

All values are means ± SD (n = 10). Values with different superscripts are significantly different among the groups by ANOVA with Duncan's multiple range test from NC at *P < 0.05, **P < 0.01; MC at #P < 0.05, ##P < 0.01; OC, &P < 0.05, &&P < 0.01.

Table 3. Co-expression of regulated genes related to lipid metabolism

Tissue	Probe set	Gene symbol	Gene title	RefSeq transcript ID	Levels
Live tissue	1367667_at	Fdps	Farnesyl diphosphate synthase	NM_031840	down
	1367707_at	Fasn	fatty acid synthase	NM_017332	down
	1387006_at	Sult2a1	Sulfotransferase family 2A, dehydroepiandrosterone (DHEA)-preferring-like 1	NM_012695	down
	1370281_at	Fabp5	Fatty acid binding protein 5, epidermal	NM_145878	down
	1370355_at	Scd1	Stearoyl-coenzyme A desaturase 1	NM_139192	down
	1387123_at	Cyp17a1	Cytochrome P450, family 17, subfamily a, polypeptide 1	NM_012753	down
	1387156_at	Hsd17b2	Hydroxysteroid (17-beta) Dehydrogenase 2	NM_024391	down
	1370566_at	Rdh2	Retinol dehydrogenase 2	NM_199208	down
	1374914_at	Ppard	Peroxisome proliferator-activated receptor delta	XM_001078083 ///	down
	1380013_at	Pnpla3	Patatin-like phospholipase domain containing 3	XM_343302	up
	1388108_at	Elovl6	ELOVL family member 6, elongation of long chain fatty acids (yeast)	NM_134383 ///	up
				XM_001075165	
Adipose tissues	1369179_a_at	Pparg	Peroxisome proliferator-activated receptor gamma	NM_001145366 ///	down
				NM_001145367 ///	
				NM_013124	
	1367585_a_at	Atplal	ATPase, Na ⁺ /K ⁺ transporting, alpha 1 polypeptide	NM_012504	down
	1367609_at	Mif	Macrophage migration inhibitory factor	NM_031051	down
	1367894_at	Insig1	Insulin induced gene 1	NM_022392	down
	1370862_at	ApoE	Apolipoprotein E	J02583	down
	1371691_at	Rarres2	Retinoic acid receptor responder (tazarotene induced) 2	BI282993	down
	1371963_at	Pcca	Propionyl-coenzyme A carboxylase, alpha polypeptide	BF395042	down
	1375034_at	Pla2g15	Phospholipase A2, group XV	A1410383	up
	1387132_at	Lipe	Lipase, hormone sensitive	NM_012859	up
	1387365_at	Nr1h3	Nuclear receptor subfamily 1, group H, member 3	NM_031627	up
	1379075_at	Mboat2	Membrane-bound O-acyltransferase domain containing 2	A1501287	up
1382680_at	Adfp	Adipose differentiation-related protein	BG673602	up	
1386960_at	Slc37a4	Solute carrier family 37 (glucose-6-phosphate transporter), member 4	NM_031589	up	

Discussion

With the dramatically increasing prevalence of obesity, the urgent need for new strategies to combat the growing epidemic emerges. Therefore, in the present study, we isolated polyphenols and polysaccharides from oolong tea

and investigated the anti-obesity capabilities of the components. In the present study, TWH, TWL, TPPH, TPPL, and TPSM effectively prevented rat body weight increase relative to the weight of the MC group. Moreover, the tea water extract and polyphenols presented dose-dependent

effects; the high-dose green tea water extract or polysaccharide was more efficacious in preventing obesity than the other treatments tested. Nevertheless, TPSH and TPSL did not significantly change the rat body weight.

He et al. reported that oolong tea could reduce the weight of rats by suppressing food intake (27). Kao et al. also observed a reduction in food intake after the administration of EGCG present in TPP (26). We also observed a decrease in weight gain induced by polyphenols, polysaccharide, or the combination of TPS and TPP, which is relevant in food utilization.

Xu et al. reported that green tea extract, polysaccharide, and polyphenols exhibit anti-inflammatory activities (28). Our results indicated that polyphenols, polysaccharide, or the combination of TPS and TPP can significantly reduce serum and liver triglyceride levels. Furthermore, the TPSL group effectively increased serum T-SOD levels.

Numerous studies on genetic, metabolic, hormonal, behavioral, social, and cultural aspects have been conducted to increase our understanding of the cause and treatment of obesity (29, 30). The physiological and molecular changes observed in our high-fat-diet-induced obese rat model provided useful insight into the development of obesity in humans. In the present study, we showed that the expression of a number of genes involved in lipid metabolism was altered in the MC group, which further demonstrated the usefulness of this high-fat diet model. In addition, a total of 24 obesity-related genes showed significant changes in liver and epididymal adipose tissues in the TPPL, TPSL, and TPSM groups compared with the MC group. Considerable evidence from the KEGG website reveals that these genes play important roles in the pathogenesis of obesity. The pathways participated in by the genes include fatty acid biosynthesis, steroid hormone biosynthesis, unsaturated fatty acid biosynthesis, fatty acid elongation, glycerolipid metabolism, and glycerophospholipid metabolism.

Conclusions

In summary, crude old oolong tea extract prevented body weight gain in male Sprague–Dawley rats, in which polyphenols and polysaccharide may play an important role, particularly the combination of polyphenols and polysaccharide. Multiple factors in oolong tea were determined to contribute to the anti-obesity effects in the present research. Each main ingredient in oolong tea contributed to the anti-obesity function, and every ingredient has potential beneficial effects in achieving weight loss, such as reducing food utilization, lowering serum triglyceride levels, inhibiting fatty acid absorption, and regulating relevant gene expression. Therefore, the combination of polysaccharide and polyphenols might be a potential therapy to treat obesity, and further clinical studies are needed in this regard.

Authors' contributions

All authors were involved in the study design and collaborated to write this article. T.W. analyzed the data, J.X.R.L. and Y.C. interpreted the data, T.W. and J.X. coordinated the research, and M.Z. was primarily responsible for the final content.

Conflict of interest and funding

No potential conflict of interest was reported by the authors. This work was supported by the Beijing Advanced Innovation Center for Food Nutrition and Human Health (Grant No. 20161025), Research Project of Tianjin Education Commission (Grant No. 2017ZD02), Innovation of Modern Agricultural Project (Grant No. F18R02), and the National Natural Science Foundation of China (Grant No. 31501475).

References

1. Upadhyay J, Farr O, Perakakis N, Ghaly W, Mantzoros C. Obesity as a Disease. *Med Clin North Am* 2018; 102: 13–33. doi:10.1016/j.mcna.2017.08.004
2. Eckel RH, Kahn SE, Ferrannini E, Goldfine AB, Nathan DM, Schwartz MW, et al. Obesity and type 2 diabetes: what can be unified and what needs to be individualized? *J Clin Endocrinol Metab* 2011; 96: 1654–63. doi:10.1210/jc.2011-0585
3. Stimpson E, Patel J, Kittleson M, Rafiei M, Osborne A, Lee F, et al. The obesity paradox. *J Heart Lung Transplant* 2013; 32: S212. doi:10.1016/j.healun.2013.01.531
4. Colman E, Golden J, Roberts M, Egan A, Weaver J, Rosebraugh C. The FDA's assessment of two drugs for chronic weight management. *N Engl J Med* 2012; 367: 1577–9. doi:10.1056/NEJMp1211277
5. Khoja SS, Piva SR, Toledo FG. Physical activity in obesity and diabetes. *Obesity: Springer, Cham*; 2016, pp. 321–33.
6. Saunders KH, Umashanker D, Igel LI, Kumar RB, Aronne LJ. Obesity Pharmacotherapy. *Med Clin North Am* 2018; 102: 135–48. doi:10.1016/j.mcna.2017.08.010
7. Mohamed GA, Ibrahim SRM, Elkhayat ES, El Dine RS. Natural anti-obesity agents. *Bulletin of Faculty of Pharmacy, Cairo University*. 2014; 52: 269–84. doi:10.1016/j.bfopcu.2014.05.001
8. Wu T, Yin J, Zhang G, Long H, Zheng X. Mulberry and cherry anthocyanin consumption prevents oxidative stress and inflammation in diet-induced obese mice. *Mol Nutr Food Res* 2016; 60: 687–94. doi:10.1002/mnfr.201500734
9. Igarashi Y, Obara T, Ishikuro M, et al. Randomized controlled trial of the effects of consumption of 'Yabukita' or 'Benifuuki' encapsulated tea-powder on low-density lipoprotein cholesterol level and body weight. *Food Nutr Res*. 2017; 61: 1334484. doi:10.1080/16546628.2017.1334484
10. Ng KW, Cao ZJ, Chen HB, Zhao ZZ, Zhu L, Yi T. Oolong tea: a critical review of processing methods, chemical composition, health effects, and risk. *Crit Rev Food Sci Nutr* 2017; 1–24. doi:10.1080/10408398.2017.1347556
11. Yang M, Wang C, Chen H. Green, oolong and black tea extracts modulate lipid metabolism in hyperlipidemia rats fed high-sucrose diet. *J Nutr Biochem*. 2001; 12: 14–20.
12. Suzuki T, Miyoshi N, Hayakawa S, Imai S, Isemura M, Nakamura Y. Health benefits of tea consumption. *Beverage Impacts Health Nutr Springer*; 2016, p. 49–67.

13. Yi T, Zhu L, Peng W-L, He X-C, Chen H-L, Li J, et al. Comparison of ten major constituents in seven types of processed tea using HPLC-DAD-MS followed by principal component and hierarchical cluster analysis. *LWT - Food Sci Technol* 2015; 62: 194–201. doi:10.1016/j.lwt.2015.01.003
14. Zhang X, Chen Y, Zhu J, Zhang M, Ho CT, Huang Q, et al. Metagenomics analysis of Gut Microbiota in a high fat diet-Induced obesity mouse model fed with (-)-Epigallocatechin 3-O-(3-O-Methyl) Gallate (EGCG3''Me). *Mol Nutr Food Res* 2018; 1800274.
15. Friedrich M, Petzke KJ, Raederstorff D, Wolfram S, Klaus S. Acute effects of epigallocatechin gallate from green tea on oxidation and tissue incorporation of dietary lipids in mice fed a high-fat diet. *Int J Obes (Lond)* 2012; 36: 735–43. doi:10.1038/ijo.2011.136
16. Huvaere K, Nielsen JH, Bakman M, Hammershoj M, Skibsted LH, Sorensen J, et al. Antioxidant properties of green tea extract protect reduced fat soft cheese against oxidation induced by light exposure. *J Agr Food Chem* 2011; 59: 8718–23. doi:10.1021/jf201139e
17. Yang B, Kortessniemi M. Clinical evidence on potential health benefits of berries. *Curr Opin Food Sci* 2015; 2: 36–42. doi:10.1016/j.cofs.2015.01.002
18. Rumpel W, Seale J, Clevidence B, Judd J, Wiley E, Yamamoto S, et al. Oolong tea increases metabolic rate and fat oxidation in men. *J Nutr* 2001; 131: 2848–52. doi:10.1093/jn/131.11.2848
19. Kovacs EM, Lejeune MP, Nijs I, Westerterp-Plantenga MS. Effects of green tea on weight maintenance after body-weight loss. *Br J Nutr* 2004; 91: 431–7. doi:10.1079/BJN20041061
20. Nagao T, Komine Y, Soga S, Meguro S, Hase T, Tanaka Y, et al. Ingestion of a tea rich in catechins leads to a reduction in body fat and malondialdehyde-modified LDL in men. *Am J Clin Nutr* 2005; 81: 122–9. doi:10.1093/ajcn/81.1.122
21. Venkatakrishnan K, Chiu HF, Cheng JC, Chang YH, Lu YY, Han YC, et al. Comparative studies on the hypolipidemic, antioxidant and hepatoprotective activities of catechin-enriched green and oolong tea in a double-blind clinical trial. *Food Funct* 2018; 9: 1205–13. doi:10.1039/c7fo01449j
22. Han LK, Takaku T, Li J, Kimura Y, Okuda H. Anti-obesity action of oolong tea. *Int J Obesity Related Metab Disord: J Int Assoc Study Obesity* 1999; 23: 98–105.
23. Kuo KL, Weng MS, Chiang CT, Tsai YJ, Lin-Shiau SY, Lin JK. Comparative studies on the hypolipidemic and growth suppressive effects of oolong, black, pu-erh, and green tea leaves in rats. *J Agr Food Chem* 2005; 53: 480–9. doi:10.1021/jf049375k
24. Ikeda I, Hamamoto R, Uzu K, Imaizumi K, Nagao K, Yanagita T, et al. Dietary gallate esters of tea catechins reduce deposition of visceral fat, hepatic triacylglycerol, and activities of hepatic enzymes related to fatty acid synthesis in rats. *Biosci Biotechnol Biochem* 2005; 69: 1049–53.
25. Rains TM, Agarwal S, Maki KC. Antiobesity effects of green tea catechins: a mechanistic review. *J Nutr Biochem* 2011; 22: 1–7. doi:10.1016/j.jnutbio.2010.06.006
26. Kao YH, Hiipakka RA, Liao S. Modulation of endocrine systems and food intake by green tea epigallocatechin gallate. *Endocrinology* 2000; 141: 980–7. doi:10.1210/endo.141.3.7368
27. He RR, Chen L, Lin BH, Matsui Y, Yao XS, Kurihara H. Beneficial effects of oolong tea consumption on diet-induced overweight and obese subjects. *Chin J Integr Med* 2009; 15: 34–41. doi:10.1007/s11655-009-0034-8
28. Xu Y, Zhang M, Wu T, Dai S, Xu J, Zhou Z. The anti-obesity effect of green tea polysaccharides, polyphenols and caffeine in rats fed with a high-fat diet. *Food Funct* 2015; 6: 297–304. doi:10.1039/c4fo00970c
29. Lu C, Zhu W, Shen CL, Gao W. Green tea polyphenols reduce body weight in rats by modulating obesity-related genes. *PLoS One* 2012; 7: e38332. doi:10.1371/journal.pone.0038332
30. Szulinska M, Stepień M, Kregielska-Narozna M, Suliburska J, Skrypnik D, Bak-Sosnowska M, et al. Effects of green tea supplementation on inflammation markers, antioxidant status and blood pressure in NaCl-induced hypertensive rat model. *Food Nutr Res* 2017; 61: 1295525. doi:10.1080/16546628.2017.1295525

***Min Zhang**

Tianjin University of Science and Technology
Tianjin 300457
P.R. China
Email: zm0102@tust.edu.cn

Sodium and potassium urinary excretion and their ratio in the elderly: results from the Nutrition UP 65 study

Pedro Moreira^{1,2,3*}, Ana S. Sousa^{1,4}, Rita S. Guerra¹, Alejandro Santos^{1,5}, Nuno Borges^{1,6}, Cláudia Afonso¹, Teresa F. Amaral^{1,7} and Patrícia Padrão^{1,2}

¹Faculdade de Ciências da Nutrição e Alimentação, Universidade do Porto, Porto, Portugal; ²EPIUnit – Instituto de Saúde Pública, Universidade do Porto, Porto, Portugal; ³Centro de Atividade Física, Saúde e Lazer; Universidade do Porto, Porto, Portugal; ⁴Escola Superior de Saúde, Instituto Politécnico de Leiria, Leiria, Portugal; ⁵I3S-Instituto de Investigação e Inovação em Saúde, Porto, Portugal; ⁶CINTESIS–Centre for Health Technology and Services Research, Porto, Portugal; ⁷UISPA-IDMEC, Faculdade de Engenharia, Universidade do Porto, Porto, Portugal

Abstract

Background: We aimed to describe urinary sodium and potassium excretion and their ratio in a representative sample of Portuguese elderly population, according to sociodemographic characteristics and weight status.

Methods: A cluster sampling approach was used, representing older Portuguese adults (≥ 65 years) according to age, sex, education level, and regional area within the Nutrition UP 65 study. This cross-sectional evaluation was conducted in 2015 and 2016. From a sample size of 1,500 participants, 1,318 were eligible for the present analysis, 57.3% were women, and 23.5% were aged ≥ 80 years. Sodium and potassium consumption was evaluated through one 24 h urinary excretion. Inadequate sodium intake was defined as $\geq 2,000$ mg/day, inadequate potassium intake was considered as $< 3,510$ mg/day, and inadequate sodium-to-potassium ratio was defined as > 1 , according to the World Health Organization cutoffs.

Results: The proportion of the participants with an inadequate intake was 80.0% in women and 91.5% in men (sodium), 96.2% of women and 79.4% of men (potassium), and 98.4% of women and 99.1% of men (sodium-to-potassium ratio). Higher sodium adequacy was observed among the older elderly, unmarried, with lower household income, and underweight/normal weight. Higher potassium adequacy was observed in the younger elderly, married, and with higher income.

Conclusion: The majority of the Portuguese elderly population was classified as having inadequate sodium, potassium, and sodium-to-potassium ratio urinary excretion. Therefore, strategies for reducing sodium and increasing potassium intake are priorities in the Portuguese elderly population.

Keywords: *Sodium, potassium, sodium-to-potassium ratio, elderly, urinary excretion*

Over the past 25 years, the estimated deaths attributed to high blood pressure have increased considerably worldwide (1). In Portugal, despite improvements in the treatment of hypertension (2) and the decrease in the mean systolic blood pressure in adults, including elders, between 1990 and 2015 (1), cerebrovascular diseases are still the leading causes of death (2).

Jointly, cardiovascular diseases (CVDs) and cancer are responsible for 54% of all deaths (3). These two groups of diseases also share some important risk factors (4), and high sodium intake is recognized to increase the risk of fatal stroke, fatal coronary heart disease (5), cancer of the nasopharynx and stomach (6), and type 2 diabetes (7).

Potassium is also a critical mineral when assessing the health effects of sodium consumption, considering that this nutrient may mitigate the negative effects of excessive sodium intake by reducing blood pressure and thus preventing stroke (8, 9).

Additionally, the ratio of Na/K may be more reliable to assess the risk of CVD and CVD-related mortality than either sodium or potassium intake alone (10). However, studies on the relations of Na/K ratio with stroke or cardiovascular-related mortality have been sparse (11). To decrease blood pressure and risk of CVD, stroke, and coronary heart disease in adults, the WHO recommends a reduction to less than 2,000 mg/day of sodium (5) and

a potassium intake of at least 3,510 mg/day (12). If individuals consume the amounts of sodium and potassium recommended by the WHO, the molar Na/K ratio will be approximately one to one, a ratio that is considered positive for health (5, 12). In this sense, lowering the Na/K ratio may reduce CVD risk and mortality (11), particularly in the elderly (13), although studies on the optimal relation between Na and K intake are still scarce (11).

Current estimates of sodium and potassium intake in a survey conducted between 2011 and 2012 in a representative sample of adults (18–90 years) from the Portuguese continental area estimated a mean 24 h urinary sodium excretion of 4,197 mg/day (10.7 g of salt) (14). In this study (14), mean 24 h urinary potassium excretion was 2,828 mg/day, making the Na/K ratio for all samples 2.5. In this study, data on sodium and potassium intake was provided for the overall sample, not allowing the characterization of older subjects.

The health in Portugal has improved considerably in the last decades (15), and the average life expectancy in the Portuguese population was 80.6 years in 2015 (16). However, the lack of data on sodium, potassium, and Na/K ratio intake in the elderly remains a challenge for the Portuguese region. The objective of our study is to describe 24 h urinary sodium and potassium excretion and their ratio in a representative sample of Portuguese elders, according to sociodemographic characteristics and weight status. The present study is a subproject of the Nutrition UP 65 study, whose protocol is published elsewhere (17).

Methods

Study design and sampling

A cross-sectional observational study was conducted in Portugal in a sample of 1,500 older Portuguese adults, ≥65 years old. To achieve a nationally representative sample of older Portuguese adults, a quota sampling approach was adopted using data from Census 2011 regarding sex, age, educational level, and regional area (defined in the Nomenclature of Territorial Units for Statistical purposes – NUTS II).

The potential participants were contacted by the interviewers, who provided information about the study purpose and methodology and invited them to participate. Individuals presenting any condition that precluded the collection of urine, such as dementia or urinary incontinence, were excluded from the study.

Data were collected between December 2015 and June 2016.

Ethics

This research was conducted according to the guidelines established by the Declaration of Helsinki and the study protocol was approved by the Ethics Committee of the Department of Social Sciences and Health (Ciências Sociais e Saúde) from the Faculdade de Medicina da

Universidade do Porto (no. PCEDCSS – FMUP 15/2015) and by the Portuguese National Commission of Data Protection (no. 9427/2015). All participants, or two representatives per participant, were asked to read and sign a duplicated informed consent form.

Data collection

Sociodemographic data and nutritional status were collected using a structured questionnaire. Eight previously trained registered nutritionists were responsible for the questionnaire's application and also by the anthropometric data collection.

Sociodemographic data included information on sex, age, regional area, education, marital status, residence type, and household income. The regional areas used are defined in NUTS II: Alentejo, Algarve, Azores, Lisbon Metropolitan Area, Center, Madeira, and North (18). Educational level was determined by the number of completed school years, and the following categories were used: no formal education, 1–3, 4, 5–11, and ≥12 years of school. Marital status was categorized as single, married or in a common-law marriage, divorced, or widowed. Residence type was defined as home or institution. Self-reported data regarding the presence of chronic diseases was also collected.

Body mass index (BMI) was computed using the standard formula [body weight (kg) /standing height² (m)], and participants were classified according to WHO cutoff values.

Anthropometric measurements were collected following standard procedures (19). Standing height was obtained with a calibrated stadiometer (Seca 213) with 0.1 cm resolution. For participants with visible kyphosis or when it was impossible to measure standing height due to a participant's paralysis or due to mobility or balance limitations, height was obtained indirectly from non-dominant hand length (in centimeters), measured with a calibrated caliper from Fervi Equipment (Fervi Equipment, Vignola, Italy) with 0.1 cm resolution (20). Body weight (in kilograms) was measured with a calibrated portable electronic scale (Seca 803) (SECA GmbH, Hamburg, Germany) with 0.1 kg resolution, with the participants wearing light clothes. When it was not possible to weigh a patient, for the same reasons that prevented standing height measurement, body weight was estimated from mid-upper arm and calf circumferences (21). Mid-upper arm and calf circumferences were measured with a metal tape measure from Lufkin (Lufkin W606 PM, Lufkin, Sparks, Maryland, USA) with 0.1 cm resolution.

The volume of urine in a 24 h period was collected for each participant. The interviewers gave the participants oral and written instructions on how to proceed for the collection and storage of the volume of 24 h urine. A 24 h urine container was also provided. A certified laboratory, Labco (Lisbon, Portugal), was responsible for urine sample collection and analysis. Urinary creatinine

was measured by the Jaffe method. A urine sample was considered inadequate if the creatinine level was <0.4 g/24 h for women or <0.6 g/24 h for men (22) or if the volume collected was <500 ml (23).

Sodium intake was evaluated after converting 24 h urinary sodium excretion, and excessive sodium intake was defined as $\geq 2,000$ mg/day, according to the World Health Organization cutoffs (5). Potassium intake was also evaluated by 24 h urinary potassium excretion and was considered low if $<3,510$ mg/day. Na/K ratio >1 was defined as inadequate.

Statistical analysis

Categorical variables were reported as frequencies. According to the normality of variable distribution, evaluated through Kolmogorov–Smirnov test, results were described as median and interquartile range (IQR).

Monthly household income was summarized using the following cutoffs: $<€500$, $€500$ – $€999$, and $\geq €1,000$. Of the included participants, 645 (48.9%) did not know or preferred not to declare their income and thus they were allocated in a separate category.

Sodium and potassium intake, Na/K ratio median value, and the frequency of patients presenting inadequacy were compared across age groups, education, marital status, residence type, household income, and also for BMI using Kruskal–Wallis or Mann–Whitney test for continuous variables and Pearson chi-squared or Fisher's exact test for categorical variables.

Results were considered significant when $p < 0.05$. Statistical analyses were conducted using the Software Package for Social Sciences for Windows (version 23.0, 2012, IBM (SPSS, Inc, an IBM Company, Chicago, IL)).

Results

From the 1,500 individuals recruited, 178 were excluded because their urine samples were inadequate. Four other participants were excluded due to the impossibility of either measuring or estimating weight. The final study sample was composed of 1,318 participants, median (IQR) age equal to 73 (10) years, age ranging between 65 and 94 years, 57.3% women. Based on self-reported data, 65.2% participants ($n = 859$) reported having high blood pressure. Moreover, almost all participants (97.5%) mentioned presenting at least one chronic disease or prolonged health issue; eight participants did not know or preferred not to respond.

Compared to the final sample, the excluded participants were older, median (IQR) = 79 (12) years *versus* median (IQR) = 73 (10) years ($p < 0.001$), had attained lower educational level ($p = 0.007$), were less likely to be married or in a common-law marriage ($p < 0.001$), and were more likely to live in an institution ($p < 0.001$) and to have lower household income or to not declare their household income ($p < 0.001$).

All the analyses performed were stratified by sex. Regarding potassium intake and Na/K analyses displayed for men, one participant presenting a value of 0 mg/24 h potassium was excluded.

Height was estimated from hand length for 25 participants and weight was estimated from mid-upper arm and calf circumferences for 12 participants.

The older Portuguese adults within the present sample presented a median (IQR) sodium excretion of 3,368 (1,848) mg/day [equivalent to a median (IQR) salt excretion of 8.42 (4.62) g/day], a median (IQR) potassium intake of 2,262 (1,131) mg/day, and a median (IQR) Na/K of 2.33 (1.07).

Concerning sodium, 80% of women and 91.5% of men presented excessive intake. Otherwise, only 3.8% of women and 20.6% of men had an adequate potassium intake. Also, 98.4% of women and 99.1% of men presented Na/K ≥ 1 .

As displayed in Table 1, among women, sodium intake decreased with age. Women aged 80 or more years presented a lower frequency of inadequate sodium intake than women aged 65–79 years. Notwithstanding this, potassium intake decreased across the two age groups and almost all (99.5%) women aged 80 or more years presented inadequate potassium intake. Women with no formal education presented lower potassium intake than women who attended school. However, no significant associations were found between education and sodium intake. Women who were married or in a common-law marriage presented higher sodium intake than single, divorced, or widowed women and the same tendency was observed for potassium intake. Women living at home ingested more sodium than those institutionalized. However, concerning the two residence types, no significant differences were found regarding potassium intake. Concerning household income, the highest sodium intake was observed for women with $\geq €1,000$ and the lowest potassium intake was observed for women with $\leq €499$ and for those who did not declare the household income. Sodium intake increased across BMI categories, with obese women presenting a higher frequency of inadequacy than underweight/normal and overweight women. Regarding potassium intake, no significant differences were observed across BMI categories. Concerning Na/K, there were no significant differences among women for any of the studied characteristics, with an exception for residence type: institutionalized women presented lower Na/K than women living at home.

The results for men are presented in Table 2. Men aged 80 years or more presented lower sodium intake and also lower potassium intake than men aged 65–79 years. No differences were observed concerning education level for sodium intake. However, similarly to women, men with no formal education presented lower potassium intake than those who attended school. Both sodium and potassium intakes were higher for married men or those in a common-law marriage than for those who were single,

Table 1. Sodium intake, potassium intake, and sodium-to-potassium ratio (Na/K) in 755 older Portuguese women, ≥65 years old, participating in a cross-sectional observational study

Age, years ^a	Sodium intake, mg/day (n = 755)		Potassium intake, mg/day (n = 755)		Na/K (n = 755)	
	Median (IQR)	Inadequate (≥2,000) n (%)	Median (IQR)	Inadequate (<3,500) n (%)	Median (IQR)	>1n (%)
65–79	3,008 (1,532)	459 (82.0)	2,106 (897)	532 (95.0)	2.38 (1.10)	550 (98.2)
≥80	2,552 (1,168)	145 (74.4)	1,755 (780)	194 (99.5)	2.31 (1.02)	193 (99.0)
p	n.s.	<0.05	<0.05	<0.05	n.s.	n.s.
Education, years						
0	2,572 (1,860)	91 (72.8)	1,755 (1092)	121 (96.5)	2.50 (1.12)	122 (97.6)
1–3	3,064 (1,780)	132 (78.1)	1,950 (819)	161 (95.3)	2.43 (1.23)	166 (98.2)
4	2,856 (1,464)	290 (82.4)	2,106 (780)	339 (96.3)	2.33 (1.03)	346 (98.3)
5–11	2,692 (1,168)	66 (83.5)	1,989 (780)	76 (96.2)	2.28 (0.91)	79 (100)
≥12	2,760 (924)	25 (83.3)	1,989 (721.5)	29 (96.7)	2.10 (1.30)	79 (100)
p	n.s.	n.s.	<0.05	n.s.	n.s.	n.s.
Marital status						
Single/divorced/widowed	2,712 (1,428)	359 (76.4)	1,930.5 (897)	454 (96.6)	2.35 (1.11)	461 (98.1)
Married/common-law marriage	3,088 (1,452)	245 (86.0)	2,145 (780)	272 (95.4)	2.44 (1.00)	282 (98.9)
p	<0.05	<0.05	<0.05	n.s.	n.s.	n.s.
Residence						
Home	2,856 (1,520)	582 (80.9)	2,028 (897)	690 (96.0)	2.40 (1.07)	707 (98.3)
Care home	2,200 (1,328)	22 (61.1)	1,794 (828.8)	36 (100)	1.99 (0.96)	36 (100)
p	<0.05	<0.05	n.s.	n.s.	<0.05	n.s.
Income, €						
≤499	2,876 (1580)	130 (78.8)	1,950 (1014)	163 (98.8)	2.40 (1.24)	161 (97.6)
500–999	2,936 (1388)	147 (86.5)	2,184 (711.8)	163 (95.9)	2.37 (1.10)	169 (99.4)
>1,000	3,040 (1,660)	65 (87.8)	2,086.5 (858)	69 (93.2)	2.38 (1.15)	72 (97.3)
Unknown/no response	2,656 (1,520)	262 (75.7)	1,950 (867.8)	331 (95.7)	2.34 (0.98)	341 (98.6)
p	<0.05	<0.05	<0.05	n.s.	n.s.	n.s.
BMI, kg/m ²						
Underweight/normal	2,400 (1,492)	74 (72.5)	1,911 (750.8)	100 (98.0)	2.23 (1.13)	98 (96.1)
Overweight	2,748 (1,480)	242 (77.1)	2,028 (897)	305 (97.1)	2.28 (0.96)	308 (98.1)
Obese	2,996 (1,756)	288 (85.0)	2,028 (936)	321 (94.7)	2.49 (1.12)	337 (99.4)
p	<0.05	<0.05	n.s.	n.s.	n.s.	n.s.

Note: 2,000 mg sodium = 5 g salt (NaCl).

n.s. – non significant

BMI, body mass index; IQR, interquartile range.

^a65–79 years: n = 560; ≥80 years: n = 195.

divorced, or widowed. Also, a lower proportion of men who were married or in a common-law marriage presented inadequate potassium intake. Institutionalized men presented lower sodium intake than those living at home, whereas no differences were found regarding potassium intake. Men in the lowest category of household income presented the lowest sodium intake and also the lowest potassium intake. Sodium intake increased across BMI categories but no differences were observed for potassium intake. Similarly to what was observed among women regarding Na/K, only residence type presented significant differences, with a lower Na/K for institutionalized men.

Discussion

Our results have shown that above 64 years, 80% of the women and 91.5% of the men exceeded the current guideline on sodium consumption (5), while for potassium 96.2% of women and 79.48% of men did not meet the recommendation, and only 0.9–1.6% met the WHO reference Na/K ratio (12). Mean sodium and potassium intakes in men and women were well below the values reported for the general Portuguese adult population by the Physa Study (mean intakes for sodium were 4,268 mg in men and 4,094 mg in women and for potassium 2,980 mg in men and 2,940 mg in women) (16); however, these results are difficult to compare with our findings, since the results were not stratified

Table 2. Sodium intake, potassium intake, and sodium-to-potassium ratio (Na/K) in 563 older Portuguese men, ≥ 65 years old, participating in a cross-sectional observational study

Age, years ^a	Sodium intake, mg/day (<i>n</i> = 563)		Potassium intake, mg/day (<i>n</i> = 562)		Na/K (<i>n</i> = 562)	
	Median (IQR)	Inadequate ($\geq 2,000$) <i>n</i> (%)	Median (IQR)	Inadequate ($< 3,500$) <i>n</i> (%)	Median (IQR)	$> 1n$ (%)
65–79	3,812 (2,052)	416 (92.0)	2,730 (1,365)	351 (77.8)	2.31 (1.04)	448 (99.3)
≥ 80	3,484 (1,684)	99 (89.1)	2,496 (1,014)	95 (85.6)	2.24 (1.12)	109 (98.2)
<i>p</i>	< 0.05	n.s.	< 0.05	n.s.	n.s.	n.s.
Education, years						
0	3,416 (1,440)	44 (91.7)	2,340 (897)	43 (89.6)	2.44 (1.21)	48 (100)
1–3	3,774 (1,808)	69 (93.2)	2,691 (1,365)	58 (79.5)	2.32 (1.18)	73 (100)
4	3,860 (2,152)	284 (90.2)	2,769 (1,443)	241 (76.5)	2.25 (1.04)	310 (98.4)
5–11	3,768 (1,964)	90 (94.7)	2,730 (1,014)	77 (81.1)	2.29 (0.84)	95 (100)
≥ 12	3,628 (1,940)	28 (90.3)	2,379 (975)	27 (87.1)	2.13 (1.25)	91 (100)
<i>p</i>	n.s.	n.s.	< 0.05	n.s.	n.s.	n.s.
Marital status						
Single/divorced/widowed	3,288 (1,668)	174 (88.8)	2,379 (1,014)	172 (88.2)	2.35 (1.14)	195 (100)
Married/common-law marriage	3,952 (2,064)	340 (92.9)	2,886 (1,326)	273 (74.6)	2.27 (1.02)	361 (98.6)
<i>p</i>	< 0.05	n.s.	< 0.05	< 0.05	n.s.	n.s.
Residence						
Home	3,768 (1,952)	504 (91.8)	2,652 (1,248)	434 (79.2)	2.31 (1.05)	543 (99.1)
Care home	2,668 (1,320)	11 (78.6)	2,574 (1,267.5)	12 (85.7)	1.59 (0.90)	14 (100)
<i>p</i>	< 0.05	n.s.	n.s.	n.s.	< 0.05	n.s.
Household income, €						
≤ 499	3,276 (1,812)	46 (86.8)	2,418 (1,101.8)	46 (88.5)	2.36 (1.05)	50 (96.2)
500–999	3,908 (2,168)	109 (92.4)	2,691 (1,218.8)	96 (81.4)	2.39 (0.93)	118 (100)
$> 1,000$	4,096 (1,584)	91 (97.8)	3,003 (1,287)	66 (71.0)	2.20 (0.98)	93 (100)
Unknown/no response	3,648 (2,036)	269 (90.0)	2,535 (1,287)	238 (79.6)	2.24 (1.12)	296 (99.0)
<i>p</i>	< 0.05	n.s.	< 0.05	n.s.	n.s.	n.s.
BMI, kg/m ²						
Underweight/normal	3,324 (1,616)	89 (89.9)	2,457 (1,287)	84 (84.8)	2.18 (0.88)	93 (99.0)
Overweight	3,780 (1,932)	261 (91.9)	2,613 (1,326)	225 (79.5)	2.34 (1.16)	280 (98.9)
Obese	3,908 (2,188)	165 (91.7)	2,749.5 (1,238.3)	137 (76.1)	2.30 (0.97)	179 (99.4)
<i>p</i>	< 0.05	n.s.	n.s.	n.s.	n.s.	n.s.

Note: 2,000 mg sodium = 5 g salt (NaCl).

BMI, body mass index; IQR, interquartile range.

n.s. – non significant

a65–79 years: *n* = 451; ≥ 80 years: *n* = 112.

by age in the latter study and subjects above 64 years of age represented only 23.3% of the total sample.

The present results reinforce the view that the vast majority of the world's population have a sodium intake within the range of 2.5–5 g (24), which is far from the recommendation of no more than 2 g of sodium per day. However, it is worth mentioning that the current cutoffs regarding the recommended sodium and sodium-to-potassium ratio intakes are still controversial, and some authors (25) argue that a U-shaped curve describes the risk association of dietary sodium intake with CVD and all-cause mortality. Furthermore, a recent publication (26) assessed the associations of

sodium intake with cardiovascular events, and this research is recognized as the largest individual-level data study relating sodium intake to CVD events and mortality; for those individuals without hypertension, compared with 4–5 g/day, higher sodium excretion was not associated with risk of the primary composite outcome (≥ 7 g/day), whereas an excretion of less than 3 g/day was associated with a significantly increased risk (26). However, the methodology of the previous study has been criticized particularly for the use of a morning spot urine sample to estimate usual salt intake and for the use of Kawasaki formula to estimate salt intake in individuals (27).

In addition, the vast majority of elderly Portuguese participants who reported having high blood pressure also reported the use of antihypertensive drugs (91.3%). This fact may contribute to an explanation for the apparently high age of the Portuguese even in the presence of high sodium intake.

Moreover, the existence of unknown confounding factors that make the population resistant to the adverse effects of high sodium intake is also a possibility (28, 29), and some authors have provided new insights into confounding variables involved in the control of sodium homeostasis that should be considered in future studies aiming to address public health issues about recommended salt intake (30).

Notwithstanding this, the current recommendations, which are internationally accepted (5), indicate the reduction of salt intake at population level as a public health priority (27).

In WHO European member states with salt consumption assessed by 24 h urinary excretion, estimates ranged between 8.25 and 18 g/day, with no member states meeting recommended levels (31). In the global report of Powles et al. (32) describing national sodium intakes by urine collection in 187 countries, the mean values in 2010 were 3.95 g/day (10.6 g salt/day), with the intake being about 10% higher in men than in women, while the differences by age were minor. In this systematic analysis, sodium intakes were higher in Eastern Europe (>4.2 g/day) than in Central Europe (3.9–4.2 g/day), and in Western Europe intakes ranged from 3.4 to 3.8 g/day. No stratification for sodium and potassium intakes after age 65 was provided in these previous mentioned reports.

Despite the heterogeneity between different populations, in the vast majority of populations, sodium consumption is well above recommended levels, while potassium intake is far below the minimum reference intake. Consequently, as in our study, the Na/K molar ratio tends to be much higher than the WHO recommendation.

The intake of sodium and potassium was similar across education groups, but consumption was lower in the older group (80 years or more) in both genders, which may be related to the expected decline in energy intake in this age group, considering the reduction of energy requirements (resting metabolic rate, thermogenesis, and physical activity) with aging (33) and, consequently, the lower intake of these two micronutrients, since they may be positively correlated with overall energy intake (34, 35). Nevertheless, the above-mentioned factors acting together in these two nutrients may have contributed to maintaining the approximate values for the Na/K ratio in the two age groups (65–79 and ≥80 years).

Married subjects from both sexes exhibited the worst nutritional adequacy for sodium and potassium intake, although no significant differences in Na/K ratio was observed in relation to their non-married counterparts. Married

people have been described as having a significant advantage in health (36). Conversely, the divorced, separated, and widowed may have compromised health (36) and higher mortality (36, 37), as well as poorer diet quality (38), consuming more industrial meals and fewer homemade foods (39). However, the higher intakes of sodium and lower intakes of potassium in married subjects, in the present study, may reflect unhealthy dietary choices influencing the intake of those nutrients. Although little is known about the relation between marital status and sodium and potassium intake in the elderly, Kutob et al. (40) reported a worse diet quality in married women in comparison to those who were divorced/separated, and this data may highlight current social changes of being married, divorced, separated, never married, or widowed that may impact long-held assumptions about marital status and nutrition-related health (41, 42). Single elders may be prone to adapt their food choices in order to satisfy their personal needs (42), possibly being nutritionally conscious, which may contribute to better adequacy of sodium and potassium.

We also found that institutionalized elderly participants of both sexes presented lower sodium intakes and Na/K ratios, which could be related to the variety of chronic conditions that may put them under health care needs (43), and concurrent lower salt intake than noninstitutionalized subjects.

Sodium and potassium intakes exhibited opposite directions according to income categories. Higher incomes were associated with higher frequency of sodium inadequacy and lower prevalence of potassium inadequacy. Higher-income persons are more likely to consume a healthy diet than lower income people, and the diet of high-income groups is reported to be higher in potassium (44), in line with our findings. Regarding sodium, income has been described as a variable that does not affect 24 h urinary sodium excretion (45), although in a recent systematic review and meta-analysis to assess socioeconomic determinants of sodium intake in adult populations of high-income countries (46), about two-thirds showed higher sodium intake in subjects with low socioeconomic conditions.

Dietary sodium is strongly related to energy intake (35) due to its inclusion in a wide variety of foods and food preparations (10), and dietary sodium is sometimes described as having a detrimental impact on overweight and obesity in the life cycle, including in adults (47–50), although no studies have specifically addressed this association in persons above 65 years old. In our study, the median sodium intake increased with increasing BMI categories in both sexes, and sodium inadequacy also increased in women with increasing BMI categories (from normal/underweight to obesity). Sodium intake is recognized as a factor that may increase the risk of obesity (51) as a consequence of increased thirst and fluid intake (52), namely of sugary drinks, or as a result of the consumption of energy-dense foods that are also

rich in sodium (for example, cheese or chips) (53, 54), or even through a direct effect on obesity (47, 53). However, since sodium intake, similar to overweight and obesity, is strongly related to energy intake, energy consumption may act as a confounder in the association between sodium and body mass, and, considering the absence of data on energy intake in the present study, no further analysis was performed to assess the independent association of sodium intake with overweight/obesity adjusting for energy intake.

Considering the high levels of sodium and potassium inadequacy in the present study, one can expect that extraordinary efforts should be made to simultaneously decrease sodium and increase potassium intake, since these two nutrients may be positively correlated (34, 35). In addition, they can also be positively correlated with overall energy intake (34, 35), although this may not always happen (54). In the case of elderly persons with low energy requirements, meeting the sodium recommendation could be easier, whereas getting enough potassium may be a much more difficult task (55).

Population-based sodium reduction strategies are potentially cost-effective (56), and as a governmental food policy strategy 'soft regulation' approaches combining targeted industry agreements and public education are considered to be highly cost-effective worldwide (57). Among preventive measures, as new science has emerged, the basic messages to consumers about the health impact of a high sodium intake have evolved, focusing not only on children and adults but also on elderly people (12, 58).

Low potassium intake has been associated with hypertension and adverse cardiovascular and renal outcomes (9, 59), whereas there is high quality evidence regarding the role of an adequate potassium intake in decreasing the risk of stroke (9) and in reducing blood pressure in hypertensive subjects without adverse effect on blood lipid concentrations, catecholamine levels, or renal function in adults. Nevertheless, potassium excess can be harmful in patients with impaired potassium excretion (59), which may be the case of persons taking some drugs (for example, potassium-sparing diuretics) or having some medical conditions, such as renal disease, diabetes, or severe heart failure (60). A possible solution to achieve adequate intakes of sodium and potassium in the elderly could be the adoption of a dietary pattern based on low energy and high nutritionally dense foods, such as the DASH (Dietary Approaches to Stop Hypertension) diet (61) or the Mediterranean diet (62), adopting healthy cooking practices. However, economic constraints may also be a barrier, considering the higher economic costs of adopting low energy dense and high nutritionally dense food patterns (63), particularly in the case of a potassium-dense diet (64) or a Mediterranean eating style (65).

Some limitations have to be acknowledged. The Nutrition UP 65 study is a cross-sectional study and therefore

no causal association between sodium and potassium urinary excretion and the associated factors can be inferred. Another possible limitation of the present study is that the present sample, although it can be regarded as large, only comprises 0.075% of the older Portuguese population. Also, the study included a single 24 h urine collection, which may not represent the usual dietary intake of subjects. However, since the study include a large representative sample of the Portuguese elderly population, the impact of the latter limitation is minimized. To the best of our knowledge, this is the first study presenting nationwide results of 24 h urinary excretion of sodium and potassium and the respective Na/K ratio, specifically for the elderly population, which we consider to be the main strength of the present work.

At least eight in every ten elderly Portuguese participants did not meet the sodium intake maximum recommendation, whereas nine out of ten participants did not meet the minimum potassium intake reference, and virtually all the elderly had an inadequate Na/K ratio. Therefore, reducing sodium and increasing potassium intake must be seen as key priorities in the Portuguese elderly population.

Conflict of interest and funding

Nutrition UP 65 is funded by Iceland, Liechtenstein, and Norway through European Economic Area (EEA) Grants in 85% and by Faculdade de Ciências da Nutrição e Alimentação, Universidade do Porto in 15%. Iceland, Liechtenstein, and Norway sponsor initiatives and projects in various program areas, primarily focusing on reducing economic and social disparities. The European Economic Area Grants are managed by Administração Central do Sistema de Saúde through the Programa Iniciativas em Saúde Pública.

References

1. Forouzanfar MH, Liu P, Roth GA, Ng M, Biryukov S, Marczak L, et al. Global burden of hypertension and systolic blood pressure of at least 110 to 115 mm Hg, 1990–2015. *JAMA* 2017; 317(2): 165–82. doi: 10.1001/jama.2016.19043. PubMed PMID:28097354.
2. Providencia R, Goncalves L, Ferreira MJ. [Cerebrovascular mortality in Portugal: are we overemphasizing hypertension and neglecting atrial fibrillation?]. *Rev Port Cardiol* 2013; 32(11): 905–13. doi: 10.1016/j.repc.2013.04.010. PubMed PMID:24246719.
3. Bordalo A. A Saúde dos Portugueses. Perspetiva 2015 (The health of Portuguese. Perspective 2015). Direção Geral da Saúde, Lisboa; 2015.
4. Pereira M, Peleteiro B, Capewell S, Bennett K, Azevedo A, Lunet N. Changing patterns of cardiovascular diseases and cancer mortality in Portugal, 1980–2010. *BMC Public Health* 2012; 12: 1126. doi: 10.1186/1471-2458-12-1126. PubMed PMID:-23273040PubMed Central PMCID: PMC3560231. eng.
5. WHO. Guideline: sodium intake for adults and children. Geneva: WHO; 2012.

6. World Cancer Research Fund International. Cancer prevention and survival. London: World Cancer Research Fund International; 2017.
7. Hu G, Jousilahti P, Peltonen M, et al. Urinary sodium and potassium excretion and the risk of type 2 diabetes: a prospective study in Finland. *Diabetologia* 2005; 48(8): 1477–83. doi: 10.1007/s00125-005-1824-1. PubMed PMID:15971060.
8. McDonough AA, Veiras LC, Guevara CA, Ralph DL. Cardiovascular benefits associated with higher dietary K⁺ vs. lower dietary Na⁺: evidence from population and mechanistic studies. *Am J Physiol Endocrinol Metab* 2017; 312(4): E348–56. doi: 10.1152/ajpendo.00453.2016. PubMed PMID:-28174181PubMed Central PMCID: PMC5406991.
9. Aburto NJ, Hanson S, Gutierrez H, Hooper L, Elliott P, Cappuccio FP. Effect of increased potassium intake on cardiovascular risk factors and disease: systematic review and meta-analyses. *BMJ* 2013; 346: f1378. doi: 10.1136/bmj.f1378.
10. Bailey RL, Parker EA, Rhodes DG, Goldman JD, Clemens JC, Moshfegh AJ, et al. Estimating sodium and potassium intakes and their ratio in the American diet: data from the 2011–2012 NHANES. *J Nutr* 2016; 146: 745–750. doi: 10.3945/jn.115.221184.
11. Okayama A, Okuda N, Miura K, Okamura T, Hayakawa T, Akasaka H, et al. Dietary sodium-to-potassium ratio as a risk factor for stroke, cardiovascular disease and all-cause mortality in Japan: the NIPPON DATA80 cohort study. *BMJ Open* 2016; 6(7): e011632. doi: 10.1136/bmjopen-2016-011632. PubMed PMID:27412107PubMed Central PMCID: PMC4947715.
12. WHO. Guideline: potassium intake for adults and children. Geneva: WHO; 2012.
13. Chang H-Y, Hu Y-W, Yue C-SJ, et al. Effect of potassium-enriched salt on cardiovascular mortality and medical expenses of elderly men. *Am J Clin Nutr* 2006; 83(6): 1289–96.
14. Polonia J, Martins L, Pinto F, Nazare J. Prevalence, awareness, treatment and control of hypertension and salt intake in Portugal: changes over a decade. The PHYSA study. *J Hypertens* 2014; 32(6): 1211–21. doi: 10.1097/HJH.0000000000000162. PubMed PMID:24675681.
15. Santana P. Ageing in Portugal: regional inequities in health and health care. *Soc Sci Med* 2000; 50(7–8): 11.
16. Santos FF Md. Esperança de vida à nascença: total e por sexo (base: triénio a partir de 2001): PORDATA. Base de Dados de Portugal Contemporâneo; 1/9/2017. Available from: [http://www.pordata.pt/Portugal/Espana%20de%20vida%20total%20e%20por%20sexo%20\(base%20tri%C3%A9nio%20a%20partir%20de%202001\)-418](http://www.pordata.pt/Portugal/Espana%20de%20vida%20total%20e%20por%20sexo%20(base%20tri%C3%A9nio%20a%20partir%20de%202001)-418)
17. Amaral TS, Santos A, Guerra RS, Sousa AS, Álvares L, Valdivieso R, et al. Nutritional strategies facing an older demographic: the nutrition UP 65 study protocol. *JMIR Res Protoc* 2016; 5(3): e184.
18. Instituto Nacional de Estatística. Censos 2011 Resultados Definitivos. Instituto Nacional de Estatística, I.P. (Ed.) Lisboa; 2012.
19. Stewart A, Marfell-Jones M, Olds T, et al. International standards for anthropometric assessment. Potchefstroom, South Africa: International Standards for Anthropometric Assessment; 2011.
20. Guerra RS, Fonseca I, Pichel F, Restivo MT, Amaral TF. Hand length as an alternative measurement of height. *Eur J Clin Nutr* 2014; 68(2): 229–33. PubMed PMID: 24169457; Eng.
21. Chumlea WC, Guo S, Roche AF, Steinbaugh ML. Prediction of body weight for the nonambulatory elderly from anthropometry. *J Am Diet Assoc* 1988; 88(5): 564–8. PubMed PMID: 3367012; eng.
22. ARUP Laboratories. Laboratory test directory – creatinine, 24-hour urine 1/9/2017. Available from: <http://ltd.aruplab.com/Tests/Pub/0020473> [cited 2016]
23. Stuver SO, Lyons J, Coviello A, Fredman L. Feasibility of 24-hr urine collection for measurement of biomarkers in community-dwelling older adults. *J Appl Gerontol* 2016; 36. doi: 10.1177/0733464815624153. PubMed PMID: 26759387; Eng.
24. Mente A, O'Donnell M, Rangarajan S, Dagenais G, Lear S, McQueen M, et al. Normal range of human dietary sodium intake: a perspective based on 24-hour urinary sodium excretion worldwide. *Am J Hypertens* 2013; 26(10): 5.
25. Graudal NJ, Jürgens G, Baslund B, Alderman MH. Compared with usual sodium intake, low- and excessive-sodium diets are associated with increased mortality: a meta-analysis. *Am J Hypertens* 2014; 27(9): 8.
26. Mente A, O'Donnell M, Rangarajan S, et al. Associations of urinary sodium excretion with cardiovascular events in individuals with and without hypertension: a pooled analysis of data from four studies. *Lancet* 2016; 388(10043): 465–75. doi: 10.1016/s0140-6736(16)30467-6. PubMed PMID:27216139; eng.
27. Cappuccio FP, Campbell NR. Population dietary salt reduction and the risk of cardiovascular disease: a commentary on recent evidence. *J Clin Hypertens (Greenwich)* 2017; 19(1): 4–5. doi: 10.1111/jch.12917. PubMed PMID:27677605; eng.
28. Alderman MH. Dietary sodium: paradigm shifts from public health to clinical medicine. *Lancet* 2016; 388(10056): 2110. doi: 10.1016/s0140-6736(16)31914-6. PubMed PMID:27968745; eng.
29. Cappuccio FP. Pro: reducing salt intake at population level: is it really a public health priority? *Nephrol Dial Transplant* 2016; 31(9): 1392–6. doi: 10.1093/ndt/gfw279. PubMed PMID:27488355; eng.
30. Titze J, Dahmann A, Lerchl K, Kopp C, Rakova N, Schroder A, et al. Spooky sodium balance. *Kidney Int* 2014; 85(4): 759–67. doi: 10.1038/ki.2013.367. PubMed PMID: 24107854; eng.
31. Mapping salt reduction initiatives in the WHO European Region. WHO Regional Office for Europe; Copenhagen. 2013.
32. Powles J, Fahimi S, Micha R, Khatibzadeh S, Shi P, Ezzati M, et al. Global, regional and national sodium intakes in 1990 and 2010: a systematic analysis of 24 h urinary sodium excretion and dietary surveys worldwide. *BMJ Open* 2013; 3(12): e003733. doi: 10.1136/bmjopen-2013-003733. PubMed PMID:-24366578PubMed Central PMCID: PMC3884590.
33. Food and Nutrition Board. Energy. In: A Report of the Panel on Macronutrients SoURLoNaLaUoDRI, The Standing Committee on the Scientific Evaluation of Dietary Reference Intakes, ed. Dietary reference intakes for energy, carbohydrate, fiber, fat, fatty acids, cholesterol, protein, and amino acids (macronutrients). The National Academies Press, Washington DC; 2005, pp. 107–264.
34. Espeland MA, Kumanyika S, Wilson AC, Reboussin DM, Easter L, Self M, et al. Statistical issues in analyzing 24-hour dietary recall and 24-hour urine collection data for sodium and potassium intakes. *Am J Epidemiol* 2001; 155(13): 996–1006.
35. Whelton PK, Appel LJ, Sacco RL, Anderson CA, Antman EM, Campbell N, et al. Sodium, blood pressure, and cardiovascular disease: further evidence supporting the American Heart Association sodium reduction recommendations. *Circulation* 2012; 126(24): 2880–9. doi: 10.1161/CIR.0b013e318279acbf. PubMed PMID:23124030.
36. Su D, Stimpson JP, Wilson FA. Racial disparities in mortality among middle-aged and older men: does marriage matter? *Am J Mens Health* 2015; 9(4): 289–300. doi: 10.1177/1557988314540199. PubMed PMID:24963098.

37. Floud S, Balkwill A, Canoy D, Wright FL, Reeves GK, Green J, et al. Marital status and ischemic heart disease incidence and mortality in women: a large prospective study. *BMC Med*. 2014; 12: 42. doi: 10.1186/1741-7015-12-42. PubMed PMID:-24618083PubMed Central PMCID: PMCPMC4103700. eng.
38. Heuberger R, Wong H. The association between depression and widowhood and nutritional status in older adults. *Geriatr Nurs*. 2014; 35(6): 428–33. doi: 10.1016/j.gerinurse.2014.06.011. PubMed PMID:25085716.
39. Shahar DR, Schultz R, Shahar A, Wing RR. The effect of widowhood on weight change, dietary intake, and eating behavior in the elderly population. *J Aging Health*. 2001; 13(2): 189–99. PubMed PMID: 11787511; eng.
40. Kutob RM, Yuan NP, Wertheim BC, Sbarra DA, Loucks EB, Nassir R, et al. Relationship between marital transitions, health behaviors, and health indicators of postmenopausal women: results from the women's health initiative. *J Women's Health* (2002). 2017; 26(4): 313–20. doi: 10.1089/jwh.2016.5925. PubMed PMID:28072926PubMed Central PMCID: PMCPMC5397241. eng.
41. Liu H, Umberson DJ. The times they are a changin': marital status and health differentials from 1972 to 2003. *J Health Soc Behav* 2008; 49(3): 239–53. doi: 10.1177/002214650804900301. PubMed PMID:18771061PubMed Central PMCID: PMCPMC3150568. eng.
42. Vesnaver E, Keller HH, Sutherland O, Maitland SB, Locher JL. Food behavior change in late-life widowhood: a two-stage process. *Appetite* 2015; 95: 399–407. doi: 10.1016/j.appet.2015.07.027. PubMed PMID:26232138PubMed Central PMCID: PMCPMC4589507.
43. Elmstahl S. Energy expenditure, energy intake and body composition in geriatric long-stay patients. *Compr Gerontol A* 1987; 1(3): 118–25. PubMed PMID: 3134130; eng.
44. Nikolic M, Glibetic M, Gurinovic M, Milesevic J, Khokhar S, Chillo S, et al. Identifying critical nutrient intake in groups at risk of poverty in Europe: the CHANCE project approach. *Nutrients* 2014; 6(4): 1374–93. doi: 10.3390/nu6041374. PubMed PMID:24699195PubMed Central PMCID: PMCPMC4011040.
45. Hong JW, Noh JH, Kim DJ. Factors associated with high sodium intake based on estimated 24-hour urinary sodium excretion: the 2009–2011 Korea National Health and Nutrition Examination Survey. *Medicine (Baltimore)* 2016; 95(9): e2864. doi: 10.1097/MD.0000000000002864. PubMed PMID:26945369PubMed Central PMCID: PMCPMC4782853.
46. de Mestral C, Mayen AL, Petrovic D, Marques-Vidal P, Bochud M, Stringhini S. Socioeconomic determinants of sodium intake in adult populations of high-income countries: a systematic review and meta-analysis. *Am J Public Health* 2017; 107(4): 563. doi: 10.2105/AJPH.2016.303629a. PubMed PMID:28272962; eng.
47. Larsen SC, Angquist L, Sorensen TI, Heitmann BL. 24h urinary sodium excretion and subsequent change in weight, waist circumference and body composition. *PLoS One*. 2013; 8: e69689. doi: 10.1371/journal.pone.0069689.
48. Venezia A, Barba G, Russo O, Capasso C, De Luca V, Farinaro E, et al. Dietary sodium intake in a sample of adult male population in southern Italy: results of the Olivetti Heart Study. *Eur J Clin Nutr* 2010;64(5):518–24. doi: 10.1038/ejcn.2010.22. PubMed PMID:20216559; eng.
49. Song HJ, Cho YG, Lee HJ. Dietary sodium intake and prevalence of overweight in adults. *Metabolism* 2013; 62(5): 703–8. doi: 10.1016/j.metabol.2012.11.009. PubMed PMID: 23357528; eng.
50. Kang YJ, Wang HW, Cheon SY, Lee HJ, Hwang KM, Yoon HS. Associations of obesity and dyslipidemia with intake of sodium, fat, and sugar among Koreans: a qualitative systematic review. *Clin Nutr Res* 2016; 5(4): 290–304. doi: 10.7762/cnr.2016.5.4.290. PubMed PMID:27812518; PubMed Central PMCID: PMCPMC 5093226.
51. Grimes CA, Riddell LJ, Campbell KJ, Nowson CA. Dietary salt intake, sugar-sweetened beverage consumption, and obesity risk. *Pediatrics* 2013; 131(1): 14–21. doi: 10.1542/peds.2012-1628. PubMed PMID:23230077.
52. He FJ, Markandu ND, Sagnella GA, et al. Effect of salt intake on renal excretion of water in humans. *Hypertension* 2001; 38(3): 317–20. PubMed PMID: 11566897; eng.
53. He FJ, Markandu ND, Sagnella GA, MacGregor GA. High salt intake: independent risk factor for obesity? *Hypertension*. 2015;66(4):843–9. doi: 10.1161/hypertensionaha.115.05948. eng.
54. Choi Y, Lee JE, Chang Y, Kim MK, Sung E, Shin H, et al. Dietary sodium and potassium intake in relation to non-alcoholic fatty liver disease. *Br J Nutr* 2016; 116(8): 1447–56. doi: 10.1017/S0007114516003391. PubMed PMID:27725000.
55. Drewnowski A, Maillot M, Rehm C. Reducing the sodium-potassium ratio in the US diet: a challenge for public health. *Am J Clin Nutr* 2012; 96(2): 439–44. doi: 10.3945/ajcn.111.025353. PubMed PMID:22760562PubMed Central PMCID: PMCPMC3396449.
56. Hope SF, Webster J, Trieu K, Pillay A, Ieremia M, Bell C, et al. A systematic review of economic evaluations of population-based sodium reduction interventions. *PLoS One* 2017; 12(3): e0173600. doi: 10.1371/journal.pone.0173600. PubMed PMID:28355231PubMed Central PMCID: PMCPMC5371286.
57. Webb M, Fahimi S, Singh GM, Khatibzadeh S, Micha R, Powles J, et al. Cost effectiveness of a government supported policy strategy to decrease sodium intake: global analysis across 183 nations. *BMJ* 2017; 356: i6699. doi: 10.1136/bmj.i6699. PubMed PMID:28073749PubMed Central PMCID: PMCPMC5225236 www.icmje.org/coi_disclosure.pdf and declare: financial support from the National Institutes of Health for the submitted work. DM reports ad hoc honorariums or consulting fees from Boston Heart Diagnostics, Haas Avocado Board, Astra Zeneca, GOED, DSM, and Life Sciences Research Organization, none of which were related to topics of dietary sodium. The other authors report no financial relationships with any organizations that might have an interest in the submitted work in the previous three years.
58. Institute of Medicine. *Strategies to Reduce Sodium Intake in the United States*. In: Henney JE, Taylor CL, Boon CS, eds. Washington, DC: The National Academies Press; 2010.
59. Rodan AR. Potassium: friend or foe? *Pediatr Nephrol* 2016; 32. doi: 10.1007/s00467-016-3411-8. PubMed PMID: 27194424; PubMed Central PMCID: PMCPMC5115995.
60. Panel on Dietary Reference Intakes for Electrolytes and Water SCotSEoDRI. Potassium. In: Food and Nutrition Board, ed. *Dietary reference intakes for water, potassium, sodium, chloride, and sulfate*. National Academy of Sciences, 2005, Washington DC. pp. 186–268.
61. Taylor EN, Stampfer MJ, Mount DB, Curhan GC. DASH-style diet and 24-hour urine composition. *Clin J Am Soc Nephrol* 2010; 5(12): 2315–22. doi: 10.2215/CJN.04420510. PubMed PMID:20847091PubMed Central PMCID: PMCPMC2994094.
62. Fearat C, Alles B, Merle B, Samieri C, Barberger-Gateau P. Adherence to a Mediterranean diet and energy, macro-, and micronutrient intakes in older persons. *J Physiol Biochem*

- 2012; 68(4): 691–700. doi: 10.1007/s13105-012-0190-y. PubMed PMID:22760695.
63. Faria AP, Albuquerque G, Moreira P, Rosário R, Araújo A, Teixeira V, et al. Association between energy density and diet cost in children. *Porto Biomed J.* 2016; 1(3): 106–11. doi: 10.1016/j.pbj.2016.08.005.
64. Drewnowski A, Rehm CD, Maillot M, Monsivais P. The relation of potassium and sodium intakes to diet cost among U.S. adults. *J Hum Hypertens* 2015; 29(1): 14–21. doi: 10.1038/jhh.2014.38. PubMed PMID:24871907PubMed Central PMCID: PMC4247818.
65. Albuquerque G, Moreira P, Rosário R, Araújo A, Teixeira VH, Lopesf O, et al. Adherence to the Mediterranean diet in children: Is it associated with economic cost? *Porto Biomed J* 2017; 2(4): 115–19. doi: 0.1016/j.pbj.2017.01.009.

***Pedro Moreira**

Faculdade de Ciências da Nutrição e Alimentação
Universidade do Porto Rua Roberto Frias, s/n PT-4200-465
Porto Portugal
Email: pedromoreira@fcna.up.pt

WWT

Mung bean proteins and peptides: nutritional, functional and bioactive properties

Zhu Yi-Shen^{1*}, Sun Shuai¹, Richard FitzGerald²

¹College of Biotechnology and Pharmaceutical Engineering, Nanjing Tech University, Nanjing, China; ²Life Science Department, University of Limerick, Limerick, Ireland

Abstract

To date, no extensive literature review exists regarding potential uses of mung bean proteins and peptides. As mung bean has long been widely used as a food source, early studies evaluated mung bean nutritional value against the Food and Agriculture Organization of the United Nations (FAO)/the World Health Organization (WHO) amino acids dietary recommendations. The comparison demonstrated mung bean to be a good protein source, except for deficiencies in sulphur-containing amino acids, methionine and cysteine. Methionine and cysteine residues have been introduced into the 8S globulin through protein engineering technology. Subsequently, purified mung bean proteins and peptides have facilitated the study of their structural and functional properties. Two main types of extraction methods have been reported for isolation of proteins and peptides from mung bean flours, permitting sequencing of major proteins present in mung bean, including albumins and globulins (notably 8S globulin). However, the sequence for albumin deposited in the UniProt database differs from other sequences reported in the literature. Meanwhile, a limited number of reports have revealed other useful bioactivities for proteins and hydrolysed peptides, including angiotensin-converting enzyme inhibitory activity, anti-fungal activity and trypsin inhibitory activity. Consequently, several mung bean hydrolysed peptides have served as effective food additives to prevent proteolysis during storage. Ultimately, further research will reveal other nutritional, functional and bioactive properties of mung bean for uses in diverse applications.

Keywords: *nutrition; protein extraction; functionality; globulins; angiotensin converting enzyme inhibitory activity; trypsin inhibitory activity; anti-fungal activity*

Many health organisations worldwide have recommended increased intake of plant-based foods to improve the prevention of chronic diseases and to improve overall human health. As a result, a variety of plant-based functional foods have been introduced into health care programmes (1). One such crop that has exhibited health benefits is mung bean [*Vigna radiata* (L.)], which is a summer pulse crop with a short growth cycle (70–90 days). It is a widely cultivated plant in many Asian countries as well as in dry regions of southern Europe and warmer parts of Canada and the United States. As an important plant-derived food resource (1), mung bean (2) is well known for its detoxification bioactivities. In addition, it has been used for treating numerous other conditions ranging from enhancement of human mental function to alleviation of heat stroke (3). The overall nutritional properties of mung beans have been recently reviewed by Dahiya et al. (4). Due to its high

nutritional value, (5) especially in seeds, mung bean has served as an important food/feed source for humans and animals. Mung bean seeds contain about 20.97–31.32% protein (6), compared to 18–22% (7) and 20–30% (8) for the protein content in soy and kidney beans, respectively. Moreover, protein content of mung bean seeds is about twofold higher than in the cereal seed maize, with a lower storage protein content (7 to 10%) (9) and significantly higher protein content than observed for conventional root crops (10).

Although high levels of proteins and amino acids in mung beans (11) are believed to be the main contributors to its nutritional content, a low methionine content and the presence of trypsin inhibitor (12) in mung bean seed are thought to be responsible for its low protein efficiency ratio (PER). Meanwhile, mung bean proteins and peptides have also been reported to possess angiotensin-converting enzyme (ACE) inhibitory activity, as well as

anti-fungal and/or antibacterial activities (3). Although major past use of mung bean seeds has been as a food resource, more recently mung bean extracts, especially protein and peptide isolates, have gained increasing attention for additional diverse applications.

Nutritional properties of the mung bean proteins

As mentioned above, mung bean seeds are particularly rich in protein, containing about 20.97–31.32% protein content (6). Mubarak (13) reported a chemical score of 76% for mung bean amino acids, which was calculated based on the Food and Agriculture Organisation of the United Nations (FAO)/the World Health Organisation (WHO) (14) guidelines. Therefore, due to its high protein content and digestibility, consumption of mung bean seeds in combination with cereals has been recommended to significantly increase the quality of protein intake as part of a vegetarian diet (3). To characterise this nutritional content more specifically, Kudre et al. (10) analysed the protein composition of isolates from mung bean seeds. The total protein content in mung bean protein isolates (MBPI) was 87.8%, with a total amino acid content of 800.2 mg g⁻¹ (Table 1). Essential amino acids constituted 43.5% of total amino acids in MBPI, whereas sulphur-containing amino acids constituted approximately 1.6% of total MBPI amino acids.

Specifically, the essential amino acids such as leucine, lysine and phenylalanine/tyrosine were predominant,

followed by valine, isoleucine and histidine (Table 1). In addition, the aromatic amino acid content of MBPI was 12.1%, in which phenylalanine and tyrosine constitutes 11.3% (90.3 of 800.2 mg g⁻¹). Indeed, the total essential amino acid content of MBPI exceeds the FAO/WHO recommendations (15). Conversely, values for threonine, tryptophan and total sulphur-containing amino acids (methionine and cysteine) were nutritionally inadequate (Table 1).

The protein content of mung bean has been reported to be negatively correlated with the content of lysine and threonine (4), whereas the latter has been positively correlated with methionine content. These results suggest that increase in methionine content is accompanied by decreased total protein content in mung bean. Therefore, the reverse scenario of high protein content in mung bean seed probably reflects low methionine content (16, 17). In addition, low levels of threonine, tryptophan and sulphur-containing amino acids (methionine and cysteine), compared to the FAO/WHO recommended values (Table 1), were reported in MBPI. However, Khalil (18) reported that the threonine content was 140.88% of the value provided by the FAO/WHO, as compared to 83.53% reported by Kudre et al. (10).

Although mung bean seeds are rich in protein, the deficiency in the sulphur-containing amino acids (methionine and cysteine) places the nutritional quality of mung bean seeds on par with other legumes (19). To address

Table 1. Amino acids in mung bean protein isolates with levels comparing the ones adapted from FAO/WHO (15) guidelines: (10)]

MBPI levels	Amino acids	MBPI (mg g ⁻¹)	FAO/WHO (mg g ⁻¹)
Overview	Total amino acids	800.2	
	Total essential amino acids	348.2 (43.51%) ^a	
	Total aromatic amino acids	96.7 (12.08%) ^a	
	Total sulfur amino acids	13.0 (1.62%) ^a	
Higher levels	Phenylalanine + Tyrosine	90.3	63
	Leucine	74	66
	Lysine	62.4	58
	Valine	46.3	35
	Isoleucine	39.1	28
	Histidine	27.9	19
Lower levels	Threonine	28.4	34
	Methionine + cysteine	13	25
	Tryptophan	6.4	11
Not mentioned by the FAO/WHO	Glutamic acid/glutamine	125.4	
	Aspartic acid/asparagine	85.3	
	Arginine	64.4	
	Serine	38.5	
	Alanine	36.6	
	Glycine	32.2	
	Proline	30	

MBPI, mung bean protein isolates.

^aPercent of amino acids, relative to total amino acids in MBPI.

the lack of sulphur-containing amino acids, methionine was successfully introduced into 8S α globulin, a major mung bean protein, using protein engineering (20). Consequently, the nutritional quality of the modified protein containing increased methionine in terms of amino acid score improved from 41 to 145%. In a similar vein, Torio et al. (11) reported another protein engineering method that introduced free sulfhydryl groups and disulphide bonds to generate cysteine-modified mung bean 8S α globulin to improve nutritional quality.

Meanwhile, the presence of hydrophobic amino acids has been reported to contribute greatly to the thermal and/or conformational stability of globulins to boost yield (10). Consequently, hydrophobic amino acid content increased to 53.1% in MBPI after substitution of charged amino acids with hydrophobic amino acids.

In addition to the amino acids evaluated using FAO/WHO (15) guidelines mentioned above, other important amino acids omitted from the guidelines should also be mentioned (Table 1). Three of these, glutamic acid, glutamine and arginine, are abundant in mung bean seeds and are thought to be important for brain development, exhibiting neuro-protective functions in infants (21). In addition, dietary glutamine can improve gastrointestinal barrier integrity by reducing systemic infections, and by stimulating lymphocyte proliferation, monocyte function and T cell 1 helper cytokine responses that may improve brain growth. Glutamine can also reduce systemic inflammation by decreasing the production of pro-inflammatory cytokines (IL-8 and IL-6). Arginine also has some benefits and has been shown to increase cerebral blood flow and increase nitric oxide production to help decrease necrotising enterocolitis incidence.

As mentioned above, non-genetically engineered mung bean proteins contain adequate amounts of most essential amino acids, with the exception of the sulphur-containing

amino acids (methionine and cysteine). Methionine and cysteine have previously been obtained dietarily by sulphur-containing amino acids but deficient in lysine (4). A 7:3 ratio of rice protein has been recommended as an optimal ratio for consumption (22).

Mung bean seed proteins

Mung bean seeds are rich in storage proteins, which account for about 85% of total protein (9). The crop's major seed storage proteins include albumins, globulins and prolamins, which are soluble in water, in dilute saline and in alcohol–water mixtures, respectively (23). Globulin and albumin, which make up over 60 and 25% of total mung bean protein, respectively, represent the main mung bean storage proteins. Prolamin, however, has not yet been isolated and characterised from mung bean. Aside from these major proteins, components comprising the other 15% of mung bean protein components have not yet been extensively studied to date, except for trypsin inhibitor (24), non-specific lipid transfer proteins (nsLTP) (25) and thiamine-binding proteins (26) (Table 2).

Three types of globulins present in mung bean seed have been characterised and are designated as basic-type (7S), vicilin-type (8S) and legumin-type (11S) globulins (5, 27), comprising 3.4%, 89.0% (5, 27) and 7.6% (w/w) of total mung bean globulin content, respectively (27).

In mature seeds, the major storage protein is 8S globulin, which is the most reported globulin in mung bean proteins (28). No disulphide linkages exist in 8S globulin, due to the lack of cysteine content (19, 27, 29). The 8S globulin consists of four subunits with molecular masses ranging from 26 to 60 kDa, as observed using SDS-PAGE analysis (16, 27, 29). Mendoza et al. (27) has determined the N-terminal amino acid sequences of the four mung bean 8S globulin subunits, which are EDKEEQ (60 kDa), IDAAEVSVSRGKNNPFYFNN (48 kDa),

Table 2. The composition of major protein fractions and individual protein components in mung bean [*Vigna radiata* (L.)]

Types	Proteins	Subunits	Molecular weight
Storage proteins [85% (9) in overall proteins]	Globulins [60% (9) in overall proteins]	Globulin 7S	28kD (27)
			16kD (27)
			8S α 5.2kD (19)
		Globulin 8S	8S α ' 5.2kD (19)
			8S β 5.2kD (19)
		Albumin [25% (9) in overall proteins]	Globulin 11S
24kD (27)			
Other proteins (15% in overall proteins)	Trypsin inhibitor		14kD (24)
		Non-specific lipid transfer peptide (nsLTP)	9.03kD (25)
		Thiamine-binding proteins (TBP)	72.6kD (26)
		Others	

SKTLSSQNEPFLRLN (32 kDa) and IDGAEVSVSRGKNNP (26 kDa).

Three highly conserved isoforms of the 8S globulin have been classified as 8S α (UniProt ID: B1NPN8_VIGRA), 8S α' (UniProt ID: Q198W4_VIGRA) and 8S β (UniProt ID: Q198W3_VIGRA) (9, 19). Bernardo et al. (19) studied the amino acid sequence homologies of these three isoforms, which were found to be 91–92% between 8S α and 8S α' , 87% between 8S α and 8S β , and 86–88% between 8S α' and 8S β . Another study showed, using the SignalP website server (30), that 8S α , 8S α' and 8S β signal peptide sequences mapped to residues 1–25, 1–24 or 1–25, and 1–23, respectively.

The detailed structure of 8S α globulin has been reported to consist of three subunits, each subunit containing two modules. X-ray crystallographic analysis has demonstrated that each module consists of a β -barrel domain and an extended loop domain (5). The overall 8S α globulin structure exhibits 68% sequence identity and structural similarity (a root-mean-square deviation of 0.6 Å) with soybean β -conglycinin β (soybean 7S globulin), and both proteins share surface hydrophobicity characteristics. However, analysis of cavity size and other structural features derived from the mung bean 8S α globulin crystal structure suggests that the thermal stability of 8S α globulin is lower than that of soybean β -conglycinin β .

Methionine and cysteine residues have been introduced into the 8S α globulin through protein engineering. Analysis of the methionine-modified mung bean protein, which can possess up to 10 additional methionine residues (20), indicates that the modified 8S α globulin exhibits improved structural stability versus the wild-type protein, as assessed by differential scanning calorimetry (DSC). Notably, no allergenic potential has been identified in either wild-type or modified protein. Meanwhile, a report by Torio et al. (11) demonstrated improved structural stability and improved heat-induced gelation properties for cysteine-modified mung bean 8S α globulin versus wild-type protein.

To our knowledge, only a limited number of reports covering the characteristics of mung bean 7S and 11S globulins exist. Mendoza et al. (27) used SDS-PAGE to show that the two bands yielded from 11S globulin were of 40 kDa and 24 kDa in size, whereas the two bands yielded from 7S globulin were of 28 kDa and 16 kDa in size. The N-terminal amino acid sequences for these four bands were determined to be NYVMN-PAYVLMKPTQKDAAL (for the 28 kDa subunit) and STTVGHSGTMMIST (for the 16 kDa subunit) of 7S globulin and SSSSTNNRF [for the 40 kDa acidic subunit (29)] and GLEETIXSSK [for the 24 kDa basic subunit (29)] for the 11S globulin. The presence of disulphide bridges in these 7S and 11S globulins was demonstrated using SDS-PAGE with and without β -mercaptoethanol. The 7S and 11S globulins each exhibited only one band in

the absence of β -mercaptoethanol, but two bands in the presence of the reducing agent. Meanwhile, mung bean globulins possessing higher 11S to 7S globulin ratios were reported to exhibit improved functionalities, for example, solubility and emulsifying activities (29).

Research on mung bean storage proteins has also provided information about this major group of globulins. In one study, Ericson et al. (16) used sucrose gradient centrifugation to show that 8S and 11S globulins account for approximately 85 and 15% of total globulins, respectively. In addition, the acidic nature of 11S globulins was shown to be less pronounced than that of 8S globulins, due to the greater relative prevalence of disulphide bridges between individual acidic and basic polypeptides in 11S versus 8S globulins (29).

Only a limited number of studies have been carried out regarding mung bean albumin, resulting in deposition of only one albumin sequence in the UniProt database (mung bean seed albumin, UniProt ID: Q43680_VIGRR). However, the reference cited for that entry was not accepted by *Plant Molecular Biology*. Another mung bean albumin sequence in the UniProt database (albumin 1, UniProt ID: ALB1_VIGRR) does not match with the mung bean sequence reported by Yamazaki et al. (31), the reference cited in the UniProt sequence database.

Functional properties of MBPI

Functional properties of proteins play a significant role as additives for food processing applications. Therefore, it is necessary to study the physicochemical characteristics of MBPI as food ingredients (32). Recently, several reports have been published regarding functional properties of mung bean proteins (33–35), including protein solubility, water absorption capacity (WAC), oil absorption capacity (OAC), foaming capacity (FC) and foam stability (FS), emulsifying activity (EA) and emulsifying stability (ES), and thermal properties. Consequently, such protein or peptide properties can improve the functionality of food processing applications; for example, the emulsifying property of the protein helps to stabilise emulsions, beverages or foams to prolong food shelf life (33). Functional improvements by MBPI would make it more applicable as food supplements.

1. Protein solubility

Solubility is considered as an important functional property of proteins, because it acts as a vital factor of the sensory quality attributes of foods (36). This property is the thermodynamic index of the equilibrium between protein–protein and protein–solvent interactions. Variations in factors, such as temperature, pH, ion strength, freezing, heating and drying, lead to changes in proteins' structural conformations, which in turn affect protein functionality (37). Additionally, pH value is an important

index of protein solubility to determine the behaviour of protein isolate in food process.

Due to electrostatic repulsion and hydration, the solubility of MBPI had been higher at pH values of 2, 10 and 12 than that of other pH values; for example, at pH 4, the lowest solubility was observed and aggregation occurs (38). Du et al. (35) determined that the minimum solubility of MBPI appeared at pH 4.6, which is the isoelectric point. The protein solubility of untreated MBPI was improved by additional heating from 61.5 to 65.6%, which is attributed to increases in charged residues on the MBPI surface, as a result of protein denaturation and/or unfolding (32). Butt and Batool (39) reported that protein solubility of MBPI was 72% at pH 7. Kudre et al. (10) determined maximum protein solubility of MBPI as 70.6% at pH 10 (Table 3). They also demonstrated that solubility of MBPI could be improved with the aid of NaCl at an appropriate concentration. Liu et al. (33) demonstrated that the solubility of mung bean 8S globulin ranged from 51.59 to 74.33%, with an average of 64.21%.

2. WAC and OAC

WAC or OAC is defined as the absorbed amount of water or fat per gram of protein, as protein has both hydrophilic and hydrophobic properties to interact with water and oil in foods. WAC is a useful indication to predict moisture loss if protein isolates can be incorporated into various food products. And OAC can reflect the hydrophobic capacity of protein. A strong negative correlation was found between WAC and OAC (33).

Brishti et al. (38) determined that the WAC and OAC of MBPI were 3.33 g g⁻¹ and 3.00 g g⁻¹ proteins, respectively. The results imply that MBPI could contribute to the improvement of textural and sensory qualities during processing of fabricated foods because of the proteins capability of retaining water and reducing interfacial tension in an emulsion system. However, Du et al. (35) measured that the highest WAC was 2.62 mL g⁻¹, and the OAC was from 9.5 to 10.5 g g⁻¹ except at the protein concentration of 1.5%. Butt and Batool (39) reported that WAC and OAC of MBPI were 163 and 113%, respectively (Table 3). In these three reports, similar preparation procedures of MBPI were applied as base extraction and acid precipitation. Liu et al. (33) determined that average WAC and OAC of mung bean 8S globulin were 1.92 g g⁻¹ and 3.07 mL g⁻¹, respectively. The varied values of WAC might be due to the protein structure and amount of polar amino acids, whereas the OAC difference might be due to the difference in nonpolar side chains binding the oil.

3. FC and FS

Foamability depends on air-liquid interface hydrophobicity, flexibility of protein molecules, protein solubility and denaturability (40). FC describes the stabilising

Table 3. Functional properties of mung bean protein isolates

	Protein solubility (%)	Water absorption capacity	Oil absorption capacity	Emulsion activity (%)	Emulsion stability (%)	Foam capacity (v/v, %)	Foam stability (v/v, %)	thermal properties	References
MBPI	—	3.33 ± 0.57 g g ⁻¹	3.00 ± 0.00 g g ⁻¹	63.18 ± 0.38 ^a 72.03 ± 0.53 ^b	62.75 ± 0.43 ^a 66.50 ± 1.37 ^b	89.66 ± 0.57	80.83 ± 1.04 ^c	157.90 ± 0.17°C ^d	(38)
MBPI	—	2.62 ml g ⁻¹	10.5	—	—	26	76.9	—	(35)
MBPI	61.6 ± 1.5/65.6 ± 2.1 ^e	—	—	—	—	—	—	100.8 ± 1.1°C ^d	(32)
MBPI	70.6	—	—	—	—	—	—	—	(10)
MBPI	72 ± 4.44	163 ± 10.05%	113 ± 6.84%	41.10 ± 1.87	21.00 ± 1.29	110 ± 6.78	58 ± 3.58	—	(39)
Globulins	92–99	—	—	90–120	—	—	—	80.8–83.0°C ^d	(29)
8S globulin	51–75	1.37–2.14 g g ⁻¹	1.90–3.84 g g ⁻¹	1.54–5.55	45–78	47–106	39–97	—	(33)

MBPI, mung bean protein isolates.

^a In distilled water; ^b in 3% NaCl; ^c after 15 min; ^d denaturation peak temperature; ^e untreated/heated.

ability of proteins by the amount of interfacial area per unit weight or concentration, and is related to molecular flexibility, charge density and hydrophobicity. And FS is the stabilising ability of proteins to the foam against gravitational and mechanical stresses as the effectiveness of whipping agents relies on their capability to preserve the whip as long as possible, which is affected by rheological properties of protein films, film elasticity and the magnitude of disjoining pressure between the protein layers (40).

Brishti et al. (38) reported that FC and FS of MBPI were 89.66 and 80.83% after 15 min of standing time, respectively. Butt and Batool (39) reported that FC and FS of MBPI were 110 and 58%, respectively. Due to different blending methods and different concentrations of MBPI, Du et al. (35) reported MBPI with 26% FC and 76.9% FS after 10 min of standing time, respectively (Table 3). This lower FC value might be caused by the high levels of hydrophobic amino acids after homogenisation at 10,000 rpm for 1 min. On the contrary, high FS could be due to the formation of a cohesive continuous network with high elasticity by MBPI, which shows optimum intermolecular interactions and creates stable foams at the air-liquid interface. Liu et al. (33) found significant positive correlation between FC and FS of mung bean 8S globulin with average 69.63% FC and 61.61% FS, respectively.

4. EA and ES

Emulsifying properties of proteins are also affected by the adsorption ratio of protein at the oil-water interface, the adsorbed amount of protein, interfacial rearrangement of conformation, the reduction degree in interfacial tension and formation of cohesive film (40). In a stabilised solution, EA represents the maximum interfacial area per unit weight of protein, and ES is the measure of the steadiness of emulsion formed by protein.

In 3% NaCl and in distilled water, EA and ES of MBPI were found to be 72.03 and 63.18, and 66.50 and 62.75%, respectively (38) (Table 3). Butt and Batool (39) reported that EA and ES of MBPI was 41.10 and 21%, respectively (Table 3). Liu et al. (33) determined that average EA index and ES of mung bean 8S globulin from different mung bean cultivars were 3.46 m² g⁻¹ and 63.15%, respectively. In chopped and fabricated meat-based products, EA and ES are critical factors. Since EA and ES of MBPI had been rather high comparing to other legumes (38), MBPI can be applied in both formation and stabilisation of fluid emulsion during the production of heat-treated textured vegetable proteins.

5. Thermal properties

The thermal properties of proteins, for example, denaturation of proteins, are often determined as an endothermic

peak on the thermogram by DSC (41). Brishti et al. (38) reported that the denaturation temperature of MBPI was at 157.90°C, which is a transition temperature accompanied by rupture of intramolecular bonds when MBPI are heated from native to denatured state. Tang et al. (29) determined that the denaturation temperature of mung bean globulins was from 80.8 to 83.0°C (Table 3). Tang et al. (40) found that disulphide bonds within the protein molecule contribute to the thermal stability of protein. Kudre et al. (10) stated that the high thermal stability attribute could be due to the disulphide bonds, whereas the presence of salt bridges in the hydrophobic clefts of protein structure makes it more thermostable. In the process of optimisation of temperature, such as extrusion and heat treatment, the analysis of thermal properties of MBPI serves as an important tool.

Extraction of mung bean proteins and peptides

Extraction of mung bean proteins has been widely studied. As a key step in mung bean protein research, many methods of protein extraction have been established. These methods are classified into two types, salt extraction methods and methods consisting of base extraction and acid precipitation. In order to isolate specific mung bean proteins, additional steps have been added to separation procedures, for example, heat treatment and Sephadex G-50 separation were used as additional steps for trypsin inhibitor isolation (24).

1. Salt extraction method

Johns et al. (42) reported an extraction method using a saturated ammonium sulphate solution. Mung bean proteins have also been extracted in 5% NaCl solutions, which was the optimum NaCl concentration to achieve a maximum total protein dissolution of 87.5%. Globulins have also been precipitated using saturated ammonium sulphate solution with concentrations of 20 and 65% for precipitating α -globulin and β -globulin, respectively, after which albumin was recovered from the dialysed supernatant liquid and isolated by coagulation. The yields of α -globulin and β -globulin were 0.35 and 5.75% (w/w), respectively, based on the dry weight of mung bean flour extracted, whereas the albumin yield ranged from 0.02 to 0.05% (w/w) of dry flour weight.

Using a different strategy, Rahma et al. (43) used a salt extraction method involving micellisation of mung bean proteins from a 0.5 mol L⁻¹ sodium chloride water solution. The procedure consisted of extraction, centrifugation, filtration and micellisation steps. The micellised protein was separated by centrifugation, washed with water and redissolved at pH 7 by addition of sodium hydroxide. Basic 7S globulin was subsequently found to be easily extracted with 0.15 mol L⁻¹ NaCl, whereas 11S globulin was extracted using 0.35 mol L⁻¹ NaCl.

2. The method of base extraction and acid precipitation

Rahma et al. (43) also established a method of base extraction and acid precipitation, and compared it to the salt extraction method outlined above. Briefly, the procedure included alkaline water extraction at pH 8 (using a flour to water ratio of 1:20 w/v) followed by isoelectric precipitation at pH 4.5, washing, re-dissolution at pH 7 using 0.1 mol L⁻¹ sodium hydroxide and centrifugation. Ultimately, 7S globulin, a predominant storage protein, was isolated using this method and 11S globulin was also isolated and determined to be a disulphide-linked polypeptide chain.

Comparative analysis suggested that the salt extraction method was much better for enrichment of the 7S globulin. Meanwhile, Thompson et al. (12) reported another method of base extraction and acid precipitation for the preparation of MBPIs. Numerous parameters, including pH, temperature, extraction time and ratio of mung bean flour to solvent, were optimised to increase the yield of protein extracted from mung bean flour. The highest yield of mung bean protein was achieved with the following optimised parameters: extraction at pH 9 at 25°C for 20 min with a 1:15 ratio of mung bean flour to solvent, followed by precipitation at pH 4. Subsequently, Kudre et al. (10) and El-Adawy (44) reported similar methods for MBPI whereby mung bean seed flour was extracted with NaOH (pH 12) or 0.1 mol L⁻¹ NaOH (pH 9), respectively. Next, both extractions were precipitated with HCl (pH 4.5), followed by centrifugation and washing. Kudre et al. obtained approximately 87.8% of MBPI from dry mung bean seeds, whereas El-Adawy reported an average yield of 13 g protein/100 g mung bean flour.

In addition, other methods incorporating additional steps have been used to isolate specific bioactive proteins, such as trypsin inhibitor protein (24) and nsLTP (25). Klomklao et al. (24) found that the highest trypsin inhibitor activity of 822.63 unit g⁻¹ seed and specific trypsin inhibitor activity of 31.95 unit mg⁻¹ protein were obtained using distilled water extraction. Moreover, certain salt and alkaline conditions were observed to increase protein solubility, leading to a reduction in specific trypsin inhibitor activity [as observed in other studies of other legumes (45–47)]. Subsequently, a final specific inhibitory activity of 406 unit mg⁻¹ protein was achieved after heat treatment, ammonium sulphate precipitation (30–65%) and Sephadex G-50 isolation. Ultimately, trypsin inhibitor activity was higher by about 13-fold compared to crude extract, with a yield of purified trypsin inhibitor from the extract of 30.25%. Meanwhile, Wang et al. (25) extracted anti-fungal nsLTP from ammonium sulphate precipitates coupled with purification using both CM-Sephadex C-50 and POROS-HS chromatography to isolate purified nsLTP, yielding 13 mg nsLTP from 100 g mung bean seeds.

Bioactivities of mung bean proteins and peptides

Many different kinds of bioactive proteins and peptides have been reported from mung bean seeds. These proteins and peptides exhibit bioactivities, which may be beneficial to human beings and animals, including ACE inhibitors, trypsin inhibitor and anti-fungal agents.

1. ACE inhibitory activity

Several diverse biological pathways are known to regulate blood pressure in living organisms. One pathway, the renin-angiotensin system, has been demonstrated to be acted upon by hypotensive peptides (31). Within the renin-angiotensin system, conversion of angiotensinogen to the pre-hypertensive hormone angiotensin I (DRVYIHPFHL) occurs through the action of renin secreted by the kidneys. Angiotensin I is further converted by ACE to angiotensin II (DRVYIHPF), which is the active form of the hormone, by ACE. Angiotensin II raises blood pressure by acting directly on blood vessels, sympathetic nerves and adrenal glands (48). Inhibition of ACE by ACE inhibitors is a strategy used to control hypertension.

ACE inhibitory activity is one of the main bioactivities reported for plant food-derived peptides (49). Aluko (50) reported that hydrolysed proteins from three legume sources, including mung bean, could provide ACE inhibitory activity. Indeed, food-derived ACE inhibitory peptides may be an alternative to synthetic drugs, since peptides are thought to cause fewer side effects (51). Consequently, Li et al. (52) have demonstrated that MBPI hydrolysed by Alcalase™ showed ACE inhibitory activity at a half maximal inhibitory concentration (IC₅₀) of 0.64 mg protein mL⁻¹. Using this method, the highest ACE inhibitory activity (53) was observed for a hydrolysate generated by Alcalase™ after 2 h of hydrolysis.

Meanwhile, another study demonstrated that a significant decrease in systolic blood pressure was observed in spontaneously hypertensive rats after ingestion of hydrolysed mung bean peptides. More recently, Li et al. (54) isolated three antihypertensive peptides from an Alcalase™-hydrolysed mung bean preparation using Sephadex G-15 and reverse-phase high-performance liquid chromatography (RP-HPLC) purification steps. The three peptides were identified by amino acid composition analysis and matrix-assisted-laser desorption/ionisation time-of-flight tandem mass spectrometry (MALDI-TOF MS/MS), as KDYRL, VTPALR and KLPAGTLF, with IC₅₀ values of 26.5, 82.4 and 13.4 μM, respectively. Concurrently, using a different strategy, *Lactobacillus plantarum* B1-6-fermented mung bean milk was shown to produce significantly higher ACE inhibitory activity (67.5%) at the end of fermentation. Production of inhibitory peptides coincided with the disappearance of larger/more hydrophobic peptides with the appearance of increasing

amounts of smaller/more hydrophilic peptides using RP-HPLC (55).

Using a different strategy, Mamilla et al. (56) compared mung bean grain and germinated seeds for ACE inhibitors using an *in vitro* ACE inhibition assay. Protein hydrolysates of germinated mung bean seeds showed greater than 82% ACE inhibition, reaching an IC₅₀ value of 0.025 mg mL⁻¹. However, the activities of ACE inhibitory peptides *in vitro* based on chemical tests are not always mirrored by their hypotensive effect *in vivo* on animal studies (57). Therefore, most of the presented studies should be treated with great caution due to the general poor correlation between *in vitro* biochemical assays on ACE and physiological responses *in vivo*. After all, many of the peptides, which show good activity *in vitro*, are degraded in the GI system, hence, explaining the unreliability of the assay results.

2. Trypsin inhibitory activity

Proteinase inhibitors, especially food-additive grade inhibitors, are in demand for protecting myofibrillar proteins from proteolysis by endogenous proteinases. Such inhibitors from legume sources, which generally inhibit trypsin, are safe, effective, thermally stable and inexpensive (10). For example, due to their inhibitory ability toward proteinases, trypsin inhibitors from legume seeds have been used for prevention of softening of mince or surimi gel mediated by heat-activated proteinases that are abundant in fish muscle or surimi (58). Subsequently, Sun et al. (59) reported that mung bean trypsin inhibitor additives were effective in preventing softening of surimi gel from marine fish blue scad. The fact that trypsin inhibitors from mung bean seeds are safe and effective in inhibiting trypsin activity suggests that their use as ingredients in drug formulations may prevent trypsin hydrolysis during drug administration.

Studies of purified mung bean trypsin inhibitor are beginning to shed light on this protein's specific functions. In one study, Chrispeels et al. (60) reported trypsin inhibitory activity from the mung bean seed extracts prepared by a method of base extraction and acid precipitation followed by trypsin-sepharose affinity chromatography. They found that the purified trypsin inhibitor was not a double-headed inhibitor containing inhibitory sites for both trypsin and chymotrypsin, as observed in soybean trypsin inhibitor (61). Moreover, an aliquot (2.5 µl) of the purified trypsin inhibitor solution corresponding to one unit of trypsin activity did not inhibit vicilin peptidohydrolase, the major endopeptidase in the cotyledons of mung bean seedlings. In another study, Lorensen et al. (62) reported that six species of trypsin inhibitors, one major (F) and five minor inhibitor species (A–E), were observed in mung bean seeds, with overall trypsin inhibitory activity reported to be equivalent to 1.8 U g⁻¹ of dry

seed weight. More recently, Wilson et al. (63) determined the sequences of trypsin inhibitors C, E, F using a combination of automatic solid-phase and manual sequencing techniques. Analysis of trypsin inhibitor F showed that it contains 80 amino acid residues and exhibits a high degree of identity with the other sequenced members of the Bowman-Birk family of protease inhibitors. Trypsin inhibitors E, E' and C are derived from inhibitor F by limited specific proteolysis. Notably, the majority cleavage sites noted in the F–E–C–E' inhibitors were found to occur at peptide bonds involving aspartyl residues. Currently, two sequences of trypsin inhibitors are reported in the UniProt Database (<http://www.uniprot.org/>), that is, Bowman-Birk trypsin inhibitor (UniProt ID: IBB_VIGRR) and trypsin inhibitor (UniProt ID: Q1WA44_VIGRA). High conservation of these sequences related to other trypsin inhibitors has been reported (Table 4).

3. Anti-fungal and/or antibacterial activities

The anti-fungal and antibacterial protein, nsLTP (a basic, 9.03 kDa protein), which displays anti-pathogenic activity, has been isolated from the mung bean (*Vigna radiata*) seeds (25). The nsLTP protein is able to bind and transfer a variety of very diverse lipids between membranes *in vitro* (48). The N-terminal sequence of nsLTP was determined to be MTCGQVQGNL AQCIGFLEKG G. It exerts anti-fungal action toward *Fusarium solani*, *Fusarium oxysporum*, *Pythium aphanidermatum* and *Sclerotium rolfsii* and antibacterial action against *Staphylococcus aureus*, but not *Salmonella typhimurium*. The lipid-binding ability of the protein is very similar to that of previously described lipid transfer proteins extracted from wheat and maize seeds, indicating that it possesses lipid transfer activity (64).

Ye et al. (65) isolated an anti-fungal protein, mungin, from mung bean (*Vigna radiata*) seeds. Interestingly, mungin, an 18 kDa protein, possesses a novel N-terminal sequence homologous to cyclophilins. The N-terminal sequence of mungin is PNPKVFFDMT IGGQPAGKIV FELFADTTTPR TAENFRALTT GEKGVSRGRK PL-HYHGSIFH R. Mungin was shown to have anti-fungal activity against *Rhizoctonia solani*, *Coprinus comatus* and

Table 4. The sequences of the mung bean trypsin inhibitors reported in UniProt database

UniProt ID	UniProt sequence
IBB_VIGRR	SHDEPSESSE PCCDSCDCTK SIPPECHCAN IRLNSCHSAC KSCICTRSMP GKCRCLD TDD FCYKPCESMD KD
Q1WA44_VIGRA	MMVLKVCVLV VFLVGVTTAG MDLNLQRSSH HHDSSEPSE SSEPCCDSCR CTKSIPPQCH CADIRLNSCH SACKSCMCTR SMPGKCRCLD TDDFCYKPCESMDKDDD

Botrytis cinerea and to a lesser extent on *Mycosphaerella arachidicola* and *Fusarium oxysporum*. Mungin also displayed inhibitory activity against α - and β -glucosidases but not against HIV-1 reverse transcriptase and β -glucuronidase. It is noteworthy that mungin, as a cyclophilin-like anti-fungal protein, also exhibited anti-mitogenic activity (66).

Conclusion

MBPI have been reported to possess a nutritional-balanced amino acid composition using recommended FAO/WHO guidelines, with the exception of a deficiency in except sulphur-containing amino acids. However, protein engineering technology has been applied to introduce additional methionine and cysteine residues into mung bean 8S globulin to boost the methionine percentage from 41 to 145%. In a similar way, a free sulfhydryl group (cysteine residue) was introduced and the presence of a new disulphide bond was confirmed in cysteine-modified globulin.

The functional properties of MBPI, that is, protein solubility, WAC, OAC, FC and FS, EA and ES, and thermal properties, are useful properties for food-processing applications. Studies on MBPI functionality have been carried out for the development of food industry applications.

Extraction methods have allowed purification of several mung bean proteins and peptides from mung bean flour, paving the way for functional analyses. Extraction methods that alter the ionic environment, combined with alkaline extraction and acid precipitation, have been used most often. Notably, varies extraction ratios of various mung bean proteins can be obtained using various strategies. Globulins, the major proteins present in mung beans, account for about 85% of total protein. The sub-unit structure, N-terminal amino acid sequence, structure and homology amongst the three distinct isoforms of 8Sa globulin have been described in detail. However, the reports on mung bean albumins need to be clarified.

In addition, bioactive proteins and peptides hold special interest due to their potential health benefits in addition to their known nutritional functions. Specifically, ACE inhibitor and anti-fungal activities of mung bean protein hydrolysates and peptides have medical use, whereas trypsin inhibitors in mung bean protein fractions may serve as additive for preventing food proteolysis. Therefore, mung bean proteins and their hydrolysates hold great promise as sources of compounds with significant nutritional, functional and bioactive potential uses in foods, pharmaceuticals, other products and processes.

Acknowledgements

This study was part of a project funded by the Priority Academic Program Development of Jiangsu Higher Education Institutions, China, and was supported by China Scholarship Council.

Conflict of interest and funding

The authors have not received any funding or benefits from industry or elsewhere to conduct this study.

References

1. Espin JC, Garcia-Conesa MT, Tomas-Barberan FA. Nutraceuticals: facts and fiction. *Phytochemistry* 2007; 68(22–24): 2986–3008. doi: 10.1016/j.phytochem.2007.09.014. PubMed PMID: 17976666.
2. Del Rosario RR, Flores DM. Functional properties of four types of mung bean flour. *J Sci Food Agr* 1981; 32(2): 175–80. doi: 10.1002/jfsa.2740320213.
3. Tang D, Dong Y, Ren H, Li L, He C, et al. A review of phytochemistry, metabolite changes, and medicinal uses of the common food mung bean and its sprouts (*Vigna radiata*). *Chem Central J* 2014; 8: 4. doi: 10.1186/1752-153x-8-4. PubMed PMID: WOS:000334627400001.
4. Dahiya PK, Linnemann AR, Van Boekel MA, Khetarpaul N, Grewal RB, Nout MJ. Mung bean: technological and nutritional potential. *Crit Rev Food Sci Nutr* 2015; 55(5): 670–88. doi: 10.1080/10408398.2012.671202. PubMed PMID: 24915360.
5. Itoh T, Garcia RN, Adachi M, Maruyama Y, Tecson-Mendoza EM, Mikami B, et al. Structure of 8Sa globulin, the major seed storage protein of mung bean. *Acta Crystallogr D Biol Crystallogr* 2006; 62(7): 824–32. doi: 10.1107/s090744490601804x.
6. Anwar F, Latif S, Przybylski R, Sultana B, Ashraf M. Chemical composition and antioxidant activity of seeds of different cultivars of mung bean. *J Food Sci* 2007; 72(7): S503–10. doi: 10.1111/j.1750-3841.2007.00462.x. PubMed PMID: 17995664.
7. Xu XP, Liu H, Tian LH, Dong XB, Shen SH, Qu LQ. Integrated and comparative proteomics of high-oil and high-protein soybean seeds. *Food Chem* 2015; 172: 105–16. doi: 10.1016/j.foodchem.2014.09.035. PubMed PMID: WOS:000345207200015.
8. Shevkani K, Singh N, Kaur A, Rana JC. Structural and functional characterization of kidney bean and field pea protein isolates: a comparative study. *Food Hydrocolloids* 2015; 43: 679–89. doi: 10.1016/j.foodhyd.2014.07.024. PubMed PMID: WOS:000345683500078.
9. Chen M-X, Zheng S-X, Yang Y-N, Xu C, Liu J-S, Yang W-D, et al. Strong seed-specific protein expression from the *Vigna radiata* storage protein 8SG alpha promoter in transgenic *Arabidopsis* seeds. *J Biotechnol* 2014; 174: 49–56. doi: 10.1016/j.jbiotec.2014.01.027. PubMed PMID: WOS:000333089700010.
10. Kudre TG, Benjakul S, Kishimura H. Comparative study on chemical compositions and properties of protein isolates from mung bean, black bean and bambara groundnut. *J Sci Food Agr* 2013; 93(10): 2429–36. doi: 10.1002/jfsa.6052.
11. Torio MAO, Itoh T, Garcia RN, Maruyama N, Utsumi S, Tecson-Mendoza EM. Introduction of sulfhydryl groups and disulfide linkage to mungbean 8Sa globulin and effects on physicochemical and functional properties. *Food Res Int* 2012; 45(1): 277–82. doi: 10.1016/j.foodres.2011.10.044.
12. Thompson LU. Preparation and evaluation of mung bean protein isolates. *J Food Sci* 1977; 42(1): 202–6. PubMed PMID: ISI:A1977CP78700049; English.
13. Mubarak AE. Nutritional composition and antinutritional factors of mung bean seeds (*Phaseolus aureus*) as affected by some home traditional processes. *Food Chem* 2005; 89(4): 489–95. doi: 10.1016/j.foodchem.2004.01.007. PubMed PMID: WOS:000224329600001.

14. FAO/WHO. Energy and protein requirements. Report of FAO Nutritional Meeting Series No 52, 1973. Rome: FAO.
15. FAO/WHO. Protein quality evaluation. Joint FAO/WHO. FAO Food Nutr Paper 1991; 51: 1–66. PubMed PMID: MEDLINE:1817076.
16. Ericson MC, Chrispeels MJ. Isolation and characterization of glucosamine-containing storage glycoproteins from the cotyledons of *Phaseolus aureus*. *Plant Physiol* 1973; 52(2): 98–104. doi: 10.1104/pp.52.2.98. PubMed PMID: MEDLINE:16658529.
17. Bhattacharyya SP, Biswas BB. Purification and characterization of high salt-soluble vicilin from mung bean (*Vigna radiata*). *Biochem Int* 1990; 21(4): 667–75. PubMed PMID: WOS:A1990DX01900010.
18. Khalil AA. Nutritional improvement of an Egyptian breed of mung bean by probiotic lactobacilli. *Afr J Biotechnol* 2006; 5(2): 206–12. PubMed PMID: WOS:000235140100026.
19. Bernardo AEN, Garcia RN, Adachi M, Angeles JGC, Kaga A, Ishimoto M, et al. 8S globulin of mungbean *Vigna radiata* (L.) wilczek: cloning and characterization of its cDNA isoforms, expression in *Escherichia coli*, purification, and crystallization of the major recombinant 8S isoform. *J Agr Food Chem* 2004; 52(9): 2552–60. doi: 10.1021/jf0305938. PubMed PMID: WOS:000221135100021.
20. Torio MAO, Adachi M, Garcia RN, Prak K, Maruyama N, Utsumi S, et al. Effects of engineered methionine in the 8S alpha globulin of mungbean on its physicochemical and functional properties and potential nutritional quality. *Food Res Int* 2011; 44(9): 2984–90. doi: 10.1016/j.foodres.2011.07.010. PubMed PMID: WOS:000296798300054.
21. Keunen K, van Elburg RM, van Bel F, Benders M. Impact of nutrition on brain development and its neuroprotective implications following preterm birth. *Pediatr Res* 2015; 77(1): 148–55. doi: 10.1038/pr.2014.171. PubMed PMID: WOS:000347672800007.
22. Florentino RF. Nutritional aspects of eating rice. *Philippine J Nutr* 1974; 27(4): 129–40. PubMed PMID: 1976:3502; English.
23. Shewry PR, Napier JA, Tatham AS. Seed storage proteins – Structures and biosynthesis. *Plant Cell* 1995; 7(7): 945–56. doi: 10.1105/tpc.7.7.945. PubMed PMID: WOS:A1995RM93700014.
24. Klomklao S, Benjakul S, Kishimura H, Chaijan M. Extraction, purification and properties of trypsin inhibitor from Thai mung bean (*Vigna radiata* (L.) R. Wilczek). *Food Chem* 2011; 129(4): 1348–54. doi: 10.1016/j.foodchem.2011.05.029. PubMed PMID: WOS:000294979600004.
25. Wang SY, Wu JH, Ng TB, Ye XY, Rao PF. A non-specific lipid transfer protein with antifungal and antibacterial activities from the mung bean. *Peptides* 2004; 25(8): 1235–42. doi: 10.1016/j.peptides.2004.06.004. PubMed PMID: ISI:000223926700002; English.
26. Gunarti DR, Rahmi H, Sadikin M. Isolation and purification of thiamine binding protein from mung bean. *HAYATI J Biosci* 2013; 20(1): 1–6. doi: 10.4308/hjb.20.1.1.
27. Mendoza EMT, Adachi M, Bernardo AEN, Utsumi S. Mungbean [*Vigna radiata* (L.) Wilczek] globulins: purification and characterization. *J Agr Food Chem*. 2001; 49(3): 1552–8. doi: 10.1021/Jf001041h. PubMed PMID: ISI:000168967400081; English.
28. Wang J, Tse YC, Hinz G, Robinson DG, Jiang L. Storage globulins pass through the Golgi apparatus and multivesicular bodies in the absence of dense vesicle formation during early stages of cotyledon development in mung bean. *J Exp Bot* 2012; 63(3): 1367–80. doi: 10.1093/jxb/err366. PubMed PMID: WOS:000300238400025.
29. Tang C-H, Sun X. Physicochemical and structural properties of 8S and/or 11S globulins from mungbean [*Vigna radiata*(L.) Wilczek] with various polypeptide constituents. *J Agr Food Chem*. 2010; 58(10): 6395–402. doi: 10.1021/jf904254f.
30. Nielsen H, Engelbrecht J, Brunak S, von Heijne G. Identification of prokaryotic and eukaryotic signal peptides and prediction of their cleavage sites. *Protein Eng* 1997; 10(1): 1–6. doi: 10.1093/protein/10.1.1. PubMed PMID: WOS:A1997WJ04100001.
31. Yamazaki T, Takaoka M, Katoh E, Hanada K, Sakita M, Sakata K, et al. A possible physiological function and the tertiary structure of a 4-kDa peptide in legumes. *Eur J Biochem* 2003; 270(6): 1269–1276. doi: 10.1046/j.1432-1033.2003.03489.x. PubMed PMID: ISI:000181549200024; English.
32. Tang CH, Sun X, Yin SW. Physicochemical, functional and structural properties of vicilin-rich protein isolates from three *Phaseolus* legumes: effect of heat treatment [Article]. *Food Hydrocolloid* 2009; 23(7): 1771–8. doi: 10.1016/j.foodhyd.2009.03.008. PubMed PMID: WOS:000267478400018; English.
33. Liu H, Liu H, Yan L, Cheng X, Kang Y. Functional properties of 8S globulin fractions from 15 mung bean (*Vigna radiata* (L.) Wilczek) cultivars. *Int J Food Sci Technol* 2015; 50(5): 1206–14. doi: 10.1111/ijfs.12761.
34. Tang C-H. Thermal denaturation and gelation of vicilin-rich protein isolates from three *Phaseolus* legumes: a comparative study. *LWT-Food Sci Technol* 2008; 41(8): 1380–8. doi: 10.1016/j.lwt.2007.08.025. PubMed PMID: WOS:000256831700004.
35. Du M, Xie J, Gong B, Xu X, Tang W, Li X, et al. Extraction, physicochemical characteristics and functional properties of Mung bean protein. *Food Hydrocolloid* 2018; 76(Suppl C): 131–140. doi: <https://doi.org/10.1016/j.foodhyd.2017.01.003>.
36. Suppavarasatit I, Lee S-Y, Cadwallader KR. Effect of enzymatic protein deamidation on protein solubility and flavor binding properties of soymilk. *J Food Sci* 2013; 78(1): C1–C7. doi: 10.1111/j.1750-3841.2012.03012.x.
37. Damodaran S, Parkin KL, Fennema OR. *Fennema's food chemistry*. Boca Raton, FL: CRC Press/Taylor & Francis; 2008.
38. Brishti FH, Zarei M, Muhammad SKS, Ismail-Fitry MR, Shukri R, Saari N. Evaluation of the functional properties of mung bean protein isolate for development of textured vegetable protein. *Int Food Res J* 2017; 24(4): 1595.
39. Butt MS, Batool R. Nutritional and functional properties of some promising legumes protein isolates. *Pak J Nutr* 2010; 9(4): 373–9. doi: 10.3923/pjn.2010.373.379.
40. Wright DJ, Hemmant JW. Foaming properties of protein solutions: comparison of large-scale whipping and conductimetric methods. *J Sci Food Agr* 1987; 41(4): 361–71. doi: 10.1002/jsfa.2740410408.
41. Tang CH, Chen L, Ma CY. Thermal aggregation, amino acid composition and in vitro digestibility of vicilin-rich protein isolates from three *Phaseolus* legumes: a comparative study [Article]. *Food Chem* 2009; 113(4): 957–63. doi: 10.1016/j.foodchem.2008.08.038. PubMed PMID: WOS:000261857100015; English.
42. Johns CO, Waterman HC. Some proteins from the mung bean, *Phaseolus aureus* Roxburgh. *J Biol Chem* 1920; 44: 303–17. PubMed PMID: 1921:6398; language unavailable.
43. Rahma EH, Dudek S, Mothes R, Gornitz E, Schwenke KD. Physicochemical characterisation of mung bean (*Phaseolus aureus*) protein isolates. *J Sci Food Agr* 2000; 80(4): 477–83. PubMed PMID: ISI:000085726100008; English.
44. El-Adawy TA. Functional properties and nutritional quality of acetylated and succinylated mung bean protein isolate. *Food*

- Chem 2000; 70(1): 83–91. PubMed PMID: ISI:000086844300014; English.
45. Deshpande SS, Campbell CG. Effect of different solvents on protein recovery and neurotoxin and trypsin-inhibitor contents of grass pea (*Lathyrus-sativus*). *J Sci Food Agr* 1992; 60(2): 245–9. doi: 10.1002/jfsa.2740600213. PubMed PMID: WOS:A1992KA88300012.
 46. Benjakul S, Visessanguan W, Thummaratwasik P. Isolation and characterization of trypsin inhibitors from some Thai legume seeds. *J Food Biochem* 2000; 24(2): 107–27. doi: 10.1111/j.1745-4514.2000.tb00689.x. PubMed PMID: WOS:000087229900002.
 47. Klomklao S, Benjakul S, Kishimura H, Osako K, Tanaka M. A heat-stable trypsin inhibitor in adzuki bean (*Vigna angularis*): effect of extraction media, purification and biochemical characteristics. *Int J Food Sci Technol* 2010; 45(1): 163–9. doi: 10.1111/j.1365-2621.2009.02117.x. PubMed PMID: WOS:000272655500021.
 48. Kader JC. Lipid-transfer proteins in plants. *Annu Rev Plant Phys* 1996; 47: 627–54. doi: 10.1146/annurev.arplant.47.1.627. PubMed PMID: ISI:A1996UT11900024; English.
 49. Guang C, Phillips RD. Plant food-derived angiotensin I converting enzyme inhibitory peptides [review]. *J Agr Food Chem* 2009; 57(12): 5113–20. doi: 10.1021/jf900494d. PubMed PMID: WOS:000267183800001; English.
 50. Aluko RE. Determination of nutritional and bioactive properties of peptides in enzymatic pea, chickpea, and mung bean protein hydrolysates. *J Aoac Int* 2008; 91(4): 947–56. PubMed PMID: ISI:000258270400033; English.
 51. Garcia MC, Puchalska P, Esteve C, Marina ML. Vegetable foods: a cheap source of proteins and peptides with antihypertensive, antioxidant, and other less occurrence bioactivities. *Talanta* 2013; 106: 328–49. doi: 10.1016/j.talanta.2012.12.041.
 52. Li GH, Shi YH, Liu H, Le GW. Antihypertensive effect of alcalase generated mung bean protein hydrolysates in spontaneously hypertensive rats. *Eur Food Res Technol* 2006; 222(5–6): 733–6. doi: 10.1007/s00217-005-0147-2. PubMed PMID: ISI:000235900700035; English.
 53. Liu F, Zhang XB, Lu CM, Zeng XH, Li YJ, Fu DH, et al. Non-specific lipid transfer proteins in plants: presenting new advances and an integrated functional analysis. *J Exp Bot* 2015; 66(19): 5663–81. doi: 10.1093/jxb/erv313. PubMed PMID: ISI:000362073400003; English.
 54. Li GH, Wan JZ, Le GW, Shi YH. Novel angiotensin I-converting enzyme inhibitory peptides isolated from Alcalase hydrolysate of mung bean protein. *J Peptide Sci* 2006; 12(8): 509–14. doi: 10.1002/Psc.758. PubMed PMID: ISI:000239879000003; English.
 55. Wu H, Rui X, Li W, Chen X, Jiang M, Dong M. Mung bean (*Vigna radiata*) as probiotic food through fermentation with *Lactobacillus plantarum* B1-6. *LWT – Food Sci Technol* 2015; 63(1): 445–51. doi: 10.1016/j.lwt.2015.03.011.
 56. Mamilla RK, Mishra VK. Effect of germination on antioxidant and ACE inhibitory activities of legumes. *LWT – Food Sci Technol* 2017; 75(Suppl C): 51–8. doi: 10.1016/j.lwt.2016.08.036.
 57. He H-L, Liu D, Ma C-B. Review on the angiotensin-I-converting enzyme (ACE) inhibitor peptides from marine proteins. *Appl Biochem Biotech* 2013; 169(3): 738–49. doi: 10.1007/s12010-012-0024-y.
 58. Benjakul S, Karoon S, Suwanno A. Inhibitory effects of legume seed extracts on fish proteinases. *J Sci Food Agr* 1999; 79(13): 1875–81. doi: 10.1002/(sici)1097-0010(199910)79:13<1875::aid-jfsa447>3.0.co;2-u. PubMed PMID: WOS:000082956500016.
 59. Sun L-C, Yoshida A, Cai Q-F, Liu G-M, Weng L, Tachibana K, et al. Mung bean trypsin inhibitor is effective in suppressing the degradation of myofibrillar proteins in the skeletal muscle of blue scad (*Decapterus maruadsi*). *J Agr Food Chem* 2010; 58(24): 12986–92. doi: 10.1021/jf103526e. PubMed PMID: WOS:000285236400057.
 60. Chrispeels MJ, Baumgartner B. Trypsin-inhibitor in mung bean cotyledons-purification, characteristics, subcellular-localization, and metabolism. *Plant Physiol* 1978; 61(4): 617–23. doi: 10.1104/pp.61.4.617. PubMed PMID: WOS:A1978EY11600030.
 61. Kunitz M. Crystalline soybean trypsin inhibitor: II. General properties. *J Gen Physiol* 1947; 30(4): 291–310. doi: 10.1085/jgp.30.4.291. PubMed PMID: MEDLINE:19873496; English.
 62. Lorenzen E, Prevosto R, Wilson KA. The appearance of new active forms of trypsin-inhibitor in germinating mung bean (*Vigna-radiata*) seeds. *Plant Physiol* 1981; 68(1): 88–92. doi: 10.1104/pp.68.1.88. PubMed PMID: WOS:A1981LY62800018.
 63. Wilson KA, Chen JC. Amino-acid-sequence of mung bean trypsin-inhibitor and its modified forms appearing during germination. *Plant Physiol* 1983; 71(2): 341–9. doi: 10.1104/pp.71.2.341. PubMed PMID: WOS:A1983QD06800022.
 64. Lin KF, Liu YN, Hsu STD, Samuel D, Cheng CS, Bonvin AMJJ, et al. Characterization and structural analyses of non-specific lipid transfer protein I from mung bean. *Biochemistry* 2005; 44(15): 5703–12. doi: 10.1021/Bi047608v. PubMed PMID: ISI:000228425600015; English.
 65. Ye XY, Ng TB. Mungin, a novel cyclophilin-like antifungal protein from the mung bean. *Biochem Biophys Res Commun* 2000; 273(3): 1111–15. doi: 10.1006/bbrc.2000.3067. PubMed PMID: ISI:000088363700055; English.
 66. Wang HX, Liu WK, Ng TB, Ooi VEC, Chang ST. Immunomodulatory and antitumor activities of a polysaccharide-peptide complex from a mycelial culture of *Tricholoma* sp., a local edible mushroom. *Life Sci* 1995; 57(3): 269–81. doi: 10.1016/0024-3205(95)00270-G.

***Zhu Yi-Shen**

College of Biotechnology and Pharmaceutical Engineering
Nanjing Tech University
Nanjing 211816, China
Email: zhuyish@njtech.edu.cn

Iodine content of six fish species, Norwegian dairy products and hen's egg

Ive Nerhus, Maria Wik Markhus, Bente M. Nilsen, Jannike Øyen, Amund Maage, Elisabeth Rasmussen Ødegård, Lisa Kolden Midtbø, Sylvia Frantzen, Tanja Kögel, Ingvild Eide Graff, Øyvind Lie, Lisbeth Dahl* and Marian Kjellekvold

Institute of Marine Research (IMR), Bergen, Norway

Abstract

Iodine is a trace element required for the production of thyroid hormones, essential for metabolism, growth and brain development, particularly in the first trimester of pregnancy. Milk and lean fish are the main dietary sources of iodine in the Norwegian diet. Thus, the aim of the present study was to provide updated analysed values of iodine concentration in six fish species, 27 selected Norwegian iodine-rich dairy foods and Norwegian hen's eggs. The iodine concentrations in the wild fish species varied between 18 $\mu\text{g}/100\text{ g}$ (Atlantic halibut) and 1,210 $\mu\text{g}/100\text{ g}$ (pollack). The iodine concentration of cow milk varied between 12 and 19 $\mu\text{g}/100\text{ g}$ and the iodine concentration of the eggs varied between 23 and 43 $\mu\text{g}/100\text{ g}$. The results in this study deviate somewhat from the current iodine concentrations in the Norwegian Food Composition Table. This deviation may have a large impact on the assessment of the iodine intake. Hence, updated knowledge about the variation in iodine level of fish, milk, dairy products and hen's egg are of great importance when estimating the iodine intake in the population. These data will contribute substantially to future estimations of dietary iodine intake and will be made available for the public Norwegian Food Composition Table.

Keywords: *iodine; dairy products; fish; hen's egg; ICP-MS; food analysis; food composition table*

Iodine is an important trace element in human nutrition and is essential for thyroid hormone synthesis. Thyroid hormones are involved in many cellular activities essential for normal body function. The importance of assessing iodine intake of pregnant and lactating women has become increasingly clear because of emerging evidence from cohort studies showing that even mild to moderate iodine deficiency during pregnancy is associated with poorer cognitive function and school performance in children (1–4).

Iodine in sufficient concentrations occurs naturally in only a limited variety of foods, marine fish having the highest iodine concentrations in general (5, 6). Iodine concentrations vary between and within fish species, and also seasonally and geographically location, as fish absorb iodine both from the seawater and from their food (7). Even though their iodine content is considerably lower than that of fish, milk and dairy products are the iodine sources of greatest importance due to their common

consumption in larger quantities in the Norwegian culture. The iodine concentration of milk depends on the supplementation concentration of iodine of cow feed, the amount of goitrogens in the rations, application of teat dipping containing iodine, iodine source, lactation stage, milk yield and milk processing (8). In addition, egg is a good dietary source of iodine (5, 9). To determine the iodine content of biological samples, inductively coupled plasma-mass spectrometry (ICP-MS) is the preferred method due to its precision.

Iodised salt programmes are the recommended method for providing sufficient iodine intake in a population (10). However, in countries with low availability of iodised salt, the intake of dietary iodine intake is of utmost importance. Neither household nor industrial iodisation of salt is mandatory in Norway. However, some brands have added iodine (5 mg/kg) in salt (6). Sufficient iodine intake is still challenging in population groups across the world, including countries in Europe (11, 12).

In the Norwegian diet, milk and dairy products contribute with 55% and fish contributes with 20% of the dietary iodine intake (6). Iodine was included in the Norwegian Food Composition Table in 2014. Dietary iodine sources in the Nordic countries have several similarities; in Denmark, milk and mandatory fortification of salt used in the bakery industry and household salt are the main dietary iodine sources (11, 13). In Iceland, it is fish; in Sweden, iodised salt; and in Finland, milk (11). In the United Kingdom, which is also lacking an iodised salt programme, milk and dairy products contribute most to the dietary iodine intake (4). Knowledge about current iodine content in foods is expedient for several reasons. Since there are few dietary sources of iodine, it is important and feasible to map to what extent these food groups contribute. In addition, it is important to estimate iodine intake of population groups, which will provide indications on whether additional monitoring programmes or health care information for vulnerable groups are necessary. Thus, the main aim of the present study was to provide updated data on the iodine content

of the most important iodine-rich food groups in the Norwegian diet, dairy products and lean fish. In addition, updated data on egg was provided. Since Norway is a major provider of fish to Europe, the data also have high relevance for calculations of European dietary iodine intake.

Materials and methods

Sampling of fish species

Five different species of wild fish were included in this study – Atlantic cod (*Gadus morhua*), saithe (*Pollachius virens*), haddock (*Melanogrammus aeglefinus*), pollack (*Pollachius pollachius*) and Atlantic halibut (*Hippoglossus hippoglossus*). Figure 1 illustrates sampling positions. Table 1 lists information regarding sampling period, number of positions and number of fish collected within the three major different sea areas – the Barents Sea, the Norwegian Sea and the North Sea.

The samples of wild fish analysed in this study were collected during several monitoring programmes for

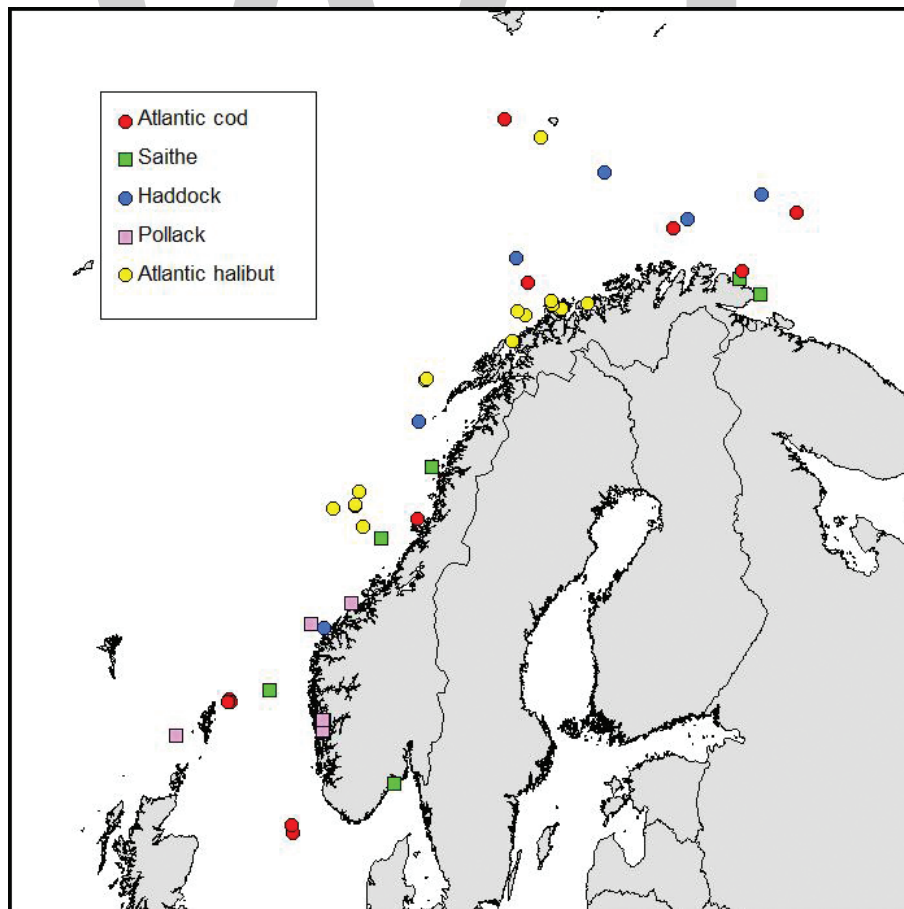


Fig. 1. Sampling positions for Atlantic cod, saithe, haddock, pollack and Atlantic halibut. Cod, saithe and haddock, 10–11 fish per position; pollack, 6–11 fish per position; Atlantic halibut, 1–2 fish per position.

Table 1. Overview of wild fish sampled for analysis of iodine content

Fish species and sampling area	Sampling period	Number of positions	Number of fish
<i>Atlantic cod (Gadus morhua)</i>		11	121
Barents Sea	January–March 2014 and February 2015	5	55
Norwegian Sea	October 2014	1	11
North Sea	August–September 2014	5	55
<i>Saithe (Pollachius virens)</i>		6	61
Barents Sea	July 2013 and June 2015	2	20
Norwegian Sea	March–April 2014	2	20
North Sea and Skagerrak	March and May 2014	2	21
<i>Haddock (Melanogrammus aeglefinus)</i>		6	65
Barents Sea	January–March 2015	4	43
Norwegian Sea	February and May 2015	2	22
<i>Pollack (Pollachius pollachius)</i>		5	41
Norwegian Sea	April and August 2014	2	17
North Sea	June 2014	1	6
Fjords in western Norway	April, October and November 2014	2	18
<i>Atlantic halibut (Hippoglossus hippoglossus)</i>		19	20
Barents Sea	September–October 2014	9	10
Norwegian Sea	August–October 2014	10	10

contaminants in wild fish in Norwegian sea areas (14–19) (Kögel, T. personal communication). The most recent samples collected for each species and area were selected, and most samples included were collected in 2014 and 2015. The sampling positions for each species were selected to obtain samples from a wide geographical area aiming to represent the normal commercial fishery catch areas. From each position, 10–11 individual fish of intermediate size were included in the study, excluding the smallest and largest fish in order to reduce the possible biological variation of the iodine concentration due to the fish size. However, if less than 10 fish were collected at a particular position, all fish were included into the study regardless of size. For Atlantic halibut, only one (or in one case two) fish were collected at each position. To obtain representative results for this species, 10 fish from the Barents Sea and 10 fish from the Norwegian Sea were included, selecting fish with weights between 11 and 40 kg, which is the most common commercial weight class for this species.

Furthermore, samples of 40 farmed Atlantic halibut were collected at three different fish farms in the western part of Norway in March, June and July 2014 and in April, August and September 2015. In addition to the fish samples taken in the field, 10 different products of canned tuna, from seven different brands, were purchased in various supermarkets in Bergen in November 2015.

Preparation of fish

Samples of Atlantic cod, saithe, pollack and haddock were frozen as whole fish at -20°C before being shipped

to the Institute of Marine Research, Bergen, Norway. For Atlantic halibut, length, weight and sex of each fish were recorded immediately after capture, and from each fish, a sample including the head and a 20–30 cm section anterior of the head was frozen and shipped to the laboratory. The samples of wild Atlantic halibut were thawed and a sample of about 200 g muscle tissue from the lean part of the fillet (B-cut) on the upper, ventral side of the fish anterior of the pectoral fin of each fish (20) was homogenised. The samples of cod, saithe, haddock and pollack were thawed, and the length, weight and sex of each fish was determined. The fish were filleted, skinned and about 200 g of muscle tissue from each individual fish was homogenised. The wet homogenised fish samples were freeze-dried, ground to a fine powder, homogenised again and kept dry pending analysis. Analyses of wild fish were performed on individual fish samples. The samples of farmed Atlantic halibut were thawed, filleted and skinned. Muscle samples from five fish collected at the same fish farm at the same time were pooled and homogenised. The pooled samples were freeze-dried, ground to a fine powder, homogenised again and kept dry pending analysis. For the canned tuna, any oil or water in the respective products was removed before the samples were homogenised and freeze-dried.

Sampling of dairy products

Seven different types of cow milk, one type of soy milk, two different types of cream milk and 17 other dairy products were included (Table 2). All products were produced in Norway with the exception of soy milk and two types of cream cheese. During the last years, alternative 'dairy'

Table 2. Norwegian milk and dairy products sampled for analysis of iodine content

Dairy product	n	Description and fat content
<i>Milk</i>		
Low-fat milk, TINE	9	Cow milk, 1.2% fat
Skimmed milk, TINE	9	Cow milk, 0.1% fat
Organic low-fat milk, TINE	9	Cow milk, 1.2% fat
Organic low-fat milk, Røros Meieri	9	Cow milk, 1.2% fat
Low-fat milk, Q	9	Cow milk, 1.0% fat
Skimmed milk, Q	9	Cow milk, 0.5% fat
Chocolate-flavoured low-fat milk, Q	3	Cow milk, 1.2% fat
Soy milk, Alpro	3	Soy beans, 1.8% fat
<i>Probiotic milk with LGG</i>		
Biola with blueberry flavour, TINE	3	Cow milk, 0.1% fat
<i>Yoghurt</i>		
'Go'morgen' with flavour, TINE	3	Cow milk and contains müsli, 3% fat
Yoghurt with natural flavour, TINE	3	Cow milk, 3.4% fat
<i>White-coloured solid cheese</i>		
'Norvegia', TINE	3	Cow milk, 2% fat
'Jarlsberg', TINE	3	Cow milk, 27% fat
'Norsk gulost', Synnøve Finden	3	Cow milk, 26% fat
<i>White soft and cream cheeses</i>		
Brie, Arla Foods, HØNG	3	Ripened cheese of pasteurised cow milk, 34%
Camembert, TINE	3	Ripened cheese of pasteurised cow milk, 28%
Soft, cream cheese, 'Snøfrisk', TINE	3	Cream cheese of goat milk, 25% fat
Soft, cream cheese, 'Philadelphia', Mondalez	3	Cream cheese of cow milk, 23.5% fat
<i>Whey cheese</i>		
'Gudbrandsdalsost', TINE	3	Cow milk and goat milk, 29% fat
'Fløtemysost', TINE	3	Cow milk, 27% fat
'Ekte geitost', TINE	3	Goat milk, 27% fat
<i>Other dairy products</i>		
Cream milk, TINE	9	Cream milk, 38% fat
Cream milk, TINE	9	Cream milk, 20% fat
Crème fraîche, TINE	3	Curdled cream, 35% fat
Cottage cheese, TINE	3	Cheese product, 4.3% fat
Curd with natural flavour, TINE	3	Curd/Quark, 8.1% fat
Sour cream, TINE	3	Sour cream, 18% fat

products, such as soy and oat milk, have become popular. Therefore, soymilk with natural flavour was selected for analysis based on supermarket volume. Information regarding producer, country of production, batch number, best before date and place of sampling were registered. All products were purchased with three different batch numbers at supermarkets in Bergen, Norway and stored in a refrigerator (4°C) prior to homogenisation.

Preparation of dairy products

The homogenisation procedure of cow milk, chocolate-flavoured milk, cream milk, soy milk and probiotic milk (liquids) consisted of the following steps: a subsample of 200 mL from each of three different batch numbers were mixed in a glass bottle, resulting in one

pooled sample of 600 mL. From this, two subsamples were frozen pending analysis (12.5 mL) and one for back up (50 mL). Three pooled samples were analysed at each sampling occasion. Furthermore, cow milk and cream milks were sampled at three different occasions of the year (Table 6).

The homogenisation procedure of yoghurts, sour cream, crème fraîche, cottage cheese, brie, camembert and solid cheeses consisted of the following steps: three items of each product were mixed and homogenised in a kitchen machine (Braun, lab.nr 1598), resulting in one pooled sample. Two sub-samples of 12.5 mL and 50 mL were collected, one for freeze-drying, pending analysis, and one for backup, respectively. All backups were stored in -80°C freezer.

A subsample of the dairy products (except probiotic milk, cow milk, chocolate-flavoured cow milk, soymilk and cream milks) was freeze-dried for minimum 24 h at -20°C or -80°C , (Labconco Freezone, 18 liter, model 775030).

Sampling of hen's egg

Eggs from three different Norwegian producers were purchased in shops in Bergen in April 2016 and in Bergen and Oslo April 2017. Based on information on their market share, the brand with the highest market share was selected. Each box of egg consisted of 6 or 12 eggs and in total 33 boxes were purchased (Table 8). Eggs purchased in 2016 were stored at -80°C until analysis and the sample from 2017 was stored fresh at 4°C until analysis.

Preparation of hen's eggs

Each pooled hen's egg sample from 2016 consisted of 36 eggs from three different boxes (same brand), while each pooled hen's egg sample from 2017 consisted of 18 eggs from three different boxes (same brand). The pooled egg samples were homogenised using a kitchen whisk.

Iodine analysis and accuracy of the measurements

The iodine content was determined using inductive coupled plasma-mass spectrophotometry (ICP-MS). Tetra methyl ammonium hydroxide (TMAH) and water were added to the samples before extraction at $90^{\circ}\text{C} \pm 3^{\circ}\text{C}$ for 3 h. Dried samples from individual fish were analysed with one analytical replicate per fish. Pooled samples from milk and dairy products and eggs were analysed with two analytical replicates per sample. Limit of quantification (LOQ) is $0.32 \mu\text{g/L}$, or 0.04 mg/kg dry weight. Limit of detection (LOD) is $0.01 \mu\text{g/L}$. The measurement uncertainty differs depending on the concentration range and is set to 40% for concentrations between LOQ and $10 \times \text{LOQ}$, and 15% for concentrations $>10 \times \text{LOQ}$. The measurement range lies between 0.04 and 90 mg/kg dry weight. The measurement uncertainty is based on the control card of the method along with participation in proficiency tests. ICP-MS is commonly used for the quantitative determination of iodine in biological samples due to its high sensitivity and selectivity (7). Although there are several methods to determine iodine, the sensitivity for iodine in ICP-MS is superior compared to other

techniques (21). The freeze-drying method and the ICP-MS method used in this study are accredited according to ISO 17025. Measurement uncertainty is based on internal reproducibility, taken from the control chart of the method along with results from participation in proficiency testing. The method is robust when performed according to the method description. The results obtained from determining iodine content in standard reference materials are listed in Table 3.

Statistical analyses

Iodine concentrations in fish of each species sampled in different areas and during different months of the year were compared using one-way ANOVA followed by Tukey's HSD multiple comparison test. Because of heteroscedasticity, iodine concentrations were log transformed prior to analysis. The relationships between iodine concentration and fish length and condition ($K\text{-factor} = 100 \times \text{weight}/\text{length}^3$), respectively, were examined for each species using Pearson's linear correlation analysis. Statistical analyses were performed using Statistica 64, version 13.

Results and discussion

Iodine content of fish

The average iodine content in fish fillet varied from $21 \mu\text{g}/100 \text{ g}$ wet weight (ww) in Atlantic halibut to $790 \mu\text{g}/100 \text{ g}$ ww in pollack (Table 4). There was a large variation between individuals within the same species, and between fish of the same species from different geographical areas and/or sampling months (Figure 2). From this dataset, we could not detect any consistency between fish species with regard to which areas or months showed the highest iodine contents. Because this research question was not taken into account during the planning of the sampling and because the main fishery in different areas take place during different times of the year, many of the samples were taken during different months of the year in the different areas. In several cases this precluded the analysis of whether observed differences were geographical or seasonal. For example, Atlantic cod from the North Sea appeared to have lower iodine concentrations than cod from the Barents Sea or the Norwegian Sea. However,

Table 3. Iodine content in standard reference materials compared with the analysed value and the measured value over time

Reference material	Analysed mean value	Certified value	Measured mean value	RSD %
Skimmed milk powder (ERM-BD 150)	$1.50 \pm 0.09 \text{ mg/kg}$ ($n = 12$)	$1.73 \pm 0.14 \text{ mg/kg}$	NA	NA
Fish Muscle (ERM-BB 422)	$1.23 \pm 0.05 \text{ mg/kg}$ ($n = 12$)	$1.4 \pm 0.4 \text{ mg/kg}$	$1.26 \pm 0.20 \text{ mg/kg}$ ($n = 209$)	10

All values are mean values \pm standard deviation (SD). Skimmed milk was used for analysing dairy products and fish muscle for analysing fish and egg. NA, not analysed; RSD, relative standard deviation.

Table 4. Iodine content of five different fish species sampled in different geographical areas

Fish species	Catch area	n	Mean \pm SD $\mu\text{g}/100\text{ g}$	Min.–max. $\mu\text{g}/100\text{ g}$	Mean weight kg	Mean length cm	Food Composition Table ^a $\mu\text{g}/100\text{ g}$	Sjomatdata ^b
Atlantic cod	All areas	121	190 \pm 160	22–720	2.8	64	119 ^c	93
Atlantic cod	Barents Sea	55	250 \pm 140	47–720	1.8	59		
Atlantic cod	Norwegian Sea	11	400 \pm 190	100–700	3.3	69		
Atlantic cod	North Sea	55	96 \pm 100	22–680	3.6	68		
Saithe	All areas	61	280 \pm 190	35–820	1.7	53	93 ^d	23
Saithe	Barents Sea	20	410 \pm 200	92–820	1.4	48		
Saithe	Norwegian Sea	20	210 \pm 150	35–620	3.0	67		
Saithe	North Sea and Skagerrak	21	220 \pm 170	46–560	0.8	43		
Haddock	All areas	65	400 \pm 500	35–2,200	1.4	50	320 ^e	n.a.
Haddock	Barents Sea	43	180 \pm 160	35–830	1.1	47		
Haddock	Norwegian Sea	22	830 \pm 650	150–2,200	2.1	56		
Pollack	All areas	41	790 \pm 690	48–3,000	2.1	59	143 ^f	70
Pollack	Norwegian Sea	17	550 \pm 430	100–2,000	2.3	56		
Pollack	North Sea	6	210 \pm 160	48–500	2.7	67		
Pollack	Fjords in western Norway	18	1,210 \pm 770	497–3,000	1.7	59		
Atlantic halibut	All areas	20	21 \pm 11	10–45	21	115	10 ^g	n.a.
Atlantic halibut	Barents Sea	10	23 \pm 11	13–45	24	122		
Atlantic halibut	Norwegian Sea	10	18 \pm 9	10–37	17	109		

Mean \pm SD and range (minimum–maximum) are given. Catch area, number of fish (n), mean weight and length of the fish within each area and Food Composition Table (Norwegian Food Safety Authority 2016).

^aNorwegian Food Composition Table (30.05.2017), www.matvaretabellen.no

^b<https://sjomatdata.nifes.no/#search/> (14.03.2018)

^cCod, wild, raw; analysed value from www.sjomatdata.no

^dSaithe, raw; analysed value from www.sjomatdata.no (12.07.2010)

^eHaddock, raw; Public Health England and Institute of food research (2015), McCance and Widdowson's The Composition of Foods, Seventh summary edition. Cambridge: The Royal Society of Chemistry. Literature source.

^fPollack, raw; French Agency for Food, Environmental and Occupational Health safety, French Food Composition Table – Ciquai 2012.

^gHalibut, Atlantic, raw; Mattilsynet og Sosial- og helsedirektoratet, Analyseprosjekt 2006–2009, Div. fiskeslag.

Publisert rapport (2012); 'Nutritional composition of selected wild and farmed raw fish'.

n.a. – not available.

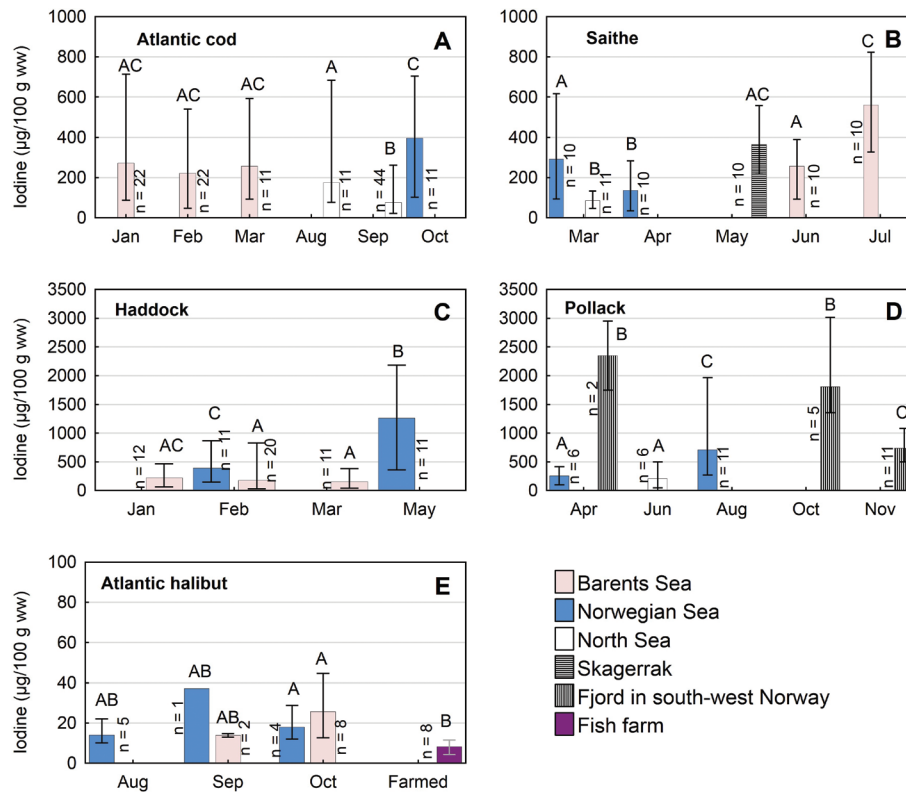


Fig. 2. Concentrations of iodine ($\mu\text{g}/100\text{ g ww}$) in A) Atlantic cod (*Gadus morhua*), B) saithe, (*Pollachius virens*), C) haddock (*Melanogrammus aeglefinus*), D) pollack (*Pollachius pollachius*) and E) Atlantic halibut (*Hippoglossus hippoglossus*) sampled during different months in different areas. Mean, minimum and maximum values are given. Significant differences between groups on \log_{10} -transformed concentrations (one-way ANOVA followed by Tukey HSD) are indicated with different letters. Notice different scaling on the y-axis for the different species.

most of the samples from the North Sea were taken in September, when no cod were caught in the other two areas (Figure 2A). These cod, caught in September, were relatively large and in good condition (Supplementary Table 1), and since both length and K -factor were negatively correlated with iodine content of cod ($r = -0.38$ and -0.35 , $p < 0.001$; Supplementary Figures 1 and 2), this may be a possible explanation for the low levels of iodine in cod from the North Sea, particularly in September. In saithe and haddock, iodine concentrations appeared to be higher later in the year, from May on, compared to earlier in the year (Figure 2B,C). For haddock, this could be an effect of spawning, as haddock spawn during April–May (22). If reserves are depleted during spawning to the extent that the total muscle mass is reduced, this could lead to a relative up-concentration of elements such as iodine. The condition (K -factor) of the haddock with the highest iodine concentrations, sampled in the Norwegian Sea in May, was indeed reduced (0.96) relative to the haddock sampled in February (1.37; Supplementary Table 1). Saithe spawn earlier in the year, during February–March (22), and the relatively lower concentrations in April compared to later in the year are thus probably not

due to spawning. However, iodine is at least partly accumulated from the diet (7), and perhaps increasing iodine content through spring and summer may be caused by enhanced uptake through the feeding season. The condition of the saithe increased slightly as the iodine concentrations increased from March through to July, and in saithe there was a positive correlation between iodine content and K -factor ($r = 0.53$, $p < 0.001$; Supplementary Figure 2). In pollack, iodine concentrations were significantly higher in a fjord in southwest Norway both in April and October as compared to all other months in all other areas (Figure 2). These were by far the highest iodine concentrations overall in the study, with mean concentrations of 2,350 and 1,800 $\mu\text{g}/100\text{ g}$ in April and October, respectively. Both pollack sampled in April and October were from the same fjord, but the number of fish were low, only seven fish. Pollack from the Norwegian Sea had significantly lower iodine concentrations in April than in August. Condition (K -factor) for the pollack from April was, however, high (Supplementary Table 1). This may have been mature fish with large gonads, since pollack spawn during March and April. The high concentrations of iodine in fjords compared to the open sea has limited value

for nutritional calculations, as the catch volume of fish from the open sea is much higher than that from the fjords. Fish absorb iodine both from the seawater and from their diet (7). Differences in preferred or available prey for different species and for fish of the same species from different areas may contribute to the large variation in iodine content. The iodine content in Atlantic halibut was low both in the Barents Sea and in the Norwegian Sea, and in both areas the iodine content was much lower than in the four lean codfish investigated. This may be due to a higher fat content in Atlantic halibut than in the four other fish species, since earlier reports have shown that fatty fish generally contain less iodine than lean fish (6). Even though it was the leaner part of the Atlantic halibut muscle (B-cut) (20) that was analysed in this study, the fat content in this part of halibut muscle typically lies between 3 and 5 g per 100 g muscle tissue (23). This is considerably higher than the fat content of the four other species, which typically contain about 0.8–1.5 g fat per 100 g muscle tissue (23). The reason why fatty fish contain lower concentrations of iodine is unknown. The iodine content in muscle of farmed Atlantic halibut was even lower than in wild Atlantic halibut, with an average of 7.8 µg/100 g and a range between 4.4 and 11 µg/100 g for the eight pooled samples (Figure 2). The difference may be due to a higher fat content in muscle of farmed halibut compared to wild halibut, but may also be caused by a low iodine content or bioavailability in the fish feed used for Atlantic halibut in fish farms. For salmon, it has been shown that fish muscle is responsive to iodine supplementations in feed to a certain degree (24). Furthermore, there was a general trend of declining concentrations of iodine in fish feed in Norway during 2000–2006, probably due to reduced use of fish meal in feed production (25). However, there must be other bio-

chemical mechanisms explaining the rather large differences in iodine content between codfish and halibut.

Table 5 lists iodine contents of 10 canned tuna products from seven different producers, and mean concentrations of the different products varied from 2 to 10 µg/100 g. The concentrations we measured in this study are lower than those of similar products listed with the following concentrations in the Norwegian Food Composition Table: 26 µg/100 g (in water, drained), 10 µg/100 g (in jelly), 26 µg/100 g (in oil, drained) and 10 µg/100 g (in oil, not drained) (26). In addition, the iodine content in tuna was generally lower than in the other fish species in this study (Table 4). Canned tuna may contain different species of tuna, which is one possible explanation for the variation. Unfortunately, the products analysed in this study were not declared with species, catch area or fish size, factors that may affect iodine content.

Iodine content of milk and cream milk

Table 6 summarises the results for cow milk and cream milk from the present study, showing the seasonal variation of iodine content in the different products. The table also lists iodine concentrations from the Norwegian Food Composition Table.

In this study, mean iodine concentrations of summer milk and fall milk were lower than in winter milk, with values between 12 and 17 µg/100 g in summer and fall milk and between 16 and 20 µg/100 g in winter milk, respectively (Table 6). This difference may be explained by a longer period of outdoor pasture feeding and/or differences in the access to iodine fortified cow feed (27). Previous studies have shown seasonal variation of the iodine content in milk with significantly higher iodine concentration in winter milk compared to spring milk or summer milk (27,

Table 5. Iodine content (mean ± SD) of different types of canned tuna ($n = 3$) purchased in food shops in Bergen, Norway

Type of tuna product (product brand)	Mean ± SD µg/100 g wet weight	Food Composition Table ^a µg/100 g	Sjomatdata ^b
In water (Rema 1000)	9 ± 3	26 ^c	9
In water (Coop)	8 ± 1.5	26 ^c	9
In water (Eldorado)	8 ± 1	26 ^c	9
In water (First Price)	10 ± 1	26 ^c	9
In water (Luxus)	2 ± 1	26 ^c	9
In jelly (Rema 1000)	8 ± 4	10 ^d	8
In oil (Coop)	7 ± 1	25 ^c	8
In oil (Eldorado)	8 ± 2	25 ^c	8
In olive oil (Ortiz)	10 ± 3	n.a.	10
In vegetable oil (Ramirez)	8 ± 1	25 ^c	8

Mean based on three items from different batch numbers.

^aNorwegian Food Composition Table (30.05.2017), www.matvaretabellen.no.

^b<https://sjomatdata.nifes.no/#search/> (14.03.2018).

^cLivsmiddelsverket. Livsmiddelsdatabas, versjon 2013.01.10. www.slv.se.

^dStatens råd for ernæring og fysisk aktivitet og Statens næringsmiddeltilsyn. Analyseprosjekt 2000. Div. matvarer. Internt notat.

n.a. – not available.

Table 6. Comparison of iodine content ($\mu\text{g}/100\text{ g}$ wet weight) of cow milk and cream milk including seasonal variation and producer, compared with declared values and values listed in the Norwegian Food Composition Table

Dairy product (product brand)	Mean ^a \pm SD	Mean ^a \pm SD	Mean ^a \pm SD	Mean ^a \pm SD	Mean
Low-fat milk 1.2% fat (TINE)	September–October 2015 ^b 11.7 \pm 0.6	January–February 2016 ^b 16 \pm 1	June–August 2016 ^b 13 \pm 1	Declaration from producer 20	20 ^d
Skimmed milk 0.7% fat (TINE)	13 \pm 2	16 \pm 1	14 \pm 2	20	20 ^d
Organic low-fat milk 1.2% fat (TINE)	16 \pm 6	20 \pm 2	15 \pm 2	20	20 ^d
Organic low-fat 1.2% fat (Røros Meieri)	NA	NA	17 ^e	-	20 ^d
Low-fat milk 1.0% fat (Q)	12.3 \pm 0.6	18 \pm 2	12.7 \pm 0.6	16	16 ^d
Skimmed milk 0.7% fat (Q)	12 \pm 0	19 \pm 1	13 \pm 0	16	20 ^d
Cream milk 38% (TINE)	September–October 2015 ^b 7.53 \pm 0.06	January–February 2016 ^b 10.3 \pm 0.6	June–July 2016 ^b 9 \pm 1	-	12 ^d
Food Cream milk 20% fat (TINE)	September–October 2015 ^f 11 \pm 2	December 2015–March 2016 ^f 12 \pm 0	May–June 2016 ^f 11 \pm 0	-	16 ^d

^aMean based on three pooled samples

^bDue to short durability, the months in each column illustrates both the production, 'best before' and shopping month for all milks and the cream milk.

^cNorwegian Food Composition Table (30.05.2017), www.matvaretabellen.no

- not declared

NA Not-Analysed

^dData from the food industry, analysed values.

^eMean from one pooled sample, hence no SD.

^fDue to long durability in food cream milk, the months illustrated are based on the production month.

^gDue to smaller production lines of both types of cream milks, the months of sampling and analysis (Table 6) were not always the same as for cow milk.

28). Due to short durability, the months in each column illustrates both the production, 'best before' and shopping month for all milks and the cream milk. Due to long durability in food cream milk, the months illustrated are based on the production month. Due to smaller production lines of both types of cream milks, the months of sampling and analysis (Table 6) were not always the same as for cow milk.

Iodine content of organic milk

In this study, the iodine concentration of the organic milk was equal to or somewhat higher than the conventional milks within the same seasons (Table 6). This result is in contrast to earlier studies from the United Kingdom (29). However, since we have analysed pooled samples, the number of items are too low and statistical analysis is not applicable. Different practices in organic and conventional farms include routine use, or no use, of vitamins and minerals and the use of fresh foods, among other things, which may be restricted in organic farms. Hence, deficiencies in some minerals can occur in organic farms (29). Rasmussen et al. (30) suggest several explanations for the lower iodine content of their organic milk, less use of iodine-containing mineral mixtures being one of them. In the present study, higher use of such mixtures might be a reason for higher concentrations of iodine in organic milk.

Iodine content of other dairy products

The concentration of iodine in Norwegian dairy products are summarised in Table 7. The iodine content were compared to the declaration and to the concentration listed in the Norwegian Food Composition Table (26).

The highest iodine concentrations in the dairy products were found in whey cheese, with concentrations from 100 to 450 µg/100 g (Table 7). In cheese manufacturing, the iodine from milk follows into the whey and not into the curd (9) which is an explaining factor as to why the brown-coloured whey cheese is a rich source of iodine. This type of brown whey cheese is typical in the Norwegian diet. The results from this study show that brown coloured whey cheese is a good source of iodine, which is in accordance with the Norwegian Food Composition Table (26) and a similar study from Norway (27). The presence of goat milk in some of the whey cheeses may also have a positive influence on the concentrations of iodine. This is illustrated by the relatively higher concentrations in both the white-coloured cheese *Snøfrisk* and the brown-coloured whey cheese *Ekte geitost* – both made of goat milk. The latter had more than four times higher concentrations of iodine than the brown-coloured cheese *Flotemysost*, which is prepared from cow milk. In addition, *Gudbrandsdalsost* contains some goat milk, which may be the reason why this cheese has a higher concentration of iodine than *Flotemysost*. In accordance with previous analysis of cheese (6), the iodine content did not vary with fat content

of the cheese (fat content listed in Table 1). Commonly, cow milk and cream milks are used as a base in the production of other dairy products, which is the reason for analysing these products in only one season. Any seasonal differences found in cow milk and cream milk are assumed to be reflected in dairy products. It is important to have updated data on iodine content of these foods because of the great variation between products (31).

Analysed concentrations versus declared concentrations of iodine content

The mandatory nutrition declaration of foods in Norway does not include iodine. A large deviation range is accepted by the food safety authorities regarding declaration of minerals. Thus, we cannot conclude that the new analysis is different from the iodine values declared on the products. To minimise seasonal variations, the iodine intake of cows could be controlled, as discussed by Troan et al. (8). Regarding the declared concentrations, one of the producers in this study have based their declaration on their latest analysis of milk from summer and winter 2012. Another producer in this study has based their latest declaration on analysis from 2012 to 2013 (8). Respectively, the first producer has two dairies (one based in south western Norway and one based in eastern Norway), while the latter producer has dairies placed across the country.

Analysed concentrations versus Norwegian Food Composition Table iodine content

In this study, the mean concentrations of iodine in wild fish were higher than those in the Food Composition Table (Table 4). Thus, estimated intake of iodine from lean fish may be underestimated in dietary surveys from Norway. The range and standard deviations in this study were quite wide. Since concentrations in the Food Composition Table are mean concentrations, analysis of a representative number of samples is necessary in order to estimate intake with high quality. The results for other dairy products than milk in this study were mostly lower than the Food Composition Table (Table 7). In this study, dairy products were sampled and analysed only in autumn, which might be one factor explaining the lower values. In accordance with earlier findings, the iodine varies with seasons, however the seasonal differences are less clear in the present study compared with earlier findings. To reflect the true variation, the Food Composition Table information of nutrient concentrations should include range values.

Iodine content of hen's eggs

Table 8 lists updated concentrations of iodine of different types of egg compared to the Food Composition Table. Concentrations measured in whole eggs in this study varied from 23 to 43 µg/100 g, and the values given in the Food Composition Table were within this range, with 35 and 38.5 µg/100 g. Whole eggs from one of the producers

Table 7. Comparison of iodine content ($\mu\text{g}/100\text{ g}$ wet weight) from the present study compared with the product declaration and the Norwegian Food Composition Table

Dairy product	Mean ^a ($\mu\text{g}/100\text{ g}$ wet weight)	Declaration from producer	Food Composition Table ^b
<i>Cow milk with flavour and alternative milk</i>			
Chocolate-flavoured low-fat cow milk, Q	17	-	18 ^c
Soy milk with natural flavour, Alpro	<2	-	1 ^d
<i>Probiotic milk with LGG</i>			
'Biola' with blueberry flavour, TINE	14	16	16 ^c
<i>Yoghurt</i>			
'Go'morgen' with flavour, TINE	13	-	14 ^e
Yoghurt with natural flavour, TINE	18	-	13 ^e
<i>White-coloured solid cheese</i>			
'Norvegia', TINE	14	31	31 ^c
'Jarlsberg', TINE	14	32	37 ^c
'Norsk gulost', Synnoeve Finden	19	-	-
<i>White soft and cream cheeses</i>			
Brie, Arla Foods	13	-	43 ^c
Camembert, TINE	18	45	45 ^c
Soft, cream cheese, 'Snøfrisk', TINE	46	49	49 ^c
Soft, cream cheese, 'Philadelphia', Mondalez	14	-	7 ^f
<i>Whey cheese</i>			
'Gudbrandsdalsost', TINE	140	166	166 ^c
'Fløtemysost', TINE	100	135	135 ^c
'Ekte geitost', TINE	450	307	306.6 ^{c,g}
<i>Other dairy products</i>			
Crème fraîche, TINE	10	-	12 ^c
Cottage cheese, TINE	15	-	14 ^h
Curd with natural flavour, TINE	16	-	20 ^c
Sour cream, TINE	9	-	12 ^c

^aMean based on two replicates per pooled sample (one pooled sample consists of three items of three different batch numbers)

^bNorwegian Food Composition Table (30.05.2017), www.matvaretabellen.no

^cData from the food industry.

^dPublic Health England og Institute of food research (2015). McCance and Widdowson's The Composition of Foods, Seventh summary edition. Cambridge: The Royal Society of Chemistry.

^eThe value is calculated from similar foods.

^fLivsmiddelsverket. Livsmiddelsdatabas, versjon 2016.02.17.

^gGoat cheese, whey

LGG, *Lactobacillus rhamnosus GG*

- no declaration

^hDanmarks Fødevarerforsknig. Fødevardatabanken, versjon 7.01 (2009).

from 2016 had lower iodine concentrations than those from the same producer in 2017. This is interesting and may be due to natural variation or changes in ingredients of the hen's feed. The latter is unfortunately unknown to the authors as this topic is outside the scope of this manuscript. None of the producers have declared iodine contents. Iodine concentrations of eggs in this study were lower as compared to the results from a previous study in Norway where mean concentrations were $45\ \mu\text{g}/100\text{ g}$ (range $39\text{--}52\ \mu\text{g}/100\text{ g}$, $n = 90$) (6). Regarding iodine, a larger portion is contained in yolk (32). This was also shown in our results, where yolk had iodine concentrations of 57 and $78\ \mu\text{g}/100\text{ g}$ and egg white only 2.4 and

$3.0\ \mu\text{g}/100\text{ g}$ (Table 8). In this study, separate analysis of egg yolk and egg white was only carried out for conventional eggs, while whole egg was analysed for both conventional and organic eggs.

Conclusion

The fish analysed not only showed a large variation in iodine content between different species but also between individuals within the same species and between locations and/or sampling seasons. Despite these differences, applying our new values would influence intake estimates considerably. Regarding dairy products, the results confirm previous data on seasonal variation of iodine

Table 8. Comparison of mean iodine content ($\mu\text{g}/100\text{ g}$) in different conventional and organic hen's eggs

Type of hen's egg (producer)	New analysis			Food Composition Table ^a		
	Whole egg	Egg white	Yolk	Whole egg	Egg white	Yolk
Conventional (Prior), 2016 ^b	23	2.4	57 ^b	35 ^c	3.4 ^c	80.2 ^c
Conventional (Prior), 2017 ^d	43	NA	NA			
Conventional (Den stolte hane), 2016 ^b	33	3	78			
Conventional (Den stolte hane), 2017 ^d	41	NA	NA			
Organic (Prior), 2016 ^b	43	NA	NA	38.5 ^c		
Organic (Prior), 2017 ^d	40	NA	NA			
Organic (Den stolte hane), 2016 ^b	40	NA	NA			
Organic (Den stolte hane), 2017 ^d	31	NA	NA			

^aNorwegian Food Composition Table (30.05.2017), www.matvaretabellen.no

^bThe sample consists of 36 eggs.

^cCalculated mean from the Analyses project 2016–2017. Analysis of eggs and chicken (2017): The Norwegian Food Safety Authorities.

^dEach sample consists of 18 eggs ($n = 2$).

NA not analysed.

content in milk. This study provided updated data of the iodine concentration in six fish species, 27 selected Norwegian iodine-rich dairy foods and Norwegian hen's eggs, which will be made available for the public Food Composition Table.

Acknowledgement

A special thanks to the personnel at the laboratory at Institute of Marine Research, for preparing and analysing the samples, and personnel on the Reference fleet and research vessels, who collected the wild fish analysed in this study. In addition, thank you to Ellen Kielland at the Norwegian Food Safety Authority for collaboration with the sampling of egg. The Norwegian Seafood Research Fund (FHF) financially supported this trial (grant number: 901038).

References

- Abel MH, Caspersen IH, Meltzer HM, Haugen M, Brandlistuen RE, Aase H, et al. Suboptimal maternal iodine intake is associated with impaired child neurodevelopment at 3 years of age in the Norwegian Mother and Child Cohort Study. *J Nutr* 2017; 147(7): 1314–24.
- Hynes KL, Otahal P, Hay I, Burgess JR. Mild iodine deficiency during pregnancy is associated with reduced educational outcomes in the offspring: 9-year follow-up of the gestational iodine cohort. *J Clin Endocrinol Metab* 2013; 98(5): 1954–62.
- Pearce EN, Lazarus JH, Moreno-Reyes R, Zimmermann MB. Consequences of iodine deficiency and excess in pregnant women: an overview of current knowns and unknowns. *Am J Clin Nutr* 2016; 104(Suppl 3): 918S–23S.
- Bath SC, Rayman MP. Iodine deficiency in the U.K.: an overlooked cause of impaired neurodevelopment? *Proc Nutr Soc* 2013; 72(2): 226–35.
- Gunnarsdottir I, Gustavsdottir AG, Thorsdottir I. Iodine intake and status in Iceland through a period of 60 years. *Food Nutr Res* 2009; 53: 1925.
- Dahl L, Johansson L, Julshamn K, Meltzer HM. The iodine content of Norwegian foods and diets. *Public Health Nutr* 2004; 7(4): 569–76.
- Julshamn K, Dahl L, Eckhoff K. Determination of iodine in seafood by inductively coupled plasma/mass spectrometry. *J AOAC Int* 2001; 84(6): 1976–83.
- Troan G, Dahl L, Meltzer HM, Abel MH, Indahl UG, Haug A, et al. A model to secure a stable iodine concentration in milk. *Food Nutr Res* 2015; 59: 29829.
- Haldimann M, Alt A, Blanc A, Blondeau K. Iodine content of food groups. *J Food Compos Anal* 2005; 18(6): 461–71.
- WHO, UNICEF, ICCID. Assessment of iodine deficiency disorders and monitoring their elimination: a guide for programme managers. Geneva: World Health Organization; 2007.
- Nystrom HF, Brantsaeter AL, Erlund I, Gunnarsdottir I, Hulthen L, Laurberg P, et al. Iodine status in the Nordic countries – past and present. *Food Nutr Res* 2016; 60: 31969.
- Volzke H, Caron P, Dahl L, de Castro JJ, Erlund I, Gaberscek S, et al. Ensuring effective prevention of iodine deficiency disorders. *Thyroid* 2016; 26(2): 189–96.
- Rasmussen LB, Carle A, Jorgensen T, Knudsen N, Laurberg P, Pedersen IB, et al. Iodine intake before and after mandatory iodization in Denmark: results from the Danish Investigation of Iodine Intake and Thyroid Diseases (DanThyr) study. *Br J Nutr* 2008; 100(1): 166–73.
- Julshamn K, Duinker A, Nilsen BM, Frantzen S, Maage A, Valdernesnes S, et al. A baseline study of levels of mercury, arsenic, cadmium and lead in Northeast Arctic cod (*Gadus morhua*) from different parts of the Barents Sea. *Mar Pollut Bull* 2013; 67(1–2): 187–95.
- Julshamn K, Duinker A, Nilsen BM, Nedreaas K, Maage A. A baseline study of metals in cod (*Gadus morhua*) from the North Sea and coastal Norwegian waters, with focus on mercury, arsenic, cadmium and lead. *Mar Pollut Bull* 2013; 72(1): 264–73.
- Frantzen S, Maage A. Fremmedstoffer i villfisk med vekt på kystnære farvann [Contaminants in wild caught fish with emphasis on coastal waters. Tusk, ling and bycatch species. Results for samples collected during 2013–2015]. Brosme, lange og bifangstarter. 2016. Available from: <https://nifes.hi.no/report/rapport-villfisk-2016/>
- Nilsen BM, Nedreaas K, Maage A. Kartlegging av fremmedstoffer i Atlantisk kveite (*Hippoglossus hippoglossus*). [Baseline study of contaminants in Atlantic halibut (*Hippoglossus hippoglossus*)]. 2016. Available from: <https://nifes.hi.no/report/atlantisk-kveite-sluttrapport/>

18. Nilsen BM, Julshamn K, Duinker A, Nedreaas K, Maage A. Basisundersøkelse av fremmedstoffer i sei (*Pollachius virens*) fra Nordsjøen. [Baseline study of contaminants in saithe (*Pollachius virens*) from the North Sea]. 2013. Available from: <https://nifes.hi.no/report/basisundersokelse-av-fremmedstoffer-i-sei-pollachius-virens-fra-nordsjoen/>
19. Nilsen BM, Julshamn K, Duinker A, Nedreaas K, Maage A. Basisundersøkelse av fremmedstoffer i sei (*Pollachius virens*) fra Norskehavet og Barentshavet. [Baseline study of contaminants in saithe (*Pollachius virens*) from the Norwegian Sea and the Barents Sea]2013. Available from: <https://nifes.hi.no/report/basisundersokelse-fremmedstoffer-sei-norskehavet-barentshavet/>
20. Nortvedt R, Tuene S. Body composition and sensory assessment of three weight groups of Atlantic halibut (*Hippoglossus hippoglossus*) fed three pellet sizes and three dietary fat levels. *Aquaculture* 1998; 161(1–4): 295–313.
21. Shelor CP, Dasgupta PK. Review of analytical methods for the quantification of iodine in complex matrices. *Anal Chim Acta* 2011; 702(1): 16–36.
22. Olsen E, Aanes S, Mehl S, Holst JC, Aglen A, Gjørseter H. Cod, haddock, saithe, herring, and capelin in the Barents Sea and adjacent waters: a review of the biological value of the area. *ICES J Marine Sci* 2010; 67(1): 87–101.
23. IMR (Institute of Marine Research). Seafood data. 2018. Available from: <https://sjomatdata.nifes.no/#/substance/402/-1> [cited 19 March 2018].
24. Julshamn K, Maage A, Waagbø R, Lundebye A. A preliminary study on tailoring of fillet iodine concentrations in adult Atlantic salmon (*Salmo salar* L.) through dietary supplementation. *Aquacult Nutr* 2006; 12: 45–51.
25. Sissener NH, Julshamn K, Espe M, Maage A. Surveillance of selected nutrients, additives and undesirables in commercial Norwegian fish feeds in the years 2000–2010. *Aquacult Nutr* 2013; 19(4): 555–572.
26. Norwegian Food Safety Authority TNDoh, University of Oslo. Norwegian food composition database. 2016. Available from: <http://matvaretabellen.no/?!language=en> [cited 23 June 2017].
27. Dahl L, Opsahl JA, Meltzer HM, Julshamn K. Iodine concentration in Norwegian milk and dairy products. *Br J Nutr* 2003; 90(3): 679–85.
28. Cressey PJ. Iodine content of New Zealand dairy products. *J Food Compos Anal* 2003; 16(1): 25–36.
29. Bath SC, Button S, Rayman MP. Iodine concentration of organic and conventional milk: implications for iodine intake. *Br J Nutr* 2012; 107(7): 935–40.
30. Rasmussen LB, Larsen EH, Ovesen L. Iodine content in drinking water and other beverages in Denmark. *Eur J Clin Nutr* 2000; 54(1): 57–60.
31. Norwegian Scientific Committee for Food Safety V. Assessment of salt fortified with iodine and flouride. Available from: <https://www.vkm.no/download/18.2994e95b15cc5450716d638b/1500307741080/895624d06a.pdf>
32. Travnicek J, Kroupova V, Herzig I, Kursá J. Iodine content in consumer hen eggs. *Vet Med (Praha)* 2006; 51(3): 93.

***Lisbeth Dahl**

Institute of Marine Research P.O. Box 1870 Nordnes

NO-5817 Bergen, Norway

Email: Lisbeth.Dahl@hi.no

A novel polysaccharide from the *Sarcodon aspratus* triggers apoptosis in Hela cells via induction of mitochondrial dysfunction

Dan-Dan Wang¹, Qing-Xi Wu¹, Wen-Juan Pan¹, Sajid Hussain¹, Shomaila Mehmood¹ and Yan Chen^{1,2*}

¹School of Life Sciences, Anhui University, Hefei, China; ²Anhui Key Laboratory of Modern Biomanufacturing, Hefei, China

Abstract

Background: Polysaccharides extracted from fungus that have been used widely in the food and drugs industries due to biological activities.

Objective: The objective of the present study was to investigate the tumor-suppressive activity and mechanism of a novel polysaccharide (SAP) extracted from *Sarcodon aspratus*.

Methods: The SAP was extracted and purified using Sepharose CL-4B gel from *S. aspratus*. The cytotoxicity of SAP on cell lines was determined by MTT method. Cellular migration assays were implemented by using transwell plates. The apoptosis and mitochondrial membrane potential ($\Delta\psi_m$) of Hela cells were analyzed by flow cytometry. The western blot was used to determine the protein expression of Hela cells.

Results: The results showed that SAP with a molecular weight of 9.01×10^5 Da could significantly inhibit the growth of Hela cells *in vitro*. Three-dimensional cell culture (3D) and transwell assays showed that SAP restrained the multi-cellular spheroids growth and cell migration. Flow cytometry analysis revealed that SAP induced a loss of mitochondrial membrane potential ($\Delta\psi_m$). Western blot assays indicated that SAP promoted the release of cytochrome c, increased Bax expression, down-regulated of Bcl-2 expression and activated of caspase-3 expression.

Conclusion: This study suggested that SAP induced Hela cells apoptosis via mitochondrial dysfunction that are critical in events of caspase apoptotic pathways. The anti-tumor (Hela cells) activity of SAP recommended that *S. aspratus* could be used as a powerful medicinal mushroom against cancer.

Keywords: *Sarcodon aspratus*; mushrooms; polysaccharide; apoptosis; mitochondrial dysfunction

In recent years, various therapeutic means have contributed to the treatment and prevention of cancers, but these methods can provoke irreversible side effects. Thus, the urgent task of the new drug research is to pursue the natural alternatives with high therapeutic properties and low toxicity. With unique advantages of nontoxic and anticancer cell activities, the polysaccharides from medicinal mushrooms have attracted global interest from pharmaceutical industries as a miraculous herbal medicine (1, 2). In particular, *Ganoderma lucidum* (3), *Lentinus edodes* (4), and *Grifola frondosa* (5) are commonly known medicinal mushrooms worldwide.

Sarcodon aspratus is a famous rare delicious and edible mushroom grown mainly in the Yunnan Province, China. Earlier experiments had demonstrated that the fucogalactan isolated from *S. aspratus* triggers the release of the tumor necrosis factor- α and nitric oxide from murine

macrophages associated with antitumor effect (6). In addition, the polysaccharide from *S. aspratus* had immunostimulatory activity (7). Two polysaccharide fractions were separated from the mycelium of *S. aspratus* in our laboratory; they displayed strong tumor-suppressive activities with no cytotoxicity against normal cell lines *in vitro* (8). However, investigation on the *S. aspratus* has its main focus toward the characteristics and medicinal value of polysaccharides. There is little information related to biochemical mechanisms underlining the tumor cells apoptosis promotion by polysaccharides isolated from fruiting bodies of *S. aspratus*.

Mitochondria, as a vital organelle existing in almost all eukaryotic cells to supply energy for various activities, are viewed as central regulator of the decision between cellular survival and demise (9). There is a burgeoning interest in the scientific community to fully define the role

of mitochondria in cellular apoptosis. There is abundant evidence to demonstrate that mitochondria can release cytochrome c and other proteins to activate caspases and trigger tumor cells apoptosis (10). The experiments presented in this article provide some guidelines for elucidating the tumor-suppressive activity and mechanism of a new polysaccharide (SAP) extracted and purified from the fruiting bodies of *S. aspratus*. Given the evidence that SAP induce HeLa cells apoptosis via a mitochondrial pathway, the study will be helpful to develop novel functional foods and drugs.

Materials and methods

Materials and chemicals

The *S. aspratus* fruiting bodies were obtained from Yimeng Yisheng edible fungus cooperative (Yunnan, China). Human uterine cervix carcinoma cell line (HeLa), human hepatoma cell line (HepG-2), human stomach cancer cell line (HGC-27), and human normal liver cell line (MRC-5) were purchased from the cell bank of Shanghai Institute of Cell Biology (Shanghai, China). Sepharose CL-4B gel was obtained from Amersham (Uppsala, Sweden). Dextran standards, standard monosaccharides, 5-fluorouracil (5-Fu), 3-(4,5-dimethylthiazol-2-yl)-2,5-diphenyl tetrazoliumbromide (MTT), 5,5',6,6'-tetraethylimida-carbocyanine iodide (JC-1), and poly(2-hydroxyethylmethacrylate) (poly-HEMA) were obtained from Sigma (St. Louis, MO, USA). Fetal bovine serum (FBS) and RPMI-1640 medium were obtained from Wisten Biotechnology (WISTEN Co. Ltd., Nanjing); 24-well transwell plates were acquired from Corning (NY, USA). Anti- β -actin antibody, anti-caspase-9 antibody, anti-caspase-3 antibody, anti-Bcl-2 antibody, anti-Bax antibody, and anti-cytochrome c antibody were purchased from Abcam (Cambridge, UK). All the kits used in assays were supplied by Shanghai Beyotime Bioengineering Institute (Shanghai, China). All other chemical reagents used were of analytical grade.

Preparation and purification of *S. aspratus* polysaccharide

The fruits of *S. aspratus* (100 g) were dipped into the 95% ethanol at 70°C for 2 h to remove lipid and some colored materials. After filtering, the residue was collected and immersed into distilled water (1:5, w/v) three times at 80°C for 2 h. The supernatant was concentrated to 50 mL with a rotary evaporator at 65°C under vacuum. Then, the concentrate was added to a fourfold of 95% (v/v) ethanol and kept overnight at 4°C. The precipitates were obtained by centrifugation (4,500 rpm, 10 min) and dissolved in distilled water to remove the proteins by using Sevag method (11). After that, dialyzed against distilled water, the crude polysaccharides were obtained after the freeze-drying.

The crude polysaccharides (100 mg) were loaded on Sepharose CL-4B column (2.6 × 100 cm) equilibrated with deionized water at a flow rate of 1 mL/min. The eluting

fractions were monitored by high-performance liquid chromatography (HPLC) instrument (Agilent Technologies, Palo Alto, CA, USA). The relevant fraction was collected, concentrated, and lyophilized to obtain a brown polysaccharide (SAP), which was examined whether or not polysaccharide could inhibit the growth of cancer cells.

Molecular weight determination

Molecular weight of the polysaccharide was determined by HPLC equipped with Ultrahydrogel 1000 (300 × 7.8 mm, Tosoh Corp, Tokyo, Japan) and an evaporative light scattering detector (ELSD). Standard dextrans including T-10, T-40, T-70, T-500, and T-1000 were used as molecular mass markers. Sample solution (10 mg/mL, 10 μ L) was injected into each run and eluted with distilled water at 30°C with a flow rate of 1.0 mL/min.

Infrared spectral analysis

The construction of SAP was detected by Fourier transform infrared spectrometer (FT-IR). The sample (1.0 mg) was ground with 100 mg potassium bromide (KBr) powder and then pressed into pellets for FT-IR measurement in the frequency range of 4,000–4500 cm^{-1} .

Chemical characters of the polysaccharide

The polysaccharide content of SAP was estimated by phenol-sulfuric acid method, and the protein content was detected by Coomassie Brilliant Blue G-250 method.

The monosaccharide compositions of the polysaccharide were determined using the method reported by our laboratory (12). Briefly, the SAP (10 mg) was hydrolyzed with 2 M trifluoroacetic acid (TFA, 110°C, 6 h), and the residual acid was removed with a rotary evaporator at 65°C under vacuum. The hydrolysis product monosaccharides and standard monosaccharides (including d-fructose, d-mannose, l-rhamnose, d-glucose, d-galactose, d-xylose, and l-fucose) were derivatized to be 0.5 mol/L 1-phenyl-3-methyl-5-pyrazolone (PMP) and 0.5 mol/L NaOH incubated at 70°C for 30 min. The hydrolysates were analyzed by HPLC equipped with a ZORBAX SB-C18 column (150×4.6 nm, particle size 5 μ m, Agilent Technologies, CA, USA). The analysis was performed using gradient elution of acetonitrile (14–20–40%) and 200 mM ammonium acetate (86–80–60%) for 0–20–30 min, respectively, with the flow rate of 1.0 mL/min and UV absorbance at 245 nm.

Cell culture

The cell lines were cultured in RPMI-1640 medium containing 10% FBS at 37°C and 5% CO_2 in a humidified atmosphere incubator.

Effect of cytotoxicity of the polysaccharide

The cytotoxicity of SAP on HeLa, HepG-2, HGC-27, and MRC-5 cells was determined by MTT method (13).

A single cell was dispensed in a 96-well culture plate at density of 3×10^3 cells per well. After 24 h, cells were incubated with various concentrations of SAP (25, 50, 100, 200, and 400 $\mu\text{g}/\text{mL}$), with 5-Fu (25 $\mu\text{g}/\text{mL}$) as positive group, whereas the control group was treated with the medium, only for 48 h. The cells were incubated with 100 μL of MTT (0.5% w/v) for 4 h at 37°C in dark. After removing the supernatant, the formazan crystals in the cells were dissolved in dimethyl sulfoxide (DMSO, 100 μL /well). Then, the plates were placed in microplate reader (Epoch-2, Biotek) and the absorbance was measured at 560 nm. The cytotoxicity of SAP was expressed as percentage of cell viability as compared to control.

The effect of SAP restrains tumor migration ability

Cellular migration assays were implemented using 24-well transwell plates containing 8.0 μm pore membrane (14). The HeLa cells (5×10^4) were resuspended in serum-free medium and then added into the upper insert membrane. RPMI-1640 medium supplemented with 20% FBS was added into the bottom chamber. Cells were then treated with polysaccharide and 5-Fu for 48 h, concurrently. The cells without the treatment of SAP were used as control group. Then, the migrated cells fixed with methanol and cells localized on the bottom membrane surface. After staining with hematoxylin–eosin, the migrated cells were imaged and counted using an inverted microscope (Carl Zeiss, Oberkochen, Germany) (10 \times magnification, at least five fields per condition).

Proliferation rate of multicellular spheroids of HeLa cells

The cell culture flask, the bottom of which was coated with a layer of poly-HEMA thin film, was exposed to ultraviolet light for 3 h to ensure asepsis before use. The HeLa monolayer cells (5×10^5) were resuspended in the medium containing 5% FBS and then seeded in the cell culture flask. Cells were incubated at 37°C with 5% CO₂, and the culture medium was changed every other day (15). After 2 days, the HeLa multicellular spheroids (MCS) could self-assemble to form three-dimensional (3D) MCS. HeLa 3D tumor models maintained good structural stability for 3 days. Then, we added the water extract of SAP (200 $\mu\text{g}/\text{mL}$) and 5-Fu (25 $\mu\text{g}/\text{mL}$) to the cultures. MCS formation and growth were monitored every day; MCS of HeLa cells were examined under an inverted microscope.

Cell apoptosis analysis

To analyze apoptosis of HeLa cells, an Annexin V-FITC Apoptosis Detection Kit was used (16). HeLa cells were seeded at a density of 5×10^5 cells per well in 6-wells plate with 1.5 mL culture medium. Twenty-four hours after cell inoculation, the SAP was added to the cultures at different concentrations (50, 100, and 200 $\mu\text{g}/\text{mL}$) and

5-Fu (25 $\mu\text{g}/\text{mL}$). After 48 h, we used Annexin V-FITC Apoptosis Detection Kit to detect the cell apoptosis. The stained cells were analyzed by FACSCalibur (BD Biosciences; Ex = 488 nm; Em = 530 nm). The data were collected and analyzed using Cell Quest pro software. At least 10,000 events were evaluated.

Mitochondrial membrane potential

The mitochondrial membrane potential ($\Delta\psi\text{m}$) of HeLa cells was analyzed by JC-1. JC-1 is a lipophilic fluorochrome that is used to evaluate the status of the $\Delta\psi\text{m}$ (17). JC-1 that fluoresces in the FL-1 channel (R1), which J-aggregates, will emit red fluorescence at high membrane potential in healthy cells, and JC-1 that lacks fluorescence in the FL-2 channel (R2) is considered to correspond to mitochondrial dysfunction with a depolarized $\Delta\psi\text{m}$ which remained green fluorescence monomers. The HeLa cells were treated by the same methods as described above. They were harvested and labeled with JC-1 and then analyzed by flow cytometry. The data were collected and analyzed using Cell Quest pro software. At least 10,000 events were evaluated.

Western blot analysis

After the treatment with SAP (0, 50, 100, 200 $\mu\text{g}/\text{mL}$) for 48 h, the HeLa cells were lysed with ice-cold radioimmunoprecipitation assay (RIPA) buffer for 30 min over ice and then centrifuged at 12,000 r/min for 15 min at 4°C to obtain the cytosol fraction. In order to obtain cytochrome c protein, Cell Mitochondrial Isolation Kit was used. The protein concentration was determined with BCA Protein Assay Kit according to the manufacturer's protocol. The proteins were denatured by boiling in 1 \times loading buffer, and protein samples were separated by 12% SDS-polyacrylamide gel electrophoresis (SDS-PAGE) and electroblotted onto a 0.22 μm polyvinylidene difluoride (PVDF). Subsequently, the membrane was blocked in blocking buffer (5% skim milk with 1 \times Tris-buffered saline [TBS] containing 0.1% Tween-20) for 3 h with shaking at room temperature, followed by incubation with the primary antibodies (cytochrome c, Bcl-2, Bax, caspase-3, procaspase-9, and β -actin) overnight at 4°C. The membrane was then washed by suspending it in washing buffer (add 5 mL of 10% Tween-20 to 1,000 mL TBS), agitated for 10 min and incubated with the appropriate secondary antibodies for 3 h at room temperature. After washing twice with TBS (15 min/time), the antibody-specific protein was visualized by enhanced chemiluminescence (ECL) detection system with ECL Kit.

Statistical analysis

Results were expressed as mean \pm standard deviation (SD). The statistical significance of difference groups was evaluated by analysis of variance, followed by Service Solutions (SPSS, version 18.0) software. A value of $p < 0.05$ was regarded to be statistically significant.

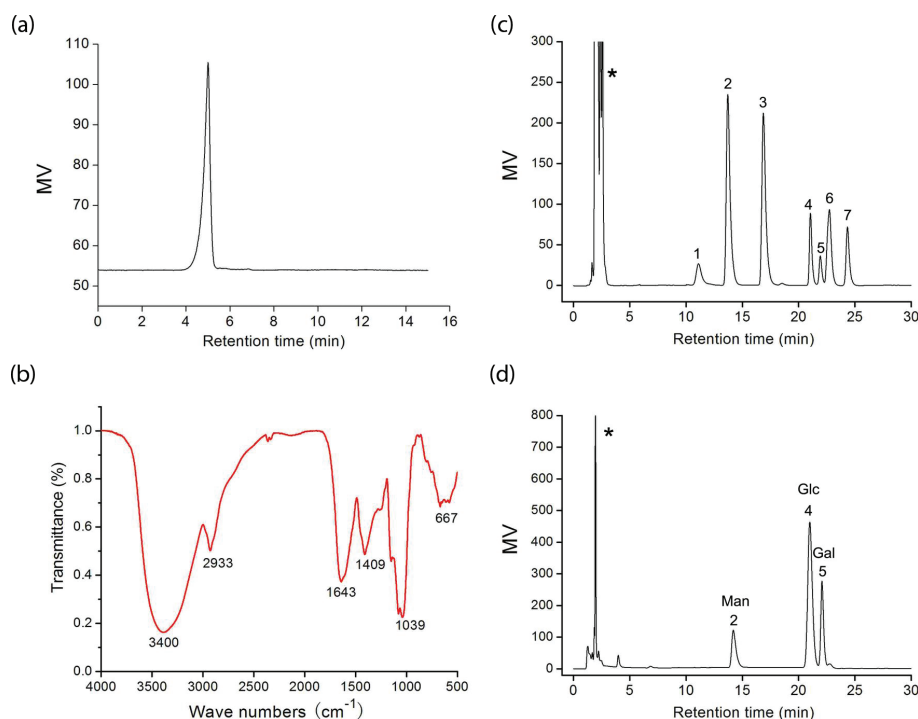


Fig. 1. (a) HPLC chromatogram of SAP; (b) FT-IR spectrum of SAP; (c) a standard mixture of monosaccharides; (d) analysis of monosaccharide composition of SAP (*-solvent peak, 1-fructose, 2-mannose, 3-rhamnose, 4-glucose, 5-galactose, 6-xylose, and 7-fucose).

Results and discussion

Preparation and chemical characters of the polysaccharide

The crude polysaccharide was isolated from the fruiting bodies of *S. aspratus* and purified by Sepharose CL-4B gel. The homogeneity and average molecular weight of the SAP were estimated using an HPLC method. SAP showed single and symmetrical peaks, indicating their homogeneity (Fig. 1a). The SAP retention time was 4.63 min. The average molecular weight of SAP fractions was estimated to be about 9.01×10^5 Da.

FT-IR has been shown to be a powerful tool for the identification of characteristic organic groups in the polysaccharide (Fig. 1b). The absorbance band at $3,400\text{ cm}^{-1}$ represented the stretching vibration of O-H in the constituent sugar residues (18). The adjacent peak at $2,933\text{ cm}^{-1}$ was found for the stretching vibration of C-H in the sugar ring (19). The relatively strong absorption peak at $1,643\text{ cm}^{-1}$ was caused by the bending vibration of C-O bonds in uronic acids. On the contrary, SAP had the absorption band centered at $1,409\text{ cm}^{-1}$ due to the C-H (deformation) (20). In addition, the absorbance of polysaccharides in the range $1,040\text{--}1,600\text{ cm}^{-1}$ was characteristic of the C-O (19). The sugar composition of SAP was identified and quantified by HPLC analysis (Fig. 1c). The results indicated that it was composed of D-galactose, D-glucose, and D-mannose with molar ratios of

1.48:4.13:1.0. The total sugar content of SAP was about 85.68% and its protein content was 4.25%.

Effect of cytotoxicity of the polysaccharide

We evaluated the cytotoxicity of SAP toward Hela, HepG-2, and HGC-27 cells by MTT (Fig. 2a). The cancer cells viability obvious descent was triggered by SAP and occurred in a dose-dependent manner in comparison with the control group. The SAP presented significantly high inhibition for Hela cells that could reach 70% at the concentration of $200\text{ }\mu\text{g/mL}$, which was in good agreement to our previous work (8). In addition, cytotoxicity of SAP toward normal cells was also determined in comparison with 5-Fu. The SAP had no cytotoxicity on MRC-5 (human normal cells) even at high concentration ($400\text{ }\mu\text{g/mL}$), but 5-Fu ($25\text{ }\mu\text{g/mL}$) killed human normal cells (Fig. 2b). Our previous study and current results indicated that polysaccharides extracted, whether from mycelium or fruiting bodies, preferably inhibit Hela cells. Based on the significant tumor-suppressive activity, Hela cells were chosen as the targeted cell line to further investigate the antitumor activity and molecular mechanism of SAP.

SAP restrains tumor migration ability

Metastasis, which is an essential character of biological behaviors in malignancies, is also the main reason for

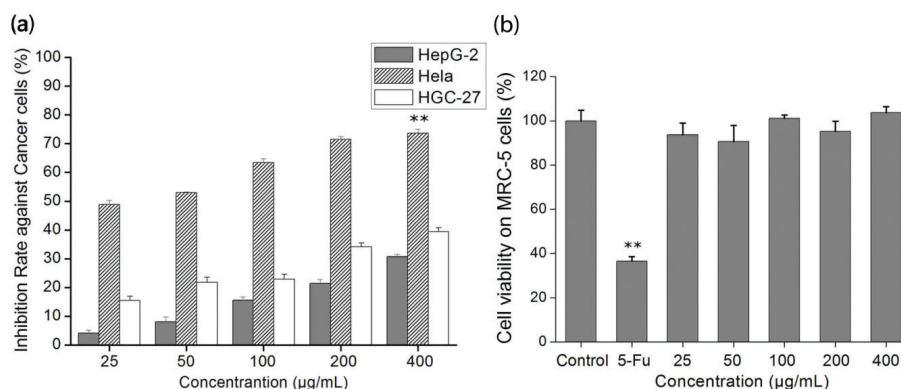


Fig. 2. The *in vitro* growth inhibition ratio of cells by SAP. (a) Cytotoxicity of SAP in HepG-2, Hela or HGC-27 cancer cells; (b) cytotoxicity of SAP at different concentrations and 5-Fu (25 µg/mL) on MRC-5 cells. The results were expressed as means \pm SD ($n = 3$) for MTT assay. (a) $**p < 0.01$ compared with HGC-27 cells. (b) $**p < 0.01$ compared with control group.

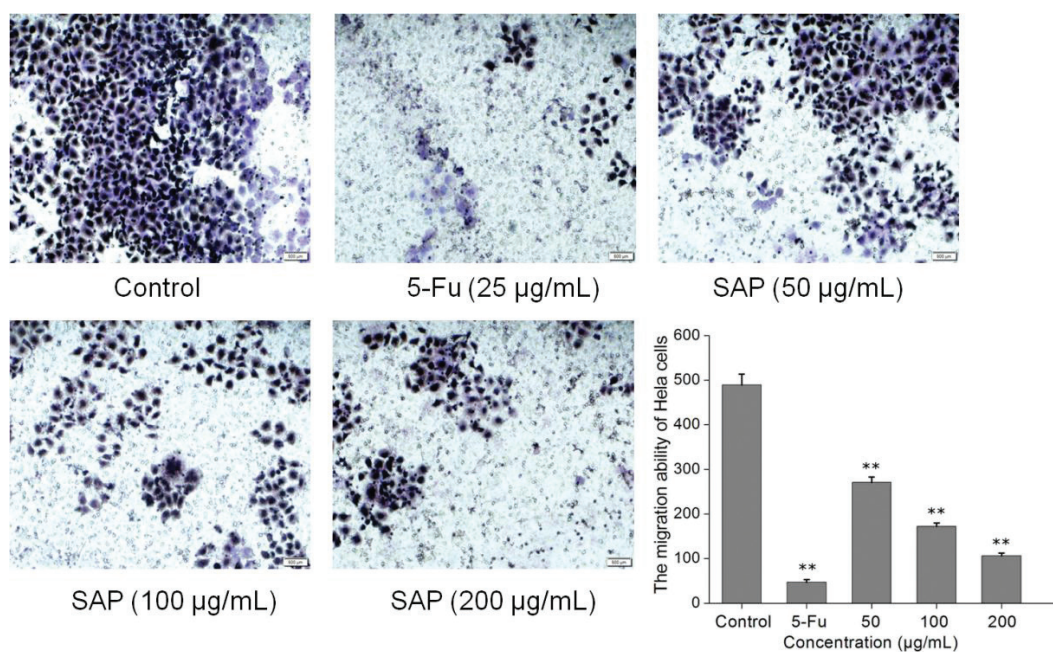


Fig. 3. The effect of SAP restrains tumor migration ability of Hela cells. Typical photos and quantification of the transwell migration assay with Hela cells co-cultured with SAP or 5-Fu. The results were expressed as means \pm SD ($n = 3$). $**p < 0.01$ compared with control group.

the death of tumor sufferers (21). We examined whether SAP could suppress the migration of Hela cells. The migrated cells were stained with hematoxylin–eosin; the transwell assay showed that migrated cells were significantly reduced with SAP (200 µg/mL) co-cultured for 48 h (Fig. 3). The migrated cells were counted by using an inverted microscope at six fields per condition; the data indicated that the SAP at low concentration (50 µg/mL) could suppress the cell migration compared with control ($p < 0.05$). These observations suggested that SAP significantly suppressed the migration ability of Hela cells.

Proliferation rate of multicellular spheroids of Hela cells

Three-dimensional (3D) cell culture has microenvironment characteristics of cells in living organisms, which is better than classic two-dimensional (2D) cell culture. MCS represent the most common use of cancer research (22–24). In addition, cancer cells in 3D environments exhibit stronger survival potential as well as more powerful chemoresistance to anticancer drugs (24). To validate the anticancer effect of SAP, we developed 3D tumor models based on human cancer cells. An inverted microscope was used to observe the morphology of Hela cells over a 4-day treatment with 200 µg/mL SAP and

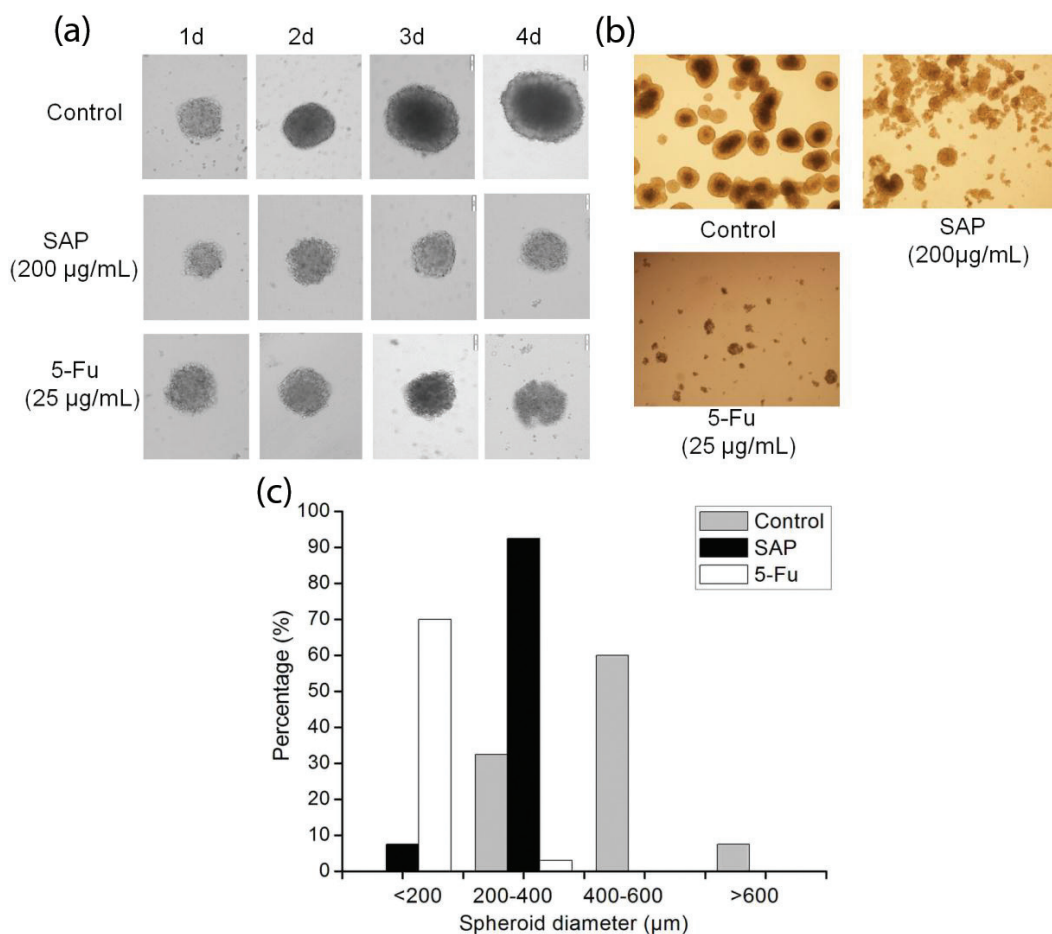


Fig. 4. The multicellular spheroids of HeLa cells were treated with 5-Fu (25 µg/mL) and SAP (200 µg/mL). (a) Cellular morphological changes during 4 days of culture in 3D constructs were observed under contrast microscope (Olympus, Japan). (b) Representative photographs of the multicellular spheroids and (c) distribution of spheroid diameter in 3D HeLa cells on day 6.

25 µg/mL 5-Fu. Diameters of HeLa MCS increased every day in control group; however, MCS in SAP-treated group were almost not increased as compared to that in the control group (Fig. 4a). To further analyze the cellular morphology in the 3D constructs, we observed a pride of MCs after 6 days (Fig. 4b). It was shown that HeLa cells formed round spheroids with smooth surface and tight cell–cell connections in the control group. Image-based nano measure analysis was used to measure the spheroid's diameter. It is obvious from Fig. 4c that MCS in the control group have shown increased diameter (>600 µm) after 6 days. On the contrary, SAP-treated MCS displayed smaller diameter (≤400 µm) as compared to the control group.

SAP induced cell apoptosis

To investigate whether SAP induced decrease in HeLa cells viability was related to cell apoptosis, HeLa cells were treated with 5-Fu and different concentrations of SAP for 48 h; the cells were stained (with Annexin V-FITC and PI) and analyzed by flow cytometry. We found that low

concentrations of SAP (50 µg/mL) induced cell apoptosis (12.31%) as compared to the control (1.47%) (Fig. 5). As a result of the treatment with SAP (200 µg/mL), the percentage of living cells significantly declined from 98.05% (control group) to 75.21%, which was close to the 5-Fu (25 µg/mL) effect (63.55%). In light of this, a conclusion could be drawn that SAP might induce HeLa cells apoptosis.

SAP induces the dissipation of mitochondrial membrane potential

Recent studies have shown that mitochondrial metabolism is a research field that has development for cancer therapy (25). Apoptosis is frequently associated with depolarization of the mitochondrial membrane potential ($\Delta\psi_m$). The majority of cells in healthy cultures will have a polarized $\Delta\psi_m$; loss of $\Delta\psi_m$ is an early event in the apoptotic process (26). In this study, the cells were stained with JC-1 according to the protocol and analyzed by flow cytometry. The change of $\Delta\psi_m$ was observed in treated HeLa cells (Fig. 6). Compared to control, the proportion of the green fluorescence of

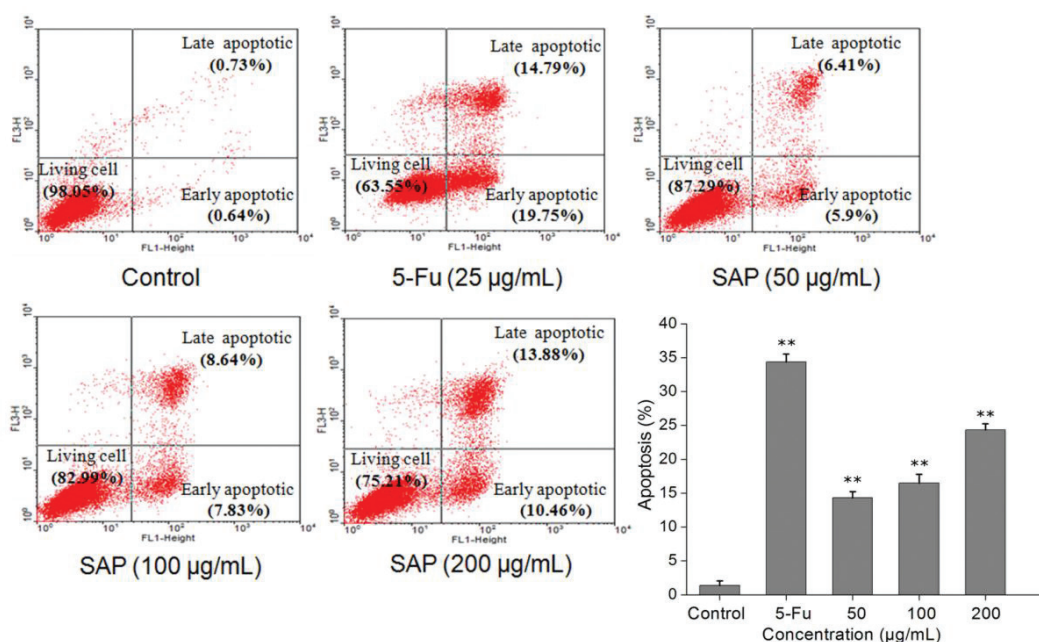


Fig. 5. The effect of SAP induces tumor cell apoptosis of HeLa cells. The cells apoptosis were monitored by flow cytometry using FACSscan (BD Biosciences). The results were expressed as means \pm SD ($n = 3$). ** $p < 0.01$ compared with control group.

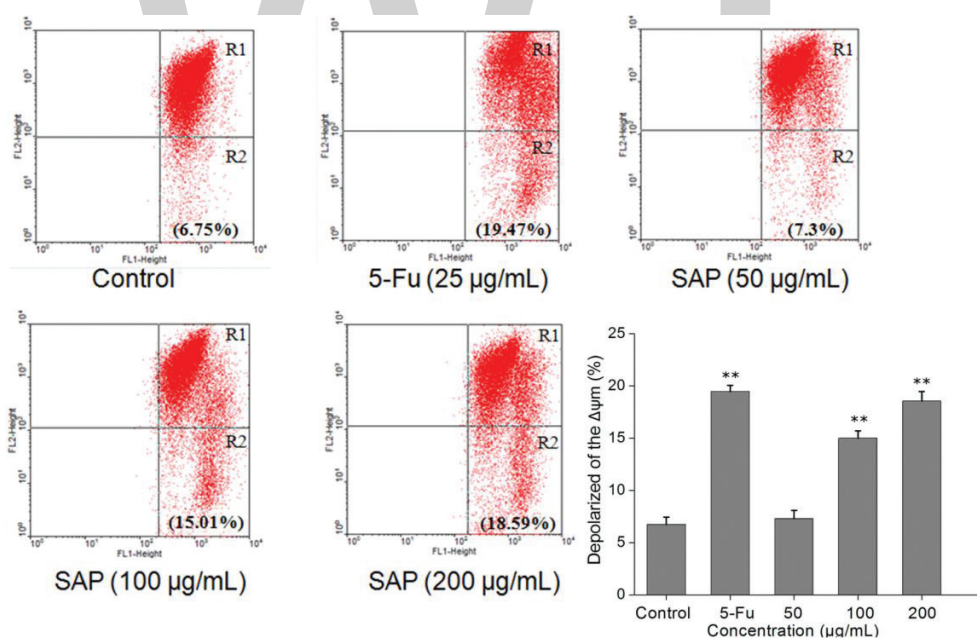


Fig. 6. Loss of mitochondrial membrane potential of HeLa cells induced by 5-Fu or different concentrations of SAP and stained by JC-1. Red/green fluorescence intensity detected by flow cytometry using FACSscan (BD Biosciences). The results were expressed as means \pm SD ($n = 3$). ** $p < 0.01$ compared with control group.

cells increased from 6.75 to 18.59% after treatment with 200 $\mu\text{g/mL}$ of SAP. Taken together, the results indicated that SAP could induce the dissipation of mitochondrial membrane potential ($\Delta\psi_m$) which facilitated the apoptosis of HeLa cells.

SAP induced cells apoptosis via regulation of cytochrome c and Bcl-2 family

A reduction in the mitochondrial membrane potential is usually accompanied by release of cytochrome c into the cytosol. The release of cytochrome c from mitochondria

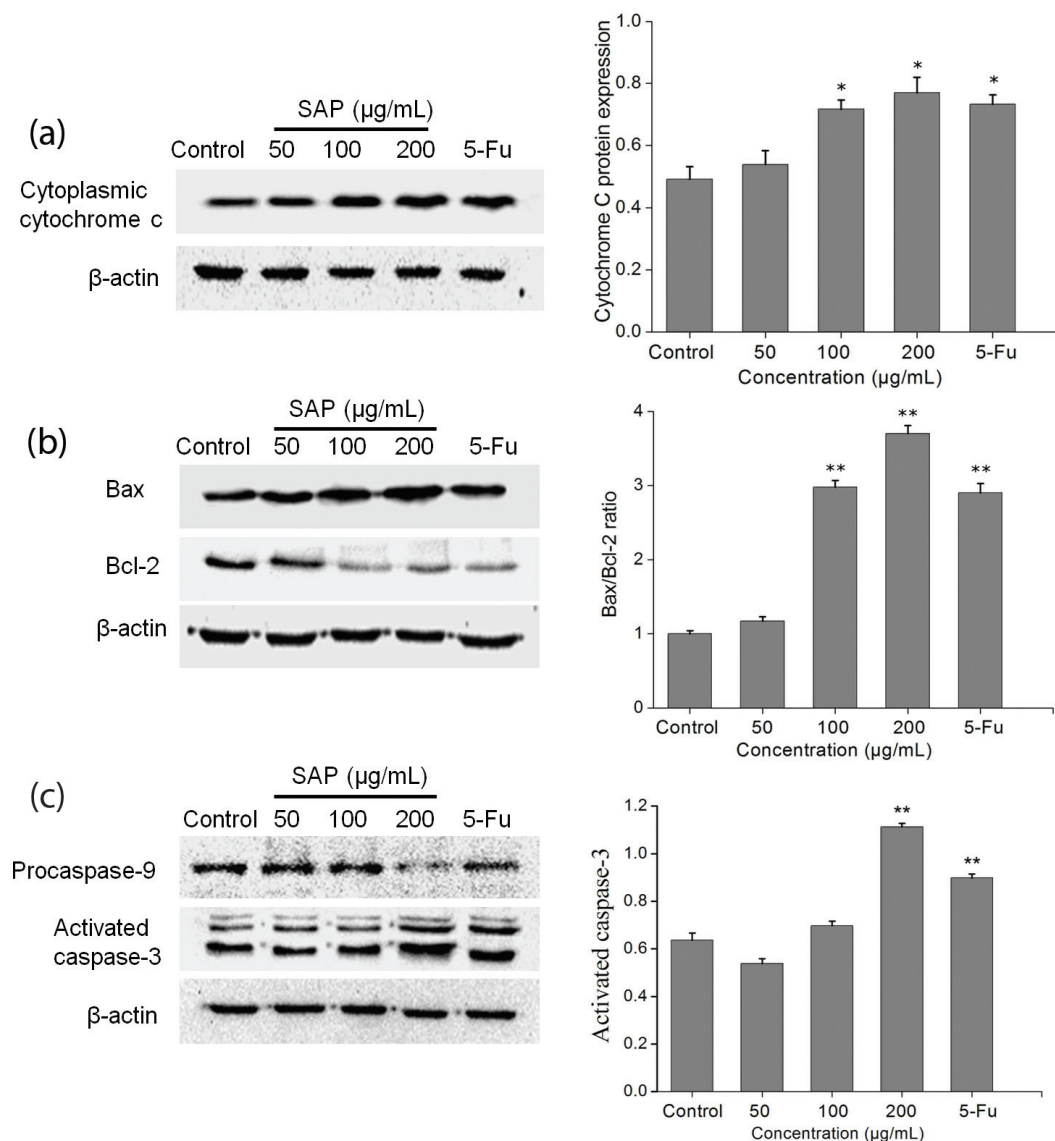


Fig. 7. Cytochrome c, Bcl-2, Bax, procaspase-9, and caspase-3 expression were analyzed by western blot. (a) SAP regulated the HeLa cells release of cytochrome c from mitochondria and (b) Bcl-2 protein family. (c) SAP regulated the HeLa cells procaspase-9 and activated caspase-3. The results were expressed as means \pm SD ($n = 3$). * $p < 0.05$ and ** $p < 0.01$ compared with control group.

is a particularly important event in the induction of apoptosis (27). Therefore, we examined the amount of cytochrome c in the cytoplasm using western blotting technique. After 48 h, a significant ($p < 0.05$) increase in cytosolic cytochrome c was observed (Fig. 7a).

On the one hand, this mitochondrial-mediated apoptosis pathway is regulated by the pro-apoptotic effectors (Bax, Bak, Bid, Bad, etc.) and the anti-apoptotic effectors (Bcl-2, Bcl-k, Bcl-w, etc.). The Bax serves as a major regulator to accelerate the permeability of mitochondria and release of cytochrome c, whereas the Bcl-2 resides in the mitochondrial wall and protects the integrity of mitochondria against cell apoptosis (28). On the other hand, Bcl-2 expression does not influence Bax expression but

inhibit activated caspase-3 expression in a dose-dependent manner (29). Therefore, the ratio of Bax/Bcl-2 is one of the decisive factors that determine cell apoptosis. With the increase in SAP concentration, the expression level of Bcl-2 gradually decreased, whereas the expression level of Bax gradually increased (Fig. 7b). The results suggested that SAP could promote apoptosis by elevating cytochrome c and Bcl-2 family.

Caspase 3 contributes to the SAP-induced HeLa cells apoptosis

Once cytochrome c is released from the mitochondria into the cytoplasm, it binds to Apaf-1 and subsequently recruits procaspase-9 to the apoptosome which can activate caspase-9 (30). The caspase-9 cleaves and activates

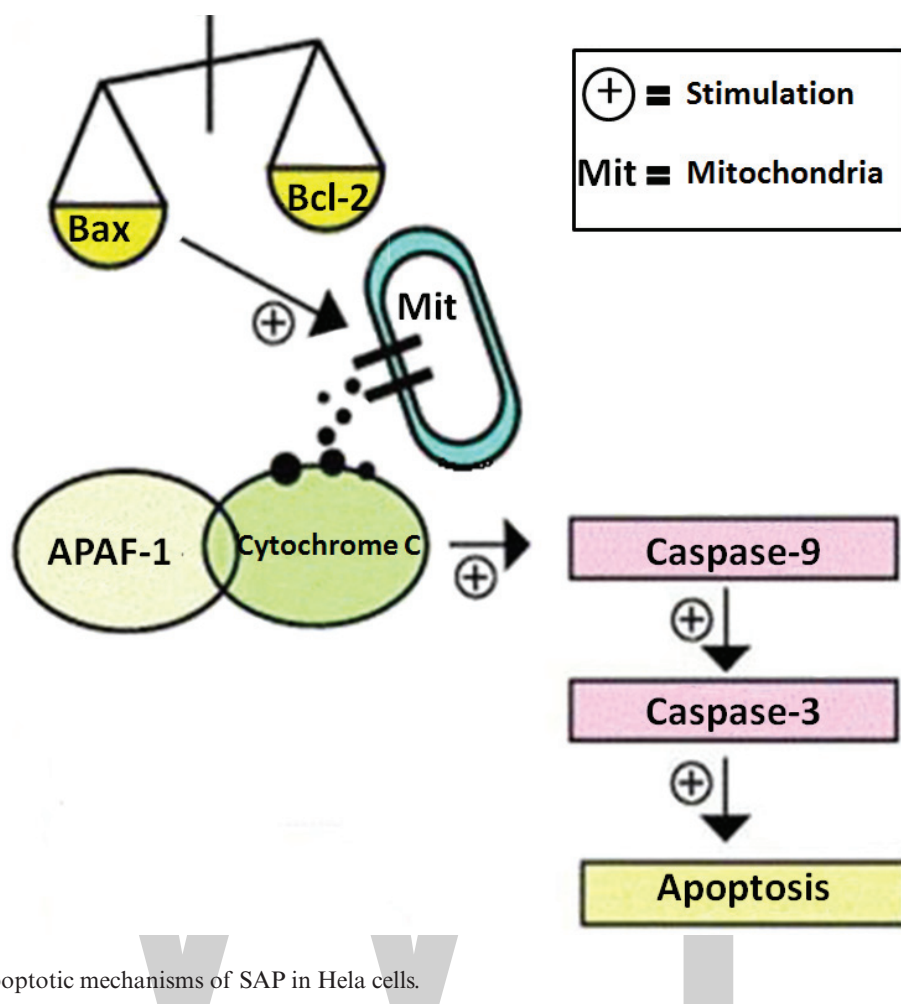


Fig. 8. Possible apoptotic mechanisms of SAP in HeLa cells.

downstream effector caspase-3. Caspase-3 is regarded as a crucial mediator of programmed cell apoptosis which has a prominent execution in the apoptotic signaling pathways (31). To investigate SAP-induced apoptosis in HeLa cells, western blot technique was used to detect the expression level of activated caspase-3 and procaspase-9. The results (Fig. 7c) indicated that during treatment with 200 $\mu\text{g}/\text{mL}$ SAP, the activation of caspase-3 prominently increased (reaching 1.77 times compared with control group), while procaspase-9 decreased dramatically. The above-mentioned results presented that SAP could regulate the activities of caspase-9 and caspase-3 and induce the HeLa apoptosis subsequently.

Conclusions

In this study, we isolated, purified, and characterized the novel polysaccharide from the fruiting bodies of *S. aspratus*. We evaluated the cancer cells cytotoxicity of SAP on tumor cells, *in vitro*. The results showed that, no matter at three-dimensional (3D) cell culture or two-dimensional (2D) cell culture, SAP (50 $\mu\text{g}/\text{mL}$) could significantly restrain the growth of tumor cells with no

cytotoxicity against normal cells. Our study investigated the apoptotic pathways by SAP in HeLa cells. Experimental results suggested that SAP caused mitochondrial dysfunction by increased expression of Bax and decreased expression of Bcl-2 which prompted release of cytochrome c from the mitochondria to the cytosol. These pro-apoptotic effectors caused recruitment of procaspase-9 which can activate caspase-9. The caspase-9 cleaves and activates downstream effector caspase-3 resulting in programmed cell apoptosis. These results speculate that SAP induces tumor cells apoptosis at least in part through the activation of caspase-3 and mitochondrial pathway (Fig. 8). In a nutshell, *S. aspratus* could be used as a potential medicinal agent for the treatment of cervical carcinoma.

Acknowledgements

This work was supported by the National Natural Science Foundation of China (31271817), the Key Project of Science and Technology of Anhui (1501031099).

Conflict of interest and funding

The authors declare that they have no conflict of interest.

References

- Vieira V, Marques A, Barros L, Barreira J, Ferreira IC. Insights in the antioxidant synergistic effects of combined edible mushrooms: phenolic and polysaccharidic extracts of *Boletus edulis* and *Marasmius oreades*. *J Food Nutr Res* 2012; 51(2): 1196.
- Ren L, Perera C, Hemar Y. Antitumor activity of mushroom polysaccharides: a review. *Food Funct* 2012; 3(11): 1118.
- Zhao L, Dong Y, Chen G, Hu Q. Extraction, purification, characterization and antitumor activity of polysaccharides from *Ganoderma lucidum*. *Carbohydr Polym* 2010; 80: 783–9.
- Santoyo S, Ramirez-Anguiano AC, Aldars-Garcia L, Reglero G, Soler-Rivas C. Antiviral activities of *Boletus edulis*, *Pleurotus ostreatus* and *Lentinus edodes* extracts and polysaccharide fractions against Herpes simplex virus type 1. *J Food Nutr Res* 2012; 51(4): 225–35.
- Liu Q, Cao XJ, Zhuang XH, Han W, Guo WQ, Xiong J, et al. Rice bran polysaccharides and oligosaccharides modified by *Griifola frondosa* fermentation: antioxidant activities and effects on the production of NO. *Food Chem* 2017; 223: 49–53.
- Mizuno M, Shiomi Y, Minato KI, Kawakami S, Ashida H, Tsuchida H. Fucogalactan isolated from *Sarcodon aspratus* elicits release of tumor necrosis factor- α and nitric oxide from murine macrophages. *Immunopharmacology* 2000; 46(2): 113–21.
- Han XQ, Wu XM, Chai XY, Chen D, Dai H, Dong HL, et al. Isolation, characterization and immunological activity of a polysaccharide from the fruit bodies of an edible mushroom, *Sarcodon aspratus* (Berk.) S. Ito. *Food Res Int* 2011; 44(1): 489–93.
- Chen Y, Hu ML, Wang C, Yang YL, Chen JH, Ding JN, et al. Characterization and in vitro antitumor activity of polysaccharides from the mycelium of *Sarcodon aspratus*. *Int J Biol Macromolec* 2013; 52: 52–8.
- Mayevsky A. Mitochondrial function and energy metabolism in cancer cells: past overview and future perspectives. *Mitochondrion* 2009; 9(3): 165–79.
- Shang D, Li Y, Wang C, Wang X, Yu Z, Fu X. A novel polysaccharide from Se-enriched *Ganoderma lucidum* induces apoptosis of human breast cancer cells. *Oncol Rep* 2011; 25: 267–72.
- Nie S, Zhang H, Li W, Xie M. Current development of polysaccharides from *Ganoderma*: isolation, structure and bioactivities. *Bioac Carbohydr Diet Fibre* 2013; 1(1): 10–20.
- Liu L, Lu YM, Li XH, Zhou LY, Yang D, Wang LM, et al. A novel process for isolation and purification of the bioactive polysaccharide TLH-3' from *Tricholoma lobayense*. *Process Biochem* 2015; 50: 1146–51.
- Wu X, Mao G, Fan Q, Zhao T, Zhao J, Li F, Yang L. Isolation, purification, immunological and anti-tumor activities of polysaccharides from *Gymnema sylvestre*. *Food Res Int* 2012; 48: 935–9.
- Li Y, He Q, Ren X, Tang X, Xu Y, Wen X, et al. MiR-145 inhibits metastasis by targeting fascin actin-bundling protein 1 in nasopharyngeal carcinoma. *PLoS One* 2015; 10(3): e122228.
- Liu H, Liu J, Qi C, Fang Y, Zhang L, Zhuo R, et al. Thermosensitive injectable in-situ forming carboxymethyl chitin hydrogel for three-dimensional cell culture. *Acta Biomater* 2016; 35: 228–37.
- Ding Q, Yang D, Zhang W, Lu Y, Zhang M, Wang L, et al. Antioxidant and anti-aging activities of the polysaccharide TLH-3 from *Tricholoma lobayense*. *Int J Biol Macromolec* 2016; 85: 133–40.
- Liao W, Lu Y, Fu J, Ning Z, Yang J, Ren J. Preparation and characterization of dictyophora indusiata polysaccharide-Zinc complex and its augmented antiproliferative activity on human cancer cells. *J Agr Food Chem* 2015; 63(29): 6525–34.
- Zhao T, Mao G, Mao R, Zou Y, Zheng D, Feng W, et al. Antitumor and immunomodulatory activity of a water-soluble low molecular weight polysaccharide from *Schisandra chinensis* (Turcz.) Baill. *Food Chem Toxicol* 2013; 55: 609–16.
- Sun X, Gao RL, Xiong YK, Huang QC, Xu M. Antitumor and immunomodulatory effects of a water-soluble polysaccharide from *Lilii Bulbus* in mice. *Carbohydr Polym* 2014; 102(1): 543–9.
- Gan D, Ma L, Jiang C, Xu R, Zeng X. Production, preliminary characterization and antitumor activity in vitro of polysaccharides from the mycelium of *Pholiota dinghuensis* Bi. *Carbohydr Polym* 2011; 84(3): 997–1003.
- Papageorgis P, Ozturk S, Lambert AW, Neophytou CM, Tzatsos A, Wong CK, et al. Targeting IL13Ralpha2 activates STAT6-TP63 pathway to suppress breast cancer lung metastasis. *Breast Cancer Res* 2015; 17: 1–15.
- Page H, Flood P, Reynaud EG. Three-dimensional tissue cultures: current trends and beyond. *Cell Tissue Res* 2013; 352(1): 123–31.
- Xu X, Farach-Carson MC, Jia X. Three-dimensional in vitro tumor models for cancer research and drug evaluation. *Biotechnol Adv* 2014; 32(7): 1256–68.
- Padron JM, Van Der Wilt CL, Smid K, Smitskamp-Wilms E, Backus HH, Pizao PE, et al. The multilayered postconfluent cell culture as a model for drug screening. *Crit Rev Oncol Hematol* 2000; 36: 141–57.
- Weinberg SE, Chandel NS. Targeting mitochondria metabolism for cancer therapy. *Nat Chem Biol* 2014; 11(1): 9–15.
- Ye RR, Tan CP, Ji LN, Mao ZW. Coumarin-appended phosphorescent cyclometalated iridium(III) complexes as mitochondria-targeted theranostic anticancer agents. *Dalton Trans* 2016; 45(33): 13042–51.
- Tian Y, Zhao Y, Zeng H, Zhang Y, Zheng B. Structural characterization of a novel neutral polysaccharide from *Lentinus giganteus* and its antitumor activity through inducing apoptosis. *Carbohydr Polym* 2016; 154: 231–40.
- Hata AN, Engelman JA, Faber AC. The BCL2 family: key mediators of the apoptotic response to targeted anticancer therapeutics. *Cancer Discov* 2015; 5(5): 475–87.
- Zhao H, Yenari MA, Cheng D, Sapolsky RM, Steinberg GK. Bcl-2 overexpression protects against neuron loss within the ischemic margin following experimental stroke and inhibits cytochrome c translocation and caspase-3 activity. *J Neurochem* 2003; 85(4): 1026–36.
- Wu C, Lee S, Malladi S, Chen M, Mastrandrea NJ, Zhang Z, et al. The Apaf-1 apoptosome induces formation of caspase-9 homo- and heterodimers with distinct activities. *Nat Commun* 2016; 7: 13565.
- Galluzzi L, Kepp O, Kroemer G. Caspase-3 and prostaglandins signal for tumor regrowth in cancer therapy. *Oncogene* 2012; 31(23): 2805–8.

*Yan Chen

School of Life Sciences, Anhui University,
Hefei 230601, China
Email: chenyan91030@yahoo.com

PERMISSIONS

All chapters in this book were first published in F&NR, by Swedish Nutrition Foundation; hereby published with permission under the Creative Commons Attribution License or equivalent. Every chapter published in this book has been scrutinized by our experts. Their significance has been extensively debated. The topics covered herein carry significant findings which will fuel the growth of the discipline. They may even be implemented as practical applications or may be referred to as a beginning point for another development.

The contributors of this book come from diverse backgrounds, making this book a truly international effort. This book will bring forth new frontiers with its revolutionizing research information and detailed analysis of the nascent developments around the world.

We would like to thank all the contributing authors for lending their expertise to make the book truly unique. They have played a crucial role in the development of this book. Without their invaluable contributions this book wouldn't have been possible. They have made vital efforts to compile up to date information on the varied aspects of this subject to make this book a valuable addition to the collection of many professionals and students.

This book was conceptualized with the vision of imparting up-to-date information and advanced data in this field. To ensure the same, a matchless editorial board was set up. Every individual on the board went through rigorous rounds of assessment to prove their worth. After which they invested a large part of their time researching and compiling the most relevant data for our readers.

The editorial board has been involved in producing this book since its inception. They have spent rigorous hours researching and exploring the diverse topics which have resulted in the successful publishing of this book. They have passed on their knowledge of decades through this book. To expedite this challenging task, the publisher supported the team at every step. A small team of assistant editors was also appointed to further simplify the editing procedure and attain best results for the readers.

Apart from the editorial board, the designing team has also invested a significant amount of their time in understanding the subject and creating the most relevant covers. They scrutinized every image to scout for the most suitable representation of the subject and create an appropriate cover for the book.

The publishing team has been an ardent support to the editorial, designing and production team. Their endless efforts to recruit the best for this project, has resulted in the accomplishment of this book. They are a veteran in the field of academics and their pool of knowledge is as vast as their experience in printing. Their expertise and guidance has proved useful at every step. Their uncompromising quality standards have made this book an exceptional effort. Their encouragement from time to time has been an inspiration for everyone.

The publisher and the editorial board hope that this book will prove to be a valuable piece of knowledge for researchers, students, practitioners and scholars across the globe.

LIST OF CONTRIBUTORS

Alessandro Attanzio, Luisa Tesoriere, Sonya Vasto, Anna Maria Pintaudi, Maria A. Livrea and Mario Allegra

Dipartimento di Scienze e Tecnologie Biologiche, Chimiche e Farmaceutiche, Università degli Studi di Palermo, Palermo, Italy

W. Martens, M. A. Karim and M. U. H. Joardder

Science and Engineering Faculty, Queensland University of Technology 2 George street, Brisbane, QLD 4001, Australia

Nghia Duc Pham

Science and Engineering Faculty, Queensland University of Technology 2 George street, Brisbane, QLD 4001, Australia

Engineering Faculty, Vietnam National University of Agriculture, Vietnam

Hwa Joung Lee, Rihua Cui, Ja Young Jeon, Hae Jin Kim and Kwan-Woo Lee

Department of Endocrinology and Metabolism, Ajou University School of Medicine, Suwon, Republic of Korea

Sung-E Choi and Yup Kang

Department of Physiology, Ajou University School of Medicine, Suwon, Republic of Korea

Tae Ho Kim

Division of Endocrine and Metabolism, Department of Internal Medicine, Seoul Medical Center, Seoul, Republic of Korea

Stina Engelheart and Robert Brummer

School of Medical Sciences, Örebro University, Örebro, Sweden

Huandong Zhao

Key Laboratory of Nanobiological Technology of Chinese Ministry of Health, Xiangya Hospital, Central South University, Changsha, China

School of Pharmaceutical Sciences, Central South University, Changsha, China

Yuxiang Chen

School of Pharmaceutical Sciences, Central South University, Changsha, China

Jian Li and Yang Chen

Institute of Biomedical Engineering, Xiangya Hospital, Central South University, Changsha, China

Juan Zhao

Department of Clinical Laboratory, Xiangya Hospital, Central South University, Changsha, China

Caiping Ren

Cancer Research Institute, Collaborative Innovation Center for Cancer Medicine, Key Laboratory for Carcinogenesis of Chinese Ministry of Health, School of Basic Medical Science, Central South University, Changsha, China

Nurhayati Zainal Abidin

Institute of Biological Sciences, Faculty of Science, University of Malaya, Kuala Lumpur, Malaysia

Annie George

Institute of Biological Sciences, Faculty of Science, University of Malaya, Kuala Lumpur, Malaysia Biotropics Malaysia Berhad, Lot 21, Jalan U1/19, Section U1, Hicom-Glenmarie Industrial Park, 40150 Shah Alam, Malaysia

Jay Udani

Agoura Hills, CA, USA

Ashril Yusof

Exercise Science, Sports Centre, University of Malaya, 50603 Kuala Lumpur, Malaysia

Koichi Misawa

Biological Science Laboratories, Kao Corporation, Ichikai-machi, Haga-gun, Tochigi, Japan

Hiroko Jokura

Lifestyle Research Center, Kao Corporation, Tokyo, Japan

Akira Shimotoyodome

Health Care Food Research Laboratories, Kao Corporation, Tokyo, Japan

Liu Xianchu and Liu Ming

Institute of Physical Education, Hunan University of Arts and Science, Hunan Province, Changde, China Key Laboratory of Physical Fitness and Exercise Rehabilitation of Hunan Province, Hunan Normal University, Changsha, China

Liu Xiangbin and Zheng Lan

Key Laboratory of Physical Fitness and Exercise Rehabilitation of Hunan Province, Hunan Normal University, Changsha, China

Inger Aakre, Maria Wik Markhus, Marian Kjellevoid and Lisbeth Dahl

Food Security and Nutrition, Institute of Marine Research, Bergen, Norway

Vibeke Moe and Lars Smith

Department of Psychology, University of Oslo, Oslo, Norway

Yao Jiang, Chuhan Fu and Zhengquan Su

Guangdong Engineering Research Center of Natural Products and New Drugs, Guangdong Pharmaceutical University, Guangzhou, China

Guangdong Metabolic Diseases Research Center of Integrated Chinese and Western Medicine, Key Unit of Modulating Liver to Treat Hyperlipemia SATCM (State Administration of Traditional Chinese Medicine), Guangdong Pharmaceutical University, Guangzhou, China

Jiao Guo

Guangdong Metabolic Diseases Research Center of Integrated Chinese and Western Medicine, Key Unit of Modulating Liver to Treat Hyperlipemia SATCM (State Administration of Traditional Chinese Medicine), Guangdong Pharmaceutical University, Guangzhou, China

Guihua Liu

Shenzhen Center for Disease Control and Prevention, Shenzhen, China

Byung-Hyun Park

Department of Biochemistry, Chonbuk National University Medical School, Jeonju, Jeonbuk, Republic of Korea

Ui-Jin Bae

Department of Biochemistry, Chonbuk National University Medical School, Jeonju, Jeonbuk, Republic of Korea

Clinical Trial Center for Functional Foods, Chonbuk National University Hospital, Jeonju, Jeonbuk, Republic of Korea

Eun-Soo Jung and Su-Jin Jung

Clinical Trial Center for Functional Foods, Chonbuk National University Hospital, Jeonju, Jeonbuk, Republic of Korea

Soo-Wan Chae

Clinical Trial Center for Functional Foods, Chonbuk National University Hospital, Jeonju, Jeonbuk, Republic of Korea

Department of Pharmacology, Chonbuk National University Medical School, Jeonju, Jeonbuk, Republic of Korea

Xin Wu, Chuan-qi Xie, Qiang-qiang Zhu, Ming-yue Wang, Bin Sun, Yan-ping Huang, Chang Shen and Meng-fei An

Key Laboratory of Pu-erh Tea Science, Ministry of Education, Yunnan Agricultural University, Kunming, China

College of Food Science and Technology, Yunnan Agricultural University, Kunming, China

Yun-li Zhao

Key Laboratory of Pu-erh Tea Science, Ministry of Education, Yunnan Agricultural University, Kunming, China

College of Food Science and Technology, Yunnan Agricultural University, Kunming, China

State Key Laboratory of Phytochemistry and Plant Resources in West China, Kunming Institute of Botany, Chinese Academy of Sciences, Kunming, China

Xuan-jun Wang and Jun Sheng

Key Laboratory of Pu-erh Tea Science, Ministry of Education, Yunnan Agricultural University, Kunming, China

College of Science, Yunnan Agricultural University, Kunming, China

State Key Laboratory for Conservation and Utilization of Bio-Resources in Yunnan, Kunming, China

Xiujing Dou, Junlan Han, Qiuyuan Ma, Baojing Cheng, Anshan Shan, Nan Gao and Yu Yang

Institute of Animal Nutrition, Northeast Agricultural University, Harbin, China

Xiaobin Zhang, Zhenhuan Song, Yuanyuan You and Tianfeng Chen

The First Affiliated Hospital, and Department of Chemistry, Jinan University, Guangzhou 510632, China

Xiaoling Li

Institute of Food Safety and Nutrition, Jinan University, Guangzhou 510632, China

Anthony O. Obilana and Victoria A. Jideani

Food Technology Department, Cape Peninsula University of Technology, Bellville Campus, Cape Town, South Africa

Barthi Odhav

Biotechnology and Food Technology Department, Durban University of Technology, Durban, South Africa

Tao Wu and Min Zhang

Beijing Advanced Innovation Center for Food Nutrition and Human Health, Beijing Technology and Business University, Beijing, China
State Key Laboratory of Food Nutrition and Safety, Tianjin University of Science and Technology, Tianjin, China
Tianjin Food Safety & Low Carbon Manufacturing Collaborative Innovation Center, Tianjin, China

Jinling Xu, Yijun Chen and Rui Liu

State Key Laboratory of Food Nutrition and Safety, Tianjin University of Science and Technology, Tianjin, China

Pedro Moreira

Faculdade de Ciências da Nutrição e Alimentação, Universidade do Porto, Porto, Portugal
EPIUnit – Instituto de Saúde Pública, Universidade do Porto, Porto, Portugal
Centro de Atividade Física, Saúde e Lazer, Universidade do Porto, Porto, Portugal

Patrícia Padrão

Faculdade de Ciências da Nutrição e Alimentação, Universidade do Porto, Porto, Portugal
EPIUnit – Instituto de Saúde Pública, Universidade do Porto, Porto, Portugal

Rita S. Guerra and Cláudia Afonso

Faculdade de Ciências da Nutrição e Alimentação, Universidade do Porto, Porto, Portugal

Ana S. Sousa

Faculdade de Ciências da Nutrição e Alimentação, Universidade do Porto, Porto, Portugal
Escola Superior de Saúde, Instituto Politécnico de Leiria, Leiria, Portugal

Alejandro Santos

Faculdade de Ciências da Nutrição e Alimentação, Universidade do Porto, Porto, Portugal
I3S-Instituto de Investigação e Inovação em Saúde, Porto, Portugal

Nuno Borges

Faculdade de Ciências da Nutrição e Alimentação, Universidade do Porto, Porto, Portugal
CINTESIS–Centre for Health Technology and Services Research, Porto, Portugal

Teresa F. Amaral

Faculdade de Ciências da Nutrição e Alimentação, Universidade do Porto, Porto, Portugal
UISPA-IDMEC, Faculdade de Engenharia, Universidade do Porto, Porto, Portugal

Zhu Yi-Shen and Sun Shuai

College of Biotechnology and Pharmaceutical Engineering, Nanjing Tech University, Nanjing, China

Richard FitzGerald

Life Science Department, University of Limerick, Limerick, Ireland

Ive Nerhus, Maria Wik Markhus, Bente M. Nilsen, Jannike Øyen, Amund Maage, Elisabeth Rasmussen Ødegård, Lisa Kolden Midtbø, Sylvia Frantzen, Tanja Kögel, Ingvild Eide Graff, Øyvind Lie, Lisbeth Dahl and Marian Kjellevoid

Institute of Marine Research (IMR), Bergen, Norway

Dan-Dan Wang, Qing-Xi Wu, Wen-Juan Pan, Sajid Hussain and Shomaila Mehmood

School of Life Sciences, Anhui University, Hefei, China

Yan Chen

School of Life Sciences, Anhui University, Hefei, China
Anhui Key Laboratory of Modern Biomanufacturing, Hefei, China

Index

A

Amino Acid, 76, 96, 146, 149-151, 154, 175-177, 180-183
Ascorbic Acid, 3-4, 10, 15, 19, 49, 151

B

Bile Acid, 86-87, 94, 99-100
Bitter Melon Extract, 21-22
Blood Lipid, 101, 156, 170
Body Mass Index, 2, 32, 47-48, 64-65, 79, 85, 165, 167-168

C

C-reactive Protein, 1-2, 7-8, 33
Cactus Pear Diet, 1-4
Cathepsin K, 110-111, 113, 117-120
Chitooligosaccharide, 86
Comprehensive Geriatric Assessment, 31, 35
Coupled Plasma Mass-spectrometry, 77-78
Creatine Phosphokinase, 70

D

D-galactose, 37-38, 45, 199
Dietary Iodine Intake, 77, 185-186
Dried Kiwifruit, 11, 13

E

Endoplasmic Reticulum, 21, 29-30
Epidermal Growth Factor Receptor, 121
Epididymal Fat, 23, 25
Erythrocyte Sedimentation Rate, 1
Eurycoma Longifolia, 47-48, 61-62

F

Fasting Blood Glucose, 101, 105
Fatty Acid Elongation, 156, 162
Fetal Bovine Serum, 102, 112, 122, 135, 199
Finger Millet, 151, 155
Fluoxetine, 47, 60-61
Food Composition Table, 78, 185-186, 190, 192-196

G

Gene Expression, 29, 86-88, 94-96, 99, 118, 122, 124-128, 130-132, 156, 158, 162
Glucose-dependent Insulinotropic Peptide, 63
Glutathione Peroxidase, 37-38, 71
Grape Seed Proanthocyanidin Extract, 62, 70, 72-76
Green Tea Aqueous Extract, 110-111, 119

H

Hepatic Steatosis, 27, 29, 101, 105-106
High Fat Diet, 22, 29-30, 99, 101
High-performance Liquid Chromatography, 102, 134-135
Host Defense Peptides, 121, 132-133
Hyperglycemia, 29-30, 45, 63-64, 68-69, 101

I

Inadequate Iodine Intake, 77, 83-84
Inadequate Potassium Intake, 164, 166-167
Indicaxanthin, 2, 4, 6-8
Inflammatory Cytokines, 2, 4, 45, 72-73, 121, 130
Iodine-rich Foods, 79, 81-82

L

Lactic Acid Level, 70
Lipid Homeostasis, 21, 30
Liver X Receptor Alpha, 86, 96
Low-density Lipoprotein, 3, 48, 65, 86, 92, 96, 100, 157, 162

M

Malnutrition, 31-36
Malondialdehyde, 37-38, 45, 70-71, 157, 163
Metabolic Panel, 47-48
Metabolic Syndrome, 1, 29-30, 70
Mitochondrial Membrane Potential, 198, 200, 203-204
Morus Alba L, 101
Mulberry Leaf Extract, 101-102, 104, 108-109
Mung Bean Proteins, 174-175, 177, 179-180, 182

N

Nonalcoholic Fatty Liver Disease, 21, 29-30, 99
Nutrient Reference Values, 151

O

Olfactory Function, 35
Oolong Tea, 134-135, 143, 156-157, 159-163
Oxidative Stress, 2, 7-8, 27, 30, 37-38, 43-46, 70-71, 73-76, 134, 144, 162

P

Pearl Millet, 145-146, 148-155
Penicillin, 22, 102, 122, 135-136
Phoenix Dan Cong Tea, 134-136, 143
Placebo, 47-68, 108
Postmenopausal Osteoporosis, 110, 115, 119

Postprandial Hyperglycemia, 63, 69

R

Reactive Oxygen Species, 23-24, 117, 134, 144

Rice Bran Triterpenoids, 63, 66, 68

S

Sarcodon Aspratus, 198, 207

Sarcopenia, 33, 35, 99

Sertraline, 47, 60

Serum Lipid Levels, 26, 86, 90

Sodium Phenylbutyrate, 121-122

Somatic Disorders, 31-34

Steroid Hormone Biosynthesis, 156

T

Theophylline, 136-137

Toll-like Receptor, 121, 133

Total Polyphenol Content, 10, 15, 135

Triglyceride, 21, 23, 64, 66, 68, 86, 92, 100, 103, 106, 157-158, 162

Triterpene Alcohol, 63-64, 69

Trypsin Inhibitory Activity, 174, 181

Tumour Necrosis Factor, 1

U

Urinary Iodine Concentration, 77-78, 80-82, 85

Urinary Sodium, 164-165, 171-172

V

Vitamin D Receptor, 122, 133

W

Walnut Oil Capsule, 37-39

WWT